EVALUATION OF THE IMMUNOGENICITY OF T AND B CELL EPITOPES FROM THE S AND M PROTEINS OF SARS-COV-2 WUHAN AND OMICRON STRAINS IN BALB/C MICE

KANWAL KHALID

SCHOOL OF MEDICAL AND LIFE SCIENCES
SUNWAY UNIVERSITY
MALAYSIA

2024

EVALUATION OF THE IMMUNOGENICITY OF T AND B CELL EPITOPES FROM THE S AND M PROTEINS OF SARS-COV-2 WUHAN AND OMICRON STRAINS IN BALB/C MICE

KANWAL KHALID

DISSERTATION SUBMITTED IN FULFILMENT OF THE REQUIREMENTS FOR THE DEGREE OF MASTER OF SCIENCE IN LIFE SCIENCES

SCHOOL OF MEDICAL AND LIFE SCIENCES
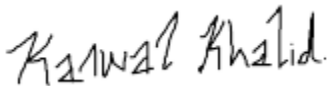## SUNWAY UNIVERSITY
MALAYSIA

2024

ORIGINAL LITERARY WORK DECLARATION

Name of Candidate : Kanwal Khalid

IC /Passport No : NU4129023

Student ID : 19115914

Name of Degree : Masters in Life Sciences

Title of Dissertation : Evaluation of the Immunogenicity of T and B Cell Epitopes from the S and M proteins of SARS-CoV-2 Wuhan and Omicron Strains in BALB/c Mice

I do solemnly and sincerely declare that:

1. I am the sole author/writer of this Work;

2. This Work is original;

3. Any use of any work in which copyright exists was done by way of fair dealing and for permitted purposes and any excerpt or extract from, or reference to or reproduction of any copyright work has been disclosed expressly and sufficiently and the title of the Work and its authorship have been acknowledged in this Work;

4. I do not have any actual knowledge nor do I ought reasonably to know that the making of this work constitutes an infringement of any copyright work;

5. I hereby assign all and every right in the copyright to this Work to the Sunway University (SunU), who henceforth shall be owner of the copyright in this Work and that any reproduction or use in any form or by any means whatsoever is prohibited without the written consent of Sunway University having been first had and obtained;

6. I am fully aware that if in the course of making this Work I have infringed any copyright whether intentionally or otherwise, I may be subject to legal action or any other action as may be determined by Sunway University.

_____
Candidate's Signature   Date: 9th November 2023

Subscribed and solemnly declared before,

_____
Witness's Signature   Date: 10th November 2023

Name   : Associate Professor Dr Hwang Jung Shan
Designation : Associate Professor, School of Medical and Life Sciences, Sunway University
Witness will be the supervisor

ABSTRACT

The coronavirus disease (COVID-19) caused by the severe acute respiratory syndrome coronavirus 2 (SARS-CoV-2) has resulted in numerous infections and deaths. The emergence of SARS-CoV-2 variants of concern (VOCs) resulted in reductions in the protective efficacies of current mRNA and viral-vectored vaccines targeting the spike (S) protein from the SARS-CoV-2 Wuhan strain. A more promising strategy involves targeting highly conserved and immunogenic sequences from SARS-CoV-2 structural proteins to produce immune responses against the Wuhan strain and circulating VOCs. Recombinant protein vaccines could serve as a valuable vaccine development platform based on their high stability, safety, and immunogenicity in clinical development. This research project aimed to develop a recombinant protein vaccine against SARS-CoV-2. Antigens were identified through literature mining and derived from the SARS-CoV-2 S and membrane (M) in the form of six peptides specifying highly conserved B cell and T cell epitopes. The expressed recombinant protein of interest, GST-6Phis, was purified through ammonium sulfate precipitation, gel filtration, immobilized metal affinity chromatography (IMAC), nickel-nitrilotriacetic acid (Ni-NTA) histidine affinity chromatography, and a protein concentrator. Four groups of 5 BALB/c mice each were intramuscularly or intranasally immunized with 10 μg GST-6Phis or with PBS. Cellular and humoral responses were evaluated at 42 days' post-immunization. Intramuscular administration of GST-6Phis resulted in IFN-γ secreting $CD4^+$ T cells, while intranasal administration produced IFN-γ secreting $CD8^+$ T cells. Robust IgG antibody responses, as represented by absorbance values and mean reciprocal antibody titers, resulted from the intramuscular and intranasal administration of GST-6Phis. Sera obtained from mice immunized both intramuscularly and intranasally with GST-6Phis contained neutralizing antibodies against the SARS-CoV-2 Wuhan strain, while intramuscular administration produced neutralizing

antibodies against Omicron. In conclusion, the recombinant protein vaccine demonstrated the promise of utilizing conserved and immunogenic epitopes to produce immune responses against both the SARS-CoV-2 Wuhan and Omicron strains.

ACKNOWLEDGMENTS

My heartfelt appreciation to Distinguished Professor Poh Chit Laa, my main supervisor, for providing me with the invaluable opportunity to expand my research skills and knowledge, and for her unwavering support and constructive feedback that made the successful completion of my Master's research project.

My deepest thanks to my current main supervisor, Associate Prof. Dr. Hwang Jung Shan, and co-supervisor Dr. Ong Seng-Kai for their invaluable guidance and insightful comments on how to improve the quality of my research.

I would also like to thank Dr. Lim Hui Xuan for her assistance and guidance on how to effectively conduct mice immunizations and improve my research skills.

I am deeply grateful to my parents, Dr. Khalid Osman and Dr. Nargis Iqbal, and to my brother, Hamza Khalid for their unwavering support throughout my educational journey. I am truly appreciative that my parents have worked tirelessly to provide for me and have sacrificed considerably so that my brother and I could get a quality education.

I am profoundly grateful to my beloved cat, Suzen Suza, who holds a special place as both my best friend and an important member of my family. Her devoted companionship over the course of 18 years has left an indelible mark on my life.

TABLE OF CONTENTS

LIST OF TABLES

LIST OF FIGURES

live CD3$^+$ T cells, and CD3$^+$CD4$^+$ T cells producing IFN-γ. **(B)** Representative plots showing the percentage of IFN-γ production by CD4$^+$ T cells in splenocytes of BALB/c mice immunized intramuscularly with PBS, intramuscularly with GST-6Phis, and intranasally with PBS, and intranasally with GST-6Phis. The quadrant G+- shows CD4$^+$ T cells scored negative for IFN-γ production while G++ shows CD4$^+$ T cells scored positive for IFN-γ production **(C)** Comparative percentages of IFN-γ secreting CD4$^+$ T cells in splenocytes in mice immunized intramuscularly with PBS, intramuscularly with GST-6Phis, and intranasally with PBS, and intranasally with GST-6Phis. Data from triplicate assays were plotted using GraphPad Prism 8.02 software (GraphPad Software Inc., San Diego, CA, USA) and expressed as mean (± SD) (T-test: * $p < 0.05$) (NS: not significant).

LIST OF ABBREVIATIONS

COVID-19	Coronavirus Disease 2019
SARS-CoV-2	Severe Acute Respiratory Syndrome Coronavirus 2
WHO	World Health Organization
IV	Inactivated Vaccine
LAV	Live attenuated vaccine
VOC	Variants of concern
FDA	Food and Drug Administration
EMA	European Medicines Agency
GMT	Geometric Mean Titre
FRNT50	50% Focus Reduction Neutralisation Test
ºC	degree Celsius
IFN-γ	Interferon gamma
ORF	Open-reading frame
IMAC	Immobilized metal affinity chromatography
Ni-NTA	Nickel-nitrilotriacetic acid
µg	Microgram
µL	Microlitre
CMV	Cytomegalovirus
SDS	Sodium Dodecyl Sulfate
S	Spike
M	Membrane

N	Nucleocapsid
E	Envelope
ACE2	Angiotensin-converting enzyme 2
NTD	NH-2 terminal domain
RBD	Receptor-binding domain
LB	Luria-Bertani
TMPRSS2	Transmembrane serine protease 2
DNA	Deoxyribonucleic acid
mRNA	Messenger ribonucleic acid
RNA	Ribonucleic acid
LPS	Lipopolysaccharide
GST	Glutathione S-transferase
His	Histidine
TNF	Tumor Necrosis Factor
CTL	Cytotoxic T lymphocyte.
MHC	Major histocompatibility complex
T_{fr}	Foxp3$^+$ T follicular regulatory
T_{fh}	T follicular helper
HEK	Human embryonic kidney
APC	Antigen-presenting cells
LNP	Lipid nanoparticle
NIAID	National Institute of Allergy and Infectious Diseases
rpm	Revolutions per minute

ICS	Cytokine staining
ELISA	Enzyme-linked immunosorbent assay
ELISpot	Enzyme-linked immunosorbent spot
RBDHRP	HRP-conjugated RBD
SDS-PAGE	Sodium dodecyl-sulfate polyacrylamide gel electrophoresis
IPTG	Isopropyl β-D-1-thiogalactopyranoside
IN RP	Intranasal GST-6Phis recombinant protein
IM RP	Intramuscular GST-6Phis recombinant protein
IN PBS	Intranasal PBS
IM PBS	Intramuscular PBS
UM	University Malaya
CV	Column volumes
PVDF	Polyvinylidene difluoride
GISAID	Global Initiative on Sharing All Influenza Data
TMB	3,3'5,5'-Tetramethylbenzidine
PBS	Phosphate buffered saline
BSA	Bovine serum albumin
CH	Central helix
VLP	Virus-like particle
Sf9	Spodoptera frugiperda
UV	Ultraviolet
SDS	Sodium dodecyl-sulfate
T7 promoter	T7 RNA polymerase

T7 terminator	Tφ transcription terminator
TSP	Total soluble proteins
NTA	Nitrilotriacetic acid
IDA	Iminodiacetic acid

CHAPTER 1: INTRODUCTION

The COVID-19 which was caused by the novel etiological agent, the SARS-CoV-2 originated in Wuhan City, China in December 2019. COVID-19 spread across the globe at an alarmingly accelerated rate (Sannathimmappa & Nambiar, 2020). On March 11, 2020, the World Health Organization (WHO) officially classified the global COVID-19 outbreak as a pandemic (Cucinotta & Vanelli, 2020). Academic groups and pharmaceutical companies actively collaborated at an unprecedented pace in history to develop effective vaccines against SARS-CoV-2 (Ahmed et al., 2021). These vaccine candidates were based on vaccine platforms such as messenger ribonucleic acid (mRNA) and viral-vectored and also conventional ones such as the inactivated and protein subunit. These vaccine candidates were licensed under emergency approval for large-scale public immunizations (Shahcheraghi et al., 2021). Notably, all these vaccine candidates were based on the S glycoprotein of the SARS-CoV-2 Wuhan strain (Martínez-Flores et al., 2021). Indeed, these vaccine candidates conferred high levels of protection against infections caused by the SARS-CoV-2 Wuhan strain (El Sahly et al., 2022; Falsey et al., 2021).

1.1 Problem statement

Reported vaccine efficacies of the licensed vaccines against the SARS-CoV-2 Wuhan strain were high. For example, mRNA-1273, BNT162b2, ChAdOx1 nCoV-19, and BBIBP-CorV showed a protective efficacy of 94.1%, 95%, 90%, and 78.1%, respectively (Puranik et al., 2021; Voysey et al., 2021; Zhang et al., 2022). However, the SARS-CoV-2 is subjected to spontaneous mutations due to the replication process carried out by the viral ribonucleic acid (RNA) polymerase (Cosar et al., 2022). Throughout the duration of the pandemic, there has been a consistent evolution of the SARS-CoV-2, resulting in the emergence of Alpha, Beta, Gamma, Delta, and Omicron VOCs that are different in genome sequences when compared to the original

SARS-CoV-2 Wuhan strain (Farhud & Mojahed, 2022). The majority of these mutations primarily were located in the S gene (Magazine et al., 2022).

The emergence of SARS-CoV-2 VOCs is associated with a reduction in the protective efficacies of current vaccines. Decreased efficacies of the mRNA-1273, BNT162b2, ChAdOx1 nCoV-19, BBIBP-CorV vaccines against SARS-CoV-2 VOCs have been reported (Tseng et al., 2022). The emergence and dissemination of SARS-CoV-2 variants pose a significant challenge in effectively preventing and controlling the pandemic through immunizations with vaccines based on the S protein of the SARS-CoV-2 Wuhan strain. Therefore, despite the existence of effective vaccines against the SARS-CoV-2 Wuhan strain, the number of infections and deaths attributable to SARS-CoV-2 VOCs continued to increase. As of 14 June 2023, there were 767,984,989 infections and 6,943,390 deaths associated with COVID-19 (WHO, 2023a). The COVID-19 pandemic has demonstrated a significant propensity for causing harm to the health and well-being of individuals as well as inducing financial repercussions, economic crises, and leading to the widespread implementation of stringent lockdown measures (Belitski et al., 2022; Dai et al., 2021; Hill, 2022; Shang et al., 2021). There is a high probability of the emergence of novel VOCs, characterized by multiple mutations in the S protein. Consequently, this could potentially render current vaccines less effective against these novel VOCs with modified S proteins, thereby increasing susceptibility to infection and the potential for immune escape.

Vaccine development approaches involving mRNA, DNA, or recombinant protein serve as a promising solution against the problem of emerging SARS-CoV-2 VOCs and the associated reduction in the protective efficacies of current vaccines against SARS-CoV-2. Indeed, mRNA, deoxyribonucleic acid (DNA), and recombinant protein vaccines may be developed to incorporate different antigenic targets specific to the sequences of novel SARS-CoV-2 VOCs (Maruggi et al.,

2019; Moyle & Toth, 2013; Smith et al., 2020). Indeed, Moderna's bivalent booster vaccine, mRNA-1273.222, which consisted of the mRNA encoding the S protein from both the SARS-CoV-2 Wuhan strain and the SARS-CoV-2 Omicron BA.4/BA.5 variants, quickly progressed to phase 2/3 clinical development and demonstrated the induction of higher neutralizing antibody titers against BA.4/BA.5 compared to a booster dose of mRNA-1273 (Chalkias et al., 2022). While this proactive approach to developing vaccines is commendable, such targeted development may not be sustainable in the long run in light of the emergence of the continuously mutating SARS-CoV-2 virus. A more viable prospect for vaccine development against emerging SARS-CoV-2 VOCs is associated with the identification of highly conserved and immunogenic epitopes that may be incorporated in mRNA, DNA, or recombinant protein vaccines as antigenic determinants to develop immunization strategies effective against emerging SARS-CoV-2 VOCs.

The use of the conventional live attenuated vaccine (LAV) platform is not considered to be feasible or safe in terms of large-scale productions of LAVs to vaccinate against COVID-19 because of the danger it poses in terms of potential reversion of live attenuated viruses to virulence through mutations or recombination (Hanley et al., 2011). Moreover, in order to develop LAVs for large-scale production, the growth of the highly pathogenic live SARS-CoV-2 virus has to be conducted in large quantities which can pose an alarming problem of safety. Furthermore, installing bioreactors and engaging in extensive purification procedures to manufacture both LAVs and inactivated vaccines (IVs) is costly and may serve as a limitation for the production of the vaccine in low-income countries (Fang et al., 2022).

A modification in the antigenic region of mRNA vaccines does not change the physical and chemical properties of the vaccine and large-scale production of mRNA vaccines may be standardized and performed using a complex 1 or 2-step *in vitro* reaction and a purification

platform with steps such as DNase digestion, precipitation, chromatography, or tangential flow filtration (Rosa et al., 2021). Also, when compared to the preparation of DNA vaccines using *E. coli* which may result in endotoxin contamination, the mRNA vaccine platform is attractive in terms of safety because of minimal cell-derived impurities and contaminants. Additionally, unlike DNA vaccines, mRNA vaccines do not need to cross the nucleus and are not associated with genome integration (Rosa et al., 2021). However, mRNA vaccines require ultra-cold storage conditions of around -70°C, which limits their deployment across the globe (Uddin & Roni, 2021). An additional challenge is the lack of thermostability in mRNA vaccines. Advancements towards improvements in the thermostability of mRNA vaccines and global collaboration to facilitate their deployment in resource-limited areas are required. Viral-vectored vaccines are also associated with various drawbacks, including vector-induced immunity, impractical for use in immunocompromised individuals, inconsistent immune responses, potential genetic changes, and substantial challenges in mass production and long-term storage (Strizova et al., 2021).

This project aims to develop a recombinant protein vaccine candidate based on highly conserved and immunogenic epitopes incorporated into expression plasmids for the development of recombinant protein vaccines that could be easily modified in response to emerging VOCs. Justifications include the positive attributes of rapid development of recombinant vaccines based on different antigens and freeze-drying or lyophilization of recombinant protein vaccines. Similar to nucleic acid vaccines, recombinant protein vaccines also have the advantage of accelerated development of different vaccines based on different antigenic regions. Vaccination in low-income countries such as Ethiopia, Nigeria, Kenya, Malawi, Tanzania, Uganda, Cameroon, Mozambique, Lesotho, and India is hampered due to a lack of finances and infrastructural facilities for cold storage of mRNAvaccines (Ashok et al., 2017). In contrast, recombinant protein vaccines may be

freeze-dried or lyophilized, allowing them to be preserved in a dried powdered form and they could be used to cater to large populations in Asia and Africa.

1.2 Aims of the current research

Concerns of reduced protective efficacies of current vaccines against SARS-CoV-2 VOCs and the emergence of highly transmissible VOCs warrant the development of vaccines that could offer convenience of production at low cost and storage conditions especially for developing and under-developed nations. In particular, a promising solution lies in the utilization of highly conserved and immunodominant epitopes from S and other SARS-CoV-2 antigenic regions identified from reverse vaccinology bioinformatics approaches which could confer broad protection against the ancestral SARS-CoV-2 strain as well as VOCs.

The aim of this research study is to develop a recombinant protein vaccine against SARS-CoV-2 which is composed of highly conserved and immunogenic peptides representing B and T cell epitopes that were identified through literature mining approaches. The peptides were linked together using KK, AAY, or GPGPG linkers. The nucleotides encoding this linked sequence of six peptides were then incorporated into the pET-41a(+) vector, which was subsequently expressed in *E. coli* to produce the recombinant protein. The characterization of the recombinant expression plasmid was conducted by restriction enzyme digestions of the plasmid, followed by determination of the size of the plasmid and confirmation of the nucleotide sequence of the cloned gene of interest. The recombinant expression plasmid was grown in *E. coli* cells and the expression of the protein of interest in the crude lysate was confirmed. A purification scheme based on ammonium sulfate precipitation, gel filtration chromatography, IMAC, and a centricon protein concentrator was developed to obtain a purified protein which was further used for intramuscular and intranasal immunizations of BALB/c mice for evaluation of the elicited humoral and cellular immune

responses. The humoral responses in mice were evaluated in terms of the neutralizing and IgG antibody levels in the sera of immunized mice while cellular responses were evaluated in terms of interferon-gamma (IFN-γ) production by CD4$^+$ and CD8$^+$ T cells. This allowed a comparison to be made between the immune responses elicited from the intranasal and intramuscular administration of the recombinant protein vaccine.

1.3 Research objectives

This research project has the following objectives:

- To express and purify a recombinant protein vaccine candidate incorporating validated peptides capable of eliciting neutralizing antibodies (nAbs) and cytokines to produce humoral and cellular immune responses against SARS-CoV-2 Wuhan strain and VOCs

- To immunize BALB/c mice with the naked recombinant protein vaccine through intramuscular and intranasal administrations and conduct immunogenicity testing to evaluate humoral and cellular responses

1.4 Research questions

- Are the individual peptides representing B and T cell epitopes immunogenic and what is their global HLA population coverage?

- Is the recombinant protein vaccine safe in animal models?

- What are the levels of antibody titres (binding as well as nAbs) and cytokine production that can be elicited by the recombinant protein vaccine when administered intramuscularly and intranasally?

- Are the antigen regions encoding the B-cell epitopes of the SARS-CoV-2 genome used to develop the recombinant protein vaccine effective to elicit immune responses against the SARS-CoV-2 Wuhan and Omicron strain?

CHAPTER 2: LITERATURE REVIEW

2.1 Epidemiology

In December 2019, several cases of pneumonia were reported in Wuhan City, China. The initial cases were largely connected to the Huanan seafood wholesale market, where the sale of aquatic animals and live animals took place (Li et al., 2020a). Following the initial report from China, the disease began to spread rapidly, and the number of cases increased significantly. On 11 January 2020, the first case outside mainland China was reported in Thailand. In a matter of months, the disease had made its way to every continent except Antarctica (Dhar Chowdhury & Oommen, 2020). Multiple countries such as the European continent (276,780,884 infections and 2,253,193 deaths), the Americas (193,320,888 infections and 2,970,993 deaths), Western Pacific (207,412,892 infections and 417,658 deaths), Eastern Mediterranean (23,401,838 infections and 351,665 deaths), South-East Asia (61,208,962 infections and 808,058 deaths), and African region (9,553,390 infections and 175,443 deaths) have been affected (WHO, 2023b).

2.2 Symptoms

The type and severity of COVID-19 symptoms varied from person to person. The most commonly reported symptoms were fever, dry cough, difficulty breathing, gastrointestinal symptoms, joint and muscle pain, chest pain, altered smell and taste, and diarrhea (Aiyegbusi et al. 2021; Grant et al., 2020). Severe symptoms in line with pneumonia were reported in the second or third week of infection and were associated with reduced oxygen saturation, altered blood gas, abnormal chest X-rays, alveolar exudates, and interlobular involvement which demonstrated eventual deteriorations. Lymphopenia was usually reported with increased levels of inflammatory markers such as C-reactive protein and proinflammatory cytokines (Velavan & Meyer, 2020).

2.3 Genomic organization

The genome of the SARS-CoV-2 is a single-stranded positive-sense RNA with a size of approximately 29.9 kb (Jungreis et al., 2021). The genome is composed of two large open-reading frames, ORF1a and ORF1b, located at the 5' end. These are responsible for encoding 16 non-structural proteins ranging from NSP1 to NSP16 which are involved in the formation of a replication–transcription complex (RTC) (Alanagreh et al., 2020). The other ORFs located at the 3' end are responsible for encoding four structural proteins, namely S, envelope (E), membrane (M), and nucleocapsid (N) proteins. The M protein provides shape and structure to the viral particles, the E protein ensures proper virion assembly and release, and the N protein packages the RNA genome and enhances pathogenicity by reducing interferon production, while the S protein recognizes the angiotensin-converting enzyme 2 (ACE2) host cell receptor (Rastogi et al., 2020). The structure of the SARS-CoV-2, its genomic organization and encoded proteins are shown in **Figure 2.1**.
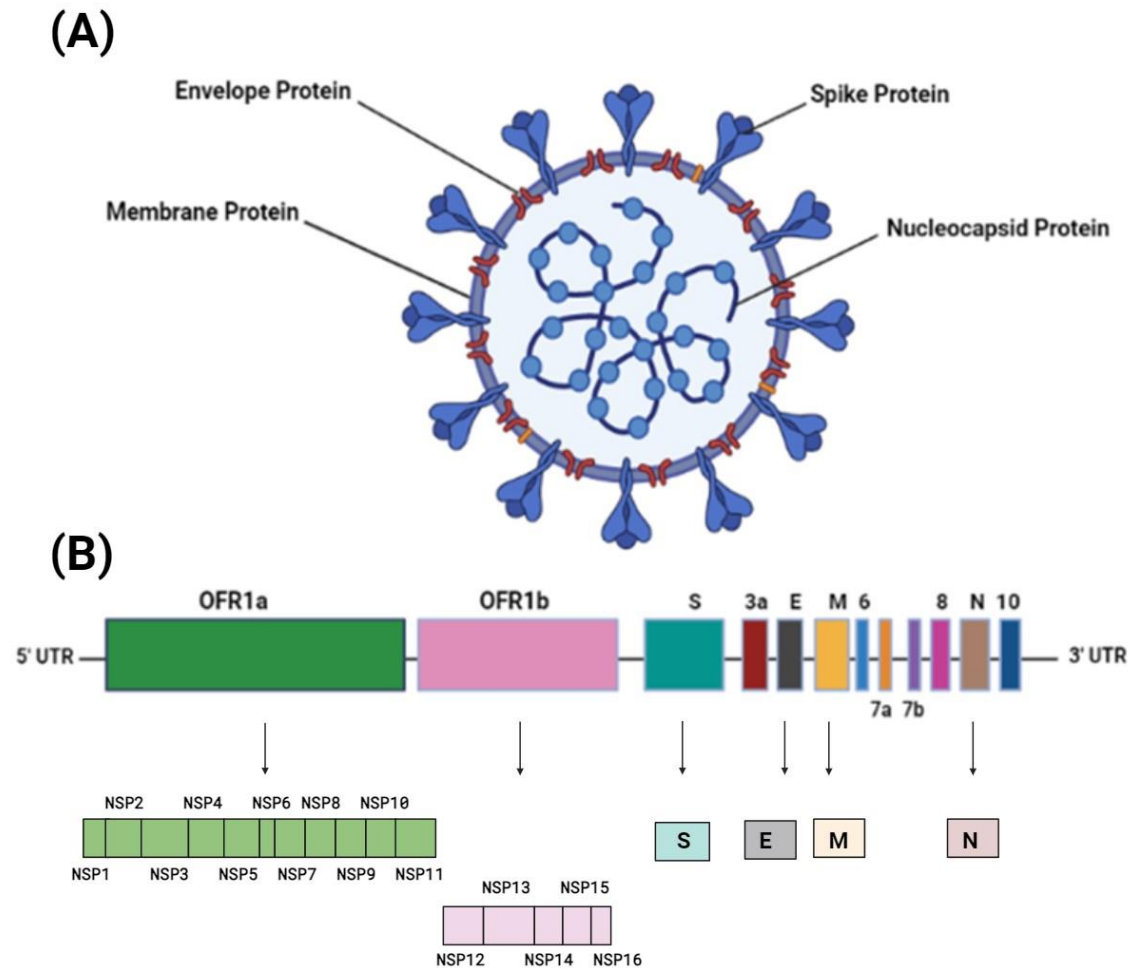
Figure 2.1. Structure (A) and genomic organization (B) of SARS-CoV-2. ORF = Open-reading frame; UTR= untranslated region;

NSP = non-structural protein; S = Spike; E = Envelope; M = Membrane; N = Nucleocapsid

2.4 The importance of the S protein and its interaction with ACE2

The S structural protein is of particular importance to vaccine design since it mediates binding and entry into the host (Shang et al., 2020). The S protein is a glycosylated type I membrane protein and consists of two subunits S1 and S2. The S protein exists in a trimeric prefusion form which is cleaved by the host furin protease into S1 and S2. The S1 subunit contains the N terminal domain (NTD) and the receptor-binding domain (RBD) which is responsible for binding to the ACE2 cell receptor (Nguyen et al., 2020) (**Figure 2.2**).
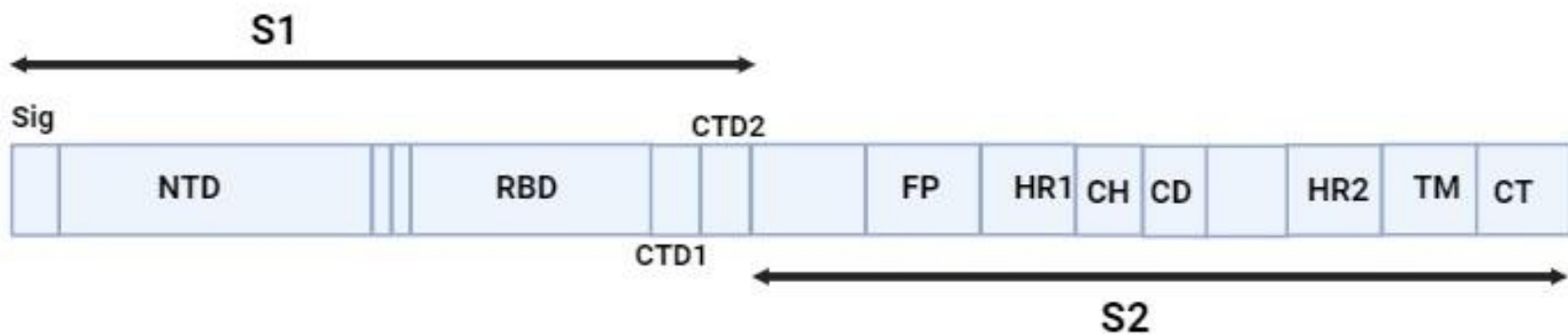
Figure 2.2. The genomic organization of the S protein of SARS-CoV-2 showing the signal peptide (Sig), NTD, RBD, C-terminal domains (CTD1 and CTD2), fusion peptide (FP), heptad repeat regions (HR1 and HR2), central helical region (CH), the connector domain (CD), transmembrane region (TM), endodomain/cytoplasmic tail (CT), and endoplasmic reticulum retention signal (ERsig)

The S protein requires priming by host cell proteases such as endosomal cysteine protease cathepsin L and the serine proteases furin and transmembrane serine protease 2 (TMPRSS2) for viral entry and membrane fusion. Priming refers to the cleavage of the S protein subunits and it was reported that S protein cleavage occurs at two sites. The first is the S1/S2 site between the S1 and S2 subunits by furin to expose the RBD in the "up" conformation and allow it to bind to the ACE2 receptor. The RBD allows the enveloped virus to bind to host cells by interacting with the ACE2 receptor expressed by host cells in the lower respiratory tract (Mariano et al., 2020) (Figure 2.3.). After the RBD binds to ACE2, additional cleavage of the S2 subunit occurs at a second specific site by the host serine protease TMPRSS2 which leads to the dissociation between S1 and S2 and produces the mature N-terminus of the fusion peptide. This allows the fusion of viral and host membranes and facilitates virus entry (**Figure 2.3.**). When the SARS-CoV-2 enters the host cell, it will release its RNA and polyproteins will be produced following translation. The RNA genome of the SARS-CoV-2 is replicated. The RNA genome of SARS-CoV-2 is replicated in the cytoplasm, where it serves as a template for translation of large replicase polyproteins. These proteins form replication–transcription complexes responsible for RNA synthesis, aided by modifications of endoplasmic reticulum membranes. This process yields full-length genome complements and subgenomic RNAs, crucial for viral protein production and assembly. Viral protein translation is regulated by programmed ribosomal frameshifting and leaky ribosomal scanning (Malone et al., 2022). This is followed by the arrangement of structural proteins formed in the host cell, followed by a release of the virus particles (Vallamkondu et al., 2020).

The binding of the RBD to the ACE2 receptor induces a conformational change in the S protein from a metastable prefusion conformation to a stabilized postfusion conformation (**Figure 2.3.**). However, the S protein may be maintained in a stabilized prefusion state. Previous structural

studies facilitated an improved understanding of the structural properties of SARS-CoV-2 S. Kirchdoerfer et al. (2017) introduced a strategy to stabilize the S protein through the introduction of two proline mutations through cryo-EM analyses of stabilized trimeric SARS-CoV S. The mRNA-1273 (Corbett et al., 2020) and BNT162b2 as well as the protein subunit vaccine by Novavax (Phase 3) utilized the two proline mutations to develop a prefusion-stabilized S protein as the main antigenic target (Dai & Gao, 2021). These mutations were made by inducing mutations in two consecutive residues (K986 and V987) in the S2 subunit located between the central helix (CH) and the heptad repeat 1 (HR1) (Dai & Gao, 2021). In contrast to the wild-type SARS-CoV-2 S protein, the SARS-CoV-2 S protein carrying two proline mutations shows an open conformation with the RBD in the 'up' position, thus allowing induction of high neutralizing antibody titers (Juraszek et al., 2021).
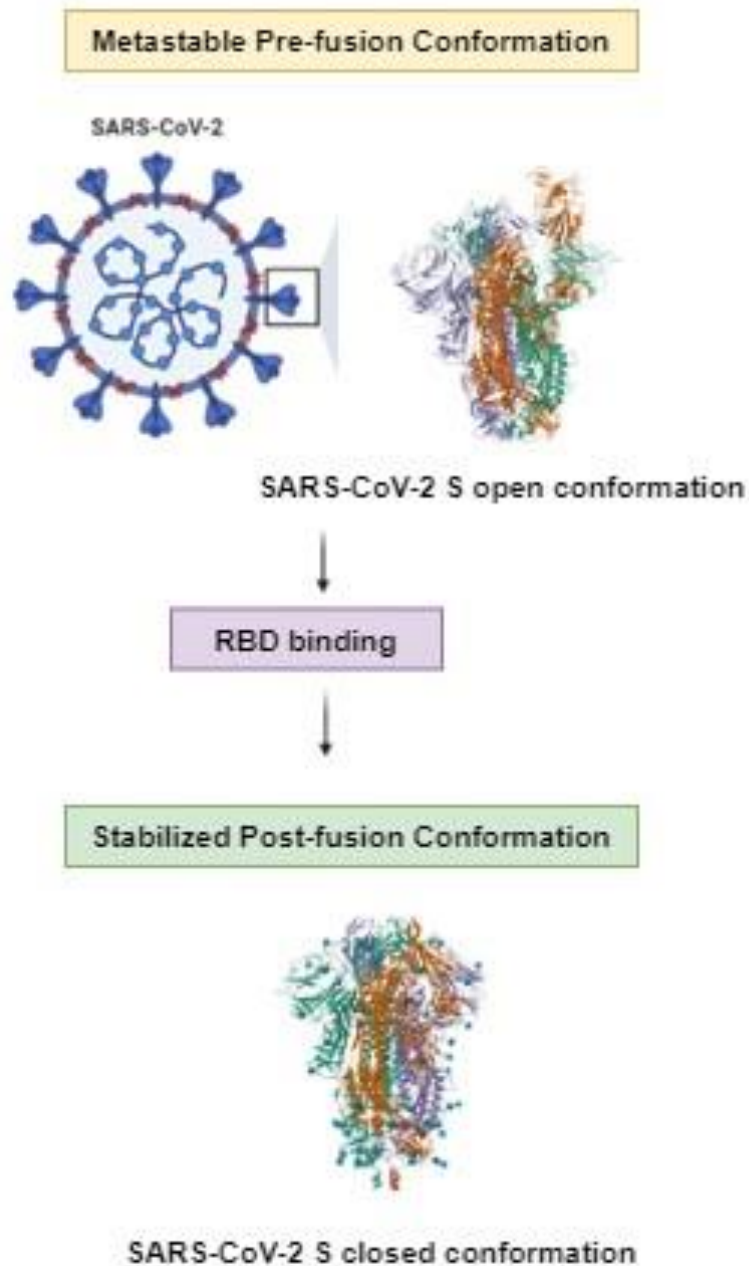
Figure 2.3. The induction of conformational changes in the S protein resulting from the binding of the RBD to the ACE2 receptor showing a pre-binding open SARS-CoV-2 conformation (PDBID: 7DDN), allowing it to bind to the ACE2 receptor and a post-binding SARS-CoV-2 S protein closed conformation (PDBID:6VXX). The open and closed structures were obtained from the Research Collaboratory for Structural Bioinformatics Protein Data Bank (RCSB PDB).

2.5 Conventional vaccine development

Conventional vaccines such as LAVs have been developed against rabies and measles and reduced the incidence of several diseases such as rubella, influenza, rotavirus, tuberculosis and typhoid (Greenwood, 2014). The inactivated polio vaccine (IPV) was shown to confer protection against symptomatic poliomyelitis and paralysis, and the live virus oral polio vaccine (OPV) provided potent intestinal immunity which was useful in preventing viral shedding and transmission of infection (Alfaro-Murillo et al., 2020). Whole live vaccines were used to immunize against pneumococcus, meningococcus and typhoid bacillus in addition to the use of a toxoid vaccine such as a tetanus toxoid, diphtheria toxoid and a killed pertussis vaccine. Sinovac Biotech and Sinopharm vaccine developed the CoronaVac and BBIBP-CorV vaccines, respectively against COVID-19.

There is preclinical research associated with the development and immunogenicity testing of LAV candidates against SARS-CoV-2. Different modifications have been employed to ameliorate the possible risk of reversion to virulence. For example, Wang et al. (2021b) utilized codon deoptimization to develop a SARS-CoV-2 LAV which resulted in prevention of reversion to virulence and potent induction of host immunogenicity. Additionally, Adler et al. (2023) demonstrated that the removal of the S protein furin cleavage site from a SARS-CoV-2 LAV may be effective in inhibiting its transmission as evidenced by the full inhibition of horizontal transmission in hamsters who were administered with the LAV vaccine candidate. Importantly, the protection offered by the vaccine against SARS-CoV-2 infection and the potency of immune responses was similar to immunogenicity elicited from the administration of the live attenuated candidate possessing the furin cleavage site. Additionally, the vaccine did not exhibit any propensity to recombine in vivo or in vitro with a field strain of SARS-CoV-2.

Another study found that the sCPD9 LAV candidate elicited superior immune responses when compared to the mRNA BNT162b2 and the Ad2-spike adenovirus-vectored vaccine when immunogenicity was evaluated in Syrian hamsters (Nouailles et al., 2023). These differences were observed in terms of effective viral clearance, decreased tissue damage, rapid pre-plasmablast development, robust mucosal humoral responses, and prompt retrieval of memory T cells from lung tissue following exposure to heterologous SARS-CoV-2. Notably, the development of an effective LAV for SARS-CoV-2 vaccine development necessitates extensive information about the viral genes and their functions to deter any potential reversion to virulence. Nevertheless, there are several SARS-CoV-2 accessory proteins whose functions are unknown (Malik, 2020).

2.6 Vaccine development against COVID-19 focusing on S protein

Upon analysis of the SARS-CoV-2 genome sequence, several academic and pharmaceutical groups developed mRNA and viral-vectored vaccines based on the S protein which was identified as a key antigenic target. Moderna and the Vaccine Research Center at the National Institute of Allergy and Infectious Diseases (NIAID) developed mRNA-1273, a lipid nanoparticle (LNP) encapsulated mRNA vaccine expressing the prefusion-stabilized S glycoprotein (Baden et al., 2021). Concurrently Pfizer and BioNTech developed BNT162b2, a lipid nanoparticle–formulated, nucleoside-modified RNA vaccine that encodes a prefusion-stabilized, membrane-anchored SARS-CoV-2 full-length S protein (Thomas et al., 2021). Viral-vectored vaccines by Janssen Pharmaceutical, CanSino Biologics, and AstraZeneca in collaboration with the University of Oxford were also developed to target the S protein. These vaccine candidates quickly obtained emergency approval by the Food and Drug Administration (FDA) and European Medicines Agency (EMA) and were administered globally for large-scale public immunizations. mRNA-

1273, BNT162b2, ChAdOx1 nCoV-19 (low-dose, followed by a standard dose), and BBIBP-CorV showed protective efficacies of 94.1% and 95.0%, 90·0%, and 78.1%, respectively (Puranik et al., 2021; Voysey et al., 2021; Zhang et al., 2022). However, multiple SARS-CoV-2 VOCs with high transmission and neutralization escape capabilities began to emerge soon after the success of the mRNA, viral-vectored, and IVs.

2.6.2 Mutations in the S protein

An important mutation that differentiated the SARS-CoV-2 Wuhan strain from the six previous coronaviruses (HCoV-229E, HCoV-OC43, SARS-CoV (SARS-CoV-1), HCoV-NL63, CoV-HKU1, and MERS-CoV) was the D614G, a S-protein mutation, associated with the carboxy(C)-terminal region of the S1 domain. The D614G mutation has been linked to reduced S1 shedding and increased infectivity, resulting in increased transmission advantage over past coronaviruses known to infect humans (Zhang et al., 2020a). The D614G was also shown to be consistently present in SARS-CoV-2 VOCs (Ahmad et al., 2022).

SARS-CoV-2 VOCs were associated with multiple mutations in the S protein. Currently, five VOCs of SARS-CoV-2 have been identified. The VOCs B.1.1.7 (UK), B.1.351, (South Africa), P.1 (Brazil), and B.1.617.2 (India) were associated with mutations leading to virus adaptations such as increased transmissibility and immune evasion (Noh et al., 2021a). For example, the B.1.1.7 variant has the following mutations: N501Y substitution in the RBD, H69/V70 deletion in the NTD, and a P681H mutation adjacent to the furin cleavage site in the S protein (Zahradník et al., 2021; Kemp et al. 2020; Planas et al., 2021). These mutations were linked to increased transmissibility of the SARS-CoV-2 variant. In particular, the H69/V70 deletion modified the conformation of the NTD loop which enhanced infectivity (Kemp et al., 2020). Furthermore, the B.1.351 variant was associated with the K417N, E484K, and N501Y mutations

while the P.1 variant carried the K417T, E484K, and N501Y substitutions in the RBD (Planas et al., 2021). A total of 9, 10, 12, 17, and 39 mutations were present in the S protein in the Alpha (B.1.1.7), Beta (B.1.351), Gamma (P.1), Delta (B.1.617.2), Omicron (B.1.1.529) VOCs, respectively (Ahmad et al., 2022). Recently, as of 15 March 2024, Omicron BA.2, BA.4 and BA.5 are no longer considered VOCs since the European Centre for Disease Prevention and Control (ECDC) has de-escalated these from the list of SARS-CoV-2 VOCs, since these parental lineages are not currently circulating (ECDC 2024). As of 9 February 2024, Variants of Interest (VOIs) include Omicron XBB.1.5, XBB.1.16, Eris EG.5, Omicron BA.2.86, and JN.1. The Omicron JN.1 variant was reported as the dominant variant in the U.S., responsible for more than 60% SARS-CoV-2 cases (WHO, 2024).

2.6.3 Reduction in protective efficacies of current vaccines in response to VOCs

Harvey et al. (2021) reasoned that since the Wuhan S glycoprotein was present as the main antigenic determinant in viral-vectored and mRNA vaccines that were first licensed under emergency use, mutations in the S protein in SARS-CoV-2 VOCs could impact antigenicity and the interaction of the S protein with the host to elicit nAbs. Indeed, mRNA-1273, BNT162b2, and ChAdOx1 nCoV-19 were soon reported to exhibit reduced protective efficacies against SARS-CoV-2 VOCs.

Collier et al. (2021) conducted *in vitro* pseudotyped neutralization assays evaluating neutralizing antibody responses following first and second immunizations using pseudoviruses expressing the SARS-CoV-2 wild-type S protein or a SARS-CoV-2 mutated S protein with 8 eight amino acid changes as present in the B.1.1.7 variant. The results showed that 16.1% of the monoclonal antibodies targeting the receptor-binding motif (RBM) had a 100-fold reduction in

neutralizing activity while 19.4% were associated with a partial 2–10-fold reduction in neutralizing activity against the B.1.1.7 VOC (Collier et al., 2021).

In participants immunized with the ChAdOx1 nCoV-19 vaccine, there was a 4-fold reduction in neutralizing activity against the B.1.351 variant; geometric mean titers reduced from 297 against the Wuhan SARS-CoV-2 to 74 against the VOC (Madhi et al., 2021). Another study reported that mutations in the Beta B.1.351 VOC could lead to a 6.4-fold reduction in geometric mean titers in the sera of individuals immunized with the mRNA-1273 vaccine (Wu et al., 2021).

The most recent is the Omicron (B.1.1.529) VOC which has emerged in multiple countries and has been repeatedly associated with a high potential for immune evasion and transmissibility (Carabelli et al., 2023; Willett et al., 2022). In particular, cross-neutralization experiments were conducted with patients infected with the SARS-CoV-2 Wuhan strain and Alpha, Beta, Gamma, and Delta VOCs demonstrated that SARS-CoV-2 Wuhan strain and Alpha, Beta, Gamma, and Delta VOCs form one antigenic cluster. However, the Omicron variant represents a separate antigenic variant and may belong to a distinct serotype compared to other SARS-CoV-2 strains (van der Straten et al., 2022). Consequently, immunity generated by Omicron infection or vaccination may not offer substantial protection against other strains, nor would immunity from previous strains be highly effective against Omicron (Suryawanshi et al., 2022).

The increased infectivity could be explained by the D614G, E484A, N501Y, K417N, Y505H, and G496S mutations that were present in Omicron and could enhance the molecular flexibility of the S protein to bind to the ACE2 receptor (Chakraborty et al., 2022). A research study conducted with 12 individuals in South Africa demonstrated that the protective efficacy of the Pfizer-BioNTech vaccine could be significantly reduced against the omicron variant (Cele et al., 2022). In individuals immunized with the Pfizer vaccine, a 22-fold reduction in the levels of

nAbs was observed in response to Omicron as compared to the prototype Wuhan strain. Geometric mean titre (GMT) of the 50% focus reduction neutralisation test (FRNT50) of nAbs in the sera of participants was 1,963 against the ancestral prototype SARS-CoV-2 strain with the D614G mutation and reduced to 89 for Omicron (Cele et al., 2022). Plaque reduction neutralization test (PRNT$_{50}$) titers associated with immunized or convalescent cohorts were significantly reduced against the Omicron variant. In fact, when compared with the neutralizing antibody titers elicited against the wild-type SARS-CoV-2, there was a 31-fold, 6.5-fold, and 10.6-fold reduction in neutralizing antibody titers after immunization with the BNT162b2 vaccine, the CoronaVac vaccine, and in COVID-19 convalescent sera against the Omicron strain (Cheng et al., 2022).

In a different study, an evaluation of neutralizing antibody titers against the SARS-CoV-2 Wuhan strain and the Omicron BA.1, BA.2, BA.2.12.1, and BA.4 or BA.5 subvariants showed that when compared to the Wuhan strain, the neutralizing antibody titers were reduced by a factor of 6.4 against BA.1, by a factor of 7.0 against BA.2, by a factor of 14.1 against BA.2.12.1, and by a factor of 21.0 against BA.4 or BA.5. Omicron subvariants BA.2.12.1, BA.4 and BA.5 was shown to be more likely to escape neutralizations than the BA.1 subvariant. The median neutralizing antibody titer was lowered by a factor of 2.2 against the BA.2.12.1 subvariant and by a factor of 3.3 against the BA.4 or BA.5 subvariant when compared to the BA.1 subvariant (Hachmann et al., 2022). Moreover, sera from BNT162b2 and mRNA-1273 vaccinees showed a 1-3-fold decrease in neutralizing activity against a pseudovirus containing the E484K, N501Y, and a combination of K417N, E484K, and N501Y mutations. All of these mutations were present in the Omicron VOC (Wang et al., 2021a).

Apart from immune escape from antibodies elicited by B cell epitopes, the evasion of cytotoxic T lymphocyte (CTL) immunity by SARS-CoV-2 VOCs through T cell mutations in viral

epitopes has also been a serious concern. Overall, it was reported that SARS-CoV-2 variants had less than a marginal effect on the elicitation of CD4$^+$ and CD8$^+$ T cell responses in convalescent patients and vaccinees receiving the mRNA vaccines. The overall SARS-CoV-2 T cell reactivity was not considerably affected by the SARS-CoV-2 B.1.1.7, B.1.351, P.1, and CAL.20C lineages (Tarke et al., 2021). Moreover, T cell responses in terms of overall SARS-CoV-2–specific IFN-γ responses were found to be similar to those elicited from the original Wuhan strain of SARS-CoV-2 (Guo et al., 2022; Noh et al., 2021b). Noh et al. (2021b) concluded that 93% and 97% of CD4$^+$ and CD8$^+$ T cell epitopes, respectively, were largely conserved in the Alpha, Beta, Gamma, and Epsilon (B.1.429) variants. However, through mutations in the major histocompatibility complex (MHC)-I restricted viral epitope genes, there is a likelihood for SARS-CoV-2 variants to overcome CD8$^+$ T cell surveillance (Agerer et al., 2021). Agerer et al. (2021) conducted bioinformatics analysis to detect 194 SARS-CoV-2 nonsynonymous mutations from 27 CTL epitopes which reduced the binding of peptides to MHC-I. The majority of these epitopes (13 out of 27) were situated within the S protein, while the rest were spread across various other viral proteins: 6 in the N protein, 4 in ORF1ab, 3 in the M protein, and 1 in the E protein. These mutations ultimately resulted in reduced proliferation, IFN-γ production as well as lower cytotoxic activity of CD8$^+$ T cells. Given the reported reduction in T cell activity against SARS-CoV-2 VOCs, it is crucial to actively monitor T cell reactivity in the context of SARS-CoV-2 infections.

Vaccines incorporating different epitopes serve as a promising solution against the problem of emerging SARS-CoV-2 VOCs and the associated reduction in protective efficacy of currently available vaccines against SARS-CoV-2. mRNA, DNA, and recombinant protein vaccines can be developed to incorporate different antigenic targets specific to the sequence of SARS-CoV-2 VOCs (Maruggi et al., 2019; Moyle & Toth, 2013; Smith et al., 2020). Indeed, Moderna's bivalent

booster vaccine, mRNA-1273.222 which consisted of the S protein of Omicron BA.4/BA.5 quickly progressed to phase 2/3 clinical development and demonstrated the induction of higher neutralizing antibody titers against BA.4/BA.5 compared to a booster dose of mRNA-1273 (Chalkias et al., 2022). While this proactive approach to developing vaccines is commendable, such targeted adaptations may not be sustainable in the long run in light of the emergence of continuously mutating SARS-CoV-2 strains.

2.7 Identification of broadly conserved and immunogenic B and T cell epitopes

While the S protein was the main antigenic target which was used during early vaccine development initiatives against COVID-19, the emergence of SARS-CoV-2 VOCs and the reduction in protective efficacies conferred by current S-based vaccines warrants the need for new vaccine development strategies. The current research project builds on previously identified peptide sequences representing conserved and immunogenic B and T cell epitopes within the S and M proteins. Using such an approach might be useful for providing broad coverage against the SARS-CoV-2 Wuhan strain and its VOCs which would eradicate the need for multiple booster immunizations to sustain protective immunity upon the emergence of different VOCs. This strategy of identifying potential antigens and then validating them through immunogenicity and challenge studies in protective models is a strategy known as reverse vaccinology 1.0 (Burton, 2017). Well-established methods like reverse vaccinology combined with bioinformatics have brought stability and efficiency to the vaccine development process. By examining the genetic information, this approach enables the identification of specific protein components within the viral genome that are capable of eliciting robust humoral and cellular immune responses (Enayatkhani et al., 2022). This strategy shows promise in locating immunogenic and conserved

epitopes related to SARS-CoV-2, which is necessary for developing multi-epitope or subunit vaccines (da Silva et al., 2023).

2.7.1 Current research on immunoinformatics-based identification of epitopes

The development of recombinant protein vaccines against the SARS-CoV-2 Wuhan strain and its VOCs first requires the identification of epitopes from antigenic regions that would elicit broad and long-lasting immune responses. Such an approach is warranted because it shows promise in boosting the effectiveness of immunization and its breadth of protection against viral variants/subvariants that are constantly emerging and being transmitted to the community.

There is extensive research being conducted in identifying such immunogenic epitopes. For example, Heide et al. (2021) identified immunogenic epitopes from different structural proteins present in SARS-CoV-2 towards the generation of specific T cell epitopes. These epitopes were obtained from 135 overlapping 15-mer peptides spanning the envelope (E), membrane (M) and nucleoprotein (N) of SARS-CoV-2, interacting with sera from both infected and convalescent SARS-CoV-2 patients. Peptide-specific CD4$^+$ T cell responses in terms of IFN-γ production were evaluated using enzyme-linked immunosorbent spot (ELISpot) and corroborated by single-peptide intracellular cytokine staining (ICS) analysis. It was observed that 97% of the participants demonstrated the elicitation of CD4$^+$ T cell responses directed towards either the N, M or E proteins. More specifically, high response frequencies were demonstrated, with a total of 10 N, M or E-specific peptides, half of these peptides showing strong binding affinities to several HLA class II binders. Notably, three peptides Mem_P30 (aa146–160), Mem_P36 (aa176–190), and Ncl_P18 (aa86–100) were able to elicit CD4$^+$ specific T cell responses in approximately 55% of participants, showing a high population coverage. Mem_P30 and Mem_P36 belonged to the M protein and the Ncl_P18 peptide was found in the N protein. After specifying the length and HLA

restriction of the peptides, a novel DRB*11 tetramer (Mem_aa145–164) was developed and used for *ex vivo* phenotype evaluation of SARS-CoV-2-specific CD4^{+} T cells. This in-depth analysis of single T cell peptide response showed that SARS-CoV-2 infection universally primed a broad T cell response that was focused on several specific peptides found within the N, M, and E structural proteins.

As reported by Lim et al. (2022), B cell responses could be identified by epitope identification using literature mining and bioinformatics tools to identify antigenic regions capable of eliciting humoral immune responses. Although current vaccines could confer lower levels of protection against SARS-CoV-2 VOCs due to multiple mutations in antigenic regions, satisfactory protective efficacy was still observed against SARS-CoV-2 VOCs. This protection might be attributable to cellular immunity. The identification of epitopes capable of eliciting CD8^{+} specific T cell responses is promising because multifunctional CD8^{+} T cells could allow inhibition of the viral escape of SARS-CoV-2 VOCs. The existence of conserved CD8^{+} T cell epitopes could effectively compensate for the reduction in the CD8^{+} T cell activity resulting from mutations within T cell epitopes. Boni et al. (2021) demonstrated that several immunodominant CD8^{+} T cell epitopes could be found in conserved locations within the SARS-CoV-2 genome that were highly unlikely to undergo mutations without significantly impairing functional SARS-CoV-2 genes. It was significant that several of these conserved epitopes were labelled as degenerate, which enabled them to associate with several HLA class I molecules on antigen presenting cells (APCs) and interact with CD8^{+} T cell populations of various HLA restrictions at the same time. Degenerate CD8^{+} T cell epitopes were seen to be logical candidates for the development of CD8^{+} T cell response-enhanced COVID-19 vaccines.

Research has also focused on identifying CD4$^+$ T cell epitopes to provide protection against the SARS-CoV-2 Wuhan strain and its VOCs. Although the impact of mutations in the SARS-CoV-2 genome on CD4$^+$ T cell immune responses is not well understood, epitope mapping might provide useful knowledge regarding the ability of CD4$^+$ T cells to provide broad and conserved protection against VOCs. 21 epitopes in S, M, and N were identified after isolation of 159 SARS-CoV-2 CD4$^+$ T cell clones from healthcare workers who were infected with wild-type SARS-CoV-2 (D614G) in the past (Tye et al., 2022). 10 out of 17 epitopes from the S protein, were mutated in VOCs and 7 showed impaired CD4$^+$ T cell recognition. Impaired CD4$^+$ T cell recognition in response to VOCs warrants the need for the identification of broad CD4$^+$ T cell epitopes that could ameliorate immune evasion capabilities associated with SARS-CoV-2 VOCs.

The emergence of SARS-CoV-2 variants that show an increased propensity to evade antibodies has led to recurrent waves of infections with reduced vaccine efficacy. In our search for broadly protective vaccinations, there is still a crucial knowledge gap regarding the degree to which vaccine-elicited mucosal or systemic memory T cells can defend against such antibody-evasive SARS-CoV-2 variants. Using adjuvanted S protein-based vaccines that elicited potent T cell responses, Kingstad-Bakke et al. (2022) assessed whether systemic or lung-resident CD4$^+$ and CD8$^+$ T cells protected against SARS-CoV-2 variants in the presence or absence of virus-nAbs. It was observed that the elicitation of mucosal response was associated with potent viral control and protection of lung pathology through the production of nAbs. Although mucosal immunity resulted in the elicitation of mucosal memory CD8$^+$ T cells, humoral immune responses had a more prominent role in effectively neutralizing the invading virus. In fact, mucosal memory CD8$^+$ T cells were not able to confer adequate levels of protection in response to homologous SARS-CoV-

2 without CD4^{+} T cells and nAbs. Nevertheless, when virus-nAbs were not present, memory CD8^{+} T cells helped by CD4^{+} T cells were able to confer protection against the B1.351 (β) variant without symptoms of lung immunopathology. It might be useful to induce systemic and mucosal memory T cells that were directed against conserved epitopes to combat SARS-CoV-2 variants that can avoid nAbs.

2.7.2 Variability in immune responses across disease severity: Contrasts between asymptomatic vs symptomatic, recovered vs chronically infected individuals

Since the S protein of SARS-CoV-2 is implicated in the entry of the virus into the host cell, the RBD of the S1 protein has been the most prominent target for vaccine development against SARS-CoV-2 (Li et al., 2020b). Furthermore, following the isolation of antibodies from convalescent patients with high neutralizing titers, the epitopes associated with these antibodies were mapped onto the S1 region, more specifically the RBD and the NTD (Sun et al., 2020). The S protein has also been associated with the elicitation of T cell responses. Chen et al. (2021) employed an immunoinformatics approach to predict conserved B and T cell epitopes located on the S protein. MHC-I KIADYNYKL and MHC-II LEILDITPC showed a high antigenicity score of 1.6639 and 1.6390, respectively.

In a study evaluating seroprevalence of S-specific antibodies, it was reported that following infection with SARS-CoV-2, there were detectable levels of antibodies elicited against the S protein (Wajnberg, 2020). Seroprevalence studies demonstrated that the peak serum geometric mean neutralizing antibody titer of patients infected with SARS-CoV-2 admitted to the intensive care unit (ICU) was significantly higher than those not admitted to the ICU (Liu et al., 2020). nAbs were detectable in the early stage of COVID-19. They peaked around 4-5 weeks and gradually decreased within 3 months (Seow et al., 2020). Other studies have also shown neutralizing or anti-

spike antibody levels to wane quickly which may contribute to susceptibility to SARS-CoV-2 infection (Israel et al., 2021; Levin Einav et al., 2021).

Considering that S-based humoral responses may wane over time, it may be useful to explore utilizing other structural regions for their potential to elicit more sustained humoral responses. Indeed, Poland et al. (2020) found that humoral responses in the form of IgG antibodies were elicited also against the N protein (Poland et al., 2020) (**Figure 2.4.).** Xiang et al. (2021) reported that IgG antibodies elicited against the N protein and the RBD of SARS-CoV-2 were still present one-year post-infection with SARS-CoV-2. However, nAbs were only detectable in 43% of the recovering patients. Furthermore, these nAbs against the original Wuhan strain could neutralize the B.1.351 variant in only 22.6% of recovering patients (Xiang et al., 2021).
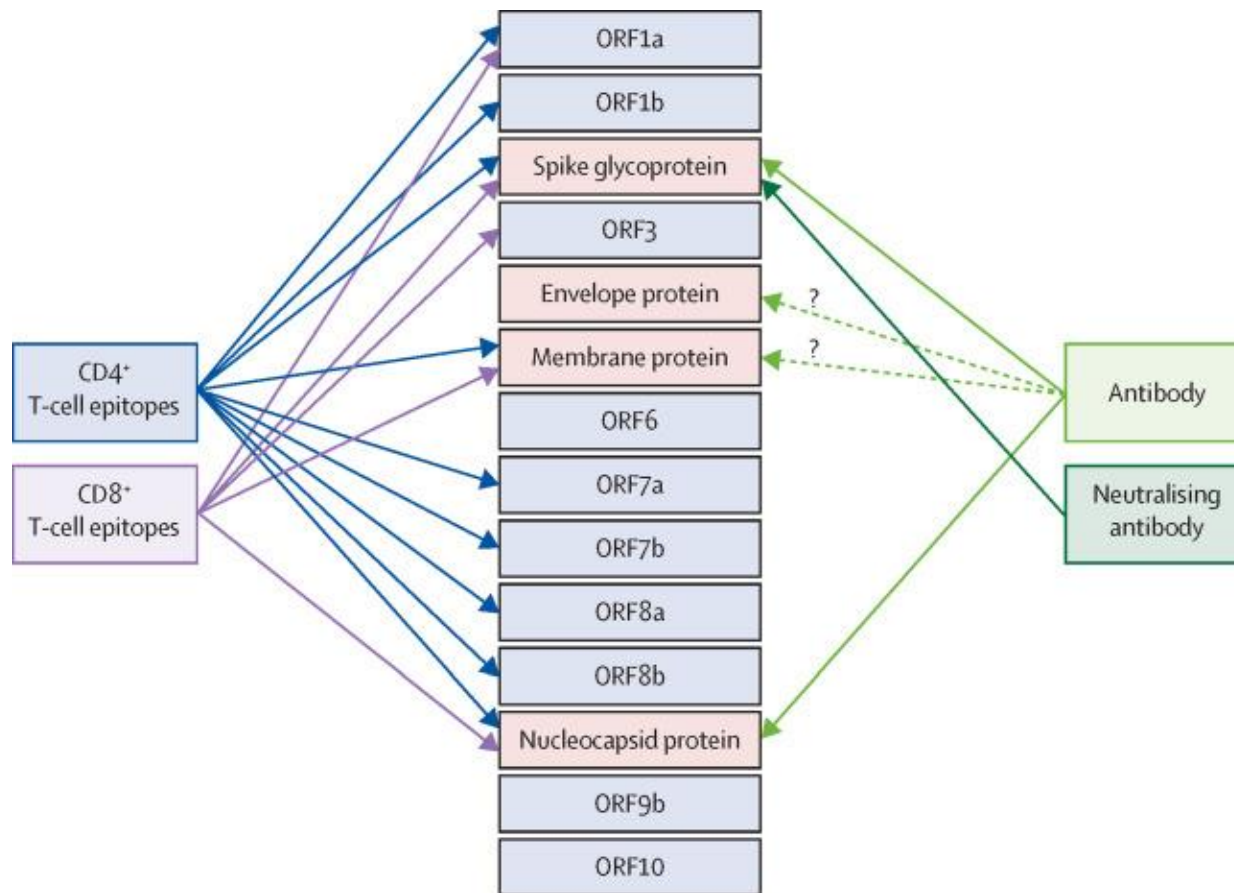
Figure 2.4. The structural, non-structural, and accessory proteins of SARS-CoV-2 other than the S protein that can elicit humoral and cellular immune responses (Adapted from Poland et al., 2020)

Enzyme-linked immunosorbent assay (ELISA) experiments, using a stabilized SARS-CoV-2 S trimer protein, yielded a positive rate of 41.5% for IgG titers ≥1:80. A significant proportion of COVID-19 IgG positive samples exhibited moderate (1:320 or 1:960) to high (1:2880) antibody titers against the S protein. Notably, plasma with IgG titers of 1:320, 1:960, or ≥1:2880 corresponded to neutralizing antibody titers of 1:30, 1:75, and 1:550, respectively (Wajnberg, 2020). Samples with IgG titers ranging from 1:960 to ≥1:2880 demonstrated effective neutralization of SARS-CoV-2 infections. In conclusion, IgG antibodies against the S protein were found to neutralize SARS-CoV-2 infection, with a strong correlation observed between IgG titers and neutralizing antibody titers (Wajnberg, 2020).

T cell responses were also associated with SARS-CoV-2 infection. When compared to healthy controls, the elevated expression levels of perforin and granzyme B in severe COVID-19 patients indicated the functionality of memory CD8$^+$ T cells and CD8$^+$PD-1$^+$CD38$^+$ T cells (Braun et al., 2020). Importantly, the number of CD4$^+$ and CD8$^+$ T cells was associated with the severity of COVID-19 disease. For example, in serious illness, the number of CD4$^+$ and CD8$^+$ T cells was significantly decreased than in moderate illnesses (Poland et al., 2020). Furthermore, Diao et al. (2020) found that the number of CD4$^+$ and CD8$^+$T cells were significantly reduced in severe disease groups when compared to mild/moderate disease groups. Lower counts of CD4$^+$ or CD8$^+$ T cells may be associated with worse prognosis following SARS-CoV-2 (Hu et al., 2020).

Zuo et al. (2021) evaluated T cell response after mild asymptomatic infection with SARS-CoV-2 by stimulation with peptides from SARS-CoV-2 proteins. The T cell count was performed using the proinflammatory cytokine interferon IFN-γ. Although T cell response was detectable in all patients, the magnitude of T cell response was significantly higher 6 months after symptomatic infection as compared to asymptomatic infection.

Quantification of SARS-CoV-2 specific $CD4^+$ and $CD8^+$ T cells and the cytokines produced by them such as IFN-γ, IL-2, IL-4, and Tumor Necrosis Factor (TNF), showed that $CD4^+$ T cells were in greater abundance than $CD8^+$ T cells. The cytokine IL-2 was prominently produced by $CD4^+$ T cells while IFN-γ was produced by $CD8^+$ T cells (Dan et al., 2021; Zuo et al., 2021). Dan et al. (2021) further reported the presence of $CD40L^+OX40^+$ T_{fh} cells several months after infection. Furthermore, $CD4^+$ T cells were shown to be involved in aiding the humoral response as T follicular helper (T_{fh}) cells provided assistance in the development of humoral immune memory. T_{fh} cells also correlated with the levels of nAbs (Dan et al., 2021).

In a study evaluating T cell responses against SARS-CoV-2 infection, it was reported that symptomatic patients showed the presence of peripheral T cell lymphopenia which was significantly associated with disease severity, length of RNA positivity, and death. The T cell count was found to be limited and preserved in asymptomatic patients. Those suffering from severe disease demonstrated strong T cell responses specific to SARS-CoV-2 infection (Shrotri et al., 2021). Moreover, in another study, T cell responses against the SARS-CoV-2 were elicited specifically in response to the structural S, M, and N proteins as well as accessory proteins in samples collected from convalescent patients (Gallais et al., 2020). Furthermore, T cell responses were determined by using IFN-γ ELISpot assays in convalescent patients (Peng et al., 2020).

Although major vaccine candidates have focused on the full-length S protein to induce B cell, $CD4^+$, and $CD8^+$ T cell immune responses, Hellerstein (2020) explain that the search for $CD4^+$ and $CD8^+$ T cell epitopes by analyzing the sera from convalescent patients shows that the immune response is not dictated solely by the S protein. Natural infection, in fact, was associated with broad epitope coverage from several regions other than the S protein. This was evidenced by the S protein being associated with only 27% of the $CD4^+$ T cell response. Interestingly the M and N

proteins accounted for 27% and 11% of the CD4$^+$ T cell response, respectively. Therefore, efficient vaccine formulation must consist of epitopes from the M, N, as well as the S protein to induce broad epitope coverage and potent humoral and cellular responses.

2.7.4 Validation of selected epitopes through incorporation in recombinant protein vaccines

Although initial findings, which utilize in silico immunoinformatic approaches associated with vaccine development and immunogenicity, can identify epitopes based on high levels of antigenicity and broad conservancy, in vivo immunogenicity experiments need to be conducted to validate these epitopes and the resulting immune responses in both animal and human models. Identification of conserved and immunogenic epitopes in combination with the incorporation of these epitopes in multi-epitope-based vaccines can allow the targeting of multiple epitopes simultaneously (Herrera et al., 2021).

As witnessed by vaccine development against SARS-CoV-2, DNA, mRNA, and recombinant protein vaccines offer certain advantages over traditional vaccine platforms in terms of convenience, potent elicited immune responses, and stronger safety profiles. DNA, mRNA, and recombinant protein vaccines may serve as antigens after processing by APCs and subsequently presented on MHC class I and class II molecules for the activation of CD4$^+$ and CD8$^+$ T cells. Specialized CD4$^+$ T cells, namely Tfh and Foxp3$^+$ T follicular regulatory (Tfr) cells, play crucial roles in facilitating germinal centre B cell formation through interactions with T and B cells. Tfh cells provide assistance to B cells through interactions between CD40L on Tfh cells and CD40 on B cells, leading to the release of cytokines such as IL-2, IL-4, IL-21, and IFN-γ. These cytokines further stimulate the formation of germinal centres, promoting maturation into plasma cells that produce memory B cells and long-lived antibody-secreting plasma cells. On the other hand, CD8$^+$ T cells directly combat infections by targeting and eliminating infected cells using perforin

and granzymes, thereby restricting the pathogen's spread within the body. The elicitation of humoral and cellular immune responses from the administration of DNA, mRNA, and recombinant protein vaccines is illustrated in **Figure 2.5.**
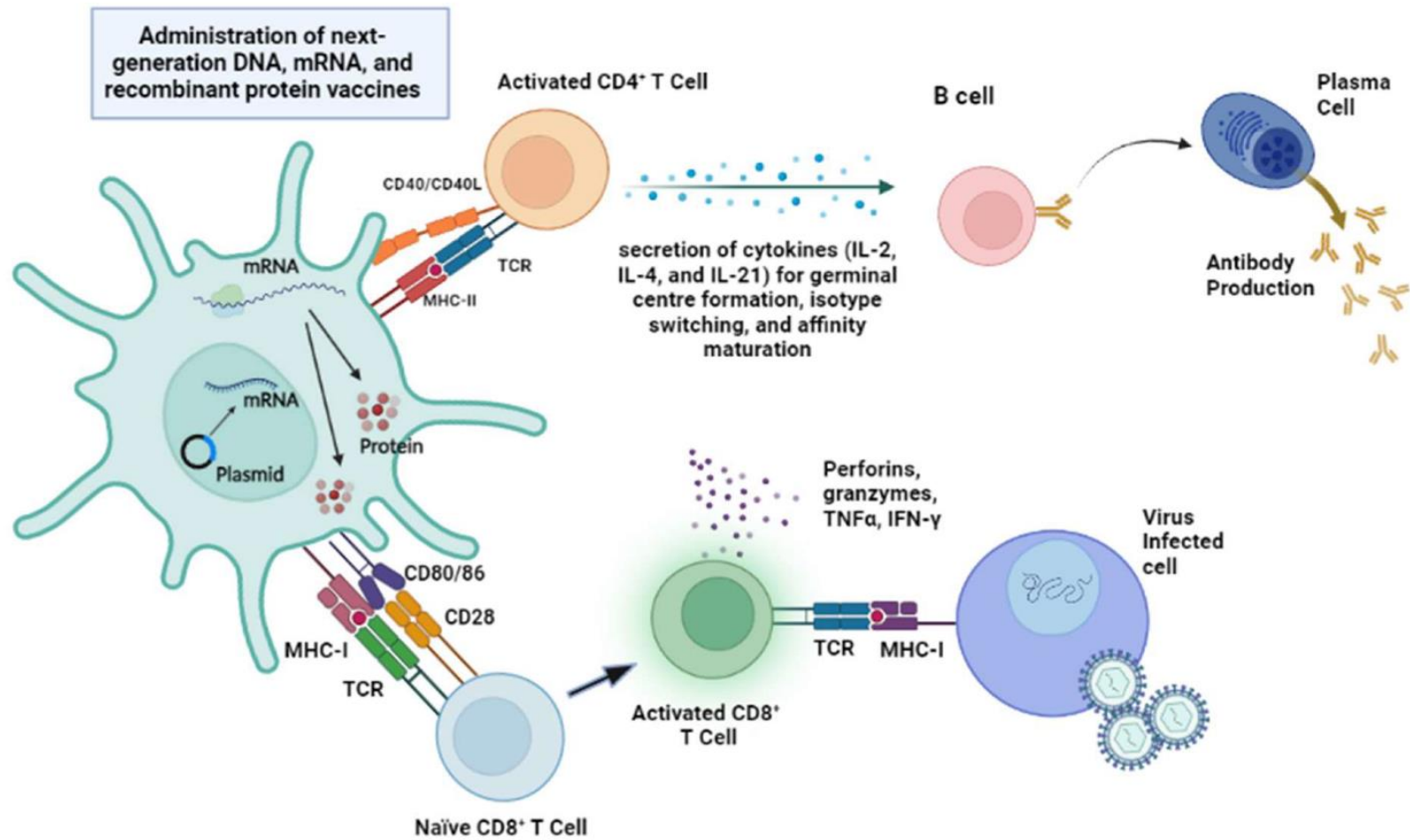
Figure 2.5. Elicitation of humoral and cellular immune responses from the administration of DNA, mRNA, and recombinant protein vaccines

Nucleic acids have also been used as therapeutics for cancer. For the purpose of cancer immunotherapy, plasmids, mRNA, and immunomodulatory DNA/RNA, can precisely transport and release therapeutics to target tissues and cells (Zhou et al., 2020). Recently, promising research has been conducted on nanoparticles which can be equipped with ligands to disrupt cell membranes and enhance nucleic acid delivery to specific cells (Mollé et al. 2023). The mRNA vaccine platform is viewed as a promising solution to develop vaccine candidates against SARS-CoV-2 at an accelerated pace. mRNA vaccines were the first vaccine candidates against SARS-CoV-2 that progressed to clinical development and received emergency use authorization (EUA) for large-scale public immunization (Barbier et al., 2022). Smith et al. (2020) explained how a number of nucleic acid vaccine candidates based on different antigenic regions could be efficiently and quickly developed when faced with emerging resistant pathogenic strains (Smith et al., 2020).

To improve immunogenicity, DNA vaccines often require the use of adjuvants, which can enhance the immune response (Tomljenovic & Shaw, 2011). Furthermore, the administration of DNA vaccines typically requires a medical device such as electroporator that can deliver electric pulses to facilitate the uptake of DNA by cells (Babuadze et al., 2022; Smith, et al., 2020; Zhao et al., 2023). Recent advances have enhanced the stability of mRNA vaccines by optimizing mRNA structure and effectively screening excipients such as modified nucleotides and sucrose. Improvements in manufacturing processes also facilitated the preparation of thermally stable mRNA vaccines with high safety and protective efficacy (Cheng et al., 2023). Increasing RNA length was shown to decrease the half-life of mRNA vaccines. The shelf life of the second-generation Moderna COVID-19 mRNA vaccine, mRNA-1283, which encodes the shorter N-terminal and receptor-binding region of the S protein, was extended from 6 to 12 months at 2–8

°C, indicating a significant improvement in mRNA stability. Sequence optimization in terms of translation efficiency and mRNA stability was also substantially enhanced by the selection of human α- and β-globin 3′ UTR sequences. Instead of using uridine triphosphate (UTP), N1-methyl pseudouridine triphosphate (m1ψTP) was used in the development of mRNA-1273 and BNT162b2. m1ψTP is associated with higher stability levels and has a superior safety profile (Cheng et al., 2023). An excipient that is frequently used to lower the temperature of crystallization and ice crystal formation in the aqueous phase is sucrose. The use of sucrose improves the freeze-thaw stability of mRNA vaccines and was used as a stabilizing agent and cryoprotectant in mRNA-1273 and BNT162b2 (Ayat et al. 2019). The distribution of vaccination services and the supply of vaccines have undergone as a result of developments in vaccine equity and factors associated with globalization such as increased international investment, harmonization of regulatory requirements across borders, and manufacture in developing nations (Omidvar Tehrani & Perkins, 2022).

Subunit vaccines stand as remarkable achievements in modern medicine, offering potent tools to immunize against infectious diseases. For example, Cervarix, Gardasil, and Gardasil-9 are three commercially available HPV preventive vaccines. These vaccines are non-infectious subunit vaccines comprising virus-like particles (VLPs) of HPV 16, 18, 31, 33, 45, 52, and 58; and HPV 6, 11, 16, and 18. 360 copies of the virus's L1 main capsid protein self-assemble to generate the VLPs. HPV L1 virus-like particle (VLP) vaccines have shown exceptional prophylactic efficacy in clinical trials and success in national vaccination programs with high coverage rates when given in a prime/boost sequence of three injections spaced six months apart (Schiller & Lowy, 2018). Moreover, Engerix-B developed by GlaxoSmithKline (GSK) and Recombivax HB developed by Merck) are two licensed recombinant subunit vaccines against hepatitis B. Both are formed up of

HBsAg that has been extracted and refined from Saccharomyces cerevisiae and are antigen suspensions that have been adjuvanted with alum (Gomez & Robinson, 2018). Engerix-B and Recombivax HB are linked to with ≥90% seroprotection rates upon primary 3-dose vaccination and adequate safety profiles, respectively (Van Den Ende et al., 2017).

The reactivity of mRNA vaccines depends on their ability to express foreign antigens, leading to the elimination of infected APCs. Although lipid nanoparticles (LNPs) can induce an acute inflammatory response, the trials conducted so far have not detected significant signs of adverse safety when employing LNPs for the delivery of small molecules, non-expressing RNAs, or RNAs encoding endogenous proteins (Krishna et al., 2016). While careful assessment of their usage is necessary, new advancements in mRNA vaccines offer potential remedies for various diseases in the context of biomedical technologies.

The development of recombinant protein vaccines has been described as a promising approach to elicit potent immune responses (Pollet et al., 2021a). They are associated with practical advantages of stability, safety, high immunogenicity with the use of adjuvants, and a proven track record in clinical development. The recombinant protein platform is considered to be safe and non-infectious. It is easier to produce a vaccine antigen as a recombinant protein when compared to LAVs and IVs (Liu, 2019). The advantage associated with immunization using recombinant protein vaccines is that they do not require the use of cold chain storage in freezers and liquid nitrogen to store and preserve the vaccine at temperatures lower than −80 °C, which suggests that they could be used to immunize populations in resource-poor third-world countries lacking cold chain facilities. Freeze-drying or lyophilization of recombinant protein vaccines has also been performed. For example, Lai et al. (2021) discussed the development of insect cell-expressed SARS-CoV-2 S protein ectodomain constructs compatible with lyophilization and storage in a dry

thermostabilized state (Lai et al., 2021). Moreover, freeze-dried, heat-stable formulations of influenza subunit vaccines were safe and immunogenic when administered to mice (Flood et al., 2016).

There are several expression systems available for the production of recombinant proteins. *E. coli* is commonly used as an expression system since it possesses unparalleled fast-growth kinetics, enabling the rapid production of recombinant proteins. Although heterologous glycoproteins can be produced using yeast, insect, and mammalian systems, the *E. coli* system is often only used to generate non-glycosylated proteins. On the other hand, improvements in *E. coli* glycosylation have been made. The N-glycosyltransferase from Actinobacillus pleuropneumoniae (ApNGT) can be co-expressed for the in vivo transfer of a glucose residue to IFNα at an NX(S/T) N-glycosylation sequon, according to Prabhu et al. (2021). Using an in vitro chemoenzymatic approach, the N-glucosylated protein was effectively elaborated with biantennary sialylated complex-type N-glycan in the second phase. It was discovered that the N-glycosylated IFNα product exhibited markedly enhanced proteolytic stability and was physiologically active. Another important advantage associated with the development of recombinant protein vaccines is the ability to obtain bacterial cultures with high cell densities, which makes it possible to produce proteins on a larger scale more effectively. *E. coli* expression systems use media that can be easily developed from inexpensive, generally accessible components, lowering production costs. Furthermore, it is simple and quick to transform *E. coli* with exogenous recombinant DNA, making it easier to introduce the required genes for protein expression (Rosano & Ceccarelli, 2016). Another useful technique for creating recombinant glycoproteins is by using Spodoptera frugiperda (Sf9) insect cells with baculovirus-mediated expression. This approach is favored due to its simplicity and rapidity in expressing foreign proteins. Moreover, it offers a high likelihood of obtaining

biologically active proteins, further contributing to its popularity in the field of protein production (Altmann et al., 2016). In general, it is true that newly produced polypeptides can be folded, modified, trafficked, and assembled by insect cells to generate very authentic, soluble end products (Kost et al., 2005). However, not all proteins can be expressed in insect cells. Proteins that need complex post-translational modifications and folding may be more suited for mammalian expression systems because insect cells are able to produce less complex N-glycans than mammalian cells (Felberbaum, 2015). In particular, the expression of membrane-active proteins in insect cells may result in misfolding of polypeptides to form non-functional protein (Liu et al., 2013).

The resemblance of protein secretion pathways between yeasts and higher eukaryotic organisms has meant that yeasts such as *Pichiapastoris* (syn *Komagataella* spp.) are now also widely recognized as favorable hosts for the production of various recombinant proteins (Thak et al., 2020). The extracellular secretion of recombinant proteins by yeasts simplifies the downstream purification process, making it more cost-effective (Pollet et al., 2021b). Nevertheless, integrative plasmids are used for transformation of *Pichia pastoris* cells for which maintaining antibiotic selection pressure after transformants have been selected is not required. Since zeomycin is costly, no antibiotic is used. The lack of antibiotic in the Yeast Extract–Peptone–Dextrose (YPD) medium means that bacterial contamination might occur (Haon et al., 2015). Furthermore, fungal bioprocessing is generally carried out in solid-state fermentation systems (SSF) and is associated with limitations such as contamination issues and low substrate utilisation rate (Arora et al., 2018).

Recombinant proteins, such as those produced in *E. coli*, require purification from mixtures of crude lysates. The process can be facilitated by the use of glutathione S-transferase (GST) or poly-histidine (His) affinity tags to enable purification through affinity chromatography (Fujita-

Yamaguchi et al., 2015, Schäfer et al., 2015). Endotoxins in Gram-negative bacteria like *E. coli* can cause inflammation and septic shock when they get into the bloodstream. This happens because the endotoxins stimulate the production of inflammatory substances by cells sensitive to lipopolysaccharide (LPS). Recombinant proteins obtained from *E. coli* often contain endotoxin contamination due to high levels of LPS in the cell wall. Even small amounts of endotoxin in recombinant protein preparations can lead to adverse reactions such as shock. Therefore, it is crucial to remove endotoxins from recombinant proteins to prevent these harmful reactions (Liu et al., 1997). Nevertheless, endotoxins may be conveniently removed from purified proteins through the use of a porous cellulose bead surface modified with covalently attached poly(ϵ-lysine) chains, which possess high binding affinity for endotoxins. The purified proteins may then be monitored for endotoxins using endotoxin quantification assays (Ghaemi et al., 2022). Additionally, recombinant protein vaccines may require the use of adjuvants to enhance and prolong the immune response. Adjuvants are added to vaccines to stimulate the immune system and have dose-sparing effects. While adjuvants can be beneficial, their use also introduces additional considerations such as safety, compatibility, and potential side effects. Adjuvants such as aluminum salts are frequently used to boost the immunogenicity of recombinant protein vaccines. Nevertheless, it is frequently noted that vaccines made with these adjuvants lose effectiveness when they are refrigerated or lyophilized. Typically, processing-related adjuvant particle aggregation is attributed to this decline in potency (Pan et al., 2021). Additionally, it has been reported that adjuvants like MF59 or alum cause localized tissue damage and cell death, which in turn creates a pro-inflammatory environment (Díaz-Dinamarca et al., 2022).

Recombinant protein vaccines offer several advantages, including their non-replicating nature and absence of infectious components. These characteristics help position them as a safer

alternative when compared to vaccines derived from live viruses. Extensive testing of this vaccine platform has demonstrated that these vaccines typically elicit only mild side effects. As a result, multiple recombinant protein vaccines have been successfully utilized in clinical settings worldwide (Pollet et al., 2021a). Due to the distinct advantages associated with the recombinant protein vaccine platform in terms of ease of production following the establishment of an effective purification strategy, a strong safety profile, the ability to elicit potent immune responses, and convenient storage at room temperature in freeze-dried form, this research project has incorporated the 6 selected epitope sequences into a recombinant expression plasmid to produce a recombinant protein vaccine. The advantages and limitations associated with the use of recombinant protein, DNA, and mRNA vaccines have been summarized in Table 2.1.

Table 2.1. The advantages and limitations associated with the use of recombinant protein, DNA, and mRNA vaccines

Vaccine	Advantages	Limitations	References
Recombinant protein vaccines	• Safe and non-infectious. • Elicit strong immune responses. • Proven track record. • Convenient storage in freeze-dried forms. • Do not require ultra-cold storage temperatures.	• Require several purification steps involving column and affinity chromatography. • Adjuvant is needed to enhance long-term immunity.	Liu (2019) Lai et al. (2021) Flood et al. (2016) Rosano & Ceccarelli, (2016) Altmann et al. (2016) Thak et al. (2020) Pollet et al. (2021a)
DNA vaccines	• Can be conveniently produced in bulk quantities compared to IVs and mRNA vaccines. • Cost-effective when compared to the complexities involved in producing IVs or mRNA vaccines. • Suitable for distribution and large-scale immunization in underdeveloped countries.	• Lower immunogenicity. • Risk of genomic integration. • Requires adjuvants for enhanced immunogenicity. • Immunizations necessitate the use of medical devices like electroporators. • Needleless patch administration is still under development.	Poland et al. (2021) Krammer (2020) Khalid & Poh (2023) Hobernik & Bros (2018) Kutzler & Weiner (2008) Tomljenovic & Shaw (2011) Al-Fattah Yahaya et al. (2023)

	• Can be conveniently produced in prokaryotic cells, like *E. coli*, or expressed in mammalian cells, such as HEK-293 T cells		
mRNA vaccines	• Accelerated development from preclinical to clinical stages using established regulatory pathways. • High levels of safety. • Effective in providing protection against COVID-19. • The nucleotide sequence of mRNA vaccines can be easily modified to target emerging resistant pathogenic strains.	• Expensive to develop and produce. • Requires ultra-low temperatures of −80°C. • The high cost and demanding storage conditions of mRNA vaccines can render them logistically inconvenient and expensive for many low-income countries.	Barbier et al. (2022) Polack et al. (2020) Baden et al. (2021) Smith, et al. (2020) Cao et al. (2021) Rosa, et al. (2021)

2.8 Current recombinant protein vaccine development landscape

The current vaccine developmental landscape against SARS-CoV-2 may be broadly divided into recombinant protein vaccines focusing on the full-length S protein, and those utilizing the RBD as the main antigenic region or virus-like particle (VLP)-based vaccines (Krammer, 2020). Recombinant protein vaccines based on the S protein were able to attain high vaccine efficacy through the use of certain alterations to the S protein. The S protein in its unmodified activated form is unstable and occurs in various conformations that do not fully expose the neutralizing epitopes. Moreover, recombinant protein vaccines such as the one developed by Novavax utilized two proline mutations to develop a prefusion-stabilized S protein as the main antigenic target. These mutations were made by introducing mutations in two consecutive residues (K986 and V987) in the S2 subunit located between the central helix (CH) and the heptad repeat 1 (HR1) (Dai & Gao, 2021). The existence of the polybasic cleavage site in SARS-CoV-2 S protein at S1/S2 has been shown to be associated with higher transmissibility, and pathogenesis, allowing the virus to evade the immune response as well as increased instability. Therefore, current S-based recombinant protein vaccines use these modifications either alone or in combination. For example, Amanat et al. (2020) demonstrated that S-based recombinant protein vaccine candidates either consisting of the polybasic cleavage site deletion or the inclusion of proline mutations were able to elicit nAbs and induce full protection of mice in *in vivo* challenge studies.

2.8.1 Novavax

A prominent example of a recombinant nanoparticle protein vaccine developed against SARS-CoV-2 is the NVX-CoV2373 developed by Novavax which was composed of the prefusion-stabilized full-length S protein of the original Wuhan strain in combination with the Matrix-M adjuvant. NVX-CoV2373 S form 27.2 nm thermostable nanoparticles that can bind

strongly to the ACE2 receptor. Promising reports in terms of safety and immunogenicity have been obtained from a phase 1–2 Trial of NVX-CoV2373. Participants were divided into groups receiving either the vaccine with or without the Matrix-M adjuvant or the placebo. The vaccine was considered to be safe as evidenced by a complete absence of serious side effects along with minimal reactogenicity which was enhanced upon the administration of the adjuvant. Moreover, potent humoral and cellular responses were elicited upon the administration of the vaccine. The groups receiving vaccine formulated with the Matrix-M adjuvant elicited geometric mean anti-S IgG antibody titer of 63,160 and neutralization responses of 3906 that were higher than in convalescent patients recovering from symptomatic COVID-19. In conclusion, the vaccine was shown to be safe and capable of eliciting strong immune responses in immunized adults in a Phase 1–2 trial (Keech et al., 2020).

Heath et al. (2021) detailed the safety, efficacy, and immunogenicity data acquired following the administration of the NVX-CoV2373 vaccine in a larger cohort of adults in a phase 3 clinical trial. Participants of the study were either immunized using two 5 μg doses of NVX-CoV2373 or administered the placebo. Efficacy studies showed that SARS-CoV-2 infections were observed in 10 participants from the vaccine group and in 96 from the placebo group. An extremely positive vaccine efficacy of 96.4% was reported against the SARS-CoV-2 Wuhan strain. It was noteworthy that vaccine efficacy was reduced to 86.3% by the Alpha B.1.1.7 VOC. All five cases of severe infections belonged to participants in the placebo group. Furthermore, adverse effects were mild and transient in nature.

2.8.2 RBD Recombinant SARS-CoV-2 vaccine (Sf9 Cell)

A promising vaccine candidate against SARS-CoV-2 is the recombinant peptide vaccine focusing on the full RBD as the main antigenic region produced by baculovirus expressed in Sf9

cells. Being developed by West China Hospital in collaboration with Sichuan University, the vaccine candidate has shown promising results in phase 1 and phase 2 clinical trials in terms of safety and immunogenicity evaluated after full vaccination in adults. Although side effects such as pain at the site of injection, fever, cough, and fatigue were reported, laboratory parameters in terms of blood cell counts (white blood cell, lymphocyte, neutrophil, platelet, and hemoglobin) liver function tests (alanine aminotransferase, aspartate aminotransferase, and total bilirubin), kidney function tests (creatinine), blood coagulation tests (prothrombin and activated partial thromboplastin time) and other biochemical markers (blood sugar, urine protein, and urine erythrocyte) did not significantly alter as compared to the naïve group receiving the placebo (Meng et al., 2021). Moreover, potent humoral responses were elicited in both phase 1 and phase 2 clinical trials in terms of binding antibodies produced against the RBD. In phase 1, the high-dose group receiving 3 doses of the vaccine at days 0, 14, and 28 showed the highest binding antibody geometric mean titre of 1282.1, followed by the high-dose group receiving 2 doses of the vaccine at days 0 and 28 with a binding antibody geometric mean titre of 96.9, lastly by the low-dose group receiving 2 doses of the vaccine at days 0 and 28 with a binding antibody geometric mean titre of 39.3. Neutralizing antibody responses against the live virus showed that the neutralizing antibody geometric mean titre (102.9) elicited in the high-dose group was significantly higher than in the low-dose (1.2) and placebo (0.7) groups (Meng et al., 2021). Furthermore, an evaluation of cellular immune responses in phase 1 clinical trial showed that the highest levels of IFN-γ were recorded at day 14 after vaccination. Approximately, 25.2 spot-forming cells were observed in the low-dose group (days 0 and 28), followed by 21.8 in the high-dose group (day 0 and 28), 39.9 in the high-dose group (days 0, 14, and 28), and 9.1 in the placebo group (Meng et al., 2021). Similarly, in phase 2, the high-dose group receiving 3 doses of the vaccine at days 0, 14, and 28

46

showed the highest binding antibody with a geometric mean titre of 1099.9, followed by the low-dose group receiving 3 doses of the vaccine with a binding antibody geometric mean titre of 156.2. The high-dose group receiving 2 doses of the vaccine showed a binding antibody geometric mean titre of 135.9 and the low-dose group showed a binding antibody geometric mean titre of 40.0. Neutralizing antibody levels were highest (102.6) in the high-dose group receiving 3 doses, followed by a significant reduction in groups receiving 3 low doses (8.1), 2 high-doses (3.6), and 2 low doses (1.9) (Meng et al., 2021). The recombinant protein vaccine is currently in a phase 3 clinical trial (WHO, 2023).

2.8.3 VAT00008 adjuvanted with AS03

The SARS-CoV-2 S recombinant protein vaccine VAT00008, developed by Sanofi Pasteur and GlaxoSmithKline was tested in various formulations either with the AF03 or AS03 adjuvant. Safety testing demonstrated that while local and systemic reactions were reported, there were no serious adverse effects occurring due to vaccine administration. There was higher reactogenicity upon vaccine administration in the 50 year-old and older age group. Moreover, immunogenicity testing showed that a single dose was not adequate in terms of the production of nAbs. The administration of two vaccine doses was able to elicit effective neutralizing antibody responses. For participants aged 18-49, neutralizing antibody titres were reported to be 13.1 for the low-dose (1.3 μg) group adjuvanted with AF03, 20.5 in the low-dose group adjuvanted with AS03, 43.2 in the high-dose (2.6 μg) group adjuvanted with AF03, 75.1 in the high-dose group adjuvanted with AS03, 5.00 in the high-dose group without adjuvant, and also 5.00 in the placebo group. For older participants with ages 50 and above, neutralizing antibody titres were reported to be 8.62 for the low-dose (1·3 μg) group adjuvanted with AF03, 12.9 in the low-dose group adjuvanted with AS03, 12.3 in the high-dose (2·6 μg) group adjuvanted with AF03, 52.3 in the high-dose group adjuvanted

with AS03, 5.00 in the high-dose group without adjuvant, and also 5·00 in the placebo group. Due to the relatively higher humoral immune responses elicited as a result of immunization with the vaccine adjuvanted with the AS03, the collaborators decided to proceed with this formulation for future clinical trials (Goepfert et al. 2021). The vaccine showed tolerable levels of safety and high elicited immune responses in the phase 2 clinical trial when adjuvanted with AS03. Adverse side effects upon immunization were reported to be transient and mostly mild to moderate. The second immunization increased both the frequency and intensity of the adverse effects reported. Moreover, humoral responses in terms of neutralizing antibody titres were reported to be significantly higher in participants immunized with the vaccine as compared to participants receiving the placebo. Neutralizing antibody geometric mean titres were recorded to be 3143 in the low-dose group, and 2338 in the medium-dose group, with the highest being 7069 in the high-dose group (Sridhar et al., 2022).

2.8.4 UB612

The UB-612 multi-epitope recombinant protein vaccine was associated with the use of specific immunogenic peptides from the S protein, RBD of S1 linked to a single chain Fc domain of human IgG1 (S1-RBD-sFc), peptides specifying CD4$^+$ and CD8$^+$ T cells from the S2 subunit, as well as those from the M and N protein The vaccine also employs the use of an aluminum phosphate adjuvant and CpG1 which produces a Th1 polarized response. Phase I/II trial results of UB-612 no related serious adverse events, durable neutralizing activity and broad T cell responses against SARS-CoV-2 Delta and Omicron VOCs (Wang et al., 2022). Following primary immunization, a booster dose of the UB-612 vaccine led to an increase in neutralizing antibody levels by 131-, 61-, and 49-fold against Wuhan SARS-CoV-2, Omicron BA.1 and BA.2

variants, respectively with 95% efficacy against symptomatic Wuhan strain SARS-CoV-2 (Guirakhoo et al., 2022).

Indeed, the current developmental landscape of vaccine development against SARS-CoV-2 reflected that recombinant protein vaccines were being quickly progressed to the clinical stage. As many as 16 vaccine candidates had already progressed to phase 3 clinical trial with 1 vaccine candidate in phase 4 being approved for global immunizations under emergency use as of 8th March 2022 (WHO, 2023). **Table 2.2.** provides a comprehensive overview of the clinical development of recombinant protein vaccines against SARS-CoV-2.

Table 2.2. An overview of the clinical development of recombinant protein vaccines against SARS-CoV-2

#	Type of Vaccine Candidate	Number of Doses	Route of administration	Developers	Clinical Trial Phase	NCT #
1.	MVC-COV1901 (S-2P protein + adjuvant CpG 1018)	2	IM	Medigen Vaccine Biologics + Dynavax + National Institute of Allergy and	Phase 4	NCT05079633
2.	SARS-CoV-2 rS/Matrix M1-Adjuvant (Full-length recombinant SARS CoV-2	2	IM	Anhui Zhifei Longcom Biopharmaceutical + Institute of Microbiology,	Phase 3	NCT04611802
3.	Recombinant SARS-CoV-2 vaccine (CHO Cell)	2-3	IM	Sanofi Pasteur + GSK	Phase 3	ChiCTR2100050849
4.	VAT00008: SARS-CoV-2 S protein with adjuvant	2	IM	Clover Biopharmaceuticals Inc./Dynavax	Phase 3	PACTR202011523101903*
5.	CpG 1018/Alum-adjuvanted Recombinant SARS-CoV-2 Trimeric S-protein Subunit Vaccine (SCB-2019)	2	IM	Vaxine Pty Ltd./CinnaGen Co.	Phase 3	NCT05012787
6.	COVAX-19® Recombinant S protein + adjuvant	2	IM	Instituto Finlay de Vacunas	Phase 3	IRCT20150303021315N24
7.	FINLAY-FR-2 anti-SARS-CoV-2 Vaccine (RBD chemically	2	IM	Federal Budgetary Research Institution State Research Center of Virology and Biotechnology "Vector"	Phase 3	RPCEC00000354

	conjugated to tetanus toxoid plus adjuvant)					
8.	EpiVacCorona (EpiVacCorona vaccine based on peptide antigens for the prevention of COVID-19)	2	IM	Federal Budgetary Research Institution State Research Center of Virology and Biotechnology "Vector"	Phase 3	NCT04780035
9.	RBD (baculovirus production expressed in Sf9 cells)	2	IM	West China Hospital + Sichuan University	Phase 3	NCT04887207
10.	UB-612 (Multitope peptide based S1-RBD-protein based vaccine)	2	IM	Vaxxinity	Phase 3	NCT05293665
11.	CIGB-66 (RBD+aluminium hydroxide)	3	IM	Center for Genetic Engineering and Biotechnology (CIGB)	Phase 3	RPCEC00000359
12.	BECOV2	2	IM	Biological E. Limited	Phase 3	CTRI/2021/08/036074
13.	Recombinant Sars-CoV-2 S protein, Aluminum adjuvanted (Nanocovax)	2	IM	Nanogen Pharmaceutical Biotechnology	Phase 3	NCT04922788
14.	S-268019	2	IM	Shionogi	Phase 3	NCT05212948
15.	GBP510	2	IM	SK Bioscience Co., Ltd. and CEPI	Phase 3	NCT05007951
16.	Razi Cov Pars	3	IM	Razi Vaccine and Serum Research Institute	Phase 3	IRCT20210206050259N3
17.	EuCorVac-19	2	IM	POP Biotechnologies and EuBiologics Co.,Ltd	Phase 3	NCT05572879
18.	ReCOV	2	IM	Jiangsu Rec-Biotechnology	Phase 3	NCT05398848

19.	Recombinant SARS-CoV-2 Fusion Protein Vaccine (V-01)	2	IM	Livzon Pharmaceutical	Phase 3	NCT05096832
20.	Recombinant SARS-CoV-2 Vaccine (CHO cell)	2	IM	National Vaccine and Serum Institute, China; Beijing Zhong Sheng Heng Yi	Phase 3	NCT05599516
21.	RBD protein recombinant SARS-CoV-2 vaccine (Noora Vaccine)	3	IM	Bagheiat-allah University of Medical Sciences/AmitisGen	Phase 3	IRCT20210620051639N3
22.	COVID-19 Vaccine Hipra	2	IM	Laboratorios Hipra, S.A.	Phase 3	NCT05246137
23.	SCTV01C	1	IM	Sinocelltech Ltd.	Phase 3	NCT05308576
24.	SARS-CoV-2 Recombinant Vaccine adjuvanted With Alum+CpG 1018	2	IM	PT Bio Farma	Phase 3	NCT05433285
25.	MF59 adjuvanted SARS-CoV-2 Sclamp vaccine	2	IM	CSL Ltd. + Seqirus + University of Queensland	Phase 2/3	NCT04806529
26.	SARS-CoV-2 Protein Subunit Recombinant Vaccine	2	IM	PT Bio Farma	Phase 2/3	NCT05313035
27.	PIKA-Adjuvanted Recombinant SARS-CoV-2 S Protein Subunit Vaccine	2	IM	Yisheng Biopharma	Phase 2/3	NCT05463419
28.	ARVAC-CG	2	IM	Laboratorio Pablo Cassara S.R.L.	Phase 2/3	NCT05752201

29.	Convacell	2	IM	St. Petersburg Research Institute of Vaccines and Sera	Phase 2/3	NCT05726084
30.	FINLAY-FR1 anti-SARS-CoV-2 Vaccine (RBD + adjuvant)	2	IM	Instituto Finlay de Vacunas	Phase 2	RPCEC00000366
31.	SARS-CoV-2-RBD-Fc fusion protein (AKS-452)	1-2	IM	University Medical Center Groningen + Akston Biosciences Inc.	Phase 2	NCT05124483
32.	COVAC-1 and COVAC-2 sub-unit vaccine (S protein) + SWE adjuvant	2	IM	University of Saskatchewan	Phase 2	NCT05209009
33.	SCB-2020S, an adjuvanted recombinant SARS-CoV-2 trimeric S-protein (from B.1.351 variant)	2	IM	Clover Biopharmaceuticals AUS Pty Ltd	Phase 2	NCT04950751
34.	V-01-351/V-01D Bivalence Vaccine (Omicron) or V-01D-351	1	IM	Livzon Pharmaceutical Group Inc.	Phase 2	NCT05273528
35.	KBP-COVID-19 (RBD-based)	2	IM	Kentucky Bioprocessing Inc.	Phase 1/2	NCT04473690
36.	IMP CoVac-1 (SARS-CoV-2 HLA-DR peptides)	1	SC	University Hospital Tuebingen	Phase 1/2	NCT04954469
37.	CIGB-669 (RBD+AgnHB)	3	IN	Center for Genetic Engineering and Biotechnology (CIGB)	Phase 1/2	RPCEC00000345

38.	QazCoVac-P - COVID-19 Subunit Vaccine	1-2	IM	Research Institute for Biological Safety Problems	Phase 1/2	NCT04930003
39.	202-CoV; SARS-CoV-2 S trimer protein + adjuvant, CpG7909.	2	IM	Shanghai Zerun Biotechnology + Walvax Biotechnology + CEPI	Phase 1/2	NCT05313022
40.	Versamune-CoV-2FC vaccine, recombinant S1 antigen	3	NR	Farmacore Biotecnologia Ltda	Phase 1/2	NCT05016934
41.	SII B.1.351 + Matrix-M1 adjuvant	2	IM	Novavax	Phase 1/2	NCT05029856
42.	SII Bivalent + Matrix-M1 adjuvant	1	IM	Novavax	Phase 1/2	NCT05029857
43.	SII B.1.617.2 + Matrix-M1 adjuvant (Delta)	1-2	IM	Novavax	Phase 1/2	NCT05029858
44.	PepGNP-SARSCoV2	2	ID	Emergex Vaccines Holding Limited	Phase 1/2	NCT05633446
45.	Betuvax-CoV-2 COVID-19 vaccine	2	IM	Human Stem Cell Institute, Russia	Phase 1/2	NCT05270954
46.	AdimrSC-2f (recombinant RBD +/- Aluminium)	NR	NR	Adimmune Corporation	Phase 1	NCT04522089
47.	MF59 adjuvanted SARS-CoV-2 Sclamp	2	IM	The University of Queensland	Phase 1	NCT04495933
48.	SK SARS-CoV-2 recombinant surface antigen protein subunit (NBP2001) + adjuvanted with alum.	2	IM	SK Bioscience Co., Ltd.	Phase 1	NCT04760743

49.	SpFN + QS21 (ALFQ) adjuvant.	2-3	IM	Walter Reed Army Institute of Research (WRAIR)	Phase 1	NCT04784767
50.	CoVepiT	1-2	SC	OSE Immunotherapeutics	Phase 1	NCT04885361
51.	CoV2-OGEN1, protein-based vaccine	1-2	Oral	USSF/Vaxform	Phase 1	NCT04893512
52.	Baiya SARS-CoV-2 VAX1, a plant-based subunit vaccine (RBD-Fc + adjuvant)	2	IM	Baiya Phytopharm Co., Ltd.	Phase 1	NCT04953078
53.	SARS-CoV-2 Vaccine (IN-B009)	2	IM	HK inno. N Corporation	Phase 1	NCT05113849
54.	DoCo-Pro-RBD-1 + MF59	1	IM	University of Melbourne	Phase 1	NCT05272605
55.	VXS-1223U Microarray patch (HD-MAP) (HexaPro)	1	ID	Vaxxas Pty Ltd	Phase 1	ACTRN12622000597796
56.	PRIME-2-CoV_Beta	2	IM	Speransa Therapeutics	Phase 1	NCT05367843
57.	ACM-SARS-CoV-2-beta ACM-CpG vaccine candidate (ACM-001)	2	IN	ACM Biolabs	Phase 1	NCT05385991
58.	OMV-linked HexaPro	1	IN	Intravacc B.V.	Phase 1	NCT05604690
59.	Recombinant SARS-CoV-2 S-Trimer Vaccine (CHO Cell) booster	1	IM	Binhui Biopharmaceutical Co., Ltd.	Phase 1	NCT05716347

Adapted from COVID-19 vaccine tracker and landscape as of March 30, 2023.

https://www.who.int/publications/m/item/draft-landscape-of-covid-19-candidate-vaccine

2.9 Rationale for utilizing highly conserved and immunogenic epitopes as vaccine antigens

Current recombinant protein vaccine development against SARS-CoV-2, consisting of the S protein, presents certain challenges. Schaub et al. (2021) asserted that the S protein is challenging to express in large quantities recombinantly because it is metastable and glycosylated. This directly relates to low production and the number of vaccine doses that can be mass-produced. Such a challenge requires a thorough evaluation of expression systems, host cell organisms, and optimization of culture conditions to maximize heterologous protein expression. Vaccines focusing on the S protein as the main antigenic region are also susceptible to a reduction in protective efficacy as a result of SARS-CoV-2 VOCs.

Vaccines focusing on only the RBD may potentially be highly susceptible to antigenic drift, whereby mutations in the SARS-CoV-2 may significantly reduce the protective efficacies of such vaccines. The SARS-CoV-2 Omicron B.1.1.529 variant was shown to have 15 mutations in the RBD. Different mutations in Omicron help it to evade neutralizing antibodies. Some mutations, such as K417N, G446S, E484A, and Q493R, mainly affected antibodies that target specific regions overlapping with the ACE2-binding motif (groups A–D). Others, including G339D, N440K, and S371L, were reported to impact a subset of neutralizing antibodies from groups E and F, but antibodies like S309 and CR3022 were less affected (Cao et al., 2022). Moreover, Greaney et al. (2021) showed that mutations such as K417 and E484 are highly effective at evading particular types of antibodies and are prevalent among many sequenced viral isolates. Following the evasion of class 2 antibodies, the immune response relies predominantly on class 1 and class 3 antibodies to combat the virus. Notably, certain emerging viral lineages carrying the E484K mutation often acquire additional mutations, such as K417N/T (seen in B.1.351 and P.1 variants), which enhance their ability to evade class 1 antibodies. Additionally, viral lineages like B.1.427/429 and B.1.617.2

possess a moderate class 3 escape mutation (L452R), while B.1.617.1 harbours both E484Q and L452R mutations. Other clusters of viral sequences exhibit mutations in epitopes targeted by class 2 and class 3 antibodies, such as E484K and R346K, further affecting antibody recognition and neutralization.

In light of mutations that can lower the protective efficacies of current vaccines, this research project aims to express a recombinant protein vaccine composed of peptides representing highly conserved and immunogenic B and T cell epitopes from SARS-CoV-2 M and N proteins. It is hypothesized that upon assessment of the neutralizing activity against the SARS-CoV-2 Wuhan and Omicron strains, the vaccine would be able to inhibit the interaction between the RBD from both strains and the ACE2 receptor.

2.10 Rationale for the use of linkers in the current study

In the current research study, peptides SB6 and SB10 were linked to each other using a KK linker. KK linkers have been used to join B cell epitopes in several studies (Ayyagari et al., 2020, Gu et al., 2017; Sarkar et al., 2020). By preventing the formation of antibodies for the peptide sequence that individual epitopes can form when they are linked linearly, KK linkers are essential in lowering junctional immunogenicity (Yano et al., 2005). Additionally, KK linkers boost immunogenicity (Li et al., 2015). Peptides B6 and B10 were connected to S1 through an AAY linker, while S1 was linked to S19 using a GPGPG linker. Subsequently, S19 was connected to S5 via an AAY linker, and S5 was linked to M1 using an AAY linker. Junctional epitopes may form if linkers are not used. These are new antigenic determinants that are created when two separate protein fragments, typically derived from different proteins, are linked together artificially. These epitopes arise at the junction where the two fragments are connected. AAY linkers enhance epitope presentation designed to minimize the formation of junctional epitopes by providing a stable and

predictable linkage between peptide fragments (Atapour et al., 2022). The AAY linker enhances epitope partitioning by attempting to make the C-terminus of CTLs more accessible for molecule-mediated binding, leading to increased epitope presentation (Hasan & Mia, 2022). In another study, GPGPG linkers used to connect the HTLs, boosted their immune response. These linkers, rich in glycine, not only improve solubility but also enhance activity, accessibility, and flexibility for neighboring domains (Tarrahimofrad et al. 2011).

CHAPTER 3: MATERIALS AND METHODS

3.1 Peptides used to develop the recombinant protein vaccine

The peptides $ST1_{258-279}$, $ST5_{1052-1073}$, $ST19_{339-371}$, MT1, $SB6_{553-568}$ and $SB10_{554-573}$ were identified though literature mining. Lim et al. (2021) comprehensively evaluated the data from 11 different publications that used bioinformatics to identify promising $CD4^+$ and $CD8^+$ T cell epitopes from the S protein of SARS-CoV-2. WTAGAAAYYVGYLQPRTFLLKY ($ST1_{258-279}$) was identified as a highly potent T cell epitope, capable of inducing both $CD4^+$ and $CD8^+$ T cell responses. It was associated with positive IFN-γ production, a high immunogenicity score of 97.729%, and a high global HLA population coverage of 99.63%. $ST5_{1052-1073}$ FPQSAPHGVVFLHVTYVPAQEK was identified as a highly potent T cell epitope, capable of inducing both $CD4^+$ and $CD8^+$ T cell responses. It was associated with positive IFN-γ production, a high immunogenicity score of 98.6%, and a high global HLA population coverage of 96.4% (Lim et al., 2021). Prioritizing the identification of epitopes from conserved regions of the SARS-CoV-2 as well as from regions associated with high viral infectivity, Yarmarkovich et al. (2020) demonstrated that viral epitope GEVFNATRFASVYAWNRKRISNCVADYSVLYNS (denoted $ST19_{339-371}$ in the current study) from the RBD of the S protein scored in the 90.9[th] percentile of T epitopes. It was also shown to be third of 1,546 epitopes scored in the S, E, and M genes for combined B and T cell epitopes, with high MHC class I coverage of 98.3%. Peptide ST19 was located between residues 325-357 of the S1 subunit of SARS-CoV-2, coinciding with part of the SARS-CoV-2 RBD.

Moreover, GEVFNATRFASVYAWNRKRISNCVADYSVLYNS was used as a peptide along with 45 other peptides which were mixed to form a multi-peptide cocktail to serve as a COVID-19 vaccine. Intramuscular administration of this COVID-19 peptide vaccine in addition

to a tetanus vaccine in horses was able to induce nAbs against the SARS-CoV-2 Delta variant (Deng & Sweeney, 2022). GLMWLSYFIASFRLFARTRSM (denoted MT1 in the current study) was identified as a $CD4^+$ T cell epitope through *in silico* predictions of potential T cell epitopes through retrieval of protein sequences from the NCBI database, analysis of average antigenic propensity and binding affinity of peptides for class II MHC, assessment of immunogenicity score and the ability to induce Th1 immune response together with IFN-γ production (Lim et al., 2021). Lastly, $SB6_{553-568}$ (TESNKKFLPFQQFGRDIA) and $SB10_{554-573}$ (ESNKKFLPFQQFGRDIADTT) were chosen as linear B cell epitopes. Amrun et al. (2020) found that patients in the ICU with severe COVID-19 had elevated IgG titers directed against the linear B cell epitope, TESNKKFLPFQQFGRDIA. Moreover, Heffron et al. (2021) utilized ultradense peptide microarray mapping to identify TESNKKFLPFQQFGRDIADTT as one of the epitopes associated with potent antibody responses as a result of SARS-CoV-2 infection. ESNKKFLPFQQFGRDIADTT was predicted as a dominant SARS-CoV B Cell Epitope as identified by the EpitopeVec software that utilizes residue properties, modified antigenicity scales, and protein language model-based representations for linear BCE predictions. Information on the sequences of the six selected peptides representing immunogenic B and T cell epitopes as well as their location on the location on SARS-CoV-2 viral genome is shown in **Table 3.1.**

Table 3.1. The sequences and location on genome of the six selected peptides representing immunogenic B and T cell epitopes

	Peptide	Peptide Sequence	Location on Genome	Type of Epitope
1.	ST1	WTAGAAAYYVGYLQPRTFLLKY	S	T Cell
2.	ST5	FPQSAPHGVVFLHVTYVPAQEK	S	T Cell
3.	MT1	GLMWLSYFIASFRLFARTRSM	M	T Cell
4.	ST19	GEVFNATRFASVYAWNRKRISNCVADYSVLYNS	S	T Cell
5.	SB6	TESNKKFLPFQQFGRDIA	S	B Cell
6.	SB10	ESNKKFLPFQQFGRDIADTT	S	B Cell

3.2 Analysis of conservancy of the 6 peptides against Omicron using the IEDB epitope conservancy analysis

Sequences of a total of 4260 SARS-CoV-2 Omicron strains were downloaded from the Global Initiative on Sharing All Influenza Data (GISAID) (https://gisaid.org/) in a FASTA format. The sequences were pasted onto a Google Colaboratory notebook along with a Python code developed by Dr Cheah Wai Ching from the Sunway University Department of Engineering to convert the nucleotide sequences to amino acid sequences. The 6 peptides were then checked to determine if they were conserved against 4,260 Omicron strains.

3.2 Construction of recombinant plasmid pET41a-GST-6PHis

Nucleotide sequences consisting of the gene of interest fused to Glutathione-S-transferase (GST) at the N terminal and to 8 histidine residues (8x His) at the C terminal were synthesized and cloned into the pET-41a (+) expression plasmid by a commercial company (GenScript, California, USA) to form the recombinant plasmid pET41a-GST-6PHis. The gene of interest consisted of nucleotide sequences encoding six peptides representing predicted immunogenic epitopes from the SARS-CoV-2 S, M, and N proteins. Peptides were joined together with AAY and GPGPG linkers (**Figure 3.1**). The expected size of the GST-6Phis recombinant protein of interest was determined to be approximately 46 kDa using the ExPASy ProtParam tool (https://web.expasy.org/protparam/)**.** The insert comprising the GST- tag linked to 6 peptides and 8 histidine residues was considered a singular transcriptional unit which was under the control of the T7 promoter. The expression of the gene insert would produce GST-6Phis with gene expression terminated at the T7 terminator. The plasmid also includes a lac operon. the lac repressor protein binds to the lac operator region of the lac operon, preventing transcription of the gene of interest. The lac operon can be induced by IPTG which will bind to the lac repressor to allow transcription.

Therefore, IPTG will be added for the expression of the gene insert. pET41a-GST-6PHis also contained nucleotides encoding kanamycin resistance genes to serve as a selection marker to enable the selection of recombinants resistant to kanamycin. The final size of the plasmid was 6181 base pairs (bp). The plasmid map for pET41a-GST-6PHis is shown in **Figure 3.2.**

The amino acid sequence of GST-6Phis expressed from the gene insert

MSPILGYWKIKGLVQPTRLLLEYLEEKYEEHLYERDEGDKWRNKKFELGLEFPNLPYYIDGDVKLTQ

SMAIIRYIADKHNMLGGCPKERAEISMLEGAVLDIRYGVSRIAYSKDFETLKVDFLSKLPEMLKMFED

RLCHKTYLNGDHVTHPDFMLYDALDVVLYMDPMCLDAFPKLVCFKKRIEAIPQIDKYLKSSKYIAWP

SB6   SB10

LQGWQATFGGGDHPPKSDGSTSLVPRGSTESNKKFLPFQQFGRDIAKKESNKKFLPFQQFGRDIADTT

ST1   ST19

AAYWTAGAAAYYVGYLQPRTFLLKYGPGPGGEVFNATRFASVYAWNRKRISNCVADYSVLYNSAAY

ST5   MT1

FPQSAPHGVVFLHVTYVPAQEKAAYGLMWLSYFIASFRLFARTRSMLVPRGSLEHHHHHHHH

The expected size of the protein expressed from the cloned gene insert = 45851.73 kDa ≈ 46 kDa

Figure 3.1. The amino acid sequence of GST-6Phis. The peptides SB6, SB10, ST1, ST19, ST5, and MT1 are labelled and underlined.

Linkers joining these peptides are shown in green. Nucleotides encoding this sequence was incorporated to form pET41a-GST-6PHis
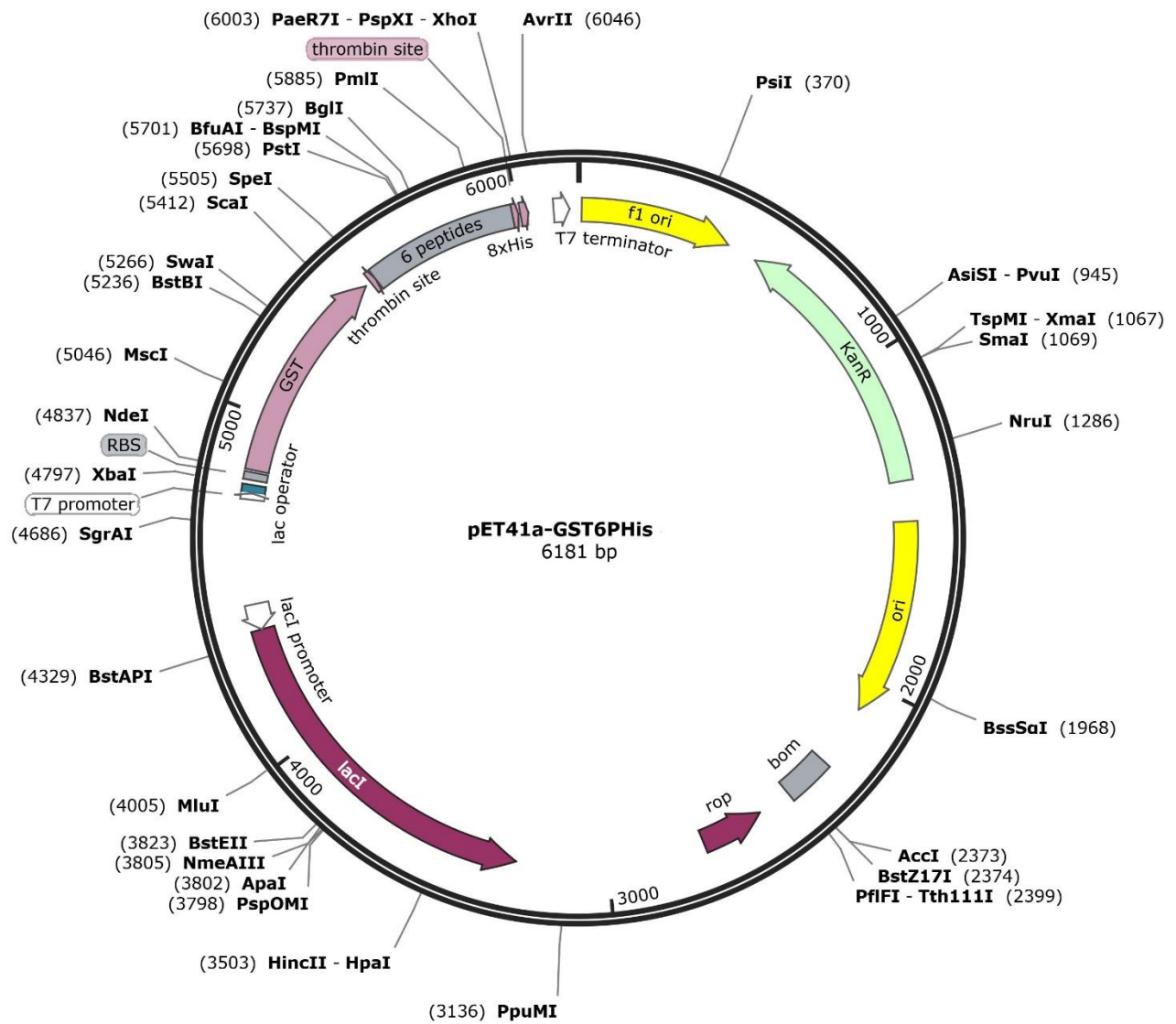
Figure 3.2. The plasmid map for pET41a-GST-6PHis generated using SnapGene Viewer

3.3 Preparation of competent *E. coli* BL21(DE3) cells

Competent *E. coli* BL21(DE3) cells were prepared using the calcium chloride method. An aliquot of 10 ml of Luria-Bertani (LB) broth was inoculated with a single colony of the desired *E. coli* strain and cultured overnight at 37°C with shaking at 200 revolutions per minute (rpm). An aliquot of 1 ml of the overnight culture was inoculated into 100 ml of sterile LB broth and cultured overnight at 37°C with shaking at 200 rpm. The culture was divided equally between two sterile 50 ml centrifuge tubes and centrifuged for 10 minutes at 7,000 rpm at 4°C (Eppendorf Centrifuge 5810/ 5810 R, Hamburg, Germany) and the supernatant was discarded. An aliquot of 20 ml of sterile, ice-cold 100 mM $CaCl_2$ was added to the cell pellets, followed by gentle resuspension. The resuspended cells were placed on ice for 15 minutes and centrifuged for 10 minutes at 7,000 rpm at 4°C after which the supernatant was discarded. An aliquot of 5 mL of sterile, ice-cold 100 mM $CaCl_2$ supplemented with 15% glycerol was added to each cell pellet, followed by gentle resuspension. The resuspended cells were divided into 100 µl aliquots in sterile, ice-cold Eppendorf tubes and stored at -80°C.

3.4 Transformation of competent *E. coli* cells

4 µg of lyophilized plasmid DNA in 1x TE buffer was added to thawed competent cells in a 1.5 ml centrifuge tube and kept on ice for 30 minutes. The tubes were subjected to heat shock at 42°C for 42 seconds. LB broth was added to each tube, followed by incubation at 37°C with shaking at 200 rpm for 60 minutes. Transformed *E. coli* cells were spread on LB + kanamycin selection plates (50 µg/ml) and incubated overnight at 37°C.

3.5 Plasmid extraction

A single colony of transformed *E. coli* was inoculated into 10 ml of LB broth supplemented with kanamycin (50 µg/ml) and incubated at 37°C with shaking at 200 rpm. Plasmid extraction

was performed using the QIAprep Spin Miniprep Kit (QIAGEN, Hilden, Germany). Following centrifugation, the pellet was mixed with Buffer P1 (resuspension buffer RNase), followed by the addition of Buffer P2 (lysis buffer). After incubation at room temperature, Neutralization Buffer N3 was added. The supernatant was collected and added to the spin column directly. PB buffer was added, followed by centrifugation to remove the ethanol residue. Elution of DNA was performed using the elution buffer. The concentration and purity of the extracted DNA was determined using the Thermo Fisher Scientific NanoDrop One (Thermo Fisher Scientific, Massachusetts, USA).

3.6 Confirming the pET41a-GST-6PHis plasmid sequencing

Characterization of pET41a-GST-6PHis was performed using restriction enzyme restriction, followed by agarose gel electrophoresis and nucleotide sequencing. In order to linearize the pET41a-GST-6PHis recombinant expression plasmid, restriction enzyme digestion was carried out with XhoI (New England Biolabs, Massachusetts, US). The agarose gel was prepared by mixing 1 g of agarose powder in 100 ml of 1xTAE buffer. The mixture was fully dissolved by heating in the microwave and then allowing the agarose to cool while occasionally swirling the mixture. SYBR green was added and then mixed properly before pouring the mixture onto the gel mould with the 8-well comb already in place. After solidification, the gel was placed in the gel tank and submerged in 1xTAE buffer. After loading molecular marker and different volumes of the DNA plasmid along with 5 µl of loading dye, the gel was run at 100 V for 60 minutes. Agarose gel electrophoresis was carried out in a 1% agarose gel at 100 mV for 60 minutes. The Invitrogen 1Kb Plus Ladder (Invitrogen, Massachusetts, USA) was used as the molecular marker for reference to indicate the size of the visualized DNA bands. The gel was visualized using G:BOX F3LFB gel

doc (Syngene, Maryland, USA). Nucleotide sequence analysis of the gene insert was conducted by a commercial company (GenScript, California, USA).

3.8 Expression of GST-6PHis from transformed *E. coli* cells and production of crude extract

A single colony of *E. coli* BL21(DE3) transformed with pET41a-GST-6PHis was inoculated into 10 ml of LB broth supplemented with 50 µg/ml kanamycin solution and incubated in a shaking incubator set at 37°C for 16 hours at 220 rpm. An aliquot of 2 ml of the overnight culture was added into 200 ml of LB broth and incubated in a shaking incubator set at 37°C and 220 rpm until the OD_{600} reached 0.4 – 0.6. IPTG induction was performed by adding 1 M IPTG solution made by dissolving 0.238 g of IPTG in 1 ml of water (Research Products International, Illinois, US) to the culture with incubation in a shaking incubator set at 37°C for 16 hours at 220 rpm. The culture was subjected to centrifugation at 10,000 rpm for 15 minutes at 4°C, followed by 6 cycles of sonication using the UP100H ultrasonic processor (Hielscher Ultrasonics, Berlin, Germany) set at 100% amplitude and a cycle of 1, followed by cooling on ice for 1 minute after each cycle. The cell debris was separated from the intracellularly expressed protein contained in the supernatant by centrifugation at 10,000 rpm for 15 minutes at 4°C.

3.7 Detection of histidine-tagged protein of interest using SDS-PAGE Coomassie and Western blot

Protein samples were mixed with the 6X loading buffer (Morganville Scientific, New Jersey, United States) in a ratio of 2:1, followed by boiling at 95°C for 15 minutes, and loading of denatured samples onto a 12% SDS-PAGE polyacrylamide gel. The resolving gel was prepared by adding 1.642 ml of water to 1.25 ml of Tris-HCl pH 8.8 resolving gel buffer (Bio-Rad, California, United States), followed by the addition of 2 ml of acrylamide (Bio-Rad, California, United States), 50 µl of 10% SDS solution (Bio-Rad, California, United States), 25 µl of 10% APS

solution (Bio-Rad, California, United States), and 5 µl of TEMED (Bio-Rad, California, United States). The stacking gel was made by adding 2.5 ml of water to 1.26 ml of Tris-HCl pH 6.8 stacking gel buffer (Bio-Rad, California, United States), followed by the addition of 660 µl of acrylamide (Bio-Rad, California, United States), 50 µl of 10% SDS solution (Bio-Rad, California, United States), 50 µl of 10% APS solution (Bio-Rad, California, United States), and 8 µl of TEMED (Bio-Rad, California, United States). Electrophoresis was carried out at 100 V for 120 minutes, followed by visualization of protein bands using Coomassie blue stain (Bio-Rad, California, US). Western blot was conducted and the separated proteins were transferred from the polyacrylamide gel onto a polyvinylidene difluoride (PVDF) membrane using the semi-dry method. The membrane was then blocked with 10% skim milk (distilled autoclaved water used as diluent) for 12 hours at 4°C to prevent nonspecific binding of antibodies, followed by adequate washing with 1X TBST. Overnight primary antibody incubation was carried out with Anti-His-Tag Antibody (Santa Cruz Biotechnology, Inc, Dallas, USA), The membrane was washed in 1X TBST. Secondary antibody incubation was performed with goat anti-mouse HRP conjugated secondary antibody (1:1000) for 45 minutes at room temperature (Invitrogen, Massachusetts, US). The blot was visualized using the G:BOX F3LFB gel doc (Syngene, Maryland, USA).

3.9 Ammonium sulfate precipitation

The crude extract was subjected to ammonium sulfate precipitation using the following concentrations: 0-20% (1.10 g of ammonium sulfate added to 10 ml of crude lysate containing 0% ammonium sulfate to get 20% saturated solution, final volume: 10.58 ml), 20-30% (0.60 g of ammonium sulfate added to 10.58 ml of solution containing 20% ammonium sulfate to get 30% saturated solution, final volume: 10.90 ml), 30-40% (0.64 g of ammonium sulfate added to 10.90 ml of solution containing 30% ammonium sulfate to get 40% saturated solution, final volume:

11.24 ml), 40-50% (0.68 g of ammonium sulfate added to 11.24 ml of solution containing 40% ammonium sulfate to get 50% saturated solution, final volume: 11.60 ml), 50-60% (0.72 g of ammonium sulfate added to 11.60 ml of solution containing 50% ammonium sulfate to get 60% saturated solution, final volume: 11.98 ml), 60-70% (0.77 g of ammonium sulfate added to 11.98 ml of solution containing 60% ammonium sulfate to get 70% saturated solution, final volume: 12.39 ml), and 70-80% (0.83g of ammonium sulfate added to 12.39 ml of solution containing 70% ammonium sulfate to get 80% saturated solution, final volume: 12.83 ml). Specified amounts of ammonium sulfate (Chemiz, Shah Alam, Malaysia) were added to the crude extract successively as described. For each ammonium sulfate concentration, the ammonium sulfate was gradually added to the crude extract with continuous stirring at 4°C. After determining the optimum ammonium sulfate concentration, the sample was centrifuged at 10,000 rpm for 15 minutes at 4°C. The pellet was dissolved in 100 µl of PBS. The supernatant was used for successive precipitations at higher ammonium sulfate concentrations. The total protein as well as the proportion of recombinant protein precipitated at each ammonium sulfate concentration were evaluated using SDS-PAGE Coomassie and Western blot.

3.10 Gel filtration chromatography

Gel filtration chromatography was used for desalting the ammonium sulfate present in the protein sample and for further fractionating the total proteins based on size exclusion to produce fractions containing GST-6Phis. A total of 5 g of the gel filtration resin, Sephadex G-75 (Sigma-Aldrich, Missouri, USA) was soaked in 500 ml of PBS overnight to swell the resin and added to an Econo-Column® (Bio-Rad, California, US). The ammonium sulfate fractionated sample was allowed to flow through and a total of 30 fractions containing 1 ml of the sample mixture were collected until 30 ml of the sample had been eluted. The concentration (mg/ml) and absorbance at

280 nm were determined for each fraction using the Thermo Fisher Scientific NanoDrop One (Thermo Fisher Scientific, Massachusetts, USA). A standard curve was constructed by plotting the absorbance at 280 nm against the elution volume using GraphPad Prism 7. SDS-PAGE Coomassie and Western blot were performed to identify specific fractions containing GST-6Phis. These fractions were then pooled together for further purification using IMAC.

3.11 IMAC

IMAC was performed using the PROTEINDEX™ HiBond™ Ni-NTA resin (Marvelgent Biosciences, Massachusetts, MA) at room temperature. The column was cleaned with 10 column volumes (CVs) of distilled water and equilibrated with 10 CVs of PBS. The pooled sample mixture was allowed to bind to the column for 30 minutes with regular gentle pipetting and then flow through the column. The sample was added to the column and placed on a shaker for 10 minutes in order to allow it to bind to the resin effectively. The flowthrough was poured back into the column followed by gentle shaking for 5 minutes. This last step was repeated a second time as well. The column was washed with Imidazole concentrations 10 mM (50 µl of 3M imidazole stock solution and 14.95 ml of PBS), 50 mM (250 µl of 3M imidazole stock solution and 14.75 ml of PBS), 100 mM (500 µl of 3M imidazole stock solution and 14.5 ml of PBS), 150 mM (750 µl of 3M imidazole stock solution and 14.25 ml of PBS), 200 mM (1000 µl of 3M imidazole stock solution and 14 ml of PBS), 250 mM (1.25 ml of 3M imidazole stock solution and 13.75 ml of PBS), and 500 mM (2.5 ml of 3M imidazole stock solution and 12.5 ml of PBS). This was done in order to wash out contaminating proteins with lower imidazole concentrations and elute GST-6Phis using higher imidazole concentrations. The crude extract, flow-through, and eluates samples were subjected to SDS-PAGE Coomassie and Western blot to detect the presence and abundance of GST-6Phis in these samples through visual inspection of bands.

3.12 Ethics statement

All animal procedures were carried out in accordance with the guidelines approved by the Animal Institutional Animal Care and Use Committee (2022-230512/SUNWAY/R/KK) of University Malaya (UM) and Sunway Research Ethics Committee (Ethics Approval No.: PGSUREC2021/043). All mice were housed in a temperature-controlled biosafety level 2 (BSL-2) animal facility at the Animal Experimentation Unit at UM.

3.13 Mice immunizations

Female BALB/c mice (6-weeks old) used in the research study were purchased from UM and immunizations were carried out at the UM animal facility. Mice were immunized intramuscularly or intranasally with 10 µg of GST-6Phis. Intramuscular immunizations were carried out by injecting 50 µl of GST-6Phis into the thigh muscle using a 26 ½ gauge needle. Intranasal immunizations were carried out by administering 10 ul to the nostril using a 10 µl micropipette. For both intramuscular and intranasal administrations, a 3-dose regimen was followed with mice being immunized at days 0, day 14, and day 28. No adjuvant was used. Mice were divided into 4 groups (n=5). Group 1 consisted of the intramuscular administration of GST-6Phis. Group 2 consisted of the intranasal administration of GST-6Phis. Group 3 and Group 4 involved the intramuscular and intranasal administration of PBS, respectively. Mouse health was monitored at day 0, day 14, day 28, and day 42 in terms of a visual inspection of mouse fur and movement. At day 42 post immunization, mice were anaesthetized by exposure to 4% isoflurane in a 1 L container for 5 minutes. A total of 1 ml of blood was collected using a 26 ½ gauge needle via cardiac puncture after mice had been anaesthetized. Cervical dislocation was performed to euthanize the mice after which spleens were removed. A graphical illustration of the immunization schedule is shown in **Figure 3.3.**
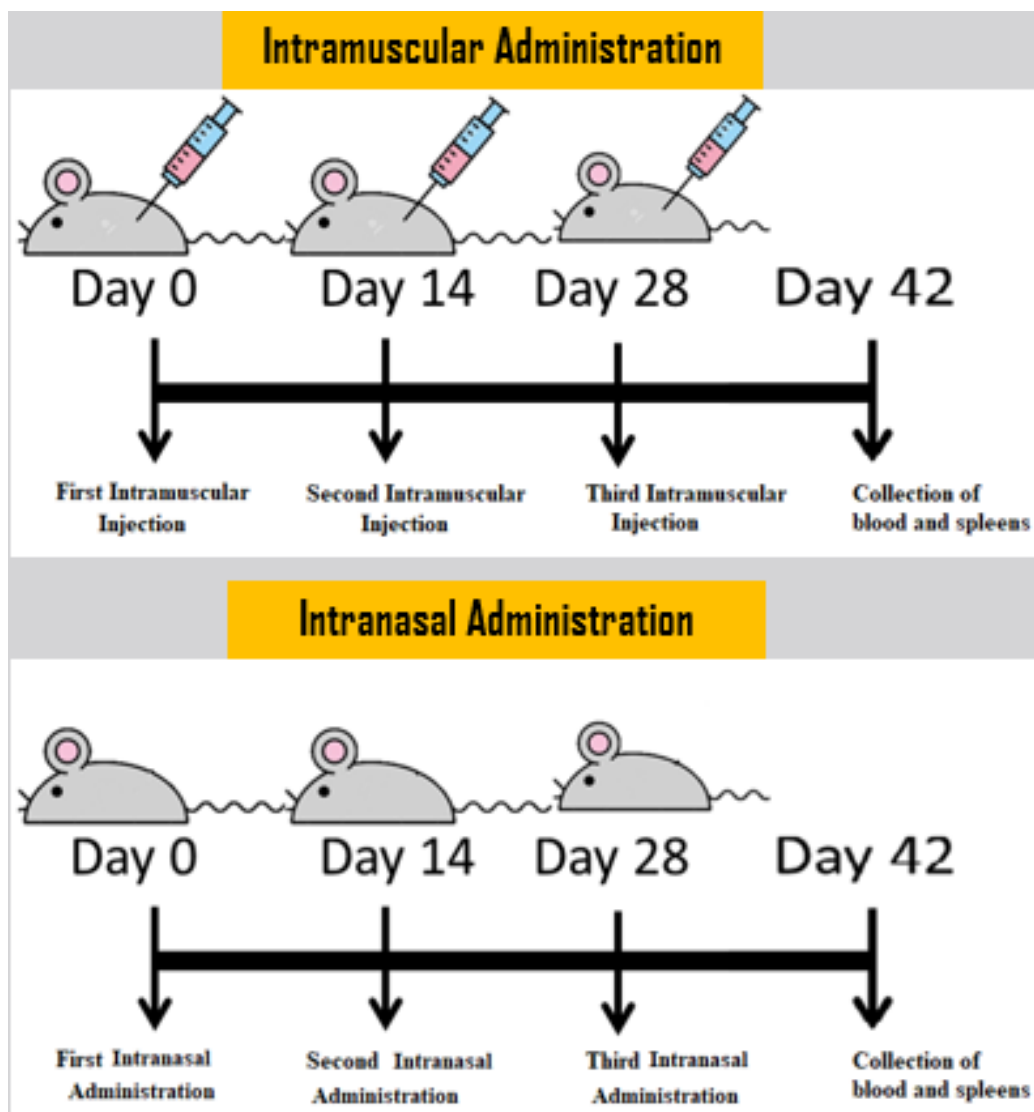
Figure 3.3. The 3-dose immunization schedule used for the intramuscular and intranasal immunizations of BALB/c mice

3.14 Evaluation of humoral responses in terms of total IgG and neutralizing antibodies

3.14.1 Detection of IgG antibodies through the ELISA

Blood samples collected from mice were centrifuged at 6,000 rpm for 15 minutes to obtain sera. A 96-well flat-bottom plate (Fisher Scientific, Pittsburgh, USA) was coated with 10 µg of GST-6Phis diluted in coating buffer made by dissolving 5.3 g of Na_2CO_3 in 900 ml distilled water,

followed by addition of 4.2 g of $NaHCO_3$ and 1 g sodium azide. The pH was adjusted to 9.6 and the volume to 1 L with additional distilled water. The plate was incubated overnight at 4°C. The contents of the wells were discarded and the plate was washed with 0.05% (v/v) Tween 20 in PBS wash [0.05% (v/v) Tween 20 in PBS]. Blocking buffer (0.5% BSA in PBS) was added, followed by incubation at 37 °C for 2 hours. Sera from immunized mice were diluted 1:50, 1:250 and 1:1000 using sample dilution buffer (20% blocking buffer in PBS) and incubated for 2 hours at 37°C. The background control consisted of wells without sera. Wells were washed with 200 µl of PBS Tween 20. Then, 100 µl of horseradish peroxidase (HRP)-conjugated goat anti-mouse IgG antibody (1:1000 dilution with sample dilution buffer) (Invitrogen, Carlsbad, CA, USA) was added and incubated at 37°C for 1 hour. Aliquots of 100 µl of 3,3'5,5'-Tetramethylbenzidine (TMB) substrate solution (SeraCare Life Sciences Inc., Milford, MA, USA) were added to each well and allowed to incubate at room temperature for 30 seconds until a blue color was observed. Lastly, 100 µl of 1M sulphuric acid (H_2SO_4) was added to the wells to stop the reaction. Absorbance was read using a Tecan Infinite M200 Pro microtiter plate reader (Tecan, Zürich, Switzerland) at 450 nm.

3.14.2 Neutralizing antibody detection using the GenScript cPass™ SARS-CoV-2 Neutralization Antibody Detection kit

The determination of the levels of neutralizing antibodies to the SARSCoV-2 Wuhan and Omicron strains in the sera of immunized mice that could inhibit the interaction between the HRP-conjugated RBD (RBDHRP) and the ACE2 receptor was performed using the FDA approved "cPASS SARS-CoV-2 Surrogate Virus Neutralization Test RUO Kit" (Cat. #L00847-A, GenScript, California, USA) (Tan et al., 2020). The kit contained the Wuhan (Accession #: NC-045512) HRPRBD antibody was prepared by diluting the stock solution in a 1:1000 ratio with the RBD dilution buffer. The capture plate consisted of microplates pre-coated with ACE2 protein. Positive and negative controls were provided as part of the kit. The A 1x wash solution consisting of Tris-buffered saline with Tween 20 at pH 8.0 was prepared by diluting it with deionised water in a 1:20 ratio. Sera from mice immunized intramuscularly and intranasally with PBS or GST-6Phis were mixed in a 1:1 ratio with the diluted RBDHRP and added to wells, followed by incubation at 37 °C for 15 minutes. Wells were washed with the wash solution and 100 µl of TMB solution. The plate was incubated in the dark for 15 minutes at room temperature, followed by the addition of 50 µl of stop solution until a yellow color was observed. The capture plate was read in a Tecan Infinite M200 Pro microtiter plate reader (Tecan, Zürich, Switzerland) at 450 nm. The experiment was repeated for the four mice groups to test neutralizing activity against the Omicron RBD. This was achieved through the use of the Omicron (Accession #: P0DTC2) HRPRBD antibody which was ordered separately (GenScript, California, USA). The determined absorbance values were used to determine the signal inhibition for the detection of nAbs calculated from the formula:

$$\% \text{ Signal Inhibition} = (1 - \frac{\text{OD value of Sample}}{\text{OD value of Negative Control}}) \times 100$$

The cutoff value for the cPass SARS-CoV-2 Neutralizing Antibody Detection Kit is 30% signal inhibition. Therefore, a signal inhibition $\geq$ 30% coincided with the positive detection of nAbs to SARSCoV-2 a signal inhibition $\leq$ 30% meant that nAbs to SARSCoV-2 were not detected in a particular serum sample.

3.15 Evaluation of cellular responses

3.15.1 Processing of murine splenocytes from immunized mice

The splenocytes used in this study were obtained from individual spleens. A total of four experimental groups were included: intramuscular GST-6Phis, intranasal GST-6Phis, intramuscular PBS, and intranasal PBS. Each group consisted of five mice, and five spleens were harvested, processed individually, and subjected to flow cytometry analysis from each mouse. Spleens removed from immunized mice were stored in incomplete RPMI 1640 media (Sigma-Aldrich, Missouri, USA) and processed for splenocyte isolation. Spleens were placed into 100 μm pore size cell strainer (BD Biosciences, New Jersey, USA), crushed with a 5 ml syringe plunger (Terumo Inc., Tokyo, Japan), washed with incomplete RPMI 1640 media, and collected into 50 ml Falcon tubes, followed by centrifugation at 3,000 rpm for 3 minutes. The supernatants were discarded and the tubes were tapped to dislodge the pellet. ACK lysing buffer (150 mM NH_4Cl, 0.1 mM $NaHCO_3$, and 10 mM EDTA) was added to the pellet to lyse the red blood cells. The RBC lysis reaction was stopped through the addition of complete RPMI 1640 media containing 10% heat-inactivated FBS, 1% Penicillin-Streptomycin, 50 μM 2-Mercaptoethanol, and 10 mMol HEPES, followed by centrifugation at 3,000 rpm for 3 minutes. The supernatants were discarded, the pelleted cells were resuspended in complete RPMI media, and subjected to a cell count using the hemocytometer. Splenocytes were seeded at 4.0 x 10^6 cells/well for flow cytometry analysis

to determine the percentage of IFN-γ producing CD3$^+$ CD4$^+$ and CD3$^+$ CD8$^+$ T cells. No cell sorting was performed prior to analysis.

3.15.2 Intracellular cytokine staining (ICS) by flow cytometry analysis

Splenocytes from the 4 groups were seeded into a 24-well plate. Each well was treated with 10 µg of GST-6Phis. A separate 24-well plate used for the positive (CD3/CD28) and negative (media only) controls and for the calibration controls (IFN, CD3, CD8, CD4). Cytokine production was induced through the addition of 50 ng/ml PMA (phorbol 12-myristate 13-acetate), 1 µg/ml ionomycin (calcium ionophore), and 1 µg/ml GolgiStop (BD Biosciences, New Jersey, USA), for five hours at 37°C. The contents of the wells were transferred to 1.5 ml microcentrifuge tubes and centrifuged at 250 rpm for 5 minutes at 4°C. The supernatants were discarded and the pellets were resuspended in 50 µl of BD Horizon™ Fixable Viability Stain 780 (FVS-780) (BD Biosciences, New Jersey, USA), followed by incubation in the dark for 30 minutes at room temperature. Stain buffer (0.1% Tween-20 in PBS) was added to the tubes to wash off extra dye, followed by centrifugation at 3,000 rpm for 3 minutes at 4°C. The supernatants were discarded and the pellets were resuspended in 100 µl of surface stain master mix containing CD3, CD4, and CD8 antibody. This was followed by incubation in the dark for 30 minutes at 4°C after which 300 µl of stain buffer was added to neutralize the surface stains. Centrifugation was at 3,000 rpm for 3 minutes at 4°C. The supernatants were discarded and the pellets were resuspended in Cytofix buffer (BD Biosciences, New Jersey, USA), followed by incubation for 30 minutes at 4°C. Cytoperm buffer was then added, followed by centrifugation at 3,000 rpm for 3 minutes at 4°C. The supernatants were discarded and the pellets were resuspended in the intracellular stain, anti-IFN- γ- PerCP-Cy5.5 conjugated antibody stain, followed by incubation in the dark for 60 minutes at 4°C. Stain buffer was introduced to counteract the intracellular stain, prevent excessive staining, and

eliminate any anti-IFN-γ-PerCP-Cy5.5 conjugated unbound antibodies. This was followed by centrifugation at 3,000 rpm for 3 minutes. Supernatants were discarded and stain buffer was added to resuspend the cells before they were transferred to FACS tubes and subjected to analysis with the BD FACSCelesta™ Flow Cytometer (BD Biosciences, New Jersey, USA). In the flow cytometry analysis, a four-step gating strategy was employed to identify $CD4^+$ and $CD8^+$T cells producing IFN-γ. Firstly, live lymphocytes were distinguished based on the addition of FVS-780 and the surface stain master mix containing CD3, CD4, and CD8 antibodies. Subsequently, singlet cells were gated using forward scatter (FSC) vs. side scatter (SSC) plots. Live $CD3^+$ T cells were then identified through the use of the surface stain master mix containing CD3 antibody. Finally, $CD3^+$ $CD4^+$ and $CD3^+$ $CD8^+$ T cells were gated based on the addition of the surface stain master mix containing CD4 and CD8 antibody, respectively. Following gating, intracellular staining with anti-IFN-γ-PerCP-Cy5.5 conjugated antibody allowed detection of IFN-γ production specifically by the $CD4^+$ and $CD8^+$ T cell subset.

3.16 Statistical analysis

Statistical analysis was performed using GraphPad Prism 8.02 software (Graph Pad Software Inc., San Diego, CA, USA). Comparisons were conducted between the intramuscular GST-6Phis and intramuscular PBS groups, as well as intranasal GST-6Phis and intranasal PBS groups. In addition, comparisons between intramuscular GST-6Phis and intranasal GST-6Phis groups were also conducted to assess differences in the immune response induced by the two immunization routes. Statistical analyses were performed using T-tests to evaluate differences between the groups.

CHAPTER 4: RESULTS

This research study builds on research conducted by Dr Lim Hui Xuan and Masters candidate Aziz Yahaya. Bioinformatics analysis by Lim et al. (2021) showed that ST1, ST5, and MT1 were both CD4+ and CD8+T cell epitopes with high global HLA population coverage and conservancy (**Appendix Figure Table S1**). Moreover, Aziz Yahaya performed validation of individual peptides in terms of IFN-γ production and neutralizing activity (**Appendix Figure S1 & S2**).

4.1 Epitope conservancy analysis against Omicron

The sequence of the 6 peptides was cross-checked with the FASTA sequences of 4,260 SARS-CoV-2 Omicron strains using the IEDB Epitope Conservancy Analysis tool. The epitope sequences of five of the six peptides from the SARS-CoV-2 Wuhan strain were highly conserved when compared with sequences of SARS-CoV-2 Omicron strains. Peptides ST1, ST5, MT1, SB6, and SB10 showed high sequence similarities of 99.30% (4,230/4,260), 99.91% (4,256/4,260), 100% (4,260/4,260), 99.79% (4,251/4,260), 99.58% (4,242/4,260) against Omicron strains, respectively. However, peptide ST19 was not conserved against the SARS-CoV-2 Omicron strains since it showed a sequence similarity of only 1.92% (82/4,260) against the SARS-CoV-2 Omicron strains (**Table 4.1**).

Table 4.1. The epitope conservancy analysis against Omicron of the six peptides that were incorporated in pET41a-GST-6PHis

	Peptide	Peptide Sequence	Antigenic Region	Percent of protein sequence matches at identity < = 100%
1.	SB6	TESNKKFLPFQQFGRDIA	S	99.79 (4,251/4,260)
2.	SB10	ESNKKFLPFQQFGRDIADTT	S	99.58 (4,242/4,260)
3.	ST1	WTAGAAAYYVGYLQPRTFLLKY	S	99.30 (4,230/4,260)
4.	ST19	GEVFNATRFASVYAWNRKRISNCVADYSVLYNS	S	1.92 (82/4,260)
5.	ST5	FPQSAPHGVVFLHVTYVPAQEK	S	99.91 (4,256/4,260)
6.	MT1	GLMWLSYFIASFRLFARTRSM	M	100 (4,260/4,260)

4.2 XhoI digestion of pET41a-GST-6PHis and analysis by agarose gel electrophoresis

The recombinant expression plasmid pET41a-GST-6PHis has a single restriction site for XhoI at position 6003 bp. Characterization of pET41a-GST-6PHis was conducted through the digestion of different concentrations of the plasmid using the restriction enzyme XhoI, followed by agarose gel electrophoresis to visualize the size of the linearized plasmid. **Appendix Figure S4** shows the result of the agarose gel electrophoresis with lane 1: 1 kb DNA ladder, lane 2: 1.12 ng/ul, lane 3: 2.24 ng/ul, lane 4: 3.36 ng/ul, lane 5: 4.48 ng/ul, lane 6: 5.60 ng/ul, and lane 7: 8.4 ng/ul of digested pET41a-GST-6PHis. All lanes showed bands adjacent to approximately 6.1 kbp representing the linearized pET41a-GST-6PHis with the thickness of the bands increasing in each successive lane due to increasing concentration of the plasmid. The result showed that the recombinant plasmid was of the right size in accordance with the size of the plasmid of 6181 bp. The recombinant plasmid was further characterized by DNA sequencing.

4.3 Nucleotide sequencing of the gene insert incorporated into pET-41a (+)

Nucleotide sequencing of the gene insert was performed to verify the fidelity of the commercially synthesized product. Nucleotides encoding the GST protein were shown in red while nucleotides encoding the six linked peptides and 8 histidine residues were shown in green and blue, respectively. The sequencing result of the gene insert demonstrated a 100% similarity with the expected sequence that was provided to the commercial company for cloning (GenScript, California, USA) (**Appendix Figure S5**).

4.4 Confirmation of the GST-6Phis in the crude lysate

Following sonication and centrifugation, the supernatant referred to as the crude lysate was subjected to analysis using SDS-PAGE Coomassie in order to confirm the expression of GST-6Phis. Visual inspection of the separated proteins on the SDS-PAGE Coomassie gel following staining with Coomassie Brilliant Blue showed a prominent band relative to the expected band size representing GST-6Phis at 46 kDa among multiple contaminating proteins (**Figure 4.1 A, Lane 1**). Moreover, Western blotting was performed to confirm the presence of GST-6Phis at 46 kDa **(Figure 4.1 B, Lane 1).**
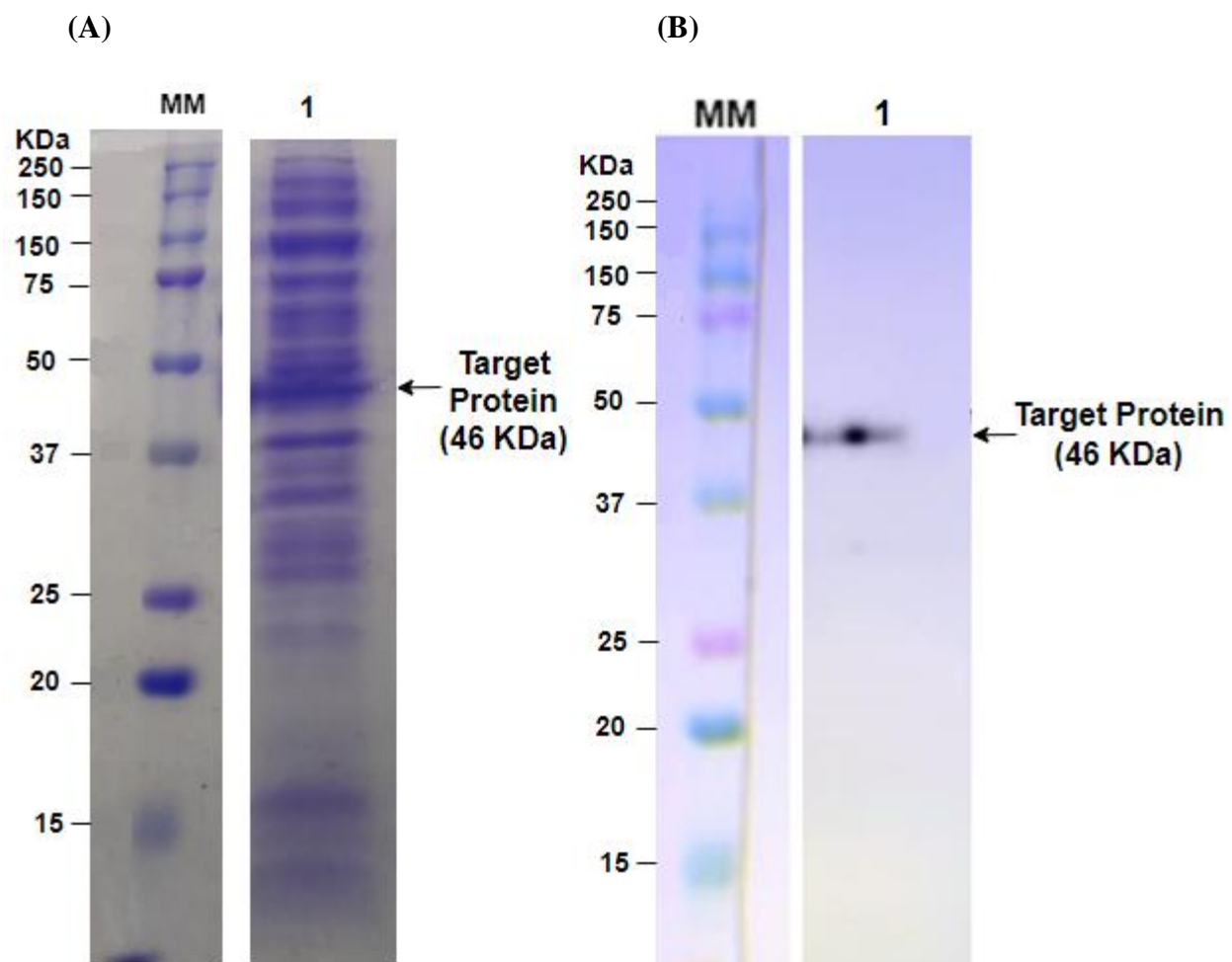
Figure 4.1. (A) SDS-PAGE Coomassie and **(B)** Western blotting the crude lysate obtained from the induction of *E. coli* cells transformed with pET41a-GST-6PHis (lane 1). Western blot was carried out using anti-His-tag antibody and detected with goat anti-mouse HRP conjugated secondary antibody. The Prestained Kaleidoscope ladder was used as the molecular marker (Lane MM).

4.5 Optimization of IPTG concentration and induction time

SDS-PAGE Coomassie and Western blot analysis were performed in order to visualize and investigate the impact of using different IPTG concentrations and induction times on the protein abundance of GST-6Phis to determine the optimum conditions for high production of GST-6Phis. IPTG concentrations of 0.2 M, 0.4 M, 0.6 M, 0.8 M, and 1 M were investigated along with induction times of 8 and 16 hours at an induction temperature of 25°C. In addition to multiple contaminating protein bands, the SDS-PAGE Coomassie profile showed a distinct band at 46 kDa which corresponded to GST-6Phis (**Figure 4.2. A)**. Western blot analysis showed that 8 hours of IPTG induction with 0.2 M IPTG resulted in a faint band at 46 kDa (**Figure 4.2. B, Lane 1**). The 46 kDa band increased in relative thickness when IPTG concentration was increased progressively from 0.2 M to 0.8 M while maintaining the induction time at 8 hours (**Figure 4.2. B, Lane 1-3**). The thickness of the 46 kDa band increased substantially when an IPTG concentration of 1 M was used with an induction time of 8 hours (**Figure 4.2. B, Lane 4**). A slight increase in relative thickness of the 46 kDa band was observed when induction was carried out with 1 M IPTG and an induction time of 16 hours (**Figure 4.2. B, Lane 5**). Therefore, it was concluded that an IPTG concentration of 1M and an induction time of 16 hours were optimum relative to the other tested conditions for the production of GST-6Phis.A
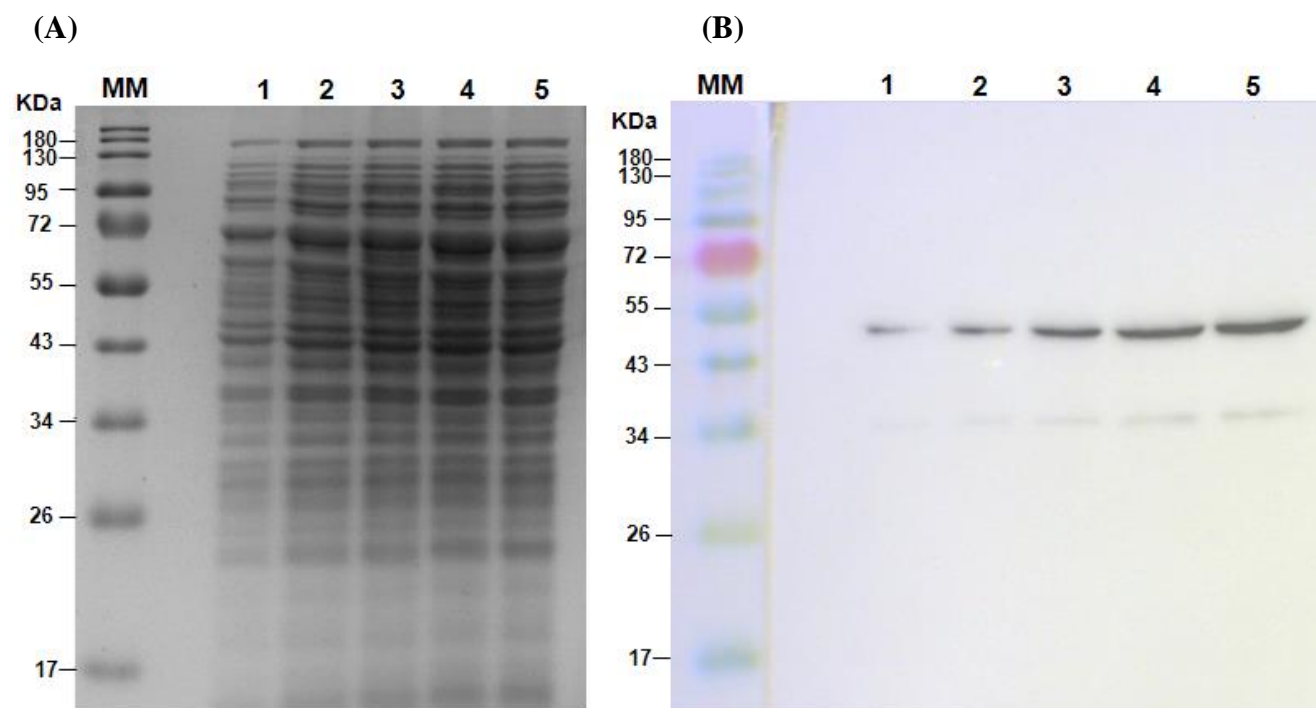
Figure 4.2. (A) SDS-PAGE Coomassie and **(B)** Western blotting for the crude lysate from *E. coli* transformed with pET41a-GST-6PHis induced with 0.2 M IPTG for 8 hours (lane 1), 0.4 M IPTG for 8 hours (lane 2), 0.8 M IPTG for 8 hours (lane 3), 1 M IPTG for 8 hours (lane 4), and 1 M IPTG for 16 hours (Lane 5). The Prestained Kaleidoscope ladder was used as the molecular marker (lane MM).

4.6 IM IPTG induction at 25°C and 30°C, followed by IMAC with a nickel-nitrilotriacetic acid (Ni-NTA) histidine affinity column

IMAC with a Ni-NTA histidine affinity column was used to purify GST-6Phis from a mixture of contaminating proteins. Purification was performed using crude lysate samples obtained from *E. coli* cells induced with 1M IPTG at induction temperatures of 25°C and 30°C. Visual inspection of the SDS-PAGE Coomassie analysis showed prominent bands at 46 kDa in the original crude lysate sample (**Figure 4.3. A, Lanes 1-8**). The flowthrough sample showed a fainter 46 kDa band at an induction temperature of 25°C (**Lane 2, Figure 4.3. B, Lane 2**) when compared to a thicker 46 kDa band at an induction temperature of 30°C (**Figure 4.3. B, Lane 6**). This indicated a higher binding affinity of GST-6Phis for the Ni-NTA resin at an induction temperature of 25°C when compared to 30°C. The wash sample showed a minimal amount of GST-6Phis (**Figure 4.3. B, Lane 3 & Lane 7**). IPTG induction at 25°C showed a more abundant amount of the eluted GST-6Phis (**Figure 4.3. B, Lane 4**) as compared to a much fainter 46 kDa band when an induction temperature of 30 °C was used (**Figure 4.3. B, Lane 8**). In conclusion, an IPTG induction temperature of 25°C was more favorable in terms of producing a greater abundance of the eluted GST-6Phis than when an induction temperature of 30°C was used.
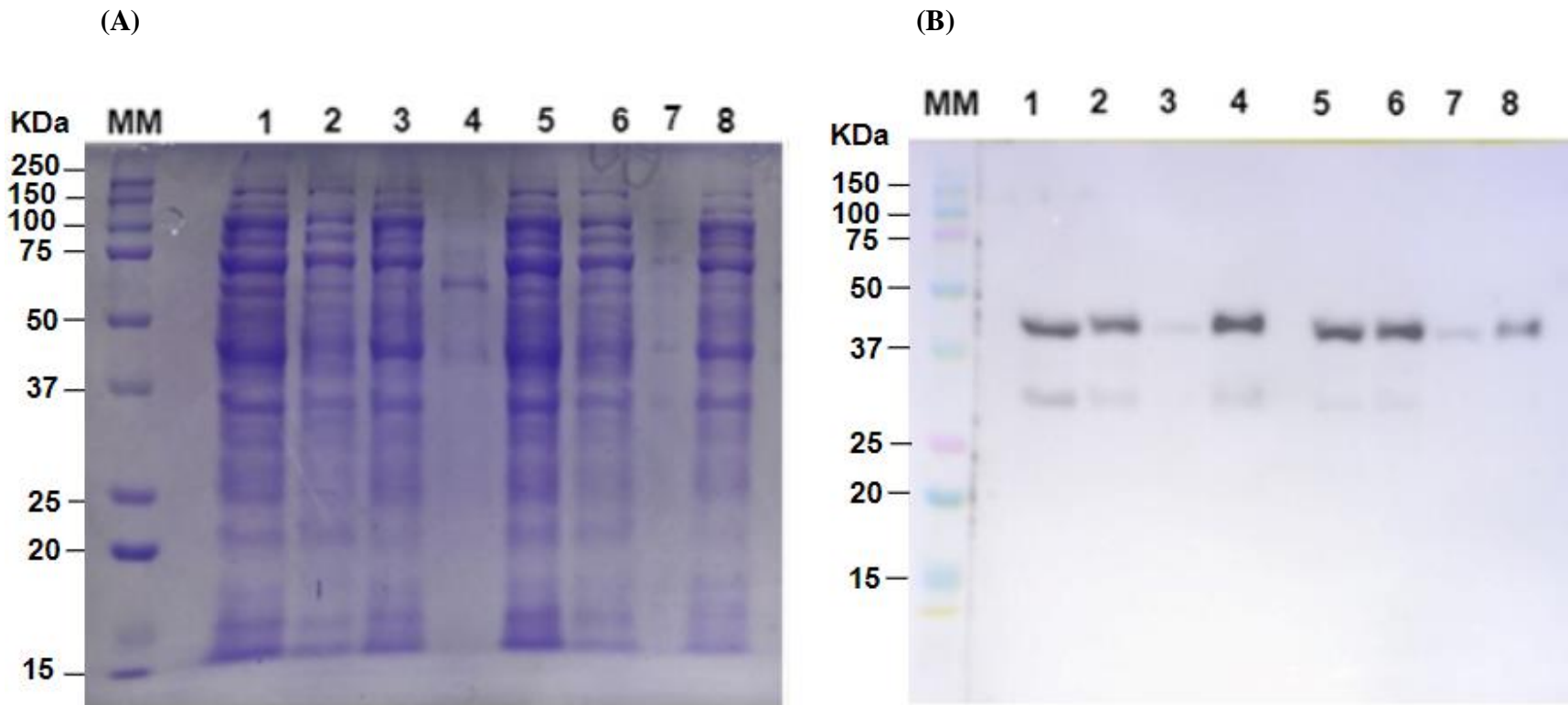
Figure 4.3. (A) SDS-PAGE Coomassie and **(B)** Western blotting of IMAC performed on crude lysate (lane 1) from *E. coli* cells induced with 1M IPTG at 25°C to produce flowthrough (lane 2), wash (lane 3), and eluate (lane 4). Another IMAC experiment was performed on crude lysate (lane 5) from *E. coli* induced with 1M IPTG at 30°C to produce the flowthrough (lane 6), wash (lane 7), and eluate (lane 8). The Prestained Kaleidoscope ladder was used as the molecular marker (lane MM).

4.7 Initial purification of GST-6Phis

Optimization was carried out to determine the best purification steps to purify GST-6PHis from bacterial crude extract. The desired purification target was 10 µg recombinant protein per 200 ml bacterial culture.

4.7.1 IMAC

IMAC with a Ni-NTA histidine affinity column was used to purify GST-6Phis from contaminating proteins expressed from *E. coli* cells transformed with pET41a-GST-6PHis and induced with 1M IPTG at an induction temperature of 25°C for 16 hours. Samples of crude extract, flowthrough, and eluates at various imidazole concentrations were analyzed. The experiment was performed using a range of imidazole concentrations from 10 mM to 500 mM in order to elucidate the imidazole concentration required for the elution of GST-6Phis free from contaminating proteins. SDS-PAGE Coomassie analysis showed that the crude lysate contained multiple contaminating proteins **(Figure 4.4. A, Lane 1)**. There was a prominent band at 46 kDa representing GST-6Phis in this fraction. The flowthrough contained significantly lower amounts of contaminating proteins as represented by much fainter bands **(Figure 4.4. A, Lane 2)**. The band at 46 kDa representing GST-6Phis significantly decreased in thickness in the flowthrough **(Figure 4.4. B, Lane 2)**. This decrease in thickness of the band at 46 kDa demonstrated that proteins in the crude lysate including GST-6Phis had bound to the Ni-NTA resin. Washing with 10 mM and 50 mM imidazole was able to elute contaminating proteins **(Figure 4.4. A, Lane 3-4)**. These fractions contained minimal amounts of GST-6Phis demonstrating that 10 mM and 50 mM imidazole were not sufficient to effectively elute GST-6Phis but were useful in removing contaminating proteins. 100 mM to 150 mM imidazole eluates showed contaminating proteins larger than 50 kDa **(Figure 4.4. A, Lane 5-6)**. These fractions also contained abundant amounts of GST-6Phis **(Figure 4.4. B, Lane 5-6)**.

Therefore, 100 mM to 150 mM imidazole concentrations could effectively elute GST-6Phis but also eluted contaminating proteins together with the protein of interest. Nevertheless, there was a faint 46 kDa band when elution was performed using 200 mM imidazole **(Figure 4.4. B, Lane 7)**. It may be concluded that elution with 50 mM imidazole would remove most impurities while further elution with 500 mM imidazole could be useful for effectively eluting a large amount of GST-6Phis in a single fraction. However, the latter would contain GST-6Phis among contaminating proteins and would require further purification.
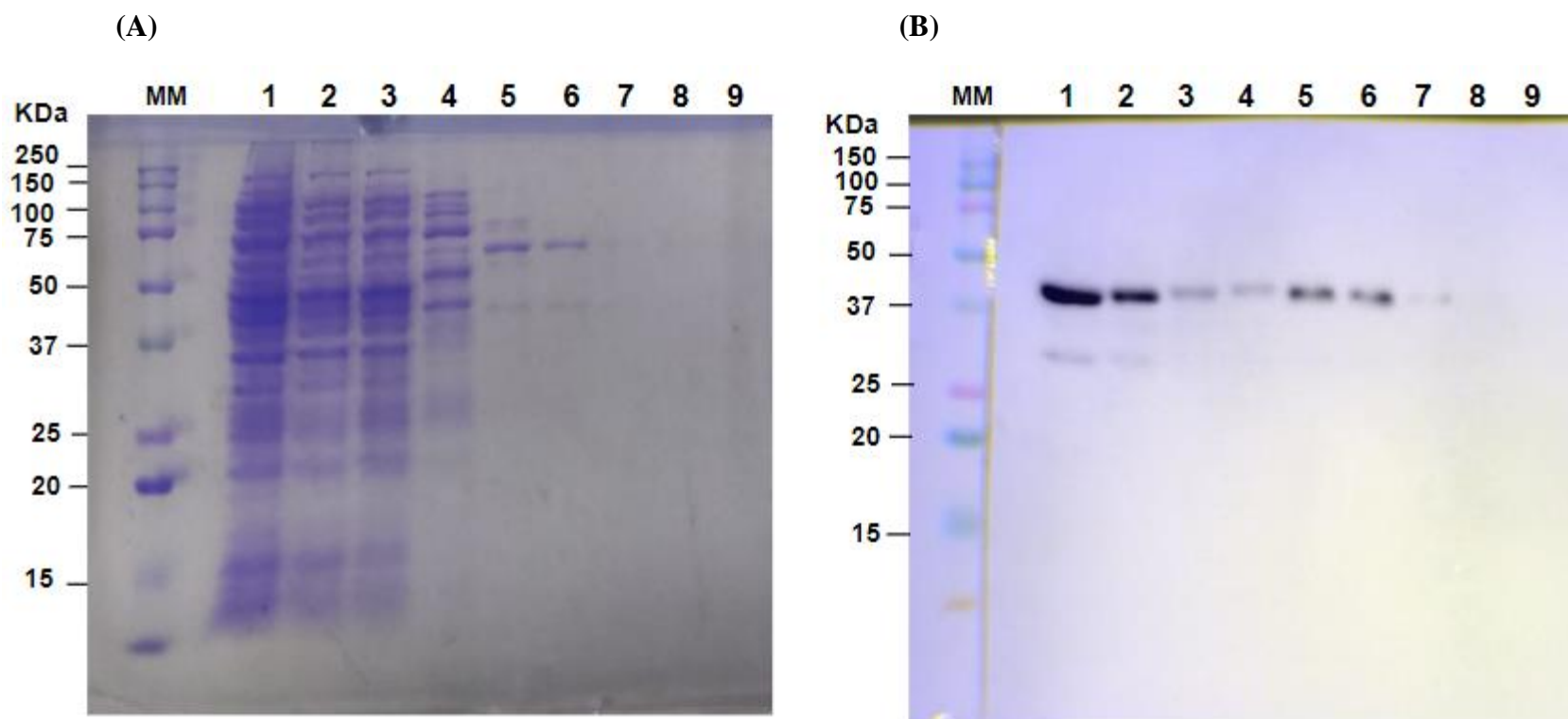
Figure 4.4. (A) SDS-PAGE Coomassie and **(B)** Western blotting from IMAC purification of crude lysate from *E. coli* transformed with pET41a-GST-6PHis; lane 1: crude lysate; lane 2: flowthrough; lane 3: elution with 10 mM imidazole; lane 4: elution with 50 mM imidazole; lane 5: elution with 100 mM imidazole; lane 6: elution with 150 mM imidazole; lane 7: elution with 200 mM imidazole; lane 8: elution with 250 mM imidazole; and lane 9: elution with 500 mM imidazole. The Prestained Kaleidoscope ladder was used as the molecular marker (Lane MM).

4.7.2 Ammonium sulphate precipitation

Ammonium sulphate precipitation was performed using 0-20%, 20-30%, 30-40%, 40-50%, 50-60%, 60-70%, and 80-90% ammonium sulphate to determine the concentration effective for the maximum precipitation of GST-6Phis. GST-6Phis was most abundantly precipitated out at 0-20%, 20-30%, and 30-40% ammonium sulphate concentrations as evidenced by thick bands at 46kDa (**Figure 4.5. B, Lane 1-3**). A very faint band at 46kDa was observed at 40-50% ammonium sulphate (**Figure 4.5. A, Lane 4**). Abundant amounts of contaminating proteins were precipitated at 50-60%, 60-70%, and 70-80% ammonium sulphate (**Figure 4.5. A, Lane 5-7**). However, no bands corresponding to 46 kDa were detected, indicating that these fractions did not contain GST-6Phis (**Figure 4.5. B, Lane 5-7**). It was concluded that the use of 40% ammonium sulphate precipitation and the exclusion of 40-50% ammonium sulphate precipitates could most efficiently concentrate a large amount of GST-6Phis and reduce the contaminating proteins present. 0-40% ammonium sulphate precipitation will, therefore, serve as the first step in the purification scheme.
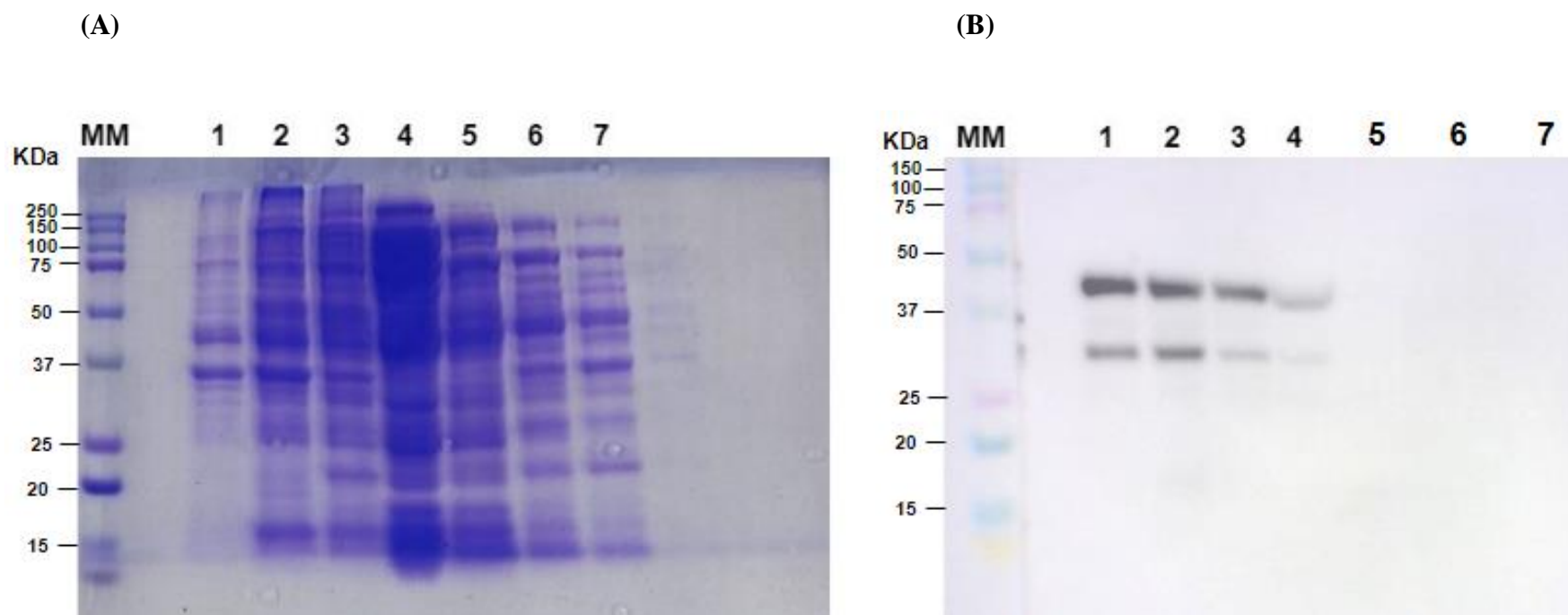
Figure 4.5. (A) SDS-PAGE Coomassie and (**B**) Western blotting of ammonium sulphate precipitates obtained from 0-20% (lane 1), 20-30% (lane 2), 30-40% (lane 3), 40-50% (lane 4), 50-60% (lane 5), 60-70% (lane 6), 70-80% (lane 7) ammonium sulphate concentrations. The Prestained Kaleidoscope ladder was used as the molecular marker (Lane MM).

4.7.3 Ammonium sulphate precipitation, followed by IMAC

The 0-40% ammonium sulphate precipitate was subjected to IMAC. SDS-PAGE Coomassie analysis showed that the 0-40% ammonium sulphate precipitate contained abundant amounts of multiple proteins (**Figure 4.6. A, Lane 1**). A prominent band at 46 kDa demonstrated that GST-6Phis was also abundantly present in this fraction among other contaminating proteins (**Figure 4.6. B, Lane 1**). The flowthrough contained significantly lower amounts of proteins as represented by much fainter bands **(Figure 4.6. A, Lane 2)**. The band at 46 kDa representing GST-6Phis was also significantly smaller in the flowthrough **(Figure 4.6. B, Lane 2)**. This decrease in band size at 46 kDa demonstrated that proteins in the crude lysate including GST-6Phis had bound to the Ni-NTA resin. Elution with 50 mM imidazole was able to elute several proteins bound to the Ni-NTA resin (**Figure 4.6. A, Lane 3**). A small amount of GST-6Phis was also eluted when 50 mM imidazole was used (**Figure 4.6. B, Lane 3**). Elution with 500 mM imidazole showed a prominent band at 46 kDa but also a band at 37 kDa (**Figure 4.6. A, Lane 4**). The band at 46 kDa represented the elution of GST-6Phis along with a contaminating protein at 37 kDa (**Figure 4.6. B, Lane 4**). However, it was worth noting that the contaminating protein larger than 50kDa that could not be removed with IMAC only was removed when IMAC was conducted after 0-40 ammonium sulfate precipitation. Nevertheless, further purification is required to remove the contaminating protein at 37 kDa.
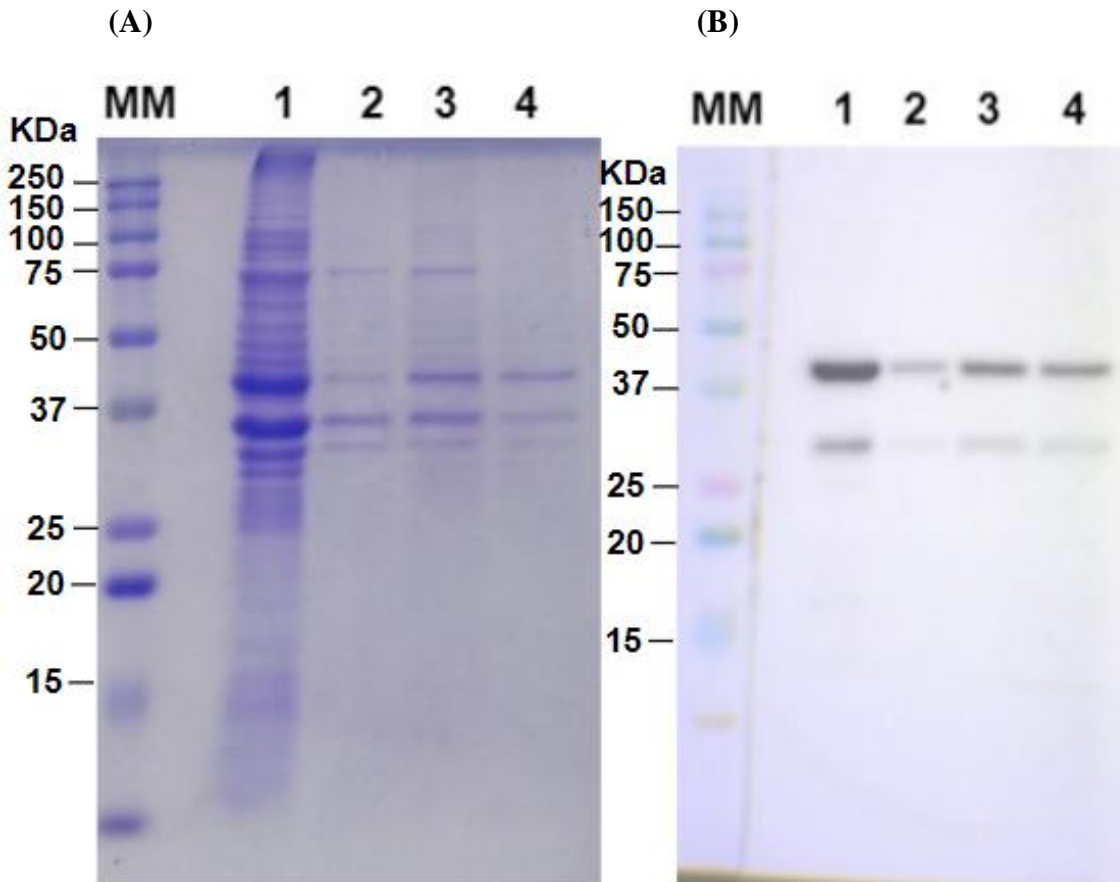
Figure 4.6. (A) SDS-PAGE Coomassie and **(B)** Western blotting of 0-40% ammonium sulphate precipitation followed by IMAC showing fractions representing the 0-40% precipitate (lane 1), flowthrough (lane 2), eluate from 50 mM imidazole elution (lane 3), and eluate from 500 mM imidazole elution (lane 4). The prestained Kaleidoscope ladder was used as the molecular marker (Lane MM).

4.8 Final purification using 0-40% ammonium sulfate precipitation, followed by gel filtration, and his-tag affinity chromatography

Precipitated proteins yielded from 0-40% ammonium sulfate precipitation (0-40%) were dissolved in 1.5 ml of PBS. Sephadex G-75 resin was swollen in PBS buffer to form a slurry which was used to pack a gel filtration column. The concentration and absorbance readings of thirty 1 ml fractions were collected from gel filtration chromatography. The absorbance of successive elutions increased sharply and reached a peak value of 31.51 mg/ml at the eluted fraction 19. The standard curve of eluted fractions plotted against Absorbance at 280 nm (A280) further corroborated that a single sharp peak was obtained at eluted fraction 19, rising sharply at eluted fraction 15 and plateauing at eluted fraction 25 (**Figure 4.7**). Analysis of the SDS-PAGE Coomassie and Western blot conducted on eluted fraction 15 through to eluted fraction 24 showed that these samples contained 46 kDa GST-6PHis along with other contaminating proteins. There were minimal amounts of GST-6Phis in eluted fractions 15 and 16 (**Figure 4.8. B, Lane 1-Lane 2**). GST-6Phis was most concentrated in eluted fraction 17 through eluted fraction 21 (**Figure 4.8. B, Lane 3-Lane 7**). There were minimal amounts of GST-6Phis in eluted fractions 22, 23, and 24 (**Figure 4.8. B, Lane 8-Lane 10**). Eluted fraction 17 through eluted fraction 21 were pooled together and subjected to IMAC.
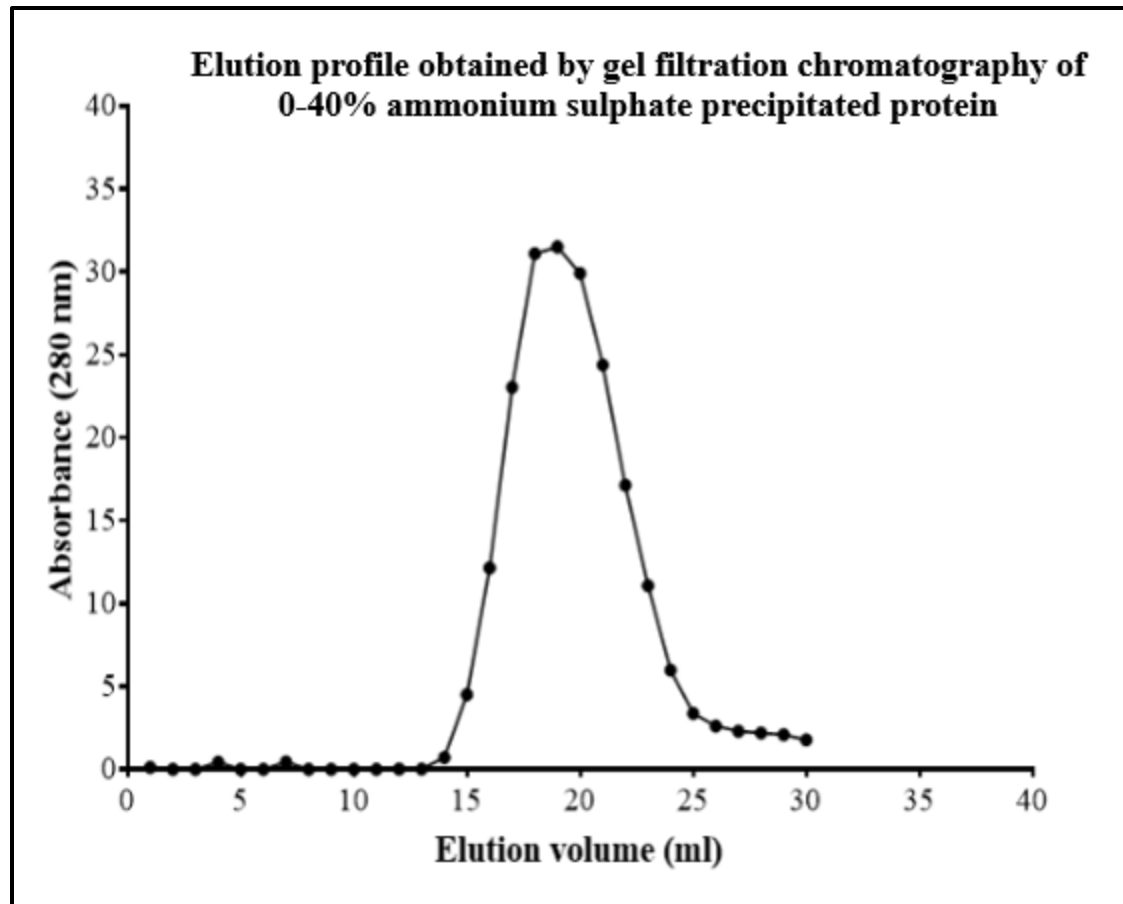
Figure 4.7. The elution profile obtained by gel filtration chromatography of the crude protein extract subjected to 0-40% ammonium

sulfate precipitation
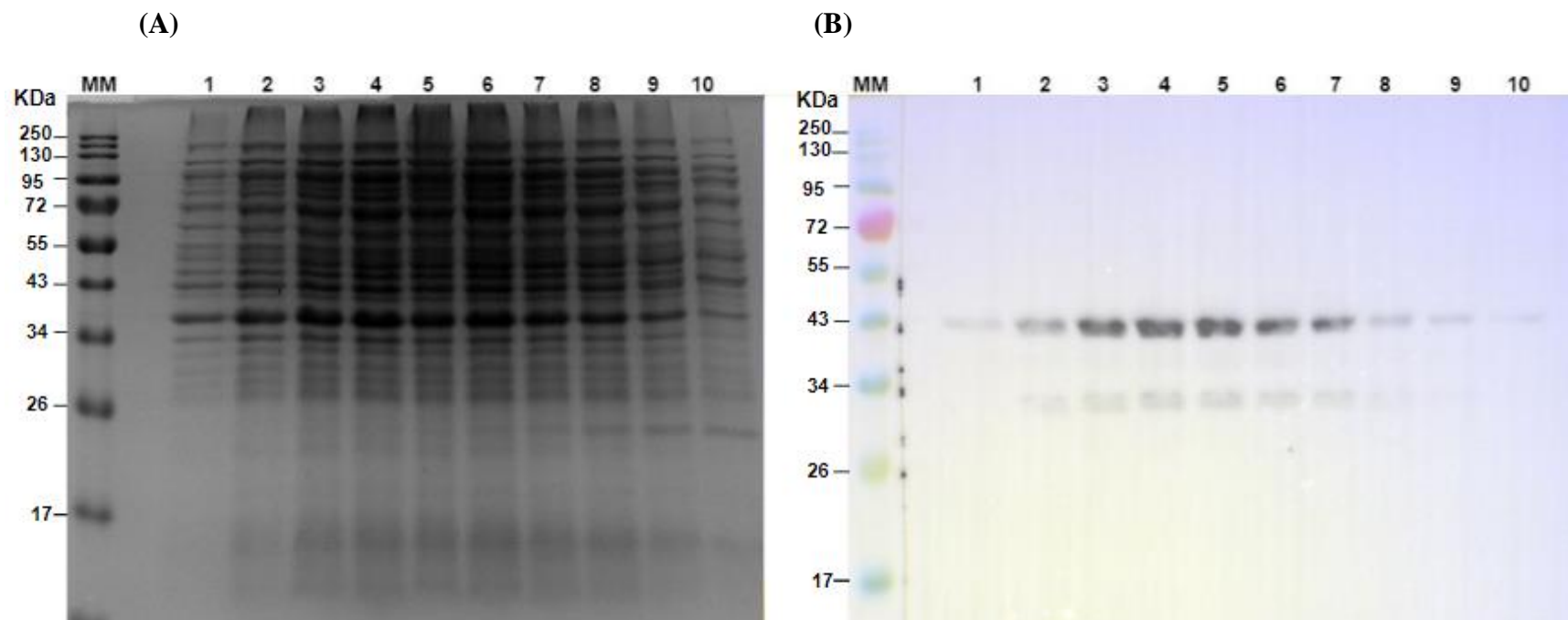
Figure 4.8. (**A**) SDS-PAGE Coomassie and (**B**) Western blotting of eluted fraction 15 (lane 1), eluted fraction 16 (lane 2), eluted fraction 17 (lane 3), eluted fraction 18 (lane 4), eluted fraction 19 (lane 5), eluted fraction 20 (lane 6), eluted fraction 21 (lane 7), eluted fraction 22 (lane 8), eluted fraction 23 (lane 9), and eluted fraction 24 (lane 10) that formed the peak of the gel filtration standard curve. The prestained Kaleidoscope ladder was used as the molecular marker (Lane MM).

97

4.9 Production of the purified GST-6Phis

      A purification scheme consisting of ammonium sulphate precipitation, gel filtration chromatography, and IMAC was developed to purify GST-6Phis from contaminating proteins expressed by pET41a-GST-6PHis. The crude lysate expressed from *E. coli* cells transformed with pET41a-GST-6PHis consisted of multiple proteins (**Figure 4.9. A, Lane 1**). GST-6Phis was also produced abundantly among several contaminating proteins (**Figure 4.9. B, Lane 1**). The crude lysate was subjected to 0-40% ammonium sulphate precipitation which served to concentrate GST-6Phis among contaminating proteins (**Figure 4.9. A, Lane 2**). GST-6Phis was abundantly present in the fraction of precipitated proteins (**Figure 4.9. B, Lane 2**). Precipitated proteins were dissolved in PBS and subjected to gel filtration and eluted fraction 17 through eluted fraction 21 were pooled together. Pooled fractions still contained contaminating proteins (**Figure 4.9. A, Lane 3**). However, GST-6Phis was abundantly observed (**Figure 4.9. B, Lane 3**). The flowthrough contained a relatively small amount of total protein when compared to the pooled gel filtration fraction (**Figure 4.9. A, Lane 4**). GST-6Phis was also shown to be less abundantly present in the flowthrough when compared to the pooled gel filtration fractions (**Figure 4.9. B, Lane 4**). This indicated the binding of proteins including GST-6Phis to the Ni-NTA resin. Elution with 50 mM imidazole was able to elute several contaminating proteins (**Figure 4.9. A, Lane 5**). This fraction also eluted a small amount of GST-6Phis (**Figure 4.9. B, Lane 5**). The eluate obtained from elution with 500 mM imidazole did not contain contaminating proteins (**Figure 4.9. A, Lane 6**). However, Western blotting analysis showed that the eluate contained GST-6Phis, albeit in a small amount (**Figure 4.9. B, Lane 6**). Since high concentrations of GST-6Phis would be required for mice immunization experiments, the eluate was passed through a 50 kDa cut-off Centricon to concentrate GST-6Phis and to remove imidazole. The concentrate was shown to contain an

abundant amount of GST-6Phis **(Figure 4.9. B, Lane 7)**. No contaminating proteins were observed **(Figure 4.9. A, Lane 7)**.
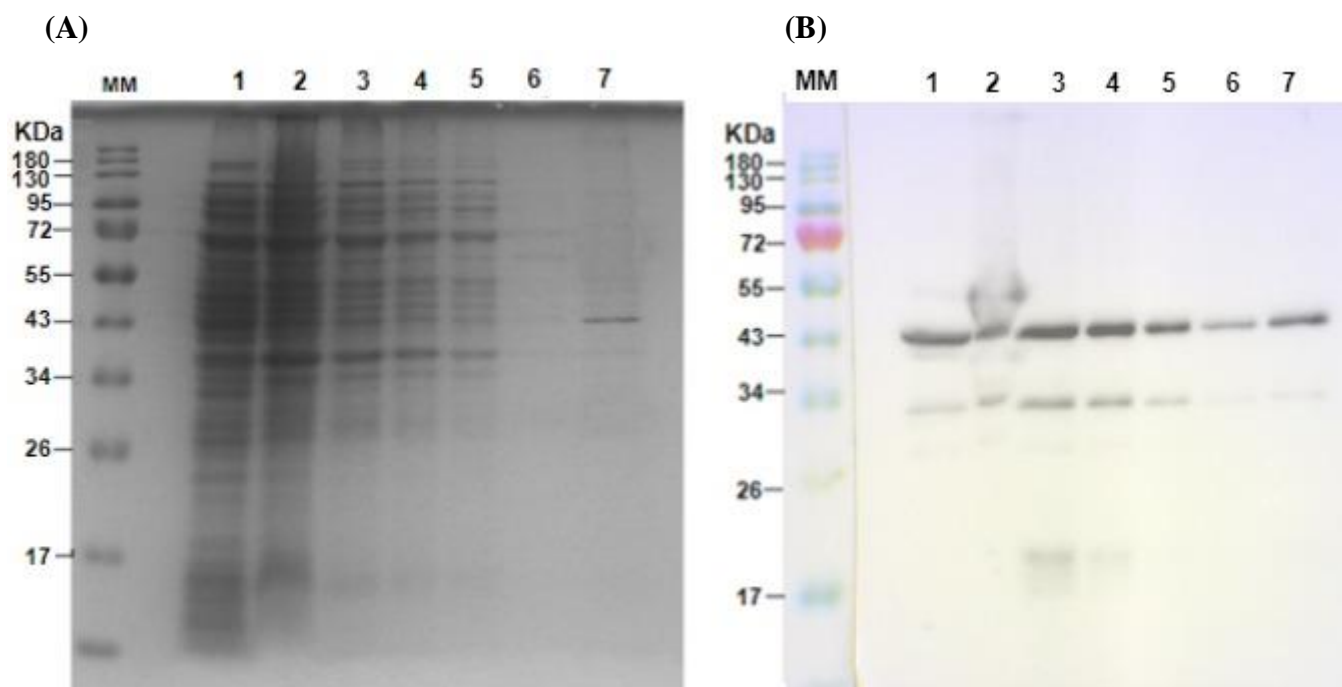
Figure 4.9. (A) The SDS-PAGE Coomassie profile and **(B)** Western blotting of crude lysate from *E. coli* transformed with pET41a-GST-6PHis (lane 1), subjected to 0-40% ammonium sulphate precipitation (lane 2), followed by gel filtration chromatography and pooling of eluted fractions 17-21 (lane 3), flowthrough (lane 4), elution with 50 mM imidazole (lane 5), elution with 50 mM imidazole (lane 6), and the concentrate from a 50 kDa cut-off Centricon to yield purified GST-6Phis. The prestained Kaleidoscope ladder was used as the molecular marker (Lane MM).

4.9 Monitoring mice health to evaluate vaccine toxicity

The health of the immunized mice was monitored throughout the 42-day immunization study. The weight of the mice increased gradually as expected and there was no drop in weight at any time. There were also no signs of ruffled feather, deceased movement or lethargy. No mice died during the study. Therefore, it was concluded that the vaccine was not toxic to mice.

4.10 High cell viability of splenocytes

Flow cytometry was used to conduct the cell viability analysis of the splenocytes obtained from mice immunized intramuscularly with PBS, mice immunized intramuscularly with the GST-6Phis, mice immunized intranasally with PBS, and mice immunized intranasally with GST-6Phis. The cell viability of the splenocytes were 85%, 82%, 80.1%, and 80.7%, respectively (**Figure 4.10**).
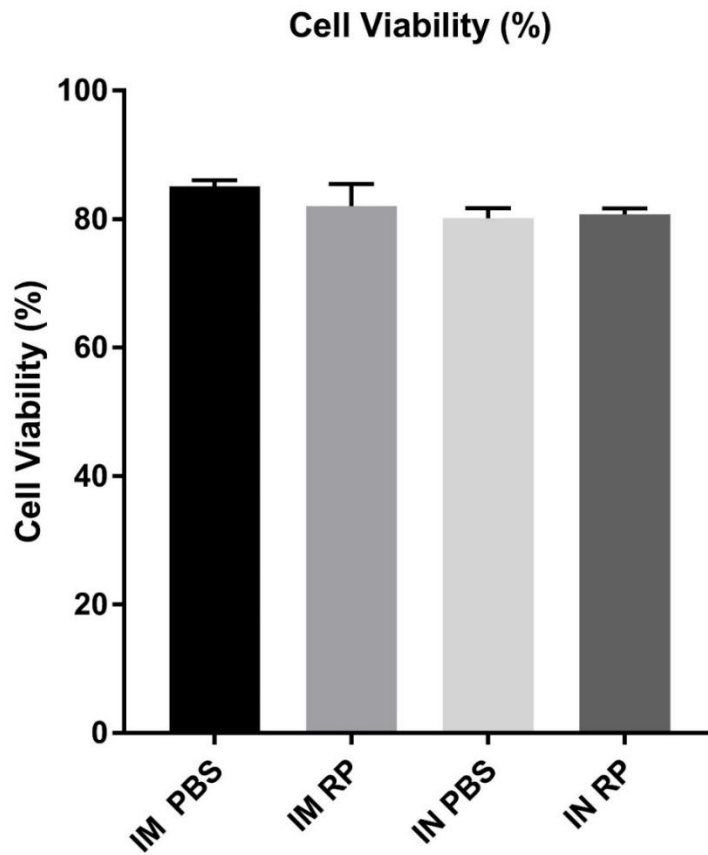
Figure 4.10. Cell viability of splenocytes from mice immunized intramuscularly with PBS (IM PBS), intramuscularly with GST-6Phis (IM RP), intranasally with PBS (IN PBS), and intranasally with GST-6Phis (IN RP)

4.11 Flow cytometry analysis of IFN-γ secreting CD3$^+$ CD4$^+$ and CD3$^+$ CD8$^+$ T cells

The intranasal and intramuscular administration of GST-6Phis was conducted in order to evaluate differences in the elicitation of immune responses attributable to differences in delivery routes relative to the negative control. Following stimulation of murine splenocytes with PMA, ionomycin, and GolgiStop to induce cytokine production, splenocytes were stained with CD3, CD4, CD8 and IFN-γ antibodies. Flow cytometry was conducted to determine the production of IFN-γ secreting CD3$^+$ CD4$^+$ and CD3$^+$ CD8$^+$ T cells from the intramuscular and intranasal administration of the GST-6Phis and PBS.

4.11.1 Production of IFN-γ secreting CD3$^+$ CD4$^+$ T cells by the respective intramuscular and intranasal administration of the GST-6Phis

A specific gating strategy was employed for ICS analysis to determine the percentage of CD4$^+$ T cells producing IFN-γ. This involved gating the lymphocyte population, followed by the singlet population, and identification of live CD3$^+$ T cells, and finally CD3$^+$ CD4$^+$ T cells (**Figure 4.11. A**). The percentage of CD3$^+$ CD4$^+$ T cells secreting IFN-γ was reported to be 0.3467% for harvested splenocytes from mice immunized intramuscularly with GST-6Phis relative to 0.21% for harvested splenocytes from mice immunized intramuscularly with PBS (**Figure 4.11. B**). Moreover, the percentage of CD3$^+$CD4$^+$ T cells secreting IFN-γ was reported to be 0.29% for harvested splenocytes from mice immunized intranasally with GST-6Phis which was similar to 0.29% that was determined from harvested splenocytes from mice immunized intranasally with PBS (**Figure 4.11. B**). Harvested splenocytes from mice immunized intramuscularly with GST-6Phis showed significantly higher production of IFN-γ secreting CD3$^+$ CD4$^+$ T cells (0.3467% of CD3$^+$CD4$^+$ T cells producing IFN-γ) relative to mice immunized intramuscularly with PBS (0.2067% of CD3$^+$CD4$^+$ T cells producing IFN-γ) (*p < 0.05) (**Figure 4.11. C**). This reflected a

percentage increase of about 67.63% higher in mice immunized with GST-6Phis compared to those immunized with PBS. However, harvested splenocytes from mice immunized intranasally with GST-6Phis recombinant protein showed no significant difference in levels of IFN-γ secreting $CD3^+ CD4^+$ T cells (0.2867% of $CD3^+ CD4^+$ T cells producing IFN-γ) relative to mice immunized intranasally with PBS (0.284% of $CD3^+ CD4^+$ T cells producing IFN-γ) (**Figure 4.11 C**).

(A)

(B)

(C)

105
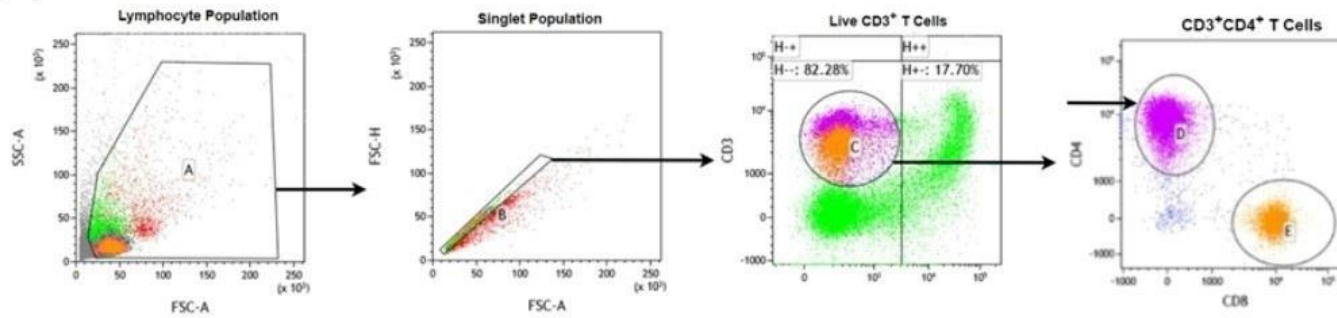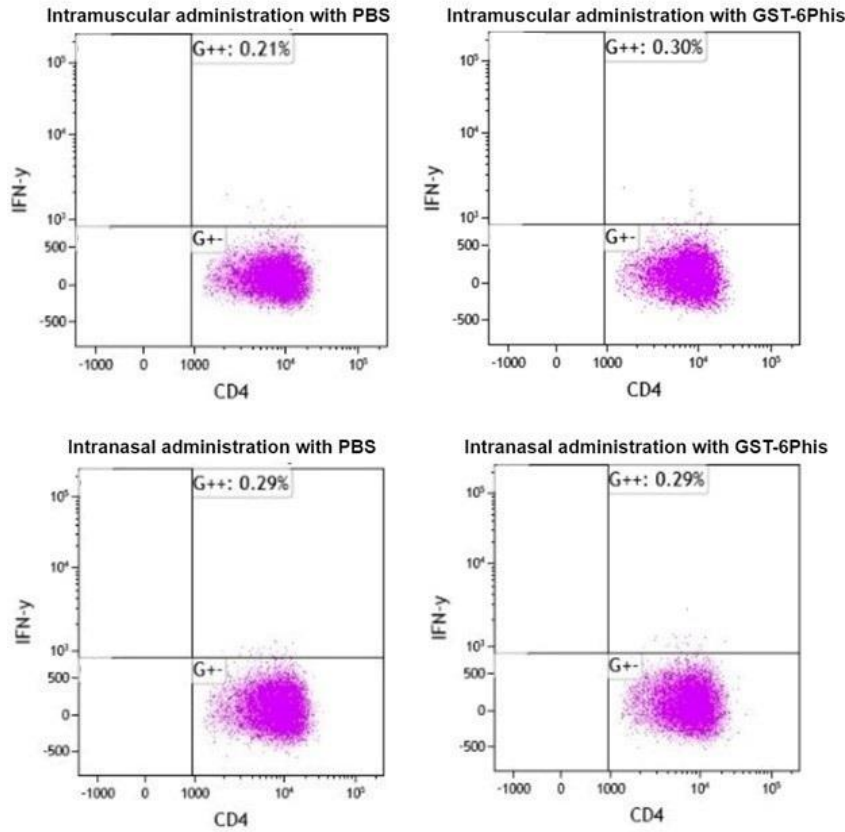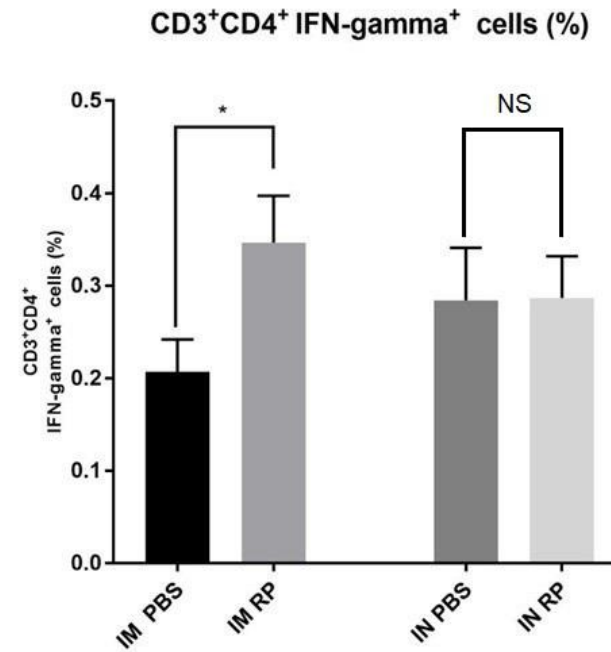
Figure 4.11. GST-6Phis elicited IFN-γ production by CD4$^+$ T cells in splenocytes of BALB/c mice that were immunized with this vaccine. BALB/c mice (n=5) were immunized with the GST-6Phis three times either with intramuscular or intranasal administration at a two-week interval. On Day 42 post-immunization, cells were harvested from the spleens of the immunized mice. **(A)** Gating strategy employed for ICS analysis of T cell subsets in flow cytometry in terms of the identification of the lymphocyte population, singlet population, live CD3$^+$ T cells, and CD3$^+$CD4$^+$ T cells producing IFN-γ. **(B)** Representative plots showing the percentage of IFN-γ production by CD4$^+$ T cells in splenocytes of BALB/c mice immunized intramuscularly with PBS, intramuscularly with GST-6Phis, and intranasally with PBS, and intranasally with GST-6Phis. The quadrant G+- shows CD4$^+$ T cells scored negative for IFN-γ production while G++ shows CD4$^+$ T cells scored positive for IFN-γ production **(C)** Comparative percentages of IFN- γ secreting CD4$^+$ T cells in splenocytes in mice immunized intramuscularly with PBS, intramuscularly with GST-6Phis, and intranasally with PBS, and intranasally with GST-6Phis. Data from triplicate assays were plotted using GraphPad Prism 8.02 software (GraphPad Software Inc., San Diego, CA, USA) and expressed as mean (± SD) (T-test: * $p < 0.05$) (NS: not significant).

4.11.2 Production of IFN-γ secreting CD3$^+$CD8$^+$ T cells by the intramuscular and intranasal administration of GST-6Phis

A specific gating strategy was employed for ICS analysis to determine the percentage of CD8$^+$ T cells producing IFN-γ. This involved gating the lymphocyte population, followed by the singlet population, identification of live CD3$^+$ T cells, and finally CD3$^+$ CD8$^+$ T cells. The percentage of CD3$^+$ CD8$^+$ T cells secreting IFN-γ was reported to be 11.44% for harvested splenocytes from mice immunized intramuscularly with GST-6Phis relative to 10.10% for harvested splenocytes from mice immunized intramuscularly with PBS (**Figure 4.12. A**). Moreover, the percentage of CD3$^+$CD8$^+$ T cells secreting IFN-γ was reported to be 13.18% for harvested splenocytes from mice immunized intranasally with GST-6Phis relative to 6.34% for harvested splenocytes from mice immunized intranasally with PBS (**Figure 4.12. A**). Harvested splenocytes from mice immunized intranasally with GST-6Phis showed highly significant production of IFN-γ secreting CD3$^+$ CD8$^+$ T cells (13.152% of CD3$^+$ CD8$^+$ T cells producing IFN-γ) when compared to mice immunized intranasally with PBS (8.8433% of CD3$^+$ CD8$^+$ T cells producing IFN-γ) (**Figure 4.12. B**). This reflected a percentage increase of 48.73% higher in mice immunized with GST-6Phis compared to those immunized with PBS. Harvested splenocytes from mice immunized intramuscularly with GST-6Phis showed higher levels of IFN-γ secreting CD3$^+$ CD8$^+$ T cells (11.587% of CD3$^+$CD8$^+$ T cells producing IFN-γ) when compared to mice immunized intramuscularly with PBS (10.073% of CD3$^+$CD8$^+$ T cells producing IFN-γ) (**Figure 4.12. B**). This reflected a fold difference of about 15.03% higher in mice immunized with GST-6Phis compared to those immunized with PBS but this difference was not statistically significant.

(A)

Intramuscular administration with PBS

F++: 10.10%

IFN-y

F+-

CD8

Intramuscular administration with GST-6Phis

F++: 11.44%

IFN-y

F+-

CD8

Intranasal administration with PBS

F++: 6.34%

IFN-y

F+-

CD8

Intranasal administration with GST-6Phis

F++: 13.18%

IFN-y

F+-

CD8

(B)

$CD3^+CD8^+$ IFN-gamma$^+$ cells (%)

NS

**

$CD3^+CD8^+$ IFN-gamma$^+$ cells (%)

IM PBS   IM RP   IN PBS   IN RP
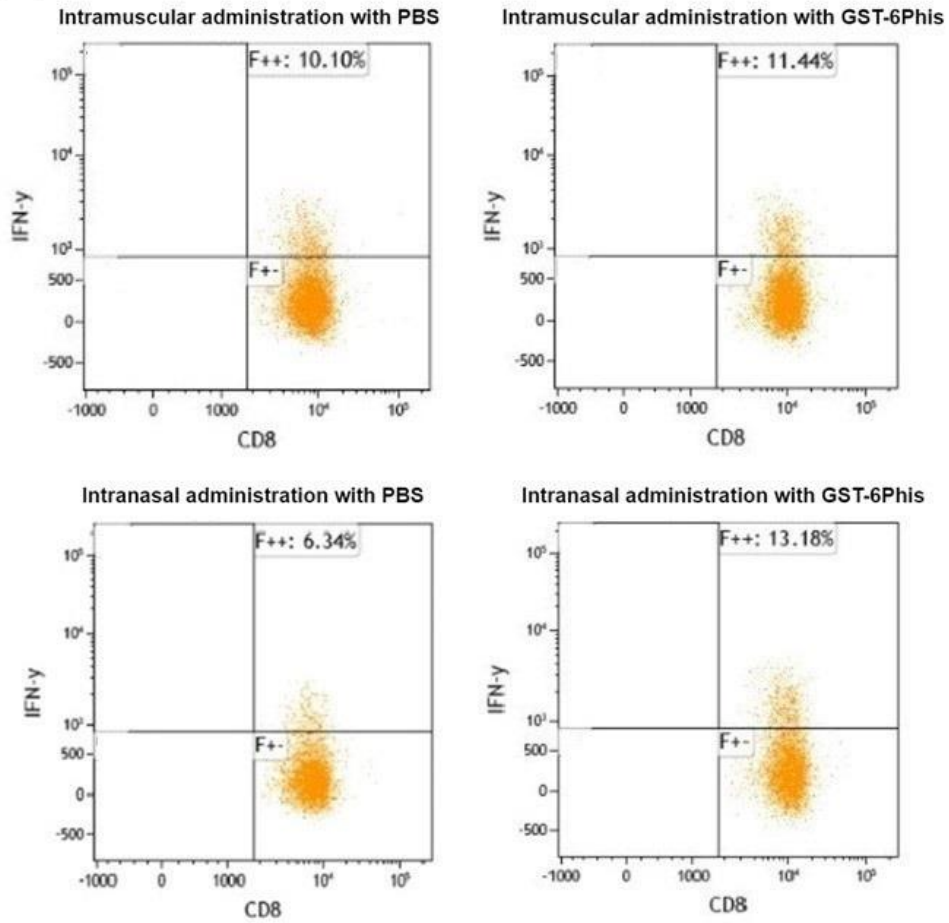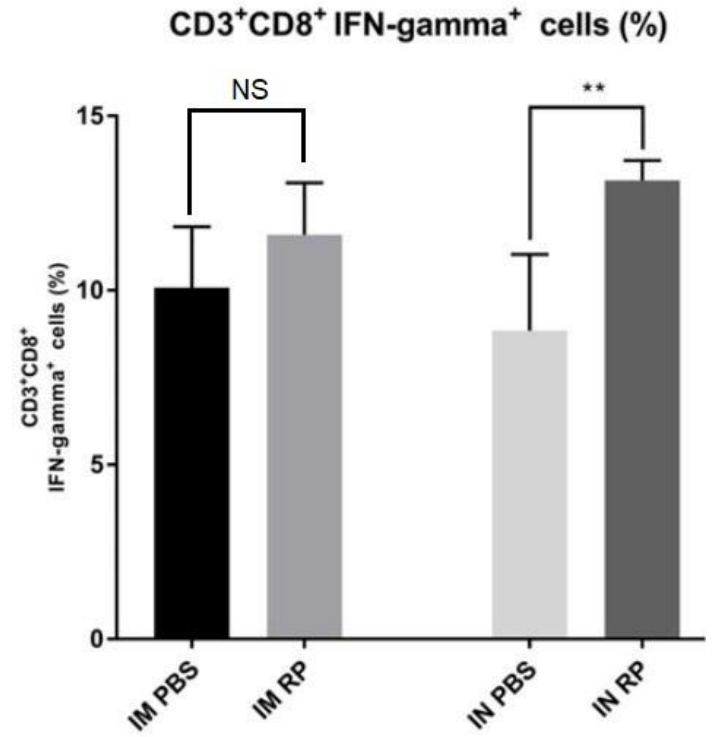
Figure 4.12. GST-6Phis elicited IFN-γ production by CD8$^+$ T cells in splenocytes of BALB/c mice that were immunized with this vaccine. BALB/c mice (n=5) were immunized with the GST-6Phis three times either with intramuscular or intranasal administration at a two-week interval. On Day 42 post-immunization, cells were harvested from the spleens of the immunized mice. **(A)** Representative plots showing the percentage of IFN-γ production by CD8$^+$ T cells in splenocytes of BALB/c mice immunized intramuscularly with PBS, intramuscularly with GST-6Phis, and intranasally with PBS, and intranasally with GST-6Phis. The quadrant F+- shows CD8$^+$ T cells scored negative for IFN-γ production while F++ shows CD8$^+$ T cells scored positive for IFN-γ production **(B)** Comparative percentages of IFN-γ secreting CD8$^+$ T cells in splenocytes in mice immunized intramuscularly with PBS, intramuscularly with GST-6Phis, and intranasally with PBS, and intranasally with GST-6Phis. Data from triplicate assays were plotted using GraphPad Prism 8.02 software (Graph Pad Software Inc., San Diego, CA, USA) and expressed as mean (± SD) (T-test: ** $p < 0.01$) (NS: not significant)

4.12 Initial sequence similarity analysis between peptides B6 and B10 and cPASS Omicron RBD

The similarity between the amino acid sequences of peptides B6 and B10 and the Omicron RBD that was utilized in the cPASS kit was determined using the EMBOSS Needle Sequence Alignment tool (https://www.ebi.ac.uk/Tools/psa/emboss_needle/). Similarity analysis was performed in order to demonstrate that peptides B6 and B10 could elicit nAbs capable of binding to the cPASS Omicron RBD to inhibit it from binding to the ACE2 receptor. Sequence similarity analysis showed that peptide B6 shared 4 amino acids with the cPASS Omicron RBD (**Figure 4.13. A**). Peptide B10 shared 8 amino acids with the cPASS Omicron RBD (**Figure 4.13. B**). This means that inhibition of the interaction between the Omicron RBD and the ACE2 receptor used in the cPASS kit by peptides B6 and B10, albeit partial, may be possible.

(A)

```
# Identity:       4/223 ( 1.8%)
# Similarity:     6/223 ( 2.7%)
# Gaps:         207/223 (92.8%)
# Score: 20.0
#
#
#=======================================
```

Query   1 --   0

Test Sequence   1 RVQPTESIVRFPNITNLCPFGEVFNATRFASVYAWNRKRISNCVADYSVL   50

Query   1 --   0

Test Sequence   51 YNSASFSTFKCYGVSPTKLNDLCFTNVYADSFVIRGDEVRQIAPGQTGKI   100

Query   1 --   0

Test Sequence 101 ADYNYKLPDDFTGCVIAWNSNNLDSKVGGNYNYLYRLFRKSNLKPFERDI   150

Query   1 --------------TESNKKFLPFQQFGRD--------------------   16
                                  .|.....:.|.|.:|..
Test Sequence 151 STEIYQAGSTPCNGVEGFNCYFPLQSYGFQPTNGVGYQPYRVVVLSFELL   200

Query   17 ----------------------   16

Test Sequence 201 HAPATVCGPKKSTNLVKNKCVNF   223

(B)

```
# Identity:        8/228 ( 3.5%)
# Similarity:     11/228 ( 4.8%)
# Gaps:          213/228 (93.4%)
# Score: 20.5
#
#
#======================================

Query            1 -------------------------------------------------    0

Test Sequence    1 RVQPTESIVRFPNITNLCPFGEVFNATRFASVYAWNRKRISNCVADYSVL   50

Query            1 -------------------------------------------------    0

Test Sequence   51 YNSASFSTFKCYGVSPTKLNDLCFTNVYADSFVIRGDEVRQIAPGQTGKI  100

Query            1 ---------------------------------------ESNKKFLPFQQ   11
                                                           :||.|  ||:
Test Sequence  101 ADYNYKLPDDFTGCVIAWNSNNLDSKVGGNYNYLYRLFRKSNLK--PFE-  147

Query           12 FGRDIADTT----------------------------------------   20
                    |||:...
Test Sequence  148 --RDISTEIYQAGSTPCNGVEGFNCYFPLQSYGFQPTNGVGYQPYRVVVL  195

Query           21 ---------------------------   20

Test Sequence  196 SFELLHAPATVCGPKKSTNLVKNKCVNF  223
```

Figure 4.13. (A) Sequence similarity between B6 and cPASS Omicron RBD **(B)** Sequence similarity between B10 and cPASS Omicron

RBD

4.13 High levels of IgG antibodies in the sera from immunized mice

An ELISA IgG assay was conducted to evaluate the levels of IgG antibodies elicited in the sera from mice immunized intramuscularly and intranasally with the recombinant protein vaccine when compared to the negative control. Sera samples from immunized mice were diluted in the ratios 1:50, 1: 250, and 1: 1000. The absorbance values of the samples were subtracted from the absorbance values of the blank wells. Significantly low absorbance readings were observed in the sera of mice who were immunized intramuscularly and intranasally with PBS across all dilutions (IM PBS 1: 50 = 0.3168; IM PBS 1: 250 = 0.2648; IM PBS 1: 1000 = 0.2345; IN PBS 1: 50 = 0.3372; IN PBS 1: 250 = 0.1744; IN PBS 1: 1000 = 0.1482), indicating minimal IgG antibody presence. In contrast, sera from mice immunized intramuscularly and intranasally with GST-6Phis exhibited substantially higher absorbance values (IM GST-6Phis 1: 50 = 1.7591; IM GST-6Phis 1: 250 = 1.6975; IM GST-6Phis 1: 1000 = 1.6694; IN GST-6Phis 1: 50 = 1.7616; IN GST-6Phis 1: 250 = 1.7307; IN GST-6Phis 1: 1000 = 1.6586), indicating a robust IgG antibody response (**Figure 4.14**). At a dilution of 1:50, the fold difference in absorbance values between mice immunized intramuscularly with the recombinant protein vaccine GST-6Phis and those immunized intramuscularly with PBS is approximately 5.56. In contrast, at the same dilution level, the fold difference for mice immunized intranasally with GST-6Phis compared to mice immunized intranasally with PBS is approximately 5.23. At a dilution of 1:250, the fold difference for IM GST-6Phis is about 6.41 when compared to mice immunized intramuscularly with PBS. The fold difference for mice immunized intranasally with GST-6Phis compared to mice immunized intranasally with PBS was approximately 9.93. At the highest dilution of 1:1000, the fold difference for the intramuscular administration of GST-6Phis was 7.12 when compared to the intramuscular administration of PBS. Similarly, the intranasal administration of GST-6Phis at this

dilution level showed a fold difference of approximately 11.20 when compared to the intranasal

administration of PBS (**Figure 4.14**).

Absorbance Values of ELISA IgG Test Against SARS-CoV-2
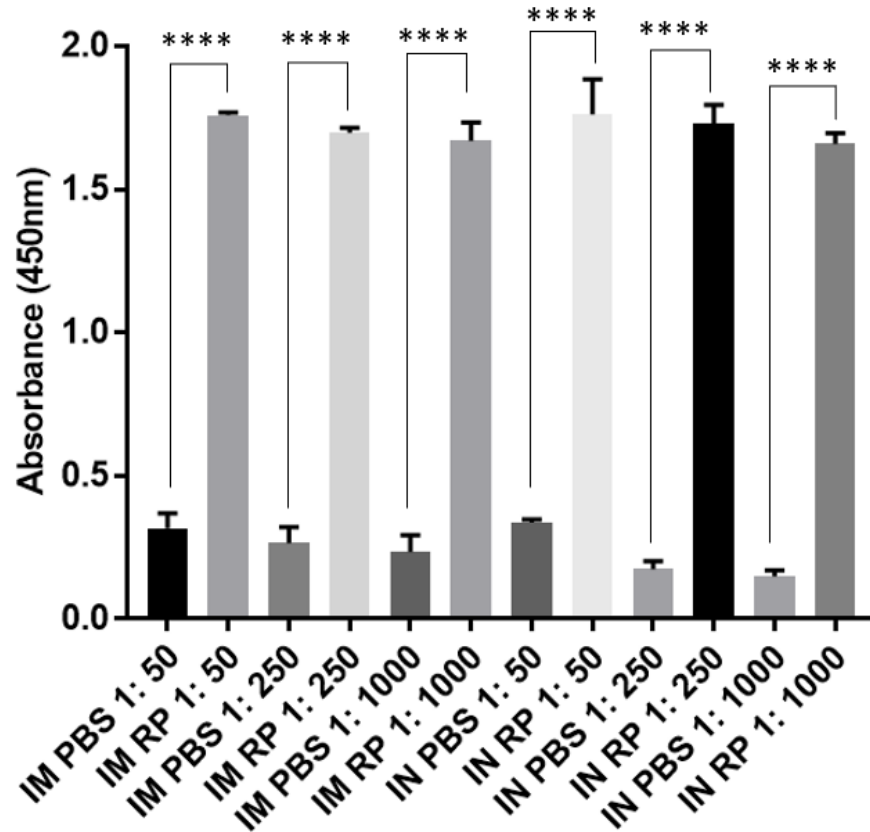

Figure 4.14. The absorbance values corresponding to levels of IgG antibodies in the sera samples of mice immunized intramuscularly with PBS (IM PBS), intramuscularly with GST-6Phis (IM RP), intranasally with PBS (IN PBS), and intranasally with GST-6Phis (IN RP). ELISA plates were coated with 10 μg of GST-6Phis diluted in coating buffer and incubated overnight. Data from triplicate assays were plotted using GraphPad Prism 8.02 software (Graph Pad Software Inc., San Diego, CA, USA) and expressed as mean (± SD) (T-test: **** $p < 0.0001$).

4.14 Determination of mean reciprocal IgG titer

In order to transform obtained absorbance (450 nm) values into the mean reciprocal IgG titers, serum dilutions 1:50, 1:250, and 1:1000 were plotted against absorbance (450 nm). The dotted line represented the cut-off value for the detection of IgG against the antigen in terms of absorbance values (0.148) (**Figure 4.15**). The cut-off value was used to determine the mean reciprocal IgG titers of undiluted sera from mice immunized intramuscularly with PBS, intramuscularly with GST-6Phis, intranasally with PBS, and intranasally with GST-6Phis. High mean reciprocal IgG titers of 1656 were found in the sera from mice immunized intramuscularly with GST-6Phis when compared to mean reciprocal IgG titers of 200 were found in the sera from mice immunized intramuscularly with PBS. This difference was statistically significant (**** $p < 0.0001$) reflecting a percentage increase of 728% (**Figure 4.16**). Similarly, high mean reciprocal IgG titers of 1646 were found in the sera from mice immunized intranasally with GST-6Phis when compared to mean reciprocal IgG titers of 233 were found in the sera from mice immunized intranasally with PBS. This difference was also statistically significant (**** $p < 0.0001$) reflecting a percentage increase of 606% (**Figure 4.16**).
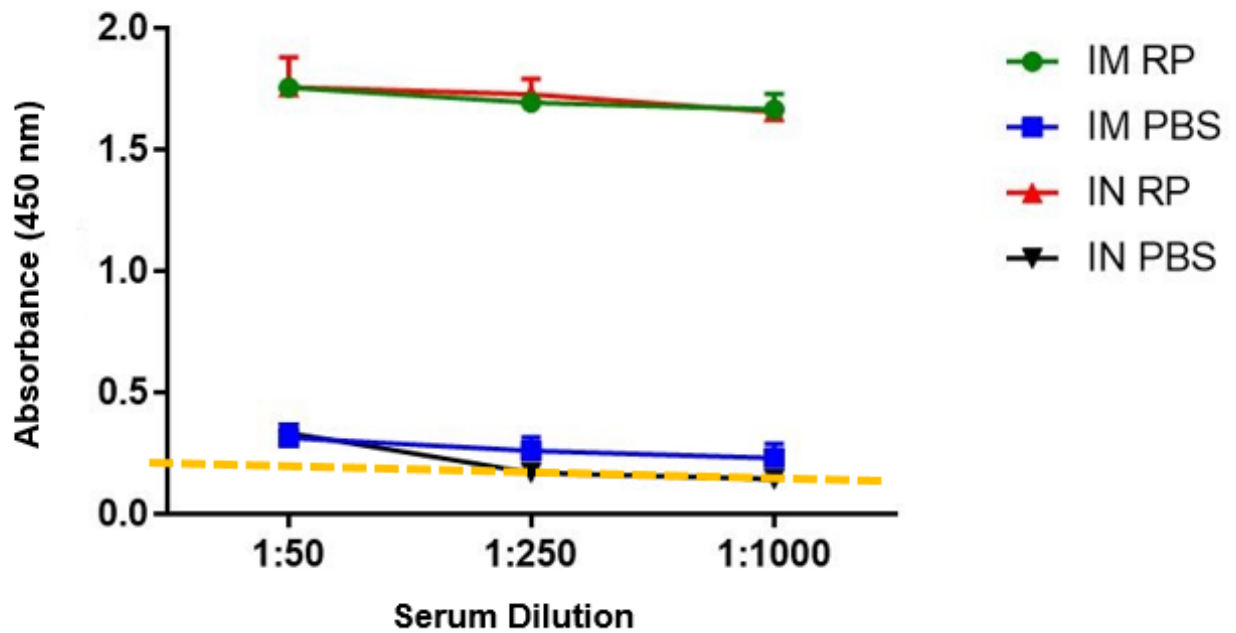
Figure 4.15. Determination of cut-off point using antigen specific IgG in different dilution of sera from mice immunized intramuscularly with PBS (IM PBS), intramuscularly with GST-6Phis (IM RP), intranasally with PBS (IN PBS), and intranasally with GST-6Phis (IN RP). The dotted line represented the cut-off value (0.148).

Mean Reciprocal IgG Antibody Titer Against SARS-CoV-2
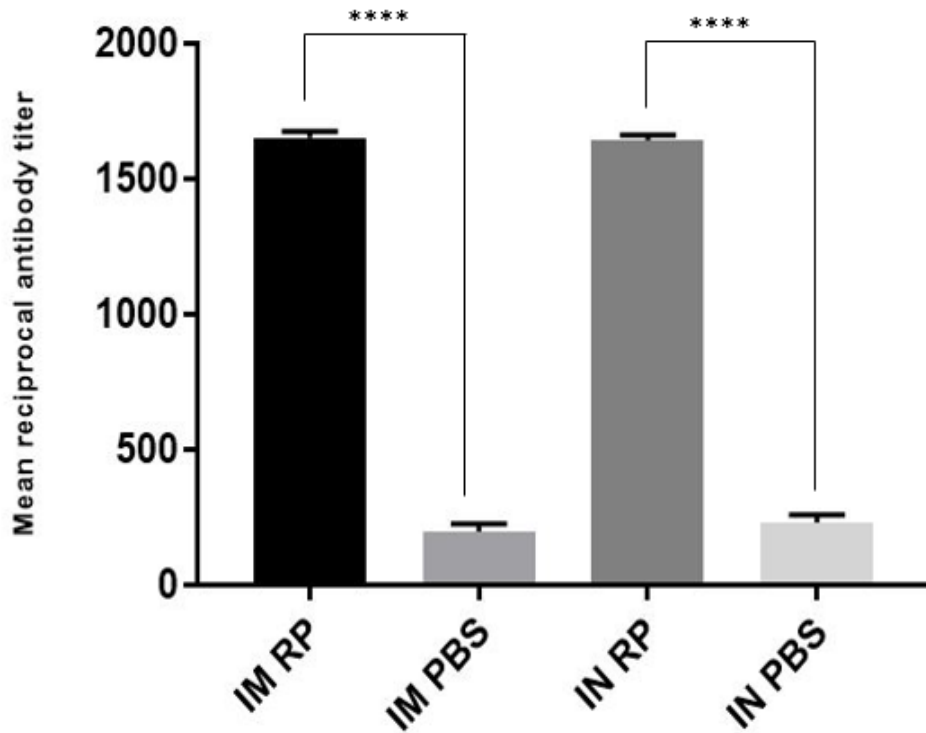
Figure 4.16. Mean reciprocal IgG titers from mice immunized intramuscularly with PBS (IM

PBS), intramuscularly with GST-6Phis (IM RP), intranasally with PBS (IN PBS), and

intranasally with GST-6Phis (IN RP). Data from triplicate assays were plotted using GraphPad

Prism 8.02 software (Graph Pad Software Inc., San Diego, CA, USA) and expressed as mean ($\pm$

SD) (T-test: **** $p < 0.0001$).

4.15 Positive detection of nAbs against the SARSCoV-2 Wuhan and Omicron strains in the sera of mice immunized with GST-6Phis

Sera from mice immunized intramuscularly and intranasally with PBS or GST-6Phis were mixed in a 1:1 ratio with the Wuhan RBDHRP and the signal inhibition of the interaction between RBD and ACE2 receptor was determined for the four mice groups. For the first experiment with the SARS-CoV-2 Wuhan RBD, sera from mice immunized intramuscularly and intranasally with PBS both showed a signal inhibition of 0. Sera from mice immunized intramuscularly and intranasally with 10 μg of GST-6Phis showed a signal inhibition of 34.6% and 30.8%, respectively. For the second experiment with the SARS-CoV-2 Omicron RBD, sera from mice immunized intramuscularly with PBS and with 10 μg of GST-6Phis showed a signal inhibition of 13% and 30%, respectively. The positive and negative control showed a signal inhibition of 97.2% and 0, respectively (**Figure 4.17**). Since the cutoff value for the cPass SARS-CoV-2 Neutralizing Antibody Detection Kit is 30% signal inhibition, it was concluded that sera obtained from the intramuscular and intranasal administration of GST-6Phis were positive for the presence of nAbs capable of blocking the binding between SARS-CoV-2 Wuhan RBD and the ACE2 receptor. Additionally, sera obtained from the intramuscular administration of GST-6Phis was scored positive for nAbs capable of interaction between SARS-CoV-2 Omicron RBD and the ACE2 receptor.
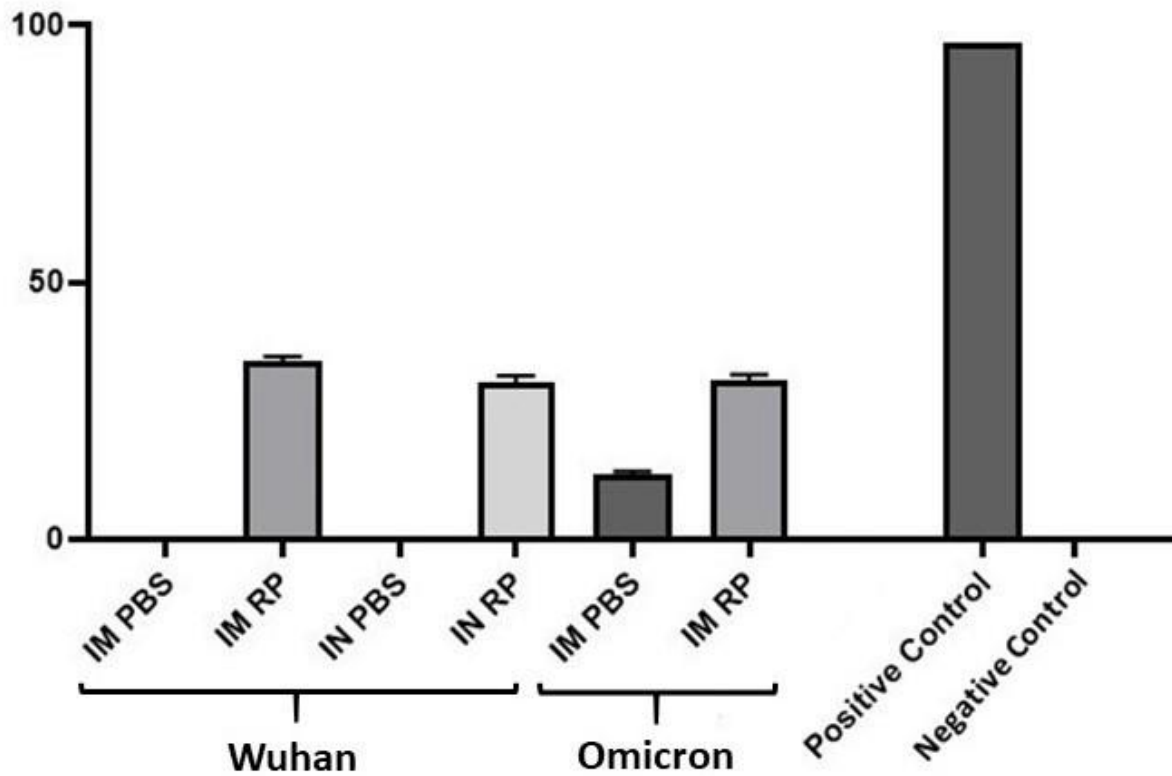
Figure 4.17. The signal inhibition of the interaction between RBD and ACE2 receptor in the sera of mice immunized intramuscularly with PBS (IM PBS), intramuscularly with GST-6Phis (IM RP), intranasally with PBS (IN PBS), intranasally with GST-6Phis (IN RP), and in the positive and negative controls

CHAPTER 5: DISCUSSION

Conservancy Analysis

The infective potential of COVID-19 is alarming since it continues to cause numerous infections and deaths across different regions of the world attributable to rapidly emerging SARS-CoV-2 VOCs. Building from preliminary experiments conducted by Dr Lim Hui Xuan and Sunway Masters candidate, Al-Fattah Yahaya, a total of six peptides designated as ST1, ST5, ST19, MT1, SB6, and SB10 were selected to develop the vaccine. Conservancy analysis against the SARS-CoV-2 Omicron showed that while ST1, ST5, MT1, SB6, and SB10 demonstrated high conservancy peptide ST19 was shown to have lost conservancy. This is understandable since S19 coincided with part of the SARS-CoV-2 RBD. Indeed, the Omicron was shown to have four significant mutations in the RBD, which represents the highest number among all VOCs. The K417/E484/N501 triad mutation and the addition of T478K in Omicron greatly impact the ability of the virus to evade immune responses (Kudriavtsev et al., 2022). The loss of conservancy of the ST19 peptide against SARS-CoV-2 Omicron VOC raises concerns about potential implications for current vaccine efficacy. Notably, ST19 was designated as a CD4$^+$ and CD8$^+$ T cell epitope and should not be able to impact the elicitation of humoral responses. Peptides B6 and B10 that were selected as B cell epitopes were shown to be highly conserved against the SARS-CoV-2 Omicron variant. Since peptides B6 and B10 were high in immunogenicity, they were able to elicit potent humoral responses against the SARS-CoV-2 Wuhan strain. Moreover, the high conservancy of B6 and B10 in the Omicron VOC would similarly confer neutralizing antibody responses against the SARS-CoV-2 Omicron variant. Even though ST19 did not maintain conservancy against the Omicron variant, it is noteworthy that the remaining five peptides were conserved against the SARS-CoV-2 Omicron variant.

This research project demonstrates a promising approach to vaccine development against SARS-CoV-2 VOCs. It involved the development of a recombinant protein vaccine incorporating the aforementioned highly conserved and immunogenic epitopes from SARS-CoV-2 structural proteins. Immunogenicity evaluation after intramuscular and intranasal administration of GST-6PHis in BALB/c mice showed that the vaccine was able to elicit immune responses against the SARS-CoV-2 Wuhan and Omicron strains.

Evaluation of Immunogenicity

Cellular Immunity

An analysis of the cell viability of splenocytes showed promising results, reinforcing the assertion of a low level of cytotoxicity which meant that most of the cells remained alive. Notably, over 80% of cells remained viable throughout the immunogenicity study. This high cell viability indicates the maintenance of cellular integrity and function and that potential endotoxin levels were low and likely not detrimental to the cells, suggesting a lower risk of endotoxicity. However, to definitively confirm endotoxin levels and their impact, it's still important to conduct specific endotoxin assessment assays to protect mice from adverse effects. A weight reduction could indicate stress, illness, or adverse reactions to treatments or conditions such as inadequate nutrition, discomfort due to the immunization process, immune responses to the treatment, or underlying health concerns. A lack of weight reduction could indeed suggest acceptable levels of endotoxicity. If endotoxin levels were elevated and causing toxicity, it could lead to adverse effects on the health and well-being of the mice, potentially resulting in weight loss. No reduction in body weight of the mice was observed at any point during the immunization study. Instead, a gradual increase in the weight of mice was noted over this period, which aligns with the natural growth progression of the mice and compared well with the untreated mice in the control group.

Flow cytometry analysis of the splenocytes from mice immunized intranasally with GST-6Phis showed a statistically significant difference of 1.485 times higher in the percentage of CD8$^+$ T cells producing IFN-γ when compared to mice immunized intranasally with PBS. The results of the current study when examined after analyzing already published data corroborate the idea that mucosal immunization might offer a more strategic advantage in fighting infection from respiratory viruses such as the SARS-CoV-2 by conferring immune protection at the site of viral entry. A local immunological response could be elicited by intranasal immunization, especially in the mucosal tissues, which might have helped to activate and attract IFN-γ producing CD8$^+$ T cells. Intranasal administration involves delivering the immunogen through the nasal mucosa, which is rich in immune cells and provides direct access to the respiratory immune system. Indeed, intranasal immunization with an RBD-based recombinant protein vaccine was able to confer elevated levels of nAbs along with mucosal secretory IgA and lung-resident memory T cells (TRM), which was attributable to local T cell proliferation (Lei et al., 2022). Additionally, it is plausible that different delivery routes could result in various kinds and degrees of immunological activation. Additional factors, such as certain cytokines and chemokines, that encourage the activation and differentiation of CD8$^+$ T cells that produce IFN-γ might be provided via intranasal immunization. It is well known that the respiratory mucosa contains a dense network of immune cells and signalling chemicals that can influence the nature of the immune response that is elicited. Different ways that antigens are introduced to the immune system can have an impact on the type of immunological response elicited. Specialized APCs in the respiratory mucosa can effectively present antigens to CD8$^+$ T cells, which may trigger a potent IFN-γ response.

However, intramuscular administration of GST-6Phis did not result in potent elicitation of T cell responses in terms of IFN-γ secreting CD3$^+$CD8$^+$ T cells. When compared to intranasal

administration of the vaccine, intramuscular administration may not provide the same level of efficient antigen presentation to CD8$^+$ T cells, leading to a weaker IFN-γ response. The muscle tissue is not a typical location for immunological responses, thus intramuscular immunization would not produce the same local immune response resulting from mucosal immunizations and might need extra steps to activate the immune cells that could produce IFN-γ. Even though intramuscular vaccines have direct exposure to professional APCs, such as dendritic cells and macrophages in muscle tissue, the processing and presentation of antigens to CD8$^+$ T cells may be suboptimal compared to mucosal routes. The efficiency of cross-presentation – the process by which exogenous antigens are presented on major histocompatibility complex class I (MHC-I) molecules – may vary in different tissues, potentially limiting CD8$^+$ T cell priming. Moreover, not all APCs in muscle tissue may be in an optimal state for antigen presentation to CD8$^+$ T cells. Dendritic cells, for instance, may exist in various differentiation states with different capacities for antigen presentation Secondary lymphoid organs (SLOs) such as lymph nodes, spleen, Peyer's patches and mucosal tissues such as the nasal associated lymphoid tissue (NALT) are able to elicit immune responses based on carefully controlled expression of cytokines and lymphoid chemokines (LTα, LTβ, RANKL, TNF, IL-7, and IL-17) (Ruddle & Akirav, 2009). Muscle tissue lacks the specialized microarchitecture and immune cell populations found in secondary lymphoid organs, which play crucial roles in T cell priming and activation. Factors such as the availability of co-stimulatory molecules, cytokine milieu, and antigen persistence may influence the quality and magnitude of CD8$^+$ T cell responses following intramuscular vaccination. No adjuvants were administered along with the vaccine in the current study. It is possible that the CD8$^+$ T cell response could be enhanced through the incorporation of adjuvants that promote

antigen cross-presentation, such as TLR3 or TLR9 agonists, which may enhance CD8$^+$ T cell responses by activating APCs and facilitate the generation of cytotoxic T lymphocytes (CTLs).

In conclusion, immune responses can vary depending on the tissue environment. Intranasal immunization might trigger a more local response with a focus on mucosal immunity, whereas intramuscular immunization could result in a more systemic response. IFN-γ production by CD8$^+$ T cells might be favoured in the mucosal environment due to the presence of certain cytokines and immune cell types that promote this response.

Flow cytometry analysis of the splenocytes from mice immunized intramuscularly with GST-6Phis showed a statistically significant difference in the percentage of CD4$^+$ T cells producing IFN-γ production when compared to mice immunized intramuscularly with PBS. The statistically significant difference in the percentage of CD4$^+$ T cells producing IFN-γ after intramuscular immunization with GST-6Phis suggests that this immunization route has effectively triggered a CD4$^+$ T cell response. This might be due to the protein's ability to stimulate APCs in the muscle tissue, resulting in the activation and differentiation of CD4$^+$ T cells into IFN-γ producing Th1 cells.

However, flow cytometry analysis of the splenocytes from mice immunized intranasally with GST-6Phis did not show a statistically significant difference in the percentage of CD4$^+$ T cells producing IFN-γ production when compared to mice immunized intranasally with PBS. The weaker IFN-γ secreting CD3$^+$CD4$^+$ T cell response observed from the intranasal route of immunization can be attributed to several route-specific factors. Mucosal tissues, such as the respiratory tract, possess unique immunological characteristics geared towards maintaining immune tolerance to harmless antigens encountered through inhalation. This environment is rich in regulatory T cells and anti-inflammatory cytokines, which may dampen the CD4$^+$ T cell

response to intranasal vaccines. Antigens delivered intranasally encounter specialized APCs, such as dendritic cells residing in the mucosal-associated lymphoid tissues (MALT). However, compared to systemic APCs encountered by intramuscular vaccines, MALT APCs may exhibit differential expression of co-stimulatory molecules and cytokines, leading to suboptimal priming of CD4^{+} T cells. T cells primed in mucosal tissues, including the respiratory tract, may exhibit preferential homing to mucosal sites rather than systemic circulation. Therefore, despite effective priming within the mucosa, CD4^{+} T cells may not efficiently traffic to peripheral lymphoid organs where they are needed for systemic immune responses. Intranasal immunization of the vaccine could incorporate the use of adjuvants which could increase the number of IFN-γ secreting CD3^{+}CD4^{+} T cell vaccines often require specific adjuvants to enhance their immunogenicity due to the tolerogenic nature of mucosal tissues. Adjuvants that promote mucosal immunity, such as cholera toxin subunit B or heat-labile enterotoxin from *E. coli*, may be necessary to overcome mucosal tolerance and elicit robust CD4 T cell responses (Thiam et al., 2015).

The current recombinant protein vaccine developmental landscape mainly consists of vaccines expressing the full-length S protein sequence or the RBD. Tian et al. (2021) reported that upon administration of the NVX-CoV2373 vaccine, IFN-γ secreting CD4^{+} and CD8^{+} T cells were observed in the spleens of mice immunized with adjuvanted NVX-CoV2373. For IFN-γ secreting CD4^{+} T cell production, levels reached as high as 3.8 IFN-γ CD4^{+} per million splenocytes (log10) as compared with the control with 2.2 IFN-γ CD4^{+} per million splenocytes (log10). Administration of adjuvanted NVX-CoV2373 resulted in 2.5 IFN-γ CD4^{+} per million splenocytes (log10). For IFN-γ secreting CD8^{+} T cell production, levels reached as high as 5.2 IFN-γ CD8^{+} per million splenocytes (log10) as compared with the control with 3.4 IFN-γ CD8^{+} per million splenocytes (log10). Administration of adjuvanted NVX-CoV2373 resulted in 4.5 IFN-γ CD8^{+} per million

splenocytes (log10). Li et al. (2021) reported that administration of the S-protein-based COVAX-19 vaccine resulted in a 30% proliferation of $CD4^+$ T cells relative to the control with approximately 3% proliferation. The proliferation of $CD8^+$ T cells was reported to be 30% relative to the control with approximately 5% proliferation. These differences were found to be statistically significant for both $CD4^+$ and $CD8^+$ T cells. Furthermore, immunogenicity testing of the RBD recombinant protein against SARS-CoV-2 developed by West China Hospital showed that the percentage of $CD4^+$ cells producing IFN-γ was approximately 5.0% when compared to the control (1.5% $CD4^+$ T cells producing IFN-γ). Similarly, the percentage of $CD8^+$ T cells producing IFN-γ was 4.0% reported to be when compared to the control (1.5% $CD8^+$ T cells producing IFN-γ) (Yang et al., 2020).

In conclusion, S-based and RBD-based recombinant protein vaccines against SARS-CoV-2 administered together with adjuvants could elicit higher percentages of $CD4^+$ and $CD8^+$ T cells. Nevertheless, the recombinant protein vaccine in the current research study was administered without the use of an adjuvant and still resulted in the elicitation of T cell responses significantly higher than the negative control. Future studies may incorporate the use of adjuvants to evaluate the increase in the percentages of $CD4^+$ and $CD8^+$ T cells producing IFN-γ. Data on T cell responses in terms of IFN-γ producing $CD4^+$ and $CD8^+$ T cells was shown to be lacking for multi-epitope vaccines such as COVAXX UB-612, EpiVacCorona, and the HLA class I and HLA-DR T cell multi-epitope vaccine. Nevertheless, the GST-6Phis recombinant protein vaccine offers certain benefits in terms of convenience and practicality of production over current multi-epitope vaccines such as COVAXX UB-612, EpiVacCorona, and the HLA class I and HLA-DR T cell which are all synthesized using synthetic peptides. Large-scale production of such multi-epitope vaccines is costly and time-consuming. In contrast, the GST-6Phis recombinant protein vaccine

could conveniently be scaled to produce large quantities of the vaccine for large-scale public use. The incorporation of adjuvants could additionally significantly bolster the immune response to produce large quantities of the vaccine for public use.

Humoral Immunity

In the current research study, both intranasal and intramuscular administration of GST-6Phis resulted in the elicitation of high IgG antibody levels. It is important to compare the IgG antibody titers elicited from the administration of GST-6Phis to those elicited from the administration of other recombinant proteins in BALB/c mice. Immunogenicity data in mice showed that intramuscular NVX-CoV2373 immunization resulted in anti-S IgG production of approximately 5 anti-SARS-CoV-2 S IgG half-maximal inhibitory concentration (IC50) log10. Overall the addition of adjuvants was shown to further improve immunogenicity. For example, mice that were immunized with the 0.1 μg, 1 μg, or 10 μg of NVX-CoV2373 adjuvanted with Matrix-M had significantly higher anti-S IgG titers ($p \leq 0.00006$) when compared with mice that had been immunized with 10 μg of unadjuvanted NVX-CoV2373 which reflected a tenfold or more dose sparing attributable to the Matrix-M adjuvant (Tian et al., 2021).

Evaluation of the immunogenicity of the Covax-19 vaccine expressing the full-length S protein as reported by Li et al. (2021) showed that serum IgG levels measured as absorbance at 450 nm were approximately 0.7 for mice immunized with 1 μg of the RBD vaccine alone, 2.0 for mice immunized with 1 μg of the RBD vaccine and Advax adjuvant (delta inulin polysaccharide particles formuated with Toll-like receptor 9 (TLR9)-active oligonucleotide, CpG55.2), and rising to 2.8 for mice immunized with 5 μg of the RBD vaccine and Advax adjuvant., furthermore, in the study evaluating the immunogenicity of an RBD recombinant protein against SARS-CoV-2 developed by West China Hospital, Yang et al. (2020) reported serum IgG levels measured as

absorbance at 450 nm. Administration of 10 µg of the RBD vaccine with 50 µl of Al(OH)3 resulted in 0.3 IgG antibody titers in terms of absorbance (450 nm) values at 1:50 dilution of immune sera. Data on antibody titer elicited from the administration of 10 µg of the RBD vaccine without adjuvant was not provided.

Immunogenicity evaluation in terms of S1-RBD-specific IgG antibody responses was conducted upon the administration of 3 µg, 9 µg or 30 µg of the COVAXX UB-612 multi-epitope vaccine in BALB/c mice. The results showed that S1-RBD-specific IgG antibody titers measured at Week 3 had a significant dose-dependent response trend (* $p < 0.05$ between 3 and 9 µg administration of the vaccine and *** $p < 0.005$ between 3 and 30 µg administration of the vaccine. at week three S1-RBD-specific IgG antibody responses were detected at approximately 1.5 for 3 µg, 2.0 for 9 µg, and 3.0 for 30 µg S1-RBD-specific IgG (Log10) (Guirakhoo et al., 2021).

Another multiepitope vaccine candidate against SARS-CoV-2 consisted of SARS-CoV-2 S, M, and N fused together to form an S-N-M construct) consisting of CTLs, HTLs, and linear B lymphocyte epitopes. the multiepitope S-N-M construct adjuvanted with Montanide 720 was able to significantly induce total IgG production. Evaluation of S-N-M-specific IgG levels was assessed in terms of absorbance at 450 nm. three weeks after administration of the vaccine, IgG levels reached absorbance at 450 nm levels higher than 3.0 three weeks after vaccine administration and dropped to approximately 2.7 three months after the last vaccine administration. Absorbance values were significantly higher than those compared with the administration of PBS (Khairkhah et al., 2022).

It is worth noting that the current study assessed IgG responses in terms of absorbance (450 nm) as well as in terms of mean reciprocal IgG titer. However, NVX-CoV2373 and COVAXX UB-612 measured IgG levels in terms of antigen-specific log10 values which makes it challenging

to make direct comparisons with the IgG results of the current study. Nevertheless, valid comparisons may be made in terms of IgG production between the current study and other recombinant protein immunogenicity results. The S-N-M multi-epitope vaccine and the Covax-19 vaccine resulted in higher absorbance levels upon administration of the highest adjuvanted vaccine dosage. Nevertheless, GST-6Phis fared better than the RBD vaccine developed by West China Hospital with substantially higher absorbance (450 nm) values even without the use of an adjuvant.

Moreover, it was noteworthy that other vaccine candidates conducted mice immunizations after incorporating adjuvants to improve the immune response. However, the current study did not incorporate adjuvants and the purified protein of interest was directly injected into mice. Despite the elicitation of significantly higher IgG levels as indicated by absorbance and mean reciprocal absorbance values than the control, it is reasoned that the use of adjuvants in future experiments may further boost total IgG responses.

The cPASS kit which was specially designed to gain insights into neutralizing antibody activity within the laboratory without the need for live virus challenge studies showed that sera obtained from BALB/c mice immunized both intramuscularly and intranasally with GST-6Phis tested positive for the existence of nAbs capable of inhibiting the interaction between the SARS-CoV-2 Wuhan RBD and the ACE2 receptor while only sera obtained from BALB/c mice immunized intramuscularly with GST-6Phis tested positive for the existence of nAbs against the Omicron strain.

Other studies have pseudovirus and live virus studies to determine neutralizing activity. For example, immunization with 10 µg of NVX-CoV2373 adjuvanted with Matrix-M elicited nAbs that inhibited interaction between the SARS-CoV-2 RBD and the ACE2 host receptor 21–

28 days after a single priming dose (Tian et al., 2021). Similarly, mice immunized with the RBD-based vaccine consisted of nAbs capable of neutralizing infection when tested with pseudovirus and live virus studies (Yang et al., 2020). The Covax-19 S protein-based vaccine elicited high levels of nAbs that not only neutralized infection by the B.1.319 virus but also by the B.1.1.7 strain (Li et al., 2021). The COVAXX UB-612 vaccine also elicited potent levels of nAbs in the sera of immunized mice.

However, recombinant protein vaccine development was primarily focused on the S protein or the RBD of the S1 SARS-CoV-2 subunit. Nevertheless, the recombinant protein vaccine in the research study consisted of conserved B and T cell epitopes. Intramuscular and intranasal administration of the recombinant protein vaccine resulted in nAbs capable of inhibiting the binding of SARS-CoV-2 Wuhan RBD to the ACE2 host cell receptor. Additionally, intramuscular administration of the recombinant protein vaccine was also able to inhibit the binding of SARS-CoV-2 Omicron RBD to the ACE2 host cell receptor. This represents a major finding, demonstrating the ability of the vaccine to provide cross-protection against the Omicron VOC attributable to the incorporation of conserved epitopes in the B6 and B10 peptides.

It has been well established that when antigens are introduced directly at a mucosal surface, they can have a significant impact on the elicitation of adaptive immune responses (Iwasaki, 2016). Different immune cells are present at the respective sites and there is also variability in how the immune system responds to these cells. The current research study demonstrated that intranasal immunization resulted in stronger $CD8^+$ T cell response when compared to $CD8^+$ T cell responses elicited from the intramuscular route of immunization.

Cokarić Brdovčak et al. (2022) evaluated B and T cell responses following immunization of BALB/c mice with ChAdOx1-S using the intranasal and intramuscular routes. Intranasal

administration of ChAdOx1-S was able to elicit superior mucosal immune responses. Significantly higher percentages of epitope-specific CD8$^+$ T cells were observed in the lungs of mice immunized intranasally with ChAdOx1-S. immunization with ChAdOx1-S resulted in the elicitation of CD8$^+$ T cells in both mice immunized intranasally and intramuscularly with the vaccine, there were significantly higher percentages of epitope-specific CD8 T cells in the lungs showing a tissue-resident phenotype in mice immunized intranasally than mice immunized intramuscularly with the vaccine.

In the context of the research objectives, the significant IgG antibody response to GST-6Phis as well as the presence of neutralizing antibodies holds promising implications. The presence of specific IgG antibodies suggested the potential for protective immunity against the target pathogen. Further investigations could explore the functional attributes of these antibodies, such as their ability to neutralize the antigen or enhance phagocytosis, shedding light on the mechanisms underlying the postulated protection. Building upon these findings, future research endeavours could investigate the durability and longevity of the IgG antibody response following immunization with GST-6Phis. Additionally, studies focusing on the efficacy of the vaccine in live challenges could provide valuable insights into its mechanism of protection. Moreover, the IgG responses were elicited against the B6 and B10 SARS-CoV-2 epitopes. These findings align with the primary objective of the research study, which aims to show that the vaccine can confer humoral responses against specific epitopes from the SARS-CoV-2 viral protein. Both intramuscular and intranasal administration of the recombinant protein vaccine was able to induce an IgG antibody response which indicates its suitability for protecting against targeted B cell epitopes. The neutralizing potential of the vaccine against the Wuhan and Omicron strains further demonstrates the completion of the objectives of the study.

Recommendations for future studies

Glycosylation is a critical post-translational modification (PTM) that is essential for the proper folding, stability, and function of many eukaryotic proteins. E. coli, being a prokaryotic system, lacks the machinery for performing glycosylation. Alternatives include mammalian cell lines (CHO or HEK293 cells), insect cells (Baculovirus expression system), or yeast (*Pichia pastoris* or *Saccharomyces cerevisiae*) which are known for their complex glycosylation capabilities.

The cytotoxicity of GST-6Phis was not evaluated before administering it to mice. This decision was influenced by constraints which would significantly delay the duration of the Masters research project. Moreover, the literature was extensively studied to determine the amount of recombinant protein that could be safely administered to mice. Indeed, the administration of 10 μg of the NVX-CoV2373 vaccine was well tolerated and immunogenic (Tian et al., 2021). Using an amount supported by the literature was deemed to be reasonable to keep the cytotoxicity of the vaccine at low levels.

Nevertheless, it is recognized that the cell viability of splenocytes may also be effectively measured using the MTT assay. For example, Alnuqaydan et al. (2022) isolated splenocytes (lymphocytes) from BALB/c mice and determined cell viability. This was done by plating splenocytes on a cell culture plate. Plated cells were exposed to different amounts of Withaferin A, followed by incubation and the addition of MTT. The absorbance at 570 nm was measured using an ELISA plate reader, and the data was analysed to determine the percentage of viable cells. Future studies that have more flexible study time frames could conduct cytotoxicity evaluation before administration of the vaccine to animal models.

Another limitation of the study was that endotoxicity levels of GST-6Phis were not assessed before the immunogenicity study. The decision to not conduct an endotoxicity study was influenced by practical considerations of time constraints and budget limitations. Conducting an endotoxicity study requires resources in terms of time, funding, and specialized assays. Given the constraints that were faced, other aspects of the research were prioritized to obtain significant results in terms of IFN-γ production by $CD4^+$ and $CD8^+$ T cells, nAbs, and IgG antibodies. These assays could be effectively conducted within the available resources.

Nevertheless, in future preclinical investigations conducted on a larger scale and involving larger animal models, it is recommended to incorporate an endotoxicity study into the experimental design. Such a study would contribute to a more comprehensive understanding of the potential effects of endotoxins on the experimental outcomes. By assessing endotoxicity levels, researchers can ensure the safety and accuracy of their findings, further enhancing the reliability and translational relevance of the study's results.

Moreover, it is recognized that the sample size of the experiment was small and kept small to a manageable size. There were a total of only 20 mice for the 4 groups (n=5). The limitation arising from the small sample size of 20 mice in this study introduces challenges when attempting to extend the study's findings to a broader population. A smaller sample size raises several concerns. Notably, the precision and accuracy of the data could be compromised, leading to reduced confidence in the extent to which the results accurately depict real-world situations. Additionally, the implications and broader applicability of the study's outcomes might be restricted due to the limited number of subjects.

According to Hackshaw (2008), small sample sizes lack reliability and the adoption of a 95% confidence interval is advised to enhance result dependability. The utilization of a small

sample size can complicate result interpretation, as drawing meaningful conclusions from the collected data becomes challenging. Hackshaw (2008) further clarifies that research data guide the prediction of the true effect by evaluating the observed estimate and the 95% confidence intervals. In the context of the mice immunization study, this limitation is particularly relevant. The small sample size curtails our capacity to confidently extend findings to a larger population, especially considering the intrinsic variability among individual mice. Future endeavours involving larger mouse cohorts would facilitate a more comprehensive exploration of immunization effects, thereby strengthening the basis for deriving accurate and dependable conclusions.

In the future, research efforts equipped with adequate resources and a broader time frame may increase the size of the mouse cohort. A larger number of mice in the study could offer enhanced statistical power, enabling a more robust analysis of the immunization effects. This increase in sample size could lead to a more representative and reliable depiction of the population under study, mitigating potential biases arising from the inherent variability among individual mice. Additionally, a larger sample size can augment the precision of estimations, bolstering the confidence levels in the observed outcomes. By addressing the current limitation of a small sample size, future investigations would be better poised to draw substantiated conclusions with greater generalizability, thus contributing to the advancement of knowledge in the field of mice immunization studies.

In response to the evolving nature of SARS-CoV-2 and the rapid emergence of new and potentially more challenging variants, innovative approaches are needed to effectively combat the ongoing COVID-19 pandemic. Reverse vaccinology has emerged as a promising strategy in this context. Within the SARS-CoV-2 genome and VOCs, researchers can pinpoint certain viral components that are conserved, such as essential protein sections or epitopes that are critical for

135

viral entry, replication, or immune evasion. Scientists can create vaccines that vigorously stimulate immune responses against a wide range of strains, including new variants, by focusing on these essential components. This proactive strategy enables vaccine development tactics and design flexibility to potentially reduce the impact of new SARS-CoV-2 mutations. Although the current research project focuses on the incorporation of identified epitopes to develop recombinant protein vaccines, future efforts should also explore the incorporation of such epitopes into DNA, mRNA, and viral-vectored vaccines.

CHAPTER 6: CONCLUSION

This research study demonstrates the effectiveness of the use of highly conserved and immunogenic peptides representing B and T cell epitopes to develop vaccines to confer protection against the SARS-CoV-2 Wuhan and Omicron strains. The six peptides selected through literature mining approaches were used to develop a recombinant protein vaccine. When the GST-6Phis protein of interest was used to immunize BALB/c mice through the intramuscular and intranasal routes, it resulted in the elicitation of both cellular and immune responses. While immunization through the intramuscular route was effective in producing IFN-γ secreting $CD3^+$ $CD4^+$ T cells, intranasal immunization resulted in the induction of IFN-γ secreting $CD3^+$ $CD8^+$ T cells. Moreover, both intranasal and intramuscular immunizations with GST-6P were associated with high IgG antibody responses in terms of mean reciprocal antibody titers. Furthermore, both immunization routes produced nAbs against the SARS-CoV-2 Wuhan strain, while intramuscular immunization resulted in nAbs against Omicron. It may be said that the intramuscular route was more effective in terms of neutralizing potential of the immune response. The results indicate that epitope-based vaccines may be a promising way to immunize against emerging VOCs based on the identification of broadly conserved and immunogenic B and T cell epitopes.

REFERENCES

Alfaro-Murillo, J. A., Ávila-Agüero, M. L., Fitzpatrick, M. C., Crystal, C. J., Falleiros-Arlant, L. H., & Galvani, A. P. (2020). The case for replacing live oral polio vaccine with inactivated vaccine in the Americas. *Lancet (London, England), 395*(10230), 1163–1166. https://doi.org/10.1016/S0140-6736(20)30213-0

Al-Fattah Yahaya, A. A., Khalid, K., Lim, H. X., & Poh, C. L. (2023). Development of next generation vaccines against SARS-CoV-2 and variants of concern. *Viruses*, *15*(3), 624.

Altmann, F., Staudacher, E., Wilson, I. B., & März, L. (1999). Insect cells as hosts for the expression of recombinant glycoproteins. *Glycotechnology*, 29-43.

Agerer, B., Koblischke, M., Gudipati, V., Montaño-Gutierrez, L. F., Smyth, M., Popa, A., Genger, J. W., Endler, L., Florian, D. M., Mühlgrabner, V., Graninger, M., Aberle, S. W., Husa, A. M., Shaw, L. E., Lercher, A., Gattinger, P., Torralba-Gombau, R., Trapin, D., Penz, T., Barreca, D., et al. (2021). SARS-CoV-2 mutations in MHC-I-restricted epitopes evade CD8(+) T cell responses. *Sci Immunol*, *6*(57). https://doi.org/10.1126/sciimmunol.abg6461

Ahmed, S., Khan, S., Imran, I., Al Mughairbi, F., Sheikh, F. S., Hussain, J., Khan, A., & Al-Harrasi, A. (2021). Vaccine development against COVID-19: Study from pre-clinical phases to clinical trials and global use. *Vaccines*, *9*(8). https://doi.org/10.3390/vaccines9080836

Aiyegbusi, O. L., Hughes, S. E., Turner, G., Rivera, S. C., McMullan, C., Chandan, J. S., Haroon, S., Price, G., Davies, E. H., Nirantharakumar, K., Sapey, E., & Calvert, M. J. (2021). Symptoms, complications and management of long COVID: A review. *J R Soc Med*, *114*(9), 428-442. https://doi.org/10.1177/01410768211032850

Alanagreh, L., Alzoughool, F., & Atoum, M. (2020). The human coronavirus disease COVID-19: Its origin, characteristics, and insights into potential drugs and its mechanisms. *Pathogens*, *9*(5). https://doi.org/10.3390/pathogens9050331

Alnuqaydan, A. M., Almutary, A., Bhat, G. R., Mir, T. A., Wani, S. I., Rather, M. Y., Mir, S. A., Alshehri, B., Alnasser, S., Ali Zainy, F. M., & Rah, B. (2022). Evaluation of the cytotoxic, anti-inflammatory, and immunomodulatory effects of Withaferin A (WA) against lipopolysaccharide (LPS)-induced inflammation in immune cells derived from BALB/c mice. *Pharmaceutics*, *14*(6), 1256. https://doi.org/10.3390/pharmaceutics14061256

Amanat, F., Strohmeier, S., Rathnasinghe, R., Schotsaert, M., Coughlan, L., García-Sastre, A., & Krammer, F. (2020). Introduction of two prolines and removal of the polybasic cleavage site leads to optimal efficacy of a recombinant spike based SARS-CoV-2 vaccine in the mouse model. *bioRxiv*, 2020.09.16.300970. https://doi.org/10.1101/2020.09.16.300970

Arora, S., Rani, R., & Ghosh, S. (2018). Bioreactors in solid state fermentation technology: Design, applications and engineering aspects. *Journal of Biotechnology, 269*, 16-34.

Atapour, A., Vosough, P., Jafari, S., & Sarab, G. A. (2022). A multi-epitope vaccine designed against blood-stage of malaria: an immunoinformatic and structural approach. *Scientific Reports, 12*(1), 11683. https://doi.org/10.1038/s41598-022-15956-3

Ayat, N. R., Sun, Z., Sun, D., Yin, M., Hall, R. C., Vaidya, A. M., Liu, X., Schilb, A., Scheidt, J., & Lu, Z. R. (2019). Formulation of biocompatible targeted ECO/siRNA nanoparticles with long-term stability for clinical translation of RNAi. *Nucleic Acid Therapeutics*, *29*(4), 195-207.

Ayyagari, V. S., T C, V., K, A. P., & Srirama, K. (2022). Design of a multi-epitope-based

    vaccine targeting M-protein of SARS-CoV2: An immunoinformatics approach. *Journal*

    of Biomolecular Structure & Dynamics, 40(7), 2963–2977.

    https://doi.org/10.1080/07391102.2020.1850357

Baden, L. R., El Sahly, H. M., Essink, B., Kotloff, K., Frey, S., Novak, R., Diemert, D., Spector,

    S. A., Rouphael, N., Creech, C. B., McGettigan, J., Khetan, S., Segall, N., Solis, J.,

    Brosz, A., Fierro, C., Schwartz, H., Neuzil, K., Corey, L., Gilbert, P., et al. (2021).

    Efficacy and Safety of the mRNA-1273 SARS-CoV-2 Vaccine. *N Engl J Med*, *384*(5),

    403-416. https://doi.org/10.1056/NEJMoa2035389

Barbier, A. J., Jiang, A. Y., Zhang, P., Wooster, R., & Anderson, D. G. (2022). The clinical

    progress of mRNA vaccines and immunotherapies. *Nature biotechnology*, *40*(6), 840-

    854.

Belitski, M., Guenther, C., Kritikos, A. S., & Thurik, R. (2022). Economic effects of the

    COVID-19 pandemic on entrepreneurship and small businesses. *Small Business*

    Economics, *58*(2), 593–609. https://doi.org/10.1007/s11187-021-00544-y

Boni, C., Cavazzini, D., Bolchi, A., Rossi, M., Vecchi, A., Tiezzi, C., Barili, V., Fisicaro, P.,

    Ferrari, C., & Ottonello, S. (2021). Degenerate CD8 epitopes mapping to structurally

    constrained regions of the spike protein: AT cell-based way-out from the SARS-CoV-2

    variants storm. *Frontiers in Immunology*, *12*, 730051.

Braun, J., Loyal, L., Frentsch, M., Wendisch, D., Georg, P., Kurth, F., Hippenstiel, S.,

    Dingeldey, M., Kruse, B., Fauchere, F., Baysal, E., Mangold, M., Henze, L., Lauster, R.,

    Mall, M., Beyer, K., Röhmel, J., Voigt, S., Schmitz, J., Miltenyi, S., et al. (2020). SARS-

CoV-2-reactive T cells in healthy donors and patients with COVID-
19. *Nature*, *587*(7833), 270-274.

Burton D. R. (2017). What are the most powerful immunogen design vaccine strategies? Reverse
vaccinology 2.0 shows great promise. *Cold Spring Harbor Perspectives in Biology,*
9(11), a030262. https://doi.org/10.1101/cshperspect.a030262

Carabelli, A. M., Peacock, T. P., Thorne, L. G., Harvey, W. T., Hughes, J., de Silva, T. I.,
Peacock, S. J., Barclay, W. S., de Silva, T. I., Towers, G. J., Robertson, D. L., &
Consortium, C.-G. U. (2023). SARS-CoV-2 variant biology: immune escape,
transmission and fitness. *Nature Reviews Microbiology*, *21*(3), 162-177.
https://doi.org/10.1038/s41579-022-00841-7

Cao, Y., & Gao, G. F. (2021). mRNA vaccines: A matter of delivery. *EClinicalMedicine*, *32*.

Cao, Y., Wang, J., Jian, F., Xiao, T., Song, W., Yisimayi, A., Huang, W., Li, Q., Wang, P, An,
R., Wang, J., Wang, Y., Niu, X., Yang, S., Liang, H., Sun, H., Li, T., Yu, Y., Cui, Q.,
Liu, S., et al. (2022). Omicron escapes the majority of existing SARS-CoV-2 neutralizing
antibodies. *Nature*, *602*(7898), 657-663.
https://doi.org/10.1038/s41586-021-04385-3

Cele, S., Jackson, L., Khoury, D. S., Khan, K., Moyo-Gwete, T., Tegally, H., San, J. E., Cromer,
D., Scheepers, C., Amoako, D. G., Karim, F., Bernstein, M., Lustig, G., Archary, D.,
Smith, M., Ganga, Y., Jule, Z., Reedoy, K., Hwa, S. H., Giandhari, J., et al. (2022).
Omicron extensively but incompletely escapes Pfizer BNT162b2 neutralization. *Nature*,
602(7898), 654-656. https://doi.org/10.1038/s41586-021-04387-1

Chakraborty, C., Bhattacharya, M., Sharma, A. R., & Mallik, B. (2022). Omicron (B.1.1.529) - A
new heavily mutated variant: Mapped location and probable properties of its mutations

with an emphasis on S-glycoprotein. *International Journal of Biological Macromolecules*, *219*, 980-997. https://doi.org/10.1016/j.ijbiomac.2022.07.254

Chalkias, S., Whatley, J., Eder, F., Essink, B., Khetan, S., Bradley, P., Brosz, A., McGhee, N., Tomassini, J. E., Chen, X., Zhao, X., Sutherland, A., Shen, X., Girard, B., Edwards, D. K., Feng, J., Zhou, H., Walsh, S., Montefiori, D. C., Baden, L. R., Miller, J. M., & Das, R. (2022). Safety and Immunogenicity of Omicron BA.4/BA.5 Bivalent Vaccine Against Covid-19. *medRxiv*, https://doi.org/10.1101/2022.12.11.22283166

Cheng, F., Wang, Y., Bai, Y., Liang, Z., Mao, Q., Liu, D., Wu, X., & Xu, M. (2023). Research Advances on the Stability of mRNA Vaccines. *Viruses*, *15*(3), 668. https://doi.org/10.3390/v15030668

Cheng, S. M. S., Mok, C. K. P., Leung, Y. W. Y., Ng, S. S., Chan, K. C. K., Ko, F. W., Chen, C., Yiu, K., Lam, B. H. S., Lau, E. H. Y., Chan, K. K. P., Luk, L. L. H., Li, J. K. C., Tsang, L. C. H., Poon, L. L. M., Hui, D. S. C., & Peiris, M. (2022). Neutralizing antibodies against the SARS-CoV-2 Omicron variant BA.1 following homologous and heterologous CoronaVac or BNT162b2 vaccination. *Nature Medicine*, *28*(3), 486-489. https://doi.org/10.1038/s41591-022-01704-7

Chen, Z., Ruan, P., Wang, L., Nie, X., Ma, X., & Tan, Y. (2021). T and B cell epitope analysis of SARS-CoV-2 S protein based on immunoinformatics and experimental research. *Journal of Cellular and Molecular Medicine*, *25*(2), 1274-1289. https://doi.org/10.1111/jcmm.16200

Cokarić Brdovčak, M., Materljan, J., Šustić, M., Ravlić, S., Ružić, T., Lisnić, B., Miklić, K., Brizić, I., Pribanić Matešić, M., Juranić Lisnić, V., Halassy, B., Rončević, D., Knežević, Z., Štefan, L., Bertoglio, F., Schubert, M., Čičin-Šain, L., Markotić, A., Jonjić, S., &

Krmpotić, A. (2022). ChAdOx1-S adenoviral vector vaccine applied intranasally elicits superior mucosal immunity compared to the intramuscular route of vaccination. *European Journal of Immunology*, *52*(6), 936-945. https://doi.org/https://doi.org/10.1002/eji.202249823

Collier, D. A., De Marco, A., Ferreira, I. A. T. M., Meng, B., Datir, R. P., Walls, A. C., Kemp, S. A., Bassi, J., Pinto, D., Silacci-Fregni, C., Bianchi, S., Tortorici, M. A., Bowen, J., Culap, K., Jaconi, S., Cameroni, E., Snell, G., Pizzuto, M. S., Pellanda, A. F., Garzoni, C., et al. *Nature*, *593*(7857), 136-141. https://doi.org/10.1038/s41586-021-03412-7

Corbett, K. S., Edwards, D., Leist, S. R., Abiona, O. M., Boyoglu-Barnum, S., Gillespie, R. A., Himansu, S., Schäfer, A., Ziwawo, C. T., DiPiazza, A. T., Dinnon, K. H., Elbashir, S. M., Shaw, C. A., Woods, A., Fritch, E. J., Martinez, D. R., Bock, K. W., Minai, M., Nagata, B. M., Hutchinson, et al. (2020). SARS-CoV-2 mRNA vaccine development enabled by prototype pathogen preparedness. *bioRxiv*, 2020.2006.2011.145920. https://doi.org/10.1101/2020.06.11.145920

Cosar, B., Karagulleoglu, Z. Y., Unal, S., Ince, A. T., Uncuoglu, D. B., Tuncer, G., Kilinc, B. R., Ozkan, Y. E., Ozkoc, H. C., Demir, I. N., Eker, A., Karagoz, F., Simsek, S. Y., Yasar, B., Pala, M., Demir, A., Atak, I. N., Mendi, A. H., Bengi, V. U., Cengiz Seval, G., et al. (2022). SARS-CoV-2 Mutations and their Viral Variants. *Cytokine Growth Factor Rev*, *63*, 10-22. https://doi.org/10.1016/j.cytogfr.2021.06.001

Cucinotta, D., & Vanelli, M. (2020). WHO Declares COVID-19 a Pandemic. *Acta bio-medica : Atenei Parmensis*, *91*(1), 157–160. https://doi.org/10.23750/abm.v91i1.9397

da Silva, M. K., Campos, D. M. d. O., Akash, S., Akter, S., Yee, L. C., Fulco, U. L., & Oliveira, J. I. N. (2023). Advances of reverse vaccinology for mRNA vaccine design against

SARS-CoV-2: A review of methods and tools. *Viruses*, *15*(10), 2130.

https://www.mdpi.com/1999-4915/15/10/2130

Dai, L., & Gao, G. F. (2021). Viral targets for vaccines against COVID-19. *Nature Reviews.*
Immunology, *21*(2), 73-82. https://doi.org/10.1038/s41577-020-00480-0

Dai, J., Sang, X., Menhas, R., Xu, X., Khurshid, S., Mahmood, S., Weng, Y., Huang, J., Cai, Y.,
Shahzad, B., Iqbal, W., Gul, M., Saqib, Z. A., & Alam, M. N. (2021). The Influence of
COVID-19 Pandemic on Physical Health-Psychological Health, Physical Activity, and
Overall Well-Being: The Mediating Role of Emotional Regulation. *Front Psychol*, *12*,
667461. https://doi.org/10.3389/fpsyg.2021.667461

Dan, J. M., Mateus, J., Kato, Y., Hastie, K. M., Yu, E. D., Faliti, C. E., Grifoni, A., Ramirez, S.
I., Haupt, S., Frazier, A., Nakao, C., Rayaprolu, V., Rawlings, S. A., Peters, B.,
Krammer, F., Simon, V., Saphire, E. O., Smith, D. M., Weiskopf, D., Sette, A., & Crotty,
S. (2021). Immunological memory to SARS-CoV-2 assessed for up to 8 months after
infection. *Science*, *371*(6529), eabf4063. https://doi.org/doi:10.1126/science.abf4063

Deng, W., & Sweeney, R. W. (2022). Intramuscular injection of a mixture of COVID-19 peptide
vaccine and tetanus vaccine in horse induced neutralizing antibodies against authentic
virus of SARS-CoV-2 Delta variant. *Vaccine: X*, *12*, 100230
https://doi.org/10.1016/j.jvacx.2022.100230

Dhar Chowdhury, S., & Oommen, A. M. (2020). Epidemiology of COVID-19. *Journal of*
Digestive Endoscopy, *11*(1), 3–7. https://doi.org/10.1055/s-0040-1712187

Diao, B., Wang, C., Tan, Y., Chen, X., Liu, Y., Ning, L., Chen, L., Li, M., Liu, Y., Wang, G.,
Yuan, Z., Feng, Z., Wu, Y., Chen, Y. (2020). Reduction and functional exhaustion of T

cells in patients with Coronavirus Disease 2019 (COVID-19). *Frontiers in Immunology*, *11*. https://doi.org/10.3389/fimmu.2020.00827

ECDC. (2024). SARS-CoV-2 variants of concern as of 15 March 2024. Retrieved from https://www.ecdc.europa.eu/en/covid-19/variants-concern

El Sahly, H. M., Baden, L. R., Essink, B., Montefiori, D., McDermont, A., Rupp, R., Lewis, M., Swaminathan, S., Griffin, C., Fragoso, V., Miller, V. E., Girard, B., Paila, Y. D., Deng, W., Tomassini, J. E., Paris, R., Schödel, F., Das, R., August, A., Leav, B., Miller, J. M., Zhou, H., & Pajon, R. (2022). Humoral Immunogenicity of the mRNA-1273 Vaccine in the Phase 3 Coronavirus Efficacy (COVE) Trial. *J Infect Dis*, *226*(10), 1731-1742. https://doi.org/10.1093/infdis/jiac188

Enayatkhani, M., Hasaniazad, M., Faezi, S., Gouklani, H., Davoodian, P., Ahmadi, N., Einakian, M. A., Karmostaji, A., & Ahmadi, K. (2021). Reverse vaccinology approach to design a novel multi-epitope vaccine candidate against COVID-19: An in silico study. *Journal of Biomolecular Structure & Dynamics, 39*(8), 2857–2872. https://doi.org/10.1080/07391102.2020.1756411

Falsey, A. R., Sobieszczyk, M. E., Hirsch, I., Sproule, S., Robb, M. L., Corey, L., Neuzil, K. M., Hahn, W., Hunt, J., Mulligan, M. J., McEvoy, C., DeJesus, E., Hassman, M., Little, S. J., Pahud, B. A., Durbin, A., Pickrell, P., Daar, E. S., Bush, L., Solis, J., et al. (2021). Phase 3 Safety and Efficacy of AZD1222 (ChAdOx1 nCoV-19) Covid-19 Vaccine. *N Engl J Med*, *385*(25), 2348-2360. https://doi.org/10.1056/NEJMoa2105290

Farhud, D. D., & Mojahed, N. (2022). SARS-CoV-2 notable mutations and variants: A review article. *Iran J Public Health*, *51*(7), 1494-1501. https://doi.org/10.18502/ijph.v51i7.10083

Felberbaum R. S. (2015). The baculovirus expression vector system: A commercial manufacturing platform for viral vaccines and gene therapy vectors. *Biotechnology Journal, 10*(5), 702–714. https://doi.org/10.1002/biot.201400438

Flood, A., Estrada, M., McAdams, D., Ji, Y., & Chen, D. (2016). Development of a freeze-dried, heat-stable influenza subunit vaccine formulation. *PloS one*, *11*(11), e0164692. https://doi.org/10.1371/journal.pone.0164692

Fujita-Yamaguchi, Y. (2015). Affinity chromatography of native and recombinant proteins from receptors for insulin and IGF-I to recombinant single chain antibodies. *Frontiers in Endocrinology*, *6*, 166.

Gallais, F., Velay, A., Nazon, C., Wendling, M.-J., Partisani, M., Sibilia, J., Candon, S., & Fafi-Kremer, S. (2021). Intrafamilial exposure to SARS-CoV-2 associated with cellular immune response without seroconversion, France. *Emerging Infectious Diseases*, *27*(1), 113-121. https://doi.org/10.3201/eid2701.203611

Ghaemi, A., Roshani Asl, P., Zargaran, H., Ahmadi, D., Hashimi, A. A., Abdolalipour, E., Bathaeian, S., & Miri, S. M. (2022). Recombinant COVID-19 vaccine based on recombinant RBD/nucleoprotein and saponin adjuvant induces long-lasting neutralizing antibodies and cellular immunity. *Frontiers in Immunology*, *13*, 5127.

Goepfert, P. A., Fu, B., Chabanon, A. L., Bonaparte, M. I., Davis, M. G., Essink, B. J., Frank, I., Haney, O., Janosczyk, H., Keefer, M. C., Koutsoukos, M., Kimmel, M. A., Masotti, R., Savarino, S. J., Schuerman, L., Schwartz, H., Sher, L. D., Smith, J., Tavares-Da-Silva, F., Gurunathan, S., et al. (2021). Safety and immunogenicity of SARS-CoV-2 recombinant protein vaccine formulations in healthy adults: interim results of a randomised, placebo-

controlled, phase 1-2, dose-ranging study. *The Lancet. Infectious diseases*, *21*(9), 1257–

1270. https://doi.org/10.1016/S1473-3099(21)00147-X

Gomez, P. L., & Robinson, J. M. (2018). 5 - Vaccine Manufacturing. In S. A. Plotkin, W. A.

Orenstein, P. A. Offit, & K. M. Edwards (Eds.), *Plotkin's Vaccines (Seventh Edition)* (pp.

51-60.e51). Elsevier. https://doi.org/10.1016/B978-0-323-35761-6.00005-5

Grant, M. C., Geoghegan, L., Arbyn, M., Mohammed, Z., McGuinness, L., Clarke, E. L., &

Wade, R. G. (2020). The prevalence of symptoms in 24,410 adults infected by the novel

coronavirus (SARS-CoV-2; COVID-19): A systematic review and meta-analysis of 148

studies from 9 countries. *PLoS One*, *15*(6), e0234765.

https://doi.org/10.1371/journal.pone.0234765

Greaney, A. J., Starr, T. N., Barnes, C. O., Weisblum, Y., Schmidt, F., Caskey, M., Gaebler, C.,

Cho, A., Agudelo, M., Finkin, S., Wang, Z., Poston, D., Muecksch, F., Hatziioannou, T.,

Bieniasz, P., Robbiani, D., Nussenzweig, M., Bjorkman, P., & Bloom, D., et al. (2021).

Mapping mutations to the SARS-CoV-2 RBD that escape binding by different classes of

antibodies. *Nature Communications*, *12*(1), 4196. https://doi.org/10.1038/s41467-021-

24435-8

Greenwood B. (2014). The contribution of vaccination to global health: past, present and

future. *Philosophical transactions of the Royal Society of London. Series B, Biological*

sciences, *369*(1645), 20130433. https://doi.org/10.1098/rstb.2013.0433

Gu, Y., Sun, X., Li, B., Huang, J., Zhan, B., & Zhu, X. (2017). Vaccination with a paramyosin-

based multi-epitope vaccine elicits significant protective immunity against Trichinella

spiralis infection in mice. *Frontiers in Microbiology, 8*, 1475.

Guirakhoo, F., Kuo, L., Peng, J., Huang, J.-H., Kuo, B.-S., Lin, F., Liu, Y.-J., Liu, Z., Wu, G., Ding, S., Hou, K.-L., Cheng, J., Yang, V., Jiang, H., Wang, J., Chen, T., Xia, W., Lin, E., Hung, C. H., Chen, H.-J., et al. (2021). A novel SARS-CoV-2 multitope protein/peptide vaccine candidate is highly immunogenic and prevents lung infection in an AAV hACE2 mouse model and non-human primates. *bioRxiv*, https://doi.org/10.1101/2020.11.30.399154

Guo, L., Wang, G., Wang, Y., Zhang, Q., Ren, L., Gu, X., Huang, T., Zhong, J., Wang, Y., Wang, X., Huang, L., Xu, L., Wang, C., Chen, L., Xiao, X., Peng, Y., Knight, J. C., Dong, T., Cao, B., & Wang, J. (2022). SARS-CoV-2-specific antibody and T-cell responses 1 year after infection in people recovered from COVID-19: a longitudinal cohort study. *The Lancet Microbe*, *3*(5), e348-e356. https://doi.org/10.1016/S2666-5247(22)00036-2

Hachmann, N. P., Miller, J., Collier, A. Y., Ventura, J. D., Yu, J., Rowe, M., Bondzie, E. A., Powers, O., Surve, N., Hall, K., & Barouch, D. H. (2022). Neutralization Escape by SARS-CoV-2 Omicron Subvariants BA.2.12.1, BA.4, and BA.5. *N Engl J Med*, *387*(1), 86-88. https://doi.org/10.1056/NEJMc2206576

Hanley, K. A. (2011). The double-edged sword: How evolution can make or break a live-attenuated virus vaccine. *Evolution (N Y)*, *4*(4), 635-643. https://doi.org/10.1007/s12052-011-0365-y

Haon, M., Grisel, S., Navarro, D., Gruet, A., BERRIN, J.-G., & Bignon, C. (2015). Recombinant protein production facility for fungal biomass-degrading enzymes using the yeast Pichia pastoris [Methods]. *Frontiers in Microbiology, 6*. https://doi.org/10.3389/fmicb.2015.01002

Harvey, W. T., Carabelli, A. M., Jackson, B., Gupta, R. K., Thomson, E. C., Harrison, E. M.,
Ludden, C., Reeve, R., Rambaut, A., Peacock, S. J., Robertson, D. L., & Consortium, C.-
G. U. (2021). SARS-CoV-2 variants, spike mutations and immune escape. *Nature
Reviews Microbiology*, *19*(7), 409-424. https://doi.org/10.1038/s41579-021-00573-0

Hasan, M., & Mia, M. (2022). Exploratory algorithm of a multi-epitope-based subunit vaccine
candidate against Cryptosporidium hominis: Reverse vaccinology-based
immunoinformatic approach. *International Journal of Peptide Research and
Therapeutics, 28*(5), 134. https://doi.org/10.1007/s10989-022-10438-6

Heath, P. T., Galiza, E. P., Baxter, D. N., Boffito, M., Browne, D., Burns, F., Chadwick, D. R.,
Clark, R., Cosgrove, C. A., Galloway, J., Goodman, A. L., Heer, A., Higham, A.,
Iyengar, S., Jeanes, C., Kalra, P. A., Kyriakidou, C., Bradley, J. M., Munthali, C.,
Minassian, A. M., et al. (2023). Safety and efficacy of the NVX-CoV2373 Coronavirus
Disease 2019 vaccine at completion of the placebo-controlled phase of a randomized
controlled trial. *Clinical Infectious Diseases*, *76*(3), 398-407.
https://doi.org/10.1093/cid/ciac803

Heffron, A. S., McIlwain, S. J., Amjadi, M. F., Baker, D. A., Khullar, S., Sethi, A. K.,
Palmenberg, A. C., Shelef, M. A., O'Connor, D. H., & Ong, I. M. (2021). The landscape
of antibody binding in SARS-CoV-2 infection. *bioRxiv: The preprint server for biology*,
https://doi.org/10.1101/2020.10.10.334292

Heide, J., Schulte, S., Kohsar, M., Brehm, T. T., Herrmann, M., Karsten, H., Marget, M., Peine,
S., Johansson, A. M., & Sette, A. (2021). Broadly directed SARS-CoV-2-specific CD4+
T cell response includes frequently detected peptide specificities within the membrane

and nucleoprotein in patients with acute and resolved COVID-19. PLoS pathogens, 17(9), e1009842.

Hellerstein, M. (2020). What are the roles of antibodies versus a durable, high quality T-cell response in protective immunity against SARS-CoV-2? *Vaccine: X*, *6*, 100076-100076. https://doi.org/10.1016/j.jvacx.2020.100076

Herrera L. R. M. (2021). Reverse vaccinology approach in constructing a multi-epitope vaccine against cancer-testis antigens expressed in non-small cell lung cancer. *Asian Pacific Journal of Cancer Prevention*, *22*(5), 1495–1506. https://doi.org/10.31557/APJCP.2021.22.5.1495

Hill, C. (2022). Psychological health, wellbeing and COVID-19: Comparing previously infected and non-infected South African employees. *Front Psychol*, *13*, 1013377. https://doi.org/10.3389/fpsyg.2022.1013377

Hobernik, D., & Bros, M. (2018). DNA vaccines—how far from clinical use? *International Journal of Molecular Sciences*, *19*(11), 3605.

Hu, D., Li, L., Shi, W., & Zhang, L. (2020). Less expression of CD4+ and CD8+ T cells might reflect the severity of infection and predict worse prognosis in patients with COVID-19: Evidence from a pooled analysis. *Clinica Chimica Acta*; *International Journal* of *Clinical Chemistry*, *510*, 1–4. https://doi.org/10.1016/j.cca.2020.06.040

Israel, A., Merzon, E., Schäffer, A. A., Shenhar, Y., Green, I., Golan-Cohen, A., Ruppin, E., Magen, E., & Vinker, S. (2021). Elapsed time since BNT162b2 vaccine and risk of SARS-CoV-2 infection: Test negative design study. BMJ, 375, e067873. https://doi.org/10.1136/bmj-2021-067873

Iwasaki, A. (2016). Exploiting mucosal immunity for antiviral vaccines. *Annual Review of Immunology*, *34*(1), 575-608. https://doi.org/10.1146/annurev-immunol-032414-112315

Jungreis, I., Sealfon, R., & Kellis, M. (2021). SARS-CoV-2 gene content and COVID-19 mutation impact by comparing 44 Sarbecovirus genomes. *Nature communications*, *12*(1), 2642. https://doi.org/10.1038/s41467-021-22905-7

Juraszek, J., Rutten, L., Blokland, S., Bouchier, P., Voorzaat, R., Ritschel, T., Bakkers, M. J., Renault, L. L., & Langedijk, J. P. (2021). Stabilizing the closed SARS-CoV-2 spike trimer. *Nature Communications*, *12*(1), 1-8.

Keech, C., Albert, G., Cho, I., Robertson, A., Reed, P., Neal, S., Plested, J. S., Zhu, M., Cloney-Clark, S., Zhou, H., Smith, G., Patel, N., Frieman, M. B., Haupt, R. E., Logue, J., McGrath, M., Weston, S., Piedra, P. A., Desai, C., Callahan, K., et al. (2020). Phase 1–2 Trial of a SARS-CoV-2 Recombinant Spike Protein Nanoparticle Vaccine. *New England journal of medicine*, *383*(24), 2320-2332. https://doi.org/10.1056/NEJMoa2026920

Kemp, S. A., Meng, B., Ferriera, I. A., Datir, R., Harvey, W. T., Papa, G., Lytras, S., Collier, D. A., Mohamed, A., Gallo, G., Thakur, N., Consortium, T. C.-G. U., Carabelli, A. M., Kenyon, J. C., Lever, A. M., De Marco, A., Saliba, C., Culap, K., Cameroni, E., Piccoli, L., et al. (2021). Recurrent emergence and transmission of a SARS-CoV-2 spike deletion H69/V70. *bioRxiv*, 2020.2012.2014.422555. https://doi.org/10.1101/2020.12.14.422555

Khairkhah, N., Bolhassani, A., Agi, E., Namvar, A., & Nikyar, A. (2022). Immunological investigation of a multiepitope peptide vaccine candidate based on main proteins of SARS CoV-2 pathogen. *Plos one*, *17*(6), e0268251. https://doi.org/10.1371/journal.pone.0268251

Khalid, K., & Poh, C. L. (2023). The development of DNA vaccines against SARS-CoV-2. *Advances in Medical Sciences*, *68*(2), 213-226.

Kingstad-Bakke, B., Lee, W., Chandrasekar, S. S., Gasper, D. J., Salas-Quinchucua, C., Cleven, T., Sullivan, J. A., Talaat, A., Osorio, J. E., & Suresh, M. (2022). Vaccine-induced systemic and mucosal T cell immunity to SARS-CoV-2 viral variants. Proceedings of the National Academy of Sciences, 119(20), e2118312119.

Kirchdoerfer, R. N., Wang, N., Pallesen, J., Wrapp, D., Turner, H. L., Cottrell, C. A., Corbett, K. S., Graham, B. S., McLellan, J. S., & Ward, A. B. (2018). Stabilized coronavirus spikes are resistant to conformational changes induced by receptor recognition or proteolysis. *Scientific reports*, *8*(1), 15701. https://doi.org/10.1038/s41598-018-34171-7

Kost, T. A., Condreay, J. P., & Jarvis, D. L. (2005). Baculovirus as versatile vectors for protein expression in insect and mammalian cells. *Nature Biotechnology, 23*(5), 567-575. https://doi.org/10.1038/nbt1095

Krammer, F. (2020). SARS-CoV-2 vaccines in development. *Nature*, *586*(7830), 516-527.

Krishna, M., & Nadler, S. G. (2016). Immunogenicity to biotherapeutics–the role of anti-drug immune complexes. *Frontiers in immunology*, *7*, 21.

Kudriavtsev, A. V., Vakhrusheva, A. V., Novoseletsky, V. N., Bozdaganyan, M. E., Shaitan, K. V., Kirpichnikov, M. P., & Sokolova, O. S. (2022). Immune escape associated with RBD omicron mutations and SARS-CoV-2 evolution dynamics. *Viruses*, *14*(8), 1603. https://doi.org/10.3390/v14081603

Kutzler, M. A., & Weiner, D. B. (2008). DNA vaccines: Ready for prime time? *Nature Reviews Genetics*, *9*(10), 776-788.

Lai, C. Y., To, A., Wong, T. A. S., Lieberman, M. M., Clements, D. E., Senda, J. T., Ball, A. H.,
Pessaint, L., Andersen, H., Donini, O., & Lehrer, A. T. (2021). Recombinant protein
subunit SARS-CoV-2 vaccines formulated with CoVaccine HT adjuvant induce broad,
Th1 biased, humoral and cellular immune responses in mice. *bioRxiv: The preprint server
for biology*, https://doi.org/10.1101/2021.03.02.433614

Levin Einav, G., Lustig, Y., Cohen, C., Fluss, R., Indenbaum, V., Amit, S., Doolman, R., Asraf,
K., Mendelson, E., Ziv, A., Rubin, C., Freedman, L., Kreiss, Y., & Regev-Yochay, G.
(2021). Waning immune humoral response to BNT162b2 Covid-19 vaccine over 6
months. *New England Journal of Medicine, 385*(24), e84.
https://doi.org/10.1056/NEJMoa2114583

Li, L., Honda-Okubo, Y., Huang, Y., Jang, H., Carlock, M. A., Baldwin, J., Piplani, S., Bebin-
Blackwell, A. G., Forgacs, D., Sakamoto, K., Stella, A., Turville, S., Chataway, T.,
Colella, A., Triccas, J., Ross, T. M., & Petrovsky, N. (2021). Immunisation of ferrets and
mice with recombinant SARS-CoV-2 spike protein formulated with Advax-SM adjuvant
protects against COVID-19 infection. *Vaccine, 39*(40), 5940–5953. https://doi.org//fv

Li, Q., Guan, X., Wu, P., Wang, X., Zhou, L., Tong, Y., Ren, R., Leung, K. S. M., Lau, E. H. Y.,
Wong, J. Y., Xing, X., Xiang, N., Wu, Y., Li, C., Chen, Q., Li, D., Liu, T., Zhao, J., Liu,
M., Tu, W., et al. (2020a). Early transmission dynamics in Wuhan, China, of novel
coronavirus-infected pneumonia. *New England Journal of Medicine*, *382*(13), 1199-1207.
https://doi.org/10.1056/NEJMoa2001316

Li, X., Guo, L., Kong, M., Su, X., Yang, D., Zou, M., Liu, Y., & Lu, L. (2016). Design and
evaluation of a multi-epitope peptide of human metapneumovirus. Intervirology, 58(6),
403-412.

Li, Y., Lai, D.-y., Zhang, H.-n., Jiang, H.-w., Tian, X., Ma, M.-l., Qi, H., Meng, Q.-f., Guo, S.-j.,

    Wu, Y., Wang, W., Yang, X., Shi, D.-w., Dai, J.-b., Ying, T., Zhou, J., & Tao, S.-c.

    (2020b). Linear epitopes of SARS-CoV-2 spike protein elicit neutralizing antibodies in

    COVID-19 patients. *Cellular & Molecular Immunology*, *17*(10), 1095-1097.

    https://doi.org/10.1038/s41423-020-00523-5

Lim, H. X., Lim, J., Jazayeri, S. D., Poppema, S., & Poh, C. L. (2021). Development of multi-

    epitope peptide-based vaccines against SARS-CoV-2. *Biomedical Journal*, *44*(1), 18–30.

    https://doi.org/10.1016/j.bj.2020.09.005

Lim, H. X., Masomian, M., Khalid, K., Kumar, A. U., MacAry, P. A., & Poh, C. L. (2022).

    Identification of B-cell epitopes for eliciting neutralizing antibodies against the SARS-

    CoV-2 spike protein through bioinformatics and monoclonal antibody

    targeting. *International Journal of Molecular Sciences*, *23*(8), 4341.

Liu, F., Wu, X., Li, L., Liu, Z., & Wang, Z. (2013). Use of baculovirus expression system for

    generation of virus-like particles: successes and challenges. *Protein Expression and*

    Purification, 90(2), 104–116. https://doi.org/10.1016/j.pep.2013.05.009

Liu, S., Tobias, R., McClure, S., Styba, G., Shi, Q., & Jackowski, G. (1997). Removal of

    endotoxin from recombinant protein preparations. *Clinical biochemistry*, *30*(6), 455-463.

Liu, M. A. (2019). A comparison of plasmid DNA and mRNA as vaccine

    technologies. *Vaccines*, *7*(2), 37. https://doi.org/10.3390/vaccines7020037

Liu, L., To, K. K., Chan, K. H., Wong, Y. C., Zhou, R., Kwan, K. Y., Fong, C. H., Chen, L. L.,

Choi, C. Y., Lu, L., Tsang, O. T., Leung, W. S., To, W. K., Hung, I. F., Yuen, K. Y., & Chen, Z.

(2020). High neutralizing antibody titer in intensive care unit patients with COVID-19. *Emerging*

Microbes & Infections, *9*(1), 1664–1670. https://doi.org/10.1080/22221751.2020.1791738

Madhi, S. A., Baillie, V., Cutland, C. L., Voysey, M., Koen, A. L., Fairlie, L., Padayachee, S. D., Dheda, K., Barnabas, S. L., Bhorat, Q. E., Briner, C., Kwatra, G., Ahmed, K., Aley, P., Bhikha, S., Bhiman, J. N., Bhorat, A. a. E., du Plessis, J., Esmail, A., Groenewald, M., et al. (2021). Efficacy of the ChAdOx1 nCoV-19 Covid-19 Vaccine against the B.1.351 Variant. *New England Journal of Medicine*, *384*(20), 1885-1898. https://doi.org/10.1056/NEJMoa2102214

Magazine, N., Zhang, T., Wu, Y., McGee, M. C., Veggiani, G., & Huang, W. (2022). Mutations and Evolution of the SARS-CoV-2 Spike Protein. *Viruses*, *14*(3). https://doi.org/10.3390/v14030640

Malik, Y. A. (2020). Properties of Coronavirus and SARS-CoV-2. *The Malaysian Journal of Pathology*, *42*(1), 3-11.

Malone, B., Urakova, N., Snijder, E. J., & Campbell, E. A. (2022). Structures and functions of coronavirus replication-transcription complexes and their relevance for SARS-CoV-2 drug design. *Nature Reviews. Molecular Cell Biology*, *23*(1), 21–39. https://doi.org/10.1038/s41580-021-00432-z

Martínez-Flores, D., Zepeda-Cervantes, J., Cruz-Reséndiz, A., Aguirre-Sampieri, S., Sampieri, A., & Vaca, L. (2021). SARS-CoV-2 Vaccines Based on the Spike Glycoprotein and Implications of New Viral Variants. *Frontiers in Immunology*, *12*, 701501. https://doi.org/10.3389/fimmu.2021.701501

Maruggi, G., Zhang, C., Li, J., Ulmer, J. B., & Yu, D. (2019). mRNA as a transformative technology for vaccine development to control infectious diseases. *Molecular Therapy*, *27*(4), 757-772. https://doi.org/https://doi.org/10.1016/j.ymthe.2019.01.020

Meng, F. Y., Gao, F., Jia, S. Y., Wu, X. H., Li, J. X., Guo, X. L., Zhang, J. L., Cui, B. P., Wu, Z. M., Wei, M. W., Ma, Z. L., Peng, H. L., Pan, H. X., Fan, L., Zhang, J., Wan, J. Q., Zhu, Z. K., Wang, X. W., & Zhu, F. C. (2021). Safety and immunogenicity of a recombinant COVID-19 vaccine (Sf9 cells) in healthy population aged 18 years or older: two single-center, randomised, double-blind, placebo-controlled, phase 1 and phase 2 trials. *Signal transduction and targeted therapy*, *6*(1), 271. https://doi.org/10.1038/s41392-021-00692-3

Mollé, L. M., Smyth, C. H., Yuen, D., & Johnston, A. P. R. (2022). Nanoparticles for vaccine and gene therapy: Overcoming the barriers to nucleic acid delivery. *WIREs Nanomedicine and Nanobiotechnology*, *14*(6), e1809. https://doi.org/10.1002/wnan.1809

Moyle, P. M., & Toth, I. (2013). Modern Subunit Vaccines: Development, Components, and Research Opportunities. *ChemMedChem*, *8*(3), 360-376. https://doi.org/https://doi.org/10.1002/cmdc.201200487

Noh, J. Y., Jeong, H. W., & Shin, E.-C. (2021a). SARS-CoV-2 mutations, vaccines, and immunity: implication of variants of concern. *Signal Transduction and Targeted Therapy*, *6*(1), 203. https://doi.org/10.1038/s41392-021-00623-2

Noh, J. Y., Jeong, H. W., Kim, J. H., & Shin, E.-C. (2021b). T cell-oriented strategies for controlling the COVID-19 pandemic. *Nature Reviews Immunology*, *21*(11), 687-688. https://doi.org/10.1038/s41577-021-00625-9

Nouailles, G., Adler, J. M., Pennitz, P., et al. (2023). Live-attenuated vaccine sCPD9 elicits superior mucosal and systemic immunity to SARS-CoV-2 variants in hamsters. *Nature Microbiology, 8(5), 860-874. https://doi.org/10.1038/s41564-023-01352-8*

Omidvar Tehrani, S., & Perkins, D. D. (2022). Community health resources, globalization, trust in science, and voting as predictors of COVID-19 vaccination rates: A global study with implications for vaccine adherence. *Vaccines*, *10*(8), 1343. https://doi.org/10.3390/vaccines10081343

Orenstein, W. A., & Ahmed, R. (2017). Simply put: Vaccination saves lives. *Proceedings of the National Academy of Sciences*, *114*(16), 4031-4033.

Otto, S. P., Day, T., Arino, J., Colijn, C., Dushoff, J., Li, M., Mechai, S., Van Domselaar, G., Wu, J., Earn, D. J. D., & Ogden, N. H. (2021). The origins and potential future of SARS-CoV-2 variants of concern in the evolving COVID-19 pandemic. *Current Biology: CB*, *31*(14), R918–R929. https://doi.org/10.1016/j.cub.2021.06.049

Park, S.-R., Lim, C.-Y., Kim, D.-S., & Ko, K. (2015). Optimization of Ammonium Sulfate Concentration for Purification of Colorectal Cancer Vaccine Candidate Recombinant Protein GA733-FcK Isolated from Plants [Methods]. *Frontiers in Plant Science*, *6*. https://doi.org/10.3389/fpls.2015.01040

Peng, Y., Mentzer, A. J., Liu, G., Yao, X., Yin, Z., Dong, D., Dejnirattisai, W., Rostron, T., Supasa, P., Liu, C., López-Camacho, C., Slon-Campos, J., Zhao, Y., Stuart, D. I., Paesen, G. C., Grimes, J. M., Antson, A. A., Bayfield, O. W., Hawkins, D. E. D. P., Ker, D.-S., et al. (2020). Broad and strong memory CD4+ and CD8+ T cells induced by SARS-CoV-2 in UK convalescent individuals following COVID-19. *Nature Immunology*, *21*(11), 1336-1345. https://doi.org/10.1038/s41590-020-0782-6

Planas, D., Bruel, T., Grzelak, L., Guivel-Benhassine, F., Staropoli, I., Porrot, F., Planchais, C., Buchrieser, J., Rajah, M. M., Bishop, E., Albert, M., Donati, F., Prot, M., Behillil, S., Enouf, V., Maquart, M., Smati-Lafarge, M., Varon, E., Schortgen, F., Yahyaoui, L., et al.

(2021). Sensitivity of infectious SARS-CoV-2 B.1.1.7 and B.1.351 variants to neutralizing antibodies. *Nature Medicine*, *27*(5), 917-924. https://doi.org/10.1038/s41591-021-01318-5

Polack, F. P., Thomas, S. J., Kitchin, N., Absalon, J., Gurtman, A., Lockhart, S., Perez, J. L., Pérez Marc, G., Moreira, E. D., & Zerbini, C. (2020). Safety and efficacy of the BNT162b2 mRNA Covid-19 vaccine. *New England Journal of Medicine, 383*(27), 2603-2615.

Poland, G. A., Ovsyannikova, I. G., & Kennedy, R. B. (2020). SARS-CoV-2 immunity: review and applications to phase 3 vaccine candidates. *The Lancet*, *396*(10262), 1595-1606.

Pollet, J., Chen, W. H., & Strych, U. (2021a). Recombinant protein vaccines, a proven approach against coronavirus pandemics. *Advanced Drug Delivery Reviews*, *170*, 71-82. https://doi.org/10.1016/j.addr.2021.01.001

Pollet, J., Chen, W. H., Versteeg, L., Keegan, B., Zhan, B., Wei, J., Liu, Z., Lee, J., Kundu, R., Adhikari, R., Poveda, C., Villar, M. J., de Araujo Leao, A. C., Altieri Rivera, J., Momin, Z., Gillespie, P. M., Kimata, J. T., Strych, U., Hotez, P. J., & Bottazzi, M. E. (2021b). SARS CoV-2 RBD219-N1C1: A yeast-expressed SARS-CoV-2 recombinant receptor-binding domain candidate vaccine stimulates virus neutralizing antibodies and T-cell immunity in mice. *Human Vaccines & Immunotherapeutics, 17*(8), 2356–2366. https://doi.org/10.1080/21645515.2021.1901545

Prabhu, S. K., Yang, Q., Tong, X., & Wang, L. X. (2021). Exploring a combined Escherichia coli-based glycosylation and in vitro transglycosylation approach for expression of glycosylated interferon alpha. *Bioorganic & Medicinal Chemistry*, *33*, 116037. https://doi.org/10.1016/j.bmc.2021.116037

Puranik, A., Lenehan, P. J., Silvert, E., Niesen, M. J. M., Corchado-Garcia, J., O'Horo, J. C., Virk, A., Swift, M. D., Halamka, J., Badley, A. D., Venkatakrishnan, A. J., & Soundararajan, V. (2021). Comparison of two highly-effective mRNA vaccines for COVID-19 during periods of Alpha and Delta variant prevalence. *medRxiv*. https://doi.org/10.1101/2021.08.06.21261707

Rastogi, M., Pandey, N., Shukla, A., & Singh, S. K. (2020). SARS coronavirus 2: from genome to infectome. *Respiratory Research*, *21*(1), 318. https://doi.org/10.1186/s12931-020-01581-z

Rosa, S. S., Prazeres, D. M. F., Azevedo, A. M., & Marques, M. P. C. (2021). mRNA vaccines manufacturing: Challenges and bottlenecks. *Vaccine*, *39*(16), 2190-2200. https://doi.org/10.1016/j.vaccine.2021.03.038

Rosano, G. L., & Ceccarelli, E. A. (2014). Recombinant protein expression in Escherichia coli: advances and challenges. *Frontiers in Microbiology*, *5*, 172. https://doi.org/10.3389/fmicb.2014.00172

Ruddle, N. H., & Akirav, E. M. (2009). Secondary lymphoid organs: Responding to genetic and environmental cues in ontogeny and the immune response. *Journal of Immunology*, *183*(4), 2205–2212. https://doi.org/10.4049/jimmunol.0804324

Sannathimmappa, M., & Nambiar, V. (2020). COVID-19: An Insight into SARS-CoV2 Pandemic Originated at Wuhan City in Hubei Province of China. *Journal of Infectious Diseases and Epidemiology*, *6*. https://doi.org/10.23937/2474-3658/1510146

Sarkar, B., Ullah, M. A., Johora, F. T., Taniya, M. A., & Araf, Y. (2020). Immunoinformatics-guided designing of epitope-based subunit vaccines against the SARS Coronavirus-2 (SARS-CoV-2). *Immunobiology, 225*(3), 151955.

Schäfer, F., Seip, N., Maertens, B., Block, H., & Kubicek, J. (2015). Purification of GST-tagged proteins. In *Methods in enzymology* (Vol. 559, pp. 127-139). Academic Press.

Schaub, J. M., Chou, C. W., Kuo, H. C., Javanmardi, K., Hsieh, C. L., Goldsmith, J., DiVenere, A. M., Le, K. C., Wrapp, D., Byrne, P. O., Hjorth, C. K., Johnson, N. V., Ludes-Meyers, J., Nguyen, A. W., Wang, N., Lavinder, J. J., Ippolito, G. C., Maynard, J. A., McLellan, J. S., & Finkelstein, I. J. (2021). Expression and characterization of SARS-CoV-2 spike proteins. *Nature Protocols*, *16*(11), 5339–5356. https://doi.org/10.1038/s41596-021-00623-0

Schiller, J., & Lowy, D. (2018). Explanations for the high potency of HPV prophylactic vaccines. *Vaccine*, *36*(32 Pt A), 4768–4773. https://doi.org/10.1016/j.vaccine.2017.12.079

Seow, J., Graham, C., Merrick, B., Acors, S., Pickering, S., Steel, K. J. A., Hemmings, O., O'Byrne, A., Kouphou, N., Galao, R. P., Betancor, G., Wilson, H. D., Signell, A. W., Winstone, H., Kerridge, C., Huettner, I., Jimenez-Guardeño, J. M., Lista, M. J., Temperton, N., Snell, L. B., et al. (2020). Longitudinal observation and decline of neutralizing antibody responses in the three months following SARS-CoV-2 infection in humans. *Nature Microbiology*, *5*(12), 1598-1607. https://doi.org/10.1038/s41564-020-00813-8

Shang, J., Wan, Y., Luo, C., Ye, G., Geng, Q., Auerbach, A., & Li, F. (2020). Cell entry mechanisms of SARS-CoV-2. *Proceedings of the National Academy of Sciences*, *117*(21), 11727-11734. https://doi.org/10.1073/pnas.2003138117

Shang, Y., Li, H., & Zhang, R. (2021). Effects of pandemic outbreak on economies: Evidence from business history context. *Frontiers in Public Health*, *9*. https://doi.org/10.3389/fpubh.2021.632043

Shahcheraghi, S. H., Ayatollahi, J., Aljabali, A. A., Shastri, M. D., Shukla, S. D., Chellappan, D. K., Jha, N. K., Anand, K., Katari, N. K., Mehta, M., Satija, S., Dureja, H., Mishra, V., Almutary, A. G., Alnuqaydan, A. M., Charbe, N., Prasher, P., Gupta, G., Dua, K., Lotfi, M., Bakshi, H. A., & Tambuwala, M. M. (2021). An overview of vaccine development for COVID-19. *Ther Deliv*, *12*(3), 235-244. https://doi.org/10.4155/tde-2020-0129

Shilling, P. J., Mirzadeh, K., Cumming, A. J., Widesheim, M., Köck, Z., & Daley, D. O. (2020). Improved designs for pET expression plasmids increase protein production yield in Escherichia coli. *Communications Biology*, *3*(1), 214. https://doi.org/10.1038/s42003-020-0939-8

Shrotri, M., van Schalkwyk, M. C. I., Post, N., Eddy, D., Huntley, C., Leeman, D., Rigby, S., Williams, S. V., Bermingham, W. H., Kellam, P., Maher, J., Shields, A. M., Amirthalingam, G., Peacock, S. J., & Ismail, S. A. (2021). T cell response to SARS-CoV-2 infection in humans: A systematic review. *PLOS ONE*, *16*(1), e0245532. https://doi.org/10.1371/journal.pone.0245532

Smith, T. R. F., Patel, A., Ramos, S., Elwood, D., Zhu, X., Yan, J., Gary, E. N., Walker, S. N., Schultheis, K., Purwar, M., Xu, Z., Walters, J., Bhojnagarwala, P., Yang, M., Chokkalingam, N., Pezzoli, P., Parzych, E., Reuschel, E. L., Doan, A., Tursi, N., et al. (2020). Immunogenicity of a DNA vaccine candidate for COVID-19. *Nature Communications*, *11*(1), 2601. https://doi.org/10.1038/s41467-020-16505-0

Strizova, Z., Smetanova, J., Bartunkova, J., & Milota, T. (2021). Principles and challenges in anti-COVID-19 vaccine development. *International Archives of Allergy and Immunology*, *182*(4), 339-349.

Smith, T. R., Patel, A., Ramos, S., Elwood, D., Zhu, X., Yan, J., Gary, E. N., Walker, S. N., Schultheis, K., & Purwar, M. (2020). Immunogenicity of a DNA vaccine candidate for COVID-19. *Nature Communications*, *11*(1), 2601.

Song, S., Madewell, Z. J., Liu, M., Longini, I. M., & Yang, Y. (2023). Effectiveness of SARS-CoV-2 vaccines against Omicron infection and severe events: a systematic review and meta-analysis of test-negative design studies. *Frontiers in Public Health*, *11*, 1195908. https://doi.org/10.3389/fpubh.2023.1195908

Sun, C. J., Pan, S. P., Xie, Q. X., & Xiao, L. J. (2004). Preparation of chitosan-plasmid DNA nanoparticles encoding zona pellucida glycoprotein-3α and its expression in mouse. *Molecular Reproduction and Development: Incorporating Gamete Research*, *68*(2), 182-188.

Sun, Y., Kobe, B., & Qi, J. (2020). Targeting multiple epitopes on the spike protein: a new hope for COVID-19 antibody therapy. *Signal Transduction and Targeted Therapy*, *5*(1), 208. https://doi.org/10.1038/s41392-020-00320-6

Suryawanshi, R. K., Chen, I. P., Ma, T., Syed, A. M., Brazer, N., Saldhi, P., Simoneau, C. R., Ciling, A., Khalid, M. M., Sreekumar, B., Chen, P. Y., Kumar, G. R., Montano, M., Gascon, R., Tsou, C. L., Garcia-Knight, M. A., Sotomayor-Gonzalez, A., Servellita, V., Gliwa, A., Nguyen, J., et al. (2022). Limited cross-variant immunity from SARS-CoV-2 Omicron without vaccination. *Nature*, *607*(7918), 351-355. https://doi.org/10.1038/s41586-022-04865-0

Tarke, A., Sidney, J., Methot, N., Yu, E. D., Zhang, Y., Dan, J. M., Goodwin, B., Rubiro, P.,
Sutherland, A., Wang, E., Frazier, A., Ramirez, S. I., Rawlings, S. A., Smith, D. M., da
Silva Antunes, R., Peters, B., Scheuermann, R. H., Weiskopf, D., Crotty, S., Grifoni, A.,
& Sette, A. (2021). Impact of SARS-CoV-2 variants on the total CD4(+) and CD8(+)
T cell reactivity in infected or vaccinated individuals. *Cell Reports Medicine*, *2*(7),
100355. https://doi.org/10.1016/j.xcrm.2021.100355

Tarrahimofrad, H., Rahimnahal, S., Zamani, J., Jahangirian, E., & Aminzadeh, S. (2021).
Designing a multi-epitope vaccine to provoke the robust immune response against
influenza A H7N9. *Scientific Reports, 11*(1), 24485. https://doi.org/10.1038/s41598-021-
03932-2

Thak, E. J., Yoo, S. J., Moon, H. Y., & Kang, H. A. (2020). Yeast synthetic biology for designed
cell factories producing secretory recombinant proteins. *FEMS Yeast Research*, *20*(2),
foaa009.

Thiam, F., Charpilienne, A., Poncet, D., Kohli, E., & Basset, C. (2015). B subunits of cholera
toxin and thermolabile enterotoxin of Escherichia coli have similar adjuvant effect as
whole molecules on rotavirus 2/6-VLP specific antibody responses and induce a Th17-
like response after intrarectal immunization. *Microbial Pathogenesis*, *89*, 27-34.
https://doi.org/10.1016/j.micpath.2015.08.013

Thomas, S. J., Moreira, E. D., Jr., Kitchin, N., Absalon, J., Gurtman, A., Lockhart, S., Perez, J.
L., Pérez Marc, G., Polack, F. P., Zerbini, C., Bailey, R., Swanson, K. A., Xu, X.,
Roychoudhury, S., Koury, K., Bouguermouh, S., Kalina, W. V., Cooper, D., Frenck, R.
W., Jr., Hammitt, L. L., Türeci, Ö., et al. (2021). Safety and efficacy of the BNT162b2

mRNA COVID-19 vaccine through 6 months. *New England Journal of Medicine, 385*(19), 1761-1773. https://doi.org/10.1056/NEJMoa2110345

Tian, J.-H., Patel, N., Haupt, R., Zhou, H., Weston, S., Hammond, H., Logue, J., Portnoff, A. D., Norton, J., Guebre-Xabier, M., Zhou, B., Jacobson, K., Maciejewski, S., Khatoon, R., Wisniewska, M., Moffitt, W., Kluepfel-Stahl, S., Ekechukwu, B., Papin, J., Boddapati, S., et al. (2021). SARS-CoV-2 spike glycoprotein vaccine candidate NVX-CoV2373 immunogenicity in baboons and protection in mice. *Nature Communications, 12*(1), 372. https://doi.org/10.1038/s41467-020-20653-8

Tomljenovic, L., & A Shaw, C. (2011). Aluminum vaccine adjuvants: Are they safe? *Current Medicinal Chemistry*, *18*(17), 2630-2637.

Tseng, H. F., Ackerson, B. K., Luo, Y., Sy, L. S., Talarico, C. A., Tian, Y., Bruxvoort, K. J., Tubert, J. E., Florea, A., Ku, J. H., Lee, G. S., Choi, S. K., Takhar, H. S., Aragones, M., & Qian, L. (2022). Effectiveness of mRNA-1273 against SARS-CoV-2 Omicron and Delta variants. *Nature Medicine*, *28*(5), 1063-1071. https://doi.org/10.1038/s41591-022-01753-y

Tye, E. X., Jinks, E., Haigh, T. A., Kaul, B., Patel, P., Parry, H. M., Newby, M. L., Crispin, M., Kaur, N., & Moss, P. (2022). Mutations in SARS-CoV-2 spike protein impair epitope-specific CD4+ T cell recognition. *Nature Immunology, 23*(12), 1726-1734. https://doi.org/10.1038/s41590-022-01351-7

Vallamkondu, J., John, A., Wani, W. Y., Ramadevi, S. P., Jella, K. K., Reddy, P. H., & Kandimalla, R. (2020). SARS-CoV-2 pathophysiology and assessment of coronaviruses in CNS diseases with a focus on therapeutic targets. *Biochimica et biophysica acta.*

Molecular Basis of Disease, *1866*(10), 165889.

https://doi.org/10.1016/j.bbadis.2020.165889

Van Den Ende, C., Marano, C., Van Ahee, A., Bunge, E. M., & De Moerlooze, L. (2017). The

immunogenicity and safety of GSK's recombinant hepatitis B vaccine in adults: a

systematic review of 30 years of experience. *Expert Review of Vaccines*, *16*(8), 811-832.

https://doi.org/10.1080/14760584.2017.1338568

van der Straten, K., Guerra, D., van Gils, M. J., Bontjer, I., Caniels, T. G., van Willigen, H. D.

G., Wynberg, E., Poniman, M., Burger, J. A., Bouhuijs, J. H., van Rijswijk, J., Olijhoek,

W., Liesdek, M. H., Lavell, A. H. A., Appelman, B., Sikkens, J. J., Bomers, M. K., Han,

A. X., Nichols, B. E., Prins, M., et al. (2022). Antigenic cartography using sera from

sequence-confirmed SARS-CoV-2 variants of concern infections reveals antigenic

divergence of Omicron. *Immunity*, *55*(9), 1725-1731.e1724.

https://doi.org/10.1016/j.immuni.2022.07.018

Velavan, T. P., & Meyer, C. G. (2020). The COVID-19 epidemic. *Tropical Medicine &*

International Health, *25*(3), 278-280. https://doi.org/10.1111/tmi.13383

Voysey, M., Clemens, S. A. C., Madhi, S. A., Weckx, L. Y., Folegatti, P. M., Aley, P. K.,

Angus, B., Baillie, V. L., Barnabas, S. L., Bhorat, Q. E., Bibi, S., Briner, C., Cicconi, P.,

Collins, A. M., Colin-Jones, R., Cutland, C. L., Darton, T. C., Dheda, K., Duncan, C. J.

A., Emary, K. R. W., et al. (2021). Safety and efficacy of the ChAdOx1 nCoV-19 vaccine

(AZD1222) against SARS-CoV-2: An interim analysis of four randomised controlled

trials in Brazil, South Africa, and the UK. *The Lancet*, *397*(10269), 99-111.

https://doi.org/10.1016/S0140-6736(20)32661-1

Wang, Z., Schmidt, F., Weisblum, Y., Muecksch, F., O. Barnes, C., Finkin, S., Schaefer-Babajew, D., Cipolla, M., Gaebler, C., Lieberman, J., Oliveira, T., Yang, Z., Abernathy, M., Huey-Tubman, K., Hurley, A., Turroja, M., West, K., Gordon, K., Millard, K., Ramos, R., et al., (2021a). mRNA vaccine-elicited antibodies to SARS-CoV-2 and circulating variants. *Nature*, *592*(7855), 616-622.

Wang, S., Wang, C. Y., Kuo, H. K., Peng, W. J., Huang, J. H., Kuo, B. S., Lin, F., Liu, Y. J., Liu, Z., Wu, H. T., Ding, S., Hou, K. L., Cheng, J., Yang, Y. T., Jiang, M. H., Wang, M. S., Chen, T., Xia, W. G., Lin, E., Hung, C. H., et al. (2022). A novel RBD-protein/peptide vaccine elicits broadly neutralizing antibodies and protects mice and macaques against SARS-CoV-2. *Emerging Microbes & Infections*, *11*(1), 2724–2734. https://doi.org/10.1080/22221751.2022.2140608

Wang, Y., Yang, C., Song, Y., et al. (2021b). Scalable live-attenuated SARS-CoV-2 vaccine candidate demonstrates preclinical safety and efficacy. Proceedings of the National Academy of Sciences of the United States of America, 118(29), e2102775118. https://doi.org/10.1073/pnas.2102775118

Wajnberg, A., Amanat, F., Firpo, A., Altman, D. R., Bailey, M. J., Mansour, M., McMahon, M., Meade, P., Mendu, D. R., Muellers, K., Stadlbauer, D., Stone, K., Strohmeier, S., Simon, V., Aberg, J., Reich, D. L., Krammer, F., & Cordon-Cardo, C. (2020). Robust neutralizing antibodies to SARS-CoV-2 infection persist for months. *Science*, *370*(6521), 1227-1230. https://doi.org/doi:10.1126/science.abd7728

Wei, Z., He, J., Wang, C., Bao, J., Leng, T., & Chen, F. (2022). The importance of booster vaccination in the context of Omicron wave. *Frontiers in Immunology*, *13*, 977972. https://doi.org/10.3389/fimmu.2022.977972

WHO. (2023). *WHO coronavirus (COVID-19) dashboard*. https://covid19.who.int/

WHO. (2024). Tracking SARS-CoV-2 variants. Retrived from

https://www.who.int/activities/tracking-SARS-CoV-2-variants

Willett, B. J., Grove, J., MacLean, O. A., Wilkie, C., De Lorenzo, G., Furnon, W., Cantoni, D.,
Scott, S., Logan, N., Ashraf, S., Manali, M., Szemiel, A., Cowton, V., Vink, E., Harvey,
W. T., Davis, C., Asamaphan, P., Smollett, K., Tong, L., Orton, R., et al. (2022). SARS-
CoV-2 Omicron is an immune escape variant with an altered cell entry pathway. *Nature
Microbiology*, *7*(8), 1161-1179. https://doi.org/10.1038/s41564-022-01143-7

Wong, C., Piedra, P. A., Frieman, M. B., Massare, M. J., Fries, L., Bengtsson, K. L., Stertman,
L., Ellingsworth, L., Glenn, G., & Smith, G. (2021). SARS-CoV-2 spike glycoprotein
vaccine candidate NVX-CoV2373 immunogenicity in baboons and protection in mice.
Nature Communications, 12(1), 372. https://doi.org/10.1038/s41467-020-20653-8

Wood, D. W. (2014). New trends and affinity tag designs for recombinant protein
purification. *Current opinion in structural biology*, *26*, 54-61.

Wu, K., Werner, A. P., Moliva, J. I., Koch, M., Choi, A., Stewart-Jones, G. B. E., Bennett, H.,
Boyoglu-Barnum, S., Shi, W., Graham, B. S., Carfi, A., Corbett, K. S., Seder, R. A., &
Edwards, D. K. (2021). mRNA-1273 vaccine induces neutralizing antibodies against
spike mutants from global SARS-CoV-2 variants. *bioRxiv*, 2021.2001.2025.427948.
https://doi.org/10.1101/2021.01.25.427948

Xiang, T., Liang, B., Fang, Y., Lu, S., Li, S., Wang, H., Li, H., Yang, X., Shen, S., Zhu, B.,
Wang, B., Wu, J., Liu, J., Lu, M., Yang, D., Dittmer, U., Trilling, M., Deng, F., & Zheng,
X. (2021). Declining levels of neutralizing antibodies against SARS-CoV-2 in

convalescent COVID-19 patients one year post symptom onset. *Frontiers in Immunology*, *12*, 708523. https://doi.org/10.3389/fimmu.2021.708523

Yang, J., Wang, W., Chen, Z., Lu, S., Yang, F., Bi, Z., Bao, L., Mo, F., Li, X., Huang, Y., Hong, W., Yang, Y., Zhao, Y., Ye, F., Lin, S., Deng, W., Chen, H., Lei, H., Zhang, Z., Luo, M., et al. (2020). A vaccine targeting the RBD of the S protein of SARS-CoV-2 induces protective immunity. *Nature*, *586*(7830), 572-577. https://doi.org/10.1038/s41586-020-2599-8

Yano, A., Onozuka, A., Asahi-Ozaki, Y., Imai, S., Hanada, N., Miwa, Y., & Nisizawa, T. (2005). An ingenious design for peptide vaccines. *Vaccine, 23*(17-18), 2322-2326.

Yarmarkovich, M., Warrington, J. M., Farrel, A., & Maris, J. M. (2020). A SARS-CoV-2 vaccination strategy focused on population-scale immunity. *SSRN*, 3575161. https://doi.org/10.2139/ssrn.3575161

Zahradník, J., Marciano, S., Shemesh, M., Zoler, E., Chiaravalli, J., Meyer, B., Dym, O., Elad, N., & Schreiber, G. (2021). SARS-CoV-2 RBD in vitro evolution follows contagious mutation spread, yet generates an able infection inhibitor. *bioRxiv*. https://doi.org/10.1101/2021.01.06.425392

Zhang, L., Jackson, C. B., Mou, H., Ojha, A., Rangarajan, E. S., Izard, T., Farzan, M., & Choe, H. (2020a). The D614G mutation in the SARS-CoV-2 spike protein reduces S1 shedding and increases infectivity. *bioRxiv : the preprint server for biology*. https://doi.org/10.1101/2020.06.12.148726

Zhang, Y., Belayachi, J., Yang, Y., Fu, Q., Rodewald, L., Li, H., Yan, B., Wang, Y., Shen, Y., Yang, Q., Mu, W., Tang, R., Su, C., Xu, T., Obtel, M., Mhayi, A., Razine, R., Abouqal, R., Zhang, Y., & Yang, X. (2022). Real-world study of the effectiveness of BBIBP-CorV

(Sinopharm) COVID-19 vaccine in the Kingdom of Morocco. *BMC Public Health*, *22*(1),

    1584. https://doi.org/10.1186/s12889-022-14016-9

Zhou, S., Chen, W., Cole, J., & Zhu, G. (2020). Delivery of nucleic acid therapeutics for cancer

    immunotherapy. *Medicine in Drug Discovery*, *6*, 100023.

    https://doi.org/10.1016/j.medidd.2020.100023

Zuo, J., Dowell, A. C., Pearce, H., Verma, K., Long, H. M., Begum, J., Aiano, F., Amin-

    Chowdhury, Z., Hoschler, K., Brooks, T., Taylor, S., Hewson, J., Hallis, B., Stapley, L.,

    Borrow, R., Linley, E., Ahmad, S., Parker, B., Horsley, A., Amirthalingam, G., Brown,

    K., Ramsay, M. E., Ladhani, S., & Moss, P. (2021). Robust SARS-CoV-2-specific T cell

    immunity is maintained at 6 months following primary infection. *Nature Immunology*,

    22(5), 620-626. https://doi.org/10.1038/s41590-021-00902-8

Table S1. The prediction results for linear B cell and CD4+- & CD8+- T cell epitopes in the S, M, and N proteins (Lim et al., 2021)

Peptide	Sequence	Linear B cell	Start-End (Amino Acid Length)	CD4+ T cell epitopes				CD8+ T-cell epitopes	Global HLA Population coverage (%)	Conservancy
				Percentile rank	IC50 value (nM)	IFN-γ Prediction	Immunogenicity score	Prediction score		
ST1	WTAGAAAYYVGYLQPRTFLLKY	No	258-279 (22)	3.80	42	Positive	97.729	1.5152	99.63	98 %
ST2	NYNYLYRLFRKSNLKPFERDISTEI	Yes	448-472 (25)	0.20	8	Positive	81.4673	1.9496	97.95	87.33 %
ST3	SYGFQPTNGVGYQPYRVVVLSFELLHAPAT	Yes	494-523 (30)	0.24	5	Positive	99.222	1.8786	98.57	63.33 %
ST4	FPQSAPHGVVFLHVTYVPAQEK	No	1052-1073 (22)	7.90	67	Positive	98.6684	1.043	96.41	70 %
ST5	CASYQTQTNSPRRARSVASQSIIAYTMSL	Yes	671-99 (29)	5.00	27	Positive	99.0918	1.369	91.87	96 %
MT1	GLMWLSYFIASFRLFARTRSM	Yes	89-109 (21)	1.6	40	Positive	92.9583	1.003	93.45	100 %
NT1	AALALLLLDRLNQLE	No	217-231 (35)	1.00	48	Positive	98.2915	1.2648	93.45	98.67 %
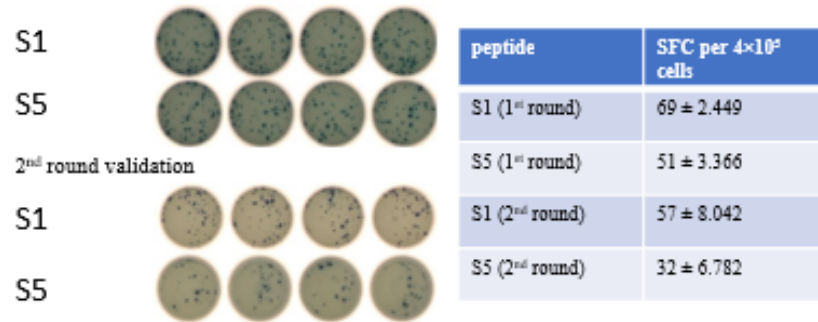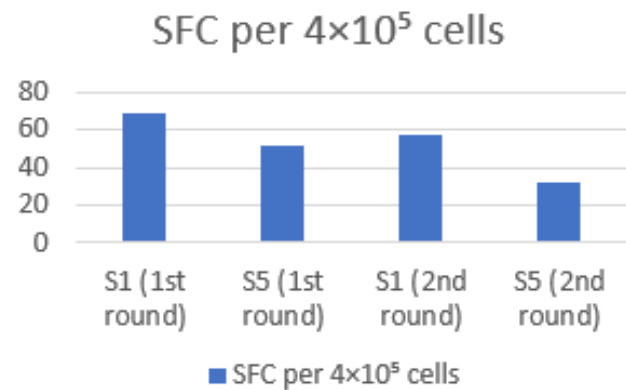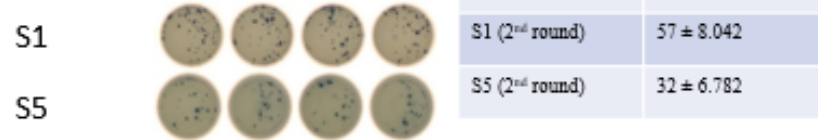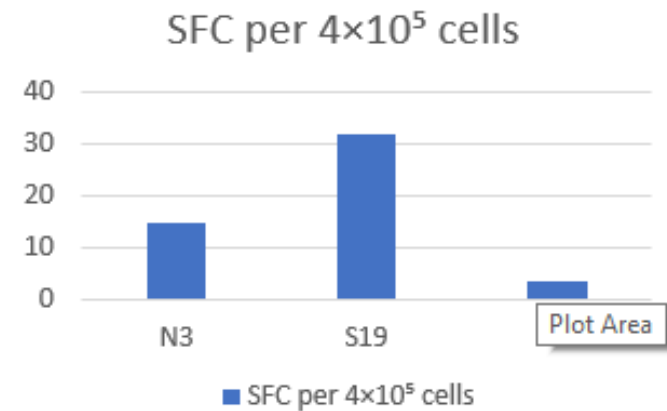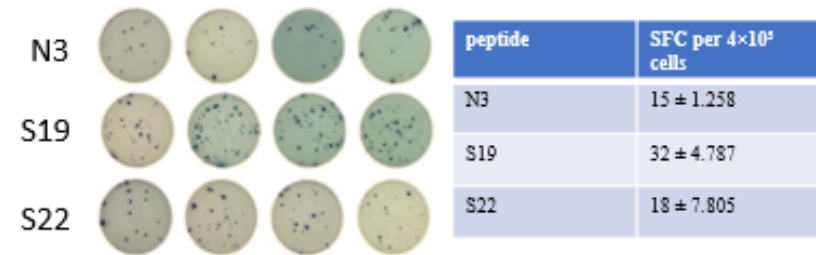
Figure S1. Validation of individual T cell epitopes in terms of IFN-γ production performed by Yahaya and Lim (2021) (unpublished data)

cPass SVNT assay for NtAb (B-cell epitope detection) of Murine sera

Peptide B6

Dilution ratio	OD value at 450 nm	Percentage of inhibition
1:2	0.8004	51.88
1:5	0.8847	46.82
1:10	0.9971	40.06
1:20	1.0768	35.27
1:40	1.261	24.20
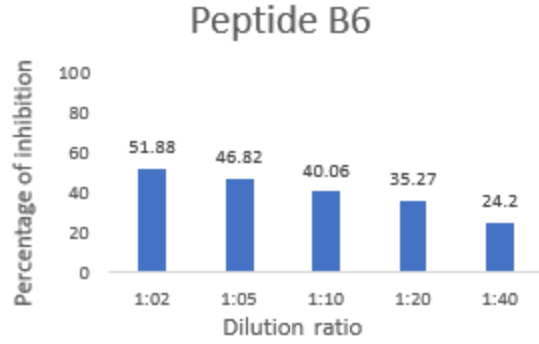
Peptide B10

Dilution ratio	OD value at 450 nm	Percentage of inhibition
1:2	0.962	42.17
1:5	1.0031	39.70
1:10	1.1039	33.64
1:20	1.1922	28.33
1:40	1.2215	26.57
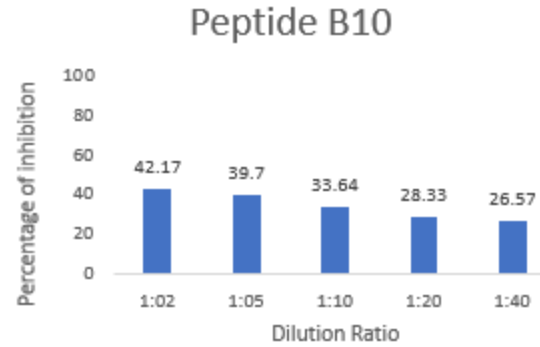
Figure S2. Validation of individual B cell epitopes in terms of neutralizing activity performed by Yahaya and Lim (2021) (unpublished data)
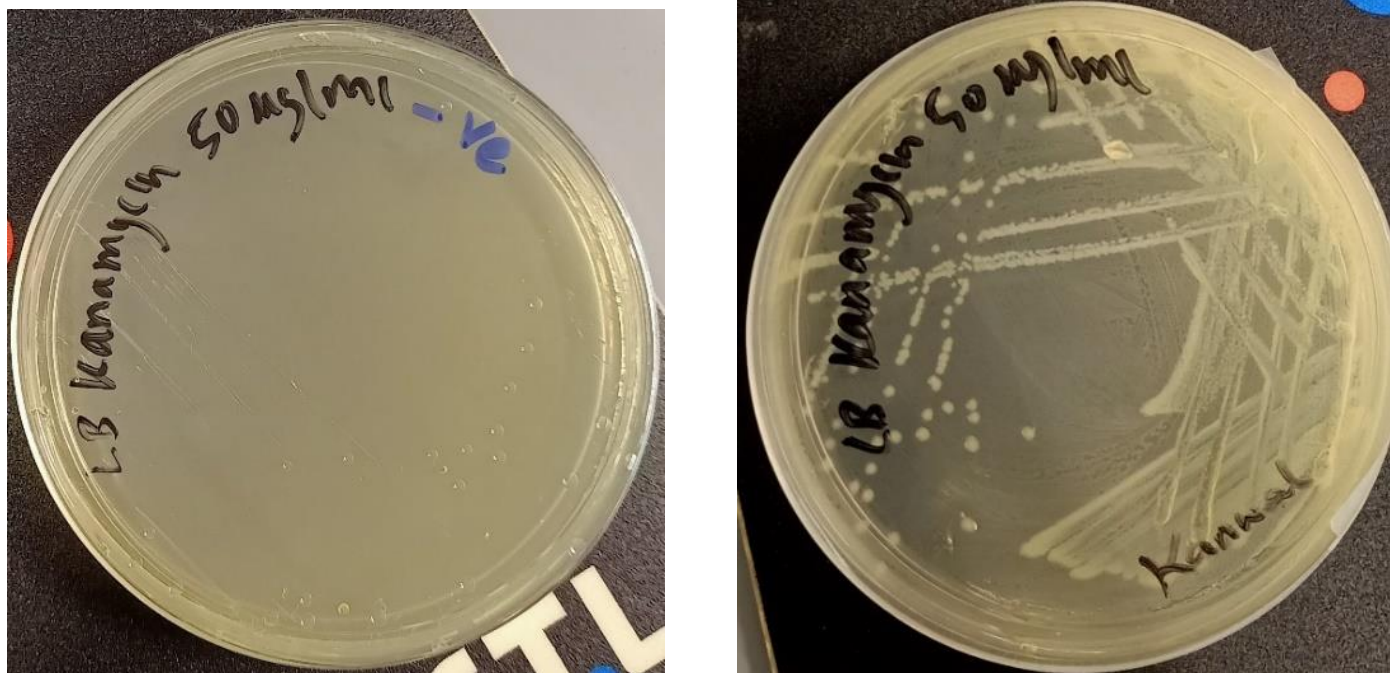
Figure S3. (A) LB kanamycin (50 μg/ml) plates containing untransformed competent *E. coli* BL21(DE3) cells (**B**) LB kanamycin (50 μg/ml) plates containing competent *E. coli* BL21(DE3) cells transformed with pET41a-GST-6PHis

(B)
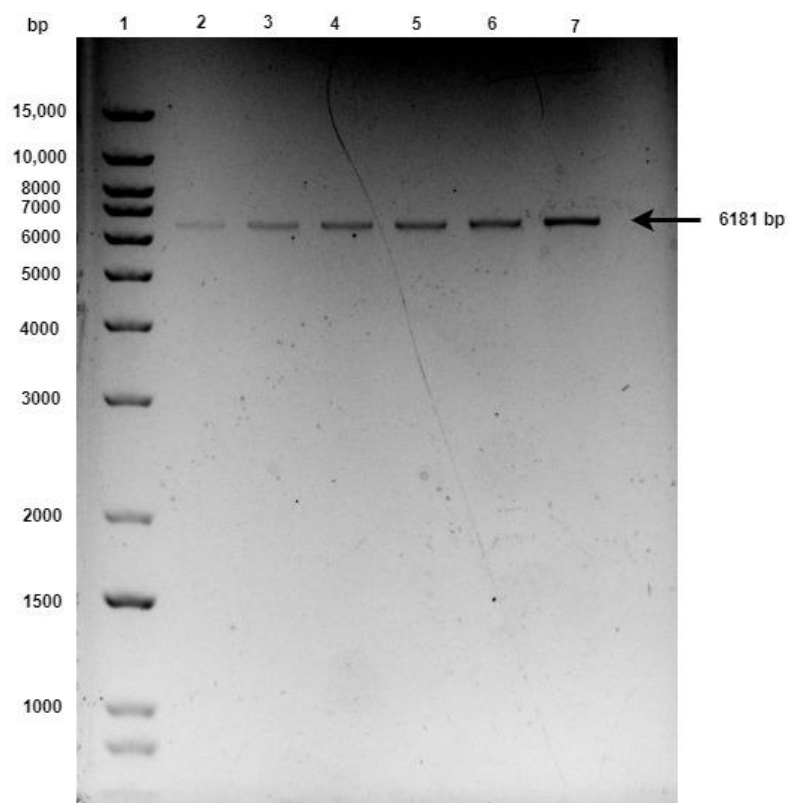
Figure S4. The agarose gel electrophoresis of XhoI digested pET41a-GST-6PHis. Lane 1: 1 kb molecular weight marker. Lane 2: 1.12 ng/ul pET41a-GST-6PHis, Lane 3: 2.24 ng/ul pET41a-GST-6PHis, Lane 4: 3.36 ng/ul pET41a-GST-6PHis, Lane 5: 4.48 ng/ul pET41a-GST-6PHis, Lane 6: 5.60 ng/ul pET41a-GST-6PHis, Lane 7: 8.4 ng/ul pET41a-GST-6PHis

GST   **6 peptide protein of interest**   **8xHistidine**

```
GenScript  ATGTCCCCTATACTAGGTTATGGAAAATTAAGGGCCTTGTGCAACCCACTCGACTTCTTTTTGGAATATC  60
Designed   ATGTCCCCTATACTAGGTTATGGAAAATTAAGGGCCTTGTGCAACCCACTCGACTTCTTTTTGGAATATC  4839
           *********************************************************************

GenScript  TTGAAGAAAAATATGAAGAGCATTTGTATGAGCGCGATGAAGGTGATAAATGGCGAAACAAAAAGTTT  120
Designed   TTGAAGAAAAATATGAAGAGCATTTGTATGAGCGCGATGAAGGTGATAAATGGCGAAACAAAAAGTTT  4899
           *********************************************************************

GenScript  GAATTGGGTTTGGAGTTTCCCAATCTTCCTTATTATATTGATGGTGATGTTAAATTAACACAGTCTATGGC  180
Designed   GAATTGGGTTTGGAGTTTCCCAATCTTCCTTATTATATTGATGGTGATGTTAAATTAACACAGTCTATGGC  4959
           *********************************************************************

GenScript  CATCATACGTTATATAGCTGACAAGCACAACATGTTGGGTGGTTGTCCAAAAGAGCGTGCAGAGATTTC  240
Designed   CATCATACGTTATATAGCTGACAAGCACAACATGTTGGGTGGTTGTCCAAAAGAGCGTGCAGAGATTTC  5019
           *********************************************************************

GenScript  AATGCTTGAAGGAGCGGTTTTGGATATTAGATACGGTGTTTCGAGAATTGCATATAGTAAAGACTTTGA  300
Designed   AATGCTTGAAGGAGCGGTTTTGGATATTAGATACGGTGTTTCGAGAATTGCATATAGTAAAGACTTTGA  5079
           *********************************************************************

GenScript  AACTCTCAAAGTTGATTTTCTTAGCAAGCTACCTGAAATGCTGAAAATGTTCGAAGATCGTTTATGTCAT  360
Designed   AACTCTCAAAGTTGATTTTCTTAGCAAGCTACCTGAAATGCTGAAAATGTTCGAAGATCGTTTATGTCAT  5139
           *********************************************************************

GenScript  AAAACATATTTAAATGGTGATCATGTAACCCATCCTGACTTCATGTTGTATGACGCTCTTGATGTTGTTTT  420
Designed   AAAACATATTTAAATGGTGATCATGTAACCCATCCTGACTTCATGTTGTATGACGCTCTTGATGTTGTTTT  5199
           *********************************************************************

GenScript  ATACATGGACCCAATGTGCCTGGATGCGTTCCCAAAATTAGTTTGTTTTAAAAAACGTATTGAAGCTATC  540
Designed   ATACATGGACCCAATGTGCCTGGATGCGTTCCCAAAATTAGTTTGTTTTAAAAAACGTATTGAAGCTATC  5319
           *********************************************************************

GenScript  CCACAAATTGATAAGTACTTGAAATCCAGCAAGTATATAGCATGGCCTTTGCAGGGCTGGCAAGCCACG  600
Designed   CCACAAATTGATAAGTACTTGAAATCCAGCAAGTATATAGCATGGCCTTTGCAGGGCTGGCAAGCCACG  5379
           *********************************************************************

GenScript  TTTGGTGGTGGCGACCATCCTCCAAAATCGGATGGTTCAACTAGTCTGGTGCCACGCGGATCCACCGAG  660
Designed   TTTGGTGGTGGCGACCATCCTCCAAAATCGGATGGTTCAACTAGTCTGGTGCCACGCGGATCCACCGAG  5439
           *********************************************************************

GenScript  AGCAACAAGAAATTCCTGCCGTTTCAGCAGTTCGGTCGTGACATCGCCAAGAAAGAAAGCAACAAGAA  720
Designed   AGCAACAAGAAATTCCTGCCGTTTCAGCAGTTCGGTCGTGACATCGCCAAGAAAGAAAGCAACAAGAA  5499
           *********************************************************************
```

175

```
GenScript   ATTTCTGCCGTTCCAGCAGTTTGGCCGCGACATTGCTGATACCACCGCGGCCTACTGGACCGCGGGTGC     780
Designed    ATTTCTGCCGTTCCAGCAGTTTGGCCGCGACATTGCTGATACCACCGCGGCCTACTGGACCGCGGGTGC     5559
            *********************************************************************

GenScript   TGCCGCG TACTATGTGGGCTACCTGCAGCCGCGTACCTTCCTGCTGAAGTATGGCCCCGGCCCAGGCG     840
Designed    TGCCGCG TACTATGTGGGCTACCTGCAGCCGCGTACCTTCCTGCTGAAGTATGGCCCCGGCCCAGGCG     5619
            *********************************************************************

GenScript   GCGAGGTGTTCAACGCCACCCGCTTTGCGAGCGTGTATGCTTGGAACCGTAAACGCATCAGCAACTGC     960
Designed    GCGAGGTGTTCAACGCCACCCGCTTTGCGAGCGTGTATGCTTGGAACCGTAAACGCATCAGCAACTGC     5739
            *********************************************************************

GenScript   GTGGCGGATTACAGCGTGCTGTATAACAGCGCCGCTTATTTTCCACAGAGCGCGCCGCACGGTGTGGT     1020
Designed    GTGGCGGATTACAGCGTGCTGTATAACAGCGCCGCTTATTTTCCACAGAGCGCGCCGCACGGTGTGGT     5799
            *********************************************************************

GenScript   GTTTCTGCACGTGACCTATGTGCCGGCTCAGGAAAAGGCGGCTTACGGCCTGATGTGGCTGAGCTACT     1080
Designed    GTTTCTGCACGTGACCTATGTGCCGGCTCAGGAAAAGGCGGCTTACGGCCTGATGTGGCTGAGCTACT     5859
            *********************************************************************

GenScript   TCATCGCCAGCTTCCGTCTGTTTGCGCGTACCCGCAGCATGCTGGTGCCACGCGGATCCCTCGAGCACC     1140
Designed    TCATCGCCAGCTTCCGTCTGTTTGCGCGTACCCGCAGCATGCTGGTGCCACGCGGATCCCTCGAGCACC     5919
            *********************************************************************

GenScript   ACCACCACCACCACCAC     1194
Designed    ACCACCACCACCACCAC     5973
            ********************
```

Figure S5. Nucleotide sequencing results of the cloned gene insert incorporated into pET41a-GST-6PHis

PUBLICATIONS

1. Lim, H. X., Masomian, M., Khalid, K., Kumar, A. U., MacAry, P. A., & Poh, C. L. (2022). Identification of B-Cell Epitopes for Eliciting Neutralizing Antibodies against the SARS-CoV-2 Spike Protein through Bioinformatics and Monoclonal Antibody Targeting. *International Journal of Molecular Sciences*, *23*(8), 4341. https://doi.org/10.3390/ijms23084341

2. Al-Fattah Yahaya, A. A., Khalid, K., Lim, H. X., & Poh, C. L. (2023). Development of Next Generation Vaccines against SARS-CoV-2 and Variants of Concern. *Viruses*, *15*(3), 624. https://doi.org/10.3390/v15030624

3. Khalid, K., & Poh, C. L. (2023). The development of DNA vaccines against SARS-CoV-2. *Advances in Medical Sciences*, *68*(2), 213–226. https://doi.org/10.1016/j.advms.2023.05.003

4. Khalid, K., & Poh, C. L. (2023). The Promising Potential of Reverse Vaccinology-Based Next-Generation Vaccine Development over Conventional Vaccines against Antibiotic-Resistant Bacteria. *Vaccines*, *11*(7), 1264. https://doi.org/10.3390/vaccines11071264

5. Khalid, K., Lim, H. X., Anwar, A., Tan, S. H., Hwang, J. S., Ong, S. K., & Poh, C. L. (2024). Preclinical Development of a Novel Epitope-based DNA Vaccine Candidate against SARS-CoV-2 and Evaluation of Immunogenicity in BALB/c Mice. *AAPS PharmSciTech, 25*(3), 60. https://doi.org/10.1208/s12249-024-02778-x

Review

Identification of B-Cell Epitopes for Eliciting Neutralizing Antibodies against the SARS-CoV-2 Spike Protein through Bioinformatics and Monoclonal Antibody Targeting

Hui Xuan Lim [1], Malihe Masomian [1], Kanwal Khalid [1], Asqwin Uthaya Kumar [1], Paul A. MacAry [2] and Chit Laa Poh [1],*

[1] Centre for Virus and Vaccine Research, School of Medical and Life Sciences, Sunway University, Bandar Sunway, Petaling Jaya 47500, Selangor, Malaysia; huixuanl@sunway.edu.my (H.X.L.); malihem@sunway.edu.my (M.M.); 19115914@imail.sunway.edu.my (K.K.); asqwin22@hotmail.com (A.U.K.)

[2] Life Sciences Institute, National University of Singapore, Singapore 119077, Singapore; micpam@nus.edu.sg

* Correspondence: pohcl@sunway.edu.my

Abstract: Severe acute respiratory syndrome coronavirus 2 (SARS-CoV-2) has caused a global public health crisis. Effective COVID-19 vaccines developed by Pfizer-BioNTech, Moderna, and Astra Zeneca have made significant impacts in controlling the COVID-19 burden, especially in reducing the transmission of SARS-CoV-2 and hospitalization incidences. In view of the emergence of new SARS-CoV-2 variants, vaccines developed against the Wuhan strain were less effective against the variants. Neutralizing antibodies produced by B cells are a critical component of adaptive immunity, particularly in neutralizing viruses by blocking virus attachment and entry into cells. Therefore, the identification of protective linear B-cell epitopes can guide epitope-based peptide designs. This study reviews the identification of SARS-CoV-2 B-cell epitopes within the spike, membrane and nucleocapsid proteins that can be incorporated as potent B-cell epitopes into peptide vaccine constructs. The bioinformatic approach offers a new in silico strategy for the mapping and identification of potential B-cell epitopes and, upon in vivo validation, would be useful for the rapid development of effective multi-epitope-based vaccines. Potent B-cell epitopes were identified from the analysis of three-dimensional structures of monoclonal antibodies in a complex with SARS-CoV-2 from literature mining. This review provides significant insights into the elicitation of potential neutralizing antibodies by potent B-cell epitopes, which could advance the development of multi-epitope peptide vaccines against SARS-CoV-2.

Keywords: B-cell epitope; vaccine; SARS-CoV-2; spike protein

1. Introduction

Severe acute respiratory syndrome coronavirus 2 (SARS-CoV-2) first emerged in December 2019 in the Chinese city of Wuhan (Hubei Province), and it has led to a serious global health problem, causing a pandemic with over 452 million infections and high mortality, with more than 6.02 million deaths as of 11 March 2022.

The most common symptoms reported for SARS-CoV-2 infections are fever, dry cough, difficulty in breathing, and muscle pain, which may potentially worsen to pneumonia, renal failure, and death in severe cases [1,2]. Pneumonia was reported as the initial clinical symptom that indicated SARS-CoV-2 infection. Gastrointestinal symptoms were also observed. With a mean incubation period of five days, symptoms are observed in less than a week. In severe cases, dyspnoea and chest symptoms associated with pneumonia were reported in 75% of patients, as confirmed by computed tomography (CT) scans [3]. Severe symptoms in line with pneumonia were usually reported in the second or third week and were associated with reduced oxygen saturation, abnormal chest X-rays, alveolar exudates, and interlobular involvement, which demonstrated deterioration. Lymphopenia

was reported with increased levels of inflammatory markers such as C-reactive protein and proinflammatory cytokines [4].

2. Genomic Structure of SARS-CoV-2

The SARS-CoV-2 genome consists of a single-stranded positive-sense RNA with a size of approximately 29.9 kB [5]. Two large open-reading frames (ORFs) comprising 70% of the genome, namely ORF1a and ORF1b, are located at the 5′ end (Figure 1). They are responsible for encoding 16 non-structural proteins, ranging from NSP1 to NSP16, which are involved in the formation of a replication–transcription complex (RTC). The RTC is associated with genome transcription and replication. The NSP genes have other diverse functions in terms of the proteins they encode, such as the cleavage of polypeptides and inhibition of the host immune response [6]. The other ORFs located at the 3′ end occupy 30% of the genome and are responsible for encoding four structural proteins, namely spike (S), envelope (E), membrane (M), and nucleocapsid (N) proteins (Figure 1). The S protein recognizes the angiotensin-converting enzyme 2 (ACE2) receptor, the M protein provides shape and structure to the viral particles, the E protein ensures proper virion assembly and release, and the N protein packages the RNA genome and enhances the pathogenicity by reducing interferon production. The 3′ UTR also encodes six accessory proteins labelled 3a, 6, 7a, 7b, 8, and 10 in Figure 1, but their functions are not fully known [7].
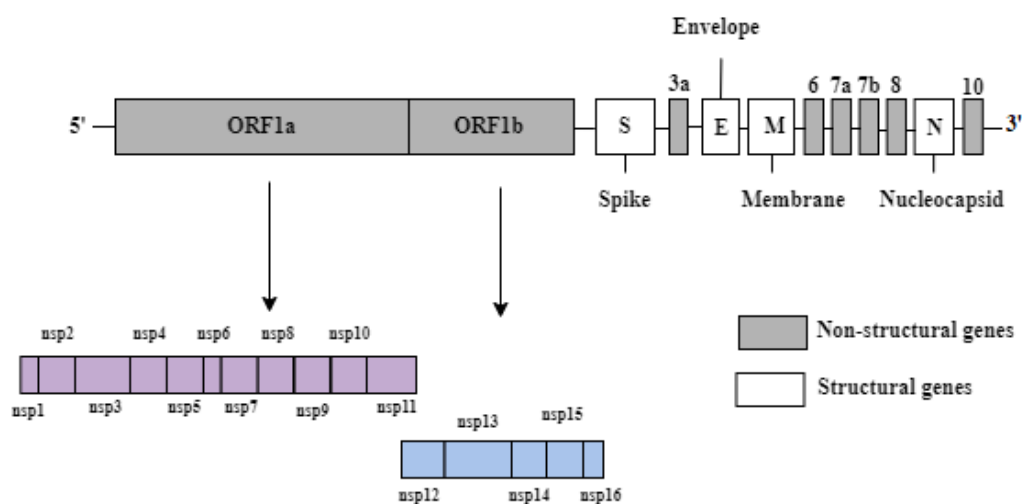
Figure 1. The genomic structure of SARS-CoV-2.

3. Viral Binding and Entry into Host Cell and the SARS-CoV-2 Lifecycle

An understanding of the functional characteristics of the S protein in the lifecycle of SARS-CoV-2 is essential, since the S protein mediates the binding of the virus and its entry into the host cells [8]. The S glycoprotein is a glycosylated type I membrane protein and consists of two subunits, S1 and S2. The S protein exists in a trimeric prefusion form, which is cleaved by a host furin protease into S1 and S2. The S1 subunit contains the NH-2 terminal domain (NTD) and the receptor-binding domain (RBD). The latter is a crucial structural component that is responsible for binding to the ACE2 cell receptor [9].

The S protein requires priming by host cell proteases such as endosomal cysteine protease cathepsin L and the serine proteases furin and TMPRSS2 in order to facilitate viral entry and membrane fusion. Cleavage of the S protein is known to occur at two sites. The first is the S1/S2 site by furin, which exposes the RBD in the "up" conformation and allows it to bind to the ACE2 receptor. The RBD promotes the binding of the enveloped virus to host cells by interacting with the ACE2 receptor expressed in the lower respiratory tract. After the RBD binds to ACE2, an additional cleavage of the S2 subunit occurs at a second specific site of the fusion peptide by the host serine protease TMPRSS2, which triggers the dissociation between S1 and S2. Cleavage at the S2 site produces the mature N-terminus of

the fusion peptide, allowing the fusion of viral and host membrane, thus facilitating virus entry. When SARS-CoV-2 enters the host cell, it will release its RNA, and polyproteins will be produced following translation. The RNA genome of SARS-CoV-2 is replicated to yield genomic RNA, which is encapsidated by the viral structural proteins formed in the host cell. The newly assembled viral particles are released by exocytosis [2].

The spike glycoprotein is composed of two subunits, S1 and S2. It is an important antigenic determinant capable of inducing a protective immune response. The S1 subunit contains the RBD, which is the main target for SARS-CoV-2-neutralizing antibodies and convalescent serum titres against the RBD correlated well with neutralization titres [10]. The RBD in the SARS-CoV-2 spike protein is a crucial antigenic region, as it contains the interacting surface for ACE2 binding [11]. In addition, the RBD was reported to be immunodominant in the humoral response and accounted for 90% of neutralizing activities [12]. Therefore, most of the current SARS-CoV-2 vaccines were designed to target the S protein as an antigen to elicit humoral immune responses.

4. Current Status of SARS-CoV-2 Vaccine

The urgency of combating COVID-19 has fast-tracked vaccine development. RNA vaccines such as mRNA vaccines were rapidly manufactured, and they elicited strong humoral immune responses in clinical trials. The WHO reported a total of 140 vaccines candidates in clinical trials using various platforms by January 2022. The majority of the vaccine candidates are protein subunit vaccines (34%), RNA vaccines (17%), and non-replicating viral vectored vaccines (14%). Among the 10 vaccines approved for use by the World Health Organization (WHO), two were mRNA vaccines (BNT162b2 Pfizer and mRNA-1273 Moderna); three were non-replicating viral vector vaccines (Janssen Ad26.CoV2.S, Astrazeneca AZD1222, and Covishield); three were inactivated vaccines (CoronaVac, BBIBP-CorV, and Covaxin); and two were protein subunit vaccines (Novavax NVX-CoV2373 and COVOVAX). These vaccines have now been administered to millions of people globally, but the protective efficacies of COVID-19 vaccines have been reported to decline due to the emergence of new variants of concern (VOC). Pfizer's BNT162b2 and Moderna's mRNA-1273 vaccines were at least 10 times less effective against the B.1.351 (beta) variant. Ad26.COV2.S elicited 5.0- and 3.3-fold lower neutralizing antibody titres against the B.1.315 (beta) and P.1 (gamma) variants, respectively [2]. The efficacy of Astra Zeneca's ChAdOx1 against the B.1.617.2 (delta) variant was 59.8% and only 22% against the B.1.351 (beta) variant [3,4]. More recently, the B.1.1.625 (Omicron) variant has already become the dominant variant of concern in many countries. The efficacy of Pfizer's vaccine was reduced to 70% during the proxy Omicron period in South Africa [13]. Two doses of Pfizer vaccine were reported to elicit 41-fold less neutralizing antibodies against the Omicron variant [14]. Sera from vaccinees who received two doses of ChAdOx1-S and BNT162b2 were found to neutralize the Omicron variant to a much lesser extent when compared to the other variants (alpha, beta, or delta) [15]. The development of a vaccine for each major type of SARS-CoV-2 variant is impractical. A different strategy necessitates the search for highly conserved B-cell epitopes is a prerequisite for constructing an efficient multi-epitope peptide vaccine that can confer broad and long-term protection against the SARS-CoV-2 variants. This will halt the need to revaccinate with the current SARS-CoV-2 vaccines, which were developed based on the S antigen of the "Wuhan" strain, or for the vaccine manufacturers to continue making new vaccines to keep up with the emergence of new variants.

Since mRNA vaccine platforms are available, Pfizer and Moderna are more likely to develop Omicron-based vaccines. Pfizer and Moderna are currently developing vaccines based on the Omicron genome. Pfizer has initiated a clinical study to evaluate the safety, tolerability, and immune response of an Omicron-specific vaccine in healthy adults from 18 to 55 years of age [16], while the Omicron-specific vaccine candidate developed by Moderna (mRNA-1273.529) is undergoing evaluation in a Phase II clinical study [17].

The neutralization of Omicron variants in individuals receiving mRNA-1273 or BNT162b boosters were four to six-fold lower than the wild-type [18], but vaccinees are still protected from severe disease and hospitalizations. However, neutralization titres against the Omicron variant 6 months after the third (booster) dose of mRNA-1273 vaccine declined 6.3-fold from the peak titres assessed 1 month after the booster injection [19]. Although protection against Omicron could be provided by the third dose of the mRNA-1273 vaccine, the decrease in titres observed after 6 months might lead to the requirement for the use of a new Omicron-based vaccine to increase the duration of protection.

5. Approaches to Rational Design of Peptide Vaccines

New vaccine technologies based on subunit proteins or peptides require the identification of suitable antigens. Peptide-based vaccines are safer when compared to traditional vaccines (live attenuated and inactivated) due to minimal allergic and toxic properties [20]. The identification of peptide epitopes using phage display libraries, overlapping peptides that cover the whole length of the protein, or peptide arrays are costly and laborious. Recent advancements of bioinformatics approaches utilizing computational algorithms such as BepiPred, ABC pred, Discotope, and CBtope rely on amino acid sequences or 3D structures to predict B-cell epitopes [21]. The process of peptide vaccine development involves the identification of peptides specifying immunodominant epitopes according to the selected criteria, such as surface accessibility, high hydrophilicity, and antigenicity [22,23]. Multiple peptides were then joined with appropriate linkers and inserted into the expression vector pET-28a(+) so that the vaccine can be expressed in the bacterial system [24]. However, even though bioinformatics approaches will enable the predictions of potential antigenic epitopes, the immunogenicity of the epitopes has to be experimentally validated. Potent B-cell epitopes targeted by monoclonal antibodies are more likely to be conformational, which are difficult to incorporate into multi-epitope peptide-based vaccines. Short peptides comprising linear amino acids from discontinuous regions of the conformational epitopes can be incorporated into peptide-based vaccines. Hence, there is the need to identify B-cell epitopes from bioinformatics (prediction or validation) and monoclonal antibody targeting.

6. Identification of SARS-CoV-2 B-Cell Epitopes within S, M, and N Proteins from the Combination of Bioinformatics and In Vitro Neutralization Assays

Infection with SARS-CoV-2 initiates an immune response that leads to the production of binding antibodies. However, not all binding antibodies can block viral entry and replication. The subpopulation of binding antibodies known as neutralizing antibodies (nAbs) can neutralize the virus and thus prevent virus infection. They are elicited by neutralizing B-cell epitopes. The identification of epitopes that can induce robust B-cell responses is a prerequisite for designing epitope-based vaccines. Linear B-cell epitopes can be incorporated easily in the multi-epitope peptide vaccine to induce humoral responses. Besides linear epitopes, conformational B-cell epitopes can be identified by prediction methods such as ElliPro. In a recent study by Dong et al. (2020), three linear B-cell epitopes were selected for in silico cloning using the expression vector PET28a(+) [25]. However, further validations of the efficacy of the vaccines will be required. Conformational epitopes are more likely to be grated onto scaffolds such as virus-like particles [26] rather than being incorporated into multi-epitope peptide-based vaccines. Therefore, we focus on the search for immunogenic linear B-cell epitopes, which are highly conserved against SARS-CoV-2 for constructing an efficient multi-epitope peptide vaccine.

Poh et al. (2020) identified two immunodominant linear B-cell epitopes, S14P5 and S21P2, which were present on the SARS-CoV-2 S glycoprotein, by using pools of overlapping linear B-cell peptides spanning the entire S glycoprotein of SARS-CoV-2. Sera depleted of antibodies targeting either peptides S14P5 or S21P2 led to a >20% reduction in pseudotyped lentivirus neutralization, validating that antibodies targeting these two linear S epitopes are important for neutralizing SARS-CoV-2. Based on peptide arrays, Farrera-

Soler et al. (2020) identified three immunodominant linear epitopes ($S_{655-672}$, $S_{787-822}$, and $S_{1147-1158}$), which were recognized in >40% of COVID-19 patients. Two of these epitopes ($S_{655-672}$ and $S_{787-822}$) corresponded to key proteolytic sites on the spike proteins S1/S2 and S2, which have been shown to play a critical role in efficient viral entry [27]. Lu et al. (2021) predicted a total of 33 B-cell epitopes based on the 3D structure of the S, M, E, and N proteins, which were further elucidated by computational simulations on epitope surface accessibility. Six immunodominant linear B-cell epitopes were discovered: three were from the S protein; one from M; and two from N proteins ($S_{556-570}$, $S_{675-689}$, $S_{721-733}$, $M_{183-197}$, $N_{152-170}$, and $N_{357-373}$). However, the epitopes from the N protein are unlikely to be immunodominant B-cell epitopes, as the N protein is encapsidated within the virion and is inaccessible to antibody binding. The peptide $S_{556-570}$ was also identified in a previous study as an immunodominant epitope that was able to elicit neutralizing antibodies [28]. As the $S_{556-570}$ epitope is localized close to the RBD, it is plausible that antibodies binding to this region might sterically hinder the binding of SARS-CoV-2 to the ACE2 receptor, thereby abolishing the virus infection [29]. Among the 33 predicted epitopes, four peptides (S_{92-106}, $S_{139-153}$, $S_{439-454}$, and $S_{455-469}$) were able to elicit the production of neutralization antibodies against both D614 and G614 SARS-CoV-2 pseudoviruses with an inhibition rate of 40–50%. Epitope S_{63-85} induced the highest neutralizing effect on G614 SARS-CoV-2 pseudoviruses with an antibody titre of 1:80 [30].

It has been shown that 90% of neutralizing antibodies (nAbs) elicited against SARS-CoV-2 in COVID-19 patients were targeted at the RBD of the S glycoprotein [12]. Thus, profiling B-cell epitopes using sera from animals immunized with overlapping peptides spanning the RBD could reveal the molecular determinants of antigenicity. Three linear peptides specifying B-cell epitopes (R345, R405, and R465) were shown to elicit strong and specific IgG antibody responses from the SARS-CoV-2 S1 protein [31]. Another three B-cell epitopes present in the RBD, CoV2_S-10, CoV2_S-11, and CoV2_S-13, were identified by immunoinformatic predictions and confirmed by ELISA with sera from *Macaca fascicularis* vaccinated with a SARS-CoV-2 RBD subunit vaccine in the study published by Kanok-porn Polyiam et al. (2021). In addition, the peptide $S_{404-424}$ was also shown to elicit neutralizing antibodies in mice [32]. The epitope $S_{809-826}$ (PSKPSKRSFIEDLLFNKV), which overlapped with the CoV2_S-17 epitope, has been demonstrated as a neutralizing epitope in humans [28]. Two epitopes that overlap with CoV2_S-20 (NNTVYDPLQPELDSFKEELD-KYFKNHTSPDVDLGDISGI) have previously been characterized as immunodominant, as well as neutralizing [33,34]. The B-cell epitopes identified from the literature were mapped on the SARS-CoV-2 S monomer (Figure 2A), while the linear B-cell epitopes in the RBD targeted by monoclonal antibodies mined from the literature were mapped on the structure of the SARS-CoV-2 RBD and ACE2 complex (Figure 2B).
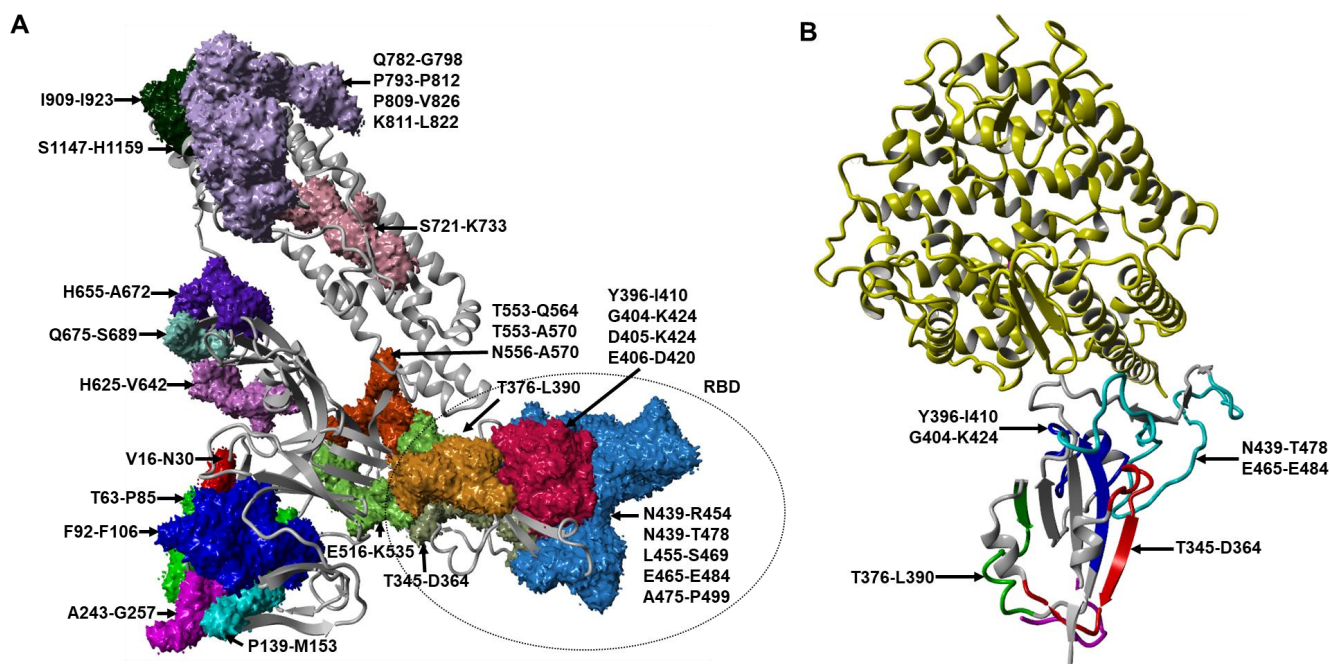
Figure 2. (**A**) The localization of B-cell epitopes mapped on the SARS-CoV-2 S monomer in closed conformation are represented by the amino residue number (PDB ID: 6ZB5/A). (**B**) Locations of B-cell epitopes targeted by monoclonal antibodies in the structure of ACE2 in complex with the SARS-CoV-2 RBD (PDB ID: 7DQA). ACE2 is shown in yellow, while the RBD is in grey colour.

7. Monoclonal Antibodies against SARS-CoV-2 RBD Protein

Neutralizing antibody-mediated immunity protects an individual from viral infections by interfering with virus–host cell interactions required for viral attachment or entry. The majority of monoclonal antibodies isolated to date specifically target the RBD on the spike protein that allows SARS-CoV-2 to interact with the ACE2 receptor. Three monoclonal antibodies (15G9, 12C10, and 10D2) targeting the peptides R345, R405, and R465, respectively, were shown to inhibit the RBD–ACE2 interaction with an inhibition rate of 20–60%. This finding is consistent with a previous study where mAB 12C10 and mAb 10D2 exhibited 20–40% neutralization capacity [30]. Among the three mAbs, 12C10, which targeted the peptide R405, could strongly bind to both the SARS-CoV and SARS-CoV-2 S proteins, indicating that 12C10 is a cross-reactive antibody [31]. Antibodies targeting epitopes CoV2_S-10 and CoV2_S-11 were shown to inhibit RBD–ACE2 interactions [35]. The neutralizing potency of the antibody against epitope CoV2_S-10 was consistent with previous studies that reported an inhibition rate of 40% [30,31]. Monoclonal antibody B38, which could neutralize SARS-CoV-2, showed interactions with multiple residues in the RBD [36]. Murine antibodies induced by peptides $S_{406–420}$ (EVRQIAPGQTGKIAD), $S_{439–454}$ (NNLDSKVGGNYNYLYR), and $S_{455–469}$ (LFRKSNLKPFERDIS), which corresponded to the epitopes present in CoV2_S-10 and CoV2_S11, were able to inhibit SARS-CoV-2 pseudovirus infections [30]. Wan et al. (2020) identified 11 potent neutralizing antibodies from 11 convalescent patients, and these also targeted three epitopes present in the RBD of the spike protein [37]. Amongst the three antibodies, antibody 414-1 showed the best neutralizing activity with an IC_{50} at 1.75 nM. Antibody 553-15 could substantially potentiate several other antibodies to have higher neutralizing abilities, while 515-5 showed cross-neutralizing activity towards the SARS-CoV pseudovirus. Two linear epitopes in the RBD were reported in the study of Makdasi et al. (2021). One of these epitopes spanning amino acids $S_{376–390}$ (TFKCYGVSPTKLNDL) was targeted by antibodies 24 and 67, while the second epitope $S_{396–410}$ (YADSFVIUGDEVRQI) was targeted by antibodies 69 and 90. The actual length of the second epitope could be further narrowed down to include only amino acids $S_{404–410}$

(GDEVRQI) after visualizing the epitopes present on the crystal structure of the spike protein, as the first eight amino acids of the peptides were not exposed to the surface of the spike trimer [38]. The second epitope had seven overlapping amino acids with the epitopes $S_{404-424}$ (GDEVRQIAPGQTGKIADYNYK) reported in a previous study [35]. Six representative epitopes covering the two hot spots (aa 525–685 and aa 770–829) across the S protein were selected from the screening of 211 peptides using peptide microarrays. Among the six selected epitopes, the antibodies against the three epitopes S_{1-93}, S_{1-105}, and S_{2-78} exhibited potent neutralizing activities with virus inhibitory efficiencies of 51%, 35%, and 35%, respectively. The antibody targeting S_{1-93} and $S_{553-564}$ (TESNKKFLPFLPFQQ) showed the highest neutralizing capacity, which is consistent with the findings of a recent study [28].

Two potent neutralizing monoclonal antibodies, B38 and H4, which targeted different RBD sites, were capable of neutralizing live SARS-CoV-2 virus (IC_{50} = 0.177 µg/mL for B38 and 0.896 µg/mL for H4) [39]. The crystal structure of the RBD-B38 complex showed that most of the residues on the B38-binding epitope overlapped with the RBD–ACE2-binding interface, suggesting that B38 neutralized SARS-CoV-2 infection by functionally mimicking ACE2 to bind to RBD and blocked RBD–ACE2 binding. Importantly, a single dose of B38 or H4 (25 mg/kg) was demonstrated to reduce lung viral loads by 32.8% and 26% in mice, respectively, when compared to the untreated group [39].

CB6 was identified from the PBMCs of a COVID-19 convalescent patient by using the recombinant RBD of the SARS-CoV-2 S protein to screen memory B cells from PBMCs. Shi et al. (2020) showed that CB6 exhibited an effective neutralization of live SAS-CoV-2 infection of Vero-E6 cells with a neutralizing dose (ND50) of 0.036 ± 0.007 µg/mL. Structural studies revealed that B6 recognized an epitope that overlapped with angiotensin-converting enzyme 2 (ACE2)-binding sites in the SARS-CoV-2 receptor binding domain and thereby interfered with virus–receptor interactions by both steric hindrance and direct competition for interface residues. CB6 effectively reduced the viral loads and lessened infection-related lung damage in rhesus macaques [40].

Noy-Porat et al. (2020) isolated and characterized eight SARS-CoV-2-neutralizing monoclonal antibodies (nMAbs) that targeted four distinct epitopes on the RBD. These antibodies were selected from a phage display library constructed using peripheral circulatory lymphocytes collected from SARS-CoV-2 patients. Monoclonal antibodies MD45, MD67, MD62, and MD65 displayed the highest neutralizing potency, with a neutralization dosage (NT_{50}) of 2.1, 1.9, 1.6, and 0.22 µg/mL, respectively. MD65 exhibited the highest neutralization capacity amongst all the monoclonal antibodies by completely inhibiting the binding of RBD to the ACE2 receptor [41].

A total of 25 mAbs were isolated from Epstein–Barr virus-immortalized memory B cells of a SARS-CoV-infected patient in 2003. S309 was the only mAb that had potent neutralizing activities against SARS-CoV-2 and SARS-CoV pseudoviruses, as well as the live SARS-CoV-2, by engaging the receptor-binding domain of the S glycoprotein. MAb S309 was shown to neutralize MLV-based SARS-CoV S-glycoprotein-pseudotyped viruses with IC_{50} of 120–180 ng/mL and displayed more potent neutralizing capability towards the live SARS-CoV-2 (2019n-CoV/USA_WA1/2020) with an IC_{50} of 79 ng/mL [42].

SARS-CoV-2 S protein-specific B cells were subsequently sorted for single-cell sequencing and mAb isolation. Among the 403 monoclonal antibodies isolated from three convalescent COVID-19 patients using a SARS-CoV-2-stabilized prefusion spike protein as the antigen, COVA1-18 and COVA2-15 were identified as unusually potent nMAbs targeting the RBD of the SARS-CoV-2 S protein. These mAbs showed neutralizing activities against the SARS-CoV-2 pseudoviruses in Huh7 liver cells with an IC_{50} value of 8 ng/mL and potently inhibited live SARS-CoV-2 infection in Vero-E6 cells with IC_{50} values of 7 and 9 ng/mL, respectively. Of the 19 mAbs that could inhibit SARS-CoV-2 pseudovirus infection, 14 were found to bind to the RBD [43].

A total of sixty-one neutralizing antibodies were isolated from the peripheral blood of five COVID-19 patients by sorting the S trimer-specific B cells, followed by single B cell

receptor sequencing. Nineteen antibodies potently neutralized live SARS-CoV-2 in vitro. Nine NMAbs exhibited very high potency with 50% virus-inhibitory concentrations in the neutralizing range from 0.7 to 9 ng/mL, including four that were directed against the RBD, three directed against the N-terminal domain (NTD), and two directed against the nearby quaternary epitopes. The study reported that NMAb 2–15 is by far the most potent in the literature that targeted the RBD and could neutralize both pseudotyped and live SARS-CoV-2 virus in Vero-E6 cells with IC_{50} of 5 ng/mL and 0.7 ng/mL, respectively. A single dose of NMAb 2–15 (1.5 mg/kg) could effectively confer protection against SARS-CoV-2 infection in hamsters by 4-log reductions in virus titres [44].

Pinto et al. (2021) identified five mAbs from the memory B cells from three COVID-19 convalescent donors that targeted the conserved S2 stem helix region. Amongst the five mAbs, S2P6 had exceptionally broad cross-reactivity and neutralization against the SARS-CoV-2 variants (including Alpha, Beta, Gamma, and Kappa) and other beta-coronaviruses through the inhibition of membrane fusion. S2P6 was shown to neutralize the infection of live SARS-CoV-2 viruses to Vero-E6$^+$ cells in the presence of protease TMPRSS2 with IC_{50} 1.67 μg/mL. S2P6 could neutralize SARS-CoV-2 pseudotyped with the S protein from several variants with IC_{50} ranging from 10 μg/mL to 100 μg/mL. Peptide mapping using linear 15-mers overlapping peptides revealed all five mAbs were binding to peptides $S_{1148–1156}$ (FKEELDKYF) located in the S2 subunit. This peptide had nine overlapping amino acids with the B-cell epitopes reported in the studies of Farrera-Soler et al. (2020) and Li et al. (2020) [27,34]. Lastly, a single dose of mAb S2P6 (20 mg/kg) could effectively confer protection against the SARS-CoV-2 Wuhan strain and B.1.351 Beta variant infections in hamsters by 2-log and 1.5-log reductions in the lung viral RNA load, respectively [45]. The efficacies of the monoclonal antibodies recognizing the RBD of the S protein were listed in Table 1.

8. Conservancy of Linear B-Cell Epitopes against SARS-CoV-2 Variants

Previous studies have demonstrated that the RBD elicited the major pool of neutralizing antibodies, but it is too risky to focus only on the RBD, especially with the continuous emergence of novel SARS-CoV-2 variants throughout the world, which contain multiple mutations in the RBD protein. Thus, it would be interesting to assess the potential epitope conservancy towards different variants and to rationally design multiepitope peptide vaccines based on the best B-cell epitope combinations. A total of 200 unique spike (S) protein sequences for 11 SARS-CoV-2 variants of concern (VOC) and variants of interest (VOI) genes were retrieved from the NCBI (https://www.ncbi.nlm.nih.gov/ (accessed on 10 August 2021)) and GISAID databases (https://www.gisaid.org/ (accessed on 6 September 2021)). The nucleotide sequences obtained from GISAID were translated to amino acid sequences using the Expasy Translate Tool (https://web.expasy.org/translate/ (accessed on 21 October 2021)). The IEDB conservancy analysis tool (http://tools.iedb.org/conservancy/ (accessed on 12 January 2022)) [46] was used to compare the degree of conservation for peptides specifying B-cell epitopes by using protein sequences of the SARS-CoV-2 Wuhan strain and variants from worldwide isolates. The conservation score of the potent peptides specifying B-cell epitopes identified from cross-referencing of all the four SARS-CoV-2 variants are listed in Table 2. Amongst the five highly conserved (100%) peptides specifying B-cell epitopes that were reported in the literature, peptide $S_{345–364}$ (TRFASVYAWNRKRIS-NCVAD) was reported to inhibit the RBD–ACE2 interaction with an inhibition rate of 60%. Thus, this peptide could improve and enhance the efficacy of the SARS-CoV-2 vaccine against the Wuhan strain and variants.

9. Conclusions

The development of an effective SARS-CoV-2 vaccine is challenging due to the emergence of SARS-CoV-2 variants. Producing a vaccine for each SARS-CoV-2 variant is impractical. A different strategy necessitates the search for highly conserved B-cell epitopes capable of eliciting neutralizing antibodies that can confer broad protection against the

SARS-CoV-2 variants. This will halt the need to revaccinate with the current SARS-CoV-2 vaccines, which were developed based on the S-antigen of the "Wuhan" strain, or for the vaccine manufacturers to continually produce new vaccines to keep up with the emergence of new variants.

B-cell epitopes can be represented as either linear or conformational. Linear B-cell epitopes consist of linear sequences of amino acids that allow the binding of target-specific antibodies, whereas conformational epitopes are composed of discontinuous residues that are brought together in close proximity to form an antigenic site. Approximately 90% of the B-cell epitopes are conformational, and only a minority of B-cell epitopes are linear [26]. We aimed to review the immunogenic linear B-cell epitopes that are highly conserved, as well as conformational B-cell epitopes targeted by monoclonal antibodies such as CB6 or S309. There are a number of commonly used B-cell epitope prediction methods with high accuracy in cross-validation, such as CBTOPE and ElliPro [26]. The methods for conformational B-cell epitope prediction are challenging, as it generally requires the knowledge of the 3D structure of proteins. Conformational B-cell epitopes are unlikely to be incorporated into multi-epitope peptide-based vaccines that generally utilize linear peptides. However, linear amino acid sequences from discontinuous regions of the conformational epitopes can be extracted and incorporated in the peptide-based vaccine design [25]. Conformational epitopes are more likely to be grafted onto suitable scaffolds like virus-like particles (VLPs) that can mimic the native antigen [26].

To date, many SARS-CoV-2-neutralizing antibodies targeting RBD have been identified from convalescent patients and vaccinees. The efficacies of the neutralizing antibodies are often abrogated by RBD mutations in the spike protein. An unusually large number of mutations are found in the Omicron variants (B.1.1.529), consisting of more than 30 mutations in the spike protein. Indeed, studies have shown that Omicron would escape the majority of potent SARS-CoV-2-neutralizing antibodies that directly interfere with the binding of ACE2 reported from the literature [47]. However, neutralizing antibodies such as S309 and CR3022, which often exhibited broad sarbecovirus-neutralizing activities, were less affected by Omicron [47]. Therefore, the combination of highly conserved peptides with potent antigenicity in generating neutralizing antibodies would provide the rational basis for vaccine designs based on these B-cell epitopes.

Table 1. Efficacies of the monoclonal antibodies recognizing the RBD of the S protein.

mAb	Sources	Target	Efficacy	Protection	Reference
B38	Peripheral blood of SARS-CoV-2-infected patients	RBD	LV neutralization: $IC_{50} = 0.177 \ \mu g/mL$	Protection of mice: Lung viral loads reduced by 32.8% compared with PBS control.	[39]
H4	Peripheral blood of SARS-CoV-2-infected patients	RBD	LV neutralization: $IC_{50} = 0.896 \ \mu g/mL$	Protection of mice: Lung viral loads reduced by 26% compared with PBS control.	[39]
414-1	Peripheral blood of SARS-CoV-2-infected patients	RBD	LV neutralization $IC_{50} = 1.75 \ nM$	N/A	[37]
MD65	Phage display library constructed using peripheral circulatory lymphocyte of SARS-CoV-2-infected patients	RBD	LV neutralization $NT_{50} = 0.22 \ \mu g/mL$	N/A	[41]

Table 1. *Cont.*

mAb	Sources	Target	Efficacy	Protection	Reference
COVA1–18	B cells of convalescent patients	RBD	PsV neutralization: $IC_{50} = 0.008$ μg/mL LV neutralization: $IC_{50} = 0.007$ μg/mL	N/A	[43]
COVA2-15	B cells of convalescent patients	RBD	PsV neutralization: $IC_{50} = 0.008$ μg/mL LV neutralization: $IC_{50} = 0.009$ μg/mL	N/A	[43]
2-15	Peripheral blood of COVID-19 patients	RBD	PsV neutralization: $IC_{50} = 0.7$ ng/mL LV neutralization: $IC_{50} = 5$ ng/mL	Protection of hamsters: Viral RNA copy numbers and infectious virus titers in lung tissues were reduced by 4 logs or more compared with the PBS control.	[44]
S309	Peripheral blood of SARS-infected patients	RBD	PsV neutralization: $IC_{50} = 120{\sim}180$ ng/mL	N/A	[42]
3F11	Humanized phage display library	RBD	PsV neutralization: $IC_{50} = 3.8$ ng/mL LV neutralization: $IC_{50} = 436$ ng/mL.	N/A	[48]
4A8	Peripheral blood of COVID-19 convalescent patients	NTD (in S1)	PsV neutralization: $EC_{50} = 49$ μg/mL LV neutralization: $EC_{50} = 0.61$ μg/mL	N/A	[49]
CR3022	Gene cloning; Protein expression	RBD	LV neutralization: $IC_{50} = {\sim}0.114$ μg/mL	N/A	
CB6	B cells of convalescent patients	RBD	PsV neutralization: $ND_{50} = 0.036$ μg/mL LV neutralization: $ND_{50} = 0.036$ μg/mL	Protection of rhesus macaques: 50 mg/kg	[40]
S2P6	Memory B cells of SARS-CoV-2 patients	S2	LV neutralization: $IC_{50} = 1.67$ μg/mL PsV D614G: $IC_{50}{\sim}10$ μg/mL PsV P.1: $IC_{50}{\sim}10$ μg/mL PsV B.1.1.7: $IC_{50}{\sim}100$ μg/mL PsV B.1.351: $IC_{50}{\sim}100$ μg/mL PsV 1.1.617: $IC_{50}{\sim}20$ μg/mL	Protection of hamsters: Viral RNA copy numbers in lung tissues were reduced by 2 logs and 1.5 logs against SARS-CoV-2 Wuhan strain and B.1.351 Beta strain.	[45]

LV: live viruses; PsV: SARS-CoV-2 pseudoviruses; N/A: data not available.

Table 2. Peptides specifying B-cell epitopes identified in SARS-CoV-2.

Protein	Monoclonal Antibody	Peptide ID	Start-End (aa)	Sequences of B-Cell Epitopes	Methods	Host	Inhibition	Conservancy (%)	Reference
S1 S2	N/A	S14P5 S21P2	553–570 809–826	TESNKKFLPFQQFGRDIA PSKPSKRSFIEDLLFNKV	Overlapping peptide library	COVID-19 sera	>20% of pseudoviruses >20% of pseudoviruses	84 100	[28]
S1 S2 S2	N/A	N/A	655–672 782–798/811–822 1147–1158	HVNNSYECDIPIGAGICA QIYKTPPIKDFG/KPSKRSFIEDLL SFKEELDKYFKN	Peptide array	COVID-19 plasma	N/A	93.50 98/100 100	[27]
S1/S2 S2	N/A	N/A	675–689 721–733	QTQTNSPRRARSVAS SVTTEILPVSMTK	Epitope predictions based on 3D protein structure, epitope surface accessibility	COVID-19 sera, BALB/c mice	~50% of G614 pseudoviruses No inhibition of D614 pseudoviruses	60.5 98.5	[30]
S1 S1 RBD RBD S1 S2 S2	N/A	N/A	16–30 243–257 406–420 475–499 556–570 793–812(N) 909–923	VNLTTRTQLPPAYTN ALHRSYLTPGDSSSG EVRQIAPGQTGKIAD AGSTPCNGVEGFNCYFPLQSYGFQP NKKFLPFQQFGRDIA PIKDFGGFN(GlcNAc)FSQILPDPSKP IGVTQNVLYENQKLI			20–40% inhibition of D614 pseudoviruses	84 85.50 88 53.50 84 99 99.50	
S1 S1 RBD RBD	N/A	N/A	92–106 139–153 439–454 455–469	FASTEKSNIIRGWIF PFLGVYYHKNNKSWM NNLDSKVGGNYNYLYR LFRKSNLKPFERDIS			40–50% inhibition of D614, G614 pseudoviruses	89.50 62 76.50 100	
S1	N/A	N/A	63–85	TWFHAIHVSGTNGTKRFDNPVLP			>80% inhibition of G614 pseudoviruses	65.50	

Table 2. *Cont.*

Protein	Monoclonal Antibody	Peptide ID	Start-End (aa)	Sequences of B-Cell Epitopes	Methods	Host	Inhibition	Conservancy (%)	Reference
RBD RBD RBD	15G9 12C10 10D2	R345 R405 R465	345–364 405–424 465–484	TRFASVYAWNRKRISNCVAD DEVRQIAPGQTGKIADYNYK ERDISTEIYQAGSTPCNGVE	Overlapping peptides covering RBD	Swine and mice	60% of RBD/ACE2 interaction 40% of RBD/ACE2 interaction 20% of RBD/ACE2 interaction	100 88 57	[31]
RBD RBD RBD	N/A	CoV2_S-10 CoV2_S-11 CoV2_S-13	404–424 439–478 516–535	GDEVRQIAPGQTGKIADYNYK NNLDSKVGGNYNYLYRLFRKSNLKPFERDISTEIYQAGST ELLHAPATVCGPKKSTNLVK	Immunoinformatic prediction (Bepipred-2.0)	Cynomolgus macaques	N/A	88 74 98.50	[35]
S1 S1 S2	N/A	S1-93 S1-105 S2-78	553–564 625–642 1148–1159	TESNKKFLPFQQ HADQLTPTWRVYSTGSNV FKEELDKYFKNH	Peptide microarray	COVID-19 sera	51% of pseudoviruses 35% of pseudoviruses 35% of pseudoviruses	99 99.5 100	[34]
RBD RBD	Ab 24 & 67 Ab 69 & 90	N/A	376–390 396–410	TFKCYGVSPTKLNDL YADSFVIRGDEVRQI	Overlapping peptides covering S protein	Rabbit sera	N/A	86.67 53.33	[38]
S2	S2P6	N/A	1148–1156	KEELDKYF	X-ray crystallography and Cryo-EM	COVID-19 sera	>90% inhibition of live viruses	100	[45]

N/A: data not available; Peptide ID: identity of peptides.

References

1. Grant, M.C.; Geoghegan, L.; Arbyn, M.; Mohammed, Z.; McGuinness, L.; Clarke, E.L.; Wade, R.G. The prevalence of symptoms in 24,410 adults infected by the novel coronavirus (SARS-CoV-2; COVID-19): A systematic review and meta-analysis of 148 studies from 9 countries. *PLoS ONE* **2020**, *15*, e0234765. [CrossRef] [PubMed]
2. Vallamkondu, J.; John, A.; Wani, W.Y.; Ramadevi, S.P.; Jella, K.K.; Reddy, P.H.; Kandimalla, R. SARS-CoV-2 pathophysiology and assessment of coronaviruses in CNS diseases with a focus on therapeutic targets. *Biochim. Biophys. Acta Mol. Basis Dis.* **2020**, *1866*, 165889. [CrossRef] [PubMed]
3. Guan, W.J.; Ni, Z.Y.; Hu, Y.; Liang, W.H.; Ou, C.Q.; He, J.X.; Liu, L.; Shan, H.; Lei, C.L.; Hui, D.S.C.; et al. Clinical characteristics of coronavirus disease 2019 in China. *N. Engl. J. Med.* **2020**, *382*, 1708–1720. [CrossRef] [PubMed]
4. Velavan, T.P.; Meyer, C.G. The COVID-19 epidemic. *Trop. Med. Int. Health* **2020**, *25*, 278–280. [CrossRef]
5. Jungreis, I.; Sealfon, R.; Kellis, M. SARS-CoV-2 gene content and COVID-19 mutation impact by comparing 44 Sarbecovirus genomes. *Nat. Commun.* **2021**, *12*, 2642. [CrossRef]
6. Alanagreh, L.; Alzoughool, F.; Atoum, M. The human coronavirus disease COVID-19: Its origin, characteristics, and insights into potential drugs and its mechanisms. *Pathogens* **2020**, *9*, 331. [CrossRef]
7. Rastogi, M.; Pandey, N.; Shukla, A.; Singh, S.K. SARS coronavirus 2: From genome to infectome. *Respir. Res.* **2020**, *21*, 318. [CrossRef]
8. Shang, J.; Wan, Y.; Luo, C.; Ye, G.; Geng, Q.; Auerbach, A.; Li, F. Cell entry mechanisms of SARS-CoV-2. *Proc. Natl. Acad. Sci. USA* **2020**, *117*, 11727. [CrossRef]
9. Nguyen, H.T.; Zhang, S.; Wang, Q.; Anang, S.; Wang, J.; Ding, H.; Kappes, J.C.; Sodroski, J. Spike glycoprotein and host cell determinants of SARS-CoV-2 entry and cytopathic effects. *J. Virol.* **2020**, *95*, e02304-20. [CrossRef]
10. Ahmed, S.; Khan, M.S.; Gayathri, S.; Singh, R.; Kumar, S.; Patel, U.R.; Malladi, S.K.; Rajmani, R.S.; van Vuren, P.J.; Riddell, S.; et al. A stabilized, monomeric, receptor binding domain elicits high-titer neutralizing antibodies against all SARS-CoV-2 variants of concern. *Front Immunol.* **2021**, *12*, 765211. [CrossRef]
11. Lan, J.; Ge, J.; Yu, J.; Shan, S.; Zhou, H.; Fan, S.; Zhang, Q.; Shi, X.; Wang, Q.; Zhang, L.; et al. Structure of the SARS-CoV-2 spike receptor-binding domain bound to the ACE2 receptor. *Nature* **2020**, *581*, 215–220. [CrossRef] [PubMed]
12. Piccoli, L.; Park, Y.-J.; Tortorici, M.A.; Czudnochowski, N.; Walls, A.C.; Beltramello, M.; Silacci-Fregni, C.; Pinto, D.; Rosen, L.E.; Bowen, J.E.; et al. Mapping neutralizing and immunodominant sites on the SARS-CoV-2 spike receptor-binding domain by structure-guided high-resolution serology. *Cell* **2020**, *183*, 1024–1042.e21. [CrossRef] [PubMed]
13. Collie, S.; Champion, J.; Moultrie, H.; Bekker, L.-G.; Gray, G. Effectiveness of BNT162b2 vaccine against Omicron variant in South Africa. *N. Engl. J. Med.* **2021**, *386*, 494–496. [CrossRef] [PubMed]
14. Cele, S.; Jackson, L.; Khan, K.; Khoury, D.; Moyo-Gwete, T.; Tegally, H.; Scheepers, C.; Amoako, D.; Karim, F.; Bernstein, M.; et al. SARS-CoV-2 Omicron has extensive but incomplete escape of Pfizer BNT162b2 elicited neutralization and requires ACE2 for infection. *medRxiv* **2021**. [CrossRef]
15. Rössler, A.; Riepler, L.; Bante, D.; von Laer, D.; Kimpel, J. SARS-CoV-2 omicron variant neutralization in serum from vaccinated and convalescent persons. *N. Engl. J. Med.* **2022**, *386*, 698–700. [CrossRef]
16. Pfizer and BioNTech Initiate Study to Evaluate Omicron-Based COVID-19 Vaccine in Adults 18 to 55 Years of Age. Available online: https://www.pfizer.com/news/press-release/press-release-detail/pfizer-and-biontech-initiate-study-evaluate-omicron-based (accessed on 15 February 2022).
17. New Studies Look to Assess Immunogenicity of Omicron-Based Vaccines. Available online: https://www.europeanpharmaceuticalreview.com/news/168012/studies-assess-immunogenicity-omicron-based-vaccines/ (accessed on 15 February 2022).

18. Garcia-Beltran, W.F.; St Denis, K.J.; Hoelzemer, A.; Lam, E.C.; Nitido, A.D.; Sheehan, M.L.; Berrios, C.; Ofoman, O.; Chang, C.C.; Hauser, B.M.; et al. mRNA-based COVID-19 vaccine boosters induce neutralizing immunity against SARS-CoV-2 Omicron variant. *Cell* **2022**, *185*, 457–466.e4. [CrossRef]

19. Pajon, R.; Doria-Rose, N.A.; Shen, X.; Schmidt, S.D.; O'Dell, S.; McDanal, C.; Feng, W.; Tong, J.; Eaton, A.; Maglinao, M.; et al. SARS-CoV-2 omicron variant neutralization after mRNA-1273 booster vaccination. *N. Engl. J. Med.* **2022**, *386*, 1088–1091. [CrossRef]

20. Sarma, V.R.; Olotu, F.A.; Soliman, M.E.S. Integrative immunoinformatics paradigm for predicting potential B-cell and T-cell epitopes as viable candidates for subunit vaccine design against COVID-19 virulence. *Biomed. J.* **2021**, *44*, 447–460. [CrossRef]

21. Jespersen, M.C.; Mahajan, S.; Peters, B.; Nielsen, M.; Marcatili, P. Antibody Specific B-Cell Epitope Predictions: Leveraging Information From Antibody-Antigen Protein Complexes. *Front. Immunol.* **2019**, *10*, 298. [CrossRef]

22. Kolaskar, A.S.; Tongaonkar, P.C. A semi-empirical method for prediction of antigenic determinants on protein antigens. *FEBS Lett.* **1990**, *276*, 172–174. [CrossRef]

23. Emini, E.A.; Hughes, J.V.; Perlow, D.S.; Boger, J. Induction of hepatitis A virus-neutralizing antibody by a virus-specific synthetic peptide. *J. Virol.* **1985**, *55*, 836–839. [CrossRef] [PubMed]

24. Kar, T.; Narsaria, U.; Basak, S.; Deb, D.; Castiglione, F.; Mueller, D.M.; Srivastava, A.P. A candidate multi-epitope vaccine against SARS-CoV-2. *Sci. Rep.* **2020**, *10*, 10895. [CrossRef] [PubMed]

25. Dong, R.; Chu, Z.; Yu, F.; Zha, Y. Contriving multi-epitope subunit of vaccine for COVID-19: Immunoinformatics approaches. *Front. Immunol.* **2020**, *11*, 1784. [CrossRef] [PubMed]

26. Sanchez-Trincado, J.L.; Gomez-Perosanz, M.; Reche, P.A. Fundamentals and methods for T- and B-cell epitope prediction. *J. Immunol. Res.* **2017**, *2017*, 2680160. [CrossRef]

27. Farrera-Soler, L.; Daguer, J.-P.; Barluenga, S.; Vadas, O.; Cohen, P.; Pagano, S.; Yerly, S.; Kaiser, L.; Vuilleumier, N.; Winssinger, N. Identification of immunodominant linear epitopes from SARS-CoV-2 patient plasma. *PLoS ONE* **2020**, *15*, e0238089. [CrossRef] [PubMed]

28. Poh, C.M.; Carissimo, G.; Wang, B.; Amrun, S.N.; Lee, C.Y.; Chee, R.S.; Fong, S.W.; Yeo, N.K.; Lee, W.H.; Torres-Ruesta, A.; et al. Two linear epitopes on the SARS-CoV-2 spike protein that elicit neutralising antibodies in COVID-19 patients. *Nat. Commun.* **2020**, *11*, 2806. [CrossRef]

29. Tian, X.; Li, C.; Huang, A.; Xia, S.; Lu, S.; Shi, Z.; Lu, L.; Jiang, S.; Yang, Z.; Wu, Y.; et al. Potent binding of 2019 novel coronavirus spike protein by a SARS coronavirus-specific human monoclonal antibody. *Emerg. Microbes Infect.* **2020**, *9*, 382–385. [CrossRef]

30. Lu, S.; Xie, X.X.; Zhao, L.; Wang, B.; Zhu, J.; Yang, T.R.; Yang, G.W.; Ji, M.; Lv, C.P.; Xue, J.; et al. The immunodominant and neutralization linear epitopes for SARS-CoV-2. *Cell Rep.* **2021**, *34*, 108666. [CrossRef]

31. Jiang, M.; Zhang, G.; Liu, H.; Ding, P.; Liu, Y.; Tian, Y.; Wang, Y.; Wang, A. Epitope profiling reveals the critical antigenic determinants in SARS-CoV-2 RBD-based antigen. *Front. Immunol.* **2021**, *12*, 707977. [CrossRef]

32. Li, L.; Zhao, Z.; Yang, X.; Li, W.; Chen, S.; Sun, T.; Wang, L.; He, Y.; Liu, G.; Han, X.; et al. Identification of four linear B-cell epitopes on the SARS-CoV-2 spike protein able to elicit neutralizing antibodies. *bioRxiv* **2020**. [CrossRef]

33. Yi, Z.; Ling, Y.; Zhang, X.; Chen, J.; Hu, K.; Wang, Y.; Song, W.; Ying, T.; Zhang, R.; Lu, H.; et al. Functional mapping of B-cell linear epitopes of SARS-CoV-2 in COVID-19 convalescent population. *Emerg. Microbes Infect.* **2020**, *9*, 1988–1996. [CrossRef] [PubMed]

34. Li, Y.; Lai, D.Y.; Zhang, H.N.; Jiang, H.W.; Tian, X.; Ma, M.L.; Qi, H.; Meng, Q.F.; Guo, S.J.; Wu, Y.; et al. Linear epitopes of SARS-CoV-2 spike protein elicit neutralizing antibodies in COVID-19 patients. *Cell Mol. Immunol.* **2020**, *17*, 1095–1097. [CrossRef] [PubMed]

35. Polyiam, K.; Phoolcharoen, W.; Butkhot, N.; Srisaowakarn, C.; Thitithanyanont, A.; Auewarakul, P.; Hoonsuwan, T.; Ru-engjitchatchawalya, M.; Mekvichitsaeng, P.; Roshorm, Y.M. Immunodominant linear B cell epitopes in the spike and mem-brane proteins of SARS-CoV-2 identified by immunoinformatics prediction and immunoassay. *Sci. Rep.* **2021**, *11*, 20383. [CrossRef] [PubMed]

36. Wu, F.; Wang, A.; Liu, M.; Wang, Q.; Chen, J.; Xia, S.; Ling, Y.; Zhang, Y.; Xun, J.; Lu, L.; et al. Neutralizing antibody responses to SARS-CoV-2 in a COVID-19 recovered patient cohort and their implications. *medRxiv* **2020**. [CrossRef]

37. Wan, J.; Xing, S.; Ding, L.; Wang, Y.; Gu, C.; Wu, Y.; Rong, B.; Li, C.; Wang, S.; Chen, K.; et al. Human-IgG-neutralizing monoclonal antibodies block the SARS-CoV-2 infection. *Cell Rep.* **2020**, *32*, 107918. [CrossRef]

38. Makdasi, E.; Levy, Y.; Alcalay, R.; Noy-Porat, T.; Zahavy, E.; Mechaly, A.; Epstein, E.; Peretz, E.; Cohen, H.; Bar-On, L.; et al. Neutralizing monoclonal anti-SARS-CoV-2 antibodies isolated from immunized rabbits define novel vulnerable spike-protein epitope. *Viruses* **2021**, *13*, 566. [CrossRef]

39. Wu, Y.; Wang, F.; Shen, C.; Peng, W.; Li, D.; Zhao, C.; Li, Z.; Li, S.; Bi, Y.; Yang, Y.; et al. A noncompeting pair of human neutralizing antibodies block COVID-19 virus binding to its receptor ACE2. *Science* **2020**, *368*, 1274–1278. [CrossRef]

40. Shi, R.; Shan, C.; Duan, X.; Chen, Z.; Liu, P.; Song, J.; Song, T.; Bi, X.; Han, C.; Wu, L.; et al. A human neutralizing antibody targets the receptor-binding site of SARS-CoV-2. *Nature* **2020**, *584*, 120–124. [CrossRef]

41. Noy-Porat, T.; Makdasi, E.; Alcalay, R.; Mechaly, A.; Levy, Y.; Bercovich-Kinori, A.; Zauberman, A.; Tamir, H.; Yahalom-Ronen, Y.; Israeli, M.A.; et al. A panel of human neutralizing mAbs targeting SARS-CoV-2 spike at multiple epitopes. *Nat. Commun.* **2020**, *11*, 4303. [CrossRef]

42. Pinto, D.; Park, Y.J.; Beltramello, M.; Walls, A.C.; Tortorici, M.A.; Bianchi, S.; Jaconi, S.; Culap, K.; Zatta, F.; De Marco, A.; et al. Cross-neutralization of SARS-CoV-2 by a human monoclonal SARS-CoV antibody. *Nature* **2020**, *583*, 290–295. [CrossRef]

43. Brouwer, P.J.M.; Caniels, T.G.; van der Straten, K.; Snitselaar, J.L.; Aldon, Y.; Bangaru, S.; Torres, J.L.; Okba, N.M.A.; Claireaux, M.; Kerster, G.; et al. Potent neutralizing antibodies from COVID-19 patients define multiple targets of vulnerability. *Science* **2020**, *369*, 643–650. [CrossRef] [PubMed]

44. Liu, L.; Wang, P.; Nair, M.S.; Yu, J.; Rapp, M.; Wang, Q.; Luo, Y.; Chan, J.F.; Sahi, V.; Figueroa, A.; et al. Potent neutralizing antibodies against multiple epitopes on SARS-CoV-2 spike. *Nature* **2020**, *584*, 450–456. [CrossRef] [PubMed]

45. Pinto, D.; Sauer, M.M.; Czudnochowski, N.; Low, J.S.; Tortorici, M.A.; Housley, M.P.; Noack, J.; Walls, A.C.; Bowen, J.E.; Guarino, B.; et al. Broad betacoronavirus neutralization by a stem helix-specific human antibody. *Science* **2021**, *373*, 1109–1116. [CrossRef] [PubMed]

46. Bui, H.H.; Sidney, J.; Li, W.; Fusseder, N.; Sette, A. Development of an epitope conservancy analysis tool to facilitate the design of epitope-based diagnostics and vaccines. *BMC Bioinform.* **2007**, *8*, 361. [CrossRef]

47. Cao, Y.; Wang, J.; Jian, F.; Xiao, T.; Song, W.; Yisimayi, A.; Huang, W.; Li, Q.; Wang, P.; An, R.; et al. Omicron escapes the majority of existing SARS-CoV-2 neutralizing antibodies. *Nature* **2021**, *602*, 657–663. [CrossRef]

48. Chi, X.; Liu, X.; Wang, C.; Zhang, X.; Li, X.; Hou, J.; Ren, L.; Jin, Q.; Wang, J.; Yang, W. Humanized single domain antibodies neutralize SARS-CoV-2 by targeting the spike receptor binding domain. *Nat. Commun.* **2020**, *11*, 4528. [CrossRef]

49. Chi, X.; Yan, R.; Zhang, J.; Zhang, G.; Zhang, Y.; Hao, M.; Zhang, Z.; Fan, P.; Dong, Y.; Yang, Y.; et al. A neutralizing human antibody binds to the N-terminal domain of the spike protein of SARS-CoV-2. *Science* **2020**, *369*, 650–655. [CrossRef]

Development of Next Generation Vaccines against SARS-CoV-2 and Variants of Concern

Abdul Aziz Al-Fattah Yahaya, Kanwal Khalid, Hui Xuan Lim and Chit Laa Poh *

Centre for Virus and Vaccine Research, School of Medical and Life Sciences, Sunway University, Bandar Sunway, Petaling Jaya 47500, Selangor, Malaysia
* Correspondence: pohcl@sunway.edu.my

Abstract: SARS-CoV-2 has caused the COVID-19 pandemic, with over 673 million infections and 6.85 million deaths globally. Novel mRNA and viral-vectored vaccines were developed and licensed for global immunizations under emergency approval. They have demonstrated good safety and high protective efficacy against the SARS-CoV-2 Wuhan strain. However, the emergence of highly infectious and transmissible variants of concern (VOCs) such as Omicron was associated with considerable reductions in the protective efficacy of the current vaccines. The development of next-generation vaccines that could confer broad protection against both the SARS-CoV-2 Wuhan strain and VOCs is urgently needed. A bivalent mRNA vaccine encoding the Spike proteins of both the SARS-CoV-2 Wuhan strain and the Omicron variant has been constructed and approved by the US FDA. However, mRNA vaccines are associated with instability and require an extremely low temperature ($-80\ °C$) for storage and transportation. They also require complex synthesis and multiple chromatographic purifications. Peptide-based next-generation vaccines could be developed by relying on in silico predictions to identify peptides specifying highly conserved B, CD4$^+$ and CD8$^+$ T cell epitopes to elicit broad and long-lasting immune protection. These epitopes were validated in animal models and in early phase clinical trials to demonstrate immunogenicity and safety. Next-generation peptide vaccine formulations could be developed to incorporate only naked peptides, but they are costly to synthesize and production would generate extensive chemical waste. Continual production of recombinant peptides specifying immunogenic B and T cell epitopes could be achieved in hosts such as *E. coli* or yeast. However, recombinant protein/peptide vaccines require purification before administration. The DNA vaccine might serve as the most effective next-generation vaccine for low-income countries, since it does not require an extremely low temperature for storage or need extensive chromatographic purification. The construction of recombinant plasmids carrying genes specifying highly conserved B and T cell epitopes meant that vaccine candidates representing highly conserved antigenic regions could be rapidly developed. Poor immunogenicity of DNA vaccines could be overcome by the incorporation of chemical or molecular adjuvants and the development of nanoparticles for effective delivery.

Keywords: SARS-CoV-2; variants; vaccines

1. Introduction

Considering the global spread of COVID-19 is due to its high transmissibility, there is an urgent need to rapidly develop safe and effective vaccines to curb the further spread of the virus. In particular, the alarming threat of the COVID-19 pandemic on global healthcare systems and its impact on the economy has necessitated the urgent development of effective vaccines. Thus, vaccines were developed at a rate unparalleled in the history of human vaccinology. Initial vaccine development against SARS-CoV-2 quickly progressed through the preclinical and clinical stages soon after the whole-genome sequence of the SARS-CoV-2 Wuhan strain became available [1]. Accelerated development of SARS-CoV-2 vaccines occurred as a result of collaborations between governments, universities and big pharma [2].

One such example is the Operation Warp Speed development of SARS-CoV-2 vaccine, a public and private initiative started by the United States Congress aimed to speed up the research, development, manufacturing, and distribution of vaccines. Warp-speed vaccine development against SARS-CoV-2 utilized novel and previous unlicensed platforms [3]. mRNA and viral-vectored vaccines were among the first few vaccine candidates, along with the inactivated vaccine (IV), approved for Phase III clinical development and subsequent approvals for emergency use [4].

The purpose of this paper is to review the development of next-generation vaccines against SARS-CoV-2 and the variants of concern (VOCs), with particular emphasis on vaccine platforms such as mRNA and recombinant protein or peptide-based vaccines. The vaccines described in this review are based on the latest research findings available regarding the vaccine platforms that have yet to be clinically applied to protect against SARS-CoV-2 infections. Promising vaccination approaches such as aerosolized adenovirus or AAV-based vaccines, live attenuated vaccines which could be applied intranasally, and novel vaccine platforms such as peptide-based vaccines all fall under this purview.

A search for next-generation vaccines was conducted using Google Scholar and PubMed databases. The following keyword search terms were used; "SARS-CoV-2" OR "severe acute respiratory syndrome coronavirus-2" AND "bivalent vaccine" OR "mRNA vaccine" OR "DNA vaccine" OR "inactivated vaccine" OR "multi-epitopes" OR "peptide vaccine" OR "pan-sarbecovirus". The literature was searched from December 2019 to January 2023 for peer-reviewed papers reporting next-generation SARS-CoV-2 vaccines. The International Clinical Trials Registry Platform (ICTRP) was searched through http://trialsearch.who.int/ (accessed on 1 December 2022). A total of 8275 studies were identified. After excluding duplicates and irrelevant studies based on the title and abstract screening, the final number of articles included in this review was 26.

2. SARS-CoV-2 Variants

Ever since the detection of the first SARS-CoV-2 viral variant, it became clear that a suitable naming scheme had to be implemented to designate and keep track of novel emerging variants despite the existing nomenclatures used by the GISAID and Nextstrain. Subsequent SARS-CoV-2 variants and their lineages would be denoted by the letters of the Greek alphabet [5]. This effort was supplemented with another classification system to describe the level of severity, transmissibility and epidemiological surveillance from health authorities. These variants were labelled as Variants Under Monitoring (VUM), Variants of Interest (VOI) and Variants of Concern (VOC) (source: WHO). Throughout the COVID-19 pandemic, there were 5 VOCs reported by the WHO; *viz* B.1.1.7 (Alpha), B.1.351, (Beta), P.1 (Gamma), B.1.617.2 (Delta) and B.1.1.529 (Omicron). These variants harbored multiple mutations in the S protein which were associated with increased transmissibility, virulence and immune evasion [6].

The first VOC to be recorded, the Alpha (B.1.1.7) variant, carried the signature N501Y mutation alongside the following mutations: D614G, Δ69–70 and P681H in the S protein [7–9]. These mutations were linked to increased transmissibility of the SARS-CoV-2 B.1.1.7 variant, with the D614G mutation carrying high significance due to the mutation causing the viral S protein to have a stronger affinity to the target human angiotensin-converting enzyme 2 (ACE2) protein while maintaining its existing immune escape function [10–12]. In addition, the H69-V70 deletion modified the conformation of the NTD loop, which enhanced infectivity [7].

The Beta variant from South Africa was the first variant to display increased rates of transmission among a younger, healthier population, making it more likely that they get infected. It also caused infected individuals to be more likely to be hospitalized and increased mortality rates [13]. The signature mutations were K417N, E484K, N501Y, Δ242–244, R246I and N501Y located in the RBD. The mutations N501Y and D614G present in the Alpha variant were identified to enhance the binding affinity between the S1 subunit
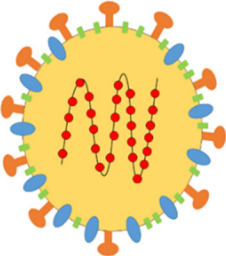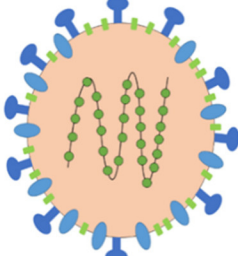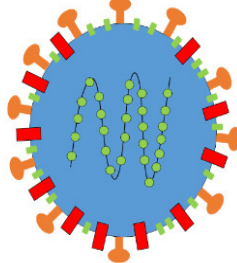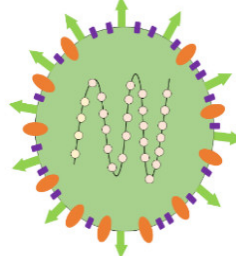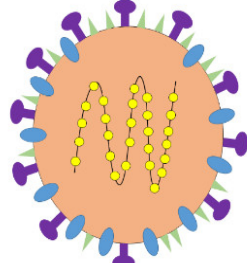
and the ACE2 receptor. The addition of the K417N and E484K mutations was reported to enhance the binding affinity of the spike and receptor further [14,15].

The Gamma variant, identified as P.1, emerged shortly after the Beta variant in October 2020. It was found to contain 12 spike protein mutations that conferred increased transmissibility and virulence in addition to facilitating viral escape. The mutations present in the RBD also included signature mutations such as N501Y, E484K and K417T, and these were also present in the previous Alpha and Beta variants [15].

The Delta variant (B.1.617.2) was first detected in India in late 2020. During the time frame between October and May 2021, Delta had spread to many other countries, causing subsequent waves of SARS-CoV-2 outbreaks [16]. The Delta strain showed that it had increased transmissibility and virulence when compared to the Alpha, Beta and Gamma variants. This was attributed to the mutations present in its spike protein. The mutations T478K, P681R and L452R present in Delta contributed to the increased infectivity [16].

The Omicron variant (B.1.1.529) was more contagious, with a higher transmissibility than the wild-type Wuhan strain and the Delta variant, and it has been the dominant strain of SARS-CoV-2 worldwide since December 2021. Omicron has evolved to give rise to five subvariants, *viz.* BA.1, BA.2, BA.3, BA.4 and BA.5. The high mutation rates in the spike (S) gene of Omicron subvariants (more than 30 mutations) affected the binding to ACE2 [17] and enabled them to escape from neutralizing antibodies [18,19]. The timeline of the emergence of SARS-CoV-2 variants as well as the amino acid changes present in SARS-CoV-2 variants in the spike (S) gene are summarized in Table 1.

Table 1. Timeline of emergence of SARS-CoV-2 variants and mutations present in Alpha. Beta, Gamma, Delta and Omicron variants in the viral spike (S) gene.

Timeline of Emergence of SARS-CoV-2 Variants				
September 2020	September 2020	October 2020	November 2020	November 2021
Alpha (B.1.1.7)	Beta (B.1.351)	Gamma (P.1)	Delta (B.1.617.2)	Omicron (B.1.1.529)
Mutations: Δ69-70, Δ144, N501Y, A570D, D614G, P681H, T716I, S982A, D1118H **Pathological effects:** i. Increased transmissibility and rate of viral replication [7] [Meng et al., 2021] ii. Increased binding affinity between RBD region and hACE-2 receptor [20,21] [Zhang et al., 2020; Harvey et al., 2020]	**Mutations:** L18F, D80A, D215G, Δ242-243, K417N, E484K, N501Y, D614G. A701V **Pathological effects:** i. Reduced protective effects of existing vaccines and monoclonal antibodies [20,22] [Zhang et al., 2020; Wibmer et al., 2021] ii. Evasion of immune responses and increased transmissibility [20,21,23] [Zhang et al., 2020; Harvey et al., 2020; Tegally et al., 2020]	**Mutations:** L18F, T20N, P26S, D138Y, R190S, K417T, E484K, N501Y, H655Y, T1027I **Pathological effects:** i. Neutralizing antibodies had reduced effectiveness due to loss of strong binding affinity [20] [Zhang et al., 2020] ii. Enhanced viral entry pathways through endosomal uptake [21] [Harvey et al., 2020]	**Mutations:** T19R, G142D, E156G, Δ157-158, L452R, T478K, D614G, P681R, D950N **Pathological effects:** i. Increased viral transmissions and virulence alongside enhanced immune escape [24,25] [Di Giarcomo et al., 2021; Tchesnokova et al., 2021] ii. Infections were more likely to result in hospitalizations and mechanical ventilation [24,25] [Di Giarcomo et al., 2021; Tchesnokova et al., 2021] iii. Evasion of immune responses [26] [Liu et al., 2021]	**Mutations:** G142D, G339D, S373P, S375F, K417N, N440K, S477N, T478K, E484A, Q493R, Q498R, N501Y, Y505H, D614G, H655Y, N679K, P681H, N764K, D796Y, Q954H, N969K **Pathological effects:** i. Mutations increased binding affinity of virus to host cells [27] [Shah et al., 2021] ii. Novel mutations present in the RBD increased transmissibility [27] [Shah et al., 2021]

3. mRNA Omicron Vaccine

Gagne et al. (2022) developed an Omicron mRNA vaccine, mRNA-1273.529, by applying a similar platform as that of the Moderna mRNA-1273 vaccine. The mRNA-1273.529 (mRNA-Omicron) vaccine encoded a full-length prefusion stabilized spike protein antigen derived from the SARS-CoV-2 Omicron variant encapsulated in lipid nanoparticles [28]. Rhesus macaques were immunized with 100 μg of mRNA-1273 vaccine at week 0 and week 4 and boosted at week 41 with 50 μg of mRNA-1274 or mRNA-Omicron. The neutralizing antibody titers against the WT strain and Omicron were higher in the sera of macaques boosted with the mRNA-Omicron vaccine; 50% inhibitory dilutions (ID_{50}) were at 5360 and 2980 when compared to those boosted with the mRNA-1273 vaccine, showing ID_{50} at 2670 and 1930, respectively. The neutralizing titers against two Omicron subvariants, BA.1 and BA.2, were comparable between groups of mice that were boosted. Viral replication in the lower airways was detected following the Omicron challenge 1 month after each booster, demonstrating that boosting with the mRNA-1273 or mRNA-Omicron vaccine conferred similar protections in the lungs against Omicron [28].

4. mRNA Bivalent Vaccines

The FDA granted an Emergency Use Authorization (EUA) for bivalent vaccines manufactured by Moderna (mRNA -1273.222) and Pfizer-BioNTech to be administered as a single booster at least two months following primary or booster vaccination [29]. The bivalent vaccine manufactured by Pfizer-BioNTech contained 15-μg of mRNA encoding the wild-type spike protein of SARS-CoV-2, and 15-μg of mRNA from the spike protein of the Omicron BA.4/BA.5 subvariants [30]. As the spike proteins in the Omicron BA. 4 and BA. 5 variants were identical, both could be targeted with a single mRNA strand. The FDA approved the bivalent BA.4/BA.5 mRNA vaccine despite the fact that the clinical trial of Pfizer BioNTech's bivalent BA.4/BA.5 mRNA vaccine was still ongoing (NCT05472038). The approval was based on the extensive safety and immunogenicity data from the monovalent mRNA vaccine as well as the clinical trial of the bivalent BA.1 vaccine and pre-clinical data obtained from immunization with the bivalent BA.4/BA.5 mRNA vaccine [29].

To evaluate the safety, tolerability and immunogenicity of the bivalent BA.4/BA.5 vaccine, the clinical Phase II/III trial (NCT05472038) enrolled about 900 healthy volunteers, aged 12 years and older in the United States, who had previously received at least three doses of an authorized COVID-19 vaccine [31]. Participants from 18 to 55 years of age were administered with either a 30-μg or 60-μg booster dose of the bivalent BA.4/BA.5 mRNA vaccine, while those aged 12 to 17 years old received a 30-μg booster dose of the same vaccine. Early data from a clinical trial involving 40 participants reported that the bivalent BA.4/BA.5 mRNA vaccine provided better protections against Omicron BA.4 and BA.5 subvariants than the original mRNA-based vaccine. The bivalent BA.4/BA.5 vaccine was well tolerated and had a similar safety profile to the original mRNA vaccine. Sera collected 7 days after a 30-μg booster dose of the bivalent BA.4/BA.5 vaccine showed a significant increase in the Omicron BA.4/BA.5-neutralizing antibody response above pre-booster levels [31]. Data regarding responses at one month post administration of the bivalent BA.4/BA.5 vaccine booster were still unavailable. Pfizer-BioNTech had initiated a similar Phase I/II/III trial (NCT05543616) in September 2022 to investigate the bivalent BA.4/BA.5 vaccine in children aged 6 months to 11 years of age. The Pfizer-BioNTech and Moderna bivalent vaccines were authorized by FDA for vaccination in children down to 6 months of age in December 2022 [32].

The Moderna bivalent vaccine, mRNA-1273.222, contained two mRNAs (1:1 ratio, 25 μg each) encoding the prefusion-stabilized spike glycoproteins of the original SARS-CoV-2 (Wuhan-Hu-1) and the Omicron variant BA.4/BA.5 [33]. Approval of the Moderna bivalent vaccine was based on pre-clinical findings for mRNA-1273.222 and data from the Phase II/III clinical trial of an mRNA-1273.214 bivalent booster vaccine targeting the Omicron BA.1 subvariant. A Phase II/III clinical trial for mRNA-1273.222 (NCT04927065) had fully enrolled 512 participants and was well in progress.

The neutralizing activities of the bivalent mRNA-1273.214 (1:1 mix of mRNAs encoding Wuhan-1 and BA.1 spike proteins) and mRNA-1273.222 (1:1 mix of mRNAs encoding the Wuhan-1 and BA.4/5 spike proteins) booster doses were higher than the mRNA-1273 booster [34]. Sera generated following the booster mRNA-1273.214 dose exhibited the greatest response against Omicron BA.1 (GMT: 13,183), but showed low activity against Omicron BA.4/5 (GMT: 293). The bivalent mRNA-1273.222 vaccine showed the highest neutralizing titers against BA.4/5 (GMT: 15,561). Boosting with mRNA bivalent vaccines slightly increased the protection of mice against lung pathology after intranasal challenge with Omicron BA.5 viruses [34].

Hajnik et al. (2022) developed an mRNA vaccine which encoded the full-length nucleocapsid protein of SARS-CoV-2 (Wuhan-Hu-1 strain) encapsulated in lipid nanoparticles (mRNA-N) [35]. In addition to mRNA-N, they also generated an mRNA vaccine encoding the full-length prefusion stabilized spike protein of SARS-CoV-2 (Wuhan-Hu-1 strain) with two proline mutations S-2P (mRNA-S), similar to the Pfizer BNT162b2 and Moderna mRNA-1273 vaccines. Mice or hamsters were immunized with two doses of mRNA-S or mRNA-S + N (1 µg of each mRNA) at week 0 and week 3, followed by a challenge with Delta and Omicron variants (2×10^4 pfu) at week 5. When compared to mRNA-S vaccination alone, the bivalent vaccine combining both mRNA-N and mRNA-S (mRNA-S + N) was demonstrated to confer protections of both the lung and upper respiratory tract against SARS-CoV-2 Omicron and Delta challenges in hamsters. The neutralizing activities in the sera of hamsters immunized with mRNA-S + N were higher against both the WT virus ($PRNT_{50}$: ~6000) and the Delta variant ($PRNT_{50}$: ~1000) when compared to mRNA vaccination alone ($PRNT_{50 \, of}$ WT: 2667, Delta: 440). Vaccination with mRNA-S + N also elicited robust S-specific and N-specific $CD4^+$ and $CD8^+$ T cell responses, as indicated by the increase in TNF-α, IFN-ɣ and IL-2 [35].

5. Inactivated Omicron Vaccine

An inactivated Omicron vaccine was developed by the China National Biotec Group Company Limited and Beijing Institute of Biological Products Company. The vaccine was produced from the Omicron BA.1 subvariant (HK-OM-P0) isolated from the throat swab of a COVID-19 patient [36]. Similar to the inactivated vaccine, Sinopharm COVID-19 Vaccine (BBIBP-CorV), derived from the original SARS-CoV-2 Wuhan strain (HB02), was cultivated in Vero cells and inactivated with β-propiolactone. A two-dose immunization with middle (6 µg) and high (12 µg) doses of the Omicron inactivated vaccine promoted the production of high levels of neutralizing antibodies against the Omicron variant (BA.1) in mice. In addition, immunization with the inactivated Omicron vaccine was shown to induce a cellular immune response, as indicated by the secretion of IFN-ɣ from T cells. The inactivated Omicron vaccine was shown to be safe and did not cause acute toxicity in rats [36]. This Omicron inactivated vaccine is currently being evaluated in Phase III clinical trial (NCT05374954) in participants aged 18 years and older with 2- or 3-dose vaccination history with the BBIBP-CorV inactivated vaccine.

6. DNA Vaccines

The DNA vaccine, ZyCoV-D, was developed by utilizing a pVAX-1 DNA plasmid vector to form a recombinant DNA plasmid consisting of the IgE signal sequence, followed by the S gene of the SARS-CoV2 prototype Wuhan strain. With favorable results in Phase I/II dose-escalation clinical trial (CTRI/2020/07/026352) and also in a Phase III clinical trial (CTRI/2020/07/026352) in 2021, the vaccine was shown to be safe and immunogenic, especially against the SARS-CoV-2 Delta variant [37].

The ZyCoV-D DNA vaccine developed by Zydus Cadila Healthcare in India is the only DNA vaccine against SARS-CoV-2 that has been approved by the Indian government for human immunizations. Consisting of the full-length spike protein (S) of the SARS-CoV-2 as the main antigenic region incorporated in the DNA plasmid vector pVAX1, the DNA vaccine showed promising results in preclinical and clinical stages. In the preclinical stage,

intradermal administration of the DNA vaccine in various animal models such as mice, guinea pigs, and rabbits at a dose of 25, 100 and 500 μg was able to elicit humoral immune antibody responses in terms of neutralizing antibodies against SARS-CoV-2, and also elicited Th-1 response as demonstrated by a 10–12-fold increase in IFN-γ production [38].

Immunogenicity testing in phase I/II clinical trials showed both humoral and cellular immune responses [39]. Seroconversion rates at Day 56 in terms of neutralizing antibody (NAB) titers were shown to be 0%, 16·67%, 20·00%, and 10·00% in the four treatment groups of participants [1 mg, Needle; 1 mg, Needle-free injection system (NFIS); 2 mg, Needle; 2 mg, Needle-free injection system (NFIS)], respectively. Seroconversion rates were much higher at Day 84, as the NAB titers were shown to be 18·18%, 16·67%, 50·00%, and 80·00% in the four treatment groups (1 mg, Needle; 1 mg, NFIS; 2 mg, Needle; 2 mg, NFIS), respectively [39]. Intradermal administrations of 2 mg of the DNA vaccine using the needle-free injection system resulted in peak cellular response in terms of IFN-γ production, with 41.5 spot-forming cells (SFC) per million PBMCs, which lasted from Day 56 to Day 84. Similar immune responses were observed upon intradermal administrations of 1 mg of the DNA vaccine, with an IFN-γ production of 73 SFC per million PBMCs.

In Phase III clinical trial, ZyCoV-D showed an efficacy of 64·9% in mild SARS-CoV-2 infections, based on 58 of 78 mild COVID-19 infections in the placebo group and 20 mild cases in those immunized with the ZyCoV-D DNA vaccine [40]. In particular, upon administration of the vaccine, the observed antibody concentrations were significantly higher in the vaccine group (952·67 EU, 95% CI 707·94–1282·00) than those observed in the placebo group (154·82 EU, 91·25–262·70). The immunogenicity response in the group that received the DNA vaccine was shown to be higher than that of the control group (IgG seroconversion 100% versus 93·33%). Cellular responses in terms of IFN-γ response at day 56 showed a 13-fold increase in SFCs per million PBMCs, while on Day 84, the response was 9·6-fold higher in terms of production of SFCs per million PBMCs when compared with the placebo group.

Other researchers have also employed the use of advanced formulations to develop DNA vaccines against SARS-CoV-2 VOCs. One such approach was the development of a more universal DNA vaccine against SARS-CoV-2 which harbored antigenic regions from multiple SARS-CoV-2 strains [41]. More specifically, the vaccine was constructed using nucleotides encoding the receptor-binding domain, membrane, and nucleoproteins from the SARS-CoV-2 prototype Wuhan strain, as well as from the Alpha and Beta variants. The administration of the vaccine induced antibodies that could neutralize the Wuhan, Beta, and Delta strains and prevented infections from SARS-CoV-2 Wuhan, Beta, Delta, and Omicron strains. Thus, humoral and cellular immune responses induced in mice immunized with the universal DNA vaccine were able to protect against the Alpha and Beta variants as well as the Wuhan strain [41]. Indeed, the DNA vaccine was also able to induce cellular responses in terms of nucleoprotein-specific T cells and contributed to 60% of the total protection conferred as a result of the administration of the vaccine [41]. Other than demonstrating that the production of T cells was essential for the resolution of the SARS-CoV-2 infection, the data also highlighted the usefulness of developing vaccines that offered broad and functional immunity against the SARS-CoV-2 Wuhan strain and its VOCs.

Jang et al. (2022) reported the development of AcHERV-COVID19S, a human endogenous retrovirus (HERV)-enveloped recombinant baculoviral DNA vaccine against SARS-CoV-2 [42]. The researchers utilized a non-replicating recombinant baculovirus that delivered the SARS-CoV-2 S gene from the Wuhan strain. In challenge studies, the administration of the AcHERV-COVID19S DNA vaccine candidate to K18-hACE2 Tg mice conferred 50% protective efficacy upon infection with the SARS-CoV-2 Delta variant. Further development of the AcHERV-COVID19D DNA vaccine involved replacing the spike (S) protein gene from the original SARS-CoV-2 Wuhan strain with the receptor binding RBD from the S1 subunit of the Delta variant. The vaccine also contained proline substitutions and the deletion of the polybasic cleavage site to enhance immunogenicity. The cross-protection offered by the AcHERV-COVID19S DNA vaccine against infections from

SARS-CoV-2 Wuhan strain and VOCs such as the Delta and Omicron strain showed that mice immunized with the AcHERV-COVID19D DNA vaccine demonstrated 100% survival when challenged with Delta and Omicron VOCs and 71.4% survival against the prototype the SARS-CoV-2 Wuhan strain [42]. The elicitation of cellular immunity was also studied by the researchers who used ELISPOT analysis to show higher levels of IFN-γ-secreting splenocytes from the spleens of C57BL/6 mice immunized with the AcHERV-COVID19S DNA vaccine as compared to naïve mice. mRNA expression levels of TNF-α, IL-2, and IL-4 were shown to be much higher in mice which had received the vaccine when compared with the control group. Immunized mice showed more potent Th1 cell immune responses and maintained a greater level of Th1 cytokine mRNA than the placebo group [42]. This data provided evidence that the goal of development of vaccines that offered cross-protection against the spread of SARS-CoV-2 VOCs could be achieved.

Recently, the development of a DNA vaccine against SARS-CoV-2 known as the pSARS2-S vaccine, which contained the S gene from the Wuhan strain and was administered through electroacupuncture in the murine model, showed that the vaccine was able to elicit high neutralizing antibody titers and IFN-γ/TNF-α-secreting CD4^{+} and CD8^{+} T cells as well as neutralizing antibodies that were able to cross-neutralize different VOCs [43]. Other approaches such as the one used by Mucker et al. (2022) employed a doggy bone DNA (dbDNA) construct which involved a novel synthetic DNA vector to develop a DNA vaccine comprising the SARS-CoV-2 spike (S) protein sequence based on the Wuhan strain. SARS-CoV-2 variants such as the Beta, Delta, and Delta[+] VOCs when tested against sera derived from hamsters immunized with the dbDNA vaccine showed that the vaccine was able to produce cross-neutralizing antibodies against SARS-CoV-2 variants other than the Wuhan strain [44].

7. Protein Subunit Vaccines

V-01D-351 is a bivalent protein-based vaccine developed by Livzon Pharmaceutical Inc., China, which contains the whole RBD protein from both Beta and Delta variants (1:1 ratio), and is armed with an interferon-α at the N terminus and dimerized by human IgG1 Fc at the C terminus, as well as a pan HLA-DR binding epitope (IFN-PADRE-RBD-Fc dimer) [45]. It is currently in a Phase II clinical trial (NCT 05273528) to assess the immunogenicity and safety of the V-01-351 bivalent protein-based vaccine in adults aged 18 years and older following vaccination with two doses of the inactivated vaccines. Participants who received the V-01D-351 booster developed potent immunogenicity against the original Wuhan strain as well as substantial cross-neutralizing responses against Delta and Omicron BA.1, indicating the presence of conserved neutralizing epitopes in Beta and Delta strains with Omicron [45]. However, there were no data regarding the neutralizing capabilities against the current Omicron BA.4 and BA.5 subvariants.

Liu et al. (2022) developed a pan-sarbecovirus vaccine by fusing the RBD from the original SARS-CoV-2 strain with a Fc fragment of human IgG, and utilized a small molecule "STING agonist CF501" as the vaccine adjuvant (CF501/RBD-Fc) [46]. This vaccine was demonstrated to elicit potent cross-neutralizing antibody responses against the live original SARS-CoV-2 strain and nine pseudotyped SARS-CoV-2 variants (Alpha, Beta, Gamma, Delta, Epsilon, Zeta, Eta, Iota and Kappa), pseudotyped SARS-CoV and SARS-related coronaviruses in rabbits and rhesus macaques. Importantly, neutralizing antibodies in the sera of rhesus macaques vaccinated with two doses of the CF501/RBD-Fc vaccine could neutralize the pseudotyped Omicron variant with an NT_{50} of 6469 on day 28 after primary vaccination [47]. Three doses of the CF501/RBD-Fc vaccine in macaques generated extremely high levels of neutralizing antibodies against the pseudotyped Omicron variant, with an NT_{50} of 35,066 at day 122 following primary vaccination. Sera from the macaques were able to neutralize the authentic Omicron variant (hCoV-19/Hong Kong/HKU-344/2021) with an NT_{50} of 9322 at day 122. The levels of neutralizing antibodies against the authentic Omicron variant remained at an NT_{50} of 2430 on day 191, implying that the CF501/RBD-Fc vaccine might provide more durable protective immunity. Vaccine-induced T cell responses

were assessed by determination of IFN-ɣ elicitation by the peripheral blood mononuclear cells (PBMCs) isolated from the macaques after primary immunization using a peptide library that spanned the full-length RBD protein [46]. CF501/RBD-Fc vaccination was shown to generate strong IFN-ɣ responses in macaques 14 days after primary vaccination, with responses remaining at a high level up to 210 days later.

8. Identification of Epitopes against SARS-CoV-2 Wuhan Strain and VOCs

The development of next-generation vaccines against the SARS-CoV-2 Wuhan strain and its VOCs first requires the identification of epitopes from antigenic regions that would elicit broad and long-lasting immune responses. Such an approach to develop next generation vaccines against SARS-CoV-2 is warranted because it shows promise in boosting the effectiveness of immunization and its breadth of protection against viral variants/subvariants that are constantly emerging and being transmitted to the community.

There is extensive research being conducted in identifying such immunogenic epitopes. For example, Heide et al. (2021) identified immunogenic epitopes from different structural proteins present in SARS-CoV-2 towards the generation of specific T cell epitopes [48]. These epitopes were obtained from 135 overlapping 15-mer peptides spanning the envelope (E), membrane (M) and nucleoprotein (N) of SARS-CoV-2, interacting with sera from both infected and convalescent SARS-CoV-2 patients. Peptide-specific CD4$^+$ T cell responses in terms of interferon-γ (IFN-γ) production were evaluated using enzyme-linked immunosorbent spot (ELISpot) and corroborated by single-peptide intracellular cytokine staining (ICS) analysis. It was observed that 97% of the participants demonstrated the elicitation of CD4$^+$ T cell responses directed towards either the N, M or E proteins. More specifically, high response frequencies were demonstrated, with a total of 10 N, M or E-specific peptides, half of these peptides showing strong binding affinities to several HLA class II binders. Notably, three peptides *viz.* Mem_P30 (aa146–160), Mem_P36 (aa176–190), and Ncl_P18 (aa86–100) were able to elicit CD4$^+$ specific T cell responses in approximately 55% of participants, showing a high population coverage. While Mem_P30 and Mem_P36 belonged to the M protein, the Ncl_P18 peptide was found in the N protein. After specifying the length and HLA restriction of the peptides, a novel DRB*11 tetramer (Mem_aa145–164) was developed and used for ex vivo phenotype evaluation of SARS-CoV-2-specific CD4$^+$ T cells. This in-depth analysis of single T cell peptide response showed that SARS-CoV-2 infection universally primed a broad T cell response that was focused on several specific peptides found within the N, M, and E structural proteins.

As reported by Lim et al. (2022), B cell responses could be identified by epitope identification using literature mining and bioinformatics tools to identify antigenic regions capable of eliciting humoral immune responses [49]. Although current vaccines could confer lower levels of protection against SARS-CoV-2 VOCs due to multiple mutations in antigenic regions, a satisfactory protective efficacy was still observed against SARS-CoV-2 VOCs. This protection might be attributable to cellular immunity. The identification of epitopes capable of eliciting CD8$^+$ specific T cell responses is promising because multifunctional CD8$^+$ T cells could allow inhibition of the viral escape of SARS-CoV-2 VOCs. The existence of conserved CD8$^+$ T cell epitopes could effectively compensate for the reduction in the CD8$^+$ T cell activity resulting from mutations within T cell epitopes. Boni et al. (2021) demonstrated that several immunodominant CD8$^+$ T cell epitopes could be found in conserved locations within the SARS-CoV-2 genome that were highly unlikely to undergo mutations without significantly impairing functional SARS-CoV-2 genes [50]. This is particularly relevant as some immunodominant CD8$^+$ T cell epitopes are located within highly conserved SARS-CoV-2 regions that could not mutate without impairing SARS-CoV-2 functionality. It was significant that several of these conserved epitopes were labelled as degenerate, which enabled them to associate with several HLA class I molecules on APCs and interact with CD8$^+$ T cell populations of various HLA restrictions at the same time. Degenerate CD8$^+$ T cell epitopes were seen to be logical candidates for the development of CD8$^+$ T cell response-enhanced next-generation COVID-19 vaccines.

Research has also focused on identifying CD4^{+} T cell epitopes to provide protection against the SARS-CoV-2 Wuhan strain and its VOCs. Although the impact of mutations in the SARS-CoV-2 genome on CD4^{+} T cell immune responses is not well-understood, epitope mapping might provide useful knowledge regarding the ability of CD4^{+} T cells to provide broad and conserved protection against VOCs. After isolating more than 100 SARS-CoV-2-specific CD4^{+} T cell clones from recovering COVID-19 patients, Long et al. (2022) mapped HLA II restrictions of 21 epitopes on three SARS-CoV-2 proteins to evaluate the breadth of immune responses. It was observed that following vaccination, responses to the spike epitopes were also observed in people who were not infected with SARS-CoV-2 [51]. In contrast to pre-existing cross-reactive coronavirus-specific T cell responses, the absence of CD4^{+} T cell cross-reactivity with endemic beta-coronaviruses suggested that these responses were generated by naive T cells. Ten of the seventeen spike epitopes had mutations in VOCs, and seven of them, including three of the four altered in Omicron, had impaired CD4^{+} T cell recognition. This showed that the identification of broad CD4^{+} T cell epitopes might be the key to limiting immune evasion capabilities associated with SARS-CoV-2 VOCs.

The emergence of SARS-CoV-2 variants that show an increased propensity to evade antibodies has led to recurrent waves of infections with reduced vaccine efficacy. In our search for broadly protective vaccinations, there is still a crucial knowledge gap regarding the degree to which vaccine-elicited mucosal or systemic memory T cells can defend against such antibody-evasive SARS-CoV-2 variants. Using adjuvanted spike protein–based vaccines that elicited potent T cell responses, Kingstad-Bakke et al. (2022) assessed whether systemic or lung-resident CD4^{+} and CD8^{+} T cells protected against SARS-CoV-2 variants in the presence or absence of virus-neutralizing antibodies [52]. It was observed that the elicitation of mucosal response was associated with potent viral control and protection of lung pathology through the production of neutralizing antibodies. Although mucosal immunity resulted in the elicitation of mucosal memory CD8^{+} T cells, humoral immune responses had a more prominent role in being able to effectively neutralize the invading virus. In fact, mucosal memory CD8^{+} T cells were not able to confer adequate levels of protection in response to homologous SARS-CoV-2 without CD4^{+} T cells and neutralizing antibodies. Nevertheless, when virus-neutralizing antibodies were not present, memory CD4^{+} and CD8^{+} T cells were able to confer protection against the B1.351 (β) variant without symptoms of lung immunopathology. It might be useful to induce systemic and mucosal memory T cells that were directed against conserved epitopes to combat SARS-CoV-2 variants that can avoid neutralizing antibodies.

Although initial findings, which utilized in silico immunoinformatic approaches associated with vaccine development and immunogenicity, have identified these epitopes based on high levels of antigenicity and broad conservancy, future studies would need to be conducted to validate these epitopes and the resulting immune responses in both animal and human models. Nevertheless, the use of bioinformatics to predict highly conserved and immunodominant epitopes capable of eliciting potent immune responses against both the SARS-CoV-2 Wuhan strain and its VOCs serves as a useful starting point, guiding the development of next-generation vaccine platforms.

9. Peptide-Based Vaccines

The concept behind a SARS-CoV-2 peptide-based vaccine is to stimulate immune cells to elicit an immune response to epitopes derived from antigenic regions of the virus. However, the main advantage of this vaccine platform over the whole S-protein or nucleic acid-based vaccines is that it could trigger specific responses to the immunogenic epitopes present as peptides. Peptide vaccines could be designed to allow the induction of CD8^{+} cytotoxic T cells (CTL) that would kill infected host cells to halt the viral replication process by incorporating CD8^{+} T cell epitopes into the vaccine design. Likewise, CD4^{+} T helper cells could also be triggered by the epitopes incorporated in the peptide vaccine being designed. Alternatively, a peptide vaccine could also be designed to induce only B cell

responses and the production of neutralizing antibodies which would prevent circulating viruses from infecting host cells. The rationale behind focusing on developing the peptide vaccine platform for immunizations against COVID-19 was to overcome the limitations of utilizing only the whole S protein of the Wuhan strain that was the target antigen in the first generation of COVID-19 vaccines. Currently, no peptide-based vaccines consisting of SARS-CoV-2 epitopes from the whole genome have been approved and applied clinically, but there are four vaccine candidates being developed based on the peptide-based vaccine platform that are currently in clinical trials.

1. CoVac-1

Heitmann et al. (2021) designed a vaccine centered on inducing a broad and long-lasting T cell immunity, as T cell epitopes were infrequently impacted by mutations present in variants of concern [53]. The vaccine prototype was composed of SARS-CoV-2 T cell epitopes derived from the viral spike (S), membrane (M), nucleocapsid (N), envelope (E) and open-reading Frame 8 (ORF8) proteins, combined with a Toll-like receptor 1/2 agonist XS15 emulsified in a Montanide ISA51VG adjuvant. This vaccine was designed to focus on antigenic peptides of SARS-CoV-2 that could be recognized by HLA-restricted T cells which would confer long-term immune protection. This vaccine prototype has recently undergone Phase I clinical trials (NCT4954469) involving 36 participants (18–80 years) in which the prototype was found to induce both multifunctional CD4$^+$ and CD8$^+$ T cell responses, targeting multiple epitopes in all the participants. Its efficacy was evaluated through comparison of IFN-γ levels from ELISPOT analysis and intracellular staining of T cells stimulated with CoVac-1 peptides against a panel of peripheral blood mononuclear cells (PBMCs) from convalescent SARS-CoV-2 patients and healthy individuals immunized with mRNA or adeno-vectored vaccines. The results reported that the immune responses mediated by CoVac-1 induced broad, potent and variant-of-concern-independent multifunctional CD4$^+$ and CD8$^+$ T cell activity. It was also found that the cells had a higher magnitude of induced immunity compared to those derived from natural infections or those from vaccinated individuals. No serious adverse reactions were found during the Phase I clinical trials even though local granuloma formations were observed in the participants post-immunization [53].

2. Peptide vaccine derived from epitopes from SARS-CoV-2 S and N proteins

This epitope-specifying peptide-based vaccine was developed as a proof of concept to determine if T cell mediated immunity was sufficient to confer protection from SARS-CoV-2 infection [54]. The authors also elaborated on this vaccine prototype, being focused specifically on T cell immunogenicity whereby 20 highly conserved peptides specifying epitopes derived from the S and N proteins were validated in murine models to stimulate long-lasting immunity through induction of cytotoxic CD8$^+$ T cells and CD4$^+$ T helper cells. All epitopes were selected with considerations of restrictions by MHC-I and MHC-II so the corresponding CD8$^+$ and CD4$^+$T cells would recognize the peptides and generate effective cellular immune responses by producing cytokines and activating co-stimulation signaling [54].

The emergence of VOCs such as Omicron has also prompted this shift towards alternative vaccine platforms such as multi-epitope peptide-based vaccines to elicit T cell-mediated immunity [55]. This might be a suitable solution to the resistance posed by the variants, as they are known to escape neutralizing antibody activities generated by current vaccines and even by natural immunity from past infections.

The authors selected the epitopes which were validated through the use of predictive in silico software, focusing on the target proteins for their conservancy and immunogenicity [54]. C57BL/6 mice were immunized twice at a 2-week interval with a peptide mixture or with individual peptides derived from either the S protein or N protein together with the CUK2 RNA adjuvant. The immunogenicity of the peptides was determined through expression of IFN-γ based on ICS flow cytometry, ELISpot and cytokine enzyme-linked immunosorbent analysis. The results indicated that four peptides (2 Spike and 2 Nucle-

ocapsid) were capable of inducing the strongest T cell-mediated responses in vivo. Mice immunized with a mixture of these four peptides and the CUK2 RNA adjuvant showed increased levels of IFN-γ-producing T cells and an increased frequency of proliferating T cells. However, there was a slight reduction in viral titers, and virus-induced injury was observed in the lungs after SARS-CoV-2 challenge. This finding indicated that the peptides might not be able to elicit immune responses to completely eliminate the virus. Currently, this vaccine candidate has only been tested in animals and there is no information regarding the efficacy of the vaccine in humans; however, the authors maintain that they are aiming to continue the development of a peptide-based vaccine based on the peptides that were validated in the murine model.

3. UB-612

UB-612 is a multi-epitope peptide-based vaccine candidate developed by Vaxxinity, USA. The UB-612 vaccine construct contained an RBD (derived from the WT Wuhan strain) which was fused to a modified single-chain human IgG1 Fc protein (S1-RBD-sFc), a UBITh1a peptide as a catalyst for T cell activation, and a mixture of five synthetic Th/CTL peptides derived from the spike protein, nucleocapsid and membrane proteins produced in CHO cells [56]. Synthetic peptides were stabilized with a negatively charged oligonucleotide (CpG1) and adsorbed on aluminum phosphate adjuvant. These peptides were found to be highly conserved across all VOCs, including Delta and Omicron variants, and were able to bind to human MHC I and II with broad HLA genetic coverage as well as induction of T cell proliferations.

UB-612 was shown to be safe and well tolerated in a Phase I/II clinical study, and it was shown to generate a lasting neutralizing antibody response with a half-life of 187 days and a sustained T cell response in individuals aged 20 to 55 (NCT04545749 and NCT04773067) [57]. Three doses of UB-612 induced significant neutralizing antibody titers against live Delta variants (VNT_{50} of 2358) when compared to live WT virus (VNT_{50} of 3992) in a Phase I study with a 100-μg booster (NCT04967742), and neutralizing titers showed only a small 1.7-fold reduction [57]. The UB-612 vaccine was found to have cross-reactive neutralizing antibody titers against pseudotyped SARS-CoV-2 variants such as Alpha, Beta, Gamma and Omicron (BA.1), when compared to the WT pseudovirus ($pVNT_{50}$ of Alpha: 9300, Beta: 4974, Gamma: 13408, Omicron: 2325 versus WT: 12778). A third dose of the UB-612 vaccine administered 7–9 months after the primary vaccination dramatically boosted neutralizing antibody titers against Omicron and the WT strain to VNT_{50} of 670 and 970, respectively, with only a small 1.4-fold reduction against the Omicron variant when compared to the 5.5-fold reductions observed in the pseudovirus assay [57,58].

The UB-612 vaccine is currently being assessed in a Phase III clinical study as a booster vaccine for vaccinees who have received primary immunizations with mRNA (Pfizer), adenovirus vectored (AstraZeneca), or inactivated virus (Sinopharm BIBP) vaccines (NCT05293665). Three doses of UB-612 at 100 μg per dose elicited neutralizing antibody titers with geometric mean titer (GMT) virus neutralization titer (VNT_{50}) at 335 against the Omicron variant, which was more than 3-fold higher than the neutralizing antibody titers observed following three doses of the Pfizer mRNA vaccine [59].

4. EpiVacCorona

This vaccine candidate was designed based on the immunodominant epitopes being presented as peptides that represented the antigenic regions [60]. These peptides were selected through computational bioinformatics with reference to X-ray diffraction analysis data of homologous SARS-CoV spike protein and the SARS-CoV-2 genetic sequence. Only epitopes that were located near the S1 and S2 sites that were vital to the virus were selected for the vaccine candidate. Computational analysis was also used to exclude potentially toxic peptides. A carrier protein derived from the SARS-CoV-2 N protein was used as a substrate onto which the selected epitopes were covalently bound. The final vaccine candidate was formulated with peptide immunogens of the S protein of the SARS-CoV-2

conjugated to a carrier protein, adjuvanted with aluminum hydroxide and administered through intramuscular injections.

Phase I/II (NCT04527575) and Phase III/IV (NCT04780035) clinical trials of EpiVac-Corona were performed in Russia in November 2020 and March 2021, respectively. In the first trial, participants were divided into a non-randomized trial (*n* = 14; Group 1) and a single-blind, placebo-controlled randomized trial (two groups: Group 2, *n* = 43; Group 3, *n* = 43). The volunteers in Group 1 received two doses of EpiVacCorona intramuscularly on Day 0 and Day 21. The participants were monitored for up to five days after each immunization for adverse reactions with standard physical, biochemical, immunological and haematological blood examinations. Following the monitoring period, with no adverse symptoms being observed, evaluation of EpiVacCorona was continued for the randomized trial whereby Group 2 participants receiving the immunization of EpiVacCorona were compared with the participants in Group 3 receiving only the placebo.

Based on the findings from each group, the vaccinees only reported mild local reactions after two immunizations. The vaccine was shown to be of low reactogenicity and was safe for use in immunizations. The most common adverse reaction was local pain at the injection site (observed in four out of 43 volunteers receiving the EpiVacCorona after the first dose and in two more patients after the second dose). All local reactions were mild and transient, lasting 1–2 days. There was one incident where a participant experienced a rise in body temperature 12 h after the first injection. However, three cases of acute respiratory viral infection (ARVI) occurred during the study, which were later confirmed to be due to COVID-19 infections.

The immunogenicity of the vaccine was evaluated by ELISA and neutralization titers. The vaccine induced IgG seroconversion by Day 42 after the first dose in 82% of the participants who had received EpiVacCorona. Neutralization assays performed in Vero E6 cells using diluted sera at 1:160 showed that all the participants had demonstrated neutralizing antibodies by Day 42 after the first immunization. The participants receiving the placebo did not show any seroconversion [60].

Phase III clinical trials were also performed in the same year, with over 3000 volunteers enrolling in the study, but the results were not made public [61]. Despite the lack of effective protection against the SARS-CoV-2 Delta strain, the vaccine had been registered with the Russian government and given emergency authorization for immunizations domestically.

10. Vectored-Based Vaccines

The majority of COVID-19 vaccinations in use are delivered intramuscularly. There are also other promising vaccination approaches such as aerosol inhalation and intranasal administrations, which could generate a mucosal immune response directly at the point of virus entry in the respiratory system. For example, two doses of aerosolized adenovirus type-5 vector-based COVID-19 vaccine (Ad5-nCov) were demonstrated to induce neutralizing antibodies and T cell responses in a Phase I clinical trial involving 130 participants [62]. However, the durability of antibodies and cellular responses as well as the cross-neutralizing activity of this vaccine against SARS-CoV-2 variants were not reported.

A single dose of intramuscular vaccination of an adeno-associated vector vaccine (AAVCOVID-1), a spike gene-based vaccine candidate encoding the S gene of the Wuhan strain, was shown to protect nonhuman primates from SARS-CoV-2 challenge after a single low dose (10^{10} genome copies) [63]. Most of the currently approved vaccines except for CanSino adenovirus type 5 (AD5)-vectored vaccine (Ad5-nCoV) or the adenovirus type 26 vectored vaccine Ad26.COV2.S (Johnson & Johnson), require two doses for full protection [64,65]. The neutralizing activities and T cell responses elicited by the AAVCOVID-1 vaccine were potent and durable for up to 11 months [63]. Importantly, the immune sera from nonhuman primates vaccinated with AAVCOVID-1 showed some degree of neutralization against all four SARS-CoV-2 variants (Alpha, Beta, Gamma and Delta) in a pseudovirus-based neutralization assay on week 14.

Modified vaccinia virus Ankara (MVA) is a highly attenuated virus strain having a replication defect in mammalian hosts [66]. MVA-SARS-2-S is a vectored vaccine based on the modified vaccinia virus Ankara that expressed the full-length SARS-CoV-2 spike (S) protein. The MVA vaccine was shown to induce SARS-CoV-2-specific T cell responses and neutralizing antibodies as well as protection of vaccinated mice from lung infections after a SARS-CoV-2 challenge. However, the durability of the cellular and humoral responses as well as the cross-neutralizing antibody responses against SARS-CoV-2 variants were not evaluated.

11. Live Attenuated Vaccines

COVI-VAC is a live attenuated vaccine candidate created by recoding of the SARS-CoV-2 WT (Wuhan strain) using the synthetic attenuated virus engineering (SAVE) strategy of codon pair bias deoptimization (CPD) [67]. The recoding of the SARS-CoV-2 genome in the COVI-VAC vaccine candidate resulted in 283 silent point mutations in the gene encoding the spike (S) protein [68]. The furin cleavage site in the spike (S) protein of COVI-VAC was also deleted to increase its safety. A single intranasal administration of COVI-VAC in Syrian golden hamsters elicited neutralizing antibodies that were as effective as the WT virus and conferred protection against WT challenge by reducing viral loads in the lung and brain [68].

cCPD9 is a live attenuated vaccine generated by genetically modifying the SARS-CoV-2 genome using codon pair deoptimization (CPD). The attenuated vaccine candidate, cCPD9, was produced by recoding nine fragments of the SARS-CoV-2 genome introduced by the reverse genetics system. A single dose of intranasal immunization with cCPD9 elicited strong neutralizing antibody responses and provided complete protection against SARS-CoV-2 challenge in hamsters [69].

However, there was no assessment of T cell responses and the durability of protective immunity for both the COVI-VAC and cCPD9 vaccine candidates. Live attenuated vaccines are considered to be the most effective vaccines because they generally elicit broad, robust and long-lasting immune responses similar to those induced by natural infections caused by the WT strain [70]. However, the safety, immunogenicity and efficacy of both live attenuated vaccine candidates should be further investigated in non-human primates and humans. The main disadvantage of live attenuated vaccines is the risk of reversion to virulence. Both COVI-VAC and cCPD9 were expected to be genetically stable due to the large number of mutations in the genome.

Another important advantage of live attenuated vaccines is that they can trigger immune responses, not only against the spike protein, but against the entire ensemble of viral proteins. Therefore, live attenuated vaccinations should be effective against all SARS-CoV-2 variants. A single intranasal droplet vaccination with sCDP9 was demonstrated to elicit strong cross-neutralizing antibody responses against the four SARS-CoV-2 variants (Alpha, Beta, Gamma and Delta) [71], whereas COVI-VAC vaccination conferred protection against heterologous challenge with the SARS-CoV-2 Beta variant (B. 1.351) in the Syrian Golden hamster model [72].

12. Discussion

Although mRNA vaccines have shown the highest efficacy and safety among the licensed COVID-19 vaccines, the disadvantages of mRNA vaccines are their high cost and low stability with short half-life. The mRNA vaccines also require extremely low temperatures ($-80\ °C$) for storage and transportation which make them unaffordable and logistically impractical for many low-income countries. We have summarized the advantages and disadvantages of each vaccine platform in Table 2. The production cost for the adenovirus vectored vaccine was lower, at $ 0.15/dose, while Pfizer and Moderna mRNA vaccines could range from $ 14.70 to $ 23.50/dose, and the DNA vaccine was priced at $ 3.53/dose [73,74].

Table 2. Advantages and disadvantages of different SARS-CoV-2 vaccine platforms.

Vaccine Platforms	Live Attenuated Vaccine	Inactivated Vaccine	mRNA Vaccine	DNA Vaccine	Peptide-Based Vaccine	Adenovirus Vectored Vaccine	Recombinant S Protein
Advantages	Simple production, easy storage, distribution and administration. Only one dose is required. Trigger immune responses against the whole virus. Considered the most effective vaccine it can elicit robust and long-lasting humoral and cellular immune responses.	Very safe because the virus is killed and no serious adverse effects. Easy for transport and storage.	Easy and quick to design. Large-scale production is feasible. Safe as no infectious virus handling is required. Can induce humoral and cellular responses.	Low cost of production. Safe and well-tolerated. Stable under room temperature at 2–8 °C Highly adaptable to the incorporation of DNA sequences of newly emerging variants of concern.	No risk of infection. Induce specific immune responses with minimal allergic and toxic properties. Highly conserved B cell epitopes can elicit cross-reactive antibodies. Highly conserved $CD4^+$ and $CD8^+$ T cell epitopes can confer broad protection. Can be incorporated in expression plasmids to produce recombinant peptides	Low cost of production. Good stability at 2–8 °C. Replication-defective vectored viruses tend to elicit stronger immune responses than killed viruses. Can induce humoral and cellular responses with a single dose of Ad5-nCoV or Ad26.COV2.S.	Focus on the most immunogenic S protein of the virus for protection. The most immunogenic vaccine platform. Incapable of causing infections.
Disadvantages	Risk of reversion to virulence.	Significant risk due to the growth of large amounts of live viruses before inactivation. The inactivation process might affect antigen immunogenicity. Adjuvants are required. Multiple doses are needed every 12 months.	High cost. mRNA vaccines exhibit instability due to liposome formulation and require storage at −80 °C. Unaffordable and logistically impractical for many low-income countries.	Lower immunogenicity. Risk of genomic integration. Require adjuvants to enhance immunogenicity. Administration requires a medical device such as an electroporator. Needless patch is still under development.	Require peptide synthesis chemically. An adjuvant maybe needed to boost immunogenicity. Lower immunogenicity than live attenuated vaccine and mRNA vaccine.	Pre-existing immunity against viral vectors can attenuate immune responses. Some candidates require storage at −20 °C. May trigger rare but serious side effects of vaccine-induced thrombotic thrombocytopenia (VITT) and blood clots.	Require multiple purification steps involving column chromatography. An adjuvant may be needed to boost long-term immunity.

The development of next-generation DNA vaccines is promising and is geared towards preventing SARS-CoV-2 VOC infections. DNA vaccines that do need extremely low temperature for storage and transportation are preferable for large-scale immunizations in underdeveloped countries that do not have sophisticated infrastructures. However, due to the small amount of antigens that could transfect target APCs in vivo, the immunogenicity of DNA vaccines must be improved by incorporating chemical, genetic, and molecular adjuvants as well as considering alternative delivery systems such as electroporation and needle-free intradermal patches to increase transfection efficiencies and the elicitation of potent immune responses.

Since the DNA vaccine platform is easily modifiable and offers convenience in plasmid design, feasible production for large-scale immunizations, and easy storage at room temperature, it has received considerable attention as a promising vaccine platform against SARS-CoV-2 and its VOCs [37]. However, DNA vaccines need to address two main concerns which involve degradation by host nucleases as well as a low APC transfection efficiency [75,76]. Nevertheless, the use of gene guns, electroporations and needle-free injections was shown to successfully address these problems to elicit potent immune responses in the clinical trials of the current DNA vaccines against SARS-CoV-2 [37]. For example, a sustained humoral response was reported following the administration of the second dose of SARS-CoV-2 DNA vaccine INO-4800. Homologous booster doses were seen to significantly augment the immune response. Increasing the dose of the vaccine from 1 mg to 2 mg was reported to significantly increase the number of cytokine producing T cells and activated CD8$^+$ T cells with lytic potential [77]. Moreover, the use of a needle-free injection system in Phase III clinical evaluation of ZyCoV-D (CTRI/2020/07/026352) showed that the administration of the DNA vaccine elicited potent immune responses, as seen from high seroconversion rates, neutralizing antibody titers and elevated IFN-γ levels compared to the placebo treatment [40].

An important issue associated with preventing the spread of infections resulting from the SARS-CoV-2 Wuhan strain and VOCs is vaccine hesitancy, which poses a global health challenge that significantly affects the spread of infections in pandemics [78]. Vaccine hesitancy and the failure to achieve good herd immunity are especially harmful for high-risk groups, such as older individuals and those with adverse health conditions [79]. The occurrence of complications such as vaccine-induced immune thrombotic thrombocytopenia (VITT) is a major contributing factor which has great potential to exacerbate vaccine hesitancy. To date, VITT has been associated only with the adenoviral vector-based platform against SARS-CoV-2. More specifically, five cases of VITT were reported among 130,000 vaccinees immunized with the ChAdOx1 CoV-19 vaccine manufactured by AstraZeneca [80]. Another vaccination with AS26.COV2.S produced by Johnson & Johnson reported 3.8 VITT cases per million vaccinees (approximately 1 in 263,000) [81]. In contrast, mRNA vaccines were not associated with such concerns of VITT. The self-adjuvating activity of the lipid nanoparticle mRNA-formulated vaccine was also reported to elicit potent antigen-specific cellular and humoral immune responses. Another disadvantage associated with the use of adenoviral vector-based vaccines is the induction of an immune response against the adenoviral vector itself [82].

The only approved DNA plasmid-based COVID-19 vaccine, the ZyCoV-D vaccine, has not had any reports of the occurrence of VITT upon administration in immunized individuals. DNA vaccines are associated with the risk of possible insertional mutagenesis. However, over the years and during the COVID-era, testing of DNA vaccines in preclinical trials did not show any insertional mutagenesis activity in terms of integration into the host genome [83].

For the elicited immune response to be sustained for longer periods of time, prime-boost regimens could be adopted. Traditionally, prime regimens were homologous, such that the same vaccine was used for priming and boosting. However, a newer, promising strategy is the combined use of a mix-and-match vaccine immunization approach which utilizes different platforms to deliver the same antigen in prime-boost vaccinations. Al-

ternatively, a heterologous prime-boost immunization approach could be adopted, using different antigens or different platforms.

The development of peptide-based vaccines for SARS-CoV-2 that incorporate antigenic structures that are easily recognizable by immune cells and could trigger rapid immune responses to the emergence of VOCs is desirable [84,85]. At the start of the pandemic, there was a motivation to develop vaccines that would protect against infection; however, the emergence of the VOCs that could resist neutralizing antibody responses triggered by the Pfizer, Moderna and AstraZeneca vaccines compromised this strategy [86–88]. Thus, peptide vaccines that could be designed to target very specific antigens and induce immunogenicity should be considered. The clinical trials for the peptide-based vaccines described in this review also showed that the development of this particular platform is progressing at an acceptable pace.

The neutralizing activities and T cell responses elicited by the adeno-associated vectored vaccine (AAVCOVID-1) were potent and durable for up to 11 months [63]. Three doses of CF501/RBD-Fc vaccinations elicited neutralizing antibodies maintained at extremely high levels in macaques for as long as 191 days (approximately 6 months). The T cell response in macaques immunized with CF501/RBD-Fc remained high at day 210 post-first immunization [46]. The available data on the durability of other vaccines were limited. Two doses of the Moderna mRNA vaccine were shown to elicit antibodies that could last for at least 6 months [89].

Development of pan-sarbecovirus or pan-β-CoV vaccines against emerging SARS-CoV-2 variants could be the best approach to developing SARS-CoV-2 vaccines [90]. A pan-sarbecovirus vaccine (CF501/RBD-Fc) was demonstrated to elicit potent cross neutralizing antibody responses against the original SARS-CoV-2 strain, nine SARS-CoV-2 variants (Alpha, Beta, Gamma, Delta, Epsilon, Zeta, Eta, Iota and Kappa), and pseudotyped SARS-CoV and SARS-related coronaviruses in rabbits and rhesus macaques [46].

Studies have reported that mucosal immune responses prevented SARS-CoV-2 replication at the entry point and reduced viral transmission [91,92]. Secretory IgA antibodies played a critical role in defense against infection at mucosal sites. However, the data on mucosal immunity for each vaccine were limited. Boosting with either the mRNA-1273 or mRNA Omicron vaccine was shown to enhance mucosal IgG antibody and neutralizing responses to WT, Beta, Delta and Omicron, with GMTs of ~10^{12} for WT, Beta and Delta and ~10^{10} for Omicron [28]. Although intramuscular vaccination with Ad5-nCoV elicited higher concentrations of RBD-binding IgA (GMT: 521 EU/mL) than the aerosolized Ad5-nCoV (GMT: 148 EU/mL) at day 28 after the first vaccination, mixed vaccinations (an intramuscular vaccination of Ad5-nCoV followed by an aerosolized Ad5-nCov booster) elicited significant levels of IgA, with a GMT of 777 EU/mL at day 28 after a booster involving aerosol vaccination [62]. A single dose of AAVCOVID vaccination elicited a detectable level of RBD-binding IgA in the bronchoalveolar lavage harvested at 5 months following immunization [63].

13. Conclusions

The COVID-19 pandemic has entered its fourth year, and there are no signs of it slowing down. The SARS-CoV-2 virus is predicted to become endemic in countries such as Israel [93]. Infectious respiratory diseases such as influenza have become endemic due to their ability to cause reinfections despite the existence of vaccines against multiple influenza serotypes and the efforts involved in vaccinating populations globally. Through re-examining the patterns of influenza infections and comparing them with SARS-CoV-2, the likelihood of achieving complete elimination of SARS-CoV-2 infections through herd immunity from vaccinations has been proven insignificant [94].

The likelihood of achieving herd immunity against SARS-CoV-2 appeared to be low due to the following reasons. Firstly, there were reports based on longitudinal observations that demonstrated that humoral responses declined over time following immunizations with currently approved vaccines against SARS-CoV-2 [95]. For example, while immu-

nization with the BNT162b2 Pfizer vaccine did lead to peak elevated levels of antibodies at weeks 4 and 5 post immunization, these titers declined shortly after. The second dose also led to elevated antibody levels, but these also decreased significantly, especially in older vaccinees [96]. Moreover, vaccine hesitancy has presented itself as a major obstacle. There were reports of the occurrence of VITT in those immunized with the adenoviral vectored-based ChAdOx1 vaccine, as well as concerns about antibody-dependent enhancement (ADE) leading to adverse effects of the mRNA vaccines. The goal of achieving herd immunity is further hampered by the emergence of new variants with immune evasion capabilities. The Omicron VOC could evade neutralization by antibodies produced in vaccinees who had received one or two doses of the vaccine, particularly when antibody titers were declining. Three doses of the spike-based vaccine may only partially protect against SARS-CoV-2 WT infection.

However, the development of next-generation vaccines capable of providing broad protection against the SARS-CoV-2 Wuhan strain and VOCs presents a promising strategy. This would involve the use of reverse vaccinology approaches that utilize in silico immunoinformatic approaches to identify highly conserved epitopes, which could be validated for their potent immunogenicity through immunizations in mice or non-human primates.

Accelerated developments in next-generation vaccine platforms showed that recombinant protein, mRNA, and DNA vaccines have advantages over traditional LAVs and IVs that utilize whole viruses. mRNA vaccines have demonstrated highly immunogenic responses that provide a high level (>94%) of immune protection against symptomatic and severe infections prior to the emergence of the Omicron variant. The mRNA platform as well as the DNA platform would allow newly validated epitope sequences to be easily incorporated through the inclusion of new gene sequences. These newly modified mRNA or DNA vaccines could be considered for development as vaccine booster doses to prevent re-infections by the WT (Wuhan) strain or by VOCs. Since mRNA vaccines require strong logistics to control their transport and storage requirements, which might hamper their usefulness and availability, DNA vaccines could offer convenience in storage and accessibility for developing countries that lack sufficient infrastructure. While recombinant protein vaccines might require extensive purification steps, they have been shown to elicit potent immune responses upon administration, and the technology of production is more amenable to low-income countries. The development of recombinant protein or peptide-based COVID-19 vaccines might set the stage for further enhancement of this platform, as the antigens encoded by the plasmid would not contain potentially harmful components, thus maintaining a stellar safety profile [97]. This trait of being able to modify the design of the DNA or recombinant peptide vaccines is of particular interest due to the benefits it entails in terms of rapidly emerging VOCs that necessitate accelerated modifications to existing antigenic sequences included in currently approved vaccines. This indicated that the antigens, once validated, might be readily incorporated in multi-epitope recombinant protein, mRNA or DNA vaccines.

Author Contributions: A.A.A.-F.Y., K.K. and H.X.L. wrote the manuscript. A.A.A.-F.Y. and H.X.L. prepared Figure. H.X.L. prepared Table. C.L.P. edited and reviewed the manuscript. All authors have read and agreed to the published version of the manuscript.

Institutional Review Board Statement: Not applicable.

Informed Consent Statement: Not applicable.

Data Availability Statement: Google Scholar (https://scholar.google.com/) and PubMed (https://pubmed.ncbi.nlm.nih.gov/) databases were used to perform literature search. The International Clinical Trials Registry Platform (ICTRP) was searched through http://trialsearch.who.int/.

Conflicts of Interest: The authors declare no conflict of interest.

References

1. Krammer, F. SARS-CoV-2 vaccines in development. *Nature* **2020**, *586*, 516–527. [CrossRef]
2. Ljungberg, K.; Isaguliants, M. DNA vaccine development at pre- and post-operation warp speed. *Vaccines* **2020**, *8*, 737. [CrossRef]
3. Kim, J.H.; Hotez, P.; Batista, C.; Ergonul, O.; Figueroa, J.P.; Gilbert, S.; Gursel, M.; Hassanain, M.; Kang, G.; Lall, B.; et al. Operation warp speed: Implications for global vaccine security. *Lancet Glob. Health* **2021**, *9*, e1017–e1021. [CrossRef]
4. Kyriakidis, N.C.; López-Cortés, A.; González, E.V.; Grimaldos, A.B.; Prado, E.O. SARS-CoV-2 vaccines strategies: A comprehensive review of phase 3 candidates. *NPJ Vaccines* **2021**, *6*, 28. [CrossRef]
5. Konings, F.; Perkins, M.D.; Kuhn, J.H.; Pallen, M.J.; Alm, E.J.; Archer, B.N.; Barakat, A.; Bedford, T.; Bhiman, J.N.; Caly, L.; et al. SARS-CoV-2 variants of interest and concern naming scheme conducive for global discourse. *Nat. Microbiol.* **2021**, *6*, 821–823. [CrossRef]
6. Noh, J.Y.; Jeong, H.W.; Shin, E.C. SARS-CoV-2 mutations, vaccines, and immunity: Implication of variants of concern. *Signal. Transduct. Target.* **2021**, *6*, 203. [CrossRef]
7. Meng, B.; Kemp, S.A.; Papa, G.; Datir, R.; Ferreira, I.; Marelli, S.; Harvey, W.T.; Lytras, S.; Mohamed, A.; Gallo, G.; et al. Recurrent emergence of SARS-CoV-2 spike deletion H69/V70 and its role in the Alpha variant B.1.1.7. *Cell Rep.* **2021**, *35*, 109292. [CrossRef] [PubMed]
8. Zahradnik, J.; Marciano, S.; Shemesh, M.; Zoler, E.; Harari, D.; Chiaravalli, J.; Meyer, B.; Rudich, Y.; Li, C.; Marton, I.; et al. SARS-CoV-2 variant prediction and antiviral drug design are enabled by RBD in vitro evolution. *Nat. Microbiol.* **2021**, *6*, 1188–1198. [CrossRef]
9. Planas, D.; Bruel, T.; Grzelak, L.; Guivel-Benhassine, F.; Staropoli, I.; Porrot, F.; Planchais, C.; Buchrieser, J.; Rajah, M.M.; Bishop, E.; et al. Sensitivity of infectious SARS-CoV-2 B.1.1.7 and B.1.351 variants to neutralizing antibodies. *Nat. Med.* **2021**, *27*, 917–924. [CrossRef] [PubMed]
10. Yurkovetskiy, L.; Wang, X.; Pascal, K.E.; Tomkins-Tinch, C.; Nyalile, T.P.; Wang, Y.; Baum, A.; Diehl, W.E.; Dauphin, A.; Carbone, C.; et al. Structural and functional analysis of the D614G SARS-CoV-2 spike protein variant. *Cell* **2020**, *183*, 739–751.e8. [CrossRef] [PubMed]
11. Korber, B.; Fischer, W.M.; Gnanakaran, S.; Yoon, H.; Theiler, J.; Abfalterer, W.; Hengartner, N.; Giorgi, E.E.; Bhattacharya, T.; Foley, B.; et al. Tracking changes in SARS-CoV-2 spike: Evidence that D614G increases infectivity of the COVID-19 virus. *Cell* **2020**, *182*, 812–827.e19. [CrossRef]
12. Flores-Vega, V.R.; Monroy-Molina, J.V.; Jimenez-Hernandez, L.E.; Torres, A.G.; Santos-Preciado, J.I.; Rosales-Reyes, R. SARS-CoV-2: Evolution and emergence of new viral variants. *Viruses* **2022**, *14*, 653. [CrossRef]
13. Dol, J.; Boulos, L.; Somerville, M.; Saxinger, L.; Doroshenko, A.; Hastings, S.; Reynolds, B.; Gallant, A.; Shin, H.D.; Wong, H.; et al. Health system impacts of SARS-CoV-2 variants of concern: A rapid review. *BMC Health Serv. Res.* **2022**, *22*, 544. [CrossRef]
14. Yadav, P.D.; Sarkale, P.; Razdan, A.; Gupta, N.; Nyayanit, D.A.; Sahay, R.R.; Potdar, V.; Patil, D.Y.; Baradkar, S.; Kumar, A.; et al. Isolation and characterization of SARS-CoV-2 Beta variant from UAE travelers. *J. Infect. Public Health* **2022**, *15*, 182–186. [CrossRef]
15. Ramesh, S.; Govindarajulu, M.; Parise, R.S.; Neel, L.; Shankar, T.; Patel, S.; Lowery, P.; Smith, F.; Dhanasekaran, M.; Moore, T. Emerging SARS-CoV-2 variants: A review of its mutations, its implications and vaccine efficacy. *Vaccines* **2021**, *9*, 1195. [CrossRef] [PubMed]
16. Tian, D.; Sun, Y.; Zhou, J.; Ye, Q. The global epidemic of the SARS-CoV-2 Delta variant, key apike mutations and immune escape. *Front. Immunol.* **2021**, *12*, 751778. [CrossRef] [PubMed]
17. Ou, J.; Lan, W.; Wu, X.; Zhao, T.; Duan, B.; Yang, P.; Ren, Y.; Quan, L.; Zhao, W.; Seto, D.; et al. Tracking SARS-CoV-2 Omicron diverse spike gene mutations identifies multiple inter-variant recombination events. *Signal. Transduct. Target. Ther.* **2022**, *7*, 138. [CrossRef]
18. Hoffmann, M.; Zhang, L.; Pohlmann, S. Omicron: Master of immune evasion maintains robust ACE2 binding. *Signal. Transduct. Target. Ther.* **2022**, *7*, 118. [CrossRef]
19. Cao, Y.; Wang, J.; Jian, F.; Xiao, T.; Song, W.; Yisimayi, A.; Huang, W.; Li, Q.; Wang, P.; An, R.; et al. Omicron escapes the majority of existing SARS-CoV-2 neutralizing antibodies. *Nature* **2022**, *602*, 657–663. [CrossRef]
20. Zhang, L.; Jackson, C.B.; Mou, H.; Ojha, A.; Peng, H.; Quinlan, B.D.; Rangarajan, E.S.; Pan, A.; Vanderheiden, A.; Suthar, M.S.; et al. SARS-CoV-2 spike-protein D614G mutation increases virion spike density and infectivity. *Nat. Commun.* **2020**, *11*, 6013. [CrossRef] [PubMed]
21. Harvey, W.T.; Carabelli, A.M.; Jackson, B.; Gupta, R.K.; Thomson, E.C.; Harrison, E.M.; Ludden, C.; Reeve, R.; Rambaut, A.; Peacock, S.J.; et al. SARS-CoV-2 variants, spike mutations and immune escape. *Nat. Rev. Microbiol.* **2021**, *19*, 409–424. [CrossRef]
22. Wibmer, C.K.; Ayres, F.; Hermanus, T.; Madzivhandila, M.; Kgagudi, P.; Oosthuysen, B.; Lambson, B.E.; de Oliveira, T.; Vermeulen, M.; van der Berg, K.; et al. SARS-CoV-2 501Y.V2 escapes neutralization by South African COVID-19 donor plasma. *Nat. Med.* **2021**, *27*, 622–625. [CrossRef] [PubMed]
23. Tegally, H.; Wilkinson, E.; Giovanetti, M.; Iranzadeh, A.; Fonseca, V.; Giandhari, J.; Doolabh, D.; Pillay, S.; San, E.J.; Msomi, N.; et al. Detection of a SARS-CoV-2 variant of concern in South Africa. *Nature* **2021**, *592*, 438–443. [CrossRef] [PubMed]
24. Di Giacomo, S.; Mercatelli, D.; Rakhimov, A.; Giorgi, F.M. Preliminary report on severe acute respiratory syndrome coronavirus 2 (SARS-CoV-2) Spike mutation T478K. *J. Med. Virol.* **2021**, *93*, 5638–5643. [CrossRef]

25. Tchesnokova, V.; Kulasekara, H.; Larson, L.; Bowers, V.; Rechkina, E.; Kisiela, D.; Sledneva, Y.; Choudhury, D.; Maslova, I.; Deng, K.; et al. Acquisition of the L452R mutation in the ACE2-binding interface of spike protein triggers recent massive expansion of SARS-CoV-2 variants. *J. Clin. Microbiol.* **2021**, *59*, e0092121. [CrossRef]

26. Liu, C.; Ginn, H.M.; Dejnirattisai, W.; Supasa, P.; Wang, B.; Tuekprakhon, A.; Nutalai, R.; Zhou, D.; Mentzer, A.J.; Zhao, Y.; et al. Reduced neutralization of SARS-CoV-2 B.1.617 by vaccine and convalescent serum. *Cell* **2021**, *184*, 4220–4236.e13. [CrossRef]

27. Shah, M.; Woo, H.G. Omicron: A heavily mutated SARS-CoV-2 variant exhibits stronger binding to ACE2 and potently escapes approved COVID-19 therapeutic antibodies. *Front. Immunol.* **2021**, *12*, 830527. [CrossRef]

28. Gagne, M.; Moliva, J.I.; Foulds, K.E.; Andrew, S.F.; Flynn, B.J.; Werner, A.P.; Wagner, D.A.; Teng, I.T.; Lin, B.C.; Moore, C.; et al. mRNA-1273 or mRNA-Omicron boost in vaccinated macaques elicits similar B cell expansion, neutralizing responses, and protection from Omicron. *Cell* **2022**, *185*, 1556–1571.e18. [CrossRef]

29. Coronavirus (COVID-19) Update: FDA Authorizes Moderna, Pfizer-BioNTech Bivalent COVID-19 Vaccines for Use as a Booster Dose. 31 August 2022. Available online: https://www.fda.gov/news-events/press-announcements/coronavirus-covid-19-update-fda-authorizes-moderna-pfizer-biontech-bivalent-covid-19-vaccines-use (accessed on 19 January 2023).

30. Pfizer and BioNTech Granted FDA Emergency Use Authorization of Omicron BA.4/BA.5-Adapted Bivalent COVID-19 Vaccine Booster for Ages 12 Years and Older. 31 August 2022. Available online: https://www.globenewswire.com/en/news-release/2022/08/31/2507787/0/en/Pfizer-and-BioNTech-Granted-FDA-Emergency-Use-Authorization-of-Omicron-BA-4-BA-5-Adapted-Bivalent-COVID-19-Vaccine-Booster-for-Ages-12-Years-and-Older.html (accessed on 19 January 2023).

31. Pfizer and BioNTech Announce Positive Early Data from Clinical Trial of Omicron BA.4/BA.5-Adapted Bivalent Booster in Individuals 18 Years and Older. 13 October 2022. Available online: https://www.globenewswire.com/en/news-release/2022/10/13/2533650/0/en/Pfizer-and-BioNTech-Announce-Positive-Early-Data-From-Clinical-Trial-of-Omicron-BA-4-BA-5-Adapted-Bivalent-Booster-in-Individuals-18-Years-and-Older.html (accessed on 19 January 2023).

32. Coronavirus (COVID-19) Update: FDA Authorizes Updated (Bivalent) COVID-19 Vaccines for Children Down to 6 Months of Age. 8 December 2022. Available online: https://www.fda.gov/news-events/press-announcements/coronavirus-covid-19-update-fda-authorizes-updated-bivalent-covid-19-vaccines-children-down-6-months (accessed on 19 January 2023).

33. European Medicines Agency Accepts Moderna's Conditional Marketing Authorization Filing for Its Omicron BA.4/BA.5 Targeting Bivalent COVID-19 Vaccine. 28 September 2022. Available online: https://investors.modernatx.com/news/news-details/2022/European-Medicines-Agency-Accepts-Modernas-Conditional-Marketing-Authorization-Filing-for-its-Omicron-BA.4BA.5-Targeting-Bivalent-COVID-19-Vaccine/default.aspx (accessed on 19 January 2023).

34. Scheaffer, S.M.; Lee, D.; Whitener, B.; Ying, B.; Wu, K.; Liang, C.-Y.; Jani, H.; Martin, P.; Amato, N.J.; Avena, L.E.; et al. Bivalent SARS-CoV-2 mRNA vaccines increase breadth of neutralization and protect against the BA.5 Omicron variant in mice. *Nat. Med.* **2022**, *29*, 247–257. [CrossRef] [PubMed]

35. Hajnik, R.L.; Plante, J.A.; Liang, Y.; Alameh, M.-G.; Tang, J.; Bonam, S.R.; Zhong, C.; Adam, A.; Scharton, D.; Rafael, G.H.; et al. Dual spike and nucleocapsid mRNA vaccination confer protection against SARS-CoV-2 Omicron and Delta variants in preclinical models. *Sci. Transl. Med.* **2022**, *14*, eabq1945. [CrossRef]

36. Zhang, Y.; Tan, W.; Lou, Z.; Zhao, Y.; Zhang, J.; Liang, H.; Li, N.; Zhu, X.; Ding, L.; Huang, B.; et al. Vaccination with Omicron inactivated vaccine in pre-vaccinated mice protects against SARS-CoV-2 prototype and Omicron variants. *Vaccines* **2022**, *10*, 1149. [CrossRef] [PubMed]

37. Chavda, V.P.; Pandya, R.; Apostolopoulos, V. DNA vaccines for SARS-CoV-2: Toward third-generation vaccination era. *Expert Rev. Vaccines* **2021**, *20*, 1549–1560. [CrossRef]

38. Dey, A.; Chozhavel Rajanathan, T.M.; Chandra, H.; Pericherla, H.P.R.; Kumar, S.; Choonia, H.S.; Bajpai, M.; Singh, A.K.; Sinha, A.; Saini, G.; et al. Immunogenic potential of DNA vaccine candidate, ZyCoV-D against SARS-CoV-2 in animal models. *Vaccine* **2021**, *39*, 4108–4116. [CrossRef]

39. Momin, T.; Kansagra, K.; Patel, H.; Sharma, S.; Sharma, B.; Patel, J.; Mittal, R.; Sanmukhani, J.; Maithal, K.; Dey, A.; et al. Safety and Immunogenicity of a DNA SARS-CoV-2 vaccine (ZyCoV-D): Results of an open-label, non-randomized phase I part of phase I/II clinical study by intradermal route in healthy subjects in India. *eClinicalMedicine* **2021**, *38*, 101020. [CrossRef]

40. Khobragade, A.; Bhate, S.; Ramaiah, V.; Deshpande, S.; Giri, K.; Phophle, H.; Supe, P.; Godara, I.; Revanna, R.; Nagarkar, R.; et al. Efficacy, safety, and immunogenicity of the DNA SARS-CoV-2 vaccine (ZyCoV-D): The interim efficacy results of a phase 3, randomised, double-blind, placebo-controlled study in India. *Lancet* **2022**, *399*, 1313–1321. [CrossRef]

41. Appelberg, S.; Ahlén, G.; Yan, J.; Nikouyan, N.; Weber, S.; Larsson, O.; Höglund, U.; Aleman, S.; Weber, F.; Perlhamre, E.; et al. A universal SARS-CoV DNA vaccine inducing highly cross-reactive neutralizing antibodies and T cells. *EMBO Mol. Med.* **2022**, *14*, e15821. [CrossRef] [PubMed]

42. Jang, Y.; Cho, H.; Chun, J.; Park, K.; Nowakowska, A.; Kim, J.; Lee, H.; Lee, C.; Han, Y.; Lee, H.J.; et al. Baculoviral COVID-19 Delta DNA vaccine cross-protects against SARS-CoV2 variants in K18-ACE2 transgenic mice. *Vaccine* **2023**, *41*, 1223–1231. [CrossRef]

43. Tzeng, T.T.; Chai, K.M.; Shen, K.Y.; Yu, C.Y.; Yang, S.J.; Huang, W.C.; Liao, H.C.; Chiu, F.F.; Dou, H.Y.; Liao, C.L.; et al. A DNA vaccine candidate delivered by an electroacupuncture machine provides protective immunity against SARS-CoV-2 infection. *NPJ Vaccines* **2022**, *7*, 60. [CrossRef] [PubMed]

44. Mucker, E.M.; Brocato, R.L.; Principe, L.M.; Kim, R.K.; Zeng, X.; Smith, J.M.; Kwilas, S.A.; Kim, S.; Horton, H.; Caproni, L.; et al. SARS-CoV-2 doggybone DNA vaccine produces cross-variant neutralizing antibodies and is protective in a COVID-19 animal model. *Vaccines* **2022**, *10*, 1104. [CrossRef] [PubMed]

45. Zhang, Z.; He, Q.; Zhao, W.; Li, Y.; Yang, J.; Hu, Z.; Chen, X.; Peng, H.; Fu, Y.X.; Chen, L.; et al. A heterologous V-01 or variant-matched bivalent V-01D-351 booster following primary series of inactivated vaccine enhances the neutralizing capacity against SARS-CoV-2 Delta and Omicron strains. *J. Clin. Med.* **2022**, *11*, 4164. [CrossRef] [PubMed]

46. Liu, Z.; Zhou, J.; Xu, W.; Deng, W.; Wang, Y.; Wang, M.; Wang, Q.; Hsieh, M.; Dong, J.; Wang, X.; et al. A novel STING agonist-adjuvanted pan-sarbecovirus vaccine elicits potent and durable neutralizing antibody and T cell responses in mice, rabbits and NHPs. *Cell Res.* **2022**, *32*, 269–287. [CrossRef]

47. Liu, Z.; Chan, J.F.; Zhou, J.; Wang, M.; Wang, Q.; Zhang, G.; Xu, W.; Chik, K.K.; Zhang, Y.; Wang, Y.; et al. A pan-sarbecovirus vaccine induces highly potent and durable neutralizing antibody responses in non-human primates against SARS-CoV-2 Omicron variant. *Cell Res.* **2022**, *32*, 495–497. [CrossRef]

48. Heide, J.; Schulte, S.; Kohsar, M.; Brehm, T.T.; Herrmann, M.; Karsten, H.; Marget, M.; Peine, S.; Johansson, A.M.; Sette, A.; et al. Broadly directed SARS-CoV-2-specific CD4+ T cell response includes frequently detected peptide specificities within the membrane and nucleoprotein in patients with acute and resolved COVID-19. *PLoS Pathog.* **2021**, *17*, e1009842. [CrossRef] [PubMed]

49. Lim, H.X.; Masomian, M.; Khalid, K.; Kumar, A.U.; MacAry, P.A.; Poh, C.L. Identification of B-cell epitopes for eliciting neutralizing antibodies against the SARS-CoV-2 spike protein through bioinformatics and monoclonal antibody targeting. *Int. J. Mol. Sci.* **2022**, *23*, 4341. [CrossRef] [PubMed]

50. Boni, C.; Cavazzini, D.; Bolchi, A.; Rossi, M.; Vecchi, A.; Tiezzi, C.; Barili, V.; Fisicaro, P.; Ferrari, C.; Ottonello, S. Degenerate CD8 epitopes mapping to structurally constrained regions of the spike protein: A T cell-based way-out from the SARS-CoV-2 variants storm. *Front. Immunol.* **2021**, *12*, 730051. [CrossRef]

51. Tye, E.X.C.; Jinks, E.; Haigh, T.A.; Kaul, B.; Patel, P.; Parry, H.M.; Newby, M.L.; Crispin, M.; Kaur, N.; Moss, P.; et al. Mutations in SARS-CoV-2 spike protein impair epitope-specific CD4+ T cell recognition. *Nat. Immunol.* **2022**, *23*, 1726–1734. [CrossRef]

52. Kingstad-Bakke, B.; Lee, W.; Chandrasekar, S.S.; Gasper, D.J.; Salas-Quinchucua, C.; Cleven, T.; Sullivan, J.A.; Talaat, A.; Osorio, J.E.; Suresh, M. Vaccine-induced systemic and mucosal T cell immunity to SARS-CoV-2 viral variants. *Proc. Natl. Acad. Sci. USA* **2022**, *119*, e2118312119. [CrossRef]

53. Heitmann, J.S.; Bilich, T.; Tandler, C.; Nelde, A.; Maringer, Y.; Marconato, M.; Reusch, J.; Jäger, S.; Denk, M.; Richter, M.; et al. A COVID-19 peptide vaccine for the induction of SARS-CoV-2 T cell immunity. *Nature* **2022**, *601*, 617–622. [CrossRef]

54. Lee, Y.-S.; Hong, S.-H.; Park, H.-J.; Lee, H.-Y.; Hwang, J.-Y.; Kim, S.Y.; Park, J.W.; Choi, K.-S.; Seong, J.K.; Park, S.-I.; et al. Peptides derived from S and N proteins of severe acute respiratory syndrome coronavirus 2 induce T cell responses: A proof of concept for T cell vaccines. *Front. Microbiol.* **2021**, *12*, 732450. [CrossRef]

55. Rosendahl Huber, S.; van Beek, J.; de Jonge, J.; Luytjes, W.; van Baarle, D. T cell responses to viral infections-opportunities for peptide vaccination. *Front. Immunol.* **2014**, *5*, 171. [CrossRef] [PubMed]

56. Wang, S.; Wang, C.Y.; Kuo, H.-K.; Peng, W.-J.; Huang, J.-H.; Kuo, B.-S.; Lin, F.; Liu, Y.-J.; Liu, Z.; Wu, H.-T.; et al. A novel RBD-protein/peptide vaccine elicits broadly neutralizing antibodies and protects mice and macaques against SARS-CoV-2. *Emerg. Microbes Infect.* **2022**, *11*, 2724–2734. [CrossRef]

57. Wang, C.Y.; Hwang, K.P.; Kuo, H.K.; Peng, W.J.; Shen, Y.H.; Kuo, B.S.; Huang, J.H.; Liu, H.; Ho, Y.H.; Lin, F.; et al. A multitope SARS-CoV-2 vaccine provides long-lasting B cell and T cell immunity against Delta and Omicron variants. *J. Clin. Investig.* **2022**, *132*, e157707. [CrossRef] [PubMed]

58. Guirakhoo, F.; Wang, S.; Wang, C.Y.; Kuo, H.K.; Peng, W.J.; Liu, H.; Wang, L.; Johnson, M.; Hunt, A.; Hu, M.M.; et al. High neutralizing antibody levels against Severe Acute Respiratory Syndrome Coronavirus 2 Omicron BA.1 and BA.2 after UB-612 vaccine booster. *J. Infect. Dis.* **2022**, *226*, 1401–1406. [CrossRef]

59. Vaxxinity's COVID-19 Vaccine Candidate UB-612 Produces High Levels of Neutralizing Antibodies against Omicron and Other Variants of Concern. 11 February 2022. Available online: https://www.biospace.com/article/releases/vaxxinity-s-covid-19-vaccine-candidate-ub-612-produces-high-levels-of-neutralizing-antibodies-against-omicron-and-other-variants-of-concern/ (accessed on 19 January 2023).

60. Ryzhikov, A.B.; Ryzhikov, E.A.; Bogryantseva, M.P.; Usova, S.V.; Danilenko, E.D.; Nechaeva, E.A.; Pyankov, O.V.; Pyankova, O.G.; Gudymo, A.S.; Bodnev, S.A.; et al. A single blind, placebo-controlled randomized study of the safety, reactogenicity and immunogenicity of the "EpiVacCorona" Vaccine for the prevention of COVID-19, in volunteers aged 18–60 years (phase I–II). *Russ. J. Infect. Immun.* **2021**, *11*, 283–296. [CrossRef]

61. Matveeva, O.; Ershov, A. Retrospective cohort study of the effectiveness of the Sputnik V and EpiVacCorona vaccines against the SARS-CoV-2 Delta variant in Moscow (June–July 2021). *Vaccines* **2022**, *10*, 984. [CrossRef] [PubMed]

62. Wu, S.; Huang, J.; Zhang, Z.; Wu, J.; Zhang, J.; Hu, H.; Zhu, T.; Zhang, J.; Luo, L.; Fan, P.; et al. Safety, tolerability, and immunogenicity of an aerosolised adenovirus type-5 vector-based COVID-19 vaccine (Ad5-nCoV) in adults: Preliminary report of an open-label and randomised phase 1 clinical trial. *Lancet Infect. Dis.* **2021**, *21*, 1654–1664. [CrossRef]

63. Zabaleta, N.; Dai, W.; Bhatt, U.; Hérate, C.; Maisonnasse, P.; Chichester, J.A.; Sanmiguel, J.; Estelien, R.; Michalson, K.T.; Diop, C.; et al. An AAV-based, room-temperature-stable, single-dose COVID-19 vaccine provides durable immunogenicity and protection in non-human primates. *Cell Host Microbe* **2021**, *29*, 1437–1453.e8. [CrossRef]

64. Zhu, F.C.; Li, Y.H.; Guan, X.H.; Hou, L.H.; Wang, W.J.; Li, J.X.; Wu, S.P.; Wang, B.S.; Wang, Z.; Wang, L.; et al. Safety, tolerability, and immunogenicity of a recombinant adenovirus type-5 vectored COVID-19 vaccine: A dose-escalation, open-label, non-randomised, first-in-human trial. *Lancet* **2020**, *395*, 1845–1854. [CrossRef]

65. Sadoff, J.; Le Gars, M.; Shukarev, G.; Heerwegh, D.; Truyers, C.; de Groot, A.M.; Stoop, J.; Tete, S.; Van Damme, W.; Leroux-Roels, I.; et al. Interim results of a phase 1-2a trial of Ad26.COV2.S COVID-19 vaccine. *N. Engl. J. Med.* **2021**, *384*, 1824–1835. [CrossRef]

66. Tscherne, A.; Schwarz, J.H.; Rohde, C.; Kupke, A.; Kalodimou, G.; Limpinsel, L.; Okba, N.M.A.; Bošnjak, B.; Sandrock, I.; Odak, I.; et al. Immunogenicity and efficacy of the COVID-19 candidate vector vaccine MVA-SARS-2-S in preclinical vaccination. *Proc. Natl. Acad. Sci. USA* **2021**, *118*, e2026207118. [CrossRef] [PubMed]

67. Coleman, J.R.; Papamichail, D.; Skiena, S.; Futcher, B.; Wimmer, E.; Mueller, S. Virus attenuation by genome-scale changes in codon pair bias. *Science* **2008**, *320*, 1784–1787. [CrossRef]

68. Wang, Y.; Yang, C.; Song, Y.; Coleman, J.R.; Stawowczyk, M.; Tafrova, J.; Tasker, S.; Boltz, D.; Baker, R.; Garcia, L.; et al. Scalable live-attenuated SARS-CoV-2 vaccine candidate demonstrates preclinical safety and efficacy. *Proc. Natl. Acad. Sci. USA* **2021**, *118*, e2102775118. [CrossRef] [PubMed]

69. Trimpert, J.; Dietert, K.; Firsching, T.C.; Ebert, N.; Thi Nhu Thao, T.; Vladimirova, D.; Kaufer, S.; Labroussaa, F.; Abdelgawad, A.; Conradie, A.; et al. Development of safe and highly protective live-attenuated SARS-CoV-2 vaccine candidates by genome recoding. *Cell Rep.* **2021**, *36*, 109493. [CrossRef]

70. Lauring, A.S.; Jones, J.O.; Andino, R. Rationalizing the development of live attenuated virus vaccines. *Nat. Biotechnol.* **2010**, *28*, 573–579. [CrossRef] [PubMed]

71. Trimpert, J.; Adler, J.M.; Eschke, K.; Abdelgawad, A.; Firsching, T.C.; Ebert, N.; Thao, T.T.N.; Gruber, A.D.; Thiel, V.; Osterrieder, N.; et al. Live attenuated virus vaccine protects against SARS-CoV-2 variants of concern B.1.1.7 (Alpha) and B.1.351 (Beta). *Sci. Adv.* **2021**, *7*, eabk0172. [CrossRef] [PubMed]

72. Kushnir, A.; Mueller, S.; Tasker, S.; Robert Coleman, J. 577. COVI-VAC™, a live attenuated COVID-19 vaccine, provides single dose protection against heterologous challenge with SARS-CoV-2 Beta (B.1.351) in the Syrian Golden hamster model. *Open Forum. Infect. Dis.* **2021**, *8* (Suppl. 1), S390. [CrossRef]

73. Light, D.W.; Lexchin, J. The costs of coronavirus vaccines and their pricing. *J. R. Soc. Med.* **2021**, *114*, 502–504. [CrossRef] [PubMed]

74. Sheridan, C. First COVID-19 DNA Vaccine Approved, Others in Hot Pursuit. 16 November 2021. Available online: https://www.nature.com/articles/d41587-021-00023-5 (accessed on 3 February 2023).

75. Shafaati, M.; Saidijam, M.; Soleimani, M.; Hazrati, F.; Mirzaei, R.; Amirheidari, B.; Tanzadehpanah, H.; Karampoor, S.; Kazemi, S.; Yavari, B. A brief review on DNA vaccines in the era of COVID-19. *Future Virol.* **2022**, *17*, 49–66. [CrossRef]

76. Hobernik, D.; Bros, M. DNA Vaccines-How Far From Clinical Use? *Int. J. Mol. Sci.* **2018**, *19*, 3605. [CrossRef]

77. Kraynyak, K.A.; Blackwood, E.; Agnes, J.; Tebas, P.; Giffear, M.; Amante, D.; Reuschel, E.L.; Purwar, M.; Christensen-Quick, A.; Liu, N.; et al. SARS-CoV-2 DNA vaccine INO-4800 induces durable immune responses capable of being boosted in a Phase 1 open-label trial. *J. Infect. Dis.* **2022**, *225*, 1923–1932. [CrossRef]

78. Galagali, P.M.; Kinikar, A.A.; Kumar, V.S. Vaccine hesitancy: Obstacles and challenges. *Curr. Pediatr. Rep.* **2022**, *10*, 241–248. [CrossRef]

79. Abdul Karim, M.; Reagu, S.M.; Ouanes, S.; Waheed Khan, A.; Smidi, W.S.; Al-Baz, N.; Alabdulla, M. Prevalence and correlates of COVID-19 vaccine hesitancy among the elderly in Qatar: A cross-sectional study. *Medicine (Baltimore)* **2022**, *101*, e29741. [CrossRef] [PubMed]

80. Schultz, N.H.; Sørvoll, I.H.; Michelsen, A.E.; Munthe, L.A.; Lund-Johansen, F.; Ahlen, M.T.; Wiedmann, M.; Aamodt, A.H.; Skattør, T.H.; Tjønnfjord, G.E.; et al. Thrombosis and thrombocytopenia after ChAdOx1 nCoV-19 vaccination. *N. Engl. J. Med.* **2021**, *384*, 2124–2130. [CrossRef] [PubMed]

81. See, I.; Lale, A.; Marquez, P.; Streiff, M.B.; Wheeler, A.P.; Tepper, N.K.; Woo, E.J.; Broder, K.R.; Edwards, K.M.; Gallego, R.; et al. Case series of thrombosis with thrombocytopenia syndrome after COVID-19 vaccination-United States, December 2020 to August 2021. *Ann. Intern. Med.* **2022**, *175*, 513–522. [CrossRef] [PubMed]

82. Verdecia, M.; Kokai-Kun, J.F.; Kibbey, M.; Acharya, S.; Venema, J.; Atouf, F. COVID-19 vaccine platforms: Delivering on a promise? *Hum. Vaccines Immunother.* **2021**, *17*, 2873–2893. [CrossRef]

83. Liu, M.A. A comparison of plasmid DNA and mRNA as vaccine technologies. *Vaccines* **2019**, *7*, 37. [CrossRef] [PubMed]

84. Di Natale, C.; La Manna, S.; De Benedictis, I.; Brandi, P.; Marasco, D. Perspectives in peptide-based vaccination strategies for syndrome coronavirus 2 pandemic. *Front. Pharmacol.* **2020**, *11*, 578382. [CrossRef] [PubMed]

85. Khairkhah, N.; Bolhassani, A.; Agi, E.; Namvar, A.; Nikyar, A. Immunological investigation of a multiepitope peptide vaccine candidate based on main proteins of SARS-CoV-2 pathogen. *PLoS ONE* **2022**, *17*, e0268251. [CrossRef]

86. Dejnirattisai, W.; Shaw, R.H.; Supasa, P.; Liu, C.; Stuart, A.S.; Pollard, A.J.; Liu, X.; Lambe, T.; Crook, D.; Stuart, D.I.; et al. Reduced neutralisation of SARS-CoV-2 omicron B.1.1.529 variant by post-immunisation serum. *Lancet* **2022**, *399*, 234–236. [CrossRef]

87. Nasreen, S.; Chung, H.; He, S.; Brown, K.A.; Gubbay, J.B.; Buchan, S.A.; Fell, D.B.; Austin, P.C.; Schwartz, K.L.; Sundaram, M.E.; et al. Effectiveness of COVID-19 vaccines against symptomatic SARS-CoV-2 infection and severe outcomes with variants of concern in Ontario. *Nat. Microbiol.* **2022**, *7*, 379–385. [CrossRef]

88. Baraniuk, C. Covid-19: How effective are vaccines against the delta variant? *BMJ* **2021**, *374*, n1960. [CrossRef]

89. Doria-Rose, N.; Suthar, M.S.; Makowski, M.; O'Connell, S.; McDermott, A.B.; Flach, B.; Ledgerwood, J.E.; Mascola, J.R.; Graham, B.S.; Lin, B.C.; et al. Antibody persistence through 6 months after the second dose of mRNA-1273 vaccine for covid-19. *N. Engl. J. Med.* **2021**, *384*, 2259–2261. [CrossRef] [PubMed]

90. Su, S.; Li, W.; Jiang, S. Developing pan-β-coronavirus vaccines against emerging SARS-CoV-2 variants of concern. *Trends Immunol.* **2022**, *43*, 170–172.

91. Smith, N.; Goncalves, P.; Charbit, B.; Grzelak, L.; Beretta, M.; Planchais, C.; Bruel, T.; Rouilly, V.; Bondet, V.; Hadjadj, J.; et al. Distinct systemic and mucosal immune responses during acute SARS-CoV-2 infection. *Nat. Immunol.* **2021**, *22*, 1428–1439. [PubMed]

92. Wang, Z.; Lorenzi, J.C.C.; Muecksch, F.; Finkin, S.; Viant, C.; Gaebler, C.; Cipolla, M.; Hoffmann, H.H.; Oliveira, T.Y.; Oren, D.A.; et al. Enhanced SARS-CoV-2 neutralization by dimeric IgA. *Sci. Transl. Med.* **2021**, *13*, eabf1555.

93. Staff, T. Omicron Wave Could Mark End of Pandemic, Israeli COVID Expert Says. *The Times of Israel*, 24 January 2022.

94. Monto, A.S. The future of SARS-CoV-2 vaccination-lessons from Influenza. *N. Engl. J. Med.* **2021**, *385*, 1825–1827. [CrossRef] [PubMed]

95. Lippi, G.; Henry, B.M.; Plebani, M. Anti-SARS-CoV-2 antibodies testing in recipients of COVID-19 vaccination: Why, when, and how? *Diagnostics* **2021**, *11*, 941. [CrossRef]

96. Ward, H.; Whitaker, M.; Flower, B.; Tang, S.N.; Atchison, C.; Darzi, A.; Donnelly, C.A.; Cann, A.; Diggle, P.J.; Ashby, D.; et al. Population antibody responses following COVID-19 vaccination in 212,102 individuals. *Nat. Commun.* **2022**, *13*, 907. [CrossRef]

97. Bagwe, P.V.; Bagwe, P.V.; Ponugoti, S.S.; Joshi, S.V. Peptide-based vaccines and therapeutics for COVID-19. *Int. J. Pept. Res. Ther.* **2022**, *28*, 94. [CrossRef]

Review article

The development of DNA vaccines against SARS-CoV-2

Kanwal Khalid, Chit Laa Poh *

Centre for Virus and Vaccine Research, School of Medical and Life Sciences, Sunway University, Bandar Sunway, Malaysia

A B S T R A C T

Background: The COVID-19 pandemic exerted significant impacts on public health and global economy. Research efforts to develop vaccines at warp speed against SARS-CoV-2 led to novel mRNA, viral vectored, and inactivated vaccines being administered. The current COVID-19 vaccines incorporate the full S protein of the SARS-CoV-2 Wuhan strain but rapidly emerging variants of concern (VOCs) have led to significant reductions in protective efficacies. There is an urgent need to develop next-generation vaccines which could effectively prevent COVID-19.
Methods: PubMed and Google Scholar were systematically reviewed for peer-reviewed papers up to January 2023.
Results: A promising solution to the problem of emerging variants is a DNA vaccine platform since it can be easily modified. Besides expressing whole protein antigens, DNA vaccines can also be constructed to include specific nucleotide genes encoding highly conserved and immunogenic epitopes from the S protein as well as from other structural/non-structural proteins to develop effective vaccines against VOCs. DNA vaccines are associated with low transfection efficiencies which could be enhanced by chemical, genetic, and molecular adjuvants as well as delivery systems.
Conclusions: The DNA vaccine platform offers a promising solution to the design of effective vaccines. The challenge of limited immunogenicity in humans might be solved through the use of genetic modifications such as the addition of nuclear localization signal (NLS) peptide gene, strong promoters, MARs, introns, TLR agonists, CD40L, and the development of appropriate delivery systems utilizing nanoparticles to increase uptake by APCs in enhancing the induction of potent immune responses.

1. Introduction

The severe acute respiratory syndrome coronavirus 2 (SARS-CoV-2) is the etiological agent of coronavirus disease 2019 (COVID-19). It has caused an alarming pandemic associated with 766,895,075 infections and 6,935,889 deaths as of 15 May 2023 [1]. The pandemic has also resulted in severe economic losses with the imposition of lockdowns, causing a debilitating burden on healthcare systems. Novel vaccines such as those based on the mRNA, viral-vectored platforms, and traditional inactivated vaccines were given emergency approval for global vaccinations. Each of the vaccine platforms has its own strengths and weaknesses. However, the emergence of SARS-CoV-2 variants of concern (VOCs) which caused continuing waves of infections and reduced protective efficacies of current vaccines against the B.1.1.7 (Alpha), B.1.351 (Beta), B.1.617.2 (Delta), and (B.1.1.529) (Omicron) variants were reported [2]. The prospect of using DNA vaccines to immunize against SARS-CoV-2 is promising because of the ease of production and reduced cost over other vaccine platforms. They can easily be modified to

incorporate different antigenic targets simply by changing the gene sequences of the DNA plasmid, making the DNA vaccine platform ideal for rapidly developing vaccines against emerging SARS-CoV-2 VOCs. Therefore, this review discusses the advantages and limitations of DNA vaccines and summarizes current DNA vaccine development against SARS-CoV-2. Furthermore, an insight into the design of DNA vaccines and the strategies to increase the immunological potency of plasmid DNA vaccines in terms of adjuvants, delivery systems, and administration routes are thoroughly reviewed.

2. Review

2.1. Mechanism of DNA vaccines

Current DNA vaccines against SARS-CoV-2 are able to elicit both humoral and cellular immune responses against the main antigen, the Spike (S) glycoprotein of the SARS-CoV-2. Eiz-Vesper et al. [3] explained that DNA vaccines which target and transfect muscle cells would likely

result in weak antigen presentation due to a lack of co-stimulatory molecules since antigen presenting cells (APCs) allow antigen presentation to major histocompatibility complex (MHC) molecules. The transfection of the recombinant DNA plasmid into professional APCs such as dendritic cells (DCs) would result in a much more potent immune response. Inside the APC, the recombinant DNA plasmid enters the nucleus so that it is transcribed to mRNA. The single stranded RNA would then exit the nucleus to undergo translation to produce the S protein in the cytoplasm which is processed inside the cell to smaller peptides to be presented to naïve B and T cells [4].

DNA vaccines can elicit cellular immune responses by binding to naïve CD4$^+$ T cells to activate them. Degradation of the S viral protein would result in the production of peptide fragments which could be presented to MHC class II molecules to form the MHC class II-peptide complex. T cell receptors (TCRs) of specific CD4$^+$ T cells are able to recognize and bind to these MHC class II-peptide complexes. This resulted in the activation of DCs through the interaction of CD40 with CD40 ligand (CD40L) on the DC. The activation of DCs led to the upregulation of CD80/CD86 which interacted with CD28 to activate naïve CD8$^+$ T cells [5]. Together with the help of CD4$^+$ T cells, activation of CD8$^+$ T cells is induced. Viral peptides are also taken up by APCs that were presented on MHC class I molecules which were recognized and bind to TCRs of CD8$^+$ T cells. The activated CD8$^+$ effector T cells then released cytotoxic granules containing perforins and granzymes and produced cytokines such as tumor necrosis factor α (TNF-α) and interferon-gamma (IFN-γ) [6].

A specialized subset of CD4$^+$ T cells known as T follicular helper (Tfh) cells aid in B cell antibody production through the formation of germinal

centres which are specialized microstructures involved in the production of long-lived antibody secreting plasma cells and memory B cells resulting from the expression of signaling lymphocyte activation molecules (SLAM)-associated protein (SAP). Cytokine-polarized CD4$^+$ memory T cell subsets such as Th1, Th2 and Th17 cells can each develop into Tfh to influence the B cell response. Tfh also promotes B cell activation through cell–cell communication such as CD40L (expressed on activated CD4$^+$ T cells) and CD40 (expressed by B cell) interactions, leading to the release of cytokines [7,8] (Fig. 1).

Tfh cells are involved in giving specialized assistance to germinal centre B cells through B and T cell interactions. Another set of cells known as Foxp3$^+$ T follicular regulatory (Tfr) cells also serve as important mediators of germinal centre regulation. Furthermore, memory CD4$^+$ T cells were also implicated in providing help to B cells in promoting earlier B cell proliferation, higher antibody levels and earlier class-switching responses when compared to naïve CD4$^+$ T cells. Memory CD4$^+$ T cells produce higher amounts and a more polarised profile of cytokines, which is believed to encourage more robust B cell antibody response and determine the antibody isotype. Current research suggests that Tfh cells produce interleukin (IL)-4 and IFN which play a key role in regulating B cell affinity development as well as immunoglobulin class switching in the germinal centre [7,8] (Fig. 1).

2.2. Advantages of DNA vaccines

The prospect of designing and constructing DNA vaccines targeting SARS-CoV-2 is attractive for a number of reasons. Firstly, the DNA vaccine platform shows great potential in eliciting both humoral and cellular
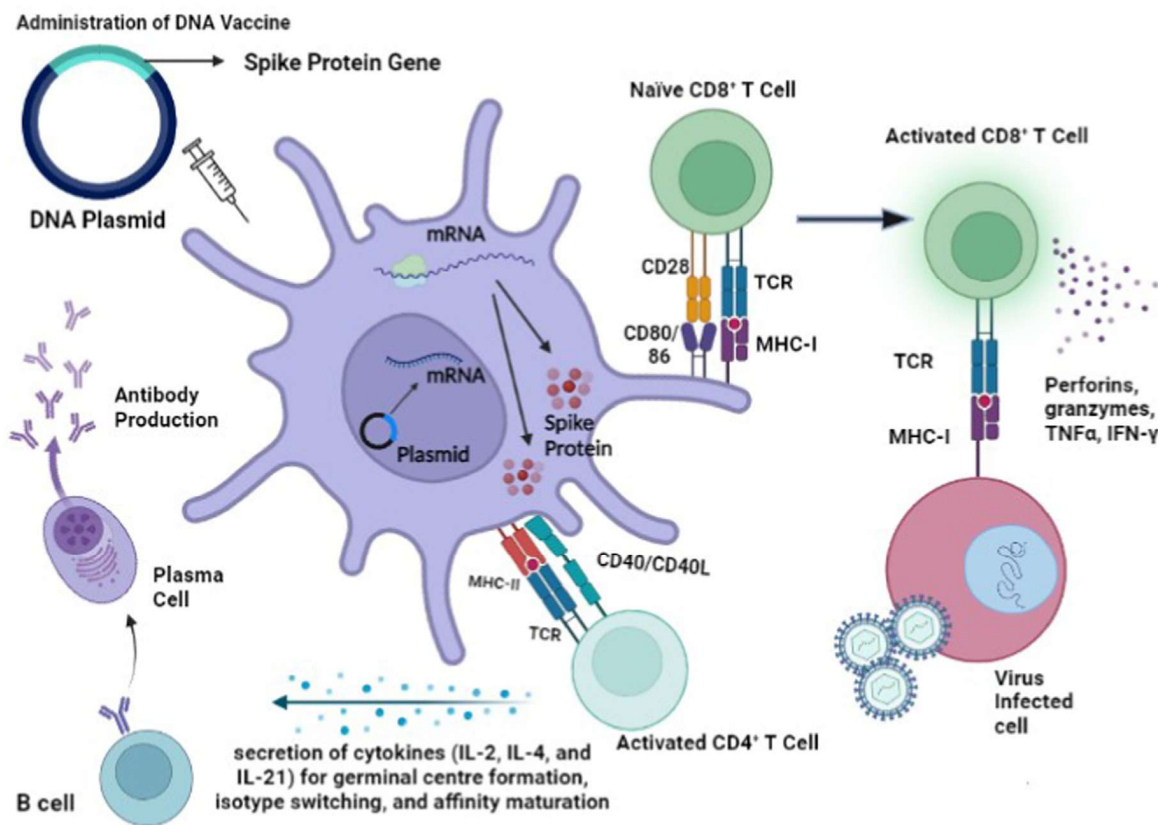
Fig. 1. The elicitation of humoral and cellular responses to DNA vaccines. CD4$^+$ T cells, such as T follicular helper (Tfh) and Foxp3$^+$ T follicular regulatory (Tfr) cells, provide specialized assistance and serve as important mediators towards the formation of germinal centre B cells through T and B cell interactions. Tfh cells also provide help to B cells through CD40L– CD40 interactions, and lead to the release of cytokines (IL-2, IL-4, and IL-21, IFN-γ). Stimulation by cytokines further promotes germination centre formation, and maturation into plasma cells which produce memory B cells and long-lived antibody secreting plasma cells. CD8$^+$ T cells directly target and kill infected cells through the production of perforin and granzymes, limiting the spread of the pathogen within the body [7,8]. Fig. 1 was produced using the graphical software Biorender (https://www.biorender.com/).

immune responses [9]. Antibodies elicited by the DNA vaccine were shown to neutralize the virus before it could gain entry into the host cell [10]. Current DNA vaccines targeting the S protein of the SARS-CoV-2 have shown effective humoral immune responses by eliciting neutralizing antibodies and cellular immune responses in terms of production of IFN-γ and IL-2 [10–13].

DNA vaccines are easier to produce in large quantities compared to the complexities of producing whole inactivated virus and mRNA vaccines [14]. Smith et al. [10] reported that DNA-based vaccines could be developed quickly since a variety of vaccine candidates could be prepared and tested using high-throughput approaches. DNA vaccines offered convenience in vaccine development. For example, a single DNA plasmid vector could be used to construct recombinant DNA plasmids containing genes encoding the whole antigen or immunogenic peptides. It is also feasible to construct a DNA plasmid expressing highly conserved peptides specifying multi-valent epitopes against the SARS-CoV-2 prototype (Wuhan strain) and VOCs.

It is relatively easy to produce the DNA vaccine in large quantities for distribution and large-scale immunizations [15]. The recombinant plasmid DNA could be conveniently produced in large quantities in bacteria such as *E. coli* and expressed in eukaryotic cells such as HEK-293 T cells [15].

The use of DNA vaccines is associated with concerns that the administered plasmid DNA might lead to possible insertional mutagenesis. However, no insertional mutagenesis activity through integration into the host genome has been reported in the development of numerous DNA vaccines against SARS-CoV-2 [16]. Insertion sequence (IS) elements which are characterized as small DNA segments encoding for proteins necessary for the mobility of the IS element are ubiquitously found in the form of bacterial mobile genetic elements and are capable of causing deleterious, neutral, or beneficial mutations [17]. Indeed, de Visser et al. [18] reported a total of 9 IS-mediated mutations occurring in the form of insertions and genetic recombination deletions to conditions of growth and starvation in *Lactococcus lactis*. Nevertheless, there have been no reports of the existence of IS elements in HEK-293 T cells which could potentially induce mutations in DNA plasmids after transfection in eukaryotic cells.

Efficient and cost-effective production of DNA vaccines for large-scale immunizations offers an attractive practical advantage. Nevertheless, Wang et al. [19] indicated that glycosylation, the binding site and adjacent amino acids could impact the binding of the S protein and the angiotensin-converting enzyme 2 (ACE2) host cell receptor. Therefore, the selection of expression systems must be carefully evaluated for the effective development of DNA vaccines against SARS-CoV-2. In a study to evaluate N-linked and O-linked glycosylations of the S protein of SARS-CoV-2 expressed in HEK-293 T cells, the expressed SARS-CoV-2 S protein showed extensive N-linked and O-linked glycosylations with the formation of N-glycans and sialylated O-glycans. Mass spectrometry using matrix-assisted laser desorption-ionization (MALDI-MS) analysis revealed that expression in HEK-293 T cells also produced α2,3- and α2,6-linked sialic acids. Various groups have successfully expressed recombinant DNA plasmids encoding the S protein in HEK-293 T cells for *in vitro* characterization of the expressed recombinant protein without the need for modifications to the recombinant DNA plasmid [10–12,20]. This suggested that HEK-293 T cells served as an excellent host for the expression of the SARS-CoV-2 S protein.

Vaccine storage is an important issue since it is directly associated with vaccine stability and the maintenance of its quality. Therefore, in order to ensure that the efficacy of mRNA vaccines is not negatively affected, cold storage at −70 °C is necessary for the preservation of the BNT162b2 mRNA-based vaccine. DNA vaccines are highly stable, less prone to degradation unlike mRNA vaccines, and do not require an extremely low temperature for storage. DNA vaccines could be stored at room temperature. Since they do not require specific cold chain storage conditions, DNA vaccines would be ideal for immunizing populations in third world countries which lack the financial resources and infrastructures to maintain cold chain distribution and storage conditions [21,22].

DNA vaccines could be stored at room temperature for as long as 6 months [23]. This presented DNA vaccines with an advantage over other vaccine platforms such as mRNA and viral-vectored vaccines since the high stability at room temperature meant that cold chain conditions were not required for transport and storage [24].

2.3. Current DNA vaccine candidates

Inovio Pharmaceuticals developed the vaccine candidate, INO-4800, a DNA based vaccine against SARS-CoV-2 which incorporated the full-length S gene in the pGX0001 vector [10]. Protein expression was confirmed by Western blot and immunofluorescence studies in the transfected HEK-293T cells. Sera from immunized mice and guinea pigs showed IgGs specific for the SARS-CoV-2 S protein. The IgG binding end-point titers showed that the SARS-CoV-2 S region (S1 + S2) as well as the receptor-binding domain (RBD) region were capable of eliciting higher levels of IgG than the IgG elicited by the S1 region alone. The antibodies in the sera derived from immunized animals could prevent the binding of the S protein to the ACE2 receptor by pseudotyped virus and confirmed the effectiveness of the neutralizing antibodies in preventing an infection. An evaluation of live virus neutralization activities conducted in C57BL/6 mice showed that the immunization with INO-4800 was able to elicit antibodies that neutralized wildtype SARS-CoV-2 virus with an average ND_{50} titer of 340. Bronchoalveolar lavage (BAL) fluid from immunized mice also showed a significant increase in IgG antibodies against the S protein from sera of immunized mice, demonstrating that such antibodies in the lungs could protect the host from lower respiratory disease. Cellular immune responses were associated with IFN-γ production and an increase in $CD4^+$ and $CD8^+$ T cells. Flow cytometric analysis of splenocytes harvested from BALB/c mice immunized with a single dose of INO-4800 showed 0.04% $CD4^+$ and 0.32% $CD8^+$ T cells producing IFN-γ after stimulation with the SARS-CoV-2 S protein antigen. Epitope mapping revealed that strong $CD4^+$ and $CD8^+$ T cell responses were associated with several epitopes from the RBD and the S2 domain [10]. INO-4800 has shown good safety and tolerability in phase 1 clinical trial. Both humoral and cellular immune responses were elicited in the 401 vaccinated human participants who received the vaccine. Recorded adverse effects were mainly grade 1 and 2 and they were not exacerbated by the higher dosage of 2.0 mg of the DNA vaccine. Levels of binding and neutralizing antibodies as well as ELISpot analysis of T cell immune responses were higher when the vaccine dose was increased from 1.0 mg to 2.0 mg [25].

Yu et al. [13] reported the development of multiple DNA vaccine candidates encoding different regions of the S protein and evaluation of immunogenicity in rhesus macaque models by Barouch's group at Harvard University. Immunizations of macaques resulted in S-specific binding antibodies and neutralizing antibodies. The levels of neutralizing antibodies against the S protein were similar to those from convalescent humans. S and RBD-specific antibodies with effector functions such as antibody-dependent neutrophil phagocytosis (ADNP), antibody-dependent complement deposition (ADCD), antibody-dependent monocyte cellular phagocytosis (ADCP), and antibody-dependent NK cell activation (IFN-γ production, CD107a degranulation, and MIP-1β expression) were observed. High levels of $IFN-γ^+$, $CD4^+$, and $CD8^+$ T cell immune responses against the whole S protein were recorded. Moreover, cellular responses of lower magnitudes were observed in macaques immunized with the S1 and RBD vaccine candidates. In challenge studies, macaques vaccinated with the S protein showed minor symptoms as well non-existing and lower SARS-CoV-2 RNA levels in the plasma, BAL, and nasopharyngeal swabs (NS), respectively when compared to controls which did not receive the vaccine. The deletion of the transmembrane domain and cytoplasmic region of the S protein elicited no protection in challenge models, demonstrating that the prefusion ectodomain stabilization was significant in eliciting immune response against SARS-CoV-2 [13].

Other DNA vaccine candidates against SARS-CoV-2 have also focused on the S protein. Chai et al. [11] reported the immunogenicity of different DNA vaccine candidates based on the S protein. The S genes and its derivatives were cloned into the DNA plasmid vector, pVAX1, and following confirmation of expression in HEK-293T cells, the recombinant plasmid DNA was administered via electroporation in mice and Syrian hamsters. Sera from the SARS-CoV-2 S protein immunized mice demonstrated antibody titers against the RBD that was able to neutralize infections caused by SARS-CoV-2. The binding of ACE2 with the RBD was observed to be blocked by the immunized mice sera. IgG and neutralizing antibody titers following SARS-CoV-2 S DNA immunization were associated with protection at 20 weeks. Moreover, the SARS-CoV-2 S recombinant DNA vaccine elicited neutralizing antibody titers against the S1 protein carrying the D614G mutation. Upon stimulation with SARS-CoV-2 S protein, high levels of Th1 type cytokines like IFN-γ and IL-2 were observed with significantly lower levels of the Th2 type cytokines such as IL-5 and IL-13 in both BALB/c and C57BL/6 mice, demonstrating that CD4$^+$ T cell responses were Th1 polarized. Challenge studies demonstrated the superiority of the DNA vaccine incorporating the full-length S protein over the RBD in terms of the significantly higher levels of anti-Spike and neutralizing antibodies. Immunizations with the recombinant S DNA vaccine resulted in 2.29 log$_{10}$ reductions of the infectious virus titer and 1.37 log$_{10}$ reductions in the number of viral RNA copies when compared to the vector control group [11].

Similarly, Prompetchara et al. [12] constructed DNA vaccine candidates carrying the full-length S, S1(pCMVkan-S1) or S2 (pCMVkan-S2). All vaccine candidates elicited high levels of S-specific binding IgGs that exhibited a balance of IgG1and IgG2a. Sera from mice immunized with S and S1 vaccine candidates were able to effectively neutralize RBD-ACE2 binding. In particular, the sera from S immunized mice demonstrated significant inhibition of RBD-ACE2 binding when compared to sera from the S1 immunizations. The levels of neutralization antibodies were the highest in the sera of S immunized mice (GMT:2551) when compared to S1 (GMT:1005) and S2 (GMT:291) immunizations. S2 immunizations were associated with non-detectable levels of inhibition of RBD-ACE2 binding as well as the lowest levels of neutralizing antibodies when compared to S1 and S immunizations. Splenocytes from mice immunized with the S DNA vaccine produced IFN-γ in response to peptide pools from the S1 or S2 regions while splenocytes from mice immunized with the S1 or S2 vaccines elicited IFN-γ in response to peptide pools from their respective regions. The highest levels of IFN-γ induced was from the S immunized mice (2991 SCF/10^6 splenocytes), followed by the S2 immunized mice (1885 SCF/10^6 splenocytes), and lastly by the S1 immunized mice (1376 SCF/10^6 splenocytes). Moreover, peptide pools associated with potent IFN-γ based on ELISpot assays were from the RBD region and the heptad repeat (HR) 1 region from the S1 and S2 regions [12].

Researchers from Osaka University presented a preclinical study to develop a recombinant DNA vaccine for SARS-CoV-2, with the S protein as the main antigen and it was designated as pVAX-1- SAR-CoV-2 S [20]. The DNA vaccine was administered to rats and humoral responses were assessed in the presence and absence of the alum adjuvant. The alum adjuvant formulated with the DNA vaccine could provide potent humoral immune response, with 666.6 μg of recombinant plasmid DNA carrying the SARS-CoV-2 S gene formulated with 66.7 μl of alum adjuvant. It was able to induce high levels of antibodies against the S and RBD proteins at week 4 through to week 16. These antibodies were able to recognize the S1 subunit carrying the D614G mutation of SARS-CoV-2. IgG2a and IgG2b were the main subclasses of produced IgG, indicating Th1 polarization. Intramuscular administration of the DNA vaccine in rats showed that IFN-γ production was significantly increased while IL4 was only slightly increased in response to immunizations with the DNA vaccines carrying the S and RBD. It was observed that DNA immunizations in rats produced sera which could decrease binding of ACE2 with the S1+S2 protein. Immunized sera when diluted 5-fold could inhibit 50% of the binding of ACE2 with the RBD protein. Sera dilutions from immunized

rats demonstrated neutralizing activities when tested with the pseudo-typed vesicular stomatitis virus (VSV) carrying the luciferase gene in Vero E6 cells. Neutralizing titers remained at an average of 98.4 at 8 weeks after immunization with the first dose of the DNA vaccine. Furthermore, body tissues and serum biochemical parameters showed that there were no toxic effects of the DNA vaccine [20].

Many other research groups are currently developing similar DNA vaccines. For example, researchers from the King Abdulaziz University developed a DNA vaccine consisting of a codon optimized S protein sequence [26]. Intramuscular immunization of BALB/c and C57BL/6J mice with 100 μg of the DNA vaccine elicited S-specific IgG antibodies and neutralizing antibodies. Moreover, the use of needle-free intradermal administration of the vaccine induced a potent Th1-biased humoral response including binding IgG antibodies, and neutralizing antibodies as well as IFN-γ, TNF-α and IL-2 cytokine production from memory CD4$^+$ and CD8$^+$ T cells when administered to BALB/c mice [26]. A DNA vaccine consisting of the S1 subunit was also able to elicit a Th1 polarized response specifically associated with IgG and neutralizing antibodies along with potent CD4$^+$ and CD8$^+$ T cell responses [27]. DNA vaccine development is also associated with different routes of administrations other than the intramuscular route. For example, the use of the Pyro-drive Jet Injector for intradermal administration of a DNA vaccine expressing the S protein resulted in potent humoral responses consisting of neutralizing antibodies without any safety concerns [28].

An evaluation of the literature on preclinical and clinical development of DNA vaccines showed that most of these vaccines were focusing on the S protein or the RBD of the S protein as the main antigenic target. The S protein of SARS-CoV-2 plays a significant role in the attachment of the virus to the ACE2 cell receptor as well as viral and host cell membrane fusion to promote the entry of the virus into the cells. Furthermore, the S protein was shown to be a prime target for eliciting neutralizing antibodies [29]. Vaccinations against SARS-CoV-2 using the full-length S protein also produced potent CD4$^+$ and CD8$^+$ T cell responses [30]. Table 1 shows the preclinical development of DNA vaccines against SARS-CoV-2 while Table 2 shows an overview of the clinical development of DNA vaccines against SARS-CoV-2.

2.4. Reduced vaccine efficacies against SARS-CoV-2 VOCs

While the vaccine candidates under emergency approval offer protection from the original SARS-CoV-2 Wuhan strain, they have been shown to exhibit reduced protective efficacies against VOCs. Indeed, current viral vectored and mRNA vaccines such as ChAdOx1 nCoV-19, BNT162b2, and mRNA-1273, which utilize the full length S protein as the main antigenic target, have been reported to demonstrate reduced protective efficacies against SARS-CoV-2 VOCs. For example, when the sera from individuals immunized with the Pfizer BNT162b2 vaccine were tested for neutralizing ability upon reinfection with SARS-CoV-2, it was observed that the neutralizing activity was reduced by 1- to 3-folds against a pseudovirus containing mutations such as E484K, N501Y, and a combination of K417 N, E484K, and N501Y mutations. In contrast, there was no reduction in neutralizing activity in response to the wild type strain and the variant with the K417 N mutation [33]. Furthermore, humoral response elicited by the mRNA vaccines was significantly reduced in response to the B.1.351 VOC. This was seen by a 9.4 fold and 10.3–12.4-fold reductions in neutralizing activities in the sera of convalescent patients and those who had received the mRNA vaccines [34]. This demonstrated that SARS-CoV-2 VOCs with mutations in the RBD were not completely neutralized by neutralizing antibodies elicited by the mRNA vaccines approved under emergency use against SARS-CoV-2.

Harvey et al. [35] also reported that since the S protein gene from the Wuhan strain was present in all of the licensed vaccines under emergency use, any mutation in the S gene of the VOC would potentially impact its interaction with neutralizing antibodies elicited by the Wuhan strain. Pseudoviruses carrying the mutations associated with the B.1.1.7 variant

Table 1
Preclinical development of DNA vaccines against SARS-CoV-2.

Name of Vaccine	Developer	Plasmid vector	Main antigenic region	Adjuvant	Mode of Administration	Reference
INO-4800	Inovio Pharmaceuticals	pGX0001	full length S gene	–	Electroporation using CELLECTRA® delivery device	[10]
SARS-CoV-2 DNA vaccine tested in Syrian hamsters	Taiwan Group	pVAX1	spike genes of SARS-CoV and SARS-CoV-2	–	Intramuscular electroporation with a BTX electroporator (ECM830)	[11]
DNA Vaccine candidates developed by Chulalongkorn University	Thailand Group	pCMVkan	full length S, S1, and S2	–	Intramuscular electroporation using TriGrid delivery system	[12]
SARS-CoV-2 Spike glycoprotein DNA plasmid vaccine	Osaka University (Japan group)	pVAX1	full length S gene	alum	Intramuscular injection	[20]
IgE-spike-S1/S2-D614G-6P-foldon	Southern University of Science and Technology, China	PCDNA3.1	S-protein S1+S2	–	Intramuscular injection	[31]
pSARS2-S	National Institute of Infectious Diseases and Vaccinology Taiwan	pVAX1	full length S gene	alum	Electroacupuncture	[32]
VIU-1005	King Abdulaziz University	pVAX1	full length S gene	–	intramuscular needle injection	[26]
pVAX-S1	King Abdulaziz University	pVAX1	S1 subunit	–	intramuscular administration using customized needle-free Tropis system	[27]
pVAX1-SARS-CoV2-co	Osaka University	pVAX1	S protein	–	Intradermal using a pyro-drive jet injector	[28]

Table 2
An Overview of the clinical development of DNA vaccines against SARS-CoV-2.

#	Type of Vaccine Candidate	Number of Doses	Route of administration	Developers	Clinical Trial Phase
1.	nCov vaccine	3	ID	Zydus Cadila	Phase 4
2.	INO-4800+electroporation	2	ID	Inovio Pharmaceuticals + International Vaccine Institute + Advaccine (Suzhou) Biopharmaceutical Co., Ltd	Phase 3
3.	AG0301-COVID19	2	IM	AnGes + Takara Bio + Osaka University	Phase 2/3
4.	GX-19 N	2	IM	Genexine Consortium	Phase 1/2
5.	GLS-5310	2	ID	GeneOne Life Science, Inc.	Phase 1/2
6.	COVID-eVax	2	IM	Takis + Rottapharm Biotech	Phase 1/2
7.	AG0302-COVID19	2–3	IM	AnGes Inc.	Phase 1/2
8.	VB10.2129	1–2	IM	Vaccibody AS	Phase 1/2
9.	VB10.2210	2	IM	Vaccibody AS	Phase 1/2
10.	Covigenix VAX-001	2	IM	Entos Pharmaceuticals Inc.	Phase 1
11.	CORVax 12	2	ID	Providence Health & Services	Phase 1
12.	bacTRL-Spike	1	Oral	Symvivo Corporation	Phase 1
13.	COVIGEN	2	ID or IM	University of Sydney, Bionet Co., Ltd Technovalia"	Phase 1
14.	COVIDITY	2	ID	Scancell Ltd	Phase 1
15.	SARS-CoV-2 DNA vaccine	2	IM	The University of Hong Kong; Immuno Cure 3 Limited	Phase 1
16.	Prophylactic pDNA Vaccine	3	IM	Imam Abdulrahman Bin Faisal University	Phase 1

Abbreviations: ID - Intradermal; IM - Intramuscular.
\Adapted from COVID-19 vaccine tracker and landscape as of September 9, 2022. https://www.who.int/publications/m/item/draft-landscape-of-covid-19-candidate-vaccines

along with the E484K mutation showed a 6.7-fold reduction in neutralization activity when sera from individuals immunized with the Pfizer BNT162b2 vaccine were tested [36]. Live virus neutralizations also showed that neutralizing titers in the sera of those immunized with the AstraZeneca ChAdOx1 nCoV-19 vaccine were 9 fold lower against the B.1.1.7 SARS-CoV-2 variant when compared to sera from vacinees immunized with the original Wuhan strain [37]. Similarly, a 6.4-fold reduction in neutralization response to the B.1.351 variant was observed in the sera of individuals vaccinated with two doses of Moderna mRNA-1273 [38].

The efficacies of the current SARS-CoV-2 vaccines were particularly challenged by mutations in the RBD which were present in variants such as B.1. 351 (Beta) and P.1 (Gamma) that could escape neutralizations. Besides immune escape mediated by B-cell epitopes, SARS-CoV-2 variants might also evade cytotoxic T lymphocyte (CTL) immunity through T cell mutations in viral epitopes which could lead to reduced CTL responses. It was reported that SARS-CoV-2 variants had a less than marginal effect on the elicitation of $CD4^+$ and $CD8^+$ T cell responses in convalescent patients and vacinees receiving the mRNA vaccines [39]. Moreover, T cell responses were found to be similar to those elicited from

the original SARS-CoV-2 Wuhan strain [40]. Noh et al. [40] concluded that $CD4^+$ and $CD8^+$ T cell epitopes were conserved. However, through mutations in the MHC-I restricted viral epitope genes, there is likelihood for SARS-CoV-2 variants to escape $CD8^+$ T cell surveillance. Agerer et al. [41] reported that some mutations in SARS-CoV-2 reduced the binding of peptides to major histocompatibility complex Class I which ultimately resulted in reduced productions of IFN-γ as well as lower cytotoxic activity of $CD8^+$ T cells. In conclusion, humoral and cellular responses elicited by the mRNA vaccine against the SARS-CoV-2 Wuhan strain offered protective immunity but VOCs were reported to reduce the neutralizing activities of the humoral responses elicited by the mRNA vaccines. Nevertheless, some studies have reported a marginal effect of VOCs on cellular responses as mutations in the MHC-I epitope genes might lower the potency of T cell responses [42].

The most recent VOC is the Omicron variant (B.1.1.529) which has emerged in multiple countries. A recent study conducted with 19 individuals in South Africa demonstrated that the protective efficacy of the Pfizer-BioNTech vaccine was significantly reduced against the omicron variant. In individuals immunized with the BNT162b2 vaccine, a 22-fold reduction in the levels of neutralizing antibodies in response to the

Omicron variant (Pango lineage B.1.1.529) was observed when compared to the prototype Wuhan strain [43].

An evaluation of neutralizing antibody titers against the SARS-CoV-2 Wuhan strain and the Omicron BA.1, BA.2, BA.2.12.1, and BA.4 or BA.5 subvariants showed that when compared to the Wuhan strain, the neutralizing antibody titers were reduced by a factor of 6.4 against BA.1, by a factor of 7.0 against BA.2, by a factor of 14.1 against BA.2.12.1, and by a factor of 21.0 against BA.4 or BA.5. Omicron subvariants BA.2.12.1, BA.4 and BA.5 were shown to be more likely to escape neutralizations than the BA.1 subvariant. The median neutralizing antibody titer was lowered by a factor of 2.2 against the BA.2.12.1 subvariant and by a factor of 3.3 against the BA.4 or BA.5 subvariant when compared to the BA.1 subvariant [44]. It was also asserted that the emergence of Omicron was met with concerns regarding reduced vaccine-induced neutralizing activities [45]. In comparison with the Delta variant, the Omicron variant significantly reduced the protective neutralizing activities of sera derived from those receiving immunizations with the current approved vaccines.

2.4.1. DNA vaccine-induced humoral and cellular immune responses against VOCs

Andrade et al. [46] evaluated the humoral and cellular responses against SARS-CoV-2 variants such as B.1.1.7 (Alpha), B.1.351 (Beta), and P.1 (Gamma) VOCs in vacinees who were immunized with the INO-4800 DNA vaccine. The evaluation of humoral responses in terms of the levels of serum IgG titers to the SARS-CoV-2 S protein from the B.1.1.7, B.1.351, and P.1 variants showed that serum IgG titers were comparable for the Wuhan, and the B.1.1.7 and B.1.351 variants. However, a 1.9-fold reduction was reported against the P.1 variant at week 8 in vacinees who received two doses of INO-4800 DNA vaccine. Pseudovirus neutralization assays showed 2.1 and 6.9-fold reductions against the B.1.1.7 and B.1.351 variants, respectively. There was no reduction in neutralizing antibodies for the P.1 variant when compared with the levels of neutralizing antibodies elicited against the Wuhan strain. However, T cell responses in terms of IFNγ and production of cytokines by CD8$^+$ cytotoxic T cells showed similar responses between the Wuhan strain and the B.1.1.7, B.1.351, and P.1 variants.

Azevedo et al. [47] investigated the efficacy of pCTV-WS, a Spike-based DNA vaccine against the Wuhan strain and the Gamma, Delta, and Omicron VOCs in transgenic (K18-hACE2) mice and hamsters. The levels of neutralizing antibodies were similar against the Wuhan and the Delta VOC. However, a 10-fold reduction in the levels of neutralizing antibodies was observed when immunized mice were challenged with the Gamma and Omicron VOCs. The T cell response was generally conserved across the different strains and played a prominent role in the reduction of viral loads and disease severity in immunized mice challenged with the Gamma or Omicron VOCs.

There are also reports showing incorporation of conserved regions from the SARS-CoV-2 into the design of the DNA vaccine that could lead to more universal and sustained immune responses in the face of emerging variants. For example, a universal SARS-CoV-2 DNA vaccine comprising antigens from immunogenic epitopes from the RBD, membrane, and nucleoprotein (NP) from the Wuhan strain, the Alpha, and the Beta variants was able to elicit cross-reactive neutralizing antibodies that successfully neutralized the Wuhan strain, Beta, Delta, and Omicron viruses *in vitro* [48]. Challenge studies showed that mice were protected from lethal infection with the SARS-CoV-2 Beta variant and NP-specific T cells alone were responsible for 60% of the conferred protection [48].

Furthermore, the administration of a pan-Spike vaccine known as INO-4802 in animal models showed the elicitation of neutralizing antibodies and T cell responses against the Wuhan strain as well as B.1.1.7, P.1, and B.1.351 VOCs with potent humoral responses induced against VOCs in priming with a heterologous wild type vaccine, and followed by INO-4802 boost administration [49].

In view of the emergence of SARS-CoV-2 variants, there is a need to incorporate highly conserved epitopes to confer broad protection against variants. DNA vaccines could offer a promising approach to develop effective vaccines, particularly against the rapidly mutating SARS-CoV-2 VOCs. DNA vaccines can easily be modified to incorporate different genes simply by changing the gene sequences of the recombinant DNA plasmid. Multiple cloning sites incorporated into the recombinant plasmid DNA can easily be used to incorporate different nucleotides encoding peptides specifying conserved immunogenic epitopes as these can be predicted from bioinformatics or through an analysis of binding sites of monoclonal antibodies found in convalescent sera [50–52]. Therefore, the DNA vaccine platform is considered an attractive and promising approach to immunize against SARS-CoV-2 due to the advantages that it offers over other vaccine platforms [10].

2.5. Limitations of DNA vaccines

DNA vaccines against infections caused by the West Nile Virus in horses and canine melanoma have been approved by the Food and Drug Administration (FDA) and the United States Department of Agriculture (USDA) for veterinary immunizations. With the exception of ZyCoV-D, no DNA vaccines have been authorized for human use. This suggests that there are limitations which have to be overcome before DNA vaccine candidates could progress to the clinic. It has been reported that pre-clinical studies demonstrated the ability of DNA vaccine candidates to elicit potent humoral and cellular responses in small animals such as mice, rats, and guinea pigs and even in non-human primates [10–13] but there are challenges in eliciting the same potency of immune responses in larger animals and humans. It was reasoned that low immunogenicity is due to the non-feasibility of upscaling plasmid DNA amounts administered in small animal models to humans [53]. Indeed, as much as 5–25 mg plasmid DNA would need to be administered to achieve the same effect [54].

Another challenge is the route of administration of DNA vaccines. All current DNA vaccines in clinical development against SARS-CoV-2 used either electroporation, intradermal, oral, or intramuscular routes to deliver the naked plasmid DNA. Another reason for low immunogenicity is the low transfection efficiency of naked plasmid DNA. The administration of naked plasmid DNA was associated with low transfection efficiency due to degradation. Indeed, the in vivo half-life of naked plasmid DNA was shown to be reduced in a few minutes following administration since it was vulnerable to degradation and removal by the reticular endothelial system (RES) [55]. DNA vaccines harbouring the DNA plasmid would need to target APCs to ensure the elicitation of potent cellular immunity [56]. The administration of naked DNA did not lead to uptake by DCs. Unsuccessful APC targeting resulted in low transfection efficiency and low immunogenicity. Moreover, several barriers have to be overcome such as penetration through the negatively charged phospholipid membrane, escape from the endosome, and entry into the nucleus.

2.6. Design of DNA vaccine and formulation improvements

Considering the potential of the SARS-CoV-2 prototype and VOCs to cause debilitating consequences to public health and wellbeing, it is essential to develop strategies to overcome the limitations of DNA vaccines so that the advantages of the platform can be used to develop effective vaccines against rapidly emerging variants. These include optimizations that might be made to the plasmid with the use of molecular or chemical adjuvants as well as exploring alternative delivery systems and routes.

2.6.1. Plasmid optimization for gene expressions

Effective construction of a recombinant DNA plasmid needs to incorporate certain genetic elements to ensure adequate protein expressions. These could include specific nucleic acid sequences that would upregulate transcriptions. An evaluation of these genetic elements is crucial to establish optimum recombinant plasmid design.

2.6.1.1. Strong promoters. It is imperative to select a promoter for efficient plasmid construction so that the transfection of the recombinant DNA plasmid into a mammalian cell line would result in both high-level and long-term transgene expressions. A promoter is defined as a specific set of nucleotides upstream of the gene of interest where RNA polymerase binds to initiate transcription. Several plasmid vectors such as pcDNA™3.1(+) and pVAX1™ were designed to contain the cytomegalovirus (CMV) promoter and enhancer for high level expression of the protein of interest when transfected into mammalian cells. However, it was observed that transcriptional silencing resulted in a reduction in the expression of recombinant gene of interest controlled by the CMV promoter following transfection as evidenced by the reduction in expression of exogenous genes driven by the CMV promoter [57]. A solution to this issue is to utilize the human elongation factor-1 alpha (hEF1α) promoter to initiate and regulate gene expression. Kim et al. [58] demonstrated high levels of gene expression in a variety of cell types using the pEF-CAT plasmid whereby the bacterial *CAT* gene of interest was ligated to specific sites within the hEF1α gene such as at the end of the TATA box, exon 1, and exon 2. The hEF1α promoter was also effective in driving gene expression when viral promoters did not drive the expression of downstream genes. Indeed, the hEF1α promoter drove the stable and high level expression of the bacterial *neo* gene more efficiently than the viral promoter of the simian virus 40 (SV40) early gene. Moreover, the CHO-derived elongation factor-1 promoter (CHEF-1) was reported to serve as a promising element to regulate high-level expression of recombinant DNA plasmids in mammalian cell lines. Expression vectors containing 5′ and 3′ flanking sequences from the CHEF1 gene had greater than 10-fold expression levels of the chemokine receptor CCR4 when compared to the CMV promoter [59]. Even though the use of such flanking sequences could enhance expression of the gene of interest, their inclusions into the vector increased the vector size which might not be ideal for transfections. Furthermore, the SV40 promoter was described to be a fairly strong promoter for the expression of therapeutic proteins in mammalian cell lines. Although it might result in comparatively lower expression, it had greater stability than the hEF1α and CMV promoters [60].

The CMV promoter was shown to be primarily responsible for the transient transcriptional expression of recombinant genes in the human embryonic kidney 293 (HEK293) cells [61]. Johari et al. [62] reported that the CMV promoter functioned by directing transcriptional expression which depended on the different components of the promoter such as the transcription factor regulatory elements (TFREs) which included AhR:ARNT, CREB, E4F, Sp1, ZBED1, JunB, c-Rel, and NF-κB. The CMV promoter could be modified or engineered to incorporate optimized binding sites. The TRFEs might also be used for the construction of synthetic promoters. The researchers found multiple suboptimal TF binding sequences including MYBL1, Oct, and E2F which might be used to further improve the transcriptional activity of the CMV promoter. The use of high-throughput parallel screening methods could be utilized to screen several hundred TFREs and evaluate their binding affinities [62].

2.6.1.2. Kozak sequence. The Kozak consensus sequence is characterized as a specific set of nucleotides that serves as the initiation site where protein translation begins in eukaryotic mRNA produced from transcription. The sequence is important for the initiation of translation and for the regulation of protein production [63]. The Kozak sequence ensures accurate translation of the protein in terms of ribosome assembly and translation initiation, considering that an incorrect initiation site might lead to the expression of non-functional proteins [64]. Plasmid vectors such as pcDNA™3.1(+) and pVAX1 are designed to require the insert to contain a Kozak consensus sequence (−6 GCCA/GCCAUGG +4) located around the initiation codon to ensure the accurate and specific initiation of translation.

An example of a Kozak sequence found in a recombinant DNA plasmid constructed using the plasmid vector pcDNA™3.1(+) is GCCACC

with the ATG initiation codon located downstream of the 6-nucleotide sequence. More specifically, for a strong consensus sequence that could strongly express the recombinant protein, the nucleotides at the +4 and −3 position (relative to the +1 assigned to the A of the initiation codon) would need to match the consensus. For effective translation, the −3 position should contain a purine base. In the absence of a purine base, a guanine should be present at +4 [65]. Recognition of AUG and alternative initiator codons is augmented by a G at position +4 but is not generally affected by the nucleotides at position +4 and + 6 [66].

2.6.1.3. Matrix attachment regions (MARs). A series of scientific discoveries have led to the incorporation of the matrix attachment regions (MARs) into mammalian expression vectors. It was observed that chromatin could be divided into topologically constrained domains separated by elements such as scaffolds of MARs [67]. Moreover, MARs were reported to be able to serve as insulator elements which prevented the spread of heterochromatin as well as gene silencing [68]. Therefore, MARs were associated with the production of an anti-silencing effect by shielding the gene of interest from the suppressive impacts of heterochromatin [69]. Mammalian expression vectors might be optimized by incorporating a variety of genetic elements to produce the right combination for optimum gene expression. MARs might be used in conjunction with strong promoters for enhancing gene expressions. For example, the incorporation of the CMV promoter to drive the expression of green fluorescent protein flanked by two different MARs or the use of SV40 promoter with two β-globin MARs substantially increased expression and stability of the transgene [70].

2.6.1.4. Introns. Intron-mediated enhancement refers to the higher level of expression of a DNA construct containing a specific intron as compared to the expression of the construct when the intron was not included [71]. The enhancement of gene expression as a result of the inclusion of certain introns has been known to occur in eukaryotes such as mammals, plants, yeast, and insects. It was reported that introns could enhance transcript levels by affecting the rate of transcription, nuclear export, transcript stability, and mRNA translation [72].

There is considerable evidence for intron mediated enhancement of gene expressions. The rate of transcription in transgenic mice was increased by 10- to 100-fold when compared to the same genes not containing introns [73]. Moreover, in eukaryotic organisms such as humans and *Saccharomyces cerevisiae*, genes that contained introns produced significantly more copies of RNA than genes lacking introns [74]. Genes that were prominently expressed were shown to contain a larger intron density in terms of the number of introns per kilobase of coding sequence when compared to genes that were weakly expressed [74].

There are also other ways in which introns could enhance gene expression. Spliceosomal introns increased gene expressions at numerous stages from transcription to translation [75]. Splicing was considered to be the crucial factor leading to the enhancement of expression of the leader intron of the Arabidopsis AtMHX gene [76]. The intron sequence showed only weak enhancement without splicing. Moreover, enhancement of gene expression was found to be strongly dependent upon intron splicing based on the analysis of mutated genes contained in rice mutants [77]. Introns are involved in enhancing gene expression and increasing gene products during multiple processes such as splicing, transcription, polyadenylation, mRNA export, and translation. Introns could contain enhancer elements to increase expression as well as sequences to enhance translation of mRNA into proteins [78].

Some genes are fully dependent on introns for their expressions and they could remain undetectable when the gene was expressed without the intron [79]. In fact, the impact of intron sequences on the expression of plasmids could be quite significant; exceeding 10-fold in some cases and depending on the right combination of factors such as the type of gene and intron in the recombinant plasmid [80]. Several studies have reported enhanced gene expression upon the inclusion of introns. A motif

derived from an intron was able to substantially enhance gene expression even when it was placed significantly downstream of the transcriptional start site [71]. Baier et al. [81] selected a group of 33 native and 13 non-native introns from highly expressed genes of *Chlamydomonas reinhardtii* with the potential to significantly increase abundance of transcripts as an efficient solution to the low transcript levels of nuclear transgenes in *C. reinhardtii*. An SV40 intron was identified as a strong intron element that effectively enhanced the expression levels of erythropoietin protein in Chinese hamster ovary (CHO) cells [82].

While it is true that the introduction of introns was reported to have a positive impact on plasmid optimization in terms of increased gene expression, there is also evidence that a larger size of the insert in the DNA plasmid vector might have a negative impact on the levels of gene expression. In an experiment where two vectors of differing plasmid lengths containing a firefly luciferase encoding gene insert were compared for levels of gene expression, it was observed that 2-fold decrease in the size of the plasmid vector backbone could increase gene expression levels by more than 10-fold in rat tenocytes *in vitro,* and rat myocardium in vivo [83]. Moreover, the administration of varying sizes of plasmid DNA into *Bacillus subtilis* ISW1214 showed that transformation efficiency was reduced with increasing size of the plasmid DNA [84]. Gene transfection efficiency was reported to be highest for the DNA plasmid shortest in size [85].

2.6.1.5. Nuclear localization signal peptides. Nuclear localization signal (NLS) peptides are characterized as short signaling molecules that facilitate the transport of substances such as proteins from the cytoplasm to the nucleus [86]. Data from several experimental investigations have shown that the addition of nuclear localization signal peptides might aid in gene delivery by enhancing the translocation of DNA to the nucleus through the nuclear membrane. The development of a capped 3.3kbp CMV-Luciferase-NLS gene incorporating a single nuclear localization signal peptide led to a remarkable enhancement of transfection efficiency [87]. This 10 to 10,000-fold increase in transfection efficiency was attributable to the NLS peptide since the introduction of a substitution mutation in the third amino acid in the NLS peptide was able to reduce the transfection efficiency to lower levels. Zanta et al. [87] reasoned that the DNA in the cytoplasm was translocated to the nucleus first by docking and then translocating through a pore in the nuclear envelope. The exogenous DNA would be present in the form of a chromatin-shaped structure inside the nucleus. The incorporation of NLS peptides into DNA vaccine has also been documented and was shown to demonstrate increased transfection efficiency of DNA in *in vitro* testing. For example, the addition of four NLS peptides, namely SV40 large T-antigen derived NLS, nucleoplasmin targeting signal, M9 sequence, and the reverse SV40 derived NLS was shown to enhance the transfection efficiency of the DNA delivery vector, LAH4, after transfection into slow-dividing epithelial cancer cells (Calu-3), macrophages (RAW264.7), DCs (JAWSII), and thymidine-induced growth-arrested cells [88]. Therefore, the use of NLS peptides in DNA vaccines against SARS-CoV-2 is a feasible option which might enhance transfection efficiency during clinical trials to elicit stronger immune responses.

2.6.1.6. Linear minimalistic (MIDGE) vectors. Current plasmid DNA vectors consist of antibiotic resistance genes that act as selection markers and allow the detection of successful transformation of plasmids for bacterial expression. However, this approach is likely to be associated with the spread of antibiotic resistance genes as the recombinant plasmid DNAs are administered to animals or humans. A suitable alternative is the use of minimalistic, immunologically-defined gene expression (MIDGE) vectors which were described as linear vectors that only consist of the sequence associated with the direct expression of the antigen which can be chemically altered to enhance the resulting immune response [89]. MIDGE vectors expressing the Leishmania homologue of receptors for activated C-kinase (LACK) antigen were shown to confer a high degree of

protection against Leishmania infection in BALB/c mice [89]. It was also observed that high levels of protection could be achieved through the use of much lower doses than what is required for traditional recombinant plasmid DNAs. Protective efficacy may be further improved through the addition of an NLS peptide to the MIDGE vector. Furthermore, MIDGE vectors could be used to elicit high levels of antigen expression both in cell cultures as well as in animal models. In particular, the development of MIDGE and MIDGE-NLS vectors encoding for the hepatitis B surface antigen (HBsAg) and subsequent immunogenicity testing showed strong humoral and cellular immune responses [90].

2.6.2. Chemical adjuvants

To date, most of the experimental preclinical DNA vaccines developed against SARS-CoV-2 were administered on their own as naked plasmid DNAs. However, it has been reported that the administration of DNA vaccines against SARS-CoV-2 together with chemical adjuvants such as Montanide, Alum, Vaxfectin might improve immunogenicity. Indeed, there is significant evidence to suggest this since the use of such chemical adjuvants showed a positive impact on immunogenicity of vaccines in the past [91,92].

2.6.2.1. Montanide. Montanide as a chemical adjuvant was shown to enhance both the humoral and the cellular immune response in murine and bovine models [93]. Moreover, DNA vaccines incorporating Montanide have been successfully commercialized for protection against the foot-and-mouth disease virus (FMDV). Furthermore, a DNA vaccine consisting of the glycoprotein D chemically adjuvanted with Montanide 903110 against the Bovine herpesvirus-1 (BoHV-1) was shown to protect against bovine infectious rhinotracheitis [92]. Cows immunized with the vaccine formulation containing Montanide effectively enhanced both the humoral and cellular response, ameliorated clinical symptoms, and significantly reduced viral excretions [92].

2.6.2.2. Alum. Considering the development of DNA vaccines against SARS-CoV-2, the only example of the use of alum administered along with recombinant SARS-CoV-2 S DNA vaccine is by researchers from Osaka University [20]. The use of aluminum salts (alum) in optimizing the humoral response in licensed DNA vaccines is well established. When a DNA vaccine encoding HBsAg was formulated with aluminum phosphate, the antibody titers were increased by 10–100 fold. The adjuvant aluminum phosphate was able to decrease the antigen dosage required by 10-fold. Boosting the adjuvanted DNA vaccine with a HBs protein was found to elicit HBs-specific IgG2a which reflected a Th1 response. The adjuvanting effect was suggested to be due to an increase in the number of T cells secreting HBs peptide antigen-specific IFN-γ and IL-2 [94].

Furthermore, a DNA vaccine against rabies adjuvanted with alum was demonstrated to provide 80% protective immunity of BALB/c mice challenged with a rabies virus strain. The immune response was observed to be Th2 polarized with increased IgG antibody titers [95]. Adjuvanting the DNA vaccine with alum was shown to elicit more potent immune responses demonstrated by an increase in the IgG antibody titer and neutralizing antibodies against rabies virus.

However, there are instances where the administration of alum with DNA vaccines failed to provide protective immunity. This was the case with the alum adjuvanted DNA vaccine against the human immunodeficiency virus (HIV) type 1 DNA vaccine. Considering that alum was present in adequately detectable levels at the injection depot, the failure to elicit sufficient levels of immunogenic humoral and cellular responses was attributed to a lack of effective interaction between the DNA vaccine and alum adjuvant [96].

2.6.2.3. Vaxfectin. Another well-known chemical adjuvant is the cationic lipid formulation, Vaxfectin, in enhancing the immunogenicity of DNA vaccines by improving delivery efficiency. This increased immunogenicity might be attributable to Vaxfectin being directly

involved in regulating immune response pathways. Several studies have also documented Vaxfectin to successfully optimize the immune response in several animal models. For example, the intradermal or intramuscular administrations of a DNA vaccine encoding the hemagglutinin (H) and fusion (F) proteins of measles virus successfully conferred protection in rhesus macaques [97]. This was demonstrated mainly by the elicitation of higher levels of neutralizing antibodies upon the administration of the DNA vaccine adjuvanted with Vaxfectin when compared to the unadjuvanted DNA vaccine. The immune response was also characterized by the rapid induction of T cells but production of IFN-γ did not increase upon treatment with Vaxfectin. Challenge studies protected the macaques from developing rash or viremia but did not confer protection against infection [97]. Nevertheless, efforts to develop a more balanced immune response consisting of the elicitation of both humoral and cellular immune response were carried out by Pan et al. [98]. In the murine model, both humoral and cellular immune responses were demonstrated by the administration of a Vaxfectin adjuvanted DNA vaccine against measles virus encoding the H and F proteins. The DNA vaccine also conferred protection against intratracheal infection and prevented the development of viremia and rashes [98].

Vaxfectin has also been incorporated as a chemical adjuvant in the development of DNA vaccines against diseases such as dengue and influenza. For example, the administration of a tetravalent dengue DNA vaccine administered with a cationic lipid-based adjuvant in a phase 1 clinical trial resulted in good safety and immunogenicity [99]. It was observed that the group of mice which were immunized three times with the high dose of the tetravalent dengue DNA vaccine adjuvanted with Vaxfectin showed the most potent IFN-γ T cell responses when compared to mice which were immunized with the DNA vaccine on its own. Moreover, a 60 μg dose of Vaxfectin adjuvanted recombinant DNA plasmid encoding highly conserved antigens namely, the NP and ion channel protein (M2) from influenza virus conferred 100% protection in mice against influenza. An evaluation of the efficacy of Vaxfectin as a chemical adjuvant suggested that on its own, Vaxfectin might be effective to optimize immunogenicity in only smaller animal models such as mice but not in larger non-human primates (NHPs) [99].

2.6.2.4. AS03. The use of emulsion based adjuvants could be administered in conjunction with DNA vaccines to enhance humoral and cellular immune responses. An investigation into the impact of the use of emulsion-based and α-tocopherol containing adjuvant Diluvac Forte® on the immunogenicity of a recombinant DNA plasmid, which encoded hemagglutinin and a non-glycosylated NP, against influenza in the murine model showed that when the naked recombinant plasmid was administered with Diluvac Forte® or an emulsion containing α-tocopherol, the humoral response was enhanced in terms of significantly elevated levels of immunoglobulin G (IgG)1 and IgG2c [100]. While AS03 has not been used for adjuvanting the current DNA vaccines against SARS-CoV-2, several recombinant protein vaccines against SARS-CoV-2 employed the use of AS03 as a vaccine adjuvant [101]. Future DNA vaccine development against SARS-CoV-2 should consider the possibility of administering DNA vaccines in a 1:1 emulsion together with AS03 which might serve as an effective adjuvant to augment the immune response elicited.

In conclusion, a number of chemical adjuvants have been incorporated in DNA vaccines and the resulted increase in immunogenicity was demonstrated in animal models. However, a number of observations were elucidated. Firstly, the immune response elicited by the administration of chemically adjuvanted DNA vaccines resulted in strong humoral responses. Secondly, the immunogenic potential of chemical adjuvants in optimizing the immune response was higher in smaller animals which brought into question their applications in DNA vaccine development and immunogenicity testing in humans. Therefore, future efforts need to focus on incorporating novel adjuvants into DNA vaccine formulations to elicit more balanced humoral and cellular immune

responses, whereby its efficacy could be evaluated in larger animal models.

Implications for the development of vaccines against the SARS-CoV-2 involve evaluating and exploring strategies that could elicit both strong antibodies and potent cellular immune responses. In light of the recent COVID-19 pandemic and the need for effective vaccines that could offer sufficient protection against the disease, the immune response must involve both the humoral and cellular immune response. It was reported that humoral response against SARS-CoV-2 in terms of IgG, total and neutralizing antibodies declined after 6 months [102]. Full resolution of SARS-CoV-2 required a Th1 polarized cellular immune response as well as the elicitation of memory B cells. An evaluation of the use of chemical adjuvants in DNA vaccines in the past showed that immune responses were mainly Th2 biased. Therefore, additional incorporation of novel adjuvants which have similar effects as the monophosphoryl lipid A (MPLA) adjuvant by shifting the immune response towards a more Th1 biased response must be explored for the future development of chemically adjuvanted DNA vaccines against SARS-CoV-2.

2.6.3. Molecular adjuvants

An understanding of the use of chemical adjuvants in formulations with DNA vaccines is needed to explain the failure to elicit optimum immunogenicity. It must be noted that chemical adjuvants are simply mixed with the DNA vaccine which might have limited interactions with the adjuvant. The use of molecular adjuvants fused to the sequence of the target gene coding for the antigen in the recombinant plasmid might overcome this problem by ensuring that the adjuvant and antigen are both expressed simultaneously, resulting in an increased interaction. Alternatively, the molecular adjuvant could be encoded by a separate plasmid which might encode Toll-like receptor agonists, cytokines, and chemokines.

CD40 is a costimulatory molecule that plays an important role in the effective functioning of the immune system. The receptor is expressed by cells of the immune system such as B cells, APCs, and macrophages [103]. It can also be expressed by other non-immune cells such as endothelial cells, smooth muscle cells, fibroblasts and epithelial cells [104]. CD4F cells could activate DCs by the interaction of its CD40 with the CD40L on the DC. Activation of DCs would result in upregulation of CD80/CD86 which interacts with CD28 on naïve CD8$^+$ T cells. The CD40L is reported to serve as an effective adjuvant capable of enhancing the immune response elicited when it is expressed as part of the DNA vaccine. For example, Tamming et al. [105] reported the protective efficacy of a DNA vaccine encoding the SARS-CoV-2 Spike glycoprotein expressed in conjunction with CD40L. It was observed that CD40L served not only as the target ligand for its costimulatory molecule but also as a molecular adjuvant. The administration of the vaccine in Syrian hamsters was associated with potent humoral responses in terms of the production of neutralizing antibodies. In the group immunized with the Spike-CD40L DNA vaccine, lung pathology was more successfully ameliorated when compared to the group of mice immunized with the DNA vaccine not adjuvanted with CD40L. Moreover, clinical trials to test the immunogenicity of GX-19, a recombinant DNA plasmid expressing the S protein together with CD40L, demonstrated the elicitation of broad binding antibody responses [106]. Moreover, when the recombinant protein SARS-CoV-2 RBD vaccine was adjuvanted with a TLR7/8 agonist formulation, alum-3M − 052, it was able to elicit a neutralizing antibody response 100 fold higher than that elicited upon the administration of the vaccine with alum alone [107].

Moreover, other sequences that might serve as molecular adjuvants to enhance the immunogenicity of DNA vaccines have been reported. For example, a novel RBD based DNA vaccine against SARS-CoV-2 elicited far more potent immune responses in terms of the production of inflammatory cytokines IL-6 and TNF-α when linked to the N-terminal inclusion of a 33-bp (11 aa) preS1 sequence of the HBV W4P variant (N-terminal HBV preS1) comparing to the weaker immune response elicited in response to the RBD-based vaccine alone. This demonstrated that the N-

terminal HBV preS1 acted as an adjuvant which enhanced immunogenicity [108].

2.6.4. Delivery systems

Apart from the type of antigen and the incorporation of an adjuvant in the vaccine design and development, the protective efficacy of the vaccine and the potency of the immune responses it could elicit depends on the type of vaccine delivery platform [109]. A promising delivery method could involve using the intranasal route to administer DNA vaccines. Currently, none of the 16 DNA vaccine candidates in clinical development have utilized the intranasal route to deliver the DNA vaccine. Nevertheless, nasal delivery could overcome problems of dependency on needles, needle-stick injuries, disposal, inconvenience, and cost. Since most SARS-CoV-2 infections originate at mucosal surfaces, the intranasal route is a promising approach to induce immune responses since it could provide a convenient and accessible route to the mucosal immune system. Mucosal surfaces are strongly associated with immune responses of the lymphoid tissues. The intranasal route of vaccination involves the mucosa-associated lymphoid tissue (MALT), known as the nasopharynx-associated lymphoid tissue (NALT). NALT is characterized as the immune system present in the nasal mucosa involving lymphoid tissue, B cells, T cells, APCs, and an epithelial layer of memory cells which are responsible to carry the antigen across the epithelium. Depending on the type of antigen, it is transported across the epithelium to interact with macrophages and DCs. The antigen is taken up by APCs and transported to the lymph nodes for presentation to T cells. Soluble antigens are endocytosed by APCs directly [110].

2.6.5. Encapsulation of DNA plasmid in poly (lactic-co-glycolic acid) PLGA

Although the DNA vaccine platform has been extensively studied for the last three decades, its clinical application is impeded by the main challenge of the vaccine antigen in not being able to reach target APCs. Different methods have been used to deliver naked DNA vaccines. Electroporation was used by Inovio pharmaceuticals to deliver the DNA vaccine INO-4800 using the CELLECTRA® delivery device [10]. This created an electrical impulse using an electroporation device to stimulate permeability of cell membranes for enhanced uptake of the DNA vaccine [111]. Although transfection efficiency is high, and the method is quick and easy, disadvantages include cell death at the site of administration and pain to the patient when the DNA vaccine is administered. Moreover, certain considerations such as the electrode shape, size, and the formulation of the DNA vaccine would need to be optimized to enhance immunogenicity [112]. Oral delivery is an interesting mode of delivery adopted by only one vaccine developer, Symvivo Corporation (Australia), to manufacture the bacTRL-Spike oral DNA vaccine. In order to be successfully delivered orally, DNA vaccines would need to be specially formulated to survive against the gastric conditions of the digestive system [113]. The Needle-Free Injection System (NFIS) was also used by Zydus Cadila Healthcare (India) to administer the ZyCoV-D DNA vaccine. Specifically, the Pharmajet Tropis® device was used to deliver the DNA vaccine intradermally through a narrow and precise fluid stream. The ZyCoV-D vaccine is the only DNA vaccine to progress to phase 4 clinical trial under Emergency Use Authorization (EUA) in India as it had previously demonstrated humoral neutralizing antibody responses and Th1 polarized cellular responses characterized by IFN-γ production in animal models [114]. Furthermore, adequate humoral and cellular immune responses were observed at day 70 after the third dose in phase 1 clinical trial. Although needle-free intradermal administration could result in efficient and painless administrations, it required expensive and sophisticated devices which might not be available in resource poor countries [115]. Mechanical delivery for plasmid DNA could also be mediated by a gene gun. Heavy metallic particles were coated with plasmid DNA and significantly reduced DNA doses which could be directly injected into the cytosol of target cells. However, the cost of the gene gun system and gold particles is high [116]. Viral vectors could be used for delivery of DNA vaccines but they were associated with safety issues such as the elicitation of unwanted immune response against the viral vector, potential reversion to virulence, and potential insertional mutagenesis. Therefore, non-viral vectors are increasingly being recognized as potential carriers for DNA vaccine delivery.

The prospect of developing nanomaterials as carriers of DNA vaccines offers several advantages over traditional naked DNA administration in terms of delivery to the target cells in the lymphoid tissues, high transfection efficiency, induction of DC maturation and antigen presentation [116,117].

Nanoparticles as carriers can prevent the DNA plasmid from potential degradation during delivery to target APCs [118]. Nanoparticle carriers which encapsulate the DNA vaccine were reported to have a size range of 10–500 nm and they were small enough to be effectively edocytosed [119]. Nanoparticles with a size less than 100 nm were observed to have increased lymphatic uptake and improved transfections of the APCs in the lymph nodes [120]. Thus, encapsulation of DNA vaccines in nanoparticles could lead to increased immunogenicity, reduced toxicity and reactogenicity, effective presentations to APCs, improved endocytosis of DNA and transport to the nucleus.

PLGA was reported to break down into lactic acid and glycolic acid. Lactic acid was reported to be further metabolized into carbon dioxide and water which were excreted from the body [121]. This feature is an added advantage in terms of safety when compared to viral vectors [116].

The synthesis of plasmid DNA is convenient and inexpensive. However, due to reports of low transfection efficiency, it is important to improve the immunogenicity of DNA vaccines through the use of different delivery systems and adjuvants. Although sophisticated equipment has been available that used different routes of administration, such as the Pharmajet Tropis® device, which used NFIS for intradermal delivery of the ZyCoV-D DNA vaccine, and the CELLECTRA® delivery device, which used electroporation to deliver the INO-4800 DNA vaccine, these were more expensive options and may not be feasible for mass vaccination [116]. In contrast, the use of PLGA NPs to encapsulate DNA could serve as a relatively inexpensive method to increase immunogenicity of administered plasmid DNA. PLGA encapsulated plasmid DNA could be conveniently produced in the laboratory using the simple manual double emulsion method or mass produced using a microfluidics system [122,123].

There are various materials that can be used as nanocarriers to encapsulate DNA vaccines. For example, plasmid DNAs were encapsulated by either proteolipid nanoparticles formulated with neutral lipid and fusion associated *trans*-membrane. Another prominent and safe approach involves the use of polymers such as PLGA and chitosan. Choosing the appropriate antigen to be expressed and the material for nanoparticle design, the nanoparticle-based vaccine could result in a timely release of the DNA payload [116].

The use of PLGA as a nanodelivery carrier is increasingly being employed to facilitate the delivery of DNA-based vaccines. PLGA is an FDA-approved biopolymer, well-known for its biodegradability, biocompatibility, and minimal toxicity which made it ideal for use as delivery vehicle. Encapsulation by PLGA also protected the DNA vaccine antigen from degradation by DNases of the host. It could also promote the long-lasting release of the DNA vaccine. This occurred through a sophisticated mechanism of hydrolysis in which the payload was released slowly [124]. This meant that special modifications are required to ensure sustained release of the payload [116].

Extensive work has been conducted involving the use of PLGA nanoparticles to encapsulate DNA plasmids. For example, Zhao et al. [125] reported the encapsulation of a recombinant DNA plasmid expressing the F gene of the Newcastle Disease Virus (pFNDV) DNA Vaccine in PLGA nanoparticles. The constructed pFNDV-PLGA nanoparticle-based DNA vaccine had a diameter of 433.5 ± 7.5 nm and a Zeta potential of +2.7 mV. The recombinant plasmid DNA demonstrated high sustainable release (93.14% of the total amount) from the pFNDV-PLGA nanoparticles. Superior and more potent immune responses were elicited

from immunization of chickens with pFNDV-PLGA nanoparticles as compared to nanoparticles containing pFNDV alone. Therefore, pFNDV-PLGA nanoparticles were associated with the elicitation of more potent cellular, humoral, and mucosal immune responses with a sustained release of the DNA payload [125].

PLGA could serve as an effective nanomaterial to encapsulate DNA vaccines which were that have been administered intranasally to elicit potent protective immune responses. Wang et al. [126] utilized chitosan-coated PLGA to encapsulate recombinant DNA plasmid encoding the FMDV capsid protein as the antigenic target and the bovine IL-6 gene to enhance the mucosal immune response. Animal models such as rats and guinea pigs were intranasally immunized with the DNA vaccine. Out of the three different expression vectors used, the recombinant plasmid constructed using the recombinant pc-P12AIL3C plasmid which contained IL-6 located between the P12A and 3C genes elicited the most potent antigen-specific serum IgG and IgA responses and the strongest titers of secretory IgA in mucosal tissues. The recombinant plasmid, pc-P12AIL3C, was able to elicit the highest levels of neutralizing antibodies and also produced the strongest cellular immune responses. Cellular immune responses were associated with T cell proliferations in response to target antigens and high levels of IFN-γ produced by CD4$^+$ and CD8$^+$ splenic T cells. Challenge studies in animal models showed that 3/5 mice were protected against FMDV infection after immunization with the pc-IL2AP12A3C DNA vaccine. This approach is particularly attractive since it points towards the increased efficacy of DNA vaccines especially when encapsulated in chitosan-coated PLGA nanoparticles, with the use of IL-6 as a molecular adjuvant to optimize the immune response. The importance of incorporating DNA vaccines into chitosan-coated PLGA nanoparticles was further demonstrated by the intranasal administration of a naked DNA vaccine against pseudorabies virus, which elicited local and systemic immune responses. A combination of the DNA vaccine with PLGA-polyethylenimine (PEI) nanoparticles further increased the time during which mucosal IgA was detectable in pigs [127].

PLGA nanoparticles could be formulated with the cationic polymer, PEI which is a synthetic polymer regarded as an efficient nanodelivery carrier due to its ability to complex with DNA and deliver the plasmid DNA into the nucleus [128]. Properties that make PEI an ideal biomaterial to be formulated in complex with DNA include its high molecular weight and branched structure. The larger molecular weight resulted in densely populated amine groups which in turn increased the cationic characteristics. This allowed the PEI complex to achieve a higher rate of transfection through the proton sponge effect associated with endosomal escape. The use of PEIs with higher molecular weight was found to induce greater toxicity, and those with lower molecular weights induced lower toxicity but with reduced transfection efficiency. Therefore, certain modifications such as increasing branching and molecular weights could be made to PEIs to incorporate polysaccharides, polymers, and disulphide bridges. Previous studies to develop DNA vaccines utilizing the PLGA-PEI complex as the nanodelivery carrier reported the induction of humoral immunity utilizing the pseudorabies glycoprotein B as the target antigen, and a H1N1 DNA vaccine was delivered through intranasal delivery [127,129].

The use of PLGA-PEI nanoparticles was reported to effectively induce DC maturation and the production of cytokines such as IL-2 and TNF-α. Approaches such as a prime boost with recombinant protein vaccines showed that the DNA vaccine was able to elicit cellular immune responses in the form of T cell mediated immunity through the production of IFN-γ [130].

3. Conclusions

The rapid emergence of SARS-CoV-2 VOCs such as the highly infectious Omicron variant has contributed to new waves of SARS-CoV-2 infections globally since late 2021. There is an urgent need to develop strategies to curb the further spread of COVID-19 as well as to curb the threat of variants that might arise in the future. The development of next generation vaccine platforms such as DNA vaccines appears to be a promising solution since DNA vaccines can be quickly developed to incorporate antigenic regions other than the full length S protein which might become ineffective in eliciting neutralizing antibodies against new VOCs. In particular, the DNA vaccine platform is associated with attributes such as its ability to incorporate different genes representing highly conserved B and T cell epitopes, high stability at room temperature, and accelerated developmental timelines to speed up their progression to clinical trials. Genetic modifications of a plasmid vector such as the insertion of the NLS peptide gene could enhance the transfection and translocation of recombinant DNA. Additional genetic modifications to increase expressions of the recombinant plasmid include the use of strong promoters, insertion of MARs, and introns. Vectors could be modified to carry molecular adjuvants such as TLR agonists and CD40L to increase immunogenicity of the DNA vaccine. With the exception of ZyCoV-D vaccine in India, no DNA vaccines have been given emergency approval under phase 4 clinical development due to limited immunogenicity in humans. This challenge might be solved through the use of chemical/molecular adjuvants and the development of appropriate delivery systems utilizing nanoparticles to increase uptake by APCs in enhancing the induction of potent immune responses.

Financial disclosure

The authors have no funding to disclose.

The author contribution

Study Design: Chit Laa Poh.
Data Collection: Kanwal Khalid.
Statistical Analysis: n/a.
Data Interpretation: Kanwal Khalid, Chit Laa Poh.
Manuscript Preparation: Kanwal Khalid.
Literature Search: Kanwal Khalid.
Funds Collection: n/a.

Declaration of competing interest

The authors declare no conflict of interests.

References

[1] WHO. WHO coronavirus (COVID-19). Dashboard 2022 [Available from: https://covid19.who.int/.

[2] Bian L, Gao F, Zhang J, He Q, Mao Q, Xu M, et al. Effects of SARS-CoV-2 variants on vaccine efficacy and response strategies. Expert Rev Vaccines 2021;20(4):365–73.

[3] Eiz-Vesper B, Schmetzer HM. Antigen-presenting cells: potential of proven und new players in immune therapies. Transfus Med Hemotherapy 2020;47(6):429–31.

[4] Shafaati M, Saidijam M, Soleimani M, Hazrati F, Mirzaei R, Amirheidari B, et al. A brief review on DNA vaccines in the era of COVID-19. Future Virol 2022;17(1):49–66.

[5] Lim TS, Goh JK, Mortellaro A, Lim CT, Hämmerling GJ, Ricciardi-Castagnoli P. CD80 and CD86 differentially regulate mechanical interactions of T-cells with antigen-presenting dendritic cells and B-cells. PLoS One 2012;7(9):e45185.

[6] Rosendahl Huber S, van Beek J, de Jonge J, Luytjes W, van Baarle D. T cell responses to viral infections - opportunities for Peptide vaccination. Front Immunol 2014;5:171.

[7] Stebegg M, Kumar SD, Silva-Cayetano A, Fonseca VR, Linterman MA, Graca L. Regulation of the germinal center response. Front Immunol 2018;9.

[8] Swain SL, McKinstry KK, Strutt TM. Expanding roles for CD4+ T cells in immunity to viruses. Nat Rev Immunol 2012;12(2):136–48.

[9] Lee LYY, Izzard L, Hurt AC. A review of DNA vaccines against influenza. Front Immunol 2018;9:1568.

[10] Smith TRF, Patel A, Ramos S, Elwood D, Zhu X, Yan J, et al. Immunogenicity of a DNA vaccine candidate for COVID-19. Nat Commun 2020;11(1):2601.

[11] Chai KM, Tzeng T-T, Shen K-Y, Liao H-C, Lin J-J, Chen M-Y, et al. DNA vaccination induced protective immunity against SARS CoV-2 infection in hamsterss. PLoS Neglected Trop Dis 2021;15(5):e0009374.

[12] Prompetchara E, Ketloy C, Tharakhet K, Kaewpang P, Buranapraditkun S, Techawiwattanaboon T, et al. DNA vaccine candidate encoding SARS-CoV-2 spike

proteins elicited potent humoral and Th1 cell-mediated immune responses in mice. PLoS One 2021;16(3):e0248007.

[13] Yu J, Tostanoski LH, Peter L, Mercado NB, McMahan K, Mahrokhian SH, et al. DNA vaccine protection against SARS-CoV-2 in rhesus macaques. Science 2020; 369(6505):806–11.

[14] Poland GA, Ovsyannikova IG, Kennedy RB. SARS-CoV-2 immunity: review and applications to phase 3 vaccine candidates. Lancet 2020;396(10262):1595–606.

[15] Krammer F. SARS-CoV-2 vaccines in development. Nature 2020;586(7830): 516–27.

[16] Liu MA. A comparison of plasmid DNA and mRNA as vaccine technologies. Vaccines (Basel) 2019;7(2).

[17] Consuegra J, Gaffé J, Lenski RE, Hindré T, Barrick JE, Tenaillon O, et al. Insertion-sequence-mediated mutations both promote and constrain evolvability during a long-term experiment with bacteria. Nat Commun 2021;12(1):980.

[18] de Visser JAGM, Akkermans ADL, Hoekstra RF, de Vos WM. Insertion-sequence-mediated mutations isolated during adaptation to growth and starvation in Lactococcus lactis. Genetics 2004;168(3):1145–57.

[19] Wang Y, Wu Z, Hu W, Hao P, Yang S. Impact of expressing cells on glycosylation and glycan of the SARS-CoV-2 spike glycoprotein. ACS Omega 2021;6(24): 15988–99.

[20] Hayashi H, Sun J, Yanagida Y, Otera T, Kubota-Koketsu R, Shioda T, et al. Preclinical study of a DNA vaccine targeting SARS-CoV-2. Curr Res Transl Med 2022;70(4):103348.

[21] Silveira MM, Moreira G, Mendonça M. DNA vaccines against COVID-19: perspectives and challenges. Life Sci 2021;267:118919.

[22] Tebas P, Kraynyak KA, Patel A, Maslow JN, Morrow MP, Sylvester AJ, et al. Intradermal SynCon® ebola GP DNA vaccine is temperature stable and safely demonstrates cellular and humoral immunogenicity advantages in healthy volunteers. J Infect Dis 2019;220(3):400–10.

[23] Song X, Xu L, Yan R, Huang X, Shah MAA, Li X. The optimal immunization procedure of DNA vaccine pcDNA–TA4–IL-2 of Eimeria tenella and its cross-immunity to Eimeria necatrix and Eimeria acervulina. Vet Parasitol 2009;159(1): 30–6.

[24] Conforti A, Marra E, Palombo F, Roscilli G, Ravà M, Fumagalli V, et al. COVID-eVax, an electroporated DNA vaccine candidate encoding the SARS-CoV-2 RBD, elicits protective responses in animal models. Mol Ther 2022;30(1):311–26.

[25] Mammen MP, Tebas P, Agnes J, Giffear M, Kraynyak KA, Blackwood E, et al. Safety and immunogenicity of INO-4800 DNA vaccine against SARS-CoV-2: a preliminary report of a randomized, blinded, placebo-controlled, Phase 2 clinical trial in adults at high risk of viral exposure. medRxiv 2021:2021. 05.07.21256652.

[26] Alamri SS, Alluhaybi KA, Alhabbab RY, Basabrain M, Algaissi A, Almahboub S, et al. Synthetic SARS-CoV-2 spike-based DNA vaccine elicits robust and long-lasting th1 humoral and cellular immunity in mice. Front Microbiol 2021:12.

[27] Alluhaybi KA, Alharbi RH, Alhabbab RY, Aljehani ND, Alamri SS, Basabrain M, et al. Cellular and humoral immunogenicity of a candidate DNA vaccine expressing SARS-CoV-2 spike subunit 1. Vaccines (Basel) 2021;9(8).

[28] Nishikawa T, Chang CY, Tai JA, Hayashi H, Sun J, Torii S, et al. Anti-CoVid19 plasmid DNA vaccine induces a potent immune response in rodents by Pyro-drive Jet injector intradermal inoculation. bioRxiv 2021;13:426436. 2021.01.

[29] Yang Y, Du L. SARS-CoV-2 spike protein: a key target for eliciting persistent neutralizing antibodies. Curr Signal Transduct Ther 2021;6(1):95.

[30] Fisher E, Padula L, Podack K, O'Neill K, Seavey MM, Jayaraman P, et al. Induction of SARS-CoV-2 protein S-specific CD8+ T cells in the lungs of gp96-Ig-S vaccinated mice. Front Immunol 2020;11:602254.

[31] Wang X, Rcheulishvili N, Cai J, Liu C, Xie F, Hu X, et al. Development of DNA vaccine candidate against SARS-CoV-2. Viruses 2022;14:1049.

[32] Tzeng T-T, Chai KM, Shen K-Y, Yu C-Y, Yang S-J, Huang W-C, et al. A DNA vaccine candidate delivered by an electroacupuncture machine provides protective immunity against SARS-CoV-2 infection. NPJ Vaccines 2022;7(1):60.

[33] Wang Z, Schmidt F, Weisblum Y, Muecksch F, Barnes CO, Finkin S, et al. mRNA vaccine-elicited antibodies to SARS-CoV-2 and circulating variants. Nature 2021; 592(7855):616–22.

[34] Wang P, Nair MS, Liu L, Iketani S, Luo Y, Guo Y, et al. Antibody resistance of SARS-CoV-2 variants B.1.351 and B.1.1.7. Nature 2021;593(7857):130–5.

[35] Harvey WT, Carabelli AM, Jackson B, Gupta RK, Thomson EC, Harrison EM, et al. SARS-CoV-2 variants, spike mutations and immune escape. Nat Rev Microbiol 2021;19(7):409–24.

[36] Collier DA, De Marco A, Ferreira IATM, Meng B, Datir RP, Walls AC, et al. Sensitivity of SARS-CoV-2 B.1.1.7 to mRNA vaccine-elicited antibodies. Nature 2021;593(7857):136–41.

[37] Madhi SA, Baillie V, Cutland CL, Voysey M, Koen AL, Fairlie L, et al. Efficacy of the ChAdOx1 nCoV-19 Covid-19 vaccine against the B.1.351 variant. N Engl J Med 2021;384(20):1885–98.

[38] Wu K, Werner AP, Moliva JI, Koch M, Choi A, Stewart-Jones GBE, et al. mRNA-1273 vaccine induces neutralizing antibodies against spike mutants from global SARS-CoV-2 variants. bioRxiv 2021;25:427948. 2021.01.

[39] Tarke A, Sidney J, Methot N, Yu ED, Zhang Y, Dan JM, et al. Impact of SARS-CoV-2 variants on the total CD4(+) and CD8(+) T cell reactivity in infected or vaccinated individuals. Cell Rep Med 2021;2(7):100355.

[40] Noh JY, Jeong HW, Shin E-C. SARS-CoV-2 mutations, vaccines, and immunity: implication of variants of concern. Curr Signal Transduct Ther 2021;6(1):203.

[41] Agerer B, Koblischke M, Gudipati V, Montaño-Gutierrez LF, Smyth M, Popa A, et al. SARS-CoV-2 mutations in MHC-I-restricted epitopes evade CD8(+) T cell responses. Sci Immunol 2021;6(57).

[42] Moss P. The T cell immune response against SARS-CoV-2. Nat Immunol 2022; 23(2):186–93.

[43] Cele S, Jackson L, Khoury DS, Khan K, Moyo-Gwete T, Tegally H, et al. Omicron extensively but incompletely escapes Pfizer BNT162b2 neutralization. Nature 2022;602(7898):654–6.

[44] Hachmann NP, Miller J, Collier AY, Ventura JD, Yu J, Rowe M, et al. Neutralization escape by SARS-CoV-2 Omicron subvariants BA.2.12.1, BA.4, and BA.5. NEJM 2022;387(1):86–8.

[45] Wilhelm A, Widera M, Grikscheit K, Toptan T, Schenk B, Pallas C, et al. Limited neutralisation of the SARS-CoV-2 Omicron subvariants BA.1 and BA.2 by convalescent and vaccine serum and monoclonal antibodies. EBioMedicine 2022: 82.

[46] Andrade VM, Christensen-Quick A, Agnes J, Tur J, Reed C, Kalia R, et al. INO-4800 DNA vaccine induces neutralizing antibodies and T cell activity against global SARS-CoV-2 variants. NPJ Vaccines 2021;6(1):121.

[47] Azevedo PO, Hojo-Souza NS, Faustino LP, Fumagalli MJ, Hirako IC, Oliveira ER, et al. Differential requirement of neutralizing antibodies and T cells on protective immunity to SARS-CoV-2 variants of concern. NPJ Vaccines 2023;8(1):15.

[48] Appelberg S, Ahlén G, Yan J, Nikouyan N, Weber S, Larsson O, et al. A universal SARS-CoV DNA vaccine inducing highly cross-reactive neutralizing antibodies and T cells. EMBO Mol Med 2022;14(10):e15821.

[49] Reed CC, Schultheis K, Andrade VM, Kalia R, Tur J, Schouest B, et al. Design, immunogenicity and efficacy of a Pan-SARS-CoV-2 synthetic DNA vaccine. bioRxiv 2021;5(11):443592.

[50] Lim HX, Masomian M, Khalid K, Kumar AU, MacAry PA, Poh CL. Identification of B-cell epitopes for eliciting neutralizing antibodies against the SARS-CoV-2 spike protein through bioinformatics and monoclonal antibody targeting. Int J Mol Sci 2022;23(8).

[51] Montes-Grajales D, Olivero-Verbel J. Bioinformatics Prediction of SARS-CoV-2 epitopes as vaccine candidates for the Colombian population. Vaccines (Basel) 2021;9(7).

[52] Polyiam K, Phoolcharoen W, Butkhot N, Srisaowakarn C, Thitithanyanont A, Auewarakul P, et al. Immunodominant linear B cell epitopes in the spike and membrane proteins of SARS-CoV-2 identified by immunoinformatics prediction and immunoassay. Sci Rep 2021;11(1):20383.

[53] Suschak JJ, Williams JA, Schmaljohn CS. Advancements in DNA vaccine vectors, non-mechanical delivery methods, and molecular adjuvants to increase immunogenicity. Hum Vaccines Immunother 2017;13(12):2837–48.

[54] Dupuis M, Denis-Mize K, Woo C, Goldbeck C, Selby MJ, Chen M, et al. Distribution of DNA vaccines determines their immunogenicity after intramuscular injection in mice. J Immunol 2000;165(5):2850–8.

[55] Hobernik D, Bros M. DNA vaccines-how far from clinical use? Int J Mol Sci 2018; 19(11).

[56] Braathen R, Spång HCL, Hinke DM, Blazevski J, Bobic S, Fossum E, et al. A DNA vaccine that encodes an antigen-presenting cell-specific heterodimeric protein protects against cancer and influenza. Mol Ther Methods Clin Dev 2020;17: 378–92.

[57] Grozdanov PN, MacDonald CC. Generation of plasmid vectors expressing FLAG-tagged proteins under the regulation of human elongation factor-1α promoter using Gibson assembly. J Vis Exp 2015;96.

[58] Kim DW, Uetsuki T, Kaziro Y, Yamaguchi N, Sugano S. Use of the human elongation factor 1α promoter as a versatile and efficient expression system. Gene 1990;91(2):217–23.

[59] Deer JR, Allison DS. High-level expression of proteins in mammalian cells using transcription regulatory sequences from the Chinese hamster ef-1α gene. Biotechnol Prog 2004;20(3):880–9.

[60] Qin JY, Zhang L, Clift KL, Hulur I, Xiang AP, Ren BZ, et al. Systematic comparison of constitutive promoters and the doxycycline-inducible promoter. PLoS One 2010;5(5):e10611.

[61] Backliwal G, Hildinger M, Chenuet S, Wulhfard S, De Jesus M, Wurm FM. Rational vector design and multi-pathway modulation of HEK 293E cells yield recombinant antibody titers exceeding 1 g/l by transient transfection under serum-free conditions. Nucleic Acids Res 2008;36(15):e96.

[62] Johari YB, Scarrott JM, Pohle TH, Liu P, Mayer A, Brown AJ, et al. Engineering of the CMV promoter for controlled expression of recombinant genes in HEK293 cells. Nat Biotechnol 2022;17(8):2200062.

[63] Kozak M. Pushing the limits of the scanning mechanism for initiation of translation. Gene 2002;299(1–2):1–34.

[64] Kozak M. Initiation of translation in prokaryotes and eukaryotes. Gene 1999; 234(2):187–208.

[65] Kozak M. Point mutations define a sequence flanking the AUG initiator codon that modulates translation by eukaryotic ribosomes. Cell 1986;44(2):283–92.

[66] Kozak M. Recognition of AUG and alternative initiator codons is augmented by G in position +4 but is not generally affected by the nucleotides in positions +5 and +6. EMBO J 1997;16(9):2482–92.

[67] Dixon JR, Selvaraj S, Yue F, Kim A, Li Y, Shen Y, et al. Topological domains in mammalian genomes identified by analysis of chromatin interactions. Nature 2012;485(7398):376–80.

[68] Girod P-A, Mermod N. Use of scaffold/matrix-attachment regions for protein production. N Compr Biochem 2003;38:359–79. Elsevier.

[69] Kim JD, Yoon Y, Hwang H-Y, Park JS, Yu S, Lee J, et al. Efficient selection of stable Chinese hamster ovary (CHO) cell lines for expression of recombinant proteins by using human interferon β SAR element. Biotechnol Prog 2005;21(3):933–7.

[70] Zhao C-P, Guo X, Chen S-J, Li C-Z, Yang Y, Zhang J-H, et al. Matrix attachment region combinations increase transgene expression in transfected Chinese hamster ovary cells. Sci Rep 2017;7(1):42805.

[71] Gallegos JE, Rose AB. An intron-derived motif strongly increases gene expression from transcribed sequences through a splicing independent mechanism in Arabidopsis thaliana. Sci Rep 2019;9(1):13777.

[72] Shaul O. How introns enhance gene expression. Int J Biochem Cell Biol 2017; 91(Pt B):145–55.

[73] Brinster RL, Allen JM, Behringer RR, Gelinas RE, Palmiter RD. Introns increase transcriptional efficiency in transgenic mice. Proc Natl Acad Sci U S A 1988;85(3): 836–40.

[74] Juneau K, Miranda M, Hillenmeyer ME, Nislow C, Davis RW. Introns regulate RNA and protein abundance in yeast. Genetics 2006;174(1):511–8.

[75] Niu D-K, Yang Y-F. Why eukaryotic cells use introns to enhance gene expression: splicing reduces transcription-associated mutagenesis by inhibiting topoisomerase I cutting activity. Biol Direct 2011;6(1):24.

[76] Akua T, Shaul O. The Arabidopsis thaliana MHX gene includes an intronic element that boosts translation when localized in a 5' UTR intron. J Exp Bot 2013;64(14): 4255–70.

[77] Morello L, Gianì S, Troina F, Breviario D. Testing the IMEter on rice introns and other aspects of intron-mediated enhancement of gene expression. J Exp Bot 2011; 62(2):533–44.

[78] Rose AB. Introns as gene regulators: a brick on the accelerator. Front Genet 2019; 9.

[79] Buchman AR, Berg P. Comparison of intron-dependent and intron-independent gene expression. Mol Cell Biol 1988;8(10):4395–405.

[80] Gallegos JE, Rose AB. The enduring mystery of intron-mediated enhancement. Plant Sci 2015;237:8–15.

[81] Baier T, Jacobebbinghaus N, Einhaus A, Lauersen KJ, Kruse O. Introns mediate post-transcriptional enhancement of nuclear gene expression in the green microalga Chlamydomonas reinhardtii. PLoS Genet 2020;16(7):e1008944.

[82] Xu D-h, Wang X-y, Jia Y-l, Wang T-y, Tian Z-w, Feng X, et al. SV40 intron, a potent strong intron element that effectively increases transgene expression in transfected Chinese hamster ovary cells. J Cell Mol Med 2018;22(4):2231–9.

[83] Boye C, Arpag S, Francis M, DeClemente S, West A, Heller R, et al. Reduction of plasmid vector backbone length enhances reporter gene expression. Bioelectrochemistry 2022;144:107981.

[84] Ohse M, Takahashi K, Kadowaki Y, Kusaoke H. Effects of plasmid DNA sizes and several other factors on transformation of Bacillus subtilis ISW1214 with plasmid DNA by electroporation. Biosci Biotechnol Biochem 1995;59(8):1433–7.

[85] Kreiss P, Mailhe P, Scherman D, Pitard B, Cameron B, Rangara R, et al. Plasmid DNA size does not affect the physicochemical properties of lipoplexes but modulates gene transfer efficiency. Nucleic Acids Res Spec Publ 1999;27(19): 3792–8.

[86] Lu J, Wu T, Zhang B, Liu S, Song W, Qiao J, et al. Types of nuclear localization signals and mechanisms of protein import into the nucleus. Cell Commun Signal 2021;19(1):60.

[87] Zanta MA, Belguise-Valladier P, Behr JP. Gene delivery: a single nuclear localization signal peptide is sufficient to carry DNA to the cell nucleus. Proc Natl Acad Sci U S A 1999;96(1):91–6.

[88] Xu Y, Liang W, Qiu Y, Cespi M, Palmieri GF, Mason AJ, et al. Incorporation of a nuclear localization signal in pH responsive LAH4-L1 peptide enhances transfection and nuclear uptake of plasmid DNA. Mol Pharm 2016;13(9):3141–52.

[89] López-Fuertes L, Pérez-Jiménez E, Vila-Coro AJ, Sack F, Moreno S, Konig SA, et al. DNA vaccination with linear minimalistic (MIDGE) vectors confers protection against Leishmania major infection in mice. Vaccine 2002;21(3–4):247–57.

[90] Moreno S, López-Fuertes L, Vila-Coro AJ, Sack F, Smith CA, Konig SA, et al. DNA immunisation with minimalistic expression constructs. Vaccine 2004;22(13–14): 1709–16.

[91] Jin H, Li Y, Ma Z, Zhang F, Xie Q, Gu D, et al. Effect of chemical adjuvants on DNA vaccination. Vaccine 2004;22(21):2925–35.

[92] Quattrocchi V, Soria I, Langellotti CA, Gnazzo V, Gammella M, Moore DP, et al. A DNA vaccine formulated with chemical adjuvant provides partial protection against bovine Herpes virus infection in cattle. Front Immunol 2017;8.

[93] Di Giacomo S, Quattrocchi V, Zamorano P. Use of adjuvants to enhance the immune response induced by a DNA vaccine against bovine Herpesvirus-1. Viral Immunol 2015;28(6):343–6.

[94] Wang S, Liu X, Fisher K, Smith JG, Chen F, Tobery TW, et al. Enhanced type I immune response to a hepatitis B DNA vaccine by formulation with calcium- or aluminum phosphate. Vaccine 2000;18(13):1227–35.

[95] Garg R, Kaur M, Saxena A, Prasad R, Bhatnagar R. Alum adjuvanted rabies DNA vaccine confers 80% protection against lethal 50 LD(50) rabies challenge virus standard strain. Mol Immunol 2017;85:166–73.

[96] Grunwald T, Ulbert S. Improvement of DNA vaccination by adjuvants and sophisticated delivery devices: vaccine-platforms for the battle against infectious diseases. Clin Exp Vaccine Res 2015;4(1):1–10.

[97] Lin WH, Vilalta A, Adams RJ, Rolland A, Sullivan SM, Griffin DE. Vaxfectin adjuvant improves antibody responses of juvenile rhesus macaques to a DNA vaccine encoding the measles virus hemagglutinin and fusion proteins. J Virol 2013;87(12):6560–8.

[98] Pan C-H, Jimenez Gretchen S, Nair N, Wei Q, Adams Robert J, Polack Fernando P, et al. Use of Vaxfectin adjuvant with DNA vaccine encoding the measles virus hemagglutinin and fusion proteins protects juvenile and infant rhesus macaques against measles virus. Clin Vaccine Immunol 2008;15(8):1214–21.

[99] Danko JR, Kochel T, Teneza-Mora N, Luke TC, Raviprakash K, Sun P, et al. Safety and immunogenicity of a tetravalent Dengue DNA vaccine administered with a cationic lipid-based adjuvant in a phase 1 clinical trial. Am J Trop Med Hyg 2018; 98(3):849–56.

[100] Karlsson I, Borggren M, Nielsen J, Christensen D, Williams J, Fomsgaard A. Increased humoral immunity by DNA vaccination using an α-tocopherol-based adjuvant. Hum Vaccines Immunother 2017;13(8):1823–30.

[101] Grigoryan L, Lee A, Walls AC, Lai L, Franco B, Arunachalam PS, et al. Adjuvanting a subunit SARS-CoV-2 vaccine with clinically relevant adjuvants induces durable protection in mice. NPJ Vaccines 2022;7(1):55.

[102] Bayart JL, Douxfils J, Gillot C, David C, Mullier F, Elsen M, et al. Waning of IgG, total and neutralizing antibodies 6 months post-vaccination with BNT162b2 in healthcare workers. Vaccines (Basel) 2021;9(10).

[103] Elgueta R, Benson MJ, de Vries VC, Wasiuk A, Guo Y, Noelle RJ. Molecular mechanism and function of CD40/CD40L engagement in the immune system. Immunol Rev 2009;229(1):152–72.

[104] Chatzigeorgiou A, Lyberi M, Chatzilymperis G, Nezos A, Kamper E. CD40/CD40L signaling and its implication in health and disease. Biofactors 2009;35(6):474–83.

[105] Tamming LA, Duque D, Tran A, Zhang W, Pfeifle A, Laryea E, et al. DNA Based Vaccine Expressing SARS-CoV-2 Spike-CD40L Fusion protein confers protection against challenge in a Syrian hamster model. Front Immunol 2021;12:785349.

[106] Ahn JY, Lee J, Suh YS, Song YG, Choi Y-J, Lee KH, et al. Safety and immunogenicity of two recombinant DNA COVID-19 vaccines containing the coding regions of the spike or spike and nucleocapsid proteins: an interim analysis of two open-label, non-randomised, phase 1 trials in healthy adults. Lancet Microbe 2022;3(3):e173–83.

[107] Routhu NK, Cheedarla N, Bollimpelli VS, Gangadhara S, Edara VV, Lai L, et al. SARS-CoV-2 RBD trimer protein adjuvanted with Alum-3M-052 protects from SARS-CoV-2 infection and immune pathology in the lung. Nat Commun 2021; 12(1):3587.

[108] Jeong H, Choi Y-M, Seo H, Kim B-J. A Novel DNA Vaccine against SARS-CoV-2 encoding a chimeric protein of its receptor-binding domain (RBD) fused to the amino-terminal region of Hepatitis B virus preS1 with a W4P mutation. Front Immunol 2021:12.

[109] Park KS, Sun X, Aikins ME, Moon JJ. Non-viral COVID-19 vaccine delivery systems. Adv Drug Deliv Rev 2021;169:137–51.

[110] Wu HY, Nguyen HH, Russell MW. Nasal lymphoid tissue (NALT) as a mucosal immune inductive site. Scand J Immunol 1997;46(5):506–13.

[111] Lambricht L, Lopes A, Kos S, Sersa G, Préat V, Vandermeulen G. Clinical potential of electroporation for gene therapy and DNA vaccine delivery. Expet Opin Drug Deliv 2016;13(2):295–310.

[112] Sardesai NY, Weiner DB. Electroporation delivery of DNA vaccines: prospects for success. Curr Opin Immunol 2011;23(3):421–9.

[113] Vela Ramirez JE, Sharpe LA, Peppas NA. Current state and challenges in developing oral vaccines. Adv Drug Deliv Rev 2017;114:116–31.

[114] Dey A, Chozhavel Rajanathan TM, Chandra H, Pericherla HPR, Kumar S, Choonia HS, et al. Immunogenic potential of DNA vaccine candidate, ZyCoV-D against SARS-CoV-2 in animal models. Vaccine 2021;39(30):4108–16.

[115] Ravi AD, Sadhna D, Nagpaal D, Chawla L. Needle free injection technology: a complete insight. Int J Pharm Investig 2015;5(4):192–9.

[116] Lim M, Badruddoza AZM, Firdous J, Azad M, Mannan A, Al-Hilal TA, et al. Engineered nanodelivery systems to improve DNA vaccine technologies. Pharmaceutics 2020;12(1):30.

[117] Farris E, Brown DM, Ramer-Tait AE, Pannier AK. Micro- and nanoparticulates for DNA vaccine delivery. Exp Biol Med 2016;241(9):919–29.

[118] Pati R, Shevtsov M, Sonawane A. Nanoparticle vaccines against infectious diseases. Front Immunol 2018;9:2224.

[119] Sousa de Almeida M, Susnik E, Drasler B, Taladriz-Blanco P, Petri-Fink A, Rothen-Rutishauser B. Understanding nanoparticle endocytosis to improve targeting strategies in nanomedicine. Chem Soc Rev 2021;50(9):5397–434.

[120] Barua S, Mitragotri S. Challenges associated with penetration of nanoparticles across cell and tissue barriers: a review of current status and future prospects. Nano Today 2014;9(2):223–43.

[121] Crotts G, Park TG. Protein delivery from poly(lactic-co-glycolic acid) biodegradable microspheres: release kinetics and stability issues. J Microencapsul 1998;15(6):699–713.

[122] Santhanes D, Wilkins A, Zhang H, John Aitken R, Liang M. Microfluidic formulation of lipid/polymer hybrid nanoparticles for plasmid DNA (pDNA) delivery. Int J Pharm 2022;627:122223.

[123] Zhao K, Li W, Huang T, Luo X, Chen G, Zhang Y, et al. Preparation and efficacy of Newcastle disease virus DNA vaccine encapsulated in PLGA nanoparticles. PLoS One 2013;8(12):e82648.

[124] Makadia HK, Siegel SJ. Poly Lactic-co-Glycolic Acid (PLGA) as biodegradable controlled drug delivery carrier. Polymers 2011;3(3):1377–97.

[125] Zhao K, Zhang Y, Zhang X, Li W, Shi C, Guo C, et al. Preparation and efficacy of Newcastle disease virus DNA vaccine encapsulated in chitosan nanoparticles. Int J Nanomed 2014;9:389–402.

[126] Wang G, Pan L, Zhang Y, Wang Y, Zhang Z, Lü J, et al. Intranasal delivery of cationic PLGA nano/microparticles-loaded FMDV DNA vaccine encoding IL-6 elicited protective immunity against FMDV challenge. PLoS One 2011;6(11): e27605.

Review

The Promising Potential of Reverse Vaccinology-Based Next-Generation Vaccine Development over Conventional Vaccines against Antibiotic-Resistant Bacteria

Kanwal Khalid and Chit Laa Poh *

Centre for Virus and Vaccine Research, School of Medical and Life Sciences, Sunway University, Bandar Sunway, Subang Jaya 47500, Malaysia; 19115914@imail.sunway.edu.my
*   Correspondence: chitlaa.poh@gmail.com

Abstract: The clinical use of antibiotics has led to the emergence of multidrug-resistant (MDR) bacteria, leading to the current antibiotic resistance crisis. To address this issue, next-generation vaccines are being developed to prevent antimicrobial resistance caused by MDR bacteria. Traditional vaccine platforms, such as inactivated vaccines (IVs) and live attenuated vaccines (LAVs), were effective in preventing bacterial infections. However, they have shown reduced efficacy against emerging antibiotic-resistant bacteria, including MDR *M. tuberculosis*. Additionally, the large-scale production of LAVs and IVs requires the growth of live pathogenic microorganisms. A more promising approach for the accelerated development of vaccines against antibiotic-resistant bacteria involves the use of in silico immunoinformatics techniques and reverse vaccinology. The bioinformatics approach can identify highly conserved antigenic targets capable of providing broader protection against emerging drug-resistant bacteria. Multi-epitope vaccines, such as recombinant protein-, DNA-, or mRNA-based vaccines, which incorporate several antigenic targets, offer the potential for accelerated development timelines. This review evaluates the potential of next-generation vaccine development based on the reverse vaccinology approach and highlights the development of safe and immunogenic vaccines through relevant examples from successful preclinical and clinical studies.

Keywords: vaccine; immunoinformatics; reverse vaccinology; antibiotics; MDR bacteria

1. Introduction

Modern medicine has undergone a revolution owing to the therapeutic use of antibiotics to treat bacterial infections [1–7]. The discovery of penicillin in 1928 marked the start of medical interventions that enabled remarkable reductions in debilitating bacterial infections such as pneumonia and tuberculosis [8,9]. As a result of antibiotics, mortality due to bacterial infections decreased significantly and the average life expectancy at birth increased from 47 to 78.8 years in the USA [10]. However, the golden age of antibiotics was abruptly halted by the emergence of MDR bacterial strains, culminating in the present antibiotic resistance crisis [10].

Medical treatments such as immunosuppressive chemotherapy against cancers, organ transplantations, and surgeries require the use of antibiotics to prevent MDR bacterial infections. MDR pathogens have been reported to cause 700,000 deaths per annum and they are anticipated to result in 10 million fatalities annually by 2050 [11]. The impact of antibiotic resistance on individual health and wellbeing as well as on the economy is disastrous, as evidenced by an estimated 1.27 million global deaths as a result of antibiotic resistance in 2019 and projected healthcare treatment costs of $300 billion to well beyond $1 trillion by 2050 [12,13].

Considering the alarming impact of the high number of infections caused by antibiotic-resistant bacteria and the high healthcare costs associated with their treatment, it is essential

to develop strategies that could reduce the incidence of diseases caused by antibiotic-resistant bacteria. The development of new and safe antibiotics is required to combat the growing number of diseases caused by pathogens resistant to existing antibiotics [14]. These antibiotics would, however, be subjected to similar selection pressures, resulting in the eventual emergence of strains becoming more resistant [14]. A promising alternative involves the development of next-generation vaccines geared towards the prevention of antimicrobial resistance due to the emergence of MDR bacteria. This review provides a comprehensive overview of preclinical and clinical vaccine development against antibiotic-resistant bacteria.

1.1. Mechanisms of Antibiotic Resistance Acquired through Horizontal Gene Transfer between Bacteria

Antibiotic resistance is due to a rise in pathogenic strains of bacteria that have developed mechanisms to considerably reduce the effectiveness of antibiotics. Studies have shown that antibiotic-resistant bacteria evade the antimicrobial action of antibiotics through antibiotic inactivation, modification of antibiotic targets such as bacterial cell walls, or through the efflux of antibiotics from bacteria [15–17]. Antibiotic resistance in bacteria can be acquired through horizontal gene transfer processes such as transformation, transduction, and conjugation. During transformation, donor bacteria release DNA fragments with resistance genes into the environment. Competent recipient bacteria can take up these fragments and integrate the resistance genes into their genome. This integration enables the recipient bacteria to produce proteins or enzymes that make them resistant to specific antibiotics. As a result, the transformed bacteria inherit antibiotic resistance, leading to the spread of resistance within bacterial populations. During transduction, bacteriophages can carry antibiotic resistance genes from a donor bacterium to a recipient bacterium. These genes can then become integrated into the recipient bacterium's chromosome. This integration allows the recipient bacterium to acquire and express the antibiotic resistance traits encoded by these genes, resulting in antibiotic resistance. During bacterial conjugation, antibiotic resistance genes are transferred through direct physical contact between the donor and the recipient bacteria. This process involves the formation of a physical bridge, called a pilus, between the two bacterial cells. The pilus facilitates the transfer of a plasmid, which carries the antibiotic resistance genes, from the donor bacterium to the recipient bacterium. Once inside the recipient bacterium, the plasmid is integrated into the chromosome [18]. These processes are illustrated in Figure 1.

1.2. Reverse Vaccinology: An Innovative Approach to Vaccine Development against Antibiotic-Resistant Bacteria

Reverse vaccinology is a groundbreaking approach in vaccine development that has revolutionized the search for effective vaccine candidates to combat antibiotic-resistant bacteria. Traditionally, vaccine development relies on cultivating and inactivating or attenuating a whole pathogen to stimulate an immune response. However, reverse vaccinology takes a different route by leveraging bioinformatics and computational analysis of pathogen genomes to identify potential vaccine targets. This innovative method focuses on identifying specific protein components, known as epitopes, within the genomes of pathogens that are most likely to result in potent immune responses. By analyzing the genetic information of the pathogen, researchers can predict and select these epitopes, paving the way for the development of multi-epitope-based vaccines [19]. This approach offers several advantages, such as the potential to simultaneously target multiple epitopes [20]. This serves as an effective way to enhance the effectiveness of vaccines developed against highly diverse and rapidly evolving antibiotic-resistant strains. Furthermore, reverse vaccinology allows for a more rapid and targeted vaccine design process, accelerating the development timeline and potentially overcoming challenges associated with traditional approaches. As antibiotic resistance continues to pose a significant threat to global health, the reverse vaccinology approach offers promising prospects in the quest for effective vaccines against antibiotic-resistant bacteria [21].
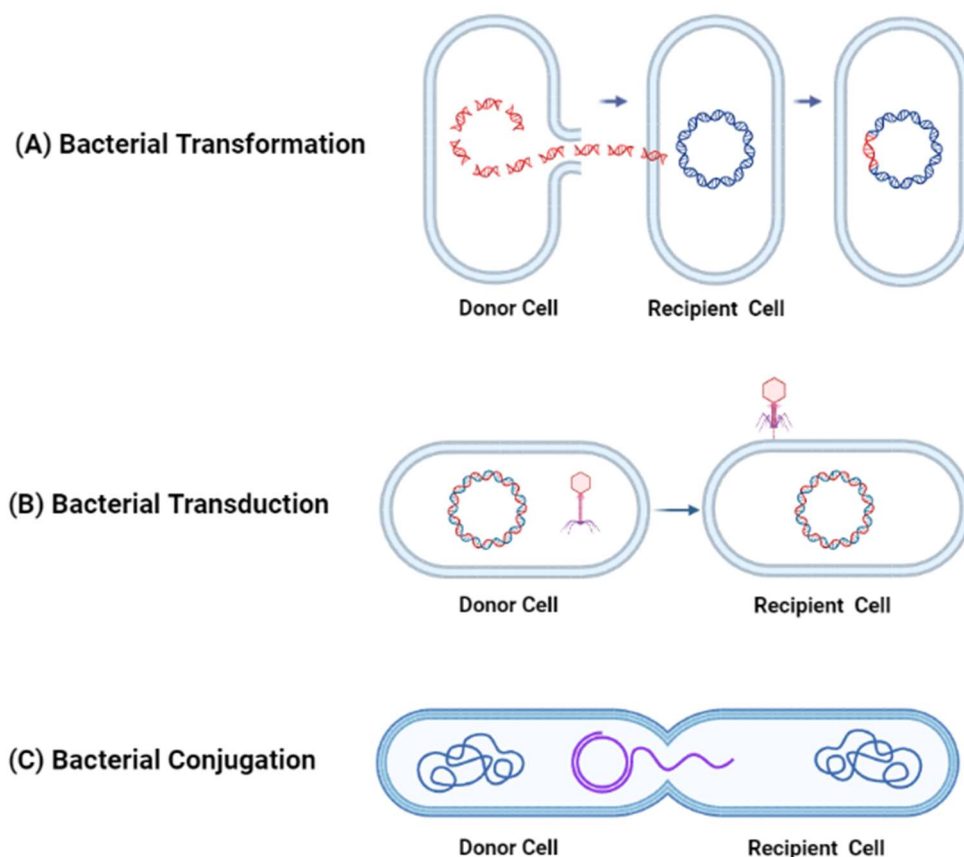
Figure 1. Mechanisms of antibiotic resistance acquired through horizontal gene transfer such as (**A**) transformation, (**B**) transduction, and (**C**) conjugation.

2. Vaccines against Antimicrobial Resistance Based on Conventional Vaccine Platforms

2.1. LAVs

Conventional vaccines such as IVs and LAVs have been developed against a number of infectious diseases caused by antibiotic-resistant bacteria. One important example is the development of LAVs against tuberculosis (TB). After the occurrence of Coronavirus disease 2019 (COVID-19), TB became the second most common cause of global mortality. Up until 2019, TB caused by the etiological agent *Mycobacterium tuberculosis* (MTB) was well known for being responsible for more than 10 million infections and the highest number of global deaths attributable to a single infectious pathogen [18]. The disease is primarily prevalent in regions of South-East Asia, Africa, and the Western Pacific. The global burden of those infected with TB has been exacerbated by the emergence of MDR tuberculosis (TB) strains, which comprise TB strains that are resistant to at least the first-line treatment drugs isoniazid and rifampicin [22].

Effective vaccines aim to stimulate protective humoral and cellular immune responses against the pathogen. LAVs have shown efficacy in protection since they can induce both potent humoral as well as cell-mediated responses. Moreover, new strategies for developing LAVs against bacteria are underway. One such strategy focused on developing LAVs that were auxotrophic for D-glutamate, which is involved in bacterial cell wall formation. LAVs against *Acinetobacter baumannii*, *Pseudomonas aeruginosa*, and *Staphylococcus aureus* not only attenuated virulence but also led to self-resolution of infections when administered to mice. Potent immune responses in terms of functional and cross-reactive antibodies as well as cellular immunity were elicited in addition to protection against *A. baumannii* AbH12O-A2 and Ab307-0294, *P. aeruginosa* PA14, and community-acquired methicillin-resistant *S. aureus* USA300LAC [23]. There are other examples of effective LAVs being developed

against bacteria. For example, anthrax vaccine adsorbed (AVA) BioThrax is a licensed avirulent vaccine recommended for the immunization of individuals aged 18–65 years for the prevention of anthrax caused by *Bacillus anthracis.*

BioThrax is composed mainly of the anthrax protective antigen (PA), while the aluminum hydroxide suspension (alhydrogel) allows adsorption of the PA, which also acts as an adjuvant. Anti-PA IgG levels were detected in more than approximately 1/3 of participants in clinical trials after a single administration. Detectable anti-PA IgG levels were observed in 95% of participants after the second dose and 100% of participants after the third administration [24,25]. The novel oral typhoid vaccine M01ZH09, as an LAV, was also shown to be safe and potently immunogenic [26].

The only available vaccine against TB is the Bacillus Calmette–Guérin (BCG) vaccine, a live attenuated strain of *Mycobacterium bovis*. The vaccine has been medically used for public immunization since 1921 [27]. BCG vaccine administration using the pulmonary mucosal delivery route conferred protection in rhesus macaques associated with production of T-helper type 17 (TH17) cells, interleukin-10, and immunoglobulin A [28]. Intravenous BCG vaccination also protected 9 out of 10 rhesus macaques from TB infection [29].

However, the BCG vaccine was reported to have lost protective efficacy against emerging TB strains. The BCG vaccine conferred lower levels of protection against a virulent TB HN878 strain that could spread to the liver and spleen. The vaccine was also unable to offer adequate protection against inflammation, weight loss, and lung and brain pathology resulting from HN878 infection [30]. While it is true that the BCG vaccine did confer partial protection in infants, there are reports indicating that the vaccine is no longer effective in protecting adolescents and adults [31]. Martinez et al. (2022) reported that the effectiveness of the BCG vaccine in protecting against all forms of TB was only 18%. The vaccine only conferred significant levels of protection in infants less than 5 years of age. The vaccine also failed to confer significant levels of protection against extrapulmonary tuberculosis. The data suggested that booster immunizations were required in older populations in order to sustain protection against TB infection [31]. While the BCG vaccine did lead to a reduction in cases of miliary tuberculosis, the vaccine conferred minimal levels of protection against primary TB infection and the reactivation of latent pulmonary tuberculosis [32,33].

Recently, another LAV candidate, known as MTBVAC, has been developed against *M. tuberculosis*. MTBVAC has shown promising results in preclinical and clinical development [34–36]. MTBVAC was shown to be an effective replacement for the BCG vaccine in a preclinical study that focused on the safety, immunogenicity, and protective efficacy of the vaccine when it was administered to newborn C57/BL6 mice [34]. No deaths or disease symptoms were reported in any of the mice immunized with the vaccine. There was also no impact on growth and organ development in mice. IFN-γ analysis after immunization demonstrated high IFN-γ production when splenocytes from mice were stimulated with Ag85B, the antigen expressed by MTB, or with purified protein derivative (PPD) as a control. An evaluation of the protective efficacy conferred by the vaccine showed that bacterial loads in the lungs and spleen were significantly reduced upon immunization with MTBVAC when compared to vaccination of mice with the BCG vaccine [34].

Preclinical studies conducted in rhesus macaques have also shown the ability of LAVs to induce potent immune responses against *M. tuberculosis*. Administration of the BCG vaccine followed by either MVA.85A, a modified vaccinia virus Ankara encoding antigen 85A, or an LAV showed that both booster doses were effective and induced strong immune responses. Evaluation of protective efficacy showed reduced pathology and chest X-ray scores, reduced lung bacterial loads, as well as increased IFN-γ production as an immune correlate of protection [37]. The discovery of MTBVAC as a live vaccine candidate as well as its development, characterization, and elicitation of immune responses in animals and humans have remarkably progressed over 25 years. The BCG vaccine is still regarded as the gold standard and phase III efficacy trials of MTBVAC have been conducted in TB-endemic countries of Sub-Saharan Africa in 2021 [38].

The development of an LAV against *S. aureus*, based on an auxotrophic mutant of *S. aureus* MRSA strain, has also been reported. Attenuation was successfully achieved through the induction of interference in D-alanine biosynthesis, which is vital for the structural integrity of bacterial cell walls and bacterial cell viability. Intravenous and intraperitoneal administrations of the attenuated vaccine strain resulted in the elicitation of potent humoral responses in terms of the production of cross-reactive antibodies produced against multiple *S. aureus* strains [39].

2.2. IVs

There are also documented examples of the use of the IV platform to develop vaccines against antibiotic-resistant bacteria. An evaluation of the immune responses and vaccine protective efficacy resulting from the immunization of BALB/cJ mice with IVs developed using whole cells of antibiotic-exposed MDR *A. baumannii* (I-M28-47-114) and non-antibiotic-exposed control (I-M28-47) showed that the IV candidate could induce clearance of bacterial pathogens as well as confer protection against MDR *A. baumannii*. Analysis of the humoral responses after vaccination showed that both vaccines could elicit high levels of IgG antibodies 5 days after immunization. Nevertheless, sera from mice immunized with the I-M28-47-114 vaccine candidate showed a much higher complement-mediated bacteriolysis rate, reaching as high as 80.7% when compared with the sera from mice immunized with I-M28-47. Macrophage-like U937 cells present in the sera of mice immunized with I-M28-47-114 showed a clearance rate of 49.3% of MDR *A. baumannii* [40].

2.3. Limitations of Conventional Vaccine Platforms

Conventional vaccine platforms such as LAVs and IVs against infectious diseases have indeed protected humans against 20 million infections and 40,000 deaths, contributing to savings of approximately USD 69 billion in healthcare and medical costs in the United States alone [41]. However, the emergence of highly infectious COVID-19 has led to the introduction of novel vaccine platforms and has also provided insight into the superiority of next-generation vaccine platforms over traditional vaccines such as LAVs and IVs. The pandemic has shed light on the limitations of traditional vaccination approaches. The use of conventional LAV platforms is not considered to be feasible or safe in terms of large-scale production of LAVs to vaccinate against viral diseases because of the danger it poses in terms of potential reversion to virulence through mutations or recombinations [42]. The development of effective LAVs necessitates making multiple mutations in the genome, including deleterious gene mutations, altered replication potential, codon deoptimization, and gene regulation by microRNAs [43]. Logically, the development of effective LAVs as vaccines could only be undertaken if there is extensive information about the bacterial genes and their functions so that any potential reversion to virulence could be prevented. This venture is made even more challenging as a result of aberrant gene expression arising from antibiotic usage, which is associated with higher rates of mutagenesis and greater virulence [44].

Although there are several examples of the use of IVs to immunize against antibiotic-resistant bacteria, it is also true that the IV platform is associated with certain limitations. One major disadvantage that IVs pose is the high toxicity of the chemical agent used to inactivate bacterial cells. For example, in order to develop the IV against MDR *A. baumannii*, Shu et al. (2016) inactivated bacterial cells using formaldehyde [40]. The challenge with using such inactivating chemical agents in IVs is that the high toxicity has to be neutralized by laboratory processes, such as removal, dilution, and/or conversion of the inactivating agent into a non-toxic form. Considering that the development of vaccines against AMR bacteria is geared towards the production of large quantities of vaccines for public immunization, these processes of growing significant amounts of bacteria could be considered to be tedious and time consuming [45]. Furthermore, the inactivation process might leave the IV significantly less immunogenic, which would necessitate the production of large amounts of vaccine antigens to induce adequate immune responses [46]. Live pathogens

are needed to be grown in large quantities in order to cater to large-scale production, which could potentially pose an alarming problem of safety to personnel working in the plant [47].

3. Current Preclinical and Clinical Development of Next-Generation Vaccines against AMR Bacteria

Considering that conventional vaccine platforms such as LAVs and IVs have major limitations, it is important to consider developing next-generation vaccines. As witnessed by the success of the novel vaccine platforms against SARS-CoV-2, next-generation vaccine development approaches offer certain advantages over traditional vaccine platforms in terms of convenience, potent elicited immune responses, and stronger safety profiles. Although novel vaccine platforms, such as mRNA and viral-vectored vaccines, have been successful in terms of potent elicited immune responses and stronger safety profiles, their effectiveness turned out to be much lower than anticipated in 2020 [48]. Also, several severe adverse effects upon vaccination, such as myocarditis, have been increasingly reported, pointing to the need for more and longer term studies for evaluating the associated risks [49]. The elicitation of humoral and cellular immune responses from the administration of next-generation vaccine platforms such as DNA, mRNA, and recombinant protein vaccines is illustrated in Figure 2.
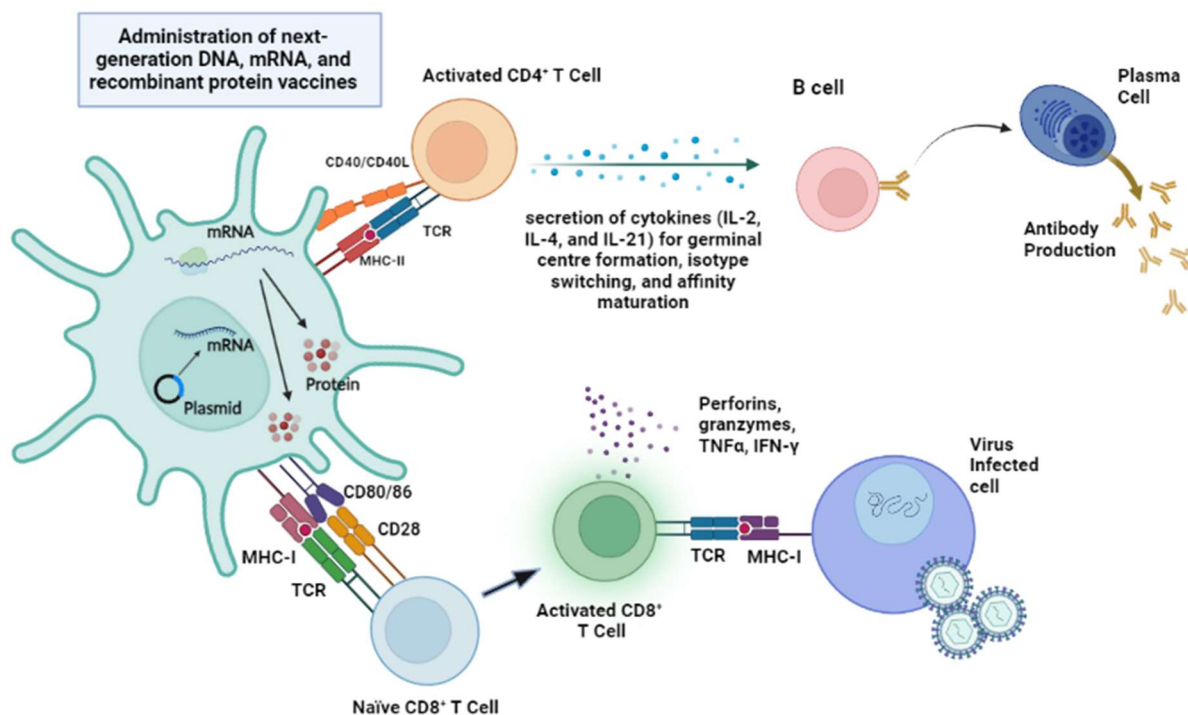
Figure 2. Elicitation of humoral and cellular immune responses from the administration of next-generation vaccine platforms such as DNA-, mRNA-, and recombinant protein vaccines. The administration of DNA vaccines requires DNA to be taken up by antigen-presenting cells (APCs) such as dendritic cells. Once inside the cell, the DNA needs to reach the nucleus to be transcribed into messenger RNA (mRNA). After transcription, the newly synthesized mRNA is transported out of the nucleus into the cytoplasm. In the cytoplasm, the mRNA serves as a template for protein synthesis. mRNA vaccines, on the other hand, can be directly translated in the cytoplasm. Once the protein is synthesized in the cytoplasm, it can undergo further modifications and processing to acquire its final functional form. These proteins can then be presented on the surface of APCs, initiating an immune response and triggering the production of specific immune cells and antibodies that provide protection against the targeted pathogen. Recombinant protein vaccines may serve as antigens after processing by APCs and subsequently presented on MHC class I and class II molecules for the activation of CD4$^+$ and CD8$^+$ T cells. Specialized CD4$^+$ T cells, namely T follicular helper (Tfh) and

Foxp3$^+$ T follicular regulatory (Tfr) cells, play crucial roles in facilitating germinal center B cell formation through interactions with T and B cells. Tfh cells provide assistance to B cells through interactions between CD40L on Tfh cells and CD40 on B cells, leading to the release of cytokines such as IL-2, IL-4, IL-21, and IFN-γ. These cytokines further stimulate the formation of germinal centers, promoting maturation into plasma cells that produce memory B cells and long-lived antibody-secreting plasma cells. On the other hand, CD8$^+$ T cells directly combat infections by targeting and eliminating infected cells using perforin and granzymes, thereby restricting the pathogen's spread within the body.

3.1. Recombinant Protein Vaccines

3.1.1. Advantages of Recombinant Protein Vaccines

The development of recombinant protein vaccines has been described as a promising approach to elicit potential immune responses, and recombinant proteins are emerging as potentially strong candidates for immunization against bacterial diseases based on the practical advantages of stability, safety, high immunogenicity with the use of adjuvants, and a proven track record in clinical development. The recombinant protein platform is considered to be safe and non-infectious. It is easier to produce a vaccine antigen as a recombinant protein when compared to LAVs and IVs [50]. The advantage associated with immunization using recombinant protein vaccines is that they do not require the use of cold chain storage in freezers and liquid nitrogen to store and preserve the vaccine at temperatures lower than −80 °C, which suggests that they could be used to immunize populations in resource-poor third world countries lacking cold chain facilities. Indeed, recombinant protein vaccines may be freeze-dried or lyophilized, allowing them to be preserved in a dried powdered form. For example, Lai et al. (2021) discussed the development of insect cell-expressed SARS-CoV-2 spike protein ectodomain constructs compatible with lyophilization and storage in a dry thermostabilized state [51]. Moreover, freeze-dried, heat-stable formulations of influenza subunit vaccines were safe and immunogenic when administered to mice [52].

There are several expression systems available for the production of recombinant proteins. *Escherichia coli* is commonly used as an expression system since it possesses unparalleled fast-growth kinetics, enabling the rapid production of recombinant proteins. The ability to achieve high cell density cultures is another significant benefit, as it enables large-scale production of proteins in a more efficient manner. Additionally, *E. coli* expression systems utilize media that can be easily formulated using readily available and inexpensive components, thereby reducing production costs. Moreover, the process of transforming *E. coli* with exogenous recombinant DNA is fast and straightforward, facilitating the introduction of the desired genes for protein expression [53]. Baculovirus-mediated expression using Spodoptera frugiperda Sf9 insect cells has emerged as a widely accepted method for producing recombinant glycoproteins. This approach is favored due to its simplicity and rapidity in expressing foreign proteins. Moreover, it offers a high likelihood of obtaining biologically active proteins, further contributing to its popularity in the field of protein production [54]. Moreover, the resemblance of protein secretion pathways between yeasts and higher eukaryotic organisms has meant that yeasts such as *Pichia pastoris* (syn *Komagataella* spp.) are now also widely recognized as favorable hosts for the production of various recombinant proteins [55]. The extracellular secretion of recombinant proteins by yeasts simplifies the downstream purification process, making it more cost effective [56].

3.1.2. Disadvantages of Recombinant Protein Vaccines

Recombinant proteins, such as those produced in *E. coli*, require purification from mixtures of crude lysates, which can be expensive and time consuming. Affinity tags are specific proteins or peptides that may be attached to the N- or C-terminus of recombinant proteins to aid in their purification. One commonly used approach is fusing the recombinant protein with glutathione S-transferase (GST) or a poly-histidine (His) tag, enabling purification through affinity chromatography [57,58].

The endotoxins found in the cell walls of most Gram-negative bacteria like *E. coli* can trigger inflammation and septic shock when these bacteria enter the bloodstream of a mammalian host. These effects are caused by endotoxins that stimulate the production and release of inflammatory mediators by host cells sensitive to lipopolysaccharide (LPS). Recombinant proteins obtained from E. coli often contain endotoxin contamination due to high levels of LPS in the cell wall. Even small amounts of endotoxin in recombinant protein preparations can lead to adverse reactions such as shock. Therefore, it is crucial to remove endotoxins from recombinant proteins to prevent these harmful reactions [59]. Nevertheless, endotoxins may be conveniently removed from purified proteins through the use of a porous cellulose bead surface modified with covalently attached poly(ε-lysine) chains, which possesses high binding affinity for endotoxins. The purified proteins may then be monitored for endotoxins using endotoxin quantification assays [60].

In conclusion, recombinant protein vaccines require multiple purification steps involving conventional column or affinity chromatography during the manufacturing process. These purification steps are essential to purify the recombinant protein of interest, but they can be time consuming, labor intensive, and costly, adding complexity to the production process. Additionally, recombinant protein vaccines may require the use of adjuvants to enhance and prolong the immune response. Adjuvants are added to vaccines to stimulate the immune system and have dose-sparing effects. While adjuvants can be beneficial, their use also introduces additional considerations such as safety, compatibility, and potential side effects.

3.1.3. Recombinant Protein Vaccine Candidates

The recently developed recombinant *Mycobacterium bovis* BCG Vaccine, VPM1002, serves as an important vaccine candidate in the late stages of clinical testing, which could potentially replace the BCG vaccine for public immunization against TB [61]. The recombinant VPM1002 vaccine was shown to be superior to the BCG vaccine in terms of immunogenicity and safety in several ways [61]. Through the characteristic expression of a hemolysin known as listeriolysin (Hly), which was isolated from *Listeria monocytogenes*, the VPM1002 vaccine candidate was able to direct the efficient translocation of antigens to the cytosol where they could be presented to CD8$^+$ T cells. It was also demonstrated that immunization with the VPM1002 vaccine candidate could elicit CD8$^+$ T cells and stimulate CD4$^+$ memory T cells, including increased production of T helper 1 (TH1) and TH17 cells, far more significantly than the administration of the BCG vaccine. The safety level associated with VPM1002 immunization was higher than that linked with BCG immunization, as evidenced by more accelerated clearance of the VPM1002 vaccine from the host cell tissue as compared to increased persistence of the BCG vaccine [62].

The main challenge associated with curbing the spread of TB is the emergence of drug-resistant TB strains, such as those associated with the Beijing/W genotype family of *M. tuberculosis*, which could potentially cause an alarmingly large number of MDR infections [63]. Indeed, the traditional BCG vaccine has significantly lost vaccine protective efficacy against *M. tuberculosis* Beijing/W genotype strains. The BCG vaccine could confer only very modest levels of protection in animal models infected with the *M. tuberculosis* Beijing/W strain [30,64]. Moreover, Grode et al. (2005) corroborated this experimental finding in BALB/c mice whereby mice immunized with the BCG vaccine showed minimal or complete lack of protection against an *M. tuberculosis* Beijing/W strain [65].

However, equipping the BCG vaccine with the membrane-perforating listeriolysin (Hly) of *L. monocytogenes* to form the Hly-secreting recombinant BCG (*hly*$^+$ rBCG) vaccine and the isogenic, urease C-deficient *hly*$^+$ rBCG (Δ*ureC hly*$^+$ rBCG) vaccine showed improved protection against *Mycobacterium tuberculosis*. The Hly-secreting recombinant BCG (*hly*$^+$ rBCG) vaccine was shown to offer significantly better protection against aerosol infection with *M. tuberculosis* than the parental BCG vaccine strain. The Δ*ureC hly*$^+$ rBCG vaccine also induced profound protection against a member of the *M. tuberculosis* Beijing/W genotype family, while the parental BCG vaccine strain failed to do so consistently [65].

Another critical subgroup at risk of infection and mortality resulting from TB are children under 15 years of age. It was observed that as many as 32,000 new infections of MDR-TB occurred in children throughout the globe [66]. Considering that therapeutic and preventive anti-TB interventions are accessible to only a small fraction of these children, current vaccines against MDR-TB are also being tested in children. After successfully progressing through the preclinical and early stages of clinical development, the VPM1002 vaccine candidate is currently being evaluated for safety and immunogenicity in infants in different regions of Africa. The results of the safety and immunogenicity of VPM1002 in phase II clinical development in 48 newborn infants immunized with the VPM1002 vaccine or the BCG Danish vaccine strain showed that whilst both vaccines were able to elicit interleukin-17 (IL-17) responses, only the VPM1002 vaccine resulted in increased stimulation of $CD8^+$ $IL-17^+$ T cells at week 16 and at the 6-month time point. Abscess formation was less commonly observed in participants immunized with the VPM1002 vaccine when compared with the BCG vaccine [62]. These results corroborated the findings obtained with the VPM1002 vaccine in phase I clinical trials conducted in adults [67]. Another phase II study for VPM1002 is ongoing [68].

In the development of promising next-generation vaccines based on recombinant plasmids against MDR-TB, Chiwala et al. (2021) developed a recombinant vaccine in which overexpressed Ag85B and Rv2628 genes were isolated from drug-resistant *M. tuberculosis* strains. The recombinant plasmid pIBCG was expressed in *E. coli* to produce RdrBCG-I [69]. After confirmation of high levels of the expression of exogenous genes from the vector pIBCG, the protein-based vaccine was administered to BALB/c mice inoculated with rifampin-resistant *M. tuberculosis*, which was also administered with a second-line anti-TB drug regimen. Upon administration of the vaccine, *M. tuberculosis* burden in the lungs was reduced by one log. Lung tissue pathology was also reduced when the vaccine was administered together with the anti-TB drugs. Administration of the recombinant protein-based vaccine led to the inhibition of *M. tuberculosis* growth and development. The expressed proteins, Ag85B and Rv2628, acted as potent antigens and led to elicitation of the Th1 immune response, which sustained the continuous inhibition of rifampin-resistant *M. tuberculosis* [69].

Recombinant protein vaccines have also been developed against *Klebsiella pneumoniae*. The high heterogeneity of *K. pneumoniae* strains is a limiting factor for the inclusion of all capsular or LPS serotypes. The YidR protein, which is highly conserved among *K. pneumoniae* strains, could serve as an effective vaccine. Rodrigues et al. (2020) developed a recombinant protein vaccine and evaluated its protection against lethal challenge with a lethal dose (LD_{100}) of K. pneumoniae in mice. Elevated levels of total serum IgG were observed in vaccinated mice when compared with naïve mice. Approximately 90% of vaccinated mice survived for 10 days following intraperitoneal challenge with *K. pneumoniae*, while non-immunized mice did not survive past 48 h following inoculation with the bacterium [70]. Thus, the Yidr recombinant protein vaccine could serve as a promising vaccine candidate against *K. pneumoniae*.

3.2. DNA Vaccines

3.2.1. Advantages of DNA Vaccines

Although clinical data on DNA vaccine development against bacteria is lacking when compared to the recombinant protein-based vaccine approach, DNA vaccine development is emerging as a promising solution to the spread of opportunistic pathogens. DNA vaccines are easier to produce in large quantities when compared to the complexities of producing IVs and mRNA vaccines [71]. It is also relatively easy to produce DNA vaccines in large quantities for distribution and large-scale immunization in under-developed countries [72]. The recombinant plasmid DNA can be conveniently produced in large quantities in bacteria, such as *E. coli*, or expressed in eukaryotic cells, such as HEK-293 T cells [72].

3.2.2. Disadvantages of DNA Vaccines

DNA vaccines, while holding great potential, also come with disadvantages. One significant drawback is their lower immunogenicity compared to traditional vaccines. DNA vaccines may not elicit robust immune responses, requiring additional measures to enhance their effectiveness [73,74]. Another concern is the risk of genomic integration, where the introduced DNA may become integrated into the recipient's genome. While the likelihood of this event is low, it is an important aspect to consider during vaccine development [75]. To improve immunogenicity, DNA vaccines often require the use of adjuvants, which can increase the immune response but may also introduce additional complexities and potential side effects [76]. Furthermore, the administration of DNA vaccines typically requires a medical device like the use of an electroporator that can deliver electric pulses to facilitate the uptake of DNA by cells [77]. This requirement may limit the accessibility and widespread use of DNA vaccines, particularly in resource-limited settings lacking such specialized equipment. Although needleless patch administration is an alternative being explored, it is still under development and not widely available.

3.2.3. DNA Vaccine Candidates

A. baumannii is an opportunistic bacterium that is resistant to 90% of commonly prescribed antibiotics. By incorporating the outer membrane protein A (OmpA) gene into the expression vector, Ansari et al. (2019) demonstrated that administration of the DNA vaccine was able to elicit both humoral and cellular immunity in terms of the production of IgM, IgG, IL-2, IL-4, IL-12, and INF-γ [78]. Furthermore, Hashemzehi et al. (2018) expressed the NlpA gene as the main antigen in expression vectors pTZ57R/T and pEGFP-C2, followed by their administration in BALB/c mice. Elevated levels of IgG, IgM, INF-γ, IL-2, IL-4, and IL-12 were observed in the immunized mice [79].

3.3. mRNA Vaccines

The development of vaccines against antibiotic-resistant bacteria is a long and arduous process. Considering the process of initial development, preclinical testing in animal models, and clinical trials involving safety and immunogenicity evaluations, vaccine development could easily take 10–15 years [80]. Due to the rapid emergence of resistant strains, the clinical progression of vaccine development involves high costs and long regulatory processes [18].

3.3.1. Advantages of mRNA Vaccines

Nevertheless, the novel mRNA vaccine platform is viewed as a promising solution to develop vaccine candidates against antibiotic-resistant bacterial strains at an accelerated pace. mRNA vaccines were the first vaccine candidates against SARS-CoV-2 that progressed to clinical development and received emergency use authorization (EUA) for large-scale public immunization. Indeed, this approval was provided only 11 months after the nucleotide sequence of the SARS-CoV-2 Wuhan strain became available in the public domain [81]. The mRNA vaccines served as highly effective and safe anti-COVID-19 vaccines but did not protect vaccinated patients from passing on the virus [82,83]. Smith et al. (2020) expressed the view that nucleic acid vaccines such as DNA and mRNA vaccines offer certain advantages that are well suited to combat rapidly emerging variants. A number of vaccine candidates could be efficiently and quickly developed, progress at an accelerated speed from the preclinical to the clinical stages through already established regulatory pathways, and be manufactured in abundant amounts for large-scale immunization [84]. Multiple mRNA vaccine candidates might be developed by simply changing the nucleotide sequence of the main antigenic region when faced with emerging resistant pathogenic strains.

3.3.2. Disadvantages of mRNA Vaccines

One notable drawback of mRNA vaccines is their inherent instability, which necessitates storage at ultra-low temperatures of around −80 °C [85]. This requirement poses

logistical challenges, particularly in regions with limited access to specialized cold chain infrastructure. Additionally, the manufacturing process for mRNA vaccines involves a complex two-step in vitro reaction and purification platform. Multiple intricate steps, including DNase digestion, precipitation, and chromatography or tangential flow filtration are required [86]. These steps can be time consuming and demanding, requiring specialized equipment and expertise. Consequently, the production costs may be higher, and the overall manufacturing process may be slower compared to conventional vaccines. Despite these challenges, ongoing research aims to address these limitations by developing new technologies that improve the stability and simplify the production process of mRNA vaccines, thereby enhancing their accessibility and scalability.

3.3.3. mRNA Vaccine Candidates

In recent years, *L. monocytogenes* has emerged as a highly pathogenic bacterium that is able to thrive even in adverse conditions such as very low temperatures and anaerobic conditions. *L. monocytogenes* is reported to be a highly virulent pathogen, as 20–30% of listeriosis cases are fatal. Efforts to develop mRNA vaccines against *L. monocytogenes* are underway. Recently, Mayer et al. (2022) identified 68 *Listeria* immunopeptides from different bacterial surface proteins that could serve as novel antigens, which were utilized in the development of lipid nanoparticle-based mRNA vaccine formulations [64]. The antigenic sequences of seven proteins were represented in nucleoside-modified mRNA encapsulated in cationic liposomes, including α-galactosylceramide (α-GC) as an adjuvant, and used for the immunization of C57BL/6J mice. The use of an adjuvant led to the activation of invariant natural killer T (iNKT) cells and specific T cell responses. Experiments showed that immunization with the top vaccine candidate, LMON_0149, was able to confer protection in mice when challenged with *L. monocytogene* due to the elicitation of strong cellular immune responses [87].

Kon et al. (2022) reported the development of an mRNA lipid nanoparticle (mRNA-LNP) vaccine against the plague, a highly infectious disease caused by the Gram-negative bacterium *Yersinia pestis* [88]. The status of *Y. pestis* as a serious bioterrorism agent is owing to its high infectivity, pathogenicity, alarming mortality, as well as the emergence of multiple antibiotic-resistant strains of *Y. pestis,* which warrants the development of an effective vaccine to prevent the occurrence of outbreaks caused by antibiotic-resistant strains of *Y. pestis.* Two mRNA-LNP vaccine candidates were constructed based on the F1 capsular antigen (caf1). One that contained the bacterial F1 capsular antigen together with a signal peptide (SP) originating from the human Ig right chain and one that contained the non-secreted ΔSP-caf1, which lacked the native signal sequence, were encapsulated in mRNA-LNP formulations and used for immunization experiments. Immunogenicity was investigated in mice that were immunized three times with 5 µg of each construct, SP-caf1-hFc or ΔSP-caf1. Potent anti-F1 humoral and antigen-specific cellular immune responses were elicited as a result of immunization with both vaccine candidates. Furthermore, challenge of the immunized mice with a high dose of virulent *Y. pestis* demonstrated that both vaccine candidates were able to offer full protection against the virulent *Y. pestis* Kimberly 53 strain. In contrast, naïve mice were not able to survive the challenge [88]. Therefore, the data indicated that the mRNA-LNP vaccine platform could serve as an effective mode of immunization against emerging bacterial strains, especially those that have acquired resistance against current antibiotics.

However, the use of LNPs in vaccines has been associated with challenges due to the occurrence of allergic reactions such as anaphylaxis. Out of the 1,893,360 initial doses of the Pfizer-BioNTech COVID-19 vaccine, there were 175 cases of severe allergic reactions. Among these, 21 cases were identified as anaphylaxis: 17 individuals had medical histories of allergies or allergic reactions, and 7 had histories of anaphylaxis. Furthermore, out of 4,041,396 recipients, 10 cases of anaphylaxis were identified: 9 individuals had documented histories of allergies or allergic reactions, and 5 had previous histories of anaphylaxis [89]. Anaphylaxis resulting from immunization with the Pfizer-BioNTech COVID-19 vaccine

was shown to be attributable to the use of polyethylene glycol (PEG). Allergy skin prick testing showed that anaphylaxis was induced when polyethylene glycol was used [90]. This underscores the importance of adhering to safety protocols during investigations, emphasizing the need for safety testing when utilizing LNPs containing PEG compounds. The advantages and limitations associated with the use of next-generation vaccines relative to conventional vaccine platforms are summarized in Table 1.

Table 1. The advantages and limitations associated with the use of next-generation vaccines relative to conventional vaccine platforms.

Vaccine	Advantages	Limitations	References
LAVs	- Ability to induce potent and long-lasting humoral and cellular responses with minimal doses. - Convenience in terms of storage, distribution, and administration. - Immune responses directed against the whole pathogen.	- Not safe for large-scale production. - Risk of potential reversion to virulence. - Necessitate extensive information about the bacterial genes and their functions. - High rates of bacterial mutations in vaccine stock strains.	[41–44]
IVs	- Safe and immunogenic. - Lack of serious side effects. - Convenience in terms of transport and storage. - Administration of a killed virus ensures safety.	- Growth of large quantities of live pathogens for large scale production could pose an alarming problem of safety to personnel working in the plant. - Extensive and tedious laboratory processes, such as removal, dilution, and/or conversion of the highly toxic inactivating chemical agents into non-toxic forms. - The inactivation process might leave the IV significantly less immunogenic. - Necessitates the production of large amounts of vaccine antigens to induce adequate immune responses.	[40,45–47]
Recombinant protein vaccines	- Safe and non-infectious. - Elicit strong immune responses. - Proven track record. - Convenient storage in freeze-dried forms. - Do not require ultra-cold storage temperatures.	- Require several purification steps involving column and affinity chromatography. - Adjuvant is needed to enhance long-term immunity.	[50–56]
DNA vaccines	- Can be conveniently produced in bulk quantities compared to IVs and mRNA vaccines. - Cost effective when compared to the complexities involved in producing IVs or mRNA vaccines. - Suitable for distribution and large-scale immunization in underdeveloped countries. - Can be conveniently produced in prokaryotic cells, like *E. coli*, or expressed in mammalian cells, such as HEK-293 T cells.	- Lower immunogenicity. - Risk of genomic integration. - Requires adjuvants for enhanced immunogenicity. - Immunizations necessitate the use of medical devices like electroporators. - Needleless patch administration is still under development.	[71–77]
mRNA vaccines	- Accelerated development from preclinical to clinical stages using established regulatory pathways. - High levels of safety. - Effective in providing protection against COVID-19. - The nucleotide sequence of mRNA vaccines can be easily modified to target emerging resistant pathogenic strains.	- Expensive to develop and produce. - Requires ultra-low temperatures of −80 °C. - The high cost and demanding storage conditions of mRNA vaccines can render them logistically inconvenient and expensive for many low-income countries.	[81–86]

3.4. Comparison between Next-Generation mRNA, Recombinant Protein, and DNA Vaccines

The COVID-19 pandemic has presented a unique opportunity to gain significant knowledge about the safety, efficacy, and breadth of the immune responses of next-generation vaccines, specifically mRNA, recombinant protein, and DNA vaccines. In recent years, the field of vaccine design has undergone a paradigm shift through the utilization of reverse vaccinology. This innovative approach aims to identify prospective vaccine candidates by employing bioinformatics analysis of the pathogen genome. The valuable insight garnered from studying these vaccines in the context of the pandemic can provide crucial aspects for next-generation vaccine development against antibiotic-resistant bacteria using the reverse vaccinology approach.

3.4.1. Safety

The reactivity of mRNA vaccines depends on their ability to express foreign antigens, leading to the elimination of infected antigen-presenting cells (APCs). Although lipid nanoparticles (LNPs) can induce an acute inflammatory response, the trials conducted so far have not detected significant signs of adverse safety when employing LNPs for the delivery of small molecules, non-expressing RNAs, or RNAs encoding endogenous proteins [91]. New advancements offer potential remedies for various disease conditions in the context of biomedical technologies. However, it is crucial to carefully assess the potential risks associated with their usage. mRNA technology, being a relatively novel approach, necessitates the consideration of safety concerns, not only in existing products but also in future developments. Therefore, it is imperative to conduct further research to ensure the safety of both current and future users of this technology.

Safety issues associated with DNA vaccines include concerns about the integration of plasmid DNA into the host genome, potential adverse immunopathological effects, the development of anti-DNA antibodies leading to autoimmune diseases, and the utilization of novel molecular adjuvants. Additionally, there is a noteworthy safety consideration regarding the potential dissemination of genetic material to the environment. This could occur through transformation of the environmental microflora, even with a limited number of complete or fragmented plasmid copies. These concerns necessitate careful evaluation during the scientific decision-making process for vaccine registration. Consequently, projects should be initiated to assess the risks associated with plasmid DNA vaccination, aiming to establish criteria for guidance and regulations for both the industry and licensing authorities [92]. So far, there has been no evidence showing plasmid integration into genomes.

Recombinant protein vaccines offer several advantages, including their non-replicating nature and absence of infectious components. These characteristics help position them as a safer alternative when compared to vaccines derived from live viruses. Extensive testing of this vaccine platform has demonstrated that these vaccines typically elicit only mild side effects. As a result, multiple recombinant protein vaccines have been successfully utilized in clinical settings worldwide [56].

3.4.2. Vaccine Protective Efficacy and Breadth of Immune Responses

With a strong record in the clinic, recombinant protein vaccines have shown high rates of protective efficacy. Indeed, recombinant protein vaccines against Pasteurella multocida, comprising the rPlpE and OmpH of P. multocida strain PMWSG-4 + adjuvant, showed efficacies of 83.33%, and 83.33%, respectively. Reverse vaccinology, when employed to clone all three immunogenic regions in order to develop a recombinant protein vaccine expressing rVacJ, rPlpE, rOmpH, and an adjuvant, led to an increase in vaccine efficacy to 100% protection [93].

Vaccine development against SARS-CoV-2 yielded important information regarding immune responses elicited upon immunization with mRNA and recombinant protein vaccines [94]. Following the initial immunization, mRNA and recombinant protein vaccines induced detectable levels of RBD-specific IgG and neutralizing antibodies, with significantly higher levels seen after the second immunization. Notably, by day 35 after the first

vaccination, the mRNA vaccine group exhibited notably elevated neutralizing antibody titers compared to the recombinant protein vaccine group. The recombinant protein vaccine group demonstrated its highest antibody titers on day 21 after the initial vaccination, whereas the mRNA vaccine group reached its peak response on day 35 following the first immunization. The recombinant protein vaccine induced a faster humoral immune response compared to the mRNA vaccine, while the mRNA vaccine required a longer duration to induce its peak immune response. Therefore, even though both platforms were able to elicit potent immune responses, the differences in terms of the time taken to reach peak immune response might differ between different vaccine platforms [94].

4. Immunoinformatic Approaches for the Development of Multi-Epitope Vaccines

4.1. Immunoinformatics Tools for Epitope Prediction and Analysis

In silico predictions and vaccinomics offer a promising strategy for the identification of specific epitopes that could serve as potent antigens capable of eliciting broad and immunological long-lasting responses against different strains of antibiotic-resistant bacteria. Information on immunogenic epitopes for vaccine development purposes may be acquired through the use of computational bioinformatics tools. Indeed, Jespersen et al. (2019) identified BepiPred, ABC pred, Discotope, and CBtope as examples of recent developments in the bioinformatics approach using computer algorithms that employed amino acid sequences or 3D structures to predict B cell epitopes [95].

Moreover, multiple databases, including MHCBN, LANL, SYFPEITHI Parker hydrophilicity, BepiPred, and the Immune Epitope Database, also serve as online tools for the prediction of B cell epitopes [96]. This strategy might prove to be more effective when compared to the use of full-length protein sequences that are highly susceptible to mutations, leading to the emergence of antibiotic-resistant bacterial strains. The literature provides extensive evidence for the development of multi-epitope vaccines against a variety of antibiotic-resistant bacteria.

4.2. Literature Review: Immunoinformatics Approaches in Vaccine Development

Dosoriti et al. (2019) employed a vaccinomics approach to yield cytotoxic and helper T cell epitopes capable of triggering a potent immune response against *Streptococcus pneumoniae* [68]. PspA and CbpA were selected as potential CTL epitopes while PhtD and PiuA were chosen as the helper T cell epitopes. The PorB protein was chosen to serve as a TLR2 agonist to increase the potency of the immune response. Molecular docking analysis confirmed that there was an appropriate and stable interaction between the vaccine and TLR2. Based on computational analysis, the chosen epitopes could be joined together with linkers to yield a multi-epitope vaccine capable of stimulating both humoral and cell-mediated immune responses against *S. pneumoniae* [97].

The spore-forming bacterium *Clostridium difficile* is known to cause diarrhea, fever, nausea, and abdominal pain. *C. difficile* is anaerobic and the spores are able to survive in the external environment for months, thereby increasing the transmissibility of the pathogen. The use of antibiotics to treat *C. difficile* infections disrupts the balance of the composition of the host microbiota in the gut. Toxin-producing *C. difficile* colonizes the gut, causing antibiotic-associated diarrhea and pseudomembranous enteritis. Furthermore, *C. difficile* is becoming increasingly resistant to antibiotics that are currently prescribed for treatment and is associated with a high rate of re-emergence following antibiotic treatment. The high morbidity and mortality of *C. difficile* in the immunocompromised patient community as well as the risk of outbreaks caused by antibiotic-resistant strains call for the urgent development of vaccines to prevent *C. difficile* infections.

Tan et al. (2022) used an immunoinformatics approach to develop a multi-epitope vaccine against *C. difficile* using the Prabi and RaptorX servers for 2D and 3D structural visualizations of the vaccine construct [98]. Molecular docking simulations were used to predict the compatibility of the interaction models of the vaccine–receptor (TLR) complex, vaccine–MHC complexes, and vaccine–B cell receptor (BCR) complex. Simulation of the

immune responses, population coverage analysis, and in silico molecular cloning were performed. Following immunoinformatics analysis, five cytotoxic T cell lymphocyte (CTL) epitopes, five helper T lymphocyte (HTL) epitopes, and seven B cell linear epitopes from the CdeC protein, which plays an essential role in spore germination, and the fliD protein, which is responsible for propagule colonization, were chosen for constructing the vaccine. The adjuvant LT-IIb was incorporated into the vaccine N-terminus through the use of the EAAAK linker to optimize the elicited immune response. Since the elicitation of intestinal mucosal immunity is integral for protection against *C. difficile*, it is necessary to assess the ability of the vaccine to induce secretory immunoglobulin A (s1gA) production by IgA plasma cells in future studies [98].

Klebsiella aerogenes is a bacterium that has acquired resistance to multiple antibiotics. It is characterized as a Gram-negative, rod-shaped anaerobe. Most *K. aerogenes* strains are resistant to β-lactams and broad-spectrum antibiotics due to the production of β-lactamases. Alzarea (2022) employed an immunoinformatics approach using in silico subtractive proteome analysis to identify vaccine targets [99]. A total of three proteins, namely Fe^{2+}–enterobactin, ABC transporter substrate-binding protein, and fimbriae biogenesis outer membrane usher protein, were shown to be antigenic. Seven epitopes were selected from these three antigens to construct a vaccine comprising seven epitopes joined together by GPGPG linkers. Moreover, the adjuvant from the B subunit of cholera toxin (CTBS) was added to the vaccine construct to enhance immunogenicity. Molecular docking analysis to test interactions of the vaccine with MHC-I, MHC-II, and TLR4 showed that the vaccine construct was able to elicit a potent immune response [100].

More recently, Albekairi et al. (2022) reported the design of a novel multi-epitope-based vaccine against *Enterobacter hormaechei* [101]. The bacterium was reported to be resistant to beta-lactam and tetracycline antibiotics and contributes to a large number of hospital-acquired infections. Reverse vaccinology and immunoinformatics approaches were used to identify the core proteome. An extracellular curlin minor subunit CsgB and two periplasmic membrane proteins were selected as the main antigens for the identification of B and T cell epitopes. In the vaccine construct, a total of three epitopes were joined together using GPGPG and EAAAK linkers to link the cholera toxin B subunit as an adjuvant to optimize the elicited immune response. Molecular docking and binding free energy calculations showed effective interactions between the vaccine construct and MHC-I, MHC-II, and TLR-4 [101]. However, such computation-based molecular simulations would require further experimental validation in vitro and in vivo.

Alshabrmi et al. (2022) reported the development of a multi-epitope vaccine against the MDR *Hafnia alvei* using epitopes from multiple proteins to yield a multi-epitope-based vaccine that was adjuvanted with a cholera toxin B subunit to optimize the immune response [102]. Further experimental validation, both in vitro and in vivo, of the computer-aided vaccine design is required.

Munia et al. (2021) employed the use of literature mining to select choline-binding protein A (CbpA) as an effective vaccine candidate to develop a multi-epitope-based vaccine (MEV) against pneumococcus [103]. An in silico approach was used to determine that the 15-mer T cell epitope (AMATGWLQYNGSWYY) showed high affinity for MHC class I and class II molecules and exhibited high population coverage. T cell-, B cell-, and IFNγ-inducing epitopes were also selected based on a strong affinity between the MEV and TLRs. It was proposed that the vaccine would induce both humoral and cell-mediated responses [103].

Kumar et al. (2019) employed a reverse vaccinology approach to develop a chimeric construct against enterobacterial pathogens by selecting peptides from known immunogenic proteins [104]. Specifically, the yersiniabactin receptor of *E. coli* UMN026 and the flagellin protein of *Stenotrophomonas maltophila* were chosen. B cell linear epitopes were predicted using the Bepipred tool, and peptide binding with a reference set of 27 alleles of MHC class I and class II molecules were analyzed. Simulation dynamics were used to validate the predicted peptide–MHC complexes. The chimeric construct was created through

in silico methods and codon optimization. The immunoinformatics analysis demonstrated that the chimeric construct, composed of gene fragments specifying a significant number of predicted peptides, was highly immunogenic. It was observed that the chimeric construct was more immunogenic, as evidenced an increase in the number of B cell and T cell epitopes and an expansion of the coverage of world populations with allelic variability [104].

4.3. Reverse Vaccinology: An Innovative Approach to Vaccine Development against Antibiotic-Resistant Bacteria

The clinical implications of developing next-generation vaccines based on reverse vaccinology in clinical practice and the field of biomedicine are significant. While initial findings from preclinical experimental studies have shown promising results in terms of vaccine development and immunogenicity, further research is needed to validate the identified epitopes and evaluate the resulting immune responses in animal models. To assess the effectiveness of the proposed vaccine candidates, challenge studies should be conducted to determine whether immunized animals are protected against lethal infections caused by pathogens such as *C. difficile*, *K. aerogenes*, *E. hormaechei*, and *H. alvei*. This step is crucial to ensuring the vaccine's efficacy and its potential to combat these specific infections.

Utilizing immunoinformatics to predict the epitopes from the antigenic regions of the respective pathogens is particularly useful for developing multi-epitope-based vaccines that target antibiotic-resistant strains. This approach enables the identification of specific epitopes that can effectively stimulate immune responses against resistant strains. Moreover, conducting a conservancy analysis of specific amino acid sequences is essential in order to include highly conserved epitopes from antigenic regions. These conserved epitopes have the potential to provide broad-spectrum protection against MDR bacteria, which is a critical aspect in combating the challenges posed by antibiotic resistance. In summary, the utilization of reverse vaccinology in the development of next-generation vaccines holds promising clinical implications. Further research involving animal models, challenge studies, and the identification of conserved epitopes would contribute to the validation and potential application of these vaccines to combat antibiotic-resistant infections in clinical practice.

5. From Research to Real-World Experience: Currently Approved and Clinical Development of Experimental Vaccines against Antibiotic-Resistant Bacteria

5.1. S. enterica Serovar Typhi

Salmonella enterica serotype *typhi*, a bacterium responsible for causing typhoid fever, infects humans when it is ingested in contaminated food and water and survives the acidic conditions in the stomach [105,106]. After entering the lymphoid tissue, infection occurs through lymphatic and hematogenous routes [107]. Typhoid emerges as a fever in the first week that progressively exacerbates to abdominal pain, constipation, and macular rashes in the second week, and to liver and spleen enlargement, ileocecal perforation, peritonitis, and septic shock in week 3. Death might result if the infection remains untreated [108,109].

A number of licensed vaccines against *Salmonella typhi* have been brought to the market for public immunization and they were divided into three categories, namely unconjugated Vi polysaccharide (ViPS) vaccine, live attenuated Ty21a vaccine, and typhoid conjugate vaccine (TCV). The FDA approved two vaccines that have been licensed for use in the USA: Ty21a, an oral attenuated live virus, and the Typhoid Vi polysaccharide vaccine, a ViPS vaccine [110,111]. The live attenuated Ty21a vaccine was shown to elicit immune responses to *S. typhi* lipopolysaccharide in the intestinal tract, thereby conferring protective immunity [112]. The elicitation of an effective immune response required four immunization doses administered on alternate days [113].

Currently, a total of five vaccine candidates against *Salmonella typhi* are in clinical development. The clinical vaccine candidate, EuTCV, which is currently in phase III clinical development, showed favorable results in a phase II/III study, demonstrating high immunogenicity in terms of seroconversion in 99.4% of immunized individuals and a reasonable safety profile. The incidence of both solicited and unsolicited treatment-emergent adverse events (TEAEs) was similar between the EuTCV and comparator Typbar-

TCV® vaccine groups. Out of a total of 444 participants, 130 (29.3%) reported unsolicited TEAEs. Among these, 87 participants (19.6%) experienced unsolicited TEAEs within 28 days after vaccination. The majority of these events (126 cases, 28.4%) occurred within 168 days post-vaccination. Most participants who reported unsolicited TEAEs had mild symptoms, with 128 individuals (28.8%) experiencing the highest grade of mild adverse events. Only 5 participants (1.1%) experienced the highest grade of moderate adverse events. No severe or life-threatening unsolicited TEAEs were reported [114]. Phase III clinical trials conducted in four hospitals in Kathmandu, Dhulikhel, Dharan, and Nepalgunj in Nepal showed that the typhoid Vi polysaccharide-diphtheria toxoid (Vi-DT) vaccine was safe in terms of an anti-Vi-IgG seroconversion rate of 99.33%, showing a good safety profile [115]. Moreover, the phase III clinical development of a Typhoid Vi conjugate vaccine (TCV) was reported to be safe, tolerable, and immunogenic in Malawian children from 9 to 12 years of age. Upon administration of TCV, there was a significant elevation of anti-Vi IgG geometric mean titers from 4·2 EU/mL at baseline to 2383·7 EU/mL at day 28 [116]. Another important candidate that is being evaluated in a phase I clinical trial consisted of a novel bivalent oral vaccine against enteric fever caused by *Salmonella typhi* and *Salmonella paratyphi* A. The vaccine incorporates two antigens, flagellin H:a and lipopolysaccharide (LPS) O:2, to target both *Salmonella typhi* and *Salmonella paratyphi* A [117]. Additionally, there are also eight vaccine candidates against *Salmonella typhi* in the preclinical stage of development.

5.2. H. influenzae Type b

In the past 20 years, there have been significant changes in the epidemiology of *Haemophilus influenzae* infections [118]. In areas where vaccines were extensively administered, invasive *H. influenzae* type b (Hib) disease in children was all but eliminated as a result of the invention and widespread use of Hib conjugate vaccines [118]. By lowering the nasopharyngeal carriage of Hib, Hib conjugate vaccines also helped to lower the number of circulating strains of the disease in the general population [119].

In addition to the three vaccine candidates in preclinical development, there are as many as 46 licensed vaccines for human use to protect against *H. influenzae* infections [120]. In fact, since the 1990s, invasive *H. influenzae* infections in children under 5 years of age had disappeared in developed countries as a result of Hib vaccine administration [121]. It has been demonstrated that vaccination against *H. influenzae* lowered the prevalence of specific drug-resistant *H. influenzae* strains [122]. The vaccine efficacy (VE) of current Hib vaccinations is approximately 94% [123]. Additionally, three of the four more promising vaccines are currently undergoing or have recently completed phase III clinical trials [120]. The pediatric hexavalent vaccine Shan 6 (NCT04429295) successfully demonstrated potent immunogenicity and a good safety profile in 2021 and is in the process of applying for New Drug Application approval [124]. Another promising candidate with its phase I clinical development conducted in 2019 is the LBVD vaccine, a combined diphtheria, tetanus, pertussis, hepatitis B, poliomyelitis, and Hib vaccine [125]. Although safe and immunogenic vaccines for Hib are available for immunization against the disease, future efforts would need to focus on immunizing more people and overcoming the challenges of global coverage in order to curb the spread of drug-resistant Hib strains [126].

5.3. S. pneumoniae

There are currently 17 vaccines targeting *S. pneumoniae* under preclinical development, all of which are in the process of being commercialized for market use [120]. While some of these vaccines are conjugate vaccines, others incorporate outer membrane vesicles, recombinant proteins, pathogen-agnostic mechanisms, and multiple antigen presentation systems [127–130]. The ability of mucosal maternal vaccination with new pneumococcal vaccines to confer protection to offspring from pneumococcal infections has also been studied in preclinical models.

Moreover, 16 vaccine candidates, including several pneumococcal conjugate vaccines, are currently undergoing clinical trials [120]. These vaccine candidates were modeled after

some licensed pneumococcal vaccines that combined the purified capsular polysaccharides of pneumococcal serotypes conjugated to a carrier protein [131]. Four vaccines, including two 13-valent vaccines, a 15-valent euPCV vaccine, and a protein-based pneumococcal vaccine, are undergoing phase I clinical trials. Notably, the protein-based pneumococcal vaccine can cover 70% of all pneumococcal serotypes (NCT04087460) [120].

A total of eight vaccines, including several pneumococcal conjugate vaccines, are undergoing phase II clinical studies. Phase II clinical trials are also being conducted for a pneumococcal protein vaccine, which was shown to provide greater protection than the current polysaccharide and conjugate vaccines (NCT01446926) [132]. A multiple antigen-presenting system used in the MAPS vaccine demonstrated proof of concept in phase I studies and has advanced to phase II. Phase III clinical trials are ongoing for four vaccine candidates, the 23-valent pneumococcal polysaccharide vaccine (PPSV23), a 5-valent pneumococcal conjugate vaccine (PCV), a 14-valent PCV (adsorbed), and a 13-valent PCV [120].

5.4. Extraintestinal Pathogenic E. coli (ExPEC)

There are four potential ExPEC vaccine candidates that have been identified in pre-clinical testing [120]. Only one of these specifically targets *Enterotoxigenic E. coli* (ETEC), *K. pneumoniae*, and uropathogenic *E. coli*. There are four ExPEC vaccine candidates in clinical studies. A phase III clinical trial (NCT04899336) for the 9-valent O-polysaccharide conjugate vaccine, ExPEC9V, started in June 2021 and is anticipated to end in May 2027 [133]. Another polysaccharide conjugate vaccine, ExPEC10V, is undergoing phase I/II clinical testing (NCT03819049) [134]. The vaccine is made up of the ExPEC serotypes O1A, O2, O4, O6A, O8, O15, O16, O18A, O25B, and O75, individually bioconjugated to a carrier protein, an exotoxin A (EPA) from *P. aeruginosa* that has undergone genetic detoxification [135].

ExPEC4V research has been suspended in favor of developing these multi-valent vaccines. Clinical development for the FimH vaccine candidate has entered phase II. FimH, a bacterial adhesin protein, served as the antigen in this vaccine together with a TLR4 agonist adjuvant [136]. The vaccine OM-89 is made up of membrane proteins from 18 different strains of *E. coli* that are heat-inactivated. A phase II clinical trial of the vaccine candidate (NCT02591901) was conducted to prevent recurrent urinary tract infections (UTIs) [137]. Whole-cell vaccines, like UroVaxom and Solco-Urovac, were thought to have less-than ideal qualities because the compositions were not well described [138].

Although the use of chemical conjugation techniques has been relatively successful in advancing vaccine production, it is expensive and technically difficult to conjugate many serotypes in a vaccine formulation [139]. In comparison with meningococcal and pneumococcal capsular polysaccharides, the O antigen is also far more difficult to purify as a polysaccharide. Due to these drawbacks and the requirement for a multivalent vaccine to effectively prevent ExPEC-associated illness, the development of an ExPEC vaccine has been subject to delay and postponement [140].

5.5. S. enterica Serovar Paratyphi A

Enteric fever is commonly caused by *Salmonella enterica* serotypes Typhi (*Salmonella* Typhi) and Paratyphi A (*Salmonella* Paratyphi A). Licensed vaccines exist for typhoid fever caused by *Salmonella* Typhi but there are currently no authorized vaccines that could protect against *Salmonella* Paratyphi A. There are currently a total of four vaccine candidates in the preclinical stages of vaccine development [120]. These vaccine candidates are bivalent in nature and were shown to protect against both *Salmonella* Typhi and *Salmonella* Paratyphi A [141].

There are a total of three candidates in clinical development. The first is the O:2, 12-TT conjugate vaccine, which was demonstrated to be safe and immunogenic in phase I/II clinical trials but failed to elicit a booster immunological response after the second dose and is currently in phase III testing. This vaccine solely targets *Salmonella* Paratyphi A. The phase I trial for the live, whole-cell attenuated CVD 1902 vaccine was completed in 2013

(NCT01129453), and the data demonstrated the safety and immunogenicity of the vaccine candidate when a single dosage was administered [142].

CVD 1902 was combined with CVD 909 to form a bivalent vaccine that targeted *Salmonella* Paratyphi A and *Salmonella* Typhi [143]. Phase IIb clinical trials were conducted for the bivalent Entervax live attenuated whole-cell vaccine targeting both *Salmonella* Paratyphi A and *Salmonella* Typhi and were proposed to end in August 2021 (NCT01405521) [144]. It was expected that vaccination against *Salmonella* Typhi would be combined with a vaccine against *Salmonella* Paratyphi A. The value of such a bivalent vaccine would be superior to either monovalent vaccine [145]. A common target for vaccines, the Vi (virulence) capsular polysaccharide, is structurally absent from *Salmonella* Paratyphi A. Since recent progress in creating the typhoid conjugate vaccine is encouraging, this has raised the possibility of generating a vaccine for *Salmonella* Paratyphi A [146].

While a number of vaccine candidates, such as conjugate, bivalent, and LAV candidates, showed promise in clinical trials, efficacy trials have not yet been conducted and so there are no licensed vaccines against *Salmonella* Paratyphi A. The challenges to the development of licensed vaccines against *Salmonella* Paratyphi A include the lack of information regarding immune correlates of protection and the absence of reliable small animal models of infection [147].

5.6. C. difficile

Five potential vaccines against *C. difficile* were undergoing preclinical testing in 2022 [90]. These vaccines utilized several distinct delivery methods, including the MAPS platform, exome-like bacterial vesicles, and *Bacillus subtilis* spores. There are at present no licensed vaccines available to prevent *C. difficile* infection. However, two recombinant vaccine candidates were undergoing clinical testing. Phase I of the GSK2904545A recombinant protein vaccine was completed in April 2022 (NCT04026009) [148]. The US FDA expedited the review of the PF-06425090 vaccine candidate in 2014. The phase III trial, which enrolled 17,500 patients, showed that administration of the vaccine candidate shortened the duration and severity of illness based on secondary endpoints, but it did not achieve the primary aim of avoiding *C. difficile* infections (NCT03090191) [149,150].

In the past ten years, research on a number of potential *C. difficile* vaccine candidates has been put on hold. Despite having demonstrated good immunogenicity and safety, the phase III trial of the ACAM-CDIFF toxoid vaccine candidate, which enrolled 9302 participants, was stopped in 2018 after interim data revealed that it was unlikely to prevent primary *C. difficile* infection (NCT01887912) [151]. The results of this trial—the first global phase III study to assess vaccination against *C. difficile* infection—highlighted the challenges involved in developing a vaccine for bacterial infections. The immunological response might have been impacted by the advanced age of the participants and the prevalence of comorbid conditions. Participants were also very susceptible to *C. difficile* infections. However, given the erratic epidemiology, a sizable population would need to be immunized. The phase II study utilizing the recombinant vaccine VLA84 was completed in 2015 (NCT02316470) [152].

Additionally, biotherapeutics and fecal microbiota transplants have recently demonstrated efficacy against *C. difficile* and may lessen the requirement for vaccination. Access to these therapies is still primarily restricted to high-income countries. Antibiotics lack effectiveness in efficiently treating *C. difficile* infections, thus alternate management techniques are critical [153]. Vaccines might aim to prevent either the first infection or the recurrence of *C. difficile* infections, which are very distinct goals. A reduction in symptoms might be achievable, according to recent results from vaccine candidates in clinical testing, but *C. difficile* might still survive in the host [154]. The successful development of a *C. difficile* toxin antibody suggests that vaccination could be effective if it could deliver local antibodies into the gut [155].

5.7. N. gonorrhoeae

Currently, there are no licensed vaccines against *N. gonorrhoeae*. Two vaccine candidates are in preclinical development against *N. gonorrhoeae* [156]. The 4CMenB vaccine, which has been approved to protect against group B meningococcal infection, might also offer protection from gonorrhea [157].

The development of an effective gonococcal vaccine faces several major obstacles, including the high degree of heterogeneity and variability of specific gonococcal antigens, the absence of known correlates of protection, a weak immune response that is mostly local, transient, and lacks immunological memory, the ability of gonococci to evade immune responses, and a lack of laboratory animal models that closely resemble human infection and disease [158,159]. These issues have led to a lack of optimism for the creation of an effective vaccine that might be used for the prevention of gonorrhea [160].

5.8. N. meningitidis

The bacterium *Neisseria meningitidis*, which causes meningitis and septicemia, is associated with high pathogenic potential based on the unpredictable emergence and circulation of serogroups [161,162]. The capsular polysaccharide (CPS) that surrounds pathogenic meningococci was shown to be essential for the survival and growth of the bacterium inside the body [163]. Serogroups A, B, C, W, X, and Y are the most common serogroups causing invasive meningococcal disease. Early efforts focused on vaccine development against *N. meningitidis* serogroups A, C, Y, and W used the CPS as the primary antigen but they were not successful in the protection of infants. This was followed by the development of polysaccharide-conjugated vaccines to serogroups A, C, W, and Y (Men ACWY) by conjugating meningococcal A, C, W, and Y polysaccharides to a diphtheria toxoid protein carrier, which was able to confer protection in young children by preventing nasopharyngeal carriage [164]. Moreover, the use of potently immunogenic and well-tolerated monovalent MenC conjugate vaccine against *N. meningitidis* serogroup C significantly reduced the incidence of *N. meningitidis* serogroup C disease in Europe and North America [165].

Monovalent MenC conjugate vaccines have demonstrated their effectiveness and safety across various age groups. The implementation of routine vaccination programs has significantly decreased the incidence of serogroup C disease in several countries, such as the UK, Spain, Italy, Greece, France, Canada, Australia, Brazil, and Argentina. Quadrivalent meningococcal conjugate vaccines offered broader protection against *N. meningitidis* serogroups A, C, Y, and W. Indeed, the approved MenACWY-CRM vaccine, which is composed of a quadrivalent meningococcal conjugate vaccine conjugated with CRM197, demonstrated the elicitation of strong immune responses following immunization [164]. Despite the existence of vaccines for multiple serogroups of *N. meningitidis*, traditional vaccines based on the B polysaccharide could not confer adequate protection against serogroup B (MenB). This was due to the similarity of the serogroup B meningococcal capsular polysaccharide with the sugars present on the surface of human cells and the likelihood of inducing an auto-immune responses, which could affect polysialic acid (PSA) located in human cells [166]. Antibodies arising from immunization with B polysaccharide could result in abnormal CNS development in the unborn child [167].

Research efforts were then focused on a reverse vaccinology approach to developing a universal *N. meningitidis* vaccine protective against serogroup B (MenB). This approach became possible due to the advent of genome sequencing and the use of in silico methods to identify surface-associated immunogenic antigens capable of inducing strong immune responses against MenB. This was followed by cloning of the selected nucleotides into plasmid expression vectors and the immunization of mice with the recombinant proteins. A universal multi-epitope vaccine known as 4CMenB was developed using three selected antigens (neisserial heparin-binding antigen or NHBA, factor H-binding protein or fHbp, and neisseria adhesin A or NadA) in combination with the outer membrane protein of a MenB strain [165]. The vaccine was capable of eliciting broad immune coverage. Following phase II and III clinical trials, the vaccine was licensed for public immunization in 2013 [165,167].

Another vaccine against *N. meningitidis* MenB that was licensed in the USA in 2014 is the bivalent rLP2086 vaccine. The vaccine contained the factor H binding protein (fHbp) from two mutant strains and gained accelerated FDA approval after it was shown to elicit potent immune responses in phase II clinical trials [168]. The human serum bactericidal assay (hSBA) was utilized to measure antibodies in vaccinees immunized with the MenB vaccine [169]. Immunogenicity and safety studies conducted in adolescents upon immunization with the bivalent rLP2086 vaccine demonstrated robust hSBA responses and the vaccine was well tolerated, with three doses eliciting the strongest immune response against MenB strains expressing vaccine-heterologous subfamily B fHbps [170].

5.9. ETEC

There are a total of ten vaccine candidates in preclinical development against ETEC. While six of these are focused only on ETEC, the rest target S. aureus, C. jejuni, or S. flexneri, in addition to ExPEC. Moreover, six vaccine candidates are in clinical development against ETEC. Three of these are combination vaccines targeting both ETEC and Shigella spp. [90]. ETVAX, an IV that showed immune responses against four E. coli strains, has progressed to phase IIb clinical development. This candidate incorporates the use of dmLT as an immunogen and an adjuvant [171–174].

Unfortunately, four vaccine candidates against ETEC that did manage to progress to clinical development were abandoned. These included TyphETEC-ZH9, a combined vaccine against typhoid and ETEC, which was successful in phase I of clinical development but was returned to the preclinical stage to also incorporate antigens targeting *Shigella* spp. [175].

An inactivated *Vibrio cholerae* vaccine candidate against ETEC, known as VLA1701, was reported to successfully pass phase II of clinical development in 2018 but was no longer included in the list of active vaccine candidates targeting ETEC [176]. Moreover, an LAV candidate known as ACE527-102, which was composed of *E. coli* CS1, CS2, CS3, and CS5, colonization factor antigen I (CFAI), and the heat-labile toxin (LT) B subunit, was able to elicit potent immune responses but could not protect immunized participants against moderate/severe diarrhea [177].

Another promising candidate, the B-subunit/whole-cell cholera vaccine, was shown to elicit immune responses capable of providing immune protection against a few ETEC strains. Protection from ETEC was demonstrated in challenge experiments. However, the resulting severe diarrhea as well as lack of knowledge about the immune correlates of protection led to the project being abandoned [178]. Nevertheless, there were promising reports that a vaccine focused on the LT toxoid and CFA antigens was able to provide protection against 80% of pathogenic ETEC strains. There is an urgent need to develop an effective vaccine for protection against ETEC in low- or middle-income countries (LMICs). The value of such a vaccine might be further enhanced by the development of a future vaccine that could protect against ETEC as well as other pathogenic bacteria [179].

5.10. K. pneumoniae

Although *K. pneumoniae* has become a significant contributor to illnesses acquired in the community, including pneumonia and pyogenic liver abscess, and serotypes K1 and K12 were determined to be the most common serotypes linked to infectious disease, there are still no vaccines currently available to prevent *K. pneumoniae* infections.

The capsule, lipopolysaccharide, siderophores, and fimbriae (also known as pili) have all been identified as virulence factors for *K. pneumoniae* so far [180]. The most extensively investigated virulence factor of these is the capsule, which is produced by gene products from the capsular polysaccharide synthesis (CPS) locus. Bacterial capsule-targeted vaccines might serve as an effective strategy to immunize against encapsulated pathogens, as evidenced by the success of capsule-targeted vaccines against *Streptococcus pneumoniae*, *Neisseria meningitides*, and *Haemophilus influenza* [181,182]. A monovalent *K. pneumoniae* K1 capsule polysaccharide (CPS) vaccine was developed in 1985 and several polyvalent

K. pneumoniae CPS vaccines were developed in 1986, but these vaccines were associated with the elicitation of only T cell responses without the elicitation of high affinity neutralizing antibodies [183–186]. (B cell responses are classified as T-dependent (T-D) or T-independent (T-I), based on the requirement for T cell help in antibody production.)

Lin et al. (2022) strongly asserted that *K. pneumoniae* CPS protein-conjugated vaccines hold promise as the solution to this problem since they might be able to elicit both humoral and cellular protective immune responses [181]. Indeed, this was demonstrated by the use of K1 (K1-ORF34) and K2 (K2-ORF16) CPS depolymerases that were discovered in phages to cleave K1 and K2 CPSs into intact structural units of oligosaccharides. To create CPS-conjugated vaccines, the resulting K1 and K2 oligosaccharides were individually conjugated with CRM197 carrier protein. Both K1 and K2 CPS-conjugated vaccines generated anti-CPS antibodies with 128-fold and 64-fold increases in bactericidal activity, respectively, compared to animals without vaccination. Challenge studies showed that the divalent vaccine (a combination of K1 and K2 CPS-conjugated vaccines) and K1 or K2 CPS-conjugated vaccines protected mice from subsequent infections of *K. pneumoniae* by the corresponding capsular type [181].

The majority (80%) of the clinical strains of *K. pneumoniae* fall into 4 of the 12 existing O serotypes [187–189]. In low-income countries, *K. pneumoniae* has been linked to a significant burden of newborn sepsis. Safety and immunogenicity results of the administration of a polyvalent *Klebsiella* vaccine comprising six serotypes of capsular polysaccharides, namely K2, K3, K10, K21, K30, and K55, demonstrated mild adverse reactions with strong immune protection. Subcutaneous immunization of 40 individuals with 50 μg of each antigen was able to elicit a 4-fold more potent immunoglobulin G (IgG) response as compared to the immune response elicited from 25 μg of each antigen [185]. Furthermore, passive protection conferred by IgGs obtained from the sera of immunized participants was observed against fatal experimental *Klebsiella* K2 burn wound sepsis [185].

Although formulations based on capsular polysaccharides have been explored, the great diversity in capsular serotypes limits vaccine coverage. There has been some progress in the development of lipopolysaccharide (LPS)-based vaccines against K. *pneumoniae*. The LPS O2a and LPS O2afg serotypes present in the majority of MDR *K. pneumoniae* strains are associated with both immune evasion and immunological responses. Human monocytes ex vivo were used to extract LPS (serotypes O1, O2a, and O2afg) from various *K. pneumoniae* strains, and the efficacy of the LPS antigens to trigger the production of pro-inflammatory cytokines and chemokines was evaluated. It was found that LPS serotypes O2afg, and to a lesser extent O2a, but not O1, failed to induce the production of pro-inflammatory cytokines and chemokines when incubated with human monocytes, which supports a function in immune evasion. Preliminary research demonstrated that LPS O1, and to a lesser extent LPS O2a, but not LPS serotypes O2afg, induced nuclear translocation of NF-B, a process that controls immune responses to infections. Investigations showed that MDR *K. pneumoniae* expressing the LPS O2afg serotypes were able to evade an early inflammatory immune response, which allowed them to methodically spread inside the host and caused various diseases associated with this bacterium [190].

The development of vaccines using LPS antigens has not yet advanced past the preclinical stage. Despite the fact that there are currently eight recognized O serotypes, epidemiologic studies indicated that four O polysaccharide serotypes (OPS) would cover 80% of clinical isolates globally. In an animal model, antibodies against subcapsular antigens, such as LPS, are protective. Researchers eliminated the lipid A moiety from LPS preparations, leaving the core and sugar repeat regions (core and O polysaccharide, or COPS) but the purified COPS and bacterial CPSs were found to be poor immunogens [191].

Chhibber et al. (2005) developed two separate KP LPS combination vaccines and demonstrated a decrease in lung bacterial load. However, ELISA antibody titers, boost responses, and rodent lethality model testing were not conducted. It was reported that O1 LPS contained in liposomes or sodium alginate microparticles was less hazardous than free LPS and induced a more favorable mucosal immune response in mice, protecting rats from

lobar pneumonia. However, the protection provided by O1 LPS vaccination or monoclonal antibodies (mAbs) against K2:O1 challenge in mice was later demonstrated by researchers to be temporary [192].

Recently, a quadrivalent conjugate vaccine comprising the four most frequent O serotypes linked to human illnesses (KP O1, O2, O3, and O5) was conjugated to either the *P. aeruginosa* flagellin A or B protein to form a vaccine. Since the lipid A portion of the LPS had been chemically removed from the COPS, it was completely detoxified and could overcome the drawbacks of LPS-based vaccines. In rabbits, immunization elicited the production of IgGs against each of the six antigens, potentially protecting mice from systemic KP infection [193].

Vaccine strategies under development against *K. pneumoniae* involve a range of different vaccine platforms, such as LAVs, IVs, outer membrane vesicles, polysaccharide- and lipopolysaccharide-based vaccines, recombinant vaccines, conjugate vaccines including PS–protein or LPS–protein fusions, and ribosomal vaccines. There have been numerous vaccine proposals put forth, some of which have advanced to clinical testing [120]. In a recent phase I/II clinical trial, KlebV4, a tetravalent bioconjugated vaccine candidate, was recently evaluated both with and without the AS03 adjuvant (NCT04959344).

Another promising approach to the design of vaccines against MDR *K. pneumoniae* involves the inactivation of bacteria using heat. The bacterial components of dead cells would still be able to elicit an immune response against pathogens. An example of a heat-killed vaccine candidate is MV140 (Uromune), which is made up of inactivated bacteria and is currently undergoing phase II clinical trials (NCT02543827, NCT04096820) [194,195]. Uromune, which contains inactivated *E. coli*, *K. pneumoniae*, *Proteus vulgaris*, and *Enterococcus faecalis*, has been licensed in Spain since 2010 but is undergoing clinical evaluation in Canada [196]. A prospective study conducted with 75 women suggested that Uromune was safe and effective at preventing UTIs in women, as evidenced by the fact that of the 75 women who completed treatment, 59 (78%) had no subsequent UTIs in the follow-up period. Prior to treatment, all women had experienced a minimum of three or more episodes of UTI during the preceding 12 months [197]. In addition, in the 2019 European Association of Urology guidelines, MV140 was suggested as an immunoactive prophylaxis to prevent the occurrence of recurrent UTIs, and it was shown in retrospective trials to be up to 90% more effective than antibiotic prophylaxis [180].

5.11. P. aeruginosa

P. aeruginosa is an important MDR pathogen capable of causing severe infections in immunocompromised individuals. The Centre for Disease Control and Prevention (CDC) has classified MDR *P. aeruginosa* as a major health concern for the past ten years due to its contribution to at least 32,600 infections, 2700 fatalities, and USD 767 million in annual healthcare costs in the US alone [198]. Patients who have recently been admitted to the intensive care unit (ICU), those with compromised immune systems, and those who have previously been exposed to antipseudomonal carbapenems and fluoroquinolones were reported to be at the highest risk of contracting infections caused by MDR and extensively drug-resistant (XDR) *P. aeruginosa* [198]. It is also associated with burn wound infections, ventilation-associated pneumonia, and chronic infections in cystic fibrosis (CF) patients [199]. Indeed, *P. aeruginosa* is well endowed with virulence factors that enable it to infect host cells and escape human adaptive immune responses, leading to the emergence of new infections [200]. One of its primary virulence factors is the type 3 secretion system (T3SS), through which it injects effector proteins directly into host cells. These effector proteins are known to affect a variety of cell functions, such as disruption of the actin cytoskeleton, which leads to apoptosis-like cell death [201].

While there are no licensed vaccines for *P. aeruginosa* at present, preclinical research on *P. aeruginosa* has advanced in the areas of antigen discovery, adjuvant use, and new delivery technologies. An experimental live vaccine against *P. aeruginosa* was developed and evaluated for immunogenicity and protective efficacy [202]. The vaccine was developed from an

auxotrophic strain of the bacterium lacking the essential enzyme involved in producing D-glutamate, a structural component of the bacterial cell wall. Therefore, while the virulence of this strain was compromised, its capacity to elicit potent and immunogenic immune responses was unaffected. When delivered intranasally, it was capable of inducing mucosal and systemic immune responses. The vaccine was shown to elicit effector memory, central memory, and IL-17A-producing CD4+ T cells. It also attracted neutrophils and mononuclear phagocytes to the airway mucosa. Following lung infection by ExoU-producing PAO1 and PA14 strains, the survival of mice was significantly increased. Protection was conferred to almost one-third of the mice infected with XDR high-risk clone ST235.

Another preclinical study utilized reductive amination to covalently bind toxin A to lipid A-free polysaccharide (PS) that was obtained from *P. aeruginosa* immunotype 5 lipopolysaccharide (LPS). The intravenously administered dose of 50 micrograms/kg body weight of the PS-toxin A conjugate vaccine was nonpyrogenic for rabbits and not harmful to animals. Upon subcutaneous delivery to human participants, the conjugate vaccine only elicited moderate, momentary reactions. Immunoglobulin G (IgG) antibodies were produced as a result of the administration of the vaccine and it counteracted toxin A's cytotoxic effects. It aided in the uptake and elimination of *P. aeruginosa* in the presence of human polymorphonuclear leukocytes. When compared to paired preimmunization serum, passively transferred IgGs extracted from the serum of an immunized donor was much more effective at preventing fatal *P. aeruginosa* burn wound sepsis [203].

The development of an effective vaccine against *P. aeruginosa* has been severely hampered by numerous issues. This pathogen is a particularly difficult target for vaccine development due to its abundance of virulence factors, a genome that facilitates adaptation to novel environments, shifting phenotypes between acute and chronic infection, and the complexity of the host immune response, among other considerations. Nevertheless, these challenges have not dissuaded efforts to develop a vaccine, but despite more than 50 years of work, clinical vaccine development for *P. aeruginosa* has been mainly ineffective. A few potential vaccines have advanced to clinical trials along the way by exploiting well-known virulence factors as vaccine antigens [204].

The mature outer membrane protein I (OprI) and the amino acids 190 to 342 of OprF from *P. aeruginosa* were combined to form the hybrid protein [Met-Ala-(His)6OprF190-342-OprI21-83], which was produced in *E. coli* and purified using Ni^{2+} chelate affinity chromatography. After safety and pyrogenicity tests in animals, eight adult human volunteers were divided into four groups and given intramuscular injections of the vaccine three times at intervals of four weeks. They were then vaccinated again six months later with either 500, 100, 50, or 20 μg of OprF-OprI adsorbed onto $Al(OH)_3$. All immunizations were safe and well tolerated. In volunteers who received the 100 μg or 500 μg dosage, there was a discernible increase in antibody titers against *P. aeruginosa* OprF and OprI after the initial vaccination. Significant antibody titers were obtained for all groups following the second vaccination. Elevated antibody titers against OprF and OprI could still be detected six months following the third vaccination. A C1q-binding assay and in vitro absorption of *P. aeruginosa* by opsonophagocytic cells were both used to demonstrate the ability of the elicited antibodies to increase complement binding and opsonization [205].

Adlbrecht et al. (2020) reported the results of a placebo-controlled, double-blind phase II/III study that was conducted to evaluate the efficacy, immunogenicity, and safety of the IC43 recombinant *P. aeruginosa* vaccine in non-surgical ICU patients [176]. The sample size of the study consisted of 800 patients between the ages of 18 to 80 years who were predicted to require mechanical ventilation for less than 48 h. The participants were randomized to receive two doses of either 100 μg of the IC43 vaccine or a saline placebo, spaced seven days apart. Safety and immunogenicity were also evaluated, showing that the rise in geometric mean OprF/I titers was 1.5-fold after the first vaccination, 20-fold at day 28, and decreased to 2.9-fold at day 180. Additionally, there was no discernible difference between the two groups in terms of overall survival or the percentage of patients with only one confirmed invasive *P. aeruginosa* infection or respiratory tract infection. It was shown that

the IC43 100 µg vaccine was well tolerated in this sizable group of critically ill, mechanically ventilated patients, Although the vaccine had a significant level of immunogenicity, it had no therapeutic advantage over a placebo in terms of overall mortality [206].

A study conducted by Shaikh et al. (2022) aimed to assess and compare the immunogenicity as well as the protective efficacy of individual and combination immunizations with PopB and OprF/I [207]. The findings indicated that only mice vaccinated with PopB/PcrH, either alone or in combination with OprF/I, exhibited a Th17 recall response from splenocytes after vaccination. Furthermore, mice that received the combination vaccine were better protected against acute lethal *P. aeruginosa*, regardless of the vaccination route, compared to those who received either vaccine alone or an adjuvant control. The vaccination also induced IgG titers against the vaccine proteins and whole *P. aeruginosa* cells. Interestingly, none of the antisera exhibited opsonophagocytic killing activity. However, antisera from mice vaccinated with vaccines containing OprF/I had the ability to block IFN-γ binding to OprF/I but exerted no protection. Thus, vaccines that combined PopB/PcrH with OprF/I and generated functional antibodies were able to offer broad and potent protection against *P. aeruginosa* pulmonary infection [207].

Reverse vaccinology techniques were employed in an experimental study to develop a potent chimeric vaccine against *P. aeruginosa* [208]. The vaccine candidate included PopB and outer membrane protein F and I (OprF/OprI) joined together using linkers. The multi-epitope vaccine, containing helper T lymphocyte (HTL), cytotoxic T lymphocyte (CTL), interferon gamma (IFN-γ), and interleukin 4 (IL-4) epitopes, was developed after performing thorough immunoinformatics analysis. This was followed by an evaluation of the physicochemical properties, allergenicity, toxicity, and antigenicity. After examination of the secondary structure, a 3D model of the tertiary structure was created, improved upon, and confirmed using computational techniques. Additionally, molecular docking and dynamics were used to determine the vaccine candidate's stability and strong protein–ligand interaction with TLR4. Additionally, pET-22b (+) was utilized in conjunction with in silico cloning to obtain optimum translation efficiency. The results showed that the chimeric vaccine had high thermostability and appropriate physicochemical properties. In particular, this vaccine candidate had a stable protein and TLR4 interaction and was sufficiently overexpressed in *E. coli.* It was also nontoxic and highly soluble. Overall, it might stimulate the immune system and suppress *P. aeruginosa* [208].

Dey et al. (2022) demonstrated that the primary membrane protein candidate of *P. aeruginosa* was a crucial factor in the susceptibility of the bacteria to antimicrobial peptides and its ability to survive inside hosts [209]. In order to create linear B cell, cytotoxic T cell, and helper T cell peptide-based vaccine constructs, the researchers carried out a computational analysis to investigate OprF and OprI, two of the key membrane proteins of *P. aeruginosa*. Twelve T cell peptides and two B cell peptides were predicted using various immunoinformatics databases, such as ABCpred (http://crdd.osdd.net/raghava/abcpred/, accessed on 14 July 2023) and the online server IEDB immune epitope database (https://www.iedb.org/, accessed on 14 July 2023). To create a high-quality three-dimensional structure of the final vaccine design, which contained epitopes, adjuvants, and linkers, simulations were used. The vaccine was shown to have the best biophysical features, including being nonallergenic, antigenic, soluble, and non-toxic. Protein–protein docking and molecular dynamics simulations revealed a robust and sustained interaction between the vaccine and TLR4 [209].

Elhag et al. (2020) also described the potential use of immunoinformatics tools to develop an epitope-based vaccine against *P. aeruginosa* [210]. The chosen vaccine target was the highly immunogenic fructose bisphosphate aldolase (FBA) of *P. aeruginosa*. Potential B and T cell epitopes were predicted using the B cell prediction method (http://tools.iedb.org/main/bcell/, accessed on 14 July 2023) while T cell epitopes were predicted using IEDB MHC I (http://tools.iedb.org/mhci/, accessed on 14 July 2023) and MHC II (http://tools.iedb.org/mhcii/, accessed on 14 July 2023) tools. Four of the MHC II epitopes and six of the MHC I epitopes from the data were reported to be promising. MHC I and

MHC II are reported to share 19 epitopes. The epitopes had a global coverage of 95.62% of the world's population. The researchers concluded that further in vivo and in vitro tests would need to be carried out to validate the vaccine's efficacy [210].

The functional amyloids of *Pseudomonas* (Faps), which are among the bacterium's biofilm components, showed a positive association with virulence and contributed to the mucoidy phenotype observed in infections in CF patients [211]. Fap proteins are viable therapeutic targets because of their extracellular accessibility, conservation among *P. aeruginosa* isolates, and relationship to the phenotype of lung infections in CF patients. Furthermore, bacterial amyloid is an option for treatment due to its documented impact on the immune response and neural function. The Fap C protein and its direct interactions were investigated to identify antigenic T cell and B cell epitopes. Epitopes and peptide adjuvants have been associated with the development of vaccination candidate structures. The vaccine candidates were validated for stability, interactions with TLRs and MHC alleles, allergenicity, physiochemical characteristics, antigenicity, and stability. Immunosimulation studies have shown that the vaccines induced a Th1-dominated response, which can help improve the prognosis of CF patients after infection [211].

5.12. S. aureus

Staphylococcus is a commensal of the human skin, but it can pose a serious threat to human health. It is known to cause nosocomial infections involving ventilator-associated pneumonia, intravenous catheter-associated infections, and post-surgical wound infections. It is estimated to cause 20,000 deaths in the USA annually [212]. Its MDR phenotype makes it one of the most difficult pathogenic bacteria to treat, in addition to its capacity to evade the immune system. Almost all antibiotics developed since the 1940s have become obsolete for the treatment of *S. aureus* infections. The first methicillin-resistant *S. aureus* (MRSA) was discovered in clinical isolates of *S. aureus* in 1961. Then, MRSA, a multi-resistant hospital disease, spread globally at an alarmingly accelerated rate. The MRSA strain Mu50, which was associated with diminished sensitivity to vancomycin, was discovered in 1997. According to the CLSI criteria, the *S. aureus* strain known as vancomycin-intermediate *S. aureus* (VISA) resulted from an adaptive mutation against vancomycin, which has long been the last line of defense against MRSA infection [213]. Considering the rapid emergence of MRSA strains showing resistance towards vancomycin, the development of safe and immunogenic vaccines for *S. aureus* is highly warranted. Despite this, there are no licensed vaccines against *S. aureus*. While previous research on vaccine development against *S. aureus* has focused on single antigen preparations, contemporary attempts prioritize the incorporation of several antigens.

Although efforts to produce a vaccine against *S. aureus* have not been successful so far, the results of preclinical and clinical trials in humans might offer some insight into the limitations. Current research seeks to find novel antigens and innovative vaccine formulations that could effectively stimulate cellular and humoral immune responses. The in vitro tissue culture and in vivo animal models used in preclinical studies to evaluate the efficacy of vaccine candidates would lead to further insight into correlates of protection. In human clinical trials, a number of new vaccine candidates are currently being examined in various target populations. Jahantigh et al. (2022) reported that there are at least five *S. aureus* vaccines currently in various stages of clinical development [214].

The two most common capsular polysaccharides, CP5 and CP8, were combined with the exotoxin A from *P. aeruginosa* in the bivalent polysaccharide vaccine candidate known as StaphVAX. CP5 and CP8 have been associated with over 80% of clinical *S. aureus* infections. The vaccine completed phase II clinical studies with positive results in chronic, ambulatory, and peritoneal dialysis patients. At 3–54 weeks after vaccination, patients who were potential candidates for cardiovascular surgery were assessed in a phase III trial. Despite good preliminary findings from phase III StaphVAX vaccine research, the FDA stated that a second phase III trial would be necessary for US registration. However, the results of the second phase III investigations revealed no difference between the StaphVAX and placebo

groups in terms of the number of *S. aureus* infections. After following up for 32, 40, and 54 weeks, it was discovered that StaphVAX reduced *S. aureus* bacteremia by 64%, 57%, and 26%, respectively. However, it was observed that antibody titers declined after 32 weeks. The second phase III StaphVAX trial with hemodialysis patients was unsuccessful [214].

The highly conserved *S. aureus* surface protein, iron-regulated surface determinant B (IsdB), is present in the V710 vaccine. In animal challenge models, the first trial of the V710 vaccine candidate demonstrated high immunogenicity. Subsequent clinical trials of the V710 vaccine candidate were conducted between 2007 and 2011. To assess the effectiveness and safety of preoperative immunization in patients undergoing cardiothoracic surgery, phase IIb/III of the experiment was launched in 2011. In patients with median sternotomies, the use of the V710 vaccine increased the mortality risk while having no effect on the frequency of significant postoperative *S. aureus* infections. These results contradicted the recommendation to administer the V710 vaccine to surgical patients [215].

The SA4Ag (PF-06290510) vaccine candidate produced by Pfizer is composed of four antigens: CRM197-conjugated anti-phagocytic capsular polysaccharides 5 and 8, the manganese transporter MntC, and the adhesion molecule ClfA. The safety, tolerability, and immunogenicity of the SA4Ag vaccine were proven by phase I/II evaluation. SA4Ag was also effective and safe for people following elective spinal fusion surgery in a phase IIb study and the evaluation is ongoing. The U.S. Food and Drug Administration (FDA) granted SA4Ag Fast Track status in February 2014. Further research revealed that the SA4Ag vaccine candidate elicited quick and strong functional immune responses in the 20- to 64- and 65- to 85-year-old age groups and had a tolerable safety profile. In animal studies, this vaccine candidate also performed well against chronic infection caused by *S. aureus*. Deep tissue infection, bacteremia, and the pyelonephritis model all showed much decreased bacterial populations after receiving the SA4Ag vaccine candidate. These encouraging preclinical SA4Ag results, however, did not demonstrate the therapeutic benefit of SA4Ag in preventing surgery-related, invasive *S. aureus* infection [216].

The GSK (GSK2392103A) vaccine candidate is a four-component Staphylococcal vaccine that contains mutant hemolysin-1 (-toxin; AT), ClfA, as well as polysaccharides 5 and 8 conjugated to the tetanus toxoid (TT) (CPS5-TT, CPS8-TT). Phase I ended in 2012, and following the initial dose, the vaccine candidate was observed to induce potent humoral immune responses [217]. The *Candida albicans* agglutinin-like sequence 3 protein (Als3p), which is the N-terminal component of the experimental vaccine NDV-3, was prepared with aluminum hydroxide (alum) adjuvant in phosphate-buffered saline (PBS). *C. albicans* and *S. aureus* cell surface proteins and Als3p share structural and sequence similarities. Consequently, both *C. albicans* and *S. aureus* infections may respond well to the NDV-3 vaccine. In the USA, NovaDigm Therapeutics finished a phase II trial for vulvovaginal candidiasis in 2016 [218].

Clegg et al. (2021) asserted that given the variety of target populations and the complexity of the diseases caused by this pathogen, a multifaceted strategy involving several therapies would be necessary. In addition to vaccines, new kinds of antibiotics, therapeutic proteins such as centyrins, monoclonal antibodies, and bacteriophage therapy are being evaluated. Some of these have undergone human testing with positive results [212].

Recombinant proteins or polysaccharide antigens of *S. aureus* have been used most frequently in clinical studies of *S. aureus* vaccines to stimulate immune responses in vaccinees. The selection of the antigen or combination of antigens to use is of the utmost significance. Surface antigens or released toxins are the protein antigens commonly targeted while developing vaccines since the immune system is able to recognize these virulence factors. Antibodies against surface antigens might also cause opsonophagocytosis and prevent adhesion and uptake, leading to the inhibition of virulence activities. Antibodies produced against secreted toxins may inhibit toxicity. The extracellular polysaccharide coating on *S. aureus* has been the target of numerous vaccine formulations that are currently undergoing clinical studies [212].

Data gathered from the immune responses that defend against invasive *S. aureus* infections, host genetic factors, and bacterial evasion mechanisms in humans are crucial for the future development of successful and effective vaccines and immunotherapies against invasive *S. aureus* infection in humans. Based on the evidence provided, it is hypothesized that staphylococcal toxins, such as superantigens and pore-forming toxins, are significant virulence factors. Targeting the neutralization of these toxins is, therefore, more likely to have therapeutic benefits than earlier attempts at opsonophagocytosis-promoting vaccines [189]. The vaccine candidates in clinical development against major bacterial pathogens are summarized in Table 2.

Table 2. Vaccine candidates in clinical development against major bacterial pathogens.

Bacterium	Vaccine Candidate	Number of Participants	Primary Outcome Measures and Data on Safety and Immunogenicity	Phase of the Study	Target Population	References
S. enterica serovar typhi	EuTCV	444	Seroconversion rate; solicited local and systemic AEs. Seroconversion in 99.4% of immunized individuals; reasonable safety profile.	Phase III NCT04830371	6 Months–45 Years	[90,219]
	Vi-DT	3071	Immunogenicity (seroconversion rate). Anti-Vi-IgG seroconversion rate of 99.33%; good safety profile.	Phase III NCT04051268	6 months–60 years	[90,220]
	Typhoid Vi conjugate vaccine	NR	Anti-Vi IgG geometric mean titers increased by 502 times, from 4·2 EU/mL to 2383·7 EU/mL at day 28; safe and tolerable.	Phase III	NR	[90]
	Entervax	99	Diagnosis of typhoid fever. No results posted.	Phase IIb NCT01405521	Adults 18–60 Years	[90,144]
	CVD 1000	96	Frequency and severity of solicited local and systemic AEs. No results posted.	Phase I NCT03981952a	Adults 18–45 Years	[90,221]
H. influenzae type b	Shan 6	460	Geometric mean concentrations (aGMCs) of Abs against pertussis antigens; potent immunogenicity; good safety profile.	Phase III NCT04429295	Healthy Infants and Toddlers in Thailand	[90,222]
	Freeze-dried Haemophilus influenzae type b (Hib) combined vaccine	NR	NR	Phase III Chi-CTR2000032281	NR	[90]
	MT-2355 (BK1310)	267	Antibody prevalence rate against anti-PRP with 1 µg/mL or higher, diphtheria toxin, pertussis, tetanus toxin, and polio virus. No results posted.	Phase III NCT03891758	Healthy Infants	[90,223]
	LBVD	460	Number of participants with antibodies (Abs) above a predefined threshold against diphtheria (D), tetanus (T), hepatitis B (Hep B), Haemophilus influenzae type b (Hib), and poliovirus (Polio) antigens. Safe and immunogenic.	Phase I NCT04429295	Healthy Infants and Toddlers in Thailand	[90,222]
S. pneumoniae	23-Valent pneumococcal polysaccharide vaccine (PPSV23)	1940	Immunogenicity study endpoint. Safety study endpoint. No results posted.	Phase III NCT04278248	healthy volunteers aged 2 Years and above	[90,224]
	15-Valent pneumococcal conjugate vaccine (PCV)	1950	Immunogenicity study endpoint. Safety study endpoint. No results posted.	Phase III NCT04357522	2 and 3-month-old Healthy Volunteers	[90,225]
	14-Valent PCV (adsorbed)	NR	NR	Phase III	NR	[90]
	13-Valent PCV	1200	Geometric mean concentration (GMC) of serotype-specific pneumococcal IgG antibody concentration ≥ 0.35 ug/mL at 30 days after primary vaccination. No results posted.	Phase III NCT02494999	healthy infants aged 2 months	[90,226]
	ASP3772	630	Safety and immunological response of PCV13, ASP3772, and PPSV23. No results posted.	Phase II NCT03803202	elderly 65 to 85	[90,227]
	Multivalent PCV	230	Pneumococcal serotype-specific IgG GMC ratios. No results posted.	Phase II NCT03467984	healthy infants	[90,228]
	Polyvalent PCV V116	600	Adverse effects and serotype-specific opsonophagocytic activity (OPA); geometric mean titers (GMTs) for the common serotypes in V116 and Pneumovax™ 23. No results posted.	Phase II NCT04168190	Healthy adults	[90,229]
	Nucovac	48	NR	Phase II CTRI/2013/ 05/003711	Healthy adults 18–65	[90]
	Pneumococcal recombinant protein vaccine (PPrV) (35)	280	Immunogenicity and adverse effects. No results posted.	Phase II NCT01446926	Healthy Adults, Toddlers and Infants	[90,230]
	SP0202, SKYPAC	750	Geometric mean (GM) of serotype-specific opsonophagocytic (OPA) titers for all pneumococcal serotypes included in the SP0202 formulations. No results posted.	Phase II NCT04583618	Adults Aged 50 to 84	[90,231]
	15-Valent PCV	140	NR	Phase II CTRI2019-02-017527	healthy subjects 2–5 years	[90]
	PF-06842433	NR	NR	Phase II EudraCT 2020-005039-59	NR	[90]

Table 2. *Cont.*

Bacterium	Vaccine Candidate	Number of Participants	Primary Outcome Measures and Data on Safety and Immunogenicity	Phase of the Study	Target Population	References
ExPEC	13-Valent PCV	237	Adverse reactions and immunogenicity. No results posted.	Phase I NCT04100772	Healthy People Aged 6 Weeks and Above	[90,232]
	Protein-based pneumococcal vaccine (PBPV)	120	Solicited and unsolicited adverse reactions; immunogenicity. No results posted.	Phase I NCT04087460	Elderly 18 to 49 years of age	[90,233]
	13-Valent PCV	NR	NR	Phase I	NR	[90]
	euPCV15	60	Incidence of solicited AEs. No results posted.	Phase I NCT04830358	Healthy Koreans 19–50 Years	[90,234]
	ExPEC9V	18556	Participants with first invasive extraintestinal pathogenic *E. coli* disease. No results posted.	Phase III NCT04899336	Adults Aged 60 Years and Older	[90,133]
	UTI Vx, FimH vaccine (FimCH)	NR	NR	Phase II	NR	[90]
	Uro-Vaxom (OM-89)	48	Checklist or consensus guidelines that can be used to measure a symptomatic urinary tract infection and practicality of carrying out a definitive randomized controlled clinical study. Urinary tract infection rates varied between different catheterization methods: male indwelling (2.72), clean intermittent (0.41), condom (0.36), female suprapubic (0.34), and normal voiding (0.06), with an overall incidence of 0.68.	Phase II NCT02591901	Adults 18–75 Years	[90,235]
	ExPEC10V (VAC52416, JNJ-69968054)	836	Safety and antibody titers. No results posted.	Phase I/II NCT03819049	Adults 60–85 Years	[90,134]
Salmonella enterica serovar Paratyphi A	O:2,12-TT	NR	NR	Phase III	NR	[90]
	Entervax	99	Diagnosis of typhoid fever. No results posted.	Phase IIb NCT01405521	Adults 18–60 Years	[90,144]
	CVD 1902	51	Safety and serum antibodies. No results posted.	Phase I NCT01129453	Adults 18–45 Years	[90,236]
C. difficile	PF-06425090 (+/− adjuvant) (62–64, 68)	17535	Number of first primary episodes of CDI. No results posted.	Phase III NCT03090191	Adults 50 and older	[90,237]
	PF-06425090 (+/− adjuvant) (62–64, 68)	140	Adverse effects. No results posted.	Phase I NCT04026009	Adults 18–70	[90,148]
N.gonorrhoeae	4CMenB (Bexsero)	652	Change in the incidence of the first episode of N. gonorrhoeae infection. Overall incidence of all episodes of N. gonorrhoeae infection. No results posted.	Phase III NCT04415424	Gay and Bisexual Men 18 to ≤50 years of age	[90,238]
ETEC	ETVAX/dmLT; ETVAX (OEV-122); ETVAX (OEV-123); ETVAX (OEV-121); (OEV-124)	NR	NR	Phase IIb PACTR202010819218562	NR	[90]
	Phase I: CfaE + mLT (ID); CssBA + dmLT; Phase II: CfaE + mLT	56	Number of adverse events and prevented diarrhea episodes. No results posted.	Phase II NCT01922856	Adults 18–50 Years	[90,239]
	Shigella-ETEC	NR	NR	Phase I	NR	[90]
	ShigETEC	NR	NR	Phase I EudraCT: 2020-000248-79	NR	[90]
K. pneumoniae	CVD 31000 (CVD 1208S-122)	54	Adverse reactions. No results posted.	Phase I NCT04634513	Adults 18–49 Years	[90,240]
	dmLT (LTR192G/L211A) (77)	75	Adverse effects and reactogenicity. No results posted.	Phase I NCT03548064	Adults 18–45 Years	[90,241]
	KlebV4	166	Adverse effects and IgG titers against *K. pneumoniae* O serotypes. No results posted.	Phase I/II NCT04959344	Adults 18–70 Years	[90,242]
P. aeruginosa	VLA43 (IC43)	803	Number of deaths until day 28. No results posted.	Phase II/III NCT01563263 (Discontinued)	Adults 18–80 Years	[90,243]
S. aureus	rTSST-1 variant vaccine (ORG28077)	140	Adverse events and fold increase of ELISA IgGs against rTSST-1. No results posted.	Phase I NCT02814708	Adults 18–64 Years	[90,244]
	GSK3878858A	632	Number of participants with solicited local adverse events. No results posted.	Phase I/II NCT04420221	Adults 18–64 Years	[90,245]

6. Conclusions

Considering the indiscriminate use of antibiotics and the increasing resistance of bacteria to them, employing new approaches for vaccines is emerging as the optimal strategy for treating and preventing bacterial infections that are resistant to antibiotics. To effectively vaccinate against antibiotic-resistant bacteria, it is crucial to utilize safe, low-risk, and low-complication vaccines. Conventional lipopolysaccharide-based and conjugate protein vaccines have been developed against rapidly mutating strains of bacteria such as *S. pneumoniae*. However, such approaches are laborious, require complex processes, and may be impractical against the rapid evolution and emergence of multiple bacterial serotypes. An effective and novel approach entails employing the reverse vaccinology method to develop subunit vaccines with minimal side effects. The advent of the COVID-19 pandemic resulted in the field of vaccine design undergoing significant transformation with the adoption of reverse vaccinology [246]. This method involves vaccinating the patient against conserved and immunogenic epitopes and antigenic determinants of the bacteria. In particular, the strategy of in silico integration of reverse vaccinology and immunoinformatics may be used to identify conserved and immunogenic epitopes that could be incorporated into next-generation multi-epitope vaccines such as recombinant protein, DNA, or mRNA vaccines [247,248]. These vaccines are amenable to accelerated developmental timelines and can quickly progress to the clinical stage in order to curb the spread of antibiotic-resistant bacterial strains. Thus, next-generation vaccines offer a promising avenue for enhancing the effectiveness and safety of vaccine candidates, ultimately contributing to improved global health outcomes.

Author Contributions: Study Design: C.L.P.; Data Collection: K.K.; Data Interpretation: K.K., C.L.P.; Manuscript Preparation: K.K.; Literature Search: K.K. All authors have read and agreed to the published version of the manuscript.

Informed Consent Statement: Not applicable.

Data Availability Statement: No new data were created.

Conflicts of Interest: The authors declare no conflict of interest.

References

1. Paterson, I.K.; Hoyle, A.; Ochoa, G.; Baker-Austin, C.; Taylor, N.G. Optimising antibiotic usage to treat bacterial infections. *Sci. Rep.* **2016**, *6*, 37853. [CrossRef] [PubMed]
2. Uddin, T.M.; Chakraborty, A.J.; Khusro, A.; Zidan, B.M.R.M.; Mitra, S.; Emran, T.B.; Dhama, K.; Ripon, M.K.H.; Gajdács, M.; Sahibzada, M.U.K.; et al. Antibiotic resistance in microbes: History, mechanisms, therapeutic strategies and future prospects. *J. Infect. Public. Health* **2021**, *14*, 1750–1766. [CrossRef] [PubMed]
3. Gao, Y.; Shang, Q.; Li, W.; Guo, W.; Stojadinovic, A.; Mannion, C.; Man, Y.G.; Chen, T. Antibiotics for cancer treatment: A double-edged sword. *J. Cancer* **2020**, *11*, 5135–5149. [CrossRef] [PubMed]
4. Heaney, A.; Trenfield, S. Antibiotic usage in first time coronary artery surgery. *J. Cardiothorac. Surg.* **2015**, *10*, A294. [CrossRef]
5. Kaviani, A.; Ince, D.; Axelrod, D.A. Management of antimicrobial agents in abdominal organ transplant patients in intensive care unit. *Curr. Transplant. Rep.* **2020**, *7*, 1–11. [CrossRef]
6. Lee, L.Y.-H.; Ha, D.L.A.; Simmons, C.; de Jong, M.D.; Chau, N.V.V.; Schumacher, R.; Peng, Y.C.; McMichael, A.J.; Farrar, J.J.; Smith, G.L.; et al. Memory T cells established by seasonal human influenza A infection cross-react with avian influenza A (H5N1) in healthy individuals. *J. Clin. Investig.* **2008**, *118*, 3478–3490. [CrossRef]
7. Gaynes, R. The discovery of penicillin—New insights after more than 75 years of clinical use. *Emerg. Infect. Dis.* **2017**, *23*, 849–853. [CrossRef]
8. Komagamine, J. The efficacy of high-dose penicillin G for pneumococcal pneumonia diagnosed based on initial comprehensive assessment at admission: An observational study. *BMC Res. Notes* **2018**, *11*, 399. [CrossRef]
9. Deshpande, D.; Srivastava, S.; Bendet, P.; Martin Katherine, R.; Cirrincione Kayle, N.; Lee Pooi, S.; Pasipanodya Jotam, G.; Dheda, K.; Gumbo, T. Antibacterial and Sterilizing Effect of Benzylpenicillin in Tuberculosis. *Antimicrob. Agents Chemother.* **2018**, *62*, e02217–e02232. [CrossRef]
10. Adedeji, W.A. The treasure called antibiotics. *Ann. Ib. Postgrad. Med.* **2016**, *14*, 56–57.
11. Liu, Y.; Li, R.; Xiao, X.; Wang, Z. Molecules that inhibit bacterial resistance enzymes. *Molecules* **2018**, *24*, 43. [CrossRef] [PubMed]

12. Schaenzer, A.J.; Wright, G.D. Antibiotic resistance by enzymatic modification of antibiotic targets. *Trends Mol. Med.* **2020**, *26*, 768–782. [CrossRef] [PubMed]
13. Soto, S.M. Role of efflux pumps in the antibiotic resistance of bacteria embedded in a biofilm. *Virulence* **2013**, *4*, 223–229. [CrossRef] [PubMed]
14. Bbosa, G.; Mwebaza, N.; Odda, J.; Kyegombe, D.; Ntale, M. Antibiotics/antibacterial drug use, their marketing and promotion during the post-antibiotic golden age and their role in emergence of bacterial resistance. *Health* **2014**, *6*, 410–425. [CrossRef]
15. O'Neill, J. Review on Antimicrobial Resistance. Antimicrobial Resistance: Tackling a Crisis for the Health and Wealth of Nations—2014 (December). Available online: http://amr-review.org (accessed on 14 July 2023).
16. Murray, C.J.L.; Ikuta, K.S.; Sharara, F.; Swetschinski, L.; Robles Aguilar, G.; Gray, A.; Han, C.; Bisignano, C.; Rao, P.; Wool, E.; et al. Global burden of bacterial antimicrobial resistance in 2019: A systematic analysis. *Lancet* **2022**, *399*, 629–655. [CrossRef]
17. Chokshi, A.; Sifri, Z.; Cennimo, D.; Horng, H. Global contributors to antibiotic resistance. *J. Glob. Infect. Dis.* **2019**, *11*, 36–42. [CrossRef]
18. Chen, W. Will the mRNA vaccine platform be the panacea for the development of vaccines against antimicrobial resistant (AMR) pathogens? *Expert. Rev. Vaccines* **2022**, *21*, 155–157. [CrossRef]
19. Enayatkhani, M.; Hasaniazad, M.; Faezi, S.; Gouklani, H.; Davoodian, P.; Ahmadi, N.; Einakian, M.A.; Karmostaji, A.; Ahmadi, K. Reverse vaccinology approach to design a novel multi-epitope vaccine candidate against COVID-19: An in silico study. *J. Biomol. Struct. Dyn.* **2021**, *39*, 2857–2872. [CrossRef]
20. Herrera, L.R.M. Reverse vaccinology approach in constructing a multi-epitope vaccine against cancer-testis antigens expressed in non-small cell lung cancer. *Asian Pac. J. Cancer Prev.* **2021**, *22*, 1495–1506. [CrossRef]
21. Tobuse, A.J.; Ang, C.W.; Yeong, K.Y. Modern vaccine development via reverse vaccinology to combat antimicrobial resistance. *Life Sci.* **2022**, *302*, 120660. [CrossRef]
22. Chakaya, J.; Khan, M.; Ntoumi, F.; Aklillu, E.; Fatima, R.; Mwaba, P.; Kapata, N.; Mfinanga, S.; Hasnain, S.E.; Katoto, P.; et al. Global tuberculosis report 2020—Reflections on the global TB burden, treatment and prevention efforts. *Int. J. Infect. Dis.* **2021**, *113* (Suppl. 1), S7–S12. [CrossRef]
23. Cabral, M.P.; García, P.; Beceiro, A.; Rumbo, C.; Pérez, A.; Moscoso, M.; Bou, G. Design of live attenuated bacterial vaccines based on D-glutamate auxotrophy. *Nat. Commun.* **2017**, *8*, 15480. [CrossRef] [PubMed]
24. Quinn, C.P.; Sabourin, C.L.; Niemuth, N.A.; Li, H.; Semenova, V.A.; Rudge, T.L.; Mayfield, H.J.; Schiffer, J.; Mittler, R.S.; Ibegbu, C.C.; et al. A three-dose intramuscular injection schedule of anthrax vaccine adsorbed generates sustained humoral and cellular immune responses to protective antigen and provides long-term protection against inhalation anthrax in rhesus macaques. *Clin. Vaccine. Immunol.* **2012**, *19*, 1730–1745. [CrossRef] [PubMed]
25. Little, S.F.; Ivins, B.E.; Webster, W.M.; Norris, S.L.; Andrews, G.P. Effect of aluminum hydroxide adjuvant and formaldehyde in the formulation of rPA anthrax vaccine. *Vaccine* **2007**, *25*, 2771–2777. [CrossRef] [PubMed]
26. Kirkpatrick, B.D.; Tenney, K.M.; Larsson, C.J.; O'Neill, J.P.; Ventrone, C.; Bentley, M.; Upton, A.; Hindle, Z.; Fidler, C.; Kutzko, D.; et al. The novel oral typhoid vaccine M01ZH09 Is well tolerated and highly immunogenic in 2 vaccine presentations. *J. Infect. Dis.* **2005**, *192*, 360–366. [CrossRef]
27. Luca, S.; Mihaescu, T. History of BCG vaccine. *Maedica* **2013**, *8*, 53–58.
28. Dijkman, K.; Sombroek, C.C.; Vervenne, R.A.W.; Hofman, S.O.; Boot, C.; Remarque, E.J.; Kocken, C.H.M.; Ottenhoff, T.H.M.; Kondova, I.; Khayum, M.A.; et al. Prevention of tuberculosis infection and disease by local BCG in repeatedly exposed rhesus macaques. *Nat. Med.* **2019**, *25*, 255–262. [CrossRef]
29. Darrah, P.A.; Zeppa, J.J.; Maiello, P.; Hackney, J.A.; Wadsworth, M.H.; Hughes, T.K.; Pokkali, S.; Swanson, P.A.; Grant, N.L.; Rodgers, M.A.; et al. Prevention of tuberculosis in macaques after intravenous BCG immunization. *Nature* **2020**, *577*, 95–102. [CrossRef]
30. Tsenova, L.; Harbacheuski, R.; Sung, N.; Ellison, E.; Fallows, D.; Kaplan, G. BCG vaccination confers poor protection against *M. tuberculosis* HN878-induced central nervous system disease. *Vaccine* **2007**, *25*, 5126–5132. [CrossRef]
31. Martinez, L.; Cords, O.; Liu, Q.; Acuna-Villaorduna, C.; Bonnet, M.; Fox, G.J.; Carvalho, A.C.C.; Chan, P.-C.; Croda, J.; Hill, P.C.; et al. Infant BCG vaccination and risk of pulmonary and extrapulmonary tuberculosis throughout the life course: A systematic review and individual participant data meta-analysis. *Lancet Glob. Health* **2022**, *10*, e1307–e1316. [CrossRef]
32. Trunz, B.B.; Fine, P.; Dye, C. Effect of BCG vaccination on childhood tuberculous meningitis and miliary tuberculosis worldwide: A meta-analysis and assessment of cost-effectiveness. *Lancet* **2006**, *367*, 1173–1180. [CrossRef] [PubMed]
33. Sathkumara, H.D.; Pai, S.; Aceves-Sánchez, M.J.; Ketheesan, N.; Flores-Valdez, M.A.; Kupz, A. BCG vaccination prevents reactivation of latent lymphatic murine tuberculosis independently of CD4(+) T cells. *Front. Immunol.* **2019**, *10*, 532. [CrossRef] [PubMed]
34. Aguilo, N.; Uranga, S.; Marinova, D.; Monzon, M.; Badiola, J.; Martin, C. MTBVAC vaccine is safe, immunogenic and confers protective efficacy against *Mycobacterium tuberculosis* in newborn mice. *Tuberculosis* **2016**, *96*, 71–74. [CrossRef] [PubMed]
35. Spertini, F.; Audran, R.; Chakour, R.; Karoui, O.; Steiner-Monard, V.; Thierry, A.-C.; Mayor, C.E.; Rettby, N.; Jaton, K.; Vallotton, L.; et al. Safety of human immunisation with a live-attenuated *Mycobacterium tuberculosis* vaccine: A randomised, double-blind, controlled phase I trial. *Lancet Respir. Med.* **2015**, *3*, 953–962. [CrossRef]

36. Arbues, A.; Aguilo, J.I.; Gonzalo-Asensio, J.; Marinova, D.; Uranga, S.; Puentes, E.; Fernandez, C.; Parra, A.; Cardona, P.J.; Vilaplana, C.; et al. Construction, characterization and preclinical evaluation of MTBVAC, the first live-attenuated *M. tuberculosis*-based vaccine to enter clinical trials. *Vaccine* **2013**, *31*, 4867–4873. [CrossRef]

37. Verreck, F.A.; Vervenne, R.A.; Kondova, I.; van Kralingen, K.W.; Remarque, E.J.; Braskamp, G.; van der Werff, N.M.; Kersbergen, A.; Ottenhoff, T.H.; Heidt, P.J.; et al. MVA.85A boosting of BCG and an attenuated, phoP deficient *M. tuberculosis* vaccine both show protective efficacy against tuberculosis in rhesus macaques. *PLoS ONE* **2009**, *4*, e5264. [CrossRef]

38. Martín, C.; Marinova, D.; Aguiló, N.; Gonzalo-Asensio, J. MTBVAC, a live TB vaccine poised to initiate efficacy trials 100 years after BCG. *Vaccine* **2021**, *39*, 7277–7285. [CrossRef]

39. Moscoso, M.; García, P.; Cabral, M.P.; Rumbo, C.; Bou, G. A D-Alanine auxotrophic live vaccine is effective against lethal infection caused by *Staphylococcus aureus*. *Virulence* **2018**, *9*, 604–620. [CrossRef]

40. Shu, M.H.; MatRahim, N.; NorAmdan, N.; Pang, S.P.; Hashim, S.H.; Phoon, W.H.; AbuBakar, S. An inactivated antibiotic-exposed whole-cell vaccine enhances bactericidal activities against multidrug-resistant *Acinetobacter baumannii*. *Sci. Rep.* **2016**, *6*, 22332. [CrossRef]

41. Orenstein, W.A.; Ahmed, R. Simply put: Vaccination saves lives. *Proc. Natl. Acad. Sci. USA* **2017**, *114*, 4031–4033. [CrossRef]

42. Vignuzzi, M.; Wendt, E.; Andino, R. Engineering attenuated virus vaccines by controlling replication fidelity. *Nat. Med.* **2008**, *14*, 154–161. [CrossRef] [PubMed]

43. Lauring, A.S.; Jones, J.O.; Andino, R. Rationalizing the development of live attenuated virus vaccines. *Nat. Biotechnol.* **2010**, *28*, 573–579. [CrossRef] [PubMed]

44. Viswanathan, V.K. Off-label abuse of antibiotics by bacteria. *Gut Microbes* **2014**, *5*, 3–4. [CrossRef] [PubMed]

45. Fertey, J.; Bayer, L.; Grunwald, T.; Pohl, A.; Beckmann, J.; Gotzmann, G.; Casado, J.P.; Schönfelder, J.; Rögner, F.H.; Wetzel, C.; et al. Pathogens inactivated by low-energy-electron irradiation maintain antigenic properties and induce protective immune responses. *Viruses* **2016**, *8*, 319. [CrossRef]

46. Burrell, C.J.; Howard, C.R.; Murphy, F.A. (Eds.) Chapter 11—Vaccines and Vaccination. In *Fenner and White's Medical Virology (Fifth Edition)*; Academic Press: London, UK, 2017; pp. 155–167.

47. Han, X.; Xu, P.; Ye, Q. Analysis of COVID-19 vaccines: Types, thoughts, and application. *J. Clin. Lab. Anal.* **2021**, *35*, e23937. [CrossRef] [PubMed]

48. Bian, L.; Gao, F.; Zhang, J.; He, Q.; Mao, Q.; Xu, M.; Liang, Z. Effects of SARS-CoV-2 variants on vaccine efficacy and response strategies. *Expert. Rev. Vaccines* **2021**, *20*, 365–373. [CrossRef]

49. Oster, M.E.; Shay, D.K.; Su, J.R.; Gee, J.; Creech, C.B.; Broder, K.R.; Edwards, K.; Soslow, J.H.; Dendy, J.M.; Schlaudecker, E.; et al. Myocarditis cases reported after mRNA-based COVID-19 vaccination in the US from December 2020 to August 2021. *JAMA* **2022**, *327*, 331–340. [CrossRef]

50. Liu, M.A. A comparison of plasmid DNA and mRNA as vaccine technologies. *Vaccines* **2019**, *7*, 37. [CrossRef]

51. Lai, C.-Y.; To, A.; Wong, T.A.S.; Lieberman, M.M.; Clements, D.E.; Senda, J.T.; Ball, A.H.; Pessaint, L.; Andersen, H.; Furuyama, W.; et al. Recombinant protein subunit SARS-CoV-2 vaccines formulated with CoVaccine HT™ adjuvant induce broad, Th1 biased, humoral and cellular immune responses in mice. *Vaccine X* **2021**, *9*, 100126. [CrossRef]

52. Flood, A.; Estrada, M.; McAdams, D.; Ji, Y.; Chen, D. Development of a freeze-dried, heat-stable influenza subunit vaccine formulation. *PLoS ONE* **2016**, *11*, e0164692. [CrossRef]

53. Rosano, G.L.; Ceccarelli, E.A. Recombinant protein expression in *Escherichia coli*: Advances and challenges. *Front. Microbiol.* **2014**, *5*, e172. [CrossRef] [PubMed]

54. Altmann, F.; Staudacher, E.; Wilson, I.B.; März, L. Insect cells as hosts for the expression of recombinant glycoproteins. *Glycoconj. J.* **1999**, *16*, 109–123. [CrossRef] [PubMed]

55. Thak, E.J.; Yoo, S.J.; Moon, H.Y.; Kang, H.A. Yeast synthetic biology for designed cell factories producing secretory recombinant proteins. *FEMS Yeast Res.* **2020**, *20*, foaa009. [CrossRef] [PubMed]

56. Pollet, J.; Chen, W.H.; Strych, U. Recombinant protein vaccines, a proven approach against coronavirus pandemics. *Adv. Drug Deliv. Rev.* **2021**, *170*, 71–82. [CrossRef]

57. Fujita-Yamaguchi, Y. Affinity chromatography of native and recombinant proteins from receptors for insulin and IGF-I to recombinant single chain antibodies. *Front. Endocrinol.* **2015**, *6*, 166. [CrossRef]

58. Schäfer, F.; Seip, N.; Maertens, B.; Block, H.; Kubicek, J. Purification of GST-tagged proteins. *Methods Enzymol.* **2015**, *559*, 127–139. [CrossRef]

59. Liu, S.; Tobias, R.; McClure, S.; Styba, G.; Shi, Q.; Jackowski, G. Removal of endotoxin from recombinant protein preparations. *Clin. Biochem.* **1997**, *30*, 455–463. [CrossRef]

60. Ghaemi, A.; Roshani Asl, P.; Zargaran, H.; Ahmadi, D.; Hashimi, A.A.; Abdolalipour, E.; Bathaeian, S.; Miri, S.M. Recombinant COVID-19 vaccine based on recombinant RBD/Nucleoprotein and saponin adjuvant induces long-lasting neutralizing antibodies and cellular immunity. *Front. Immunol.* **2022**, *13*, 974364. [CrossRef]

61. Kaufmann, S.H.; Cotton, M.F.; Eisele, B.; Gengenbacher, M.; Grode, L.; Hesseling, A.C.; Walzl, G. The BCG replacement vaccine VPM1002: From drawing board to clinical trial. *Expert. Rev. Vaccines* **2014**, *13*, 619–630. [CrossRef]

62. Loxton, A.G.; Knaul, J.K.; Grode, L.; Gutschmidt, A.; Meller, C.; Eisele, B.; Johnstone, H.; van der Spuy, G.; Maertzdorf, J.; Kaufmann, S.H.E.; et al. Safety and Immunogenicity of the recombinant *Mycobacterium bovis* BCG vaccine VPM1002 in HIV-unexposed newborn infants in South Africa. *Clin. Vaccine Immunol.* **2017**, *24*, e00439-16. [CrossRef]

63. Glynn, J.R.; Whiteley, J.; Bifani, P.J.; Kremer, K.; van Soolingen, D. Worldwide occurrence of Beijing/W strains of Mycobacterium tuberculosis: A systematic review. *Emerg. Infect. Dis.* **2002**, *8*, 843–849. [CrossRef] [PubMed]

64. Ordway, D.J.; Shang, S.; Henao-Tamayo, M.; Obregon-Henao, A.; Nold, L.; Caraway, M.; Shanley, C.A.; Basaraba, R.J.; Duncan, C.G.; Orme, I.M. Mycobacterium bovis BCG-mediated protection against W-Beijing strains of *Mycobacterium tuberculosis* is diminished concomitant with the emergence of regulatory T cells. *Clin. Vaccine Immunol.* **2011**, *18*, 1527–1535. [CrossRef] [PubMed]

65. Grode, L.; Seiler, P.; Baumann, S.; Hess, J.; Brinkmann, V.; Nasser Eddine, A.; Mann, P.; Goosmann, C.; Bandermann, S.; Smith, D.; et al. Increased vaccine efficacy against tuberculosis of recombinant *Mycobacterium bovis* bacille Calmette-Guérin mutants that secrete listeriolysin. *J. Clin. Investig.* **2005**, *115*, 2472–2479. [CrossRef] [PubMed]

66. Dodd, P.J.; Sismanidis, C.; Seddon, J.A. Global burden of drug-resistant tuberculosis in children: A mathematical modelling study. *Lancet Infect. Dis.* **2016**, *16*, 1193–1201. [CrossRef]

67. Grode, L.; Ganoza, C.A.; Brohm, C.; Weiner, J., 3rd; Eisele, B.; Kaufmann, S.H. Safety and immunogenicity of the recombinant BCG vaccine VPM1002 in a phase 1 open-label randomized clinical trial. *Vaccine* **2013**, *31*, 1340–1348. [CrossRef]

68. Cotton, M.F.; Madhi, S.A.; Luabeya, A.K.; Tameris, M.; Hesseling, A.C.; Shenje, J.; Schoeman, E.; Hatherill, M.; Desai, S.; Kapse, D.; et al. Safety and immunogenicity of VPM1002 versus BCG in South African newborn babies: A randomised, phase 2 non-inferiority double-blind controlled trial. *Lancet Infect. Dis.* **2022**, *22*, 1472–1483. [CrossRef]

69. Chiwala, G.; Liu, Z.; Mugweru, J.N.; Wang, B.; Khan, S.A.; Bate, P.N.N.; Yusuf, B.; Hameed, H.M.A.; Fang, C.; Tan, Y.; et al. A recombinant selective drug-resistant *M. bovis* BCG enhances the bactericidal activity of a second-line anti-tuberculosis regimen. *Biomed. Pharmacother.* **2021**, *142*, 112047. [CrossRef]

70. Rodrigues, M.; Yang, Y.; Meira, E.; Silva, J.; Bicalho, R. Development and evaluation of a new recombinant protein vaccine (YidR) against *Klebsiella pneumoniae* infection. *Vaccine* **2020**, *38*, 4640–4648. [CrossRef]

71. Poland, G.A.; Ovsyannikova, I.G.; Kennedy, R.B. SARS-CoV-2 immunity: Review and applications to phase 3 vaccine candidates. *Lancet* **2020**, *396*, 1595–1606. [CrossRef]

72. Krammer, F. SARS-CoV-2 vaccines in development. *Nature* **2020**, *586*, 516–527. [CrossRef]

73. Khalid, K.; Poh, C.L. The development of DNA vaccines against SARS-CoV-2. *Adv. Med. Sci.* **2023**, *68*, 213–226. [CrossRef] [PubMed]

74. Hobernik, D.; Bros, M. DNA Vaccines-How Far from Clinical Use? *Int. J. Mol. Sci.* **2018**, *19*, 3605. [CrossRef] [PubMed]

75. Kutzler, M.A.; Weiner, D.B. DNA vaccines: Ready for prime time? *Nat. Rev. Genet.* **2008**, *9*, 776–788. [CrossRef] [PubMed]

76. Tomljenovic, L.; Shaw, C.A. Aluminum vaccine adjuvants: Are they safe? *Curr. Med. Chem.* **2011**, *18*, 2630–2637. [CrossRef]

77. Al-Fattah Yahaya, A.A.; Khalid, K.; Lim, H.X.; Poh, C.L. Development of next generation vaccines against SARS-CoV-2 and variants of concern. *Viruses* **2023**, *15*, 624. [CrossRef]

78. Ansari, H.; Tahmasebi-Birgani, M.; Bijanzadeh, M.; Doosti, A.; Kargar, M. Study of the immunogenicity of outer membrane protein A (ompA) gene from *Acinetobacter baumannii* as DNA vaccine candidate in vivo. *Iran. J. Basic. Med. Sci.* **2019**, *22*, 669–675. [CrossRef]

79. Hashemzehi, R.; Doosti, A.; Kargar, M.; Jaafarinia, M. Cloning and expression of nlpA gene as DNA vaccine candidate against *Acinetobacter baumannii*. *Mol. Biol. Rep.* **2018**, *45*, 395–401. [CrossRef]

80. Han, S. Clinical vaccine development. *Clin. Exp. Vaccine Res.* **2015**, *4*, 46–53. [CrossRef]

81. Barbier, A.J.; Jiang, A.Y.; Zhang, P.; Wooster, R.; Anderson, D.G. The clinical progress of mRNA vaccines and immunotherapies. *Nat. Biotechnol.* **2022**, *40*, 840–854. [CrossRef]

82. Polack, F.P.; Thomas, S.J.; Kitchin, N.; Absalon, J.; Gurtman, A.; Lockhart, S.; Perez, J.L.; Pérez Marc, G.; Moreira, E.D.; Zerbini, C.; et al. Safety and efficacy of the BNT162b2 mRNA Covid-19 vaccine. *N. Engl. J. Med.* **2020**, *383*, 2603–2615. [CrossRef]

83. Baden, L.R.; El Sahly, H.M.; Essink, B.; Kotloff, K.; Frey, S.; Novak, R.; Diemert, D.; Spector, S.A.; Rouphael, N.; Creech, C.B.; et al. Efficacy and safety of the mRNA-1273 SARS-CoV-2 vaccine. *N. Engl. J. Med.* **2021**, *384*, 403–416. [CrossRef] [PubMed]

84. Smith, T.R.F.; Patel, A.; Ramos, S.; Elwood, D.; Zhu, X.; Yan, J.; Gary, E.N.; Walker, S.N.; Schultheis, K.; Purwar, M.; et al. Immunogenicity of a DNA vaccine candidate for COVID-19. *Nat. Commun.* **2020**, *11*, 2601. [CrossRef] [PubMed]

85. Cao, Y.; Gao, G.F. mRNA vaccines: A matter of delivery. *eClinicalMedicine* **2021**, *32*, 100746. [CrossRef] [PubMed]

86. Rosa, S.S.; Prazeres, D.M.F.; Azevedo, A.M.; Marques, M.P.C. mRNA vaccines manufacturing: Challenges and bottlenecks. *Vaccine* **2021**, *39*, 2190–2200. [CrossRef]

87. Mayer, R.L.; Verbeke, R.; Asselman, C.; Aernout, I.; Gul, A.; Eggermont, D.; Boucher, K.; Thery, F.; Maia, T.M.; Demol, H.; et al. Immunopeptidomics-based design of highly effective mRNA vaccine formulations against *Listeria monocytogenes*. *bioRxiv* **2022**, *13*, 6075. [CrossRef]

88. Kon, E.; Levy, Y.; Elia, U.; Cohen, H.; Hazan-Halevy, I.; Aftalion, M.; Ezra, A.; Bar-Haim, E.; Naidu, G.S.; Diesendruck, Y.; et al. An effective mRNA-LNP vaccine against the lethal plague bacterium. *bioRxiv* **2022**, *8*, 503096. [CrossRef]

89. Moghimi, S.M. Allergic reactions and anaphylaxis to LNP-based COVID-19 vaccines. *Mol. Ther.* **2021**, *29*, 898–900. [CrossRef]

90. Sellaturay, P.; Nasser, S.; Islam, S.; Gurugama, P.; Ewan, P.W. Polyethylene glycol (PEG) is a cause of anaphylaxis to the Pfizer/BioNTech mRNA COVID-19 vaccine. *Clin. Exp. Allergy* **2021**, *51*, 861–863. [CrossRef]

91. Krishna, M.; Nadler, S.G. Immunogenicity to biotherapeutics–the role of anti-drug immune complexes. *Front. Immunol.* **2016**, *7*, 21. [CrossRef]

92. Medjitna, T.D.; Stadler, C.; Bruckner, L.; Griot, C.; Ottiger, H.P. DNA vaccines: Safety aspect assessment and regulation. *Dev. Biol.* **2006**, *126*, 261–270; discussion 327.

93. Li, Y.; Xiao, J.; Chang, Y.F.; Zhang, H.; Teng, Y.; Lin, W.; Li, H.; Chen, W.; Zhang, X.; Xie, Q. Immunogenicity and protective efficacy of the recombinant *Pasteurella multocida* lipoproteins VacJ and PlpE, and outer membrane protein H from P. multocida A:1 in ducks. *Front. Immunol.* **2022**, *13*, 985993. [CrossRef] [PubMed]

94. Wu, Y.; Zhang, H.; Meng, L.; Li, F.; Yu, C. Comparison of immune responses elicited by SARS-CoV-2 mRNA and recombinant protein vaccine candidates. *Front. Immunol.* **2022**, *13*, 906457. [CrossRef] [PubMed]

95. Jespersen, M.C.; Mahajan, S.; Peters, B.; Nielsen, M.; Marcatili, P. Antibody specific B-cell epitope predictions: Leveraging information from antibody-antigen protein complexes. *Front. Immunol.* **2019**, *10*, 298. [CrossRef] [PubMed]

96. Rahman, M.S.; Rahman, M.K.; Saha, S.; Kaykobad, M.; Rahman, M.S. Antigenic: An improved prediction model of protective antigens. *Artif. Intell. Med.* **2019**, *94*, 28–41. [CrossRef] [PubMed]

97. Dorosti, H.; Eslami, M.; Negahdaripour, M.; Ghoshoon, M.B.; Gholami, A.; Heidari, R.; Dehshahri, A.; Erfani, N.; Nezafat, N.; Ghasemi, Y. Vaccinomics approach for developing multi-epitope peptide pneumococcal vaccine. *J. Biomol. Struct. Dyn.* **2019**, *37*, 3524–3535. [CrossRef]

98. Tan, C.; Zhu, F.; Xiao, Y.; Wu, Y.; Meng, X.; Liu, S.; Liu, T.; Chen, S.; Zhou, J.; Li, C.; et al. Immunoinformatics approach toward the introduction of a novel multi-epitope vaccine against Clostridium difficile. *Front. Immunol.* **2022**, *13*, 887061. [CrossRef]

99. Alzarea, S.I. Identification and construction of a multi-epitopes vaccine design against Klebsiella aerogenes: Molecular modeling study. *Sci. Rep.* **2022**, *12*, 14402. [CrossRef]

100. Stratmann, T. Cholera toxin subunit B as adjuvant--An accelerator in protective immunity and a break in autoimmunity. *Vaccines* **2015**, *3*, 579–596. [CrossRef]

101. Albekairi, T.H.; Alshammari, A.; Alharbi, M.; Alshammary, A.F.; Tahir Ul Qamar, M.; Ullah, A.; Irfan, M.; Ahmad, S. Designing of a novel multi-antigenic epitope-based vaccine against *E. Hormaechei*: An intergraded reverse vaccinology and immunoinformatics approach. *Vaccines* **2022**, *10*, 665. [CrossRef]

102. Alshabrmi, F.M.; Alrumaihi, F.; Alrasheedi, S.F.; Al-Megrin, W.A.I.; Almatroudi, A.; Allemailem, K.S. An in-silico investigation to design a multi-epitopes vaccine against multi-drug resistant *Hafnia alvei*. *Vaccines* **2022**, *10*, 1127. [CrossRef]

103. Munia, M.; Mahmud, S.; Mohasin, M.; Kibria, K.M.K. In silico design of an epitope-based vaccine against choline binding protein A of *Streptococcus pneumoniae*. *Inform. Med. Unlocked* **2021**, *23*, 100546. [CrossRef]

104. Kumar, A.; Harjai, K.; Chhibber, S. A multiepitopic theoretical fusion construct based on in-silico epitope screening of known vaccine candidates for protection against wide range of enterobacterial pathogens. *Human Immunol.* **2019**, *80*, 493–502. [CrossRef] [PubMed]

105. Buckner, M.M.C.; Croxen, M.; Arena, E.T.; Finlay, B.B. A comprehensive study of the contribution of *Salmonella enterica* serovar Typhimurium SPI2 effectors to bacterial colonization, survival, and replication in typhoid fever, macrophage, and epithelial cell infection models. *Virulence* **2011**, *2*, 208–216. [CrossRef] [PubMed]

106. Brockett, S.; Wolfe, M.K.; Hamot, A.; Appiah, G.D.; Mintz, E.D.; Lantagne, D. Associations among water, sanitation, and hygiene, and food exposures and typhoid fever in case-control studies: A systematic review and meta-analysis. *Am. J. Trop. Med. Hyg.* **2020**, *103*, 1020–1031. [CrossRef] [PubMed]

107. Jung, K.O.; Kim, Y.H.; Chung, S.J.; Lee, C.H.; Rhee, S.; Pratx, G.; Chung, J.K.; Youn, H. Identification of lymphatic and hematogenous routes of rapidly labeled radioactive and fluorescent exosomes through highly sensitive multimodal imaging. *Int. J. Mol. Sci.* **2020**, *21*, 7850. [CrossRef]

108. Connor, B.A.; Schwartz, E. Typhoid and paratyphoid fever in travellers. *Lancet Infect. Dis.* **2005**, *5*, 623–628. [CrossRef]

109. Ashurst, J.V.; Truong, J.; Woodbury, B. Salmonella typhi. In *StatPearls [Internet]*; StatPearls Publishing: St. Petersburg, FL, USA, 2022.

110. Hohmann, E.L.; Oletta, C.A.; Killeen, K.P.; Miller, S.I. phoP/phoQ-deleted *Salmonella typhi* (Ty800) is a safe and immunogenic single dose typhoid fever vaccine in volunteers. *J. Infect. Dis.* **1996**, *173*, 1408–1414. [CrossRef]

111. Crump, J.A.; Mintz, E.D. Global trends in typhoid and paratyphoid Fever. *Clin. Infect. Dis.* **2010**, *50*, 241–246. [CrossRef]

112. Amicizia, D.; Arata, L.; Zangrillo, F.; Panatto, D.; Gasparini, R. Overview of the impact of typhoid and paratyphoid fever: Utility of Ty21a vaccine (Vivotif®). *J. Prev. Med. Hyg.* **2017**, *58*, E1–E8.

113. Jackson, B.R.; Iqbal, S.; Mahon, B. Updated recommendations for the use of typhoid vaccine—Advisory committee on immunization practices, United States, 2015. *Morb. Mortal. Wkly. Rep.* **2015**, *64*, 305–308.

114. Choi, S.K.; Baik, Y.O.; Lee, Y.; Lee, C.; Kim, S.K.; Park, J.; Sun, M.; Jung, D.; Jang, J.Y.; Yong, T.J. A phase ii/iii, multicenter, observer-blinded, randomized, non-inferiority and safety, study of typhoid conjugate vaccine (EuTCV) compared to Typbar-TCV® in healthy 6 months-45 years aged participants. *Vaccine* **2023**, *41*, 1753–1759. [CrossRef]

115. Kumar Rai, G.; Saluja, T.; Chaudhary, S.; Tamrakar, D.; Kanodia, P.; Giri, B.R.; Shrestha, R.; Uranw, S.; Kim, D.R.; Yang, J.S.; et al. Safety and immunogenicity of the Vi-DT typhoid conjugate vaccine in healthy volunteers in Nepal: An observer-blind, active-controlled, randomised, non-inferiority, phase 3 trial. *Lancet Infect. Dis.* **2022**, *22*, 529–540. [CrossRef]

116. Nampota-Nkomba, N.; Nyirenda, O.M.; Khonde, L.; Mapemba, V.; Mbewe, M.; Ndaferankhande, J.M.; Msuku, H.; Masesa, C.; Misiri, T.; Mwakiseghile, F.; et al. Safety and immunogenicity of a typhoid conjugate vaccine among children aged 9 months to 12 years in Malawi: A nested substudy of a double-blind, randomised controlled trial. *Lancet Glob. Health* **2022**, *10*, e1326–e1335. [CrossRef] [PubMed]

117. Soulier, A.; Prevosto, C.; Chol, M.; Deban, L.; Cranenburgh, R.M. Engineering a novel bivalent oral vaccine against enteric fever. *Int. J. Mol. Sci.* **2021**, *22*, 3287. [CrossRef]

118. Agrawal, A.; Murphy, T.F. Haemophilus influenzae infections in the *H. influenzae* type b conjugate vaccine era. *J. Clin. Microbiol.* **2011**, *49*, 3728–3732. [CrossRef] [PubMed]

119. Hammitt, L.L.; Crane, R.J.; Karani, A.; Mutuku, A.; Morpeth, S.C.; Burbidge, P.; Goldblatt, D.; Kamau, T.; Sharif, S.; Mturi, N.; et al. Effect of *Haemophilus influenza* type b vaccination without a booster dose on invasive *H. influenzae* type b disease, nasopharyngeal carriage, and population immunity in Kilifi, Kenya: A 15-year regional surveillance study. *Lancet Glob. Health* **2016**, *4*, e185–e194. [CrossRef]

120. World Health Organization. *Bacterial Vaccines in Clinical and Preclinical Development 2021: An Overview and Analysis*; World Health Organization: Geneva, Switzerland, 2021.

121. Tabarani, C.; Fletcher, S.A.; Heresi, G.P.; Wootton, S.H. Invasive *Haemophilus influenza* type b in an infant during the COVID-19 pandemic: The return of diseases we hoped never to see again. *J. Pediatr. Infect. Dis.* **2022**, *41*, e30–e31. [CrossRef]

122. Jansen, K.U.; Anderson, A.S. The role of vaccines in fighting antimicrobial resistance (AMR). *Hum. Vaccin. Immunother.* **2018**, *14*, 2142–2149. [CrossRef]

123. Jackson, C.; Mann, A.; Mangtani, P.; Fine, P. Effectiveness of *Haemophilus influenzae* type b vaccines administered according to various schedules: Systematic review and meta-analysis of observational data. *Pediatr. Infect. Dis. J.* **2013**, *32*, 1261–1269. [CrossRef]

124. Obando-Pacheco, P.; Rivero-Calle, I.; Raguindin, P.F.; Martinón-Torres, F. DTaP5-HBV-IPV-Hib pediatric hexavalent combination vaccine for use in children from 6 weeks through to 4 years of age. *Expert. Rev. Vaccines* **2019**, *18*, 1115–1126. [CrossRef]

125. Klein, N.P.; Abu-Elyazeed, R.; Cheuvart, B.; Janssens, W.; Mesaros, N. Immunogenicity and safety following primary and booster vaccination with a hexavalent diphtheria, tetanus, acellular pertussis, hepatitis B, inactivated poliovirus and *Haemophilus influenzae* type b vaccine: A randomized trial in the United States. *Hum. Vaccin. Immunother.* **2019**, *15*, 809–821. [CrossRef] [PubMed]

126. Vaez, H.; Sahebkar, A.; Pourfarzi, F.; Yousefi-Avarvand, A.; Khademi, F. Prevalence of Antibiotic Resistance of *Haemophilus Influenzae* in Iran—A Meta-Analysis. *Iran. J. Otorhinolaryngol.* **2019**, *31*, 349–357. [CrossRef] [PubMed]

127. Kim, G.L.; Seon, S.H.; Rhee, D.K. Pneumonia and *Streptococcus pneumoniae* vaccine. *Arch. Pharm. Res.* **2017**, *40*, 885–893. [CrossRef] [PubMed]

128. Behrens, F.; Funk-Hilsdorf, T.C.; Kuebler, W.M.; Simmons, S. Bacterial membrane vesicles in pneumonia: From mediators of virulence to innovative vaccine candidates. *Int. J. Mol. Sci.* **2021**, *22*, 3858. [CrossRef]

129. Masomian, M.; Ahmad, Z.; Gew, L.T.; Poh, C.L. Development of next generation *Streptococcus pneumoniae* vaccines conferring broad protection. *Vaccines* **2020**, *8*, 132. [CrossRef]

130. Zhang, F.; Lu, Y.J.; Malley, R. Multiple antigen-presenting system (MAPS) to induce comprehensive B- and T-cell immunity. *Proc. Natl. Acad. Sci. USA* **2013**, *110*, 13564–13569. [CrossRef] [PubMed]

131. Pichichero, M.E. Protein carriers of conjugate vaccines: Characteristics, development, and clinical trials. *Hum. Vaccin. Immunother.* **2013**, *9*, 2505–2523. [CrossRef]

132. Brooks, W.A.; Chang, L.J.; Sheng, X.; Hopfer, R. Safety and immunogenicity of a trivalent recombinant PcpA, PhtD, and PlyD1 pneumococcal protein vaccine in adults, toddlers, and infants: A phase I randomized controlled study. *Vaccine* **2015**, *33*, 4610–4617. [CrossRef]

133. NIH. A Study of Vaccination with 9-Valent Extraintestinal Pathogenic *Escherichia coli* Vaccine (ExPEC9V) in the Prevention of Invasive Extraintestinal Pathogenic *Escherichia coli* Disease in Adults Aged 60 Years and Older with a History of Urinary Tract Infection in the Past 2 Years. Available online: https://clinicaltrials.gov/ct2/show/NCT04899336 (accessed on 21 February 2023).

134. NIH. A Study of Three Different Doses of VAC52416 (ExPEC10V) in Adults Aged 60 to 85 Years in Stable Health. Available online: https://clinicaltrials.gov/ct2/show/NCT03819049 (accessed on 21 February 2023).

135. Doua, J.; Fierro, C.; Sarnecki, M.; Spiessens, B.; Go, O.; Davies, T.; van den Dobbelsteen, G.; Poolman, J.; Haazen, W. 120. safety, reactogenicity, and immunogenicity of three different doses of VAC52416 (ExPEC10V) in adults aged 60–85 years in a randomized, multicenter, interventional, first-in-human, phase 1/2a study. *Open Forum Infect. Dis.* **2022**, *9*, ofac492.198. [CrossRef]

136. Eldridge, G.R.; Hughey, H.; Rosenberger, L.; Martin, S.M.; Shapiro, A.M.; D'Antonio, E.; Krejci, K.G.; Shore, N.; Peterson, J.; Lukes, A.S.; et al. Safety and immunogenicity of an adjuvanted *Escherichia coli* adhesin vaccine in healthy women with and without histories of recurrent urinary tract infections: Results from a first-in-human phase 1 study. *Hum. Vaccin. Immunother.* **2021**, *17*, 1262–1270. [CrossRef]

137. Wade, D.; Cooper, J.; Derry, F.; Taylor, J. Uro-Vaxom® versus placebo for the prevention of recurrent symptomatic urinary tract infections in participants with chronic neurogenic bladder dysfunction: A randomised controlled feasibility study. *Trials* **2019**, *20*, 223. [CrossRef] [PubMed]

138. Brodie, A.; El-Taji, O.; Jour, I.; Foley, C.; Hanbury, D. A retrospective study of immunotherapy treatment with Uro-Vaxom (OM-89®) for prophylaxis of recurrent urinary tract infections. *Curr. Urol.* **2020**, *14*, 130–134. [CrossRef] [PubMed]

139. Feldman, M.F.; Wacker, M.; Hernandez, M.; Hitchen, P.G.; Marolda, C.L.; Kowarik, M.; Morris, H.R.; Dell, A.; Valvano, M.A.; Aebi, M. Engineering N-linked protein glycosylation with diverse O antigen lipopolysaccharide structures in *Escherichia coli*. *Proc. Natl. Acad. Sci. USA* **2005**, *102*, 3016–3021. [CrossRef]

140. Poolman, J.T.; Wacker, M. Extraintestinal pathogenic *Escherichia coli*, a common human pathogen: Challenges for vaccine development and progress in the field. *J. Infect. Dis.* **2016**, *213*, 6–13. [CrossRef] [PubMed]

141. Baliban, S.M.; Lu, Y.J.; Malley, R. Overview of the nontyphoidal and paratyphoidal *Salmonella* vaccine pipeline: Current status and future prospects. *Clin. Infect. Dis.* **2020**, *71*, S151–S154. [CrossRef]

142. Wahid, R.; Kotloff, K.L.; Levine, M.M.; Sztein, M.B. Cell mediated immune responses elicited in volunteers following immunization with candidate live oral *Salmonella enterica serovar Paratyphi A* attenuated vaccine strain CVD 1902. *Clin. Immunol.* **2019**, *201*, 61–69. [CrossRef]

143. Shakya, M.; Neuzil, K.M.; Pollard, A.J. Prospects of future typhoid and paratyphoid vaccines in endemic countries. *J. Infect. Dis.* **2021**, *224*, S770–S774. [CrossRef]

144. NIH. Understanding Typhoid Disease after Vaccination. Available online: https://clinicaltrials.gov/ct2/show/NCT01405521 (accessed on 14 July 2023).

145. Xie, L.; Ming, L.; Ding, M.; Deng, L.; Liu, M.; Cong, Y. Paratyphoid fever A: Infection and prevention. *Front. Microbiol.* **2022**, *13*, 945235. [CrossRef]

146. Xiong, K.; Zhu, C.; Chen, Z.; Zheng, C.; Tan, Y.; Rao, X.; Cong, Y. Vi Capsular polysaccharide produced by recombinant *Salmonella enterica Serovar Paratyphi A* confers immunoprotection against infection by *Salmonella enterica Serovar Typhi*. *Front. Cell Infect. Microbiol.* **2017**, *7*, 135. [CrossRef]

147. Dobinson, H.C.; Gibani, M.M.; Jones, C.; Thomaides-Brears, H.B.; Voysey, M.; Darton, T.C.; Waddington, C.S.; Campbell, D.; Milligan, I.; Zhou, L.; et al. Evaluation of the clinical and microbiological response to *Salmonella Paratyphi A* infection in the first paratyphoid human challenge model. *Clin. Infect. Dis.* **2017**, *64*, 1066–1073. [CrossRef]

148. NIH. Safety and Immunogenicity Study of GSK's Clostridium Difficile Vaccine 2904545A when Administered in Healthy Adults Aged 18–45 Years and 50–70 Years. Available online: https://clinicaltrials.gov/ct2/show/NCT04026009 (accessed on 21 February 2023).

149. Inoue, M.; Yonemura, T.; de Solom, R.; Yamaji, M.; Aizawa, M.; Knirsch, C.; Pride, M.W.; Jansen, K.U.; Gruber, W.; Webber, C. A phase 1 randomized study assessing safety and immunogenicity of two 3-dose regimens of a *Clostridium difficile* vaccine in healthy older Japanese adults. *Vaccine* **2019**, *37*, 2600–2607. [CrossRef] [PubMed]

150. Kitchin, N.; Remich, S.A.; Peterson, J.; Peng, Y.; Gruber, W.C.; Jansen, K.U.; Pride, M.W.; Anderson, A.S.; Knirsch, C.; Webber, C. A Phase 2 Study evaluating the safety, tolerability, and immunogenicity of two 3-dose regimens of a *Clostridium difficile* vaccine in healthy US adults aged 65 to 85 years. *Clin. Infect. Dis.* **2020**, *70*, 1–10. [CrossRef] [PubMed]

151. de Bruyn, G.; Gordon, D.L.; Steiner, T.; Tambyah, P.; Cosgrove, C.; Martens, M.; Bassily, E.; Chan, E.S.; Patel, D.; Chen, J.; et al. Safety, immunogenicity, and efficacy of a *Clostridioides difficile* toxoid vaccine candidate: A phase 3 multicentre, observer-blind, randomised, controlled trial. *Lancet Infect. Dis.* **2021**, *21*, 252–262. [CrossRef] [PubMed]

152. Bézay, N.; Ayad, A.; Dubischar, K.; Firbas, C.; Hochreiter, R.; Kiermayr, S.; Kiss, I.; Pinl, F.; Jilma, B.; Westritschnig, K. Safety, immunogenicity and dose response of VLA84, a new vaccine candidate against *Clostridium difficile*, in healthy volunteers. *Vaccine* **2016**, *34*, 2585–2592. [CrossRef]

153. Spigaglia, P. Recent advances in the understanding of antibiotic resistance in *Clostridium difficile* infection. *Ther. Adv. Infect. Dis.* **2016**, *3*, 23–42. [CrossRef]

154. Riley, T.V.; Lyras, D.; Douce, G.R. Status of vaccine research and development for *Clostridium difficile*. *Vaccine* **2019**, *37*, 7300–7306. [CrossRef]

155. Humphreys, D.P.; Wilcox, M.H. Antibodies for treatment of *Clostridium difficile* infection. *Clin. Vaccine Immunol.* **2014**, *21*, 913–923. [CrossRef]

156. Semchenko, E.A.; Seib, K.L. Outer membrane vesicle vaccines for *Neisseria gonorrhoeae*. *Nat. Rev. Urol.* **2022**, *19*, 5–6. [CrossRef]

157. Mahase, E. Meningitis vaccine could protect against gonorrhoea, studies find. *BMJ* **2022**, *377*, o997. [CrossRef]

158. Edwards, J.L.; Jennings, M.P.; Apicella, M.A.; Seib, K.L. Is gonococcal disease preventable? The importance of understanding immunity and pathogenesis in vaccine development. *Crit. Rev. Microbiol.* **2016**, *42*, 928–941. [CrossRef]

159. Gottlieb, S.L.; Johnston, C. Future prospects for new vaccines against sexually transmitted infections. *Curr. Opin. Infect. Dis.* **2017**, *30*, 77–86. [CrossRef] [PubMed]

160. Unemo, M.; Sikora, A.E. Infection: Proof of principle for effectiveness of a gonorrhoea vaccine. *Nat. Rev. Urol.* **2017**, *14*, 643–644. [CrossRef] [PubMed]

161. van Deuren, M.; Brandtzaeg, P.; van der Meer, J.W. Update on meningococcal disease with emphasis on pathogenesis and clinical management. *Clin. Microbiol. Rev.* **2000**, *13*, 144–166. [CrossRef] [PubMed]

162. Booy, R.; Gentile, A.; Nissen, M.; Whelan, J.; Abitbol, V. Recent changes in the epidemiology of *Neisseria meningitidis* serogroup W across the world, current vaccination policy choices and possible future strategies. *Hum. Vaccin. Immunother.* **2019**, *15*, 470–480. [CrossRef]

163. Spinosa, M.R.; Progida, C.; Talà, A.; Cogli, L.; Alifano, P.; Bucci, C. The *Neisseria meningitidis* capsule is important for intracellular survival in human cells. *Infect. Immun.* **2007**, *75*, 3594–3603. [CrossRef] [PubMed]

164. Pace, D. Quadrivalent meningococcal ACYW-135 glycoconjugate vaccine for broader protection from infancy. *Expert. Rev. Vaccines* **2009**, *8*, 529–542. [CrossRef]

165. Serruto, D.; Bottomley, M.J.; Ram, S.; Giuliani, M.M.; Rappuoli, R. The new multicomponent vaccine against meningococcal serogroup B, 4CMenB: Immunological, functional and structural characterization of the antigens. *Vaccine* **2012**, *30* (Suppl. S2), B87–B97. [CrossRef]

166. Rivero-Calle, I.; Raguindin, P.F.; Gómez-Rial, J.; Rodriguez-Tenreiro, C.; Martinón-Torres, F. Meningococcal group B vaccine for the prevention of invasive meningococcal disease caused by *Neisseria meningitidis* serogroup B. *Infect. Drug Resist.* **2019**, *12*, 3169–3188. [CrossRef]

167. Masignani, V.; Pizza, M.; Moxon, E.R. The development of a vaccine against Meningococcus B using reverse vaccinology. *Front. Immunol.* **2019**, *10*, 751. [CrossRef]

168. McNeil, L.K.; Zagursky, R.J.; Lin, S.L.; Murphy, E.; Zlotnick, G.W.; Hoiseth, S.K.; Jansen, K.U.; Anderson, A.S. Role of factor H binding protein in *Neisseria meningitidis* virulence and its potential as a vaccine candidate to broadly protect against meningococcal disease. *Microbiol. Mol. Biol. Rev.* **2013**, *77*, 234–252. [CrossRef]

169. Kleinschmidt, A.; Vadivelu, K.; Serino, L.; Neidig, N.; de Wergifosse, B. Endogenous complement human serum bactericidal assay (enc-hSBA) for vaccine effectiveness assessments against meningococcal serogroup B. *NPJ Vaccines* **2021**, *6*, 29. [CrossRef] [PubMed]

170. Vesikari, T.; Østergaard, L.; Diez-Domingo, J.; Wysocki, J.; Flodmark, C.E.; Beeslaar, J.; Eiden, J.; Jiang, Q.; Jansen, K.U.; Jones, T.R.; et al. Meningococcal serogroup B bivalent rLP2086 vaccine elicits broad and robust serum bactericidal responses in healthy adolescents. *J. Pediatric Infect. Dis. Soc.* **2016**, *5*, 152–160. [CrossRef]

171. Svennerholm, A.M.; Lundgren, A.; Leach, S.; Akhtar, M.; Qadri, F. Mucosal immune responses against an oral enterotoxigenic *Escherichia coli* vaccine evaluated in clinical trials. *J. Infect. Dis.* **2021**, *224*, S821–S828. [CrossRef] [PubMed]

172. Akhtar, M.; Chowdhury, M.I.; Bhuiyan, T.R.; Kaim, J.; Ahmed, T.; Rafique, T.A.; Khan, A.; Rahman, S.I.A.; Khanam, F.; Begum, Y.A.; et al. Evaluation of the safety and immunogenicity of the oral inactivated multivalent enterotoxigenic *Escherichia coli* vaccine ETVAX in Bangladeshi adults in a double-blind, randomized, placebo-controlled Phase I trial using electrochemiluminescence and ELISA assays for immunogenicity analyses. *Vaccine* **2019**, *37*, 5645–5656. [CrossRef] [PubMed]

173. Qadri, F.; Akhtar, M.; Bhuiyan, T.R.; Chowdhury, M.I.; Ahmed, T.; Rafique, T.A.; Khan, A.; Rahman, S.I.A.; Khanam, F.; Lundgren, A.; et al. Safety and immunogenicity of the oral, inactivated, enterotoxigenic *Escherichia coli* vaccine ETVAX in Bangladeshi children and infants: A double-blind, randomised, placebo-controlled phase 1/2 trial. *Lancet Infect. Dis.* **2020**, *20*, 208–219. [CrossRef]

174. NIH. A Phase 2 Bridging Study to Assess the New Formulation of ETVAX. Available online: https://clinicaltrials.gov/ct2/show/NCT05178134 (accessed on 21 February 2023).

175. Steele, D.; Riddle, M.; Van De Verg, L.; Bourgeois, L. Vaccines for enteric diseases: A meeting summary. *Expert. Rev. Vaccines* **2012**, *11*, 407–409. [CrossRef]

176. NIH. Study Confirming a Human Challenge Model and Investigating the Safety of VLA1701. Available online: https://classic.clinicaltrials.gov/ct2/show/NCT03576183 (accessed on 14 July 2023).

177. Harro, C.; Chakraborty, S.; Feller, A.; DeNearing, B.; Cage, A.; Ram, M.; Lundgren, A.; Svennerholm, A.-M.; Bourgeois, A.L.; Walker, R.I. Refinement of a human challenge model for evaluation of enterotoxigenic *Escherichia coli* vaccines. *Clin. Vaccine Immunol.* **2011**, *18*, 1719–1727. [CrossRef]

178. Chakraborty, S.; Randall, A.; Vickers, T.J.; Molina, D.; Harro, C.D.; DeNearing, B.; Brubaker, J.; Sack, D.A.; Bourgeois, A.L.; Felgner, P.L.; et al. Interrogation of a live-attenuated enterotoxigenic *Escherichia coli* vaccine highlights features unique to wild-type infection. *NPJ Vaccines* **2019**, *4*, 37. [CrossRef]

179. Wolf, M.K. Occurrence, distribution, and associations of O and H serogroups, colonization factor antigens, and toxins of enterotoxigenic *Escherichia coli*. *Clin. Microbiol. Rev.* **1997**, *10*, 569–584. [CrossRef]

180. Paczosa, M.K.; Mecsas, J. Klebsiella pneumoniae: Going on the offense with a strong defense. *Microbiol. Mol. Biol. Rev.* **2016**, *80*, 629–661. [CrossRef]

181. Lin, T.-L.; Yang, F.-L.; Ren, C.-T.; Pan, Y.-J.; Liao, K.-S.; Tu, I.-F.; Chang, Y.-P.; Cheng, Y.-Y.; Wu, C.-Y.; Wu, S.-H.; et al. Development of *Klebsiella pneumoniae* capsule polysaccharide-conjugated vaccine candidates using phage depolymerases. *Front. Immunol.* **2022**, *13*, 843183. [CrossRef] [PubMed]

182. Geno, K.A.; Gilbert, G.L.; Song, J.Y.; Skovsted, I.C.; Klugman, K.P.; Jones, C.; Konradsen, H.B.; Nahm, M.H. Pneumococcal capsules and their types: Past, present, and future. *Clin. Microbiol. Rev.* **2015**, *28*, 871–899. [CrossRef] [PubMed]

183. Cryz, S.J., Jr.; Fürer, E.; Germanier, R. Safety and immunogenicity of *Klebsiella pneumoniae* K1 capsular polysaccharide vaccine in humans. *J. Infect. Dis.* **1985**, *151*, 665–671. [CrossRef] [PubMed]

184. Cryz, S.J., Jr.; Cross, A.S.; Sadoff, G.C.; Que, J.U. Human IgG and IgA subclass response following immunization with a polyvalent Klebsiella capsular polysaccharide vaccine. *Eur. J. Immunol.* **1988**, *18*, 2073–2075. [CrossRef]

185. Cryz, S.J., Jr.; Mortimer, P.; Cross, A.S.; Fürer, E.; Germanier, R. Safety and immunogenicity of a polyvalent *Klebsiella* capsular polysaccharide vaccine in humans. *Vaccine* **1986**, *4*, 15–20. [CrossRef]

186. Dintzis, R.Z. Rational design of conjugate vaccines. *Pediatr. Res.* **1992**, *32*, 376–385. [CrossRef]

187. Trautmann, M.; Ruhnke, M.; Rukavina, T.; Held, T.K.; Cross, A.S.; Marre, R.; Whitfield, C. O-antigen seroepidemiology of Klebsiella clinical isolates and implications for immunoprophylaxis of Klebsiella infections. *Clin. Diagn. Lab. Immunol.* **1997**, *4*, 550–555. [CrossRef]

188. Hansen, D.S.; Mestre, F.; Alberti, S.; Hernández-Allés, S.; Alvarez, D.; Doménech-Sánchez, A.; Gil, J.; Merino, S.; Tomás, J.M.; Benedí, V.J. *Klebsiella pneumoniae* lipopolysaccharide O typing: Revision of prototype strains and O-group distribution among clinical isolates from different sources and countries. *J. Clin. Microbiol.* **1999**, *37*, 56–62. [CrossRef]

189. Choi, M.; Hegerle, N.; Nkeze, J.; Sen, S.; Jamindar, S.; Nasrin, S.; Sen, S.; Permala-Booth, J.; Sinclair, J.; Tapia, M.D.; et al. The diversity of lipopolysaccharide (O) and capsular polysaccharide (K) antigens of invasive *Klebsiella pneumoniae* in a multi-country collection. *Front. Microbiol.* **2020**, *11*, e1249. [CrossRef]

190. Bulati, M.; Busà, R.; Carcione, C.; Iannolo, G.; Di Mento, G.; Cuscino, N.; Di Gesù, R.; Piccionello, A.P.; Buscemi, S.; Carreca, A.P.; et al. *Klebsiella pneumoniae* lipopolysaccharides serotype O2afg induce poor inflammatory immune responses ex vivo. *Microorganisms* **2021**, *9*, 1317. [CrossRef]

191. Choi, M.; Tennant, S.M.; Simon, R.; Cross, A.S. Progress towards the development of Klebsiella vaccines. *Expert. Rev. Vaccines* **2019**, *18*, 681–691. [CrossRef] [PubMed]

192. Chhibber, S.; Rani, M.; Vanashree, Y. Immunoprotective potential of polysaccharide-tetanus toxoid conjugate in *Klebsiella pneumoniae* induced lobar pneumonia in rats. *Indian. J. Exp. Biol.* **2005**, *43*, 40–45. [PubMed]

193. Hegerle, N.; Choi, M.; Sinclair, J.; Amin, M.N.; Ollivault-Shiflett, M.; Curtis, B.; Laufer, R.S.; Shridhar, S.; Brammer, J.; Toapanta, F.R.; et al. Development of a broad spectrum glycoconjugate vaccine to prevent wound and disseminated infections with *Klebsiella pneumoniae* and *Pseudomonas aeruginosa*. *PLoS ONE* **2018**, *13*, e0203143. [CrossRef] [PubMed]

194. NIH. Evaluation of the Efficacy and Safety of MV140 (MV140). Available online: https://clinicaltrials.gov/ct2/show/NCT02543827 (accessed on 14 July 2023).

195. NIH. Uromune in Treating Recurrent Urinary Tract Infections in Women. Available online: https://clinicaltrials.gov/ct2/show/NCT04096820 (accessed on 14 July 2023).

196. Nickel, J.C.; Saz-Leal, P.; Doiron, R.C. Could sublingual vaccination be a viable option for the prevention of recurrent urinary tract infection in Canada? A systematic review of the current literature and plans for the future. *Can. Urol. Assoc. J.* **2020**, *14*, 281–287. [CrossRef]

197. Yang, B.; Foley, S. First experience in the UK of treating women with recurrent urinary tract infections with the bacterial vaccine Uromune®. *BJU Int.* **2018**, *121*, 289–292. [CrossRef] [PubMed]

198. Kunz Coyne, A.J.; El Ghali, A.; Holger, D.; Rebold, N.; Rybak, M.J. Therapeutic strategies for emerging multidrug-resistant *Pseudomonas aeruginosa*. *Infect. Dis. Ther.* **2022**, *11*, 661–682. [CrossRef]

199. Elmassry, M.M.; Colmer-Hamood, J.A.; Kopel, J.; San Francisco, M.J.; Hamood, A.N. Anti-Pseudomonas aeruginosa vaccines and therapies: An assessment of clinical trials. *Microorganisms* **2023**, *11*, 916. [CrossRef]

200. de Sousa, T.; Hébraud, M.; Dapkevicius, M.; Maltez, L.; Pereira, J.E.; Capita, R.; Alonso-Calleja, C.; Igrejas, G.; Poeta, P. Genomic and metabolic characteristics of the pathogenicity in *Pseudomonas aeruginosa*. *Int. J. Mol. Sci.* **2021**, *22*, 12892. [CrossRef]

201. Hauser, A.R. The type III secretion system of *Pseudomonas aeruginosa*: Infection by injection. *Nat. Rev. Microbiol.* **2009**, *7*, 654–665. [CrossRef]

202. Cabral, M.P.; Correia, A.; Vilanova, M.; Gärtner, F.; Moscoso, M.; García, P.; Vallejo, J.A.; Pérez, A.; Francisco-Tomé, M.; Fuentes-Valverde, V.; et al. A live auxotrophic vaccine confers mucosal immunity and protection against lethal pneumonia caused by *Pseudomonas aeruginosa*. *PLOS Pathog.* **2020**, *16*, e1008311. [CrossRef]

203. Cryz, S.J., Jr.; Fürer, E.; Cross, A.S.; Wegmann, A.; Germanier, R.; Sadoff, J.C. Safety and immunogenicity of a *Pseudomonas aeruginosa* O-polysaccharide toxin A conjugate vaccine in humans. *J. Clin. Investig.* **1987**, *80*, 51–56. [CrossRef] [PubMed]

204. Killough, M.; Rodgers, A.M.; Ingram, R.J. Pseudomonas aeruginosa: Recent Advances in Vaccine Development. *Vaccines* **2022**, *10*, 1100. [CrossRef] [PubMed]

205. Mansouri, E.; Gabelsberger, J.; Knapp, B.; Hundt, E.; Lenz, U.; Hungerer, K.D.; Gilleland, H.E., Jr.; Staczek, J.; Domdey, H.; von Specht, B.U. Safety and immunogenicity of a *Pseudomonas aeruginosa* hybrid outer membrane protein F-I vaccine in human volunteers. *Infect. Immun.* **1999**, *67*, 1461–1470. [CrossRef] [PubMed]

206. Adlbrecht, C.; Wurm, R.; Depuydt, P.; Spapen, H.; Lorente, J.A.; Staudinger, T.; Creteur, J.; Zauner, C.; Meier-Hellmann, A.; Eller, P.; et al. Efficacy, immunogenicity, and safety of IC43 recombinant *Pseudomonas aeruginosa* vaccine in mechanically ventilated intensive care patients—A randomized clinical trial. *Crit. Care* **2020**, *24*, 74. [CrossRef]

207. Shaikh, M.O.F.; Schaefers, M.M.; Merakou, C.; DiBlasi, M.; Bonney, S.; Liao, T.; Zurakowski, D.; Kehl, M.; Tabor, D.E.; DiGiandomenico, A.; et al. Multicomponent *Pseudomonas aeruginosa* vaccines eliciting Th17 cells and functional antibody responses confer enhanced protection against experimental acute pneumonia in Mice. *Infect. Immun.* **2022**, *90*, e0020322. [CrossRef]

208. Sabzehali, F.; Goudarzi, H.; Salimi Chirani, A.; Yoosefi Izad, M.H.; Goudarzi, M. Development of multi-epitope subunit vaccine against *Pseudomonas aeruginosa* using OprF/OprI and PopB proteins. *Arch. Clin. Infect. Dis.* **2021**, *16*, e118243. [CrossRef]

209. Dey, J.; Mahapatra, S.R.; Patnaik, S.; Lata, S.; Kushwaha, G.S.; Panda, R.K.; Misra, N.; Suar, M. Molecular characterization and designing of a novel multiepitope vaccine construct against *Pseudomonas aeruginosa*. *Int. J. Pept. Res. Ther.* **2022**, *28*, 49. [CrossRef]

210. Elhag, M.; Alaagib, R.M.; Ahmed, N.M.; Abubaker, M.; Haroun, E.M.; Albagi, S.O.A.; Hassan, M.A. Design of epitope-based peptide vaccine against *Pseudomonas aeruginosa* fructose bisphosphate aldolase protein using immunoinformatics. *J. Immunol. Res.* **2020**, *2020*, 9475058. [CrossRef]

211. Beg, A.Z.; Farhat, N.; Khan, A.U. Designing multi-epitope vaccine candidates against functional amyloids in *Pseudomonas aeruginosa* through immunoinformatic and structural bioinformatics approach. *Infect. Genet. Evol.* **2021**, *93*, 104982. [CrossRef]

212. Clegg, J.; Soldaini, E.; McLoughlin, R.M.; Rittenhouse, S.; Bagnoli, F.; Phogat, S. *Staphylococcus aureus* vaccine research and development: The past, present and future, including novel therapeutic strategies. *Front. Immunol.* **2021**, *12*, 705360. [CrossRef]

213. Hiramatsu, K.; Katayama, Y.; Matsuo, M.; Sasaki, T.; Morimoto, Y.; Sekiguchi, A.; Baba, T. Multi-drug-resistant *Staphylococcus aureus* and future chemotherapy. *J. Infect. Chemother.* **2014**, *20*, 593–601. [CrossRef] [PubMed]

214. Jahantigh, H.R.; Faezi, S.; Habibi, M.; Mahdavi, M.; Stufano, A.; Lovreglio, P.; Ahmadi, K. The candidate antigens to achieving an effective vaccine against *Staphylococcus aureus*. *Vaccines* **2022**, *10*, 199. [CrossRef] [PubMed]

215. Anderson, A.S.; Miller, A.A.; Donald, R.G.K.; Scully, I.L.; Nanra, J.S.; Cooper, D.; Jansen, K.U. Development of a multicomponent *Staphylococcus aureus* vaccine designed to counter multiple bacterial virulence factors. *Hum. Vaccines Immunother.* **2012**, *8*, 1585–1594. [CrossRef] [PubMed]

216. Scully, I.L.; Timofeyeva, Y.; Illenberger, A.; Lu, P.; Liberator, P.A.; Jansen, K.U.; Anderson, A.S. Performance of a four-antigen *Staphylococcus aureus* vaccine in preclinical models of invasive *S. aureus* disease. *Microorganisms* **2021**, *9*, 177. [CrossRef]

217. Bhakdi, S.; Tranum-Jensen, J. Alpha-toxin of Staphylococcus aureus. *Microbiol. Rev.* **1991**, *55*, 733–751. [CrossRef]

218. Schmidt, C.S.; White, C.J.; Ibrahim, A.S.; Filler, S.G.; Fu, Y.; Yeaman, M.R.; Edwards, J.E., Jr.; Hennessey, J.P., Jr. NDV-3, a recombinant alum-adjuvanted vaccine for Candida and Staphylococcus aureus, is safe and immunogenic in healthy adults. *Vaccine* **2012**, *30*, 7594–7600. [CrossRef]

219. NIH. Non-Inferiority and Safety Study of EuTCV Compared to Typbar-TCV in Healthy 6 Months-45 Years Aged Participants. Available online: https://classic.clinicaltrials.gov/ct2/show/NCT04830371 (accessed on 14 July 2023).

220. NIH. Immunogenicity and Safety of Vi-DT (Diphtheria toxoid) Typhoid Conjugate Vaccine (Phase III). Available online: https://classic.clinicaltrials.gov/ct2/show/NCT04051268 (accessed on 14 July 2023).

221. NIH. Salmonella Conjugates CVD 1000: Study of Responses to Vaccination with Trivalent Invasive Salmonella Disease Vaccine. Available online: https://classic.clinicaltrials.gov/ct2/show/NCT03981952 (accessed on 14 July 2023).

222. NIH. Study of DTwP-HepB-Hib-IPV (SHAN6™) Vaccine Administered Concomitantly with Routine Pediatric Vaccines to Healthy Infants and Toddlers in Thailand. Available online: https://classic.clinicaltrials.gov/ct2/show/NCT04429295 (accessed on 14 July 2023).

223. NIH. Confirmatory Study of BK1310 in Healthy Infants. Available online: https://classic.clinicaltrials.gov/ct2/show/NCT03891758 (accessed on 14 July 2023).

224. NIH. Immunogenicity and Safety of 23-Valent Pneumococcal Polysaccharide Vaccine in Healthy Volunteers Aged 2 Years and Above. Available online: https://classic.clinicaltrials.gov/ct2/show/NCT04278248 (accessed on 14 July 2023).

225. NIH. Immunogenicity and Safety Study of 15-Valent Pneumococcal Conjugate Vaccine in 2-Month-Old and 3-Month-Old Healthy Volunteers. Available online: https://classic.clinicaltrials.gov/ct2/show/NCT04357522 (accessed on 14 July 2023).

226. NIH. A Phase III Clinical Trial of a 13-Valent Pneumococcal Conjugate Vaccine in Healthy Infants. Available online: https://classic.clinicaltrials.gov/ct2/show/NCT02494999 (accessed on 14 July 2023).

227. NIH. A Single Ascending Dose Study in Adults (Stage 1) and Single Ascending Dose-Finding Study (Stage 2) in Elderly Subjects with ASP3772, a Pneumococcal Vaccine. Available online: https://classic.clinicaltrials.gov/ct2/show/NCT03803202 (accessed on 14 July 2023).

228. NIH. A Study to Evaluate the Safety and Immunogenecity of LBVE(Multivalent Pneumococcal Conjugate Vaccine) in Healthy Infants. Available online: https://classic.clinicaltrials.gov/ct2/show/NCT03467984 (accessed on 14 July 2023).

229. NIH. A Phase 1/Phase 2 Study of Polyvalent Pneumococcal Conjugate Vaccine (V116) in Adults (V116-001). Available online: https://classic.clinicaltrials.gov/ct2/show/NCT04168190 (accessed on 14 July 2023).

230. NIH. Study of Investigational Pneumococcal Vaccine in Healthy Adults, Toddlers and Infants. Available online: https://classic.clinicaltrials.gov/ct2/show/NCT01446926 (accessed on 14 July 2023).

231. NIH. Study of a Pneumococcal Conjugate Vaccine in Adults Aged 50 to 84 Years. Available online: https://classic.clinicaltrials.gov/ct2/show/NCT04583618 (accessed on 14 July 2023).

232. NIH. Phase I Clinical Trial of a Candidate PCV13 in Healthy People Aged 6 Weeks and Above (PICTPCV13i). Available online: https://classic.clinicaltrials.gov/ct2/show/NCT04100772 (accessed on 14 July 2023).

233. NIH. Phase Ia Clinical Trial of a Pneumococcal Vaccine (PICTPV). Available online: https://classic.clinicaltrials.gov/ct2/show/NCT04087460 (accessed on 14 July 2023).

234. NIH. Safety and Immunogenicity of the 'EuPCV15' in Healthy Korean Adults. Available online: https://classic.clinicaltrials.gov/ct2/show/NCT04830358 (accessed on 14 July 2023).

235. NIH. Preventing UTIs in Chronic Neurogenic Bladder Dysfunction (Mix Methods) (PReSuTINeB). Available online: https://classic.clinicaltrials.gov/ct2/show/NCT02591901 (accessed on 14 July 2023).

236. NIH. Safety and Immunogenicity of CVD 1902 Oral Attenuated Vaccine to Prevent S. Paratyphi A infection. Available online: https://classic.clinicaltrials.gov/ct2/show/NCT01129453 (accessed on 14 July 2023).

237. NIH. Clostridium Difficile Vaccine Efficacy Trial (Clover). Available online: https://classic.clinicaltrials.gov/ct2/show/NCT03090191 (accessed on 14 July 2023).

238. NIH. Efficacy Study of 4CMenB (Bexsero®) to Prevent Gonorrhoea Infection in Gay and Bisexual Men (GoGoVax). Available online: https://classic.clinicaltrials.gov/ct2/show/NCT04415424 (accessed on 14 July 2023).

239. NIH. Challenge Study of an ETEC Vaccine. Available online: https://classic.clinicaltrials.gov/ct2/show/NCT01922856 (accessed on 14 July 2023).

240. NIH. Shigella CVD 31000: Study of Responses with Shigella-ETEC Vaccine Strain CVD 1208S-122. Available online: https://classic.clinicaltrials.gov/ct2/show/NCT04634513 (accessed on 14 July 2023).
241. NIH. A Double-Blind Placebo-Control Dose Escalating Study to Evaluate the Safety and Immunogenicity of dmLT by Oral, Sublingual and Intradermal Vaccination in Adults Residing in an Endemic Area. Available online: https://classic.clinicaltrials.gov/ct2/show/NCT03548064 (accessed on 14 July 2023).
242. NIH. Safety and Immunogenicity of a Klebsiella Pneumoniae Tetravalent Bioconjugate Vaccine (Kleb4V). Available online: https://classic.clinicaltrials.gov/ct2/show/NCT04959344 (accessed on 14 July 2023).
243. NIH. Confirmatory Phase II/III Study Assessing Efficacy, Immunogenicity and Safety of IC43. Available online: https://classic.clinicaltrials.gov/ct2/show/NCT01563263 (accessed on 14 July 2023).
244. NIH. Clinical Trial of the Biomed rTSST-1 Variant Vaccine in Healthy Adults. Available online: https://classic.clinicaltrials.gov/ct2/show/NCT02814708 (accessed on 14 July 2023).
245. NIH. Safety, Immunogenicity and Efficacy of GSK S. Aureus Candidate Vaccine (GSK3878858A) when Administered to Healthy Adults (Dose-Escalation) and to Adults 18 to 64 Years of Age with a Recent S. Aureus Skin and Soft Tissue Infection (SSTI). Available online: https://classic.clinicaltrials.gov/ct2/show/NCT04420221 (accessed on 14 July 2023).
246. Ong, E.; Wong, M.U.; Huffman, A.; He, Y. COVID-19 Coronavirus vaccine design using reverse vaccinology and machine learning. *Front. Immunol.* **2020**, *11*, e1581. [CrossRef]
247. Soltan, M.A.; Magdy, D.; Solyman, S.M.; Hanora, A. Design of *Staphylococcus aureus* new vaccine candidates with b and t cell epitope mapping, reverse vaccinology, and immunoinformatics. *Omics* **2020**, *24*, 195–204. [CrossRef]
248. Bianconi, I.; Alcalá-Franco, B.; Scarselli, M.; Dalsass, M.; Buccato, S.; Colaprico, A.; Marchi, S.; Masignani, V.; Bragonzi, A. Genome-based approach delivers vaccine candidates against *Pseudomonas aeruginosa*. *Front. Immunol.* **2018**, *9*, 3021. [CrossRef]

RESEARCH ARTICLE

Preclinical Development of a Novel Epitope-based DNA Vaccine Candidate against SARS-CoV-2 and Evaluation of Immunogenicity in BALB/c Mice

Kanwal Khalid[1] · Hui Xuan Lim[1,5] · Ayaz Anwar[2] · Soon Hao Tan[3] · Jung Shan Hwang[4] · Seng-Kai Ong[2] · Chit Laa Poh[1]

Abstract

The protective efficacies of current licensed vaccines against COVID-19 have significantly reduced as a result of SARS-CoV-2 variants of concern (VOCs) which carried multiple mutations in the Spike (S) protein. Considering that these vaccines were developed based on the S protein of the original SARS-CoV-2 Wuhan strain, we designed a recombinant plasmid DNA vaccine based on highly conserved and immunogenic B and T cell epitopes against SARS-CoV-2 Wuhan strain and the Omicron VOC. Literature mining and bioinformatics were used to identify 6 immunogenic peptides from conserved regions of the SARS-CoV-2 S and membrane (M) proteins. Nucleotide sequences encoding these peptides representing highly conserved B and T cell epitopes were cloned into a pVAX1 vector to form the pVAX1/S2-6EHGFP recombinant DNA plasmid vaccine. The DNA vaccine was intranasally or intramuscularly administered to BALB/c mice and evaluations of humoral and cellular immune responses were performed. The intramuscular administration of pVAX1/S2-6EHGFP was associated with a significantly higher percentage of CD8$^+$ T cells expressing IFN-γ when compared with the empty vector and PBS controls. Intramuscular or intranasal administrations of pVAX1/S2-6EHGFP resulted in robust IgG antibody responses. Sera from mice intramuscularly immunized with pVAX1/S2-6EHGFP were found to elicit neutralizing antibodies capable of SARS-CoV-2 Omicron variant with the ACE2 cell surface receptor. This study demonstrated that the DNA vaccine construct encoding highly conserved immunogenic B and T cell epitopes was capable of eliciting potent humoral and cellular immune responses in mice.

Keywords DNA vaccine · next-generation · SARS-CoV-2 · VOCs

✉ Chit Laa Poh
chitlaa.poh@gmail.com

1 Centre for Virus and Vaccine Research, School of Medical and Life Sciences, Sunway University, Bandar Sunway, 47500 Petaling Jaya, Selangor, Malaysia

2 Department of Biological Sciences, School of Medical and Life Sciences, Sunway University, Bandar Sunway, 47500 Petaling Jaya, Selangor, Malaysia

3 Department of Biomedical Science, Faculty of Medicine, University of Malaya, 50603 Kuala Lumpur, Malaysia

4 Department of Medical Sciences, School of Medical and Life Sciences, Sunway University, Bandar Sunway, 47500 Petaling Jaya, Selangor, Malaysia

5 Sunway Microbiome Centre, School of Medical and Life Sciences, Sunway University, Bandar Sunway, 47500 Petaling Jaya, Selangor, Malaysia

Introduction

COVID-19 was caused by the SARS-CoV-2 which resulted in a global pandemic, leading to extensive economic and financial downturns and a debilitating impact on public health and wellbeing [1]. As of 8 November 2024, there were more than 771,820,937 infections and 6,978,175 deaths as a result of the COVID-19 pandemic [2].

When the pandemic began, academic institutions and pharmaceutical companies collaborated at a pace unprecedented in history to develop novel mRNA and viral-vectored vaccine candidates which targeted the full-length Spike (S) protein from the SARS-CoV-2 Wuhan strain [3]. These vaccine candidates were granted emergency use authorization for global immunizations. Efficacies of the licensed vaccines against the SARS-CoV-2 Wuhan strain were high. For

example, mRNA-1273, BNT162b2, ChAdOx1 nCoV-19, and BBIBP-CorV showed protective efficacies of 94.1%, 95.0%, 90·0%, and 78.1%, respectively [4–6].

The genome of the SARS-CoV-2 is a single-stranded positive-sense RNA with a size of approximately 29.9 kB [7]. The genome comprises two large open-reading frames, ORF1a and ORF1b, positioned at the 5' end. They are responsible for encoding 16 non-structural proteins ranging from NSP1 to NSP16 which are involved in the formation of a replication–transcription complex (RTC) [8]. The other ORFs located at the 3' end are responsible for encoding four structural proteins, namely spike (S), envelope (E), membrane (M), and nucleocapsid (N) proteins. The M protein provides shape and structure to the viral particles, the E protein ensures proper virion assembly and release, and the N protein packages the RNA genome and enhances pathogenicity by reducing interferon production, while the S protein is of particular importance in vaccine design because it mediates binding and entry of the virus into the host [9, 10].

The SARS-CoV-2 is subjected to spontaneous mutations due to the replication process carried out by the viral RNA polymerase [11]. Throughout the pandemic, the SARS-CoV-2 has evolved consistently, resulting in the emergence of Alpha, Beta, Gamma, Delta, and Omicron VOCs which carried different genome sequences compared to the original SARS-CoV-2 Wuhan strain [12]. The majority of these mutations were found largely in the S gene [13].

However, the emergence of SARS-CoV-2 VOCs with multiple mutations in the S protein was associated with reduced protective efficacies of current vaccines against the Alpha, Beta, Delta, and Omicron VOCs [14–21] (Table I). Indeed, the Omicron variant (B.1.1.529) was associated with greater infectivity and immune evasion owing to the enhanced molecular flexibility of the S protein to bind to the ACE2 receptor [22–24].

mRNA-based, DNA, and recombinant protein vaccines could be developed to incorporate different antigenic targets specific to the sequences of novel SARS-CoV-2 VOCs [25–27]. Moderna's bivalent vaccine, mRNA-1273.222 which consisted of the S protein from the Wuhan strain and the Omicron BA.4/BA.5 strain, quickly progressed to phase 2/3 clinical development and demonstrated the induction of higher neutralizing antibody titers against BA.4/BA.5 variants when compared to a booster dose of mRNA-1273 [28]. Although this proactive approach to developing vaccines is commendable, such targeted adaptations might not be sustainable in the long run in light of the emergence of continuously mutating SARS-CoV-2 VOCs. Hence, the development of next-generation vaccines using highly conserved and immunogenic sequences from the SARS-CoV-2

Table I Reduction in Protective Efficacies of Current SARS-CoV-2 Vaccines

Vaccine	Reduction in neutralizing activity	Variant	Reference
BNT162b2	3.2-fold	B.1.1.7	[17]
ChAdOx1 nCoV-19	4-fold	B.1.351	[19]
mRNA-1273	6.4-fold	B.1.351	[21]
BNT162b2	22-fold	B.1.1.529	[15]
BNT162b2	31-fold	B.1.1.529	[16]
CoronaVac	6.5 fold	B.1.1.529	[16]
COVID-19 convalescent sera	10.6-fold	B.1.1.529	[16]
BNT162b2	1-3-fold	B.1.1.529	[16]

structural proteins, which were discovered by literature mining and bioinformatics tools, would be a more promising approach and would offer higher protection against the original Wuhan strain and emerging VOCs.

DNA vaccine candidates such as INO-4800 and ZyCoV-D have shown promise in clinical development against SARS-CoV-2 [29, 30]. Unlike mRNA vaccines, DNA vaccines are highly stable, less prone to degradation and do not require extreme low temperatures at -80°C for storage and transportation [31]. Moreover, DNA vaccines could be easily modified by simply changing the selected gene sequences in the DNA plasmid which could serve as up to date vaccines to effectively prevent the spread of emerging mutated VOC strains. They are also amenable to accelerated developmental timelines, allowing for rapid transition to the clinical stage. An additional advantage is the efficient large-scale and cost-effective manufacture of DNA vaccines for large-scale immunizations [27, 32]. A number of DNA vaccine candidates have shown promise in preclinical development against COVID-19 in terms of the elicitation of potent humoral and cellular immune responses and have progressed to clinical trials [27, 33–38]. However, the majority of these focus on the full length S protein sequence of the SARS-CoV-2 Wuhan strain isolated in 2019.

Most of the clinical development of DNA vaccines against SARS-CoV-2 has involved the intramuscular or intradermal administrations of the recombinant DNA plasmid. Vaccine candidates such as the pVAX-S1 vaccine developed by researchers in the King Abdulaziz University were delivered through intramuscular administration using customized needle-free Tropis system [39]. Moreover, current DNA vaccine candidates such as IN0-4800 and ZyCoV-D were both administered intradermally and utilized the CELLECTRA® delivery device and a spring-powered jet injector electroporation

device, respectively [40]. While there are a few studies evaluating elicited immune responses from DNA vaccines administered intranasally in ferrets and rhesus macaques, current research on the intranasal delivery of DNA vaccines against SARS-CoV-2 as well as evaluations of elicited immune responses as a result of intranasal delivery of DNA vaccines is lacking, particularly in clinical development [38, 41].

Intranasal administration of COVID-19 vaccines offers multiple advantages over traditional intramuscular injections. In a global context, intranasal vaccines can be easily supplied to the global population, especially to those from middle and low income countries without the need for needles. Intranasal delivery of DNA vaccines can also overcome the need for syringes or costly administration devices such as electroporators. It is cost-effective, non-invasive and does not require skilled professionals for its administration [42]. COVID-19 is a respiratory virus. The nasal mucosa serves as the first point of SARS-CoV-2 entry and viral replication before lung aspiration. The host ACE2 cell receptor is expressed in the nasal goblet as well as epithelial cells in the respiratory tract and the lungs. The nasal cavity might be the initial reservoir for seeding of the virus to the lungs. Indeed, intranasal administration of a SARS-CoV-2 vaccine elicited potent immunogenicity in both the airway mucosa and periphery in terms of T cell responses, IgG and neutralizing antibodies [43]. Moreover, potent Spike-specific IgG, IgA, and tissue-resident memory T cells were elicited in the lungs and nasal mucosa of mice immunized twice using the intranasal route with the Spike-LP-GMP vaccine. These responses lasted for at least three months [44]. Furthermore, stable protection against both the Wuhan and emerging SARS-CoV-2 strains was achieved in mice upon intranasal vaccination with ChAd-SARS-CoV-2-S [45].

Following the uptake of the vaccine antigen through the paracellular or transcellular pathway, nasally administered vaccines primarily target the nasopharynx-associated lymphoid tissue (NALT), situated beneath the mucosal lining. This region which is, part of Waldeyer's ring, encompasses the pharynx and tonsils. NALT serves as the initial site for nasal immunity, involving M cells, B cells, T cells, dendritic cells (DCs), and nearby lymph nodes. During nasal vaccination, antigens travel to NALT through specialized M cells on the follicle-associated epithelium (FAE). These M cells lack a brush border and don't secrete mucus or enzymes, aiding in antigen binding and delivery. Within NALT, dendritic cells process and present antigens, initiating immune responses. Some antigens migrate to regional lymph nodes via the major histocompatibility complex (MHC) to activate T helper cells. Activated antigen-specific CD4+ T helper cells (Th cells) interact with B cells, stimulating antibody production [46].

A total of six peptides capable of eliciting B and T cell immune responses were identified through bioinformatics and literature mining approaches. These peptides were further validated in mice to conclude that they were able to elicit potent humoral and cellular immune responses (Unpublished data).

In this study, we developed a SARS-CoV-2 recombinant DNA vaccine candidate encoding the six peptides, five of which represented highly conserved B and T cell epitopes which were immunogenic against the SARS-CoV-2 and the Omicron VOC. Reverse vaccinology bioinformatics and literature mining approaches were used to identify the peptides specifying highly conserved B cell and T cell epitopes from the SARS-CoV-2 S and M proteins. Nucleotide sequences encoding these peptides were synthesized and incorporated into a pVAX1 plasmid vector to produce the pVAX1/S2-6EHGFP recombinant DNA plasmid vaccine. We demonstrated *in vitro* protein expression after direct transfection of HEK 293T cells. The immunogenicity of the plasmid DNA vaccine candidate was analyzed for humoral and cell-mediated immune responses following intranasal and intramuscular immunizations.

Materials and Methods

Analysis of Conservancy of the 6 Peptides using the IEDB Epitope Conservancy Analysis

Sequences of a total of 4260 SARS-CoV-2 Omicron (B.1.1.529) strains were downloaded from the Global Initiative on Sharing All Influenza Data (GISAID) (https://gisaid.org/) in a FASTA format. The nucleotide sequences were then translated into amino acid sequences, followed by the extraction of spike (S) and membrane (M) protein sequences using a customized python program running in Google Colab. The IEDB Epitope Conservancy Analysis tool (https://tools.iedb.org/conservancy/) was used to determine the similarity of the 6 peptides against Omicron sequences to yield protein sequence matches at identity $< = 100\%$.

Cell Culture

Human embryonic kidney (HEK) 293T cells were maintained in Dulbecco's Modified Eagle Medium (DMEM) (Nacalai Tesque, Kyoto, Japan) which was supplemented with 10% fetal bovine serum (FBS) (Nacalai Tesque, Kyoto, Japan) and penicillin-streptomycin (1% final concentration) (Nacalai Tesque, Kyoto, Japan). HEK 293T cells were maintained in the incubator at 37°C supplemented with 5% CO_2 atmosphere.

Construction and Preparation of Recombinant Plasmid DNA pVAX1/S2-6EHGFP

Nucleotide sequences encoding peptides linked by linkers encoding AAY and GPGPG and specifying immunogenic epitopes from the SARS-CoV-2 S, M, and N proteins were cloned into the mammalian expression vector pVAX1 under the control of the cytomegalovirus immediate-early (CMV) promoter and denoted as pVAX1/S2-6EHGFP (GenScript, California, USA). The coding sequence was incorporated within the Kpn1 and EcoRI restriction site. A polyhistidine-tag consisting of nucleotide sequences encoding six histidine residues was inserted before the six peptide gene fragments encoding nucleotides. Nucleotides encoding the kanamycin resistance gene were incorporated in the plasmid vector as an antibiotic resistance selection marker to confer resistance to kanamycin.

Preparation of Competent *E. coli* TOP 10

Competent *E. coli* TOP 10 cells were prepared using the calcium chloride method. An aliquot of 10 ml of LB broth was inoculated with a single colony of the *E. coli* TOP 10 strain and cultured overnight at 37°C with shaking at 200 xg. An aliquot of 1 ml of the overnight culture was inoculated into 100 ml of LB broth and cultured overnight at 37°C with shaking at 200 xg. The culture was divided equally between two sterile 50 ml centrifuge tubes and centrifuged for 10 minutes at 7000 xg at 4°C (Eppendorf Centrifuge 5810/ 5810 R, Hamburg, Germany) and the supernatant was discarded. An aliquot of 20 ml of sterile, ice-cold 100 mM $CaCl_2$ was added to the cell pellets, followed by gentle resuspension. The suspended cells were placed on ice for 15 minutes and centrifuged for 10 minutes at 7000 xg at 4°C after which the supernatant was discarded. An aliquot of 5 ml of sterile, ice-cold 100 mM $CaCl_2$ supplemented with 15 % glycerol was added to each cell pellet and followed by gentle resuspension. The suspended cells were divided into 100 µl aliquots in sterile, ice-cold Eppendorf tubes and stored at -80°C.

Transformation of Competent *E. coli* cells

An aliquot of 2 µl of lyophilized plasmid DNA in 1x TE buffer was added to thawed competent *E. coli* TOP 10 cells in a 1.5 ml centrifuge tube and kept on ice for 30 minutes. The contents in the tubes were subjected to heat shock at 42°C for 42 seconds. An aliquot of 1 ml of trans media was added to each tube, followed by incubation at 37°C with shaking at 200 xg for 60 minutes. Aliquots of 50 µl of the transformed *E. coli* cells were spread on LB plate containing kanamycin (50 µg/ml) and incubated overnight at 37°C.

Plasmid Extraction

A single colony of transformed *E. coli* was inoculated into 10 ml of LB broth supplemented with kanamycin (50 µg/ml) and incubated at 37°C with shaking at 200 xg. The QIAprep Spin Miniprep Kit (QIAGEN, Hilden, Germany) was used for plasmid extraction. The bacterial culture was centrifuged at 10,000 xg for 5 minutes and the supernatant was discarded. The pellet was mixed with 250 µl of Buffer P1 (resuspension buffer RNase), followed by the addition of Buffer P2 lysis buffer and mixed by inversions. The mixture was incubated at room temperature for three minutes until the solution turned clear. Then 350 µl of Neutralization Buffer N3 were added to the tube and the tube was inverted 6 times. The supernatant was collected and added to the spin column directly. The column was centrifuged at 10,000 xg for 30 seconds. An aliquot of 500 µl of PB buffer was added and centrifuged at 10,000xg for 30 seconds, followed by centrifugation at 12000 xg for 1 minute to remove the ethanol residue. The column was transferred to a new Eppendorf tube and 50 µl of elution buffer was directly added to the filter of the column. The column containing the plasmid and the elution buffer was incubated for 2 minutes at room temperature and centrifuged at 12000 xg for 2 minutes. The concentration of the extracted DNA was determined using the NanoDrop One (Thermo Fisher Scientific, Massachusetts, USA).

Characterization of pVAX1/S2-6EHGFP

Characterization of the recombinant plasmid pVAX1/S2-6EHGFP was performed using restriction enzyme digestion, followed by agarose gel electrophoresis and nucleotide sequencing. In order to linearize the recombinant DNA plasmid pVAX1/S2-6EHGFP, restriction enzyme digestion was carried out with EcoRI. Agarose gel electrophoresis was carried out in a 1% agarose gel at 100 mV for 60 minutes. The Invitrogen 1Kb Plus Ladder (Invitrogen, Massachusetts, USA) was used as the molecular marker for reference to indicate the size of the visualized DNA bands. The gel was visualized using G:BOX F3LFB gel doc (Syngene, Maryland, USA). Nucleotide sequence analysis of the gene insert containing six genes in the recombinant plasmid pVAX1/S2-6EHGFP was conducted by a commercial company (GenScript, California, USA).

Transfection of HEK 293T Cells with the Recombinant DNA Plasmid pVAX1/S2-6EHGFP

The *in vitro* protein expression of the recombinant DNA plasmid pVAX1/S2-6EHGFP was evaluated in HEK 293 T cells. HEK 293 T cells were seeded into a 24-well plate at 1×10^5cfu/

ml and incubated overnight at 37°C in DMEM supplemented with 10% FBS and 1% PSA. Upon reaching 70% confluency, the HEK 293T cells were then transfected with varying concentrations of plasmid DNA (3 µg, 5 µg, 7 µg, and 10 µg) using Xfect™ Transfection Reagent (Takara Bio, Kusatsu, Japan) by following the manufacturer's protocol. The cells were incubated at 37°C in DMEM supplemented with 10% FBS and 1% PSA. Transfected HEK 293 T cells were allowed to grow for 24 hours at 37°C in DMEM supplemented with 10% FBS and 1% PSA. After 24 hours, the plate was transferred to an incubator set at 33°C for the remaining 24 hours. After 48 hours of transfection, the qualitative and quantitative transfection efficiency was determined using fluorescence microscopy and flow cytometry, respectively.

Qualitative Evaluation of Transfection Efficiency

The recombinant plasmid pVAX1/S2-6EHGFP carried a green fluorescent protein (AcGFP1) gene from *Aequorea coerulescens* with an excitation maximum of 475 nm and an emission maximum of 505 nm. Qualitative evaluation of transfection efficiency was conducted by employing fluorescent microscopy using the Nikon Inverted Microscope Eclipse Ti-S (Nikon, Kyoto, Japan) to confirm that plasmid transfection was successful. Upon successful transfection of HEK 293T cells with pVAX1/S2-6EHGFP, the AcGFP1 protein was found to be expressed under the control of the IRES2 promoter and would be visible under the FITC (fluorescein isothiocyanate) filter. Cells were also viewed under the BF (Bright Field) filter, followed by merging the FITC and BF images to determine which cells were actively expressing AcGFP1.

Quantitative Evaluation of Transfection Efficiency

Following 48 hours of transfection of HEK 293T cells with different concentrations of recombinant DNA plasmid pVAX1/S2-6EHGFP, the media was removed and the wells were washed with PBS. An aliquot of 1 ml of trypsin was added, followed by incubation at 37°C with 5% CO_2 atmosphere for 6 minutes. The cells were washed with centrifugation at 10,000 xg for 10 minutes at 4°C and fixed using the BD Cytofix/Cytoperm Fixation solution and left overnight at 4°C. Cells were centrifuged at 10,000 xg for 10 minutes at 4°C, washed with PBS, and subjected to centrifugation at 10,000 xg for 10 minutes at 4°C. Cells were suspended in FACS buffer, transferred to flow cytometer tubes, and subjected to flow cytometry using the BD FACSCelesta™ Cell Analyzer (BD Biosciences, New Jersey, USA). to quantify the number of cells expressing AcGFP1 as well as the total number of cells to determine the transfection efficiency quantitatively.

Determination of Amino Acid Sequence and Expected Protein Size of the Cloned Gene Incorporated into the DNA Plasmid Vector pVAX1

The nucleotide sequence of the cloned gene insert incorporated into the DNA plasmid vector pVAX1 was converted to its amino acid sequence using the Expasy Translate tool (https://web.expasy.org/translate/). The molecular weight of the recombinant protein of interest was determined using the amino acid sequence of the cloned gene insert using the Expasy ProtParam tool (https://web.expasy.org/protparam/).

In vitro Protein Expression of HEK 293T Cells Transfected with pVAX1/S2-6EHGFP

Following 48 hours of transfection of HEK 293T cells with different concentrations of recombinant DNA plasmid pVAX1/S2-6EHGFP, cell lysis was performed using 40 µl of cell lysis buffer and protease inhibitor. Wells were scraped and protein lysates were collected and subjected to centrifugation at 15000 xg for 15 minutes at 4°C (Eppendorf™ 5424 Microcentrifuge, Hamburg, Germany). The supernatants were subjected to SDS-PAGE and Western blot analysis.

Analysis of Samples for Detection of Histidine-Tagged Protein of Interest Using SDS-PAGE and Western Blot

Protein samples were mixed with the 6X loading buffer in a ratio of 2:1, followed by boiling at 95°C for 15 minutes, and loading of denatured samples onto a 12% polyacrylamide gel. Electrophoresis was carried out at 100 V for 120 minutes, followed by visualization of protein bands using Coomassie blue staining. Western blot was conducted and the separated proteins were transferred from the polyacrylamide gel onto a polyvinylidene difluoride (PVDF) membrane using the semi-dry method (Gravel, 2009). The membrane was then blocked with 10 % skim milk to prevent nonspecific binding of antibodies, followed by adequate washing with 1X TBST. Overnight primary antibody incubation was carried out with Anti-His-Tag Antibody (H-3): sc-8036 (1:1000) (Santa Cruz Biotechnology, Inc, Dallas, USA), followed by washing and secondary antibody incubation with anti-mouse HRP conjugated secondary antibody. The blot was visualized using the G:BOX F3LFB gel doc (Syngene, Maryland, USA).

Ethics Statement

All animal experimental procedures were carried out in accordance with the guidelines approved by the Animal Institutional Animal Care and Use Committee (FOM IACUC) (2023-20260609/SUNWAY/R/KK) of the

University Malaya (UM) and Sunway Research Ethics Committee (Ethics Approval No.: PGSUREC2021/043). All mice were housed in a temperature-controlled biosafety level 2 (BSL-2) animal facility at the Animal Experimental Unit (AEU), Faculty of Medicine, Universiti Malaya, Malaysia.

Mice Immunizations

BALB/c mice (6-8 weeks old) were purchased and immunized at the AEU, Faculty of Medicine, UM, Malaysia. For the evaluation of immunogenicity elicited by the recombinant plasmid DNA pVAX1/S2-6EHGFP, mice were randomly divided into 6 groups (n=5). Group 1, group 2, and group 3 mice were given intramuscular administrations of the naked recombinant plasmid DNA pVAX1/S2-6EHGFP, the plasmid vector pVAX1, and PBS, respectively. Mice from group 4, group 5, and group 6 were given the intranasal administrations of the naked recombinant plasmid DNA pVAX1/S2-6EHGFP, the plasmid vector pVAX1, and PBS, respectively. At day 42 post-immunization, mice were anesthetized with isoflurane for blood collection via cardiac puncture, before euthanasia by cervical dislocation after which spleens were collected.

Evaluation of Humoral Responses

Detection of Peptide-Specific IgG Antibodies Through the Enzyme-Linked Immunosorbent (ELISA) Assay

Blood samples collected from mice were centrifuged at 6000 xg for 15 minutes to obtain sera. A 96-well flat-bottom plate (Fisher Scientific, Pittsburgh, USA) was coated overnight with a mixture of peptides B6 and B10 (5 μg/peptide) at 4°C. The contents of the wells were discarded and the plate was washed with 200 μl of PBS Tween 20 wash [0.05% (v/v) Tween 20 in PBS. Aliquots of 100 μl of blocking buffer (0.5% BSA in PBS) were added to each well on the plate, followed by incubation at 37 °C for 2 hours. Sera from immunized mice were diluted using dilution buffer (20% blocking buffer in PBS) and added to wells in ratios of 1:50, 1:250 and 1:1000. A total of 12 wells were tested. Wells labelled "blank" did not contain sera and served as the negative control. Wells were washed with 200 μl of PBS Tween 20 wash, followed by the addition of 100 μl of diluted sera and incubated at 37 °C for 2 hours. Wells were washed with 200 μl of PBS Tween 20 four times, followed by the addition of 100 μl of horseradish peroxidase (HRP)-conjugated goat anti-mouse IgG antibody (Invitrogen, Calsbad, CA, USA) that had been diluted in a 1:1000 ratio in dilution buffer and incubated at 37°C for 1 hour. Aliquots of 100 μl of 3,3'5,5'-Tetramethylbenzidine (TMB) substrate solution were added to each well and contents were allowed to incubate at room temperature until a blue color was observed. Lastly, aliquots of 100 μl of 1M sulphuric acid (H_2SO_4) were added to

the wells in order to stop the reaction. Absorbance was read using a Tecan Infinite M200 Pro microtiter plate reader (Tecan, Zürich, Switzerland) at 450 nm.

Neutralizing Antibody Detection Using the GenScript cPass™ SARS-CoV-2 Neutralization Antibody Detection Kit

The determination of the levels of neutralizing antibodies to SARS-CoV-2 in the sera of immunized mice that could inhibit the interaction between RBD-HRP and the ACE2 receptor was performed using the FDA approved "cPASS SARS-CoV-2 Surrogate Virus Neutralization Test RUO Kit" (Cat. #L00847-A, Genscript) [47] . HRP-conjugated RBD (HRP-RBD) from the SARS-CoV-2 Omicron variant was prepared by diluting the stock solution in a 1:1000 ratio with the RBD dilution buffer. A 1x wash solution consisting of Tris-buffered saline with Tween 20 at pH 8.0 was prepared by diluting it with deionized water in a 1:20 ratio. Murine sera from each immunization group, negative and positive controls were mixed in a 1:1 ratio with the diluted RBD-HRP and aliquots of 100 μl were added to wells, followed by incubation at 37 °C for 15 minutes. Wells were washed with the wash solution 4 times and 100 μl of TMB solution was added to the wells. The plate was incubated in the dark for 15 minutes at room temperature, followed by the addition of 50 μl of stop solution until a yellow color was observed. Absorbance was analyzed at OD 450 nm immediately using a Tecan Infinite M200 Pro microtiter plate reader (Tecan, Zürich, Switzerland) at 450 nm. The inhibition of ACE2 receptor binding was calculated using the formula provided by the manufacturer. According to the manufacturer's specification, a positive value was interpreted as >30% of inhibition and a negative as < 30% of inhibition.

$$\%\text{Signal Inhibition} = (1 - \frac{\text{OD value of Sample}}{\text{OD value of Negative Control}}) \times 100$$

Evaluation of Cellular Responses

The intranasal and intramuscular administrations of the recombinant plasmid DNA pVAX1/S2-6EHGFP were performed in order to evaluate differences in the elicitation of immune responses attributable to differences in delivery routes relative to PBS and the empty pVAX1 vector. Following stimulation of murine splenocytes with PMA (Sigma-Aldrich, Missouri, United States), ionomycin (Sigma-Aldrich, Missouri, United States), and GolgiStop (BD Biosciences, New Jersey, USA) to induce cytokine production, splenocytes were stained with $CD3^+$, $CD4^+$, $CD8^+$ and IFN-γ antibodies. Flow cytometry was conducted to determine the percentages of IFN-γ secreting $CD3^+$ $CD4^+$ and $CD3^+$ $CD8^+$ T cells following intramuscular and intranasal

administrations of the recombinant plasmid DNA pVAX1/S2-6EHGFP, PBS, and empty pVAX1 vector.

Processing of Murine Splenocytes from Immunized Mice

Spleens removed from immunized mice were stored in incomplete RPMI 1640 media (Sigma-Aldrich, Missouri, USA) and processed for splenocyte isolation. Spleens were placed into 100 μm pore size cell strainer (BD Biosciences, New Jersey, USA), crushed with a 5 ml syringe plunger (Terumo Inc., Tokyo, Japan), washed with incomplete RPMI 1640 media, and collected into 50 mL Falcon tubes, followed by centrifugation at $3000 \times g$ for 3 minutes. The supernatants were discarded, and the tubes were tapped to dislodge the pellet. Aliquots of 7 ml of ACK lysing buffer (150 mM NH_4Cl, 0.1 mM $NaHCO_3$, and 10 mM EDTA) were added to the pellet to lyse the red blood cells. The RBC lysis reaction was stopped through the addition of complete RPMI 1640 media containing 10% heat-inactivated FBS, 1% Penicillin-Streptomycin, 50 μM 2-Mercaptoethanol, and 10 mMol HEPES), followed by centrifugation at $3000 \times g$ for 3 minutes. The supernatants were discarded, the pelleted cells were resuspended in complete RPMI media, and subjected to cell counting using the hemocytometer. Splenocytes were seeded at 4.0×10^6 cells/well for flow cytometry analysis to determine the percentage of IFN-γ expressing $CD3^+$ $CD4^+$ and $CD3^+$ $CD8^+$ T cells.

Intracellular Cytokine Staining (ICS) for Flow Cytometry Analysis

For intracellular staining, cytokine expression was induced through the addition of 50 ng/ml PMA (phorbol 12-myristate 13-acetate), 1 μg/ml ionomycin (calcium ionophore), and 1 μg/ml GolgiStop (BD Biosciences, New Jersey, USA), followed by incubation for five hours at 37°C. The stimulated cells were collected into 1.5 ml microcentrifuge tubes and centrifuged at 250 xg for 5 minutes at 4°C. The supernatants were discarded, and the pellets were resuspended in 50 μl of BD Horizon™ Fixable Viability Stain 780 (FVS-780) (BD Biosciences, New Jersey, USA) followed by incubation in the dark for 30 minutes at room temperature. Aliquots of 300 μl of stain buffer were added to the tubes to wash off any unbound antibody, followed by centrifugation at $3000 \times g$ for 3 minutes at 3°C. Surface stains were performed with each of the antibodies viz.: anti-CD3 APC conjugated antibody (Biomed Global, Kuala Lumpur, Malaysia), anti-CD4 BV786 conjugated antibody (Biomed Global, Kuala Lumpur, Malaysia), and anti-CD8A BB515 conjugated antibody (Biomed Global, Kuala Lumpur, Malaysia), were added to the cell

pellets and incubated for 30 minutes in the dark at 4°C. After 30 minutes of incubation, 300 μl of stain buffer was added to the tubes, followed by centrifugation at 400 xg for 5 minutes at 4°C. The supernatants were discarded, and the pellets were resuspended in Cytofix buffer (BD Biosciences, New Jersey, USA), followed by incubation for 30 minutes at 4°C. Aliquots of 300 μl of Cytoperm buffer were then added, followed by centrifugation at 4000 xg for 4 minutes at 4°C. The supernatants were discarded, and the pellets were resuspended in the intracellular stain, anti-IFN-γ PerCP-Cy5.5 conjugated antibody stain, followed by incubation in the dark for 60 minutes at 4°C. Aliquots of 300 μl of stain buffer were added to wash away unbound antibodies, followed by centrifugation at $3000 \times g$ for 3 minutes. Supernatants were discarded, and aliquots of 500 μl of stain buffer were added to resuspend the cells and data were acquired using the BD FACSCelesta™ Flow Cytometer (BD Biosciences, New Jersey, USA) and analyzed using the Kaluza Analysis Software (Beckman Coulter, California, United States).

Statistical Analysis

All the data were expressed as the mean value $\pm$ standard deviation (SD). Statistical analysis was performed using Graphpad Prism v8.-02 software (Graph Pad Software Inc., San Diego, CA, USA). Comparisons of the data between group were made using T-tests. The mean ($\pm$ SD) for each group was calculated, and statistical significance was assessed at $p < 0.05$ (*), $p < 0.01$ (**), $p < 0.001$ (***), and $p < 0.0001$ (****).

Results

Epitope Conservancy Analysis of Selected Peptides Against Omicron (B.1.1.529) VOC

The sequence of the 6 peptides was cross-checked with the FASTA sequences of 4260 SARS-CoV-2 Omicron strains using the IEDB Epitope Conservancy Analysis tool. Table II. showed that epitope sequences of five of the six peptides from the SARS-CoV-2 Wuhan strain were highly conserved when compared with sequences of SARS-CoV-2 Omicron strains. Peptides S1, S5, M1, B6, and B10 showed high sequence similarities of 99.30% (4230/4260), 99.91% (4256/4260), 100% (4260/4260), 99.79% (4251/4260), 99.58 % (4242/4260) against Omicron strains, respectively. However, peptide S19 was found not to be conserved against the SARS-CoV-2 Omicron strains since it showed a sequence similarity of only 1.92% (82/4260) against the SARS-CoV-2 Omicron strains.

Table II The epitope conservancy analysis of the six peptides from the SARS-CoV-2 against Omicron (B.1.1.529)

	Peptide	Peptide Sequence	Antigenic Region	Percent of protein sequence matches at identity < = 100%
1.	S1	WTAGAAAYYVGYLQPRTFLLKY	S	99.30% (4230/4260)
2.	S5	FPQSAPHGVVFLHVTYVPAQEK	S	99.91% (4256/4260)
3.	M1	GLMWLSYFIASFRLFARTRSM	M	100% (4260/4260)
4.	S19	GEVFNATRFASVYAWNRKRISNC-VADYSVLYNS	S	1.92% (82/4260)
5.	B6	TESNKKFLPFQQFGRD	S	99.79% (4251/4260)
6.	B10	ESNKKFLPFQQFGRDIADTT	S	99.58 % (4242/4260)

The six peptides were incorporated in pVAX1/S2-6EHGFP

EcoR1 Digestion of the Recombinant Plasmid pVAX1/S2-6EHGFP and Analysis by Agarose Gel Electrophoresis

The recombinant DNA plasmid pVAX1/S2-6EHGFP has a single restriction site for EcoRI at position 1220 base pairs (bp) (Fig. 1a). The recombinant DNA plasmid pVAX1/S2-6EHGFP was characterized by digesting with the restriction enzyme EcoR1. Subsequently, agarose gel electrophoresis was performed to determine the size of the linearized plasmid. Electrophoresis analysis revealed the presence of a single DNA band. Lane 1 which indicated a band at 4773 base pairs represented the linearized recombinant DNA plasmid pVAX1/S2-6EHGFP (Fig. 1b). The result showed that the recombinant DNA plasmid was of the right size in accordance with the size of the recombinant plasmid (4773 bp) as shown in the illustrated recombinant plasmid map (Fig. 1a).

Qualitative Evaluation of Transfection Efficiency

A qualitative evaluation of transfection efficiency was conducted to examine the fluorescence generated by HEK 293T cells transfected with pVAX1/S2-6EHGFP after 48 hours. The recombinant plasmid pVAX1/S2-6EHGFP contained the green fluorescent protein (AcGFP1). After incorporating optimization conditions such as lowering the culture temperature from 37°C to 33°C as well as using DMEM supplemented with 10% FBS and 1% PSA, green fluorescence signals emitted 48 hours after transfections of HEK 293T cells with the recombinant plasmid pVAX1/S2-6EHGFP were observed. The fluorescence signal emitted by HEK 293T cells transfected with different concentrations of the recombinant plasmid pVAX1/S2-6EHGFP showed that the strongest fluorescence signal was observed when transfection of HEK 293T cells was conducted with 10 µg of pVAX1/S2-6EHGFP. However, transfection with 7 µg of pVAX1/S2-6EHGFP, with 5 µg of pVAX1/S2-6EHGFP, and with 3 µg of pVAX1/S2-6EHGFP did lead to reduction in the fluorescence signals upon transfection (Fig. 2a).

Quantitative Evaluation of Transfection Efficiency

Transfection efficiency of the recombinant DNA plasmid pVAX1/S2-6EHGFP in HEK 293T cells was measured using flow cytometry after transfection with various concentrations of DNA plasmid (3 µg, 5 µg, and 7 µg) using the XfectTM Transfection Reagent (Takara Bio, Kusatsu, Japan). As a negative control, the non-transfected HEK 293T cells showed a transfection efficiency of 0.3%. The transfection efficiency of HEK 293T cells transfected with 3 µg of pVAX1/S2-6EHGFP was determined to be 14.3 %. The transfection efficiency of HEK 293T cells transfected with 5 µg of pVAX1/S2-6EHGFP increased the transfection efficiency to 22.8 %. Moreover, increasing the amount of pVAX1/S2-6EHGFP plasmid DNA further to 7 µg resulted in a prominent increase in transfection efficiency. The transfection efficiency of HEK 293T cells transfected with 7 µg of pVAX1/S2-6EHGFP was shown to be 40.6 % and increased to 49.8 % when HEK 293T cells were transfected with 10 µg of pVAX1/S2-6EHGFP. Moreover, a clear dose-dependent relationship was observed between the amount of DNA plasmid and transfection efficiency in HEK 293T cells. A proportional increase in the transfection efficiency was observed as the amount of plasmid DNA increased from 3 µg to 5 µg to 7 µg. The highest transfection efficiency achieved was when 10 µg of pVAX1/S2-6EHGFP was used for transfection (Fig. 2b).

In Vitro Protein Expression of HEK 293T Cells Transfected with pVAX1/S2-6EHGFP

In vitro protein expression was further confirmed through transfection of HEK 293T cells with varying concentrations pVAX1/S2-6EHGFP, followed by cell lysis and Western blot analysis using an anti-His-tag antibody reactive against the six histidine residues fused to the six peptides. Western blot of the lysates of HEK 293T cells transfected with 3 µg, 5 µg, 7 µg, and 10 µg of pVAX1/S2-6EHGFP revealed
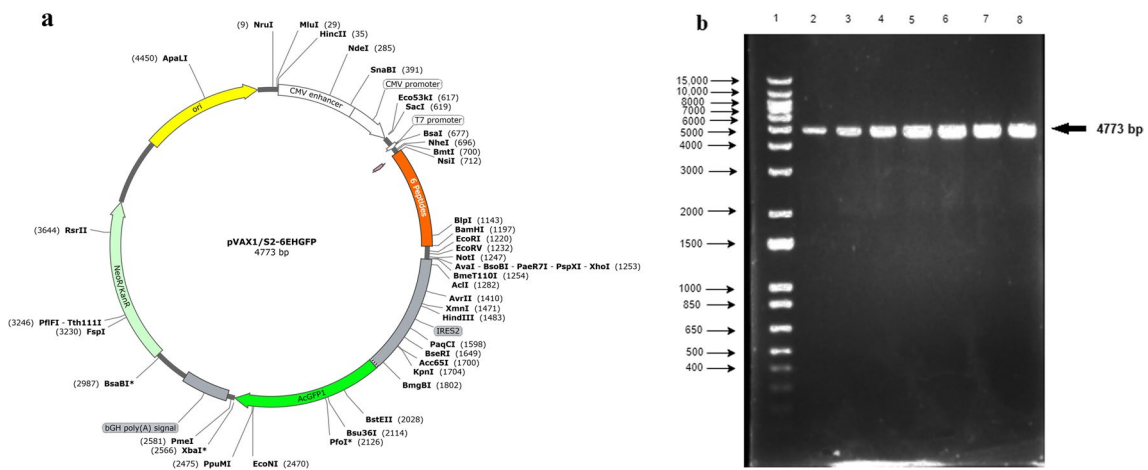
Fig. 1 **a** The plasmid map of the recombinant DNA plasmid pVAX1/S2-6EHGFP **b** Agarose gel electrophoresis of EcoR1 digested recombinant plasmid pVAX1/S2-6EHGFP, Lane MM: 1 kb molecular weight marker; Lane 1: 1 ng/µl of digested pVAX1/S2-6EHGFP
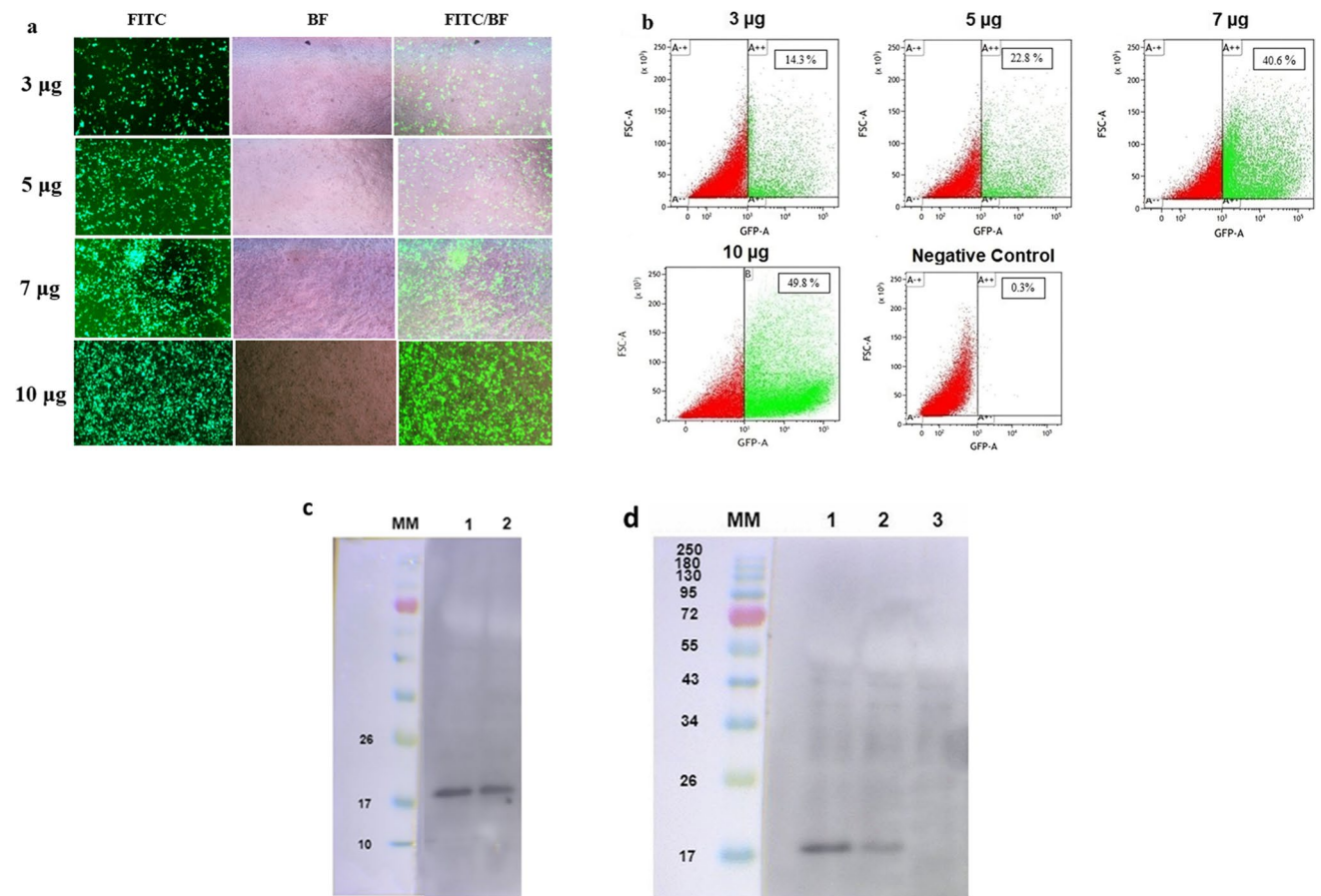

Fig. 2 **a** Fluorescent images of HEK 293T cells after 48-hour transfection with 3 µg, 5 µg, 7 µg, and 10 µg of pVAX1/S2-6EHGFP recombinant plasmid viewed under the FITC, BF, and FITC/BF merged filter **b** Flow cytometry analysis showing ratio of transfected and non-transfected HEK 293T cells transfected with 3 µg, 5 µg, 7 µg, 10 µg of pVAX1/S2-6EHGFP plasmid DNA, and the negative control of non-transfected HEK 293T cells. **c** Western blot analysis showing the *in vitro* protein expression of the cloned gene insert

after transfection of HEK 293T cells with of 10 µg (Lane 1) and 7 µg (Lane 2) of pVAX1/S2-6EHGFP. **d** The Western blot analysis showing *in vitro* protein expression of the cloned gene insert after transfection of HEK 293T cells with 5 µg (Lane 1), 3 µg (Lane 2) of pVAX1/S2-6EHGFP and the negative control of non-transfected HEK 293T cells (Lane 3). The Prestained Kaleidoscope ladder was used as the molecular marker (Lane MM)

bands equivalent to the predicted protein molecular weight of the protein of interest, 18 kDa. Transfection with 10 µg of pVAX1/S2-6EHGFP was associated with a band with the darkest intensity (Fig. 2c, **lane 1**), which was followed by bands with decreasing intensity upon transfection with 7 µg of pVAX1/S2-6EHGFP (Fig. 2c, **lane 2**). Transfection with 5 µg of pVAX1/S2-6EHGFP also generated a dark band (Fig. 2d, **lane 1**). The lightest band was observed upon transfection with 3 µg of pVAX1/S2-6EHGFP (Fig. 3d, **lane 2**). The negative control representing the protein lysate from non-transfected HEK 293T cells yielded no visible band (Fig. 2d, **lane 3**).

Mouse Weight Progression Throughout the Immunogenicity Study

The body weight progression of mice in the six experimental groups was monitored over 42 days, with measurements taken on days 0, 14, 28, and 42 post-immunization. For mice immunized intramuscularly with the recombinant DNA plasmid pVAX1/S2-6EHGFP, mice had an average weight of 21.4 g on day 0, which increased to 21.7 g on day 14, further to 21.8 g on day 28, and reached 23.5 g on day 42. For mice immunized intramuscularly with PBS, mice had an average weight of 20.4 g on day 0, which increased to 21.3 g on day

14, further to 21.6 g on day 28, and reached 22.7 g on day 42. For mice immunized intramuscularly with the empty pVAX1 vector, mice had an average weight of 20.2 g on day 0, which increased to 20.9 g on day 14, further to 21.9 g on day 28, dropping slightly to 21.6 g on day 42 (Fig. 3a). For mice immunized intranasally with the recombinant DNA plasmid pVAX1/S2-6EHGFP, mice had an average weight of 20.0 g on day 0, which increased to 20.7 g on day 14, further to 21.6 g on day 28, and reached 22.7 g on day 42. For mice immunized intranasally with PBS, mice had an average weight of 20.4 g on day 0, which increased to 21 g on day 14, further to 21.1 g on day 28, and reached 23.0 g on day 42. For mice immunized intranasally with the empty pVAX1 vector, mice had an average weight of 18.9 g on day 0, which increased to 19.2 g on day 14, further to 20.0 g on day 28, dropping slightly to 21.1 g on day 42 (Fig. 3b). The observations indicated vaccine safety and a lack of adverse side effects from the administration of the DNA vaccine by either route of administration.

Production of IFN-γ Secreting CD3$^+$CD4$^+$ T Cells by Intramuscular or Intranasal Administration of the Recombinant Plasmid DNA pVAX1/S2-6EHGFP

A specific gating strategy was employed for ICS analysis to determine the percentage of CD4$^+$ T cells producing

Fig. 3 Progression of the weight of mice immunized through **a** intramuscular (IM) or **b** intranasal (IN) route with the recombinant plasmid DNA pVAX1/S2-6EHGFP, PBS, or the empty pVAX1 vector at day 0, day 14, day 28, and day 42 post-immunization
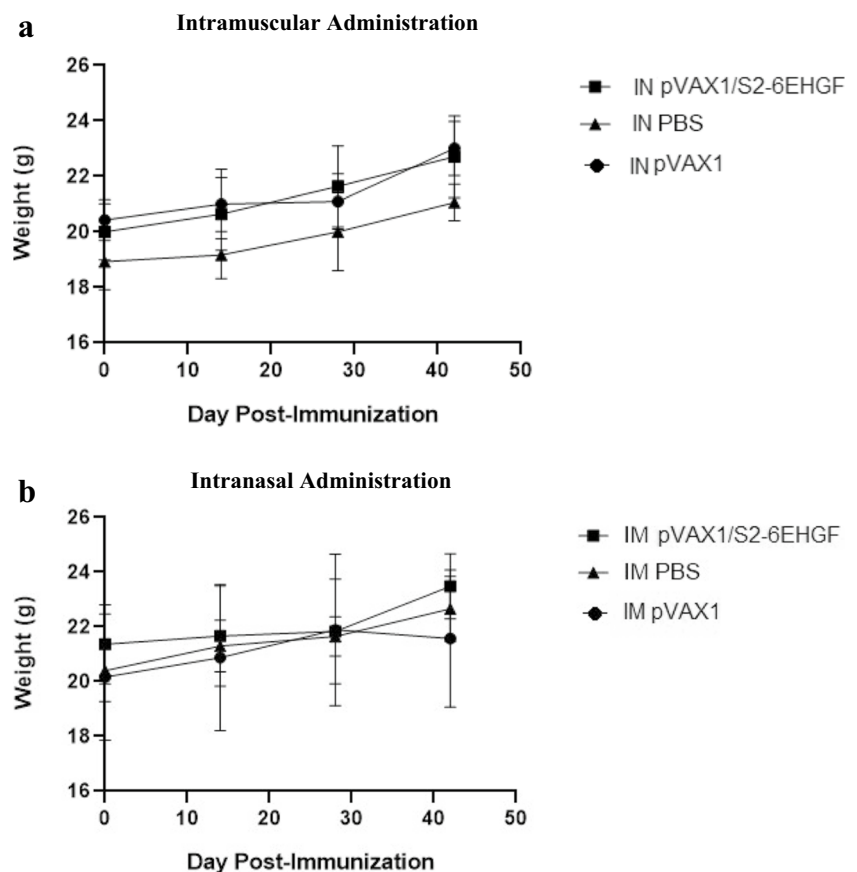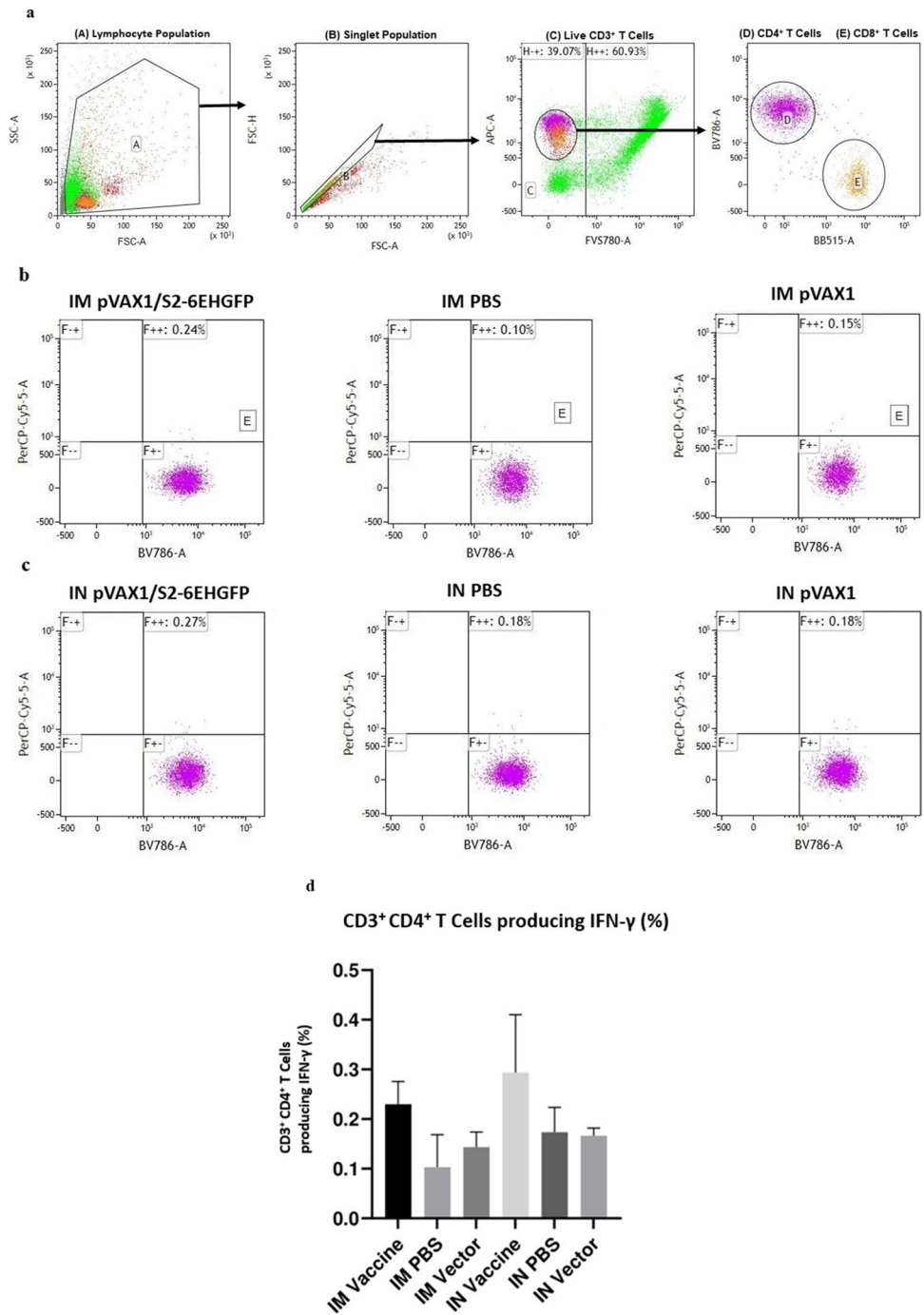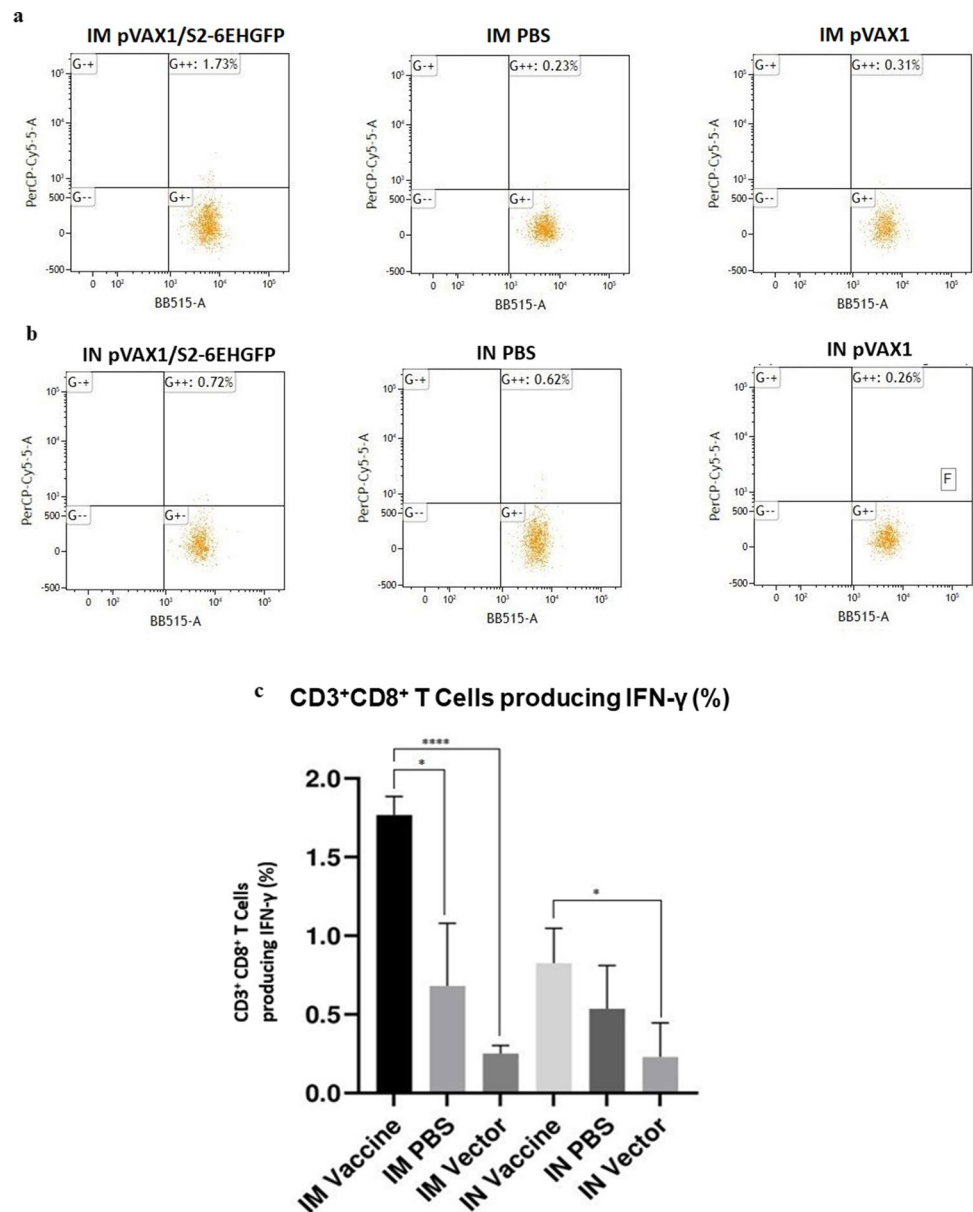
Fig. 4 The recombinant plasmid DNA pVAX1/S2-6EHGFP elicited IFN-γ production by CD4⁺ T cells in splenocytes of BALB/c mice immunized with the vaccine candidate. BALB/c mice (n=5) were immunized with the recombinant plasmid DNA pVAX1/S2-6EHGFP three times either through IM or IN administration at a two-week interval. On Day 42 post-immunization, cells were harvested from spleens of the immunized mice. **a** Gating strategy employed for ICS analysis of T cell subsets in flow cytometry in terms of the identification of the lymphocyte population, singlet population, live CD3⁺ T cells, and CD4⁺ and CD8⁺ T cells producing IFN-γ. **b** Representative plots showing the percentage of IFN-γ production by CD4⁺ T cells in splenocytes of BALB/c mice immunized intramuscularly with the recombinant plasmid DNA pVAX1/S2-6EHGFP, PBS or the empty pVAX1 vector. **c** Representative plots showing the percentage of IFN-γ production by CD4⁺ T cells in splenocytes of BALB/c mice immunized intranasally with the recombinant plasmid DNA pVAX1/S2-6EHGFP, PBS and the empty pVAX1 vector. **d** Comparative percentages of IFN-γ secreting CD4⁺ T cells in splenocytes in mice immunized with IM or IN administration with the recombinant plasmid DNA pVAX1/S2-6EHGFP, PBS, or empty pVAX1 vector. The bars indicated the mean ±SD while the error bars indicated standard deviations. Statistical significance was analyzed using paired t-tests

IFN-γ from murine splenocytes isolated from mice immunized intramuscularly or intranasally with the recombinant plasmid DNA pVAX1/S2-6EHGFP, PBS, or the empty pVAX1 vector. This involved gating the lymphocyte population, singlet population, live CD3⁺ T cells, and CD3⁺ CD4⁺ T cells producing IFN-γ (Fig. 4a). The percentage of CD4⁺ T cells secreting IFN-γ was shown to be 0.23 % for splenocytes from mice immunized intramuscularly with the recombinant plasmid DNA pVAX1/S2-6EHGFP relative to 0.10 % for splenocytes from mice immunized

intramuscularly with PBS and 0.14 % for splenocytes from mice immunized intramuscularly with the empty pVAX1 vector (Fig. 4b). The percentage of CD3⁺ CD4⁺ T cells secreting IFN-γ was at 0.29 % for splenocytes from mice immunized intranasally with the recombinant plasmid DNA pVAX1/S2-6EHGFP relative to 0.17 % for splenocytes from mice immunized intranasally with PBS and 0.16 % for splenocytes from mice immunized intranasally with the empty pVAX1 vector (Fig. 4c). An approximate percentage increase of 130% in the percentage of CD4⁺ T

Fig. 5 The recombinant plasmid DNA pVAX1/S2-6EHGFP elicited IFN-γ production by CD8$^+$ T cells in splenocytes of BALB/c mice immunized with the vaccine. BALB/c mice (n=5) were immunized IM or IN with the recombinant plasmid DNA pVAX1/S2-6EHGFP thrice with a two-week interval. On Day 42 post-immunization, cells were harvested from spleens of the immunized mice. **a** Representative plots showing the percentage of IFN-γ production by CD8$^+$ T cells in splenocytes of BALB/c mice immunized intramuscularly with the recombinant plasmid DNA pVAX1/S2-6EHGFP, PBS and the empty pVAX1 vector. **b** Representative plots showing the percentage of IFN-γ production by CD8$^+$ T cells in splenocytes of BALB/c mice immunized intranasally with the recombinant plasmid DNA pVAX1/S2-6EHGFP, PBS and the empty pVAX1 vector. **c** Comparative percentages of IFN-γ secreting CD8$^+$ T cells in splenocytes in mice immunized IM or IN with the recombinant plasmid DNA pVAX1/S2-6EHGFP, PBS, and empty pVAX1 vector. The bars indicated the mean ±SD while the error bars indicated standard deviations. Statistical significance was analyzed using paired t-tests

cells secreting IFN-γ was observed when comparing the intramuscular immunization of mice with the recombinant plasmid DNA pVAX1/S2-6EHGFP to intramuscular immunization with PBS. When comparing intramuscular immunization with the recombinant plasmid DNA to intramuscular immunization with the empty pVAX1 vector, a percentage increase of 64 % was observed (Fig. 4d). When comparing the intranasal immunization with the recombinant plasmid DNA pVAX1/S2-6EHGFP to intramuscular immunization with PBS, a percentage increase of 71 % in the percentage of CD4$^+$ T cells secreting IFN-γ was observed while a percentage increase of 81 % was observed when comparing intranasal immunization with the recombinant plasmid DNA to intramuscular immunization with the empty pVAX1 vector. While

a percentage increase was observed in the percentage of IFN-γ-secreting CD4$^+$ T cells in mice immunized with the recombinant plasmid DNA when compared to the control groups where intramuscular and intranasal administrations were used, this difference was not statistically significant (p > 0.05) (Fig. 4d).

Production of IFN-γ Secreting CD3$^+$CD8$^+$ T Cells by Intramuscular and Intranasal Administration of the Recombinant Plasmid DNA pVAX1/S2-6EHGFP

The percentage of CD8$^+$ T cells secreting IFN-γ was reported to be 1.77 % for splenocytes harvested from mice immunized intramuscularly with the recombinant plasmid DNA pVAX1/S2-6EHGFP relative to 0.68 % for splenocytes from

mice immunized intramuscularly with PBS and 0.25 % for splenocytes from mice immunized intramuscularly with the empty pVAX1 vector (Fig. 5a). Moreover, the percentage of CD8$^+$ T cells secreting IFN-γ was reported to be 0.83 % for splenocytes from mice immunized intranasally with the recombinant plasmid DNA pVAX1/S2-6EHGFP relative to 0.23 % for splenocytes from mice immunized intranasally with the empty pVAX1 vector and 0.54 % for splenocytes from mice immunized intranasally with PBS (Fig. 5b). When comparing the intramuscular immunization of mice with the recombinant plasmid DNA pVAX1/S2-6EHGFP to intramuscular immunization with PBS, a statistically significant increase of approximately 160 % was also observed in the percentage of CD8$^+$ T cells secreting IFN-γ. when comparing intramuscular immunization with the recombinant plasmid DNA to intramuscular immunization with the empty pVAX1 vector, we also observed a statistically significant increase in the percentage of CD8$^+$ T cells secreting IFN-γ, which was approximately 608% (Fig. 5c). When comparing intranasal immunization with the recombinant plasmid DNA to intranasal immunization with the empty pVAX1 vector, a statistically significant increase was observed in the percentage of CD8$^+$ T cells secreting IFN-γ, which was approximately 261 %. A percentage increase in CD8$^+$ T cells secreting IFN-γ at 54 % was also observed when comparing intranasal immunization with the recombinant plasmid DNA to intranasal immunization with PBS. However, this difference was not statistically significant ($p < 0.05$) (Fig. 5c).

High Levels of IgG Antibodies in Sera from Mice Immunized with the Recombinant Plasmid DNA pVAX1/S2-6EHGFP

An ELISA IgG assay was conducted using a 96-well ELISA plate precoated with peptides B6 and B10 to evaluate the levels of binding IgG antibodies elicited in the sera from mice immunized intramuscularly or intranasally with the recombinant plasmid DNA pVAX1/S2-6EHGFP, PBS, and empty pVAX1 vector. Sera from mice administered intramuscularly or intranasally with the recombinant plasmid DNA pVAX1/S2-6EHGFP, PBS, and empty pVAX1 vector were diluted in the ratios 1:50, 1: 250, and 1: 1000.

At 1:50 dilution, the IM Vaccine group of mice exhibited significant elevated levels of IgG antibodies, as indicated an absorbance at 450 nm (mean A450) of 1.7771, in comparison to the IM PBS group (A450 = 0.844633), with a statistically significant difference observed ($p < 0.05$) (Fig. 6). Although the IM Vaccine group demonstrated higher IgG antibody levels when compared to the group of mice administered with the vector IM (A450 = 1.144533) across the same dilution, this difference did not reach statistical significance ($p > 0.05$) (Fig. 6). At 1:250 dilutions, the group of mice receiving the vaccine IM showed significantly elevated levels of

IgG antibodies, as indicated by a mean A450 of 1.7054, in comparison to both the group of mice administered with PBS (IM) (A450 = 0.794767) and mice administered with the vector (IM) (A450 = 0.876633) with statistically significant differences were observed in both comparisons ($p < 0.05$) (Fig. 6). At 1:1000 dilution, the group of mice administered with the DNA vaccine IM exhibited significantly elevated levels of IgG antibodies, as reflected by a mean A450 of 1.5676. This was in comparison to both the IM PBS group (A450 = 0.517267) and the IM Vector group (A450 = 0.644767), with statistically significant differences observed in both comparisons ($p < 0.05$) (Fig. 6). At a 1:50 dilution, the IN Vaccine group displayed significantly elevated levels of IgG antibodies, with a mean A450 of 1.8917. This was in comparison to both the IN PBS group (A450 = 0.8201) and the IN Vector group (A450 = 0.541967), with statistically significant differences observed in both comparisons ($p < 0.05$) (Fig. 7). At 1:250 dilution, the IN Vaccine group exhibited significantly elevated levels of IgG antibodies, with a mean A450 of 1.866667. This was in comparison to both the IN PBS group (A450 = 0.794833) and the IN Vector group (A450 = 0.464), with statistically significant differences observed in both comparisons ($p < 0.05$) (Fig. 7). At 1:1000 dilution, the IN Vaccine group displayed significantly elevated levels of IgG antibodies, as indicated by a mean A450 of 1.828833. This was in comparison to both the IN PBS group (A450 = 0.645733) and the IN Vector group (A450 = 0.4573), with statistically significant differences observed in both comparisons ($p < 0.05$) (Fig. 7).

Positive Detection of Neutralizing Antibodies Against the SARS-CoV-2 Omicron Strain in the Sera of Mice Immunized Intramuscularly with the Recombinant Plasmid DNA pVAX1/ S2-6EHGFP

The ELISA IgG data showed the presence of binding IgG antibodies in the sera of mice immunized IM and IN with the recombinant plasmid DNA pVAX1/S2-6EHGFP. However, detection of significant levels of neutralizing antibodies as a subset of binding antibodies in total IgG was important. The cPass SARS-CoV-2 Neutralization Antibody Detection Kit was used to determine the levels of neutralizing antibodies effective against the SARS-CoV-2 Omicron strain in the sera of immunized mice. The neutralizing antibodies could inhibit the interaction between RBD-HPR and the ACE2 receptor.

Sera from mice immunized intramuscularly or intranasally with the recombinant plasmid DNA pVAX1/S2-6EHGFP or PBS or the empty pVAX1 vector were mixed in a 1:1 ratio with the HRP-conjugated RBD (RBD-HRP) and signal inhibition of the interaction between RBD and ACE2 receptor was determined. The positive and negative control showed signal inhibition of 96.7% and 0, respectively (Fig. 7). Sera from
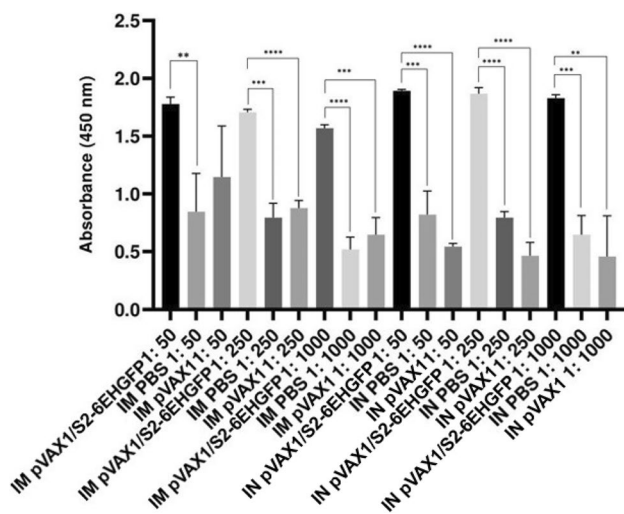
Fig. 6 Absorbance values in ELISA corresponding to the concentration of IgG antibodies in the sera of mice immunized IM or IN with the recombinant plasmid DNA pVAX1/S2-6EHGFP, PBS, and empty pVAX1 vector

Fig. 7 Inhibition of interaction between the SARS-CoV-2 Omicron strain RBD and ACE2 receptor in the sera of immunized mice with the recombinant plasmid DNA pVAX1/S2-6EHGFP, PBS, or the empty pVAX1 vector through the IM or IN administrations. Positive and negative controls were included

mice immunized intramuscularly or intranasally with PBS or the empty pVAX1 vector showed a signal inhibition of 0%, indicating that neutralizing antibodies to SARS-CoV-2 were not detected. Sera from mice immunized intramuscularly with the recombinant plasmid DNA pVAX1/S2-6EHGFP showed a signal inhibition of 31.5 %, respectively while that from mice immunized intranasally with the recombinant plasmid DNA pVAX1/S2-6EHGFP showed a signal inhibition of 29.2 %. Since the cutoff value for the cPass SARS-CoV-2 Neutralizing Antibody Detection assay was based on 30% signal inhibition, it was concluded that sera obtained from the intramuscular administration of the recombinant plasmid DNA pVAX1/S2-6EHGFP were positive for the presence of neutralizing antibodies capable of blocking the binding between SARS-CoV-2 Omicron strain RBD and the ACE2 receptor.

Discussion

The etiological agent for COVID-19, the SARS-CoV-2 continues to cause multiple infections as well as a significant morbidity and mortality toll [48]. The continuing spread of infections is attributable to SARS-CoV-2 VOCs which are associated with a potential for higher infectivity and immune invasion [49]. Although S protein based vaccines were quickly progressed through clinical development and used for public immunizations, the emergence of VOCs with multiple mutations in the S protein warrant the use of a novel approach to vaccine development. Here we have described the preclinical development of a novel COVID-19 recombinant plasmid DNA vaccine, pVAX1/S2-6EHGFP to combat the rising spread of infections caused by SARS-CoV-2 VOCs. The
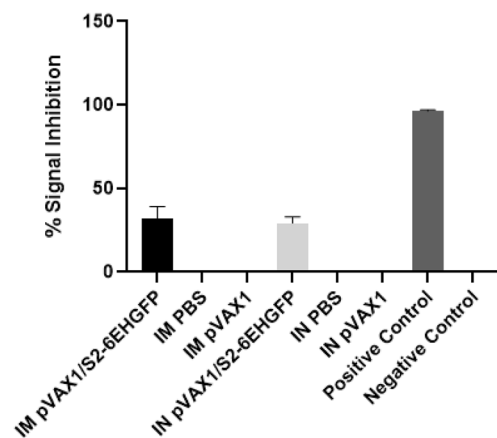
development of this vaccine amalgamates reverse vaccinology bioinformatics and literature mining approaches used for the identification of immunogenic and highly conserved epitopes together with the incorporation of selected epitopes to develop a next-generation DNA vaccine incorporating these epitopes. The design and synthesis of the vaccine was initiated upon reports of reductions in protective efficacies of current licensed BNT162b2, mRNA-1273, ChAdOx1-S vaccines as a result of the emergence of mutates SARS-CoV-2 VOCs with multiple mutations in the S protein. The data produced by this research study supports the expression and immunogenicity of the pVAX1/S2-6EHGFP recombinant plasmid DNA vaccine in the murine model. Humoral and cellular immune responses were reported upon the IM or IN administration of the pVAX1/S2-6EHGFP recombinant plasmid DNA vaccine in BALB/c mice. More specifically, administration of the vaccine and the subsequent evaluation of immune responses was conducted in accordance with clinical delivery parameters. The study assessed the production of IFN-γ by CD4$^+$ and CD8$^+$ T cells in splenocytes of immunized mice together with determination of IgG antibody levels relative to absorbance values and the presence of neutralizing antibodies blocking of ACE2/SARS-CoV-2 S protein interaction in sera of mice immunized with pVAX1/S2-6EHGFP.

Curbing the spread of infections caused by rapidly emerging SARS-CoV-2 VOCs warrants a coordinated response from the global health community and the development of novel vaccine development strategies which can elicit immune responses against both the SARS-CoV-2 prototype strain and its VOCs. In response to the emergence of highly transmissible SARS-CoV-2 VOCs such as the SARS-CoV-2 Omicron strain, we employed the use of the DNA vaccine to develop the pVAX1/S2-6EHGFP recombinant

plasmid DNA vaccine which encoded peptides representing highly conserved and immunogenic B and T cell epitopes. The design and development of the pVAX1/S2-6EHGFP recombinant plasmid DNA vaccine utilized a plug and play process such that the target antigenic sequence encoding 6 peptides from SARS-CoV-2 structural proteins was incorporated into an FDA-approved plasmid vector (pVAX1). The unique America FDA-approved pVAX1 vector was also used to express another DNA vaccine known as pVAX1-D3ME which expressed the prM and E proteins of dengue virus serotype 3 (DENV3) [50]. In the current study, the design of the pVAX1/S2-6EHGFP recombinant plasmid DNA vaccine was optimized for *in vivo* gene expression such as the inclusion of the CMV promoter, a major immediate early (MIE) enhancer-containing promoter which regulates and promotes high-level eukaryotic expression of target sequences.

Lim *et al*. (2021) utilized bioinformatics analysis to predict immunogenic B and T cell epitopes that could be used to develop a multi-epitope vaccine against SARS-CoV-2. Moreover, further literature mining performed by researchers in the Centre for Virus and Vaccine Research (CVVR) at Sunway University yielded a total of 6 peptides which represented immunogenic and highly conserved B and T cell epitopes from SARS-CoV-2 structural proteins [51, 52].

S1 WTAGAAAYYVGYLQPRTFLLKY

Lim *et al*. (2021) comprehensively evaluated the data from 11 different publications that had used bioinformatics to identify promising CD4+ and CD8+ T cell epitopes from the S protein of SARS-CoV-2. WTAGAAAYYVGYLQPRTFLLKY was identified as a highly potent T cell epitope, capable of inducing both CD4+ and C8+ T cell responses. It was associated with positive IFN-γ production, a high immunogenicity score of 97.729 %, and a high global HLA population coverage of 99.63% [52].

S5 FPQSAPHGVVFLHVTYVPAQEK

FPQSAPHGVVFLHVTYVPAQEK was identified as a highly potent T cell epitope, capable of inducing both CD4+ and C8+ T cell responses. It was associated with positive IFN-γ production, a high immunogenicity score of 98.6 %, and a high global HLA population coverage of 96.4 % [52].

S19 GEVFNATRFASVYAWNRKRISNCVADYSVLYNS

Prioritizing the identification of epitopes from conserved regions of the SARS-CoV-2 as well as from regions associated with high viral infectivity, Yarmarkovich *et al*. (2020) demonstrated that viral epitope GEVFNATRFASVYAWNRKRISNCVADYSVLYNS from the RBD of the S protein scored in the 90.9th percentile of T epitopes. It was also shown to be third of 1,546 epitopes scored in the S, E, and M genes for combined B and T cell epitopes, with high MHC class I coverage of 98.3% [53].

Moreover, GEVFNATRFASVYAWNRKRISNCVADYS-VLYNS was used as a peptide along with 45 other peptides which were mixed to form a multi-peptide cocktail to serve as a COVID-19 vaccine. Intramuscular administration of this COVID-19 peptide vaccine in addition to a tetanus vaccine in horse was able to induce neutralizing antibodies against the SARS-CoV-2 Delta variant [54].

M1 GLMWLSYFIASFRLFARTRSM

GLMWLSYFIASFRLFARTRSM was identified as a CD4+ T cell epitope through *in silico* predictions of potential T-cell epitopes through retrieval of protein sequences from the NCBI database, analysis of average antigenic propensity and binding affinity of peptides for class II MHC, assessment of immunogenicity score and the ability to induce Th1 immune response together with IFN-γ production [52].

B6 TESNKKFLPFQQFGRD & B10 ESNKKFLPFQQFGRDIADTT

Heffron *et al*. (2021) utilized ultradense peptide microarray mapping to identify ESNKKFLPFQQFGRDIADTT as one of the epitopes associated with potent antibody responses as a result of SARS-CoV-2 infection [55]. ESNKKFLPFQQF-GRDIADTT was predicted as a dominant SARS-CoV B Cell Epitope as identified by the EpitopeVec software that utilizes residue properties, modified antigenicity scales, and protein language model-based representations for linear BCE predictions.

A total of five epitopes were associated with peptides from the SARS-CoV-2 S protein. The SARS-CoV-2 S protein is characterized as a class I membrane fusion protein (Jackson *et al*., 2022). Multiple reports have established that the SARS-CoV-2 S protein interacts with the host ACE2 cell receptor to facilitate viral entry and fusion [56]. The interaction between the SARS-CoV-2 S protein and the ACE2 receptor may be blocked by the action of anti-S neutralizing antibodies [27]. *In vivo* immunogenicity studies conducted in the BAL/c mouse model reveled high levels of B6 and B10-reactive binding IgG in the serum of mice immunized with the recombinant plasmid DNA vaccine. In addition to binding IgG, antibodies, we further demonstrated that immunization with pVAX1/S2-6EHGFP induced RBD binding antibodies through an *in vitro* cPASS assay that demonstrated that these binding antibodies were able to neutralize the interaction between the SARS-CoV-2 RBD and the ACE2 receptor. Indeed, the RBD is reported to be

a target for neutralizing antibodies from SARS-CoV convalescent patients [57]. Future studies of immunogenicity testing of pVAX1/S2-6EHGFP should involve the functional demonstration of these antibodies through neutralization of SARS-CoV-2 wild-type and Omicron through live virus and pseudovirus assays in addition to assays to show competitive inhibition of SARS-CoV-2 spike protein binding to the ACE2 receptor in the presence of serum of mice immunized with the recombinant plasmid DNA vaccine. In addition to humoral immunity, cellular immune responses have also been linked with favorable recovery from SARS-CoV-2 infection [58]. In this research study, we demonstrated the induction of T cell responses against SARS-CoV-2 in terms of IFN-γ production by CD4$^+$ and CD8$^+$ T cells. Rapid cellular responses may reduce viral load and potentially slow the spread of COVID-19 and its associated SARS-CoV-2 disease.

The prospect of developing DNA vaccines for SARS-CoV-2 is attractive because the DNA vaccine platform shows great potential in eliciting both humoral and cellular immune responses [59]. MHC-I antigen presentation by non-APCs such as monocytes as well as MHC-II cross-priming and antigen presentation by dendritic cells can induce the activity of both CD4$^+$ and CD8$^+$ T cells [35]. In addition, the recognition of the antigen by B lymphocytes resulted in humoral responses [34, 37]. Current DNA vaccines targeting the S protein of the SARS-CoV-2 have shown humoral immune responses detected by ELISA in the form of neutralizing antibodies and cellular immune responses determined by ELISpot in the form of IFN-γ production [27, 33, 36, 38]. The DNA vaccine platform offers a promising solution to combat the problem of emerging SARS-CoV-2 VOCs. Multiple DNA vaccine candidates could be designed by simply changing the antigenic sequence incorporated into the plasmid vector. Smith *et al*. (2020) have reported that DNA-based vaccines could be developed quickly since a variety of different candidates could be prepared and tested using high-throughput approaches [27]. Moreover, they could be quickly progressed to the clinical stage by leveraging on established pathways.

It is relatively easy to produce the vaccine in large quantities for dissemination to the public for immunization [27, 32]. They can also be conveniently produced in large quantities using bacteria such as *E. coli* [32]. Therefore, efficient large-scale and cost-effective production of DNA vaccines for large-scale immunizations offers an attractive practical advantage. In the fields of vaccinology and immunology, vaccine storage is an important issue since it is directly associated with vaccine stability and the maintenance of its quality. Therefore, in order to ensure that the efficacy of mRNA vaccines is not negatively affected, cold storage at -70°C is necessary for the preservation of the Pfizer vaccine. DNA vaccines are highly stable, less prone to degradation

unlike mRNA vaccines, and do not require such low temperature for storage. DNA vaccines can be kept at room temperature [31]. Since they do not require specific cold chain conditions, DNA vaccines would be ideal for immunizing populations in third world countries which lack the financial resources and infrastructure to maintain cold chain conditions [31, 60]. In the current research study, immunogenicity was determined after three doses of 100 μg of the pVAX1/S2-6EHGFP recombinant plasmid DNA vaccine were administered to BALB/c mice. Future studies may be conducted to find the optimal immunogenic dose associated with the elicitation or robust immunogenic responses. This may reduce the need for multiple immunizations.

It is true that there are concerns of vaccine-induced immunopathology associated with the administration of vaccines. However, it is entirely possible that such concerns are more likely to be associated with specific vaccine platforms such as inactivated vaccines [61]. Indeed, there have been no reports of immune pathology of DNA vaccines that were tested in mice or non-human primate (NHP) models [62, 63]. Moreover, the DNA vaccine platform has shown effectiveness in models of respiratory infection, such as SARS-CoV, MERS-CoV, and RSV, by inducing Th1-type immune responses without causing immunopathology [62, 64, 65]. It is worth noting that our study's vaccine groups did not show any weight reduction following vaccine administration. This absence of weight drop among the vaccinated animals indicates a favorable safety profile for this vaccine platform in our experimental models. This finding aligns with the overall lack of observed adverse effects and suggests that the DNA vaccine platform holds promise as a safe and effective candidate. These positive safety indicators strengthen our confidence in the potential of the pVAX1/S2-6EHGFP recombinant plasmid DNA vaccine for further research and development. Future studies involving animal challenges with SARS-CoV-2 could effectively evaluate the ability of the pVAX1/S2-6EHGFP recombinant plasmid DNA vaccine to protect against the disease while also considering the potential for vaccine-enhanced disease.

Four T cell epitopes namely, S1, S5, S19, and M1 were incorporated in the pVAX1 vector as part of the vaccine design to form the pVAX1/S2-6EHGFP recombinant plasmid DNA vaccine. The IM and IN administration of pVAX1/S2-6EHGFP recombinant plasmid DNA vaccine was associated with the production of IFN-γ production by CD8$^+$ T cells. The IM and IN administration of pVAX1/S2-6EHGFP recombinant plasmid DNA vaccine also resulted in IFN-γ production by CD4$^+$ T cells, although this did not differ significantly from the control groups. Apart from T cell epitopes, two B cell epitopes namely, B6 and B10 were also to form the pVAX1/S2-6EHGFP recombinant plasmid DNA vaccine. We utilized absorbance values to demonstrate high levels of binding IgG antibodies elicited against the two B cell epitopes, B6 and B10. Both the IM and IN

administration of pVAX1/S2-6EHGFP resulted in robust levels of binding IgG antibodies in the sera of immunized mice.

The results of the neutralizing assay showed that the sera of mice immunized with the vaccine showed 30% inhibition of interaction between the SARS-CoV-2 Omicron RBD and the ACE 2 receptor. The cPASS protocol specifies that the cutoff value for the cPass SARS-CoV-2 Neutralizing Antibody Detection Kit is 30% signal inhibition. These results are promising and indicate the neutralizing potential of the humoral responses elicited by the DNA vaccine. Future studies may involve the identification of more promising B cell epitopes for inclusion in the vaccine to elicit higher percentage signal inhibition while using the cPASS kit.

The approach undertaken to develop the pVAX1/S2-6EHGFP DNA vaccine involved employing reverse vaccinology to identify highly conserved and immunogenic epitopes present in the structural proteins of SARS-CoV-2. When incorporated into the DNA, functional T cell and B cell responses were observed. This indicated that the design of the study with the use of specific epitopes could offer protection against the SARS-CoV-2 Omicron strain. This was a promising finding considering reports of reduced protective efficacies of current COVID-19 vaccines against emerging viral variants. Since these vaccines focused on the full-length S protein of the original viral strain, mutations in the S protein meant that the protective efficacies of these vaccines reduced in response to emerging variants.

In contrast, the current DNA vaccine was developed using selected highly conserved and immunogenic epitopes that were able to elicit T cell responses in terms of IFN-γ protection and cross-neutralizing activity against the Omicron variant. This demonstrates proof of concept: the inclusion of specific B cell and T cell epitopes to demonstrate cross-protection against multiple strains which will prevent the need for repeated immunizations upon emergence of each new variant. The current approach is well suited to quickly build vaccines comprising of different pathogenic to combat continuously emerging viral variants of infectious diseases through quick progression through clinical stages based on established regulatory pathways.

To date, this is the only DNA vaccine consisting of in silico predicted epitopes that is able to elicit immune responses in terms of IFN-γ producing T cells as well as humoral responses that can neutralize the SARS-CoV-2 Omicron strain. There has been one other study where Persson *et al.* (2023) reported the development of a DNA vaccine consisting of in silico epitopes protected against lethal SARS-CoV-2 infection in K18-hACE2 mice but this study only utilized T cell responses [66]. The inclusion of B cell epitopes with cross-neutralizing ability represents a forefront in vaccine design and the concept could be implemented for the development for future vaccines emerging infectious diseases.

In summary, these initial preliminary findings which described the immunogenicity of the novel COVID-19 recombinant plasmid DNA vaccine, pVAX1/S2-6EHGFP are promising, and it is especially significant that the results showed functional neutralizing antibodies and T cell responses in BALB/c mice. This research study further supports the continuing evaluation of pVAX1/S2-6EHGFP as a vaccine candidate against the SARS-CoV-2 prototype strain and VOCs. This study highlights the immunogenicity of pVAX1/S2-6EHGFP and the further evaluation of this vaccine candidate should involve challenge studies with SARS-CoV-2 prototype and the Omicron strains to establish cross-protection in multiple animal models.

Data Availability The authors confirm that the data supporting the findings of the study are available within the article and its Supplementary section. Raw data that support the findings of the study are available from the corresponding author, upon reasonable request.

Declarations

Conflict of Interest The authors declare no conflict of interest.

References

1. Sannathimmappa M, Nambiar V. COVID-19: An insight into SARS-CoV-2 pandemic originated at Wuhan City in Hubei province of China. Journal of Infectious Diseases and Epidemiology. 2020;6. https://doi.org/10.23937/2474-3658/1510146.

2. WHO: WHO coronavirus (COVID-19) dashboard. https://covid19.who.int/ (2023). Accessed.

3. Ahmed S, Khan S, Imran I, Al Mughairbi F, Sheikh FS, Hussain J, et al. Vaccine development against COVID-19: Study from pre-clinical phases to clinical trials and global use. Vaccines. 2021;9(8):836.

4. Puranik A, Lenehan PJ, Silvert E, Niesen MJM, Corchado-Garcia J, O'Horo JC, et al. Comparison of two highly-effective mRNA vaccines for COVID-19 during periods of Alpha and Delta variant prevalence. medRxiv : the preprint server for health sciences. 2021.https://doi.org/10.1101/2021.08.06.21261707.

5. Voysey M, Clemens SAC, Madhi SA, Weckx LY, Folegatti PM, Aley PK, et al. Safety and efficacy of the ChAdOx1 nCoV-19 vaccine (AZD1222) against SARS-CoV-2: an interim analysis of four randomised controlled trials in Brazil, South Africa, and the UK. Lancet. 2021;397(10269):99–111. https://doi.org/10.1016/S0140-6736(20)32661-1.

6. Zhang Y, Belayachi J, Yang Y, Fu Q, Rodewald L, Li H, et al. Real-world study of the effectiveness of BBIBP-CorV (Sinopharm) COVID-19 vaccine in the Kingdom of Morocco. BMC Pub Health. 2022;22(1):1584. https://doi.org/10.1186/s12889-022-14016-9.

7. Jungreis I, Sealfon R, Kellis M. SARS-CoV-2 gene content and COVID-19 mutation impact by comparing 44 Sarbecovirus genomes. Nat Commun. 2021;12(1):2642. https://doi.org/10.1038/s41467-021-22905-7.

8. Alanagreh L, Alzoughool F, Atoum M. The Human Coronavirus Disease COVID-19: Its Origin, Characteristics, and Insights into Potential Drugs and Its Mechanisms. Pathogens. 2020;9(5). https://doi.org/10.3390/pathogens9050331.

9. Shang J, Wan Y, Luo C, Ye G, Geng Q, Auerbach A, et al. Cell entry mechanisms of SARS-CoV-2. Proc Natl Acad Sci U S A. 2020;117(21):11727–34. https://doi.org/10.1073/pnas.2003138117.

10. Rastogi M, Pandey N, Shukla A, Singh SK. SARS coronavirus 2: from genome to infectome. Respiratory Res. 2020;21(1):318. https://doi.org/10.1186/s12931-020-01581-z.

11. Cosar B, Karagulleoglu ZY, Unal S, Ince AT, Uncuoglu DB, Tuncer G, et al. SARS-CoV-2 Mutations and their Viral Variants. Cytokine Growth Factor Rev. 2022;63:10–22. https://doi.org/10.1016/j.cytogfr.2021.06.001.

12. Farhud DD, Mojahed N. SARS-COV-2 Notable Mutations and Variants: A Review Article. Iran J Public Health. 2022;51(7):1494–501. https://doi.org/10.18502/ijph.v51i7.10083.

13. Magazine N, Zhang T, Wu Y, McGee MC, Veggiani G, Huang W. Mutations and Evolution of the SARS-CoV-2 Spike Protein. Viruses. 2022;14(3):640.

14. Agerer B, Koblischke M, Gudipati V, Montaño-Gutierrez LF, Smyth M, Popa A, et al. SARS-CoV-2 mutations in MHC-I-restricted epitopes evade CD8(+) T cell responses. Sci Immunol. 2021;6(57). https://doi.org/10.1126/sciimmunol.abg6461.

15. Cele S, Jackson L, Khoury DS, Khan K, Moyo-Gwete T, Tegally H, et al. Omicron extensively but incompletely escapes Pfizer BNT162b2 neutralization. Nature. 2022;602(7898):654–6. https://doi.org/10.1038/s41586-021-04387-1.

16. Cheng SMS, Mok CKP, Leung YWY, Ng SS, Chan KCK, Ko FW, et al. Neutralizing antibodies against the SARS-CoV-2 Omicron variant BA.1 following homologous and heterologous CoronaVac or BNT162b2 vaccination. Nature Medicine. 2022;28(3):486-9. https://doi.org/10.1038/s41591-022-01704-7.

17. Collier DA, De Marco A, Ferreira I, Meng B, Datir RP, Walls AC, et al. Sensitivity of SARS-CoV-2 B117 to mRNA vaccine-elicited antibodies. Nature. 2021;593(7857):136-41. https://doi.org/10.1038/s41586-021-03412-7.

18. Hachmann NP, Miller J, Collier A-rY, Ventura JD, Yu J, Rowe M, et al. Neutralization Escape by SARS-CoV-2 Omicron Subvariants BA.2.12.1, BA.4, and BA.5. New England Journal of Medicine. 2022;387(1):86-8. https://doi.org/10.1056/NEJMc2206576.

19. Madhi SA, Baillie V, Cutland CL, Voysey M, Koen AL, Fairlie L, et al. Efficacy of the ChAdOx1 nCoV-19 Covid-19 Vaccine against the B.1.351 Variant. New England Journal of Medicine. 2021;384(20):1885-98. https://doi.org/10.1056/NEJMoa2102214.

20. Noh JY, Jeong HW, Shin E-C. SARS-CoV-2 mutations, vaccines, and immunity: implication of variants of concern. Signal Transduct Target Therapy. 2021;6(1):203.

21. Wu K, Werner AP, Moliva JI, Koch M, Choi A, Stewart-Jones GBE, et al. mRNA-1273 vaccine induces neutralizing antibodies against spike mutants from global SARS-CoV-2 variants. bioRxiv. 2021. https://doi.org/10.1101/2021.01.25.427948.

22. Carabelli AM, Peacock TP, Thorne LG, Harvey WT, Hughes J, Peacock SJ, et al. SARS-CoV-2 variant biology: immune escape, transmission and fitness. Nat Rev Microbiol. 2023;21(3):162–77. https://doi.org/10.1038/s41579-022-00841-7.

23. Chakraborty C, Bhattacharya M, Sharma AR, Mallik B. Omicron (B.1.1.529) - A new heavily mutated variant: Mapped location and probable properties of its mutations with an emphasis on S-glycoprotein. International Journal of Biological Macromolecules. 2022;219:980-97. https://doi.org/10.1016/j.ijbiomac.2022.07.254.

24. Willett BJ, Grove J, MacLean OA, Wilkie C, De Lorenzo G, Furnon W, et al. SARS-CoV-2 Omicron is an immune escape variant with an altered cell entry pathway. Nature Microbio. 2022;7(8):1161–79. https://doi.org/10.1038/s41564-022-01143-7.

25. Maruggi G, Zhang C, Li J, Ulmer JB, Yu D. mRNA as a Transformative Technology for Vaccine Development to Control Infectious Diseases. Mole Therapy. 2019;27(4):757–72. https://doi.org/10.1016/j.ymthe.2019.01.020.

26. Moyle PM, Toth I. Modern Subunit Vaccines: Development, Components, and Research Opportunities. ChemMedChem. 2013;8(3):360–76. https://doi.org/10.1002/cmdc.201200487.

27. Smith TR, Patel A, Ramos S, Elwood D, Zhu X, Yan J, et al. Immunogenicity of a DNA vaccine candidate for COVID-19. Nature Commun. 2020;11(1):2601.

28. Chalkias S, Whatley JL, Eder F, Essink B, Khetan S, Bradley P, et al. Original SARS-CoV-2 monovalent and Omicron BA.4/BA.5 bivalent COVID-19 mRNA vaccines: phase 2/3 trial interim results. Nat Med. 2023;29(9):2325-33. https://doi.org/10.1038/s41591-023-02517-y.

29. Mammen P. Mammen J, Tebas P, Agnes J, Giffear M, Kraynyak KA, Blackwood E, et al. Safety and immunogenicity of INO-4800 DNA vaccine against SARS-CoV-2: a preliminary report of a randomized, blinded, placebo-controlled, Phase 2 clinical trial in adults at high risk of viral exposure. medRxiv. 2021:2021.05.07.21256652. https://doi.org/10.1101/2021.05.07.21256652.

30. Khobragade A, Bhate S, Ramaiah V, Deshpande S, Giri K, Phophle H, et al. Efficacy, safety, and immunogenicity of the DNA SARS-CoV-2 vaccine (ZyCoV-D): the interim efficacy results of a phase 3, randomised, double-blind, placebo-controlled study in India. Lancet. 2022;399(10332):1313–21. https://doi.org/10.1016/S0140-6736(22)00151-9.

31. Tebas P, Kraynyak KA, Patel A, Maslow JN, Morrow MP, Sylvester AJ, et al. Intradermal SynCon® Ebola GP DNA Vaccine Is Temperature Stable and Safely Demonstrates Cellular and Humoral Immunogenicity Advantages in Healthy Volunteers. J Infect Dis. 2019;220(3):400–10. https://doi.org/10.1093/infdis/jiz132.

32. Huang L, Rong Y, Pan Q, Yi K, Tang X, Zhang Q, et al. SARS-CoV-2 vaccine research and development: Conventional vaccines and biomimetic nanotechnology strategies. Asian J Pharmac Sci. 2021;16(2):136–46. https://doi.org/10.1016/j.ajps.2020.08.001.

33. Chai KM, Tzeng TT, Shen KY, Liao HC, Lin JJ, Chen MY, et al. DNA vaccination induced protective immunity against SARS CoV-2 infection in hamsterss. PLoS Negl Trop Dis. 2021;15(5):e0009374. https://doi.org/10.1371/journal.pntd.0009374.

34. Hobernik D, Bros M. DNA Vaccines—How Far From Clinical Use? Int J Molecular Sci. 2018;19(11):3605.

35. Ingolotti M, Kawalekar O, Shedlock DJ, Muthumani K, Weiner DB. DNA vaccines for targeting bacterial infections. Expert Rev Vaccines. 2010;9(7):747–63. https://doi.org/10.1586/erv.10.57.

36. Prompetchara E, Ketloy C, Tharakhet K, Kaewpang P, Buranapraditkun S, Techawiwattanaboon T, et al. DNA vaccine candidate encoding SARS-CoV-2 spike proteins elicited potent humoral and Th1 cell-mediated immune responses in mice. PLoS One. 2021;16(3):e0248007. https://doi.org/10.1371/journal.pone.0248007.

37. Tebas P, Yang S, Boyer JD, Reuschel EL, Patel A, Christensen-Quick A, et al. Safety and immunogenicity of INO-4800 DNA vaccine against SARS-CoV-2: A preliminary report of an open-label,

Phase 1 clinical trial. EClinicalMedicine. 2021;31:100689. https://doi.org/10.1016/j.eclinm.2020.100689.

38. Yu J, Tostanoski LH, Peter L, Mercado NB, McMahan K, Mahrokhian SH, et al. DNA vaccine protection against SARS-CoV-2 in rhesus macaques. Science. 2020;369(6505):806–11. https://doi.org/10.1126/science.abc6284.

39. Alluhaybi KA, Alharbi RH, Alhabbab RY, Aljehani ND, Alamri SS, Basabrain M, et al. Cellular and humoral immunogenicity of a candidate dna vaccine expressing SARS-CoV-2 spike subunit 1. Vaccines. 2021;9(8):852.

40. Yadav PD, Kumar S, Agarwal K, Jain M, Patil DR, Maithal K, et al. Needle-free injection system delivery of ZyCoV-D DNA vaccine demonstrated improved immunogenicity and protective efficacy in rhesus macaques against SARS-CoV-2. J Med Virol. 2023;95(2):e28484. https://doi.org/10.1002/jmv.28484.

41. Martins M, do Nascimento GM, Conforti A, Noll JCG, Impellizeri JA, Sanchez E, et al. A linear SARS-CoV-2 DNA vaccine candidate reduces virus shedding in ferrets. Arch Virol. 2023;168(4):124. https://doi.org/10.1007/s00705-023-05746-1.

42. Dhama K, Dhawan M. COVID-19 intranasal vaccines: current progress, advantages, prospects, and challenges. 2022;18(5):2045853. https://doi.org/10.1080/21645515.2022.2045853.

43. Schultz MD, Suschak JJ. A single intranasal administration of AdCOVID protects against SARS-CoV-2 infection in the upper and lower respiratory tracts. 2022;18(6):2127292. https://doi.org/10.1080/21645515.2022.2127292.

44. Diallo BK, Ní Chasaide C, Wong TY, Schmitt P, Lee KS, Weaver K, et al. Intranasal COVID-19 vaccine induces respiratory memory T cells and protects K18-hACE mice against SARS-CoV-2 infection. npj Vaccines. 2023;8(1):68. https://doi.org/10.1038/s41541-023-00665-3.

45. Hassan AO, Shrihari S, Gorman MJ, Ying B, Yuan D, Raju S, et al. An intranasal vaccine durably protects against SARS-CoV-2 variants in mice. Cell reports. 2021;36(4):109452. https://doi.org/10.1016/j.celrep.2021.109452.

46. Ramvikas M, Arumugam M, Chakrabarti SR, Jaganathan KS. Nasal Vaccine Delivery. Micro and Nanotechnology in Vaccine Development. 2017:279-301. https://doi.org/10.1016/B978-0-323-39981-4.00015-4.

47. Tan CW, Chia WN, Qin X, Liu P, Chen MIC, Tiu C, et al. A SARS-CoV-2 surrogate virus neutralization test based on antibody-mediated blockage of ACE2–spike protein–protein interaction. Nature Biotechnol. 2020;38(9):1073–8. https://doi.org/10.1038/s41587-020-0631-z.

48. Chang D, Chang X, He Y, Tan KJK. The determinants of COVID-19 morbidity and mortality across countries. Sci Rep. 2022;12(1):5888. https://doi.org/10.1038/s41598-022-09783-9.

49. Ao D, He X, Hong W, Wei X. The rapid rise of SARS-CoV-2 Omicron subvariants with immune evasion properties: XBB.1.5 and BQ.1.1 subvariants. MedComm (2020). 2023;4(2):e239. https://doi.org/10.1002/mco2.239.

50. Feng K, Zheng X, Wang R, Gao N, Fan D, Sheng Z, et al. Long-Term Protection Elicited by a DNA Vaccine Candidate Expressing the prM-E Antigen of Dengue Virus Serotype 3 in Mice. Front Cell Infect Microbiol. 2020;10:87. https://doi.org/10.3389/fcimb.2020.00087.

51. Lim HX, Masomian M, Khalid K, Kumar AU, MacAry PA, Poh CL. Identification of B-Cell Epitopes for Eliciting Neutralizing Antibodies against the SARS-CoV-2 Spike Protein through Bioinformatics and Monoclonal Antibody Targeting. Int Mole Sci. 2022;23(8):4341.

52. Lim HX, Lim J, Jazayeri SD, Poppema S, Poh CL. Development of multi-epitope peptide-based vaccines against SARS-CoV-2. Biomed J. 2021;44(1):18–30. https://doi.org/10.1016/j.bj.2020.09.005.

53. Yarmarkovich M, Warrington JM, Farrel A, Maris JM. Identification of SARS-CoV-2 Vaccine Epitopes Predicted to Induce Long-Term Population-Scale Immunity. Cell Reports Medicine. 2020;1(3):100036. https://doi.org/10.1016/j.xcrm.2020.100036.

54. Deng W, Sweeney RW. Intramuscular injection of a mixture of COVID-19 peptide vaccine and tetanus vaccine in horse induced neutralizing antibodies against authentic virus of SARS-CoV-2 Delta variant. Vaccine: X. 2022;12:100230. https://doi.org/10.1016/j.jvacx.2022.100230.

55. Heffron AS, McIlwain SJ, Amjadi MF, Baker DA, Khullar S, Sethi AK, et al. The landscape of antibody binding in SARS-CoV-2 infection. bioRxiv. 2021. https://doi.org/10.1101/2020.10.10.334292.

56. Dërmaku-Sopjani M, Sopjani M. Interactions between ACE2 and SARS-CoV-2 S Protein: Peptide Inhibitors for Potential Drug Developments Against COVID-19. Curr Protein Pept Sci. 2021;22(10):729–44. https://doi.org/10.2174/13892037226662109 16141924.

57. Bertoglio F, Fühner V, Ruschig M, Heine PA, Abassi L, Klünemann T, et al. A SARS-CoV-2 neutralizing antibody selected from COVID-19 patients binds to the ACE2-RBD interface and is tolerant to most known RBD mutations. Cell Rep. 2021;36(4):109433. https://doi.org/10.1016/j.celrep.2021.109433.

58. Zhou X, Ye Q. Cellular Immune Response to COVID-19 and Potential Immune Modulators. Frontiers in Immunology. 2021;12. https://doi.org/10.3389/fimmu.2021.646333.

59. Lee LYY, Izzard L, Hurt AC. A Review of DNA Vaccines Against Influenza. Front Immunol. 2018;9:1568. https://doi.org/10.3389/fimmu.2018.01568.

60. Silveira MM, Moreira G, Mendonça M. DNA vaccines against COVID-19: Perspectives and challenges. Life Sci. 2021;267:118919. https://doi.org/10.1016/j.lfs.2020.118919.

61. Antonis AF, Schrijver RS, Daus F, Steverink PJ, Stockhofe N, Hensen EJ, et al. Vaccine-induced immunopathology during bovine respiratory syncytial virus infection: exploring the parameters of pathogenesis. J Virol. 2003;77(22):12067–73. https://doi.org/10.1128/jvi.77.22.12067-12073.2003.

62. Muthumani K, Falzarano D, Reuschel EL, Tingey C, Flingai S, Villarreal DO, et al. A synthetic consensus anti–spike protein DNA vaccine induces protective immunity against Middle East respiratory syndrome coronavirus in nonhuman primates. Science translational medicine. 2015;7(301):301ra132-301ra132.

63. Yang ZY, Kong WP, Huang Y, Roberts A, Murphy BR, Subbarao K, et al. A DNA vaccine induces SARS coronavirus neutralization and protective immunity in mice. Nature. 2004;428(6982):561–4. https://doi.org/10.1038/nature02463.

64. Smith TR, Schultheis K, Morrow MP, Kraynyak KA, McCoy JR, Yim KC, et al. Development of an intradermal DNA vaccine delivery strategy to achieve single-dose immunity against respiratory syncytial virus. Vaccine. 2017;35(21):2840–7.

65. Yang J, Wang W, Chen Z, Lu S, Yang F, Bi Z, et al. A vaccine targeting the RBD of the S protein of SARS-CoV-2 induces protective immunity. Nature. 2020;586(7830):572–7. https://doi.org/10.1038/s41586-020-2599-8.

66. Persson G, Restori KH, Emdrup JH, Schussek S, Klausen MS, Nicol MJ, et al. DNA immunization with in silico predicted T-cell epitopes protects against lethal SARS-CoV-2 infection in K18-hACE2 mice. Frontiers in immunology. 2023;14. https://doi.org/10.3389/fimmu.2023.1166546.